Late Pleistocene palaeoenvironmental reconstruction of Northeastern Iberia : taxonomic, taphonomic and isotopic approach based on small-mammal assemblages

Monica Fernandez Garcia

Università degli Studi di Ferrara

DOTTORATO DI RICERCA IN SCIENZE UMANE
"International Doctorate in Quaternary and Prehistory"

In convenzione con
Muséum national d'Histoire naturelle

CICLO XXXI

COORDINATORE Prof. Trovato, Paolo

LATE PLEISTOCENE PALAEOENVIRONMENTAL RECONSTRUCTION OF NORTHEASTERN IBERIA: TAXONOMIC, TAPHONOMIC AND ISOTOPIC APPROACH BASED ON SMALL-MAMMAL ASSEMBLAGES

Settore Scientifico Disciplinare L-ANT/01

Dottoranda
Dott. FERNÁNDEZ-GARCÍA, MÓNICA

Tutori
Prof. LÓPEZ-GARCÍA, JUAN MANUEL
Prof. DENYS, CHRISTIANE
Prof. ARZARELLO, MARTA

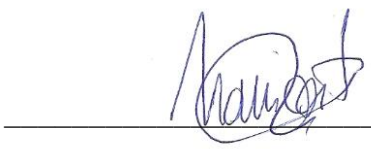

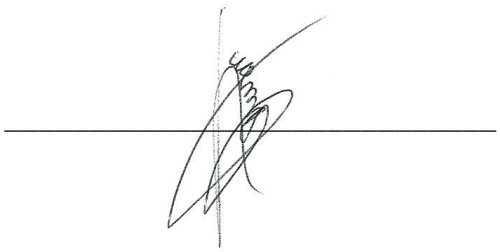

Anni 2016/2019

Cover page composition: wood mouse photograph (author: Andrew Everhale, 2001;
https://www.pinterest.es/pin/461970874258564801/),
eagle owl photograph (https://www.pinterest.es/pin/415738609333835304/) and
Neanderthal woman reproduction photograph (author: Joe McNally, 2008, National Geographic).

DOCTORAL THESIS SUPERVISED BY:

JUAN MANUEL LÓPEZ-GARCÍA

DOCTORAL THESIS TUTORIZED BY:

CHRISTIANE DENYS (MNHN)

MARTA ARZARELLO (UNIFE)

FERRARA, 29th MARCH 2019

JURY MEMBERS:

YOLANDA FERNÁNDEZ-JALVO

ANTONIO GARCÍA-ALIX

JUAN MANUEL LÓPEZ-GARCÍA

CHRISTIANE DENYS

MARTA ARZARELLO

EXTERNAL REVIEWERS:

GLORIA CUENCA-BESCÓS

ADAM NADACHOWSKI

ABSTRACT

The main objective of the PhD thesis is the reconstruction of palaeoenvironment experienced during the Late Pleistocene, mainly during Marine Isotope Stage 3 (MIS 3), at northeastern Iberia, through the combination of different ecological approaches based on small-mammal assemblages (insectivores, bats and rodents). Three archaeological sites are included: Abric Romaní rock-shelter (Capellades, Barcelona); Teixoneres cave (Moià, Barcelona) and Arbreda cave (Serinyà, Girona). It is also included a paleontological site from a close chronology, Xaragalls cave (Vimbodí-Poblet, Tarragona). The aim is the integration of the available data of the studied archaeological sequences through palaeoecological and oxygen isotope compositions analysis for increasing our knowledge about the MIS 3 environment from a regional point of view and reach a better understanding of the climatic singularities of Iberia during last Neanderthals settlements. One of the focus is fixed in oxygen isotope compositions ($\delta^{18}O$) analyzed from enamel tooth phosphates of both modern and fossil rodent remains of these localities. Taphonomic and taxonomical analyses based on small-mammals are also performed to reach a complete ecological interpretation of these sites. Other methods currently use in palaeoenvironmetal reconstructions based on small-mammal assemblages were also employed, such as mutual ecogeographic range method, habitat weighting method, chorotypes classification and bioclimatic model method. Considering the isotopic results obtained, this work shows that two main factors should be considered in Iberian palaeoenvironmental reconstructions: the possible seasonality of the rodent assemblages, derived from the predator, and the regional particularities on $\delta^{18}O$ values of meteoric waters in the Iberian Peninsula. Accordingly, a new methodological proposal for the reconstruction of palaeotemperatures from rodent tooth $\delta^{18}O$ accumulated in the Iberian Peninsula was developed and after applied to the archeological and paleontological sites studied. The recorded palaeoenvironment show globally cooler and wetter conditions than nowadays but it is detected notable climatic stability in all sites, with only slight changes related to stadial-interstadial pulsations, reflected mainly in oscitations between Mediterranean and mid-European species abundances. Woodland formations are always abundant throughout the sequences. The continuous maintenance of woodland covertures besides slight climatic variations and globally stable rodent communities, demonstrate the singularities of Iberian Peninsula, in contrast to the high climatic instability experience in Eurasia. This work highlights that a combination of different local-scale palaeoecological proxies compared to larger-scale proxies is essential to obtain faithful environmental reconstructions.

RIASSUNTO

L'obiettivo principale di questa tesi di dottorato è la ricostruzione paleoambientale registrata durante il Pleistocene superiore nella penisola Iberica nord occidentale. Principalmente si è indagato lo stadio isotopico marino 3 (MIS 3), attraverso la combinazione di differenti approcci scientifici basati sullo studio di insiemi faunistici di piccoli mammiferi (insettivori, pipistrelli e roditori). I tre siti analizzati sono: il riparo dell'Abric Romaní (Capellades, Barcellona), la grotta delle Teixoneres (Moià, Barcellona) e la grotta dell'Arbreda (Serinya, Girona). Inoltre è stato anche incluso un quarto sito paleontologico coevo, la grotta dei Xaragalls (Vimbodí-Poblet, Tarragona). L'obiettivo è quello di integrare i dati disponibili delle sequenze archeologiche con i dati derivati dell'approccio paleontologico e dell'analisi degli isotopi dell'ossigeno, per permettere l'incremento delle conoscenze ambientali del MIS 3 da un punto di vista più strettamente regionale e per comprendere meglio la singolarità climatica nell'ultima fase neandertaliana nella penisola Iberica. Lo studio si è incentrato nell'analisi isotopica dell'ossigeno ($\delta^{18}O$) dello smalto dentario sia dei roditori moderni che fossili dei suddetti siti archeologici. L'analisi tafonomica e tassonomica basata sui picoli mammiferi ha inoltre contribuito all'arricchimento delle conoscenze ecologiche, permettendo una più ampia interpretazione dei siti analizzati. Altri metodi, ugualmente utilizzati, sui resti fossili di piccoli mammiferi per la ricostruzione paleoambientale sono il metodo dell'intervalli eco-geografici comune, il metodo dell'habitat ponderato, la classificazione corotipica degli organismi e il metodo basato sul modello bioclimatico. Considerati i risultati ottenuti, questo lavoro mostra che bisogna tenere conto di due fattori importanti nella ricostruzione del paleoambiente iberico sulla base delle analisi isotopiche dell'ossigeno: la possibile stagionalità dell'accumulo di roditori, derivata dal loro predatore, e le particolarità regionali sui valori di $\delta^{18}O$ delle acque meteoriche nella penisola iberica. Una nuova proposta metodologica impiegata per la ricostruzione delle paleotemperature e ottenuta dallo studio dentario dei roditori $\delta^{18}O_p$ nella penisola iberica, dopo esser stata sviluppata, in conformità con quanto previsto, è stata applicata ai siti archeologici e paleontologici studiati. Il paleoambiente registrato mostra condizioni generalmente più fredde e più umide rispetto ad oggi ed è stata inoltre individuata una importante omogeneità climatica in tutti i siti, con leggere variazioni legate alle pulsazioni stadili-interstadiali, le quali si riflettono nelle oscillazioni tra le abbondanze di specie mediterranee e dell'Europa centrale. Le formazioni boschive sono sempre abbondanti in tutte le sequenze. La continua persistenza di coperture boschive oltre a leggere variazioni climatiche e comunita di roditori globalmente stabili, dimostra le peculiarità della Penisola Iberica, in contrasto con l'elevata instabilità climatica registrata in Eurasia. Questo lavoro sottolinea come la combinazione tra l'analisi paleoecologica su scala locale e quella su larga scala geografica, permetta essenzialmente di ottenere una ricostruzione paleoambientale più fedele.

ACKNOWLEDGEMENTS

This doctoral thesis was founded by a three-years scholarship of the Erasmus Mundus Program, obtained to develop the International Doctorate in Quaternary and Prehistory (IDQP). This scholarship gave me the opportunity to perform my research between the Università degli Studi di Ferrara (Ferrara, Italy) and the Muséum National d'Histoire Naturelle (Paris, France), but also short stays in the Université Claude Bernard (Lyon, France) and the Institut català de Paleoecologia Humana i Evolució Social (Tarragona, Spain).

Firstly, I would like to express my deepest gratitude to Dr. Juan Manuel López-García for accepting the direction of my thesis and actively helping me in its development. Without his guidance and persistent help this thesis would not have been possible. My intellectual debt is to Dr. Aurélien Royer, who generously has taught me everything about the analysis of isotopes.

I want to thank Prof. Marta Arzarello, as the coordinator of the IDQP, for assuming the coordination of this work and for help me with all the administrative procedures. Specially thanks to Prof. Benedetto Sala and Dr. Claudio Berto, for their scientific advice during my stay at the Università degli Studi di Ferrara. I am grateful also to Prof. Christiane Denys for accepting the coordination of my thesis during my stay in the Muséum National d'Histoire Naturelle. I would like to offer my special thanks to Dr. Emmanuelle Stoetzel for its guidance in the Musée de l'Homme and her scientific help.

I would like to express my gratitude to Prof. Christophe Lécuyer and to the Laboratoire de Géologie of the Université Claude Bernard for allowing me to perform the isotope analyses. Special thanks to Dr. Romain Amiot and Dr. Jean Goedert for their advices, help and supervision during the analyses.

The archaeo-paleontological sites included on this thesis are coordinated by the Institut català de Paleoecologia Humana i Evolució Social, where I have undergoned the first stage of my scientific career and where I have been welcomed whenever my research has needed it. I would like to thank those who allow me access to the material that is the object of this thesis and for its scientific help: Dr. Eudald Carbonell, Dr. Gema Chacón, Dr. Palmira Salidiè, Dr. Josep Vallverdú and Dr. Manolo Vaquero (Abric Romaní site); Dr. Jordi Rosell, Dr. Ruth Blasco and Dr. Florent Rivals (Teixoneres cave); Dr. Joaquim Soler and Dr. Narcís Soler (Arbreda cave); and, Dr. Josep Vallverdú, Dr. Sandra Bañuls, Dr. Juan Manuel López-García and Dr. Antonio Rodríguez (Xaragalls cave). The study of this material would not have been possible without intense years of field work and, therefore, I want to thank the efforts of all the people who have been involved in these excavations.

I am also grateful to Aitor Burguet Coca, Marta Puig Domènech, David Funosas, Marius Domingo de Pedro and Josep Maria Vergés for providing pellet samples. I want to thank Dr. Efstathia Robakis for accepting English revisions. Dr. Antonio Pineda-Alcalá, Dr. Ethel Allué and Dr. Florent Rivals have generously help me in the reviewing of some thesis chapters. Finally, I would like to offer my special thanks to my friend, Marc Ferrer, who patiently has helped me in the final layout of the thesis.

Una tesis es creixement professional, però és també una etapa fonamental de creixement personal i es que la vida passa en paral·lel. Els ingredients fonamentals són bons consells, generositat, amistat i constància. Les fases i els escenaris d'aquesta tesis han anat canviat, però cada experiència ha estat enriquidora, en gran part, gràcies a totes les persones que m'han acompanyat o que he anat trobant durant aquest camí, dins o fora del món acadèmic. A continuació vull dedicar unes línies a aquestes persones.

Grazie alla squadra di Ferrara (soprattutto Claudio, Elisa, Julie, Guido, Marta) per l'aiuto scientifico, ma anche per momenti di relax. Grazie soprattutto a Claudio per tutto il suo aiuto e il suo generoso consiglio. Fuori dall'UNIFE: Filippo, Claudia, Alessandro, Alice, Francesca, Nicoletta e, anche, Sofi. Abbiamo condiviso apperitivi, birre al duomo, cene improvvisate e notti fantastiche all'Arci Bolognese. A Ferrara ho conosciuto l'arrampicata, dalle persone che ho incontrato, è soprattutto con Pietro, il mio compagno di arrampicata, con cui ho condiviso preoccupazioni, birre e scampagnate. Anche grazie ai miei ex-coinquilini, che ancora dopo tanto tempo passato, loro erano lì per aiutarmi. Sixin mi dispiace per la tua bici! Ma nulla sarebbe stato lo stesso senza Manu. Sei unica, il periodo a Ferrara è stata una grandissima esperienza e molto grazie a te. Ti voglio così bene, anche se non ci sentiamo, anche se non ci vediamo. Ma vieni a Tarragona, per favore; perché non si può vivere così lotano da te!

De la meva estada a Lyon em quedo amb dues persones a nivell profesional: Aurélien i Jean. Aurélien as été un élément fondamental de cette thèse, l'isotopie c'est dur, mais moins si quelqu'un vous guide tout au long du chemin. Merci pour tous les conseils judicieux et nos longues discussions. Rendez-vous à La Balutie! Je doute que la thèse présentée ici ait été possible sans l'aide et les conseils de Jean au cours du protocole chimique et du spectromètre de masse. Merci beaucoup! A camino entre lo profesional y lo personal en Lyon, estuvo Abel, Abeider para los amigos, mi Spanish coach en la universidad de Lyon. Hubiera sido mucho más duro sin nuestras interminables charlas al olor del mate. Gracias a él conocí a Carmen, Eli, Pablo, Antonio, Natalia, Dani, Carol, Ana, Alberto, Santos, Irene y Alex (x2) y al extensísimo grupo de "españoles en Lyon". Los seis meses de estancia en Lyon hubieran sido muy aburridos sin vosotros. No sólo hemos compartido cervezas y picnics en los "quai" y en el parque de la Tête d'Or, sino que también museos, "randonnée", viajes y kayaks. Cada uno de vosotros me ha aportado mucho. Millones de gracias. Mi casa es vuestra casa.

Merci aussi à mes collègues du musée de l'Home (Gilhem, Camille, Delphine et bien d'autres), dans ce bureau fantastique surplombant la tour Eiffel. Les moments partagés avec vous ont été très amusants et j'aurais sans doute je m'aurais perdu plusieurs fois dans cet édifice labyrinthique, sans vos instructions. Merci également à Isabelle, qui m'a accueillie chez elle et qui soutient mon quotidien comme s'il s'agissait d'un membre de la famille. Vous l'avez rendu très facile, je me sentais chez moi. Gracias también a Juan y Roser, por compartir mis escasos momentos de ocio en París. Compartimos cervezas, vinos, intensas discusiones arqueológicas y políticas (como para no!) y buenas cenas en Les Fabricants.

Gracias a todo el equipo de predocs del IPHES (en especial, a Raquel, Cris, Diego, Andión, Arturo, Miguel, Paula, Iván, Jose, Carlos y Laxmi). Sois todos fundamentales, cada uno con su granito de arena y sin duda el mundo sería un lugar mejor si fuera por gente como vosotros y el mundo de la investigación sin duda. Me siento afortunada de conoceros. Esa generosidad es extensible también a muchos apreciados doctores IPHES, en especial quiero dar las gracias a Ethel, Isas, Pep, Palmira, Antonio, Lena, Rosa, Marina, Andreu, Josep Maria, Carlos, Deborah, Florent, Gema, Francesca, Quico y Anna. Siempre se obtienen ideas interesantes de las conversaciones con vosotros. Juanin gracias por tus siempre valiosísimos consejos, que me han ahorrado días enteros de trabajo. Joana compañera de batallas en Romaní, tu complicidad y consejos siempre han sido esenciales. Patri, gracias por compartir siempre tus experiencias y por tus ánimos. También quiero hacer una mención especial al grupo de micro (Juanma, Hugo, Sandra, Elisa, Almudena, Christian, Iván I, Iván II y Bisbal). Aprovecho para darte una vez más las gracias, Juanma, por esta larga trayectoria de trabajos juntos, siempre con los consejos justos, siempre dando prioridad a mi carrera científica. Sé que al inicio de mi tesis no siempre fue fácil para ti, pero siempre estuviste ahí. También mi mayor gratitud para Lluc, quien me contagio su entusiasmo por la tafonomia y me transmitio todo su extenso conocimiento. También quiero tener en cuenta en estos agradecimientos al equipazo del lavado del río en las excavacaciones de Atapuerca dirigido por nuestra amada abuela científica Gloria: Mila, Juanma, Hugo, Julia, Carmen, Ana, Mercedes, Raquel, Alicia, Cris, Pablo, Toni, Arvidas, José Luís, Javi, Cristóbal... Gracias por todos esos momentos de diversión épicos que hemos vivido. Me paso el año deseando

que sea verano, sólo para volver a reencontrarnos! También a tantas personas que he ido conociendo en sucesivas excavaciones. Por inclasificables pero destacados, Mikel y Guille os debo mencionar aquí.

Como no, gracias también al equipo de postres IPRHES: Aitor, Carol, Leo, Toni, Irene, Ana Bucchi, Edgar, Patri, Blanca, Esther, Elena, Cris... Y prometedoras incorporaciones de última hora, Antonia, Chiara, Sabrina, Anna y Adrián. Con la mayoría de vosotros, sin duda, he compartido mucho más que dulces momentos. Leito! Esas sesiones de terapia grupal compartiendo los últimos momentos, tus ánimos por siempre hacer cosas, tus divertidas expresiones canarias y tus valiosos consejos. Es siempre un placer tenerte cerca, aunque nos ha costado lo suyo los dos primeros años. Irene, Buchi y Edgar suponéis una mezcla explosiva de incalculables consecuencias, pero la diversión está asegurada. Gracias por tantos momentos divertidos. Carol, companya de piti-pauses al IPHES, on es poden gestar des de converses d'interès merament domèstic fins a profundes reflexions científiques (bé, pot ser no tant profundes). Gràcies pel coaching. Antonia, grazie mille per tutto il tuo aiuto, specialmente con la burocrazia italiana negli ultimi momenti. Y como si fueran del IPHES por causas distintas, gracias Montse y Maddalen. Montse, mi compi de yoga. Compartir ratos contigo es genial, siempre con una sonrisa y un buen consejo. De las personas más fuertes que conozco, me queda mucho que aprender de ti. Maddalen (y el ausente Toni!), los arquitectos del grupo, casi habéis completado vuestra formación en arqueología, sois conocedores de gran parte de las generaciones IPHES y por fin os llevamos a excavar. Sois una bonita válvula de escape. Y, finalmente, Toni (perdón, Dr. Pineda). 10 años ya de amistad, con infinitas experiencias compartidas desde nuestros inicios en prácticamente todo: carrera, excavaciones, máster o estancias en Ferrara. Podemos pasar meses sin vernos, pero la complicidad que hemos construido a lo largo de años se mantiene sólida como desde el primer día. Las cosas a tu lado son increíblemente sencillas y exageradamente divertidas. Gracias también por las revisiones de los capítulos y consejos de última hora. Eres nuestro doctor preferido.

Mireia, Paula, Judit, Eli i Yas. Cinc visions del món, cinc pilars en els quals recolzar-me sempre que ho he necessitat. Cadascuna diferent, cadascuna enriquidora en el seu camp. Són molts anys junts, moltes experiències, algunes molt divertides i altres menys, però que entre totes hem sabut transformar-les en creixement personal. Em sento molt afortunada de què m'hagueu acompanyat en aquest viatge i que la distancia només ens hagi enfortit. Gràcies per il·lusionar-vos amb mi. No puc ni imaginar tot el que falta per venir. Per molts anys.

Però res hagués estat possible sense el teu suport durant aquests tres anys, Aitor. Les circumstàncies del meu doctorat suposaven una aventura professional i personal i vam ser forts. En la distància, però sempre junts. Lluny, però sempre aprop. I al final del camí, dues tesis i una sola casa. Pilar fonamental personal i en molts casos professional. Mai et podré agrair tanta generositat i tantíssima paciència, però intentaré compensar-t'ho amb els mesos que queden per venir. El món es més bonic quan tu estàs aprop, perquè tu i jo som un crit.

Y, finalmente, lo más importante: mis padres. Papa, gracias por tu ambición y tu vitalidad, siempre en lucha, siempre apoyándome. Has sabido adaptarte a los diferentes momentos de estos tres últimos años, a pesar de distancia que interponía entre nosotros. Siempre con buenos consejos, intentando ofrecerme tus experiencias vitales para enriquecer la mías. Gracias por confiar en mí. Mama, gracias por tu sonrisa y siempre tu cálido abrazo. Siempre a mi lado, sin pedir nada a cambio. Siempre has creído en mí y sin tu apoyo diario dudo que hubiese llegado a donde estoy hoy en día. Sólo dos palabras; te quiero.

INDEX

Thesis structure

This PhD thesis is divided in ten chapters which combined inedited and published data. To facilitate the lecture, all material is presented in the same edition and published manuscripts can be founded in the appendices.

The first chapter, "Introduction, framework and objectives", aims to provide the essential knowledge about small-mammals assemblages, its importance for environmental reconstructions in archaeo-palaeontological contexts and the need for taphonomic studies to deal with these assemblages; as well as, the basic principles operating in oxygen isotope compositions at mid and high latitudes. Framework on the Late Pleistocene climate in Iberia and Neanderthals occupations is included. This chapter end with a brief exposition of this PhD problematic and the main objectives proposed.

The second chapter, "Material and methods synthesis", presents the main disciplines used to reach the exposed objectives and the samples included. It is provided a brief description of each of the methods employed on small-mammal remains analyzed, from recovering and analytical techniques, to methods of environmental reconstruction: taphonomy (predation and post-depositional processes), methods of landscape reconstruction (habitat weighting and diversity index) and climatic reconstruction (mutual ecogeographic range and bioclimatic model). Oxygen isotope analytical techniques, including wet chemistry procedures and palaeotemperatures reconstruction, are also explained.

The third chapter, complemented the framework studies exposed in Chapter 1, focusing on rodent communities, related to works previously published, to understand the general trends that operated in this region and the environmental lecture that provide. This work has been already published in Comptes Rendus Palevol, with the same title provided for the thesis chapter "Palaeoecological implications of rodents as proxies for the Late Pleistocene – Holocene environmental and climatic changes in northeastern Iberia". The manuscript with journal edition is included in Appendix 3.

The fourth chapter presents the small mammals from the richest level of the Abric Romaní sequence, level O. In this work, an effort to complement different ecological approaches is done, to understand the whole significance of this accumulation and its climatic signal. This work has been already published in Palaeogeography, Palaeoclimatolology, Palaeoecology, with the title "Paleoenvironmental context of Neanderthal occupations in northeastern Iberia: The small-mammal assemblage from Abric Romaní (Capellades, Barcelona, Spain)", that is maintained in this thesis chapter. The manuscript with journal edition is included in Appendix 3.

The fifth chapter is titled "Unravelling the oxygen isotope signal ($\delta^{18}O$) from rodent teeth in northeastern Iberia, and the implications for past climate reconstructions". This chapter exposed a state of the art about the oxygen isotope analyses based on rodent remains, evaluate the significance of the oxygen isotope compositions reflecting about the singularities that Iberia can suppose and asking about how the origin of the remains analyzed can affect the final palaeotemperatures estimations. One methodological proposal is presented for oxygen isotope analysis on rodent phosphate, considering Iberian context and seasonality in rodent accumulation. This protocol is after applied to one MIS 3 palaeontological site, Xaragalls cave. This works is currently under review in the journal Quaternary Science Reviews.

The following three chapters (from 6 to 9) correspond to three Late Pleistocene archaeo-

palaeontological sequences with short-term and long-term human occupation from northeastern Iberia: Abric Romaní, Teixoneres and Arbreda. These chapters are presented as scientific manuscripts, including an introduction, site description, material and methods, results exposition and a brief discussion of the own issues of the sequences. In all these chapters the oxygen isotopes analyses performed are discussed besides the taphonomic and the palaeoecological analyses. In chapter 6, "Combined palaeoecological methods using small-mammal assemblages to decipher environmental context of a long-term Neanderthal settlement in northeastern Iberia", is included all available small-mammal assemblage data from the entire excavated sequence of the Abric Romaní rock-shelter, historical and new, evaluating their origin and taphonomic history, the environmental implications and the oxygen isotope analyses performed on the richest levels. In chapter 7, "Palaeoecological reconstruction of Teixoneres site (Moià, Barcelona) based on small mammals: origin of the assemblage and palaeoclimatic inferences", previous environmental studies of small-mammal are complemented with a complete taphonomic analysis, biochemical studies and palaeotemperatures estimations. Then, in chapter 8, "Latest Pleistocene in northeastern Iberia: oxygen isotope analysis and palaeoenvironment inferences from rodent remains of Arbreda cave (Serinyà, Girona)", the palaeoclimatic conditions of Arbreda sequence are explored through oxygen isotope analysis on rodent teeth in comparison to complemenatary ecology data based on small-mammals available from the site.

The chapter 9, "General discussion", summarize and address the main aspects observed in previous chapters through a holistic interpretation, comparing and discussing general results. The discussion focuses in the oxygen isotope meaning of rodent assemblages in Iberia, in the limitations and possibilities of the palaeoclimatic methods employed through the thesis and in the environmental conditions of northeastern region of Iberia considering the implications that those have for Neanderthals subsistence. Finally, in chapter 10, "Concluding remarks and future perspectives", the central ideas exposed in the general discussion are synthetized and ways to affront aspects unresolved for this thesis are proposed.

In the appendices are provided: 1) the taxonomical criteria for the identification of the small-mammal remains from the Abric Romaní; 2) tables and figures that expand the content of the palaeoecological and taphonomic analyses presented on chapters 3-8; and, 3) the scientific manuscripts related with chapters 3 and 4.

Chapter 1.
Introduction, framework and objectives

1. Small mammals as environmental proxies

Throughout history, fossils and their origins have aroused great interest in the knowledge of the past. Currently, understanding the evolution of the species, the origin and the formation of fossils, and the environment where humans performed their activities, have also become one of the main objectives of prehistoric research. Therefore, palaeontological, taphonomic, and palaeoecological studies are common in Quaternary sites. Taking into account the constant relationship that hunter-gatherer societies maintained with the environment, obtaining information about the ecological conditions in which they developed is essential for the understanding of their subsistence strategies and their ability to adapt to the environment, centering great interest in Prehistory research during the last decades. The aim of palaeoecologial studies is to reconstruct the ecology of the past to understand evolutionary and biogeographic changes. Though these studies were traditionally based on pollen studies, there are currently many methods of palaeoecological reconstruction based on mammals. In palaeontology, most approaches are based on comparative methods and actualistic principles, which operate with taxonomic comparisons, linking fossil and modern species. Methods vary depending on the size and nature of the palaeocommunity available for research.

Archaeological studies usually establish three types of faunistic classifications related to size in order to facilitate the study of the remains: "macrofauna", "mesofauna", and "microfauna". The last category is the so-called "small vertebrates", which includes birds, amphibians, reptiles, fishes, and "small mammals". None of these classifications (e.g., "small vertebrates" and "small mammals") has a taxonomic value, but they are used in the scientific literature to indicate those orders, families, or genera in which most of the species have small size and, consequently, both the study techniques and their applications differ from those of larger specimens (Alférez, 1990; López-García, 2011). Within the small mammals, three main groups are distinguished: insectivores (moles, hedgehogs, shrews, among others), chiropters (bats), and rodents (voles, rats, mice, dormice, squirrels, among others); the lagomorphs (rabbits and hares) are sometimes also included.

Small mammals are one of the most significant groups of mammals in numbers both of species and specimens in Eurasia during the Quaternary and still today. The order Rodentia is the largest order of living mammals, includes more than 2,000 species worldwide (26 exclusively in Iberia), and are greater in number than all the other mammals combined (>42%). The order includes species mainly herbivorous (frugivores, foragers, but also omnivores) and adapted to all types of environments, from mainly terrestrial species that remain on the surface or that live underground, to arboreal or amphibious species. No less important is the order Chiroptera, comprising about 1,100 extant species (27 species in Iberia), which includes more than 20% of extant mammal species on our planet. They are the only mammals that have developed the ability of active flight, which has allowed them to occupy a great variety of ecological niches. They adopt different kinds of diets, but most species are herbivorous and frugivorous. Finally, the ancient order of Insectivora, currently known as the Eulipotyphla order, is dived into various suborders, such as Soricomorpha, which includes shrews and moles, and Erinaceomorpha, which includes hedgehogs. Both get their old name from their diet, which is based mainly on insects and constitutes one of the

lineages of current mammals of more primitive origin. They are characterized by their plantigrade feet and their dentition is made of continuous rows of teeth, which differs from the usual dental formulas (Blanco, 1998; Le Louarn and Quéré, 2003; MacDonald and Barret, 2008; Purroy and Varela, 2005; Wilson and Redeer, 2005).

When Cuvier established the principles of systematic classification in the 19th century, he insisted on the importance of studying small fossil remains, which had until then gone unnoticed (Cuvier, 1817). However, it was not until the second half of the 20th century that the study of fossil microvertebrates occupied a prominent place in the field of palaeobiology and biostratigraphy. Small mammals and especially rodents have proved to be especially useful for reconstructing the palaeoenvironment of the Quaternary (Chaline, 1988, 1970; Cuenca-Bescós et al., 2009; Hernández Fernández, 2001; Le Louarn and Quéré, 2003; López-García, 2011, among others). Several evolutionary, palaeocological, and palaeoclimatic models have been obtained from these small remains and, in biostratigraphic applications, these remains have become indispensable for determining the age of fossiliferous deposits. Currently, there are entire laboratories devoted almost exclusively to the research of small fossil vertebrates, and a great part of Vertebrate Palaeontology research relies on small vertebrates as well. Within the small mammals, Rodentia is the most studied order from the Quaternary, due to its abundant remains in fossil deposits and its indisputable biostratigraphic and palaeoecological value.

Small mammals, and particularly rodents, have very specific environmental and climatic requirements for survival. The most important factor that can affect their presence are temperature and moisture gradients, available grass and forest cover, and the quality of soils. These parameters shape the quality and availability of food resources that they require (Le Louarn and Quéré, 2003). Because of their high reproduction rates, rodents can respond quickly to environmental changes, such as seasonal fluctuations in temperature, humidity, or food availability. Moreover, their small size and the restricted territory that each rodent community inhabit, in addition to their usually short migration distances, make this group extremely good indicator of the environment at a local scale. By establishing a reciprocal relationship and considering the actualistic principle, through the knowledge of the small-mammal faunal communities in a given space and time, it is possible to deduce the dominant environment from that context in the past (Alcalde & Galobart, 2002; Chaline, 1988). Thus, considering knowledge of the current ecology of these taxa, general attributes of the palaeoenvironment can be inferred, and its variations on large time scales can be interpreted relative to climatic oscillations.

Their importance is even greater due to the wide range of geographical distribution of small mammals. In Quaternary sedimentary deposits, the abundance and richness of small mammals is usually greater than those of large mammals, allowing multiple statistical approaches and quantitative methods to be applied (Alcalde & Galobart, 2002; Chaline, 1970; 1988; López-García, 2011, among others). In addition, rodents are useful in biochronological reconstructions, since they were one of the fastest-evolving groups of mammals during the Pleistocene, despite the shortness of this period (e.g., Chaline, 1988; Cuenca-Bescós et al., 2010; Hernández-Fernández et al., 2004; Maul et al., 2014; Sesé, 2005). The study of small mammal of the past allows us to evaluate their past characteristics, such as distribution, development, evolutionary trends, diversification, or community structure (Chaline,

1970, López-Martínez, 1992). Recently, some research has shown how small-mammal diversity can be related to climatic shifts and/or anthropic pressure (Bañuls-Cardona et al., 2017; Lopez-Garcia et al., 2013). Therefore, we can confirm that small mammals provide a large amount of data on the history of the Quaternary, since they are the group that contributes most to solving questions about biochronology, palaeoclimatology and palaeoenvironment.

2. The origin of small mammals and their preservation in fossil deposits

The study of past ecosystems can be complex due to the intervention of taphonomic processes in the formation of a deposit. In any fossil association, there are differences between the recovered fossil faunal community and the community from which it originally came. The main causes of these differences are the bias inherent in the origin of the accumulation and the differential conservation of elements. Taphonomic agents could produce modifications before or after burial, which in most cases can result in a fossil assemblage not representing the exact characteristics of the original biological community, as well as possible mixtures. For these reasons, when performing rigorous palaeoecological reconstructions it is essential to know all the aspects of the environment that influence a fossil assemblage, in other words their taphonomical history, that will be mainly explained by the accumulator agent and the post-depositional processes suffered (Andrews, 1990; Denys and Patou-Mathis, 2004; Fernández-Jalvo, 1992; Fernández-López, 2000; Lyman, 1994; Scott et al., 1996).

Taphonomy is defined as the study of the passage of biological entities from the biosphere to the lithosphere; this is the investigation of the nature of the accumulation and preservation of fossil elements with the aim of understanding the factors that have influenced their conservation and destruction from the time that they were part of the living fauna community until they were recovered. Although there is some ambiguity in their differentiation, two taphonomic subsystems are generally distinguished: biostratinomy (processes that affect remains before burial) and fossil-diagenesis (processes that affect after burial) (Weigelt, 1927, Müller, 1979). From its initial definition by Efremov (1940) and the posterior pioneer and extensive taphonomic investigations on large mammals, mainly related to the classical "hunter-scavenger" debate (e.g., Ardrey, 1983; Brain, 1981), to recent redefinitions (e.g., Fernández-López, 2000), taphonomy has evolved in a systematic and methodic research, but also in its conception. Taphonomy has gone from being understood as the study of the processes that generate a loss of information during burial and fossilization to our current understanding that taphonomic alterations experienced by recovered elements can provide us valuable information about the external environment in which they occurred (Fernández-Jalvo et al., 2011; Fernández-López, 2000). In addition, during the development of this discipline, taphonomy has become multidisciplinary, since it incorporates knowledge from other sciences while providing information on past processes to disciplines such as sedimentology, micromorphology, stratigraphy, biostratigraphy, palaeoecology, archaeology and palaeobotany.

Taphonomic research was initially applied to the remains of large vertebrates, but currently is extended to numerous types of fossil records, such as the lithic industry, wood, charcoal, pollens or phytoliths. Regarding small-mammal studies, the concern for taphonomic studies appears much

later than for large vertebrate assemblages. Difficulties in the recovery of small vertebrate remains caused a certain lack of knowledge until the middle of the 20th century. Since then, the application of washing-sieving techniques has expanded the fossil records of these groups and the first questions about the origin of these small remains were posed. In addition, the small-mammal remains are particularly vulnerable to these fossilization processes due to their high fragility. The taphonomic study of small-mammal remains distinguishes the processes associated with predation (biostratinomic alterations) and the post-depositional processes that occurred after their accumulation (biostratinomic and fossil-diagenetic alterations). Pioneer studies of small-mammal remains focus on the identification of the principal agent that accumulated the small-mammal assemblages. Some have attributed their accumulation to natural causes, such as natural traps, water currents, or natural death in burrows or hibernation sites (Andrews and Cook, 1985; Denys, 1985; Kowalski, 1990; Shipman et al., 1984). However, several studies have shown that usually the main agents producing small-mammal assemblages are predators (e.g., Andrews, 1990; Bennàsar, 2010; Dodson and Wexlar, 1979; Fernández-Jalvo, 1992; Fernández-Jalvo et al., 2016; Lyman, 1994; Taylor et al., 2004).

In the 90's some research generates a great advance in the detection of the accumulator predator, mainly Andrews (1990) and Fernández-Jalvo (1992). These taphonomic approaches deduce the causes of past events through analogies with the observable processes in the present, and use the current ethology of small-mammal predators to understand their hunting habits (such as prey preferences, techniques, or hunting area extension), as well as the quantifiable aspects related to their modification of consumed remains (representation of species and elements, degrees of breakage, and digestion). The knowledge of predators' ethological characteristics allows us to evaluate the ecological bias in their prey accumulations and complement habitat inferences deduced exclusively from small mammals accumulated. Regarding the identification of post-depositional processes, most works are based on experimental work, mostly performed on remains of medium and large size (e.g., Andrews and Cook, 1985; Behrensmeyer, 1986, 1978; Bennett, 1999; Fernández-Jalvo and Andrews, 2003; Korth, 1979; Lyman, 1994; Shipman et al., 1984). The detection of these processes allows us to reconstruct the taphonomic history of the remains, evaluate the limitations of a certain association to develop ecological interpretations, and understand the processes which intervened in the formation of the site (Fernández-Jalvo, 1992).

3. Basic principles of oxygen isotope composition studies on small mammals

Interest in palaeocology, archaelogy and prehistory is extending progressively to the so-called "earth sciences". This has led to the incorporation of biochemical studies, with the aim of quantifying the qualitative changes that were initially observed in fossiliferous deposits. In the field of organic chemistry, the analysis of stable isotopes was first developed in the fields of geology, geochronology and geochemistry. The most popular application of oxygen stable isotope studies, indirectly related to archaeology, is found in the definition of the chronology of stadial and interstadial events that rely on the variations of oxygen isotope compositions recorded in planktonic and benthic foraminifera shells from ice cores (see synthesis in Dincauza, 2000). Later, they began to be applied to biochemistry, biology and ecology, and are currently applied even in the

social sciences, such as anthropology and ethnography. In the last two decades biochemical and isotopic studies have been applied to archaeological and palaeontological research with increasing intensity, for addressing subjects that extend from the estimation of absolute dating to the reconstruction of the human diet, environment, and mobility patterns (e.g., Bender, 1968; Bocherens, 1997; Hall, 1967; Lee-Thorp and van der Merwe, 1991; Schoeninger and DeNiro, 1984; Vogel and van der Merwe, 1977; see synthesis in Tornero and Saña, 2006). Most stable isotope analyses focus on four major chemical elements: carbon ($^{13}C/^{12}C$), oxygen ($^{18}O/^{16}O$), nitrogen ($^{15}N/^{14}N$), and strontium ($^{87}Sr/^{86}Sr$). Oxygen, carbon, and hydrogen are present in all forms of organic life, in their biological relationships, and in the set of chemical reactions of organic processes. The preservation of oxygen stable isotopes on animal body tissues provides information mainly about diet or environment and constitutes a powerful tool for bioarchaeological studies and for the quantification of palaeoclimate on the continental domain. Small-mammal remains frequent in Quaternary deposits can potentially address this reconstruction from local and regional contexts (Freudenthal et al., 2014; Navarro et al., 2004; Royer et al., 2014, 2013b).

Isotopes are atoms of the same chemical element, which have the same atomic number (number of protons and electrons) but whose nuclei have a different number of neutrons and therefore differ in mass number (number of neutrons and protons). Unstable isotopes can lose neutrons and become another isotope, thereby providing useful information with which to estimate past chronologies. On the contrary, the stable isotopes are equally preserved regardless of how much time has passed. Based on mass, oxygen (O) is the most abundant chemical element in the Earth, forming the main components of the hydrosphere, biosphere, and lithosphere. Oxygen can mainly occur in nature through different stable isotopes: ^{16}O (99,755%), ^{17}O (0.039%), and ^{18}O (0.206%). The ratio between ^{16}O, the lightest isotope (with 8 neutrons), and ^{18}O, the heaviest (with 10 neutrons), is the most commonly considered. As the absolute isotopic composition of a material is difficult to measure directly, isotope ratios are generally compared to that of a standard (Flanagan et al., 2005; Lécuyer, 2014). The relative abundance of ^{18}O to ^{16}O is commonly expressed in per mil (‰) relative to an international primary reference material of assigned value using the delta notation (δ), usually based on the Vienna-Standard Mean Oceanic Water (V-SMOW) (Coplen, 1995; Craig, 1961; Gonfiantini, 1978).

The difference in mass between ^{16}O and ^{18}O causes the isotopes to behave differently in chemical and physical reactions: lighter isotopes tend to react more quickly, generating a separation, which is called isotopic fractionation. This phenomenon results in the product having a greater relative abundance of light isotopes (lower $\delta^{18}O$) while the remaining substrate has a lower abundance of the light isotopes and therefore a greater relative abundance of the heavy isotopes (higher $\delta^{18}O$). At mid and high latitudes, $\delta^{18}O$ of meteoric waters ($\delta^{18}O_{mw}$) are potentially related to surface air temperatures through the year and across decades, leading to related mean annual $\delta^{18}O_{mw}$ with mean air temperatures at regional and global scales (Dansgaard, 1964; Rozanski et al., 1993) (Fig. 1.1). Meteoric water comes from evaporation from oceans, and to a lesser extent, from local evapotranspiration over continents. From a global point of view, the temperature of the air coupled to the air masses movements explains the appearance of this latitudinal gradient. The $\delta^{18}O_{mw}$

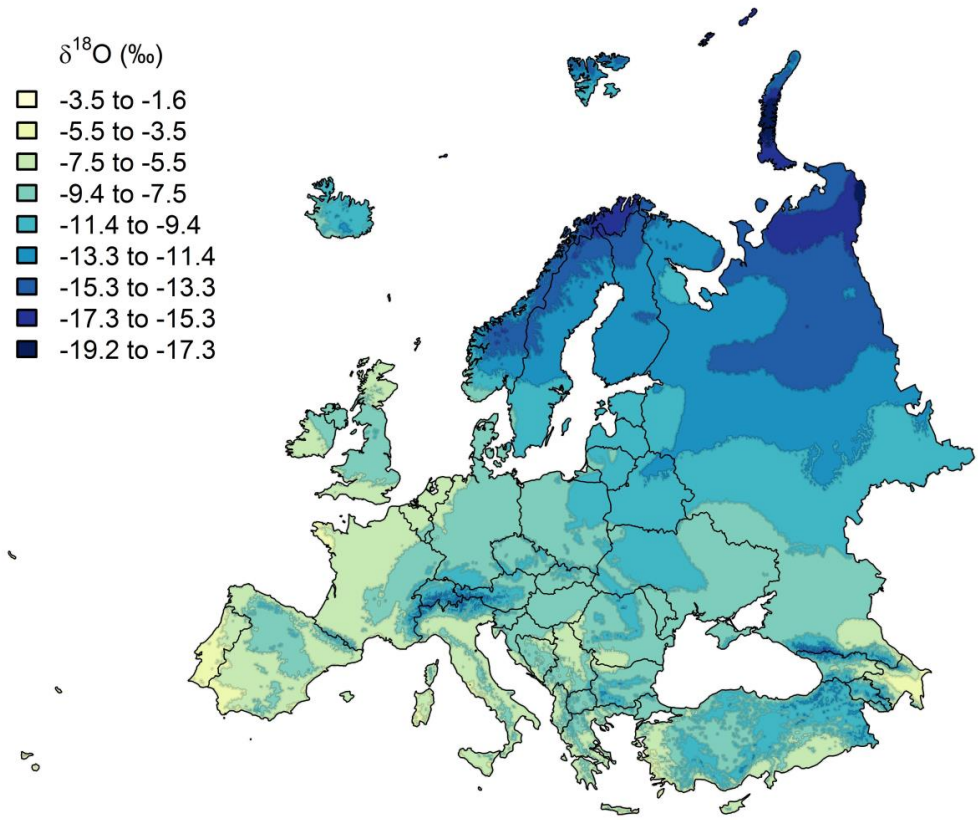

Figure 1.1 Spatial distribution of mean annual precipitation oxygen isotope compositions in Eurasia, showing latitudinal gradient. Map was obtained from http://waterisotopes.org (Bowen, 2017).

values are mainly controlled by the water vapour source, the trajectories of humid air masses, seasonal variations of precipitation and the ambient air during the process of condensation (see Dansgaard, 1964; Gat, 1996, 1980; Rozanski et al., 1993).

Accordingly, the main effects that influence $\delta^{18}O_{mw}$ in a regional-local scale are:

- Seasonality. Temperature and rainfall regimes vary between locations, but generally there is a predictable seasonal pattern, which shows higher $\delta^{18}O_{mw}$ during the warm season that decreases during the cold season, mainly as consequence of the relationship between $\delta^{18}O_{mw}$ and air temperatures.
- Continentality. The "continental effect" is driven by the depletion of $\delta^{18}O_{mw}$ in clouds as long as the distance towards the oceans increases, with decreasing $\delta^{18}O_{mw}$ values landward.
- Altitude. The "altitude effect" results from decreases in $\delta^{18}O_{mw}$ values as altitude increases. This is in response to the gradual removal of moisture from uplifted air masses with a preferential removal of the heavy isotope ^{18}O during condensation. This effect is thermo-dependent, because the condensation is caused by the decreasing temperatures associated with an increasing altitude.
- Another factor that could have an influence is the duration of precipitation, which when it is extended could lead to the "amount effect". $\delta^{18}O_{mw}$ decreases as long as rainfall amount increases, and this effect is attributed to a significant air cooling during heavy

precipitation. This effect is common in tropical areas but can occur in coasts or islands as well.

The analysis of oxygen stable isotopes can be applied to different categories of archaeological materials but are mainly centered in the organic fraction of bones and teeth. Several studies have demonstrated the relationship between stable oxygen isotopes of phosphatic tissues ($\delta^{18}O_p$) and the oxygen isotope composition of vertebrate body water, which itself is related to the composition of ingested water (from drinking water or water in food) most commonly of meteoric origin (Ayliffe et al., 1992; Longinelli, 1984; Longinelli and Nuti, 1973; Podlesak et al., 2008). Thus, the isotopic composition of animal tissues is strongly correlated with local precipitation and, thus, it is a useful proxy for reconstructing climate. Although the isotopic fractionation is kinetic (the proportions of light/heavy isotopes are maintained), $\delta^{18}O_p$ can be influenced by oxygen influxes and outfluxes (such as diet type and source of drinking water), but also by physiological factors such as body temperature and metabolism of each species (Lindars et al., 2001; Longinelli, 1984; Luz et al., 1984; Podlesak et al., 2008). These complex interdependent relationships have led to the development of taxon-dependent oxygen isotope fractionation equations relating $\delta^{18}O_p$ and $\delta^{18}O_{mw}$ (e.g., Amiot et al., 2004; Ayliffe et al., 1992; Bernard et al., 2009; D'Angela and Longinelli, 1990; Luz and Kolodny, 1985).

Some specific rodent characteristics, such as metabolic rates, rapid water turnover, and short time for mineralization of teeth, make this order very useful for climatic reconstructions based on oxygen isotopes (Blumenthal et al., 2014; Lindars et al., 2001; Podlesak et al., 2008; Royer et al., 2013a). Different oxygen isotope fractionation equations adjust to rodent teeth and bones related $\delta^{18}O_p$ to $\delta^{18}O_{mw}$ (D'Angela and Longinelli, 1990; Lindars et al., 2001; Luz and Kolodny, 1985; Navarro et al., 2004; Royer et al., 2013a) and demonstrate the relationship between the stable oxygen isotope composition of the biogenic phosphate from rodent teeth and the oxygen isotope composition of meteoric waters, which is related to past air temperatures at mid and high latitudes.

4. The Late Pleistocene climate and Neanderthal settlements

The Late Pleistocene (132-11,7 ka) is a period characterized by high climate instability with important climatic fluctuations of alternating cold and warm phases and isolated climatic episodes (see synthesis in Arribas, 2004; Arrizabalaga, 2004; Sánchez Goñi and D'Errico, 2005) (Fig. 1.2). These fluctuations most likely had impacts on flora, fauna, and human societies. Hominins, in the development of their biological and cultural evolution, had experienced these environmental changes and reacted in different ways to these new climatic scenarios. Late Pleistocene encompasses four Marine Isotope Stages (MIS; 5-2). It is considered by convention that the Late Pleistocene begins with the MIS 5e (ca. 132-116 ka), which starts at the last interglacial period of the Quaternary, traditionally called the Riss-Würm or Eemian. It is followed by four MIS 5 substages, which extend until 71 ka. This interglacial presents a strong climatic alternation, but was generally temperate, warmer, and more humid than the present-day, though some short cold episodes did occur. During the ca. 71 and 57 ka that followed MIS5, the summer insolation on the northern hemisphere was reduced and consequently the maximum extension of the polar ice caps was reached, along with a decrease in sea levels and a drastic drop in temperatures. At that point a general cold and dry trend with warm and humid

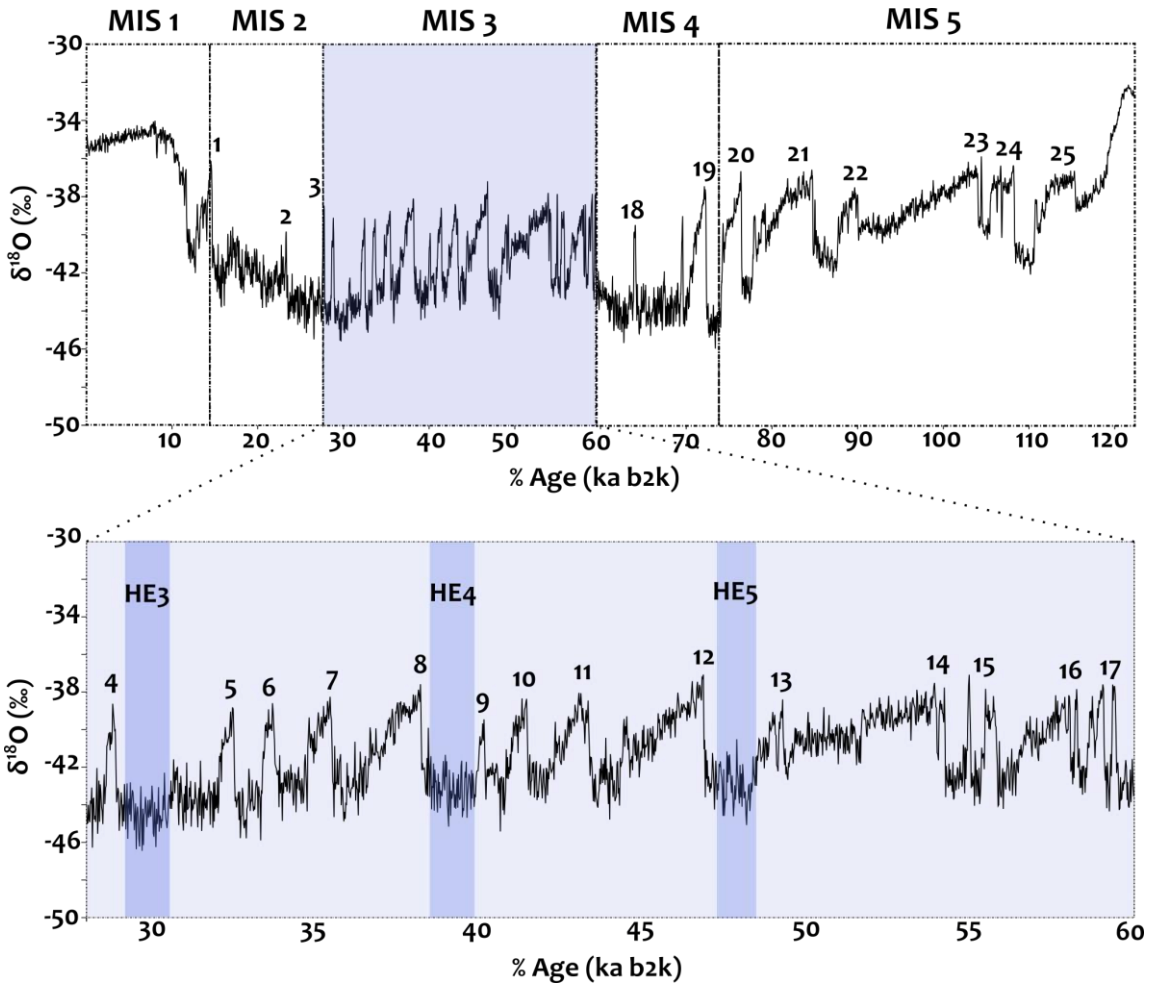

Figure 1.2 Oxygen isotope data from the NGRIP ice core from present to 123 ka (North Greenland Ice Core Project members, 2004). GICC05modelext when going beyond 60 ka b2k (summarized in Svensson et al., 2008; Wolff et al., 2010). The notation b2k implies age before 2000 AD. Greenland Interstadials (1-25) and Heinrich Events (HE) indicated. MIS, Marine Isotope Stage.

episodes was established. This trend encompassed both the very cold MIS4 (71-57 ka) episodes was established. This trend encompassed both the very cold MIS4 (71-57 ka) and the MIS3 (57-24 ka), in which temperatures slightly recovered. Near 30 ka, the most acute phase of the glaciation began at the global level, reaching its highest peak around 22-18 ka, known as the Last Glacial Maximum. It lasted about 15,000 years and corresponds to the MIS2 (24-11.7 ka).

The study of different proxies has increased our knowledge of the Quaternary environment. The main climate proxies for Late Pleistocene consist of lake sediments, speleothems, ice cores, terrestrial tracers in marine sediments, loess, palaeosoils, and glacier deposits (Moreno et al., 2014). Greenland ice-core records from the North Atlantic indicate a series of abrupt climatic fluctuations during the glacial period known as Dansgaard-Oeschger (D-O) events, during which oceanic and atmospheric conditions alternated between cold and full glacial (stadial, GS) and relatively mild (interstadial, GI) conditions (Dansgaard et al., 1982; Johnsen et al., 1992; North Greenland Ice Core Project members, 2004; Rasmussen et al., 2014; Svensson et al., 2008;

Wolff et al., 2010). These oscillations differed from the slowly varying orbital parameters that were believed to be the main drivers of climate change during this period (Milankovitch cycles). The interstadials varied in duration from around a century to many millennia, with surface air temperature (reflected in $\delta^{18}O$ values) decreasing gradually before each interstadial, which then ended in a less-pronounced but nevertheless abrupt transition to stadial conditions. Stadials are generally characterized by more stable climates than interstadials but have similarly long durations with abrupt recovery of the interstadial conditions (Dansgaard et al., 1982; Johnsen et al., 1992; Rasmussen et al., 2014). During some longer stadials, marine records from North Atlantic indicate the presence of ice rafting events, called Heinrich events (HE) (Bond et al., 1992; Heinrich, 1988). These events most likely do not span the entire stadial period and do not always show a strong response in terrestrial archives (Fletcher et al., 2010b; Moreno et al., 2014; Rasmussen et al., 2014).

In the last two decades, multidisciplinary approaches have been developed to quantify climatic parameters and improve the reconstruction of continental climate models to understand the responses of living organism to climatic changes, derived either from palaeobiological approaches (sediment pollen, mollusk, insect or mammals assemblages) or geochemical methods (stable oxygen and carbon isotopes from speleothems, sediments, mollusks, or vertebrate bones or teeth) (e.g., Fletcher et al., 2010b; Moreno et al., 2014; Rasmussen et al., 2014; Sánchez Goñi et al., 2008; Sánchez Goñi and D'Errico, 2005). The main high-resolution proxies normally used in Iberia for the study of the palaeoenvironment during MIS 3 are terrestrial records (vegetation and pollen) in marine sediments from the Alborean Sea (OPD-976; MD95-2043; Fletcher et al., 2010b; Fletcher and Sánchez-Goñi, 2008; Genty et al., 2010; Sánchez Goñi et al., 2002) and Iberian margins (MD95-2039; MD95-2042; MD04-2845; MD99-2331; Naughton et al., 2007; Roucoux et al., 2001; Sánchez-Goñi et al., 2009, 2000, 1999; Sánchez Goñi et al., 2008).

There were three Heinrich Events (HE5-H3) and fourteen interstadials (GI17-GI4) during MIS 3 (North Greenland Ice Core Project members, 2004; Rasmussen et al., 2014; Svensson et al., 2008; Wolff et al., 2010). Globally, cool and dry climates were identified in Western European sequences during GS while the climate was warmer and more humid during GI (e.g., Fletcher et al., 2010b; Moreno et al., 2014). Using pollen records, Fletcher et al. (2010) detected evidences of millennial-scale variability that matched Greenland $\delta^{18}O$ records relatively accurately. According to these pollen analyses, MIS 3 is characterized in Southern Europe by a dynamic that alternates between phases of forest development and the expansion of semi-arid areas in accordance with the warming and cooling, respectively, of the sea-surface temperatures (Fletcher et al., 2010a; Fletcher and Sánchez-Goñi, 2008; Moreno et al., 2014; Roucoux et al., 2001). During interstadials in southern Europe, warmer and humid conditions allowed for the establishment of open and discontinuous temperate forest, dominated by *Quercus* and associated thermophilus trees. The greatest developments of temperate/Mediterranean forest are experienced in the southernmost Iberian areas and the northern limit for this forest development is established in 45°N. During cooling episodes (stadials or Heinrich events) there were increments of xerophytic steppe in southern areas.

During these climatic fluctuations, Neanderthal occupations occurred in Eurasia. Neanderthals inhabited Europe for more than 100,000 years and

are usually associated with the Mousterian techno-complexes, which characterized the archaeology of the Middle Palaeolithic. During this time, Neanderthal populations extended their geographical boundaries through Europe, the Middle East and a small part of Asia. Neanderthal settlements in Iberia took place mainly during the end of MIS 5 and MIS 3 and some Iberian archaeological sites show evidence of long-term occupations of these human groups, allowing us to understand their livelihood strategies (Carbonell et al., 1996; Higham et al., 2014; Maroto et al., 2012a). Some of the main sites with human remains attributed to Neanderthals are: El Sidrón, Axlor, Mollet, Arrillor, Banyoles, Gabasa, Bolomor, Lezetxiki, Cova del Gegant, Cova Negra, El Salt, Jarama IV, Cueva del Camino, and Sima de las Palomas del Cabezo Gordo (Arsuaga et al., 2012a; 2012b; Lorenzo et al., 2012) (Fig. 1.3). Middle Palaeolithic deposits from before the Late Pleistocene are relatively scarce. They are even scarcer in the peninsular periphery, being restricted in northeastern Iberia to the terraces of Ter, Mollet, Els Vinyets, and Cova del Rinoceront (Daura et al., 2015; Maroto et al., 2012b, 2012a; Sanz et al., 2014). All of them characterized by few archaeological remains and low chrono-stratigraphic resolution, only with the exception of the Cova del Rinoceront (>200-85 ka). Therefore, it can be assumed that Neanderthal occupations in the Iberian Peninsula and, especially, in the periphery and northeastern peninsula mainly occurred during the Late Pleistocene.

The end of the Middle Palaeolithic occurred at ca. 40 ka across Europe. But late survival to this date in Iberian Peninsula is suggested by several archaeological sites: Arbreda cave (Serinyà, Girona), Cova Gran (Santa Linya, Lleida), Ermitons (La Garrotxa, Girona), Abric Romaní (Capellades, Barcelona), Els Canyars (Gavà, Barcelona) and

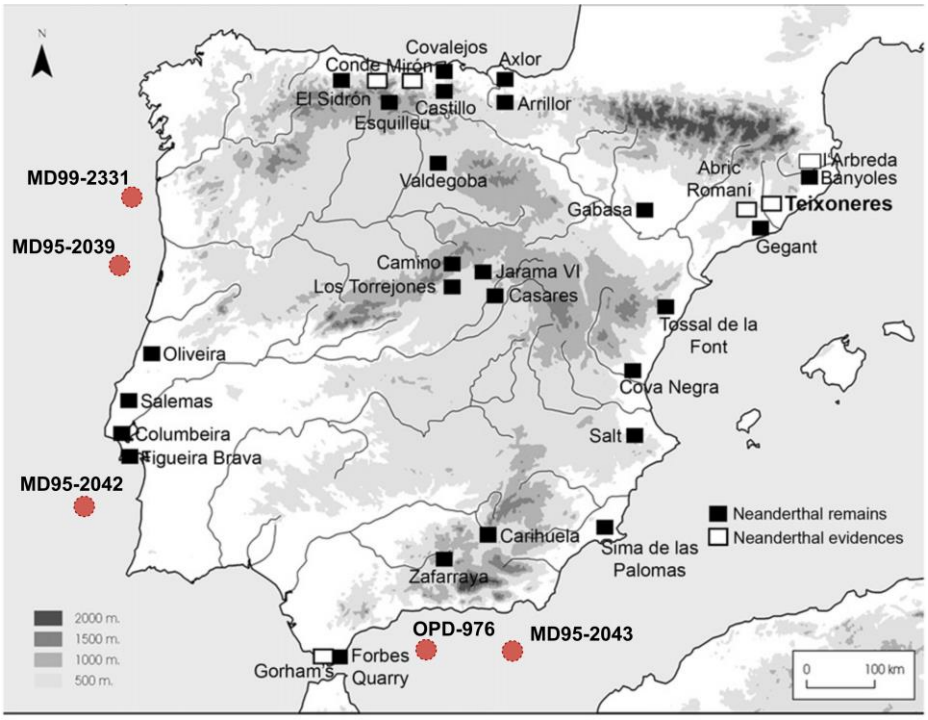

Figure 1.3 Location of some of the main sites in Iberia with Neanderthal remains or archaeological evidences. From López-García et al. (2012). Main marine cores in Atlantic Ocean and Alborean Sea are indicated by red dots.

Fuentes de San Cristobal (Aragón), in the (Asturias), Covalejos (Cantabria), El Castillo (Cantabria), Morín (Cantabria) and Lezetxiki (País Vasco), in the Cantabrian area; and, Cueva de Zafarraya (Málaga), Gorham's Cave (Gibraltar); Oliveira (Portugal), Jarama VI (Madrid) and Cabezo Gordo (Murcia) in the center and the south (synthesis in Camps and Higham, 2012; Daura et al., 2013; Maroto et al., 2012b; Martínez-Moreno et al., 2010; Vaquero and Carbonell, 2012; Wood et al., 2014). Most of the northeastern Iberian Neanderthal occupations occurred in this period, as the archaeological sites included on this PhD thesis, place in the latest stages of Neanderthals survival (Teixoneres cave and Abric Romaní) or even in the Middle-Upper Palaeolithic transition, located during MIS3-MIS2 transition (Arbreda cave).

One of the most popular topics of Prehistory studies is the connection between a changing environment and the extinction of *Homo neanderthalensis* (40–30 ka) and their substitution by the Anatomically Modern Humans that took place during the Middle–Upper Palaeolithic transition (e.g. D'Errico and Sánchez Goñi, 2003; Sepulchre et al., 2007; Staubwasser et al., 2018; Wolf et al., 2018). There has also been an interest in the modifications of the subsistence strategies as an adaptive response to changes in the environment. The Iberian Peninsula, together with Italian and Balkan Peninsulas, is commonly considered a glacial refugium during the entire Pleistocene, sheltering faunal, vegetal, and hominin species during the rigorous periods of the Last Glacial period (Finlayson et al., 2006; Hewitt, 2000; O'Regan, 2008; Sommer and Nadachowski, 2006). Some authors have connected Neanderthal relict populations with the favorable environmental conditions associated with peninsulas and the preservation of larger open woodland areas than in the rest of Europe (e.g., Finlayson et al., 2006; Finlayson and Carrión, 2007; López-García et al., 2014; Sánchez Goñi and D'Errico, 2005; Sepulchre et al., 2007; Zilhão, 2000).

5. Problematic synthesis

Neanderthal settlements in Iberia took place during the end of MIS 5 and MIS 3 and some Iberian archaeological sites show evidence of long-term occupations or repeated short-term visits of these human groups, allowing us to understand their livelihood strategies (Higham et al., 2014; Maroto et al., 2012a). A causality between millennial-scale climate cycles and the replacement of Neanderthals by modern humans in Eurasia has tentatively been suggested (D'Errico and Sánchez Goñi, 2003; Sepulchre et al., 2007; Staubwasser et al., 2018; Wolf et al., 2018). During the glacial period, Greenland ice-core records from the North Atlantic indicate a series of abrupt climatic fluctuations known as Dansgaard-Oeschger events, during which oceanic and atmospheric conditions alternated between cold and full glacial (stadial) and relatively mild (interstadial) conditions (Dansgaard et al., 1982; Johnsen et al., 1992; Rasmussen et al., 2014). Both terrestrial and marine climate provide important insights into rapid glacial changes in Southwestern Europe, in response to Dansgaard-Oeschger and Heinrich variability (e.g., Fletcher et al., 2010a; Fletcher and Sánchez-Goñi, 2008; Moreno et al., 2014; Rasmussen et al., 2014; Roucoux et al., 2001; Staubwasser et al., 2018), but the expressions of D-O scale changes differ from region to region and climatic changes had different repercussions in marine and continental domains. Moreover, there is a lack of quantitative data from 60 to 25 ka in the Mediterranean region, representing a major limitation for our ability to understand abrupt climate variability associated with D-O cycles (Fletcher et al., 2010b; Moreno et

al., 2014). Apart from pollen and charcoal studies (e.g., Carrión, 2012; Carrión et al., 2018), some testimonies of the continental domain are the small mammals collected in archaeological sites, which are strongly dependent of its environment and can improve our environmental knowledge inland in local and regional scales (e.g., Chaline, 1972; Cuenca-Bescós et al., 2011; López-García, 2011). A complete state of the art of rodent associations from northeastern Iberia during the Late Pleistocene and beginning of the Holocene is presented in Chapter 3. Indeed, geochemical approaches based on stable isotope oxygen compositions of rodent teeth, allow for the quantification of climatic parameters due to the interdependence between of climatic variables and the oxygen isotope composition of meteoric waters preserved in rodent teeth enamel (Dansgaard, 1964; García-Alix, 2015; Jeffrey et al., 2015; Longinelli and Nuti, 1973; Royer et al., 2013a, 2013b).

6. Objectives

This doctoral thesis aims to achieve a complete reconstruction of the palaeoenvironment (climate and landscape) during Late Pleistocene sequences, mainly during the Marine Isotope Stage 3 (MIS 3; ca. 60-30) at northeastern Iberia, through the combination of different disciplines based on small-mammal assemblages: taxonomy, palaeoecology, taphonomy, and oxygen isotope analyses. Three archaeological sequence are included: Abric Romaní rock-shelter (Barcelona; ca. 55-45 ka); Teixoneres cave (Barcelona, ca. 50-30 ka) and Arbreda cave (Girona, ca. 45-22 ka). These archaeological sequences studied constitute Middle Palaeolithic key sites and allow to expand the knowledge of the palaeoecological evolution of the last Neanderthal populations and their relationship with the palaeoenvironment in the Northeast of the Iberian Peninsula. It also includes a palaeontological site from a similar chronology, Xaragalls cave (Tarragona, 40-45 ka), which is rich in small-mammals remains.

The main objectives of this doctoral thesis are to:

- Complement the specific identification of small mammals from the studied sites, which provide, through their relative abundances, the necessary information to evaluate their environmental contexts. Moreover, a related goal is to deepen the knowledge of small-mammal communities of northeastern Iberia during the Late Pleistocene in order to detect regional trends in species occurrence and their environmental implications.
- Determine which is the origin of the small mammal assemblages studied and which are the implications on terms of ecology faithfulness. More knowledge of predator-prey interactions it is essential to understand the nature of these accumulations. Relatedly, a goal is to identify the post-depositional processes suffered and the fossiliferous environment in which these remains were preserved.
- Compare and test the availability of different methods of palaeotemperature reconstructions derived from small-mammal remains, comparing qualitative methods (mutual ecogeographic range and bioclimatic model methods) and quantitative methods (mainly analysis of phosphate oxygen isotopes from rodent teeth). As well as to contribute to a better understanding of oxygen isotope compositions in rodent body tissues from Iberia.
- Integrate the available data of the studied archaeological sequences from northeastern Iberia within global-scale climate changes recorded by marine pollen sediment analyses and Greenland ice cores during the last glacial.

Considering that the impact of these global climate changes is not the same at all latitudes, differences in local or regional contexts are evaluated through different scales of analyses from regional (Iberian Peninsula) to continental scale (Eurasia); testing the classical ideas of "macro-refugia" associated to Iberia during the Pleistocene.

- Understand how Neanderthal populations of northeastern Iberia were adapted to this environment and the implications the environment had for their livelihood strategies and in its disappearance at the end of MIS3. Several general questions are addressed, such as: Did harsher weather events affect these occupations? Were occupations related to favorable climatic episodes? How determinant was forest in these occupations? Were settlements favored by the existence of ecological refugia that Iberia provided? Or, did they reflect the adaptability of these hunter-gatherer groups to oscillating climatic conditions?

Chapter 2.
Material and methods synthesis

Subsequent chapters, where the precise results are presented, include their own methodological sections and a synthesis of the precise analytical methods used in each chapter. But, for the purpose of giving coherence to the different parts of this thesis, this chapter presents a brief description of the general techniques of recovery and analytical techniques of the studied small-mammal remains and a compilation of the main palaeoecological methods of reconstruction applied to faunal assemblages from archaeological or palaeontological sites. It also includes the sampling criteria for oxygen isotope analysis and the wet chemistry protocol. Statistical analyses applied to Late Pleistocene-Holocene rodent assemblages (Chapter 3) and the methods employed in the methodological proposal for oxygen isotope analysis on rodent teeth from Iberia (Chapter 5) are not included here, as they encompass specific methods explained in each chapter.

1. Main disciplines used to a multidisciplinary approach

The objectives of this thesis, explained in Chapter 1, tried to be responded with a multidisciplinary approach, throughout four main disciplines used in small-mammal research:

- **Taxonomy.** This corresponds to the first level of analysis, where the objective is the taxonomical assignation of the remains (order, family, subfamily, genus or species) and basic analysis of the fossil remains. This analysis allows to determine relative species abundances and to evaluate biogeographical distributions. Moreover, it provides us with metadata which will later be used to develop environmental reconstructions. A detailed description of the taxonomic criteria employed in the identification of the species identified is provided in Appendix 1.

- **Palaeoecology.** Small mammals have specific environmental and climatic requirements. Considering current biogeographical distribution and ecological niche preferences of fossil species, the general palaeoenvironment of a given sedimentary deposit can be inferred. Current distributions of identified species in Iberia and their ecological requirements can be found in Appendix 1. Environmental and climatic conditions prevailing during the formation of the assemblages could be inferred from quantitative (such as chorotype classifications or the Habitat Weighting Method) or qualitative methods (such as the mutual ecogeographic range method or the bioclimatic model method). Moreover, diversity and richness indexes could be applied to observe the evolution of a given sequence and establish comparisons with present-day conditions.

- **Taphonomy.** The taphonomic history of fossil remains has a special relevance to palaeoecological interpretation. The taphonomic processes that affected the studied remains, the agent responsible for their origin, and the processes suffered after the deposition of the remains at the site can be evaluated. Bearing in mind the taphonomic history of each small-mammal assemblage, the validity of the inferences reached can be ensured. The identification of the main predator itself provides palaeoecological information, whereas some taphonomic alterations that occurred during burial aid in the characterization of the fossiliferous environment.

- **Biochemistry.** The interdependent relationship between oxygen isotope composition of phosphate from tooth enamel of rodents ($\delta^{18}O_p$) and the $\delta^{18}O$ of meteoric waters ($\delta^{18}O_{mw}$), that in turn could be potentially

related to mean annual air temperatures, provides a valuable proxy to reconstruct past air temperatures in continental environments from a local to regional scale. Thus, it provides an independent method with respect to ecological methods that rely on faunal spectra. In addition, these studies require a transversal approach, which includes other disciplines such as ethology or histology.

2. Material and samples

This thesis includes three archaeological sites related with Neanderthal occupations in northeastern Iberia: Abric Romaní rock-shelter, Teixoneres cave, and Arbreda cave. One palaeontological site with a comparable chronology, Xaragalls cave, is also included (Table 2.1). Detailed description of each site is provided in their corresponding chapters (from 4 to 9). In some of these sites, previous studies of palaeoenvironmental reconstructions and/or taphonomic analyses based on small mammals have been performed. This research increases the number of identifications and complements them with new taphonomic studies of Abric Romaní and Teixoneres. Considering oxygen isotope analysis, a total of eighteen archaeological and palaeontological levels are studied, resulting in a total of 173 analysis performed: levels O, N, E, and D from Abric Romaní; levels C8, C7, C6, C5, and C4 from Xaragalls cave; levels IIIb, IIIa, IIb, and IIa from Teixoneres cave; levels H, G, F, E, and D from Arbreda cave. In addition, 14 new $\delta^{18}O$ analyses are carried out in modern rodent samples coming from modern owl pellets from *Strix aluco* and *Tyto alba*. An attempt to recover modern pellets next to fossil sites included this thesis was done, to compare oxygen isotope results from present-day materials to fossil material. Pellets were recovered from the surroundings of Teixoneres cave (Moià), Arbreda cave (Serinyà), and Xaragalls cave (Prades) (see Chapter 5-9).

3. Recovery of small-mammal remains

The small-mammal remains of the studied sites have been recovered from random sediment samples from the entire excavated surface. The specific criteria for sampling at each site is explained in each site's chapter. During the excavation process, sediment detached from the extraction of the larger remains was collected in buckets (Fig. 2.1). After, they were transported to the area intended for washing, close to a natural or artificial water course, where they were sieve-washed. Sieving is the process of passing the

	Location	Levels	Chronology	$\delta^{18}O$ samples
Abric Romaní rock-shelter	Capellades (Barcelona)	O, N, E, D	55.1-54.2 ka; 44.9-43.2 ka	38
Xaragalls cave	Vimbodí-Poblet (Tarragona)	C8, C7, C6, C5, C4	>45.1 - 45.1 ka BP	46
Teixoneres cave	Moià (Barcelona)	IIIb, IIIa, IIb, IIa	>51 ^{14}C ka BP-33 ka cal. BP	40
Arbreda cave	Serinyà (Girona)	H, G, F, E, D	41.6-27 ka cal. BP	49
Total archaeological samples				**173**
Present-day pellet samples				**14**
TOTAL				**187**

Table 2.1 Summary of biochemical samples taken from each sedimentary unit.

sediment through a determined number of superimposed sieves in decreasing mesh-size order. The limit size considered by Daams and Freudenthal (1987) is 0.5 and 0.7 mm, since smaller-sized meshes do not usually present small vertebrates remains. Through this process, it is possible to reduce the volume of the sediment, eliminating larger particles, and obtain a combination of microfossils and rock fragments, which are called "concentrated" or "levigated". The remains included in this thesis were collected by washing and sieving the sediment, with two superimposed meshes, usually 5 mm for the upper and 1 mm or 0.5 mm for the lower mesh. The concentrate from the upper mesh was sorted and removed during washing tasks, whereas concentrate from the lower meshes was collected by fractions - depending on the grain size, coarse or fine - after drying. During drying, sun exposure was avoided. Finally, bones and teeth were selected by the sorting during the field season or, later, at the Institut Català de Paleoecologia Humana i Evolució Social (IPHES, Tarragona, Spain). This technique consisted of the extraction of the vertebrate remains and other small-size archaeological remains from the gangue or mineral fraction that constituted most of the concentrate. The sorting of the fine fraction was done by hand-picking using precision tweezers and was performed with the naked eye, although it sometimes required the aid of a microscope. The separated fossil remains were stored in minigrip type bags, labeled with the precise location data of the site (at minimum: year, sedimentary units and/or subunits, square, or area of recovering and depth). Those small-mammal remains erroneously stored in "excavation level" bags have also been incorporated.

Figure 2.1 Small mammals recovering during field-work campaign at the Abric Romaní rock-shelter: sediment sampling, water-sieving and sorting.

4. Analytical techniques and identification

Firstly, the preparation of the samples for microscope observation was carried out. The procedure consisted of the classification of the different anatomical parts identified, followed by depositing the remains included in the taphonomic study in Eppendorf tubes (Ø 10 mm). In turn, the diagnostic bone elements at the species level were fixed with paste in small methacrylate boxes to facilitate their subsequent observation. The taxonomic identification and taphonomic evaluation was done with stereoscopic microscopes (*Exacta-Optech LFZ*, 10x-90x; *Olympus SZ-PT*, 18x-50x). For photographs, a color camera (*Infinity x*) was incorporated with the stereoscopic microscope (*Exacta-Optech LFZ*) that processes digital images through a computer program (*DpxView Pro*). Sometimes, photographs were taken with Dino-Lite MS35B (USB) digital microscope (Dino Capture 2.0). Occasionally, the detailed study of some remains or preparation for photographs necessitated the rewash of some remains in an ultrasonic bath (*JP SELECT FUSE*).

The small-mammal remains included in this analysis consist mainly of isolated teeth and disarticulated bones (cranial and postcranial) from insectivores, bats and rodents. The taxonomic identification was made using various anatomical atlases and reference criteria (Bab et al., 2007; Chaline, 1972; Cuenca-Bescós et al., 2014; Gosàlbez, 1987; López-García, 2011; Menu and Popelard, 1987; Nadachowski, 1982; Sevilla, 1988; among others), and by comparisons with the small-mammal reference collections available at the Institut Català de Paleoecologia Humana i Evolució Social (IPHES) and at the Università degli Studi di Ferrara (UNIFE). Specific identifications were based mainly on the best diagnostic elements: isolated teeth for Murinae, Glirinae and Sciuridae; first lower molars (m1) for Arvicolinae; mandibles, maxillae, and isolated teeth for Chiroptera and Soricomorpha; and mandibles, isolated teeth, and postcranial material for Talpidae (see Appendix 1). For the correct management of the large amount of data generated, all the taxonomic and taphonomic information was recorded in a detailed database (Excel). Each studied remain was documented individually and given a number. In this database different characteristics of the remains are categorized, such as location, anatomical and taxonomic identification, and taphonomic alterations.

5. Quantification of remains

All the remains were used for the quantification of the assemblage and were counted (NR). Each bone was identified in terms of anatomical element (NISP), but in some cases identification was not possible (Indet.). It should be specified that both NR and NISP in case of taphonomical analysis consider the recount of each analyzed item, differentiating between types of skeletal elements. Thus, dental elements were recounted as independent items, whether they were *in situ* or isolated (e.g. each tooth on a mandible is counted here as a single remain). This decision was made considering the analysis of breakage and digestion subsequently used in the taphonomic study.

The remains were grouped using the minimum number of individuals (MNI) method, determined by counting the most highly represented diagnostic element, considering laterality, for each species. In each sedimentary unit, the relative abundances were evaluated from the percentage of MNI of each species in relation to the total MNI estimated for the level. When a specific assignment was not possible, the bones

were grouped by genus (e.g. *Apodemus*), subfamily (e.g. Murinae), or order (e.g. Rodentia). Nevertheless, in Chapter 7, where taphonomic sampling does not fit the sample size of small mammals previously studied, the MNI is adapted according to the rodent remains included in the taphonomic analysis. Thus, the minimum number of elements (MNE) of dental remains based on subfamily classifications (Murinae, Arvicolinae, Glirinae), was considered in order to assess the MNI of each subunit.

6. Sampling criteria for oxygen isotope analyses

In the selection of appropriate materials for oxygen isotope compositions analyses, this study has taken methodological choices based on recommendations made by several authors.

- Teeth are preferred for isotopic studies because the mineral component is more abundant than in bones, preventing better conservation (Hillson, 2005; Zazzo et al., 2010). In addition, the exclusive use of teeth avoids variations in $\delta^{18}O$ results derived from the combination of different body tissues. Indeed, Royer et al. (2014) used a method, employed in this research, which exclusively used tooth remains for the development of their regression equation.

- The selection of continuously growing teeth during the animal's life prevents the weaning effect of some rodent teeth (Freudenthal et al., 2014; Lindars et al., 2001; Royer et al., 2013a) and allows the period just before the animal death to be recorded (Gehler et al., 2011; Jeffrey et al., 2015; Royer et al., 2013a). Moreover, the isolation of enamel from dentine is easier in incisors. Whenever possible, lower incisors were selected; since they are larger, they offer a greater amount of enamel.

- Unbroken and well-preserved remains were preferentially selected, avoiding incisors where taphonomic agents could have produced diagenetic or chemical alterations, such as soil or root etching, manganese oxide, fissures and cracks, cementation, or water abrasion (Andrews, 1990; Barham et al., 2017; Royer et al., 2014). Therefore, all remains showing digestion signs were discarded. Incisors preserved in their alveolar place are preferred because they are more protected from the chemical exchanges with sedimentary matrices (Royer et al., 2013b). Juvenile specimens were avoided, due to the incomplete mineralization process, which may cause a damping of the oxygen isotope composition (Blumenthal et al., 2014; Passey and Cerling, 2002).

- To reduce the potential effects of interspecific variability, *Apodemus sylvaticus* fossil incisors were selected in cases where there was enough material with good preservation. In some current samples this was not possible, because this species was not always present in pellets. Occasionally, other Glirinae and Arvicolinae species remains were included.

- Excluding bulk teeth analyses, each sample corresponded to a single lower incisor. A minimum number of between five and ten samples was taken from sedimentary units in order to gather a representative sample of the population; previous studies advise that a minimum of four samples is enough to bring the 95% of sub-population means within 1σ of the true population mean (Gehler et al., 2012; Lindars et al., 2001; Navarro et al., 2004; Royer et al., 2013a).

- Only enamel was crushed for the wet chemistry, avoiding dentine. For oxygen isotopic studies on fossils tooth enamel is commonly preferred, due to its inorganic

composition (mainly hydroxyapatite) that makes it less prone to suffering diagenetic alteration than bones and tooth dentine, which have a higher proportion of organic tissue (Barham et al., 2017; Kolodny et al., 1983; Lécuyer et al., 1999; Lee-Thorp and van der Merwe, 1991; Zazzo et al., 2004).

7. Wet chemistry protocol and mass spectrometer

The wet chemistry and the mass spectrometer measurements were developed in the Laboratoire de Géologie of Université Claude Bernard (Lyon, France), following the established protocol for the recovery of silver phosphate (Ag_3PO_4) crystals (Fig. 2.2). Each series consists of 10 samples (plus four external standards) and requires a four-day wet chemistry protocol, representing approximately 22-24 hours of work. In total, 19 series were performed. Time taken for preparing samples (cleaning and crushing, 3-5h/series) and sample preparation for spectrometer mass (5-8h/series) should also to be considered. Normally, the mass spectrometer took 12 min to process each aliquot (meaning approximately one hour for each sample). In total, each series took around 40-50 hours to process and a total of around 800 hours were spent on laboratory tasks.

7.1 Pretreatment of samples

Before executing a wet chemistry protocol, samples should be clean and prepared. Firstly, the rodent tooth samples were cleaned with double-deionized water (DDW) in an ultrasonic bath to remove traces of sediment. Each sample was placed in small beakers with 2ml of DDW and submitted to the vibration of the ultrasonic bat for 3 minutes and then the liquid is discarded. This operation was repeated three times for each sample. After, samples were air dried for 24 hours in a laboratory oven at 50 °C. Then, each sample was crushed in an agate mortar. For fossil samples, the enamel was separated from dentine by hand-picking with tweezers under a binocular microscope and dentine was discarded. The basal part of the enamel was always discarded, and the remaining part was gently crushed in the mortar until reaching a homogenous powdered mass. Contamination between samples was avoided by intensive cleaning of all the laboratory material used during the procedure with ethanol. Small stainless-steel laboratory spatulas were used, avoiding the use of brushes.

7.2 Wet chemistry

Enamel tooth samples were treated following the wet chemistry procedure described by Crowson et al. (1991). This procedure was slightly modified by Lécuyer et al. (1993), and subsequently adapted for small simple weights (1-3 mg apatite) by Bernard et al. (2009), Fourel et al. (2011) and Lécuyer et al. (2007). This protocol is based on the isolation of phosphate ions (PO_4^{3-}) from apatite as silver phosphate (Ag_3PO_4) crystals using acid dissolution and anion-exchange resin. Each series processed during the wet chemistry protocol consisted of fourteen samples, ten fossil or modern enamel tooth samples, plus four standards of samples of natural phosphorite (NBS120c) to ensure that no fractionation occurred during the wet chemistry. All steps of the procedure were recorded on laboratory sheets and subsequently collected in a database. This part of the procedure is carried out in a cleanroom, which is specially designed to maintain extremely low levels of pollution, such as dust, airborne organisms, or vaporized particles.

Weighting and acid dissolution. - During the first day of the protocol, samples are weighted: selecting around 3 mg of enamel powder of each sample, which is introduced in 10 ml centrifuge tubes. In a fume hood and with the necessary

Figure 2.2 Pretreatment of biochemical samples, wet chemistry protocol, and mass spectrometer procedures in the Laboratoire de Géologie of Université Claude Bernard (Lyon, France).

protection, 1ml of hydrofluoric acid (2 M HF) is added to each sample to allow the precipitation of calcium fluoride (CaF2) overnight. The ultrasonic bat is employed to accelerate the reaction in two rounds of 20 minutes.

Neutralization of the solution and isolation of phosphate ions. - The second day, the CaF2 residue precipitate is separated from phosphate solution by centrifugation of each sample at 2,500 rpm for 5 minutes (four times). The CaF2 precipitate is rinsed three times using DDW and finally rejected, whereas the rinse water containing the phosphate ions is introduced in polypropylene tubes and neutralized by adding 1 ml of potassium hydroxide (2M KOH) solution. Then, 1.5 ml of cleaned Amberlite^{TM} anion-exchange resin is added to the neutralized solution to separate the PO_4^{3-} ions. The tubes are then placed on a shaker table for at least 12 hours to promote the ion exchange process.

Elution of phosphate ions and precipitation of Ag_3PO_4 crystals. – The third day begins with checking that all the phosphate ions are adsorbed on the resin, through the application on one test sample of vanadium molybdate, a color indicator. If there is no chromatic alteration, excess solution is removed, and the resin is washed again five times with DDW to remove the last traces of ionic contaminants. All these steps are performed with micro-pipettes to maximize the final yields. To elute the phosphate ions quantitatively from the resin, 6 ml of ammonium nitrate (0.1 M NH_4NO_3) were added to bring the pH of the solution to 7.5-8.5. Tubes are once again placed on the shaker table, to accelerate the elution. After 4 hours, the resin and the phosphate solution are separated employing micro-pipettes and 1 ml of DDW to rinse the solution. The solution is placed in a 50 ml Erlenmeyer flask and, in the fume hood, 0.1 ml of ammonium hydroxide (NH_4OH) is added to raise the pH to 9-10. Then, 3 ml of an ammoniacal solution of $AgNO_3$ are added to each sample. Then, samples are placed in a thermostatic bath at 70°C for 6 hours, enabling the quantitative precipitation of millimeter-size yellowish crystals of Ag_3PO_4. The volume of solution is maintained constant during precipitation by the addition of 0.5 ml of DDW with pipettes every 15 minutes throughout the process.

Recovering of Ag_3PO_4 crystals. - The fourth day, the Ag_3PO_4 crystals are collected through a filtration system consisting of glass vacuum filter (Millipore), and washed three times with DDW. The crystals are trapped in cellulose acetate membrane filters and then air-dried at 50°C in the laboratory oven. The manual recovery of the dried crystals is carried out and they are set in small capsules. Finally, each sample is weighed, and yields are estimated, comparing the amount of sample produced with the expected according to the initial weight and theoretical amount of phosphate production.

8. Taphonomic analysis

8.1 Predation

Predation is the main factor in the accumulation of small-mammal assemblages both in modern and fossil sites (e.g., Andrews and Evans, 1983; Dodson and Wexlar, 1979; Andrews, 1990; Chaline, 1974; Denys and Patou-Mathis, 2004; Fernández-Jalvo et al., 2016; Fernández-Jalvo and Andrews, 1992). Three main groups of small-mammal predators are distinguished: 1) owls or nocturnal raptors, which swallow their prey and produce the least damage on bones and teeth; 2) diurnal raptors, which usually tear apart their prey inflicting major damage and with a more acid digestion; and, 3) small carnivores, which chew and ingest their prey, mostly producing the highest alterations on skeleton parts. Among the accumulations caused by any of these predators there is always a selection associated with the interrelation

between the predator and its prey. The factors that determine this bias are the dietary preferences of the predator, its hunting strategy, the extent and diversity of the hunting area, and prey size and habits, among others. Moreover, the predator can be considered opportunistic or selective in the selection of their prey (Andrews, 1990; Andrews and Evans, 1983).

This work follows the descriptive-analytical method established by Andrews (1990), previously prompt by some pioneering works (Andrews and Evans, 1983; Dodson and Wexlar, 1979; Korth, 1979); subsequently applied and revised by several works (e.g., Bennàsar, 2010; Comay and Dayan, 2018; Denys et al., 1996; Denys and Patou-Mathis, 2004; Desclaux et al., 2011; Fernández-Jalvo, 1992; Fernández-Jalvo et al., 2016, 1998; Fernández-Jalvo and Andrews, 1992; Laudet and Selva, 2005; Lloveras et al., 2012, 2008b, 2008a; Terry, 2007). This method was developed through the study of modern pellets and excrement of extant predators, allowing for the establishment of a series of criteria to relate the superficial alterations of the bones with a predator or a group of predators. These taphonomic analyses mainly consider three aspects to detected predation effects: anatomical representation, breakage, and corrosion by digestion. Andrews (1990) distinguished five main categories of predators based on these aspects (Table 2.2; Table 2.3).

Category 1	*Tyto alba, Asio otus, Asio flammeus , Bubo scandiacus, Strix nebulosa, Bubo lacteus*
Category 2	*Bubo bubo, Bubo africanus, Strix aluco*
Category 3	*Athene noctua, Falco tinnunculus, Falco peregrinus*
Category 4	*Circus cyaneus, Genetta genetta, Otocyon megalotis, Ichnemia albicauda*
Category 5	*Canis latrans, Vulpes vulpes, Martes martes, Alopex lagopus*

Table 2.2 General classification of predator considering their degree of modifications, following Andrews (1990).

Anatomical representation. - The presence of the anatomical elements (representation) in an assemblage will vary according to the category of predator that has produced the accumulation, but this variation can be altered by post-depositional agents. To determine the anatomical representation and the proportions of elements present, all the elements of a given sample were considered. The following indexes were estimated:

- **The relative abundance. –** This is calculated by dividing the remains recovered (NISP) for each element (i) with the expected number of this element in a completed skeleton (E) multiplied by total MNI of a giving assemblage [NISPi/(Ei*MNI)] (Dodson and Wexlar, 1979). Only those anatomical parts that are possible to relate to a taxonomic order are included (maxilla, mandible, molar, incisor, humerus, radius, ulna, femur, and tibia).
- **The PC/C index. –** This establishes a relationship between postcranial elements (PC: humerus, radius, ulna, femur, and tibia) and cranial ones (C: mandibles, maxillae and isolated molars). A correction factor was applied (x16/x10, respectively).
- **The F+H/Mx+Md index. –** This compares the proportion of femora and humeri with respect to maxillae and mandibles, as an alternative way to calculate the ratio between crania and postcrania.
- **The R+T/H+F index. –** This estimates the proportion of tibiae and radii in relation to humeri and femora. It is useful for detecting the loss of distal elements.
- **The Ms/Av or Ts/Av index. –** The proportion of isolated molars/teeth is compared with the number of empty alveoli. The result can be related to the minor or major fracture and destruction of mandibles and maxillae.

	Predator categories				
	1	2	3	4	5
IAR	**70-80%** *Tyto alba, Asio otus, Asio flammeus, Bubo scandiacus, Bubo lacteus*	**60-70%** *Bubo bubo, Bubo africanus*	**30-60%** *Strix aluco, Athene noctua*	**20-40%** *Falco tinnunculus, Falco peregrinus*	**<20%** Mammalian carnivores
PC/C index	**>200%** *Tyto alba, Asio otus, Asio flammeus, Bubo bubo, Strix nebulosa*	**100-150%** *Strix aluco, Bubo lacteus, Bubo africanus, Falco tinnunculus, Genetta genetta*	**50-70%** *Circus cyaneus, Alopex lagopus*	**<30%** *Athene noctua, Ichneumia albicauda, Canis latrans, Vulpes vulpes*	-
F+H/Mx+Md index	**>100%** *Tyto alba, Asio otus, Asio flammeus, Bubo bubo, Strix nebulosa, Otocion megalotis, Martes martes*	**80-90%** *Strix aluco, Bubo lacteus, Bubo africanus, Falco tinnunculus, Genetta genetta*	**30-50%** *Circus cyaneus, Alopex lagopus*	**<30%** *Bubo scandiacus, Athene noctua, Ichneumia albicauda, Canis latrans, Alopex/Vulpes*	-
R+T/H+F index	**85-100%** *Tyto alba, B. scandiacus, Asio otus, Bubo lacteus, Strix aluco*	**70-85%** *Asio flammeus, Bubo bubo, Strix nebulosa, Alopex, Canis latrans*	**60-70%** *Athene noctua, Falco tinnunculus*	**40-60%** *Bubo africanus, Circus cyaneus, Vulpes vulpes*	**20-40%** *Martes martes, Ichneumia albicauda, Genetta genetta, Otocyon megalotis*
Incisor breakage	**0%** *Tyto alba, Bubo scandiacus, Asio otus, Strix nebulosa*	**0-5%** *Asio flammeus, Bubo lacteus, Bubo africanus, Athene noctua*	**0-10%** *Bubo bubo, Strix aluco*	**10-20%** *Falco tinnunculus, Circus cyaneus*	**>30%** Mammalian carnivores
Molar breakage	**0%** *Tyto alba, Bubo scandiacus, Asio otus, Strix nebulosa*	**0-2%** *Asio flammeus, Bubo lacteus, Bubo africanus, Athene noctua*	**1-5%** *Bubo bubo, Strix aluco*	**10-15%** *Falco tinnunculus, Circus cyaneus*	**>20%** Mammalian carnivores
Postcranial breakage	**0%** *Tyto alba, Asio otus, Asio flammeus, Strix nebulosa, Bubo lacteus*	**10-20%** *Bubo scandiacus, Bubo bubo*	**30-60%** *Strix aluco, Bubo africanus*	**60%** *Athene noctua, Falco tinnunculus, Circus cyaneus, Ichneumia albicauda, Martes martes, Otocyon megalotis*	**>70%** *Canis latrans , Alopex/Vulpes, Martesmartes*
Incisor digestion	**5-13% / abstent-light degree** *Tyto alba, Asio flammeus*	**20-30% / light-moderate degree** *Asio otus, Bubo lacteus, Strix nebulosa, Bubo scandiacus*	**50-70% / moderate-heavy degree** *Bubo bubo, Bubo africanus, Strix aluco, Athene noctua*	**60-80% / heavy degree** *Falco tinnunculus, Falco peregrinus*	**100% / extreme degree** *Circus cyaneus* , Buteo buteo, Milvus milvus, mammalian carnivores
Molar digestion	**0-3% / abstent-light degree** *Tyto alba, Asio otus, Asio flammeus, Bubo lacteus*	**4-6% / light-moderate degree** *Bubo scandiacus, Bubo africanus, Strix nebulosa*	**11-22% / moderate-heavy degree** *Bubo bubo, Strix aluco*	**50-70% / heavy degree** *Athene noctua, Falco tinnunculus, Falco peregrinus, Circus cyaneus*	**50-100% / extreme degree** *Buteo buteo, Milvus milvus,* mammalian carnivores
Postcranial digestion	**<20%** *Tyto alba, Bubo scandiacus, Asio flammeus, Asio otus, Bubo lacteus, Strix nebulosa*	**25-50%** *Bubo bubo, Bubo africanus, Strix aluco*	**60-100%** *Athene noctua, Falco tinnunculus, Circus cyaneus*	-	**100%** Mammalian carnivores

Table 2.3 Summary of predator categories according to Andrews (1990), including the taphonomic variables considered in this work. Percentages of breakage in teeth correspond only to isolated teeth. For incisor and molar digestion categories is presented the review of Fernández-Jalvo et al. (2016), including other species and considering degree reach. It differs from Andrews (1990) in mammalian carnivores' classifications, due to these animals could be included in category 5 of extreme digestion (>50%), but some exceptions exists: viverrids and mustelids could produce extreme digestions and low percentages of digestion (20%) and some canids not reach extreme degrees.

Results of the indexes are multiplied by 100 to express results as percentages.

Breakage. **–** This is a frequent physical alteration among the fossil small-mammal assemblages, since they have fragile bones. The different types of fractures documented among remains can be useful for identifying predators because hunting strategy and form of prey ingestion vary among predators. Gastric juices tend to weaken the structure of the bone elements, making them more susceptible to subsequent fracture. However, in archaeological contexts, breakage can also occur due to taphonomic processes after the production of the accumulations. This work considers incisors, molars and femora (occasionally, humeri) for the evaluation of breakage. For each skeletal element, the number of fractured elements is compared to the total number of this type of elements (Andrews, 1990; Fernández-Jalvo and Andrews, 1992). In the case of femora, three categories are differentiated: complete elements, diaphyses, and epiphyses. Andrews (1990) notes that breakage in teeth is rare within pellets and that is greater among loose teeth (isolated), than among those that have remained inside their alveoli (*in situ*). Thus, during the recount, these two categories are considered. In the case of incisors, the rupture of the proximal edge is not considered breakage.

Digestion. **–**Digestion, derived from the action of gastric juices, will cause morphological and structural modifications which generally only affect the surface of remains. The main effects of gastric juices are corrosion and rounding. Digestion is the most reliable indicator of predation because it is the only type of alteration that cannot be confused with other agents. It is a directional and progressive process (Fernández-Jalvo et al., 2016, 2014). The acids and enzymes of the digestive process will concentrate more intensely in the most mineralized body tissues with higher inorganic content. Therefore, the enamel, the most mineralized part of the skeleton, is the most vulnerable tissue. Moreover, digestion is progressive, advancing from the bone and teeth edges (epiphysis, fracture edges, salient angles, or roots) to the internal parts. Digestion can also cause changes in the chemical composition of the affected remains, which will be manifested mainly in changes of Mg, Ca, P, and S amounts (Dauphin et al., 2003; Dauphin and Williams, 2004; Denys et al., 1996; Fernández-Jalvo et al., 2002).

The variations in the intensity of the effects of digestion will be mainly in accordance with the degree of acidity of the gastric juices, the time of digestion, and the activity of the enzymes, but also to other factors such as the age of the predator, the time since last ingestion, or even the position of the skeletal remains in the stomach of the predator (Andrews, 1990; Denys et al., 1996; Duke et al., 1975; Fernández-Jalvo, 1992; Fernández-Jalvo et al., 2002). Globally, carnivores tend to inflict higher degrees of digestion than raptors, because owls have lower gastric acidity, thereby producing less frequent and lower levels of digestion. In the present analysis, the proportion of fossil bones affected together with the degree of alteration is considered, distinguishing between light, moderate, heavy and extreme digestion (Andrews, 1990; Fernández-Jalvo et al., 2016; Fernández-Jalvo and Andrews, 1992) (Table 2.3). In this thesis, digestion analysis considers rodents, talpids, soricids, and chiropters. However, only rodent results were finally considered for recounts, due to the scarce number of talpids, soricids, and chiropters recovered. For the same reason, no differentiation has been made between isolated and *in situ* remains in the interpretations, because most teeth appeared isolated when recovered.

	Incisors	Molars			Femora and humeri
		Arvicolinae	Murinae	Insectivores	
Light	Slight corrosion or pitting and loss of enamel only from the tip of the tooth	Enamel reduction on apical edges with dentine exposed and round	Difficult to identify. Rounded and smoother-matt enamel	Any alteration can be identified	Slight corrosion in the epiphyses, mainly over the first bone patina of the femoral head or distal humerus articulation
Moderate	Enamel removed from almost half of the tooth. Dentine starts to have a wavy texture	The enamel of the apical vertices disappears, reaching half the height of the tooth, exposing the dentine	Irregular pitted enamel surface easily observed laterally at the crown-root junction	Difficult to identify. Matt surface enamel	First patina is removed, corrosion reaches the metaphysis, presenting an abraded or polished appearance. Rounded fracture-edges
Heavy	Most of the enamel is removed, forming islands. Dentine has a wavy texture	Extensive removal of enamel along the entire columns, leaving the dentin completely exposed and wavy	Enamel removed from the cusps and at crown-root junction, dentine exposed but not affected	Enamel pitted and removed from the occlusal areas at crown-root junction of the tooth. Dentine not affected	Corrosion reaches the diaphysis, presenting a wavy appearance and fracture-edges are strongly rounded
Extreme	Enamel is absent or reduced to small islands. Dentine loses its original morphology and collapses	Enamel only inward from the columns, dentine collapses, and the tooth adquires a concave shape	Enamel absent or reduced to small islands, possible collapse of dentine	Enamel absent or reduce to small island, rounded dentine and possible collapse	Pronounced irregularities in the diaphysis and edges of fracture very rounded

Table 2.4 Summary of digestion degrees inflected by predators, and identification keys for incisors, molars and postcranial remains of rodents and insectivores, based on Andrews (1990) and Fernández-Jalvo et al. (2016).

8.2 Synthesis of post-depositional alterations

After being produced, any preserved element of a fossil association will undergo changes in its composition, structure, and location, which may even lead to the destruction of a large part of the accumulated elements. Those preserved will have surface alterations related to the post-depositional agents that have intervened on them (Fernández-López, 2000). The post-depositional alterations group includes all alterations that have occurred since the small-mammal remains were accumulated by the predator until the moment they were buried. A distinction is made between biostratinomic alterations (those produced prior to burial) and fossil-diagenetic (those experienced after burial). Even so, there are some alterations whose exact moment of production is difficult to determine. The post-depositional alteration descriptions are based on small-mammal studies, together with other research focused on the study of larger fauna remains (Table 2.5). In this thesis, post-depositional taphonomic alterations have been analyzed in molars, incisors, and femora independent of taxonomic attribution. The absence/presence of the alterations were evaluated, and, in some cases, their extent and location were as well. Five burning stages were differentiated following the protocol established by Cáceres (2002) and Shipman et al. (1984). Degrees of rounding and polishing related to water abrasion were also considered, following categories defined by Cáceres (2002).

9. Palaeoecological methods

Environmental reconstruction, including landscape and climate, of studied sites has considered different quantitative methods based on the relative abundances of species. The following methods were mainly developed in this thesis at the Abric Romaní site, but previous small-mammal interpretations of Xaragalls, Texioneres, and Arbreda caves follow equivalent procedures (López-García et al., 2012a, 2012b, 2015).

	Taphonomic process	Taphonomic alteration description	Main cause	Main references
Biostratinomic alterations	**Decomposition and dispersion**	Loss of soft tissues and dispersion of bone elements. Can affect bone surfaces: perforations, tunnels or changes in mineral composition	Activity of enzymes, bacteria, fungi and insects on soft tissues	Hill, 1979; Korth, 1979; Hill and Behrensmeyer, 1965; Andrews, 1990; Fernández-Jalvo, 1992; Lyman, 1994; Turner-Walker and Jans, 2008
	Weathering	Cracking, exfoliation, splintering and peeling on the surface of the bone that increases the fragility of the remains	Meteorological agents (mainly solar radiation) and temperature-humidity changes destroy bone structure	Behrensmeyer, 1978; Andrews, 1990; Fernández-Jalvo, 1992; Lyman, 1994; Fernández-Jalvo et al., 2002; Andrews and Whybrow, 2005
	Trampling	Breakage and spatial alterations. Striations isolated or grouped, rectilinear and of variable length, width and depth. Usually, shallow and with "U" or flat sections. Random distribution	Mechanical process by which the remain rubs against sediment particles; usually by people and animals transit	Shipman and Rose, 1983; Andrews and Cook, 1985; Behresmeyer et al., 1986; Olsen and Shipman, 1988; Andrews, 1990; Domínguez-Rodrigo, 2009
	Water abrasion	Rounding and polishing, especially on edges. Random process. Micro-striations	An external physical force causes the friction of sedimentary particular contained in water, eroding bone surface. *Water can cause skeletal selection due to differential transport	Voorhies, 1969; Dodson, 1973; Wolff, 1973; Behrensmeyer, 1975; Korth, 1979; Bromage, 1984; Cáceres, 2002; Fernández-Jalvo and Andrews, 2003; Fernández-Jalvo et al., 2014
Fossil-diagenetic alterations	**Burning**	Discoloration (brown, black, grey, white). Others: structure changes, cracking, recrystallization, size reduction, deformation, fragmentation and even disintegration	Thermal alteration by direct or indirect action of fire	Shipman et al., 1984; Buikstra and Swegle, 1989; Bennet, 1999; Cáceres, 2002; Fernández-Jalvo & Avery, 2015; Fernández-Jalvo et al., 2018
	Corrosion	Root etching: sinuous and elongated grooves with irregular "U" section, variable width, length and depth and random distribution. Can cause perforations	Biochemical alteration related to plant organisms (roots, liquens, mosses, algae)	Behrensmeyer, 1978; Gordon and Buikstra, 1981; Bromage, 1984; Andrews and Cook, 1985; Courty et al., 1989; Andrews, 1990; Fernández-Jalvo, 1992; Lyman, 1994; Cáceres, 2002; Fernández-Jalvo et al., 2002; Fernández-Jalvo and Marín-Monfort, 2008
		Variable alterations: oval grooves grouped, porosity, cracks, striations, peels and small perforations. Random distribution	Biochemical process of inorganic origin relative to the substrate	
	Manganese oxide	Brown or black coloration, isolated in small areas or widespread	Chemical alteration related to bacterial activity, linked to water and humidity	Potter and Rossman, 1979; Courty et al., 1989; Fernández-Jalvo, 1992; López-González et al., 2006; Marín-Arroyo et al., 2008; 2014
	Cementation and concretions	Addition of new materials to the surface of the bone	Mineralization process. Frequently, carbonate precipitation by physical-chemical alterations of fossiliferous micro-environment (e.g., humidity changes)	Fernández-López, 2000; Courty et al., 1989

Table 2.5 Summary of the main taphonomic processes considered in the analyses in this thesis. For detailed explanation references are provided and some studies that include comprehensive reviews are recommended (Andrews, 1990; Bennàsar, 2010; Fernández-Jalvo, 1992; Fernández-Jalvo and Andrews, 2016; Lyman, 1994).

9.1 Simpson's diversity index

Species evenness and diversity were evaluated (Margalef, 1974) using Paleontological Statistics (PAST) software (Hammer et al., 2001). Williams et al. (2002) associate a highly even community with complex and heterogeneous vegetation. The evenness of a community can be represented by Simpson's Diversity Index [$(1 - \Sigma((ni/n)^2)$, where *ni* is the number of individuals of taxon *i*]. This index allows us to numerically quantify how equal communities are, and increases when the specific diversity of a community increases. Results will always be between 0 and 1; when one species is dominant over the rest of the community results are closer to 0, and when taxa are more equally represented results are closer to 1 (Simpson, 1949).

9.2 Habitat Weighting method

Landscape reconstruction was based on the Habitat Weighting method, a quantitative method employed by Evans et al. (1981) and Andrews (2006). This method is based on the distribution of each taxon in the habitat(s) in which it is currently present on the Iberian Peninsula (Palomo et al., 2007). Each species is given a maximum score of 1.00, which is divided among the habitat types according to its habitat preferences (Table 2.6).

Habitats were divided into five main types:

- **open dry**, meadows under seasonal change;
- **open humid**, evergreen meadows with dense pastures and suitable topsoil;
- **woodland**, mature forest including woodland margins and forest patches, with moderate ground cover;
- **rocky**, areas with suitable rocky or stony substratum, and
- **water**, areas along streams, lakes, and ponds.

	Chorotypes				Landscape				
	C1	C2	C3	C4	OD	OH	WO	R	WA
Crocidura russula			x		0.50		0.50		
Sorex* gr. *araneus-coronatus	x					0.50	0.50		
Sorex minutus		x				0.50	0.50		
Neomys* gr. *fodiens-anomalus	x					0.25			0.75
Talpa europaea		x				0.75	0.25		
Myotis myotis-blythii				x	0.50			0.50	
Miniopterus* cf. *schereibersii			x					1.00	
Plecotus auritus-austriacus				x			0.75	0.25	
Pipistrellus pipistrellus				x			0.50	0.50	
Nyctalus lasiopterus				x			1.00		
Arvicola sapidus				x					1.00
Microtus arvalis	x				0.50		0.50		
Microtus agrestis		x				0.50	0.50		
Iberomys cabrerae			x			0.50	0.50		
Chionomys nivalis	x							1.00	
M. (Terricola) duodecimcostatus			x			0.25	0.50	0.25	
M. (Terricola) gerbei	x					0.50	0.50		
Apodemus sylvaticus				x			1.00		
Eliomys quercinus				x			0.50	0.50	
Sciurus vulgaris				x			1.00		

Table 2.6 Species classification employed in this work according to chorotypes (C, 1-4) and weighting habitat (OD, open dry; OH, open humid; WO, woodland; R, rocky; WA, water).

9.3 Chorotypes classification

Chorotype classification relied on a quantitative method that involves the chorotypes previously established for small-mammal faunas in Catalonia by López et al. (2006) and Sans-Fuentes and Ventura (2000). These authors considered chorotypes as faunal associations with similar distributions and ecological requirements. Each taxon is assigned to one chorotype according to its current climatic requirements and geographical distribution (Fernández-García and López-García, 2013) (Table 2.6). The chorotypes differentiated are as follows:

- **Chorotype 1.** – Includes species with mid-European requirements, with low mean summer temperatures (< 20 °C), mean annual temperatures (MAT) lower than 10-12 °C, and mean annual precipitation (MAP) higher than 800 mm, and with a present-day distribution in northeastern Iberia that includes the Pyrenees, a small part of the eastern Pre-Pyrenees, and foothills lying more than 800 m above sea level.
- **Chorotype 2. –** Includes mid-European species tolerant of Mediterranean conditions, which need a high precipitation level (MAP > 600 mm) and with a broader distribution in northeastern Iberia than those of chorotype 1, extending through more southern and eastern territories. **Chorotype 3. –** Includes Mediterranean species and implies moderate temperatures (MAT > 5° C) and humid conditions (MAP < 1000 mm).
- **Chorotype 4. –** This group includes generalist species with a broad distribution or species with a particular habitat, which in general provide little climatic information.

10. Palaeotemperatures reconstruction

In the analyzed archaeological sequences – Xaragalls cave, Abric Romaní rock-shelter, Teixoneres cave, and Arbreda cave (Chapters 5 to 8) – an attempt to reconstruct past temperatures and precipitations was performed using three independent methods.

10.1 Mutual Ecogrographic Range

The mutual ecogeographic range (MER) method, previously called "mutual climatic range", is a qualitative method which determines the present-day geographical region in which a given fossil species assemblage would be located through the intersection obtained from the overlap of the current distributions of each species (Blain et al., 2009, 2016; López-García, 2011; Lyman, 2016). Careful attention is paid to ensure that the real current distribution of each species corresponds to the potential ecological distribution and has not been strongly affected by other limiting or perturbing parameters (such as human impact or predation). Accordingly, *Iberomys cabrerae* is excluded because its current distribution is influenced by anthropic factors. The little-known and generally fragmentary distribution of bat species precludes the inclusion of this order of mammals (Palomo et al., 2007). This method has already been applied to assemblages containing extant reptile and amphibian taxa (Blain et al., 2009, 2016) and to Late Pleistocene small-mammal assemblages (López-García, 2011). This method allows us to calculate several climatic parameters of a given fossil site, but mean annual temperatures (MAT) and mean annual precipitations (MAP) are used in this thesis.

10.2 Bioclimatic Model

Hernández Fernández (2001) developed a calibration dataset using mammal faunas and associated environmental data from 50 contemporary mammalian assemblages distributed all over the world. This allows fossil data to be transformed into qualitative and quantitative estimates. The bioclimatic

characterization of species is based on the climatical typology by Walter (1970). For each species, the Climatic Restriction Index (CRIi=1/n, where i is the climatic zone inhabited by the species and n is the number of climatic zones the species inhabit) was established. Thus, the bioclimatic model (BM) is based on the assignation of small-mammal species to ten different climatic zones associated with biomes mainly related to vegetation types (Hernández Fernández, 2001; Hernández Fernández et al., 2007) (Table 2.7):

- I – Equatorial – Evergreen tropical rain forest
- II – Tropical with summer rains – Tropical deciduous woodland
- II/III – Transition tropical semiarid – Savanna
- III – Subtropical arid – Subtropical desert
- IV – Subtropical with winter rains and summer drought – Sclerophyllous woodland - shrubland
- V – Warm-temperate – Temperate evergreen forest
- VI – Typical temperate – Nemoral broadleaf – deciduous forest
- VII – Arid-temperate – Steppe to cold desert
- VIII – Cold-temperate (boreal) – Boreal coniferous forest (taiga)
- IX – Polar – Tundra

Based on each species' CRI, it is possible to calculate their representation in a specific locality of each of the ten existing climates, called the Bioclimatic Component (BCi=(ΣCRIi)100/S, where S is the number of species). From the BC it is possible to estimate the MAT and MAP by means of multiple linear regression developed specifically for the order Rodentia (Hernández Fernández, 2001; Hernández Fernández et al., 2007):

$$MAT\ (^{\circ}C) = 26.686 + (0.024*II) - (0.029*II/III) - (0.024*III) - (0.074*IV) - (0.12*V) - (0.135*VI) - (0.217*VII) - (0.404*VIII) - (0.386*IX)$$

$$MAP\ (mm) = 2978.195 - (21.237*II) - (27.563*II/III) - (33.05*III) - (32.648*IV) - (6.678*V) - (5.076*VI) - (28.4*VII) - (33.109*VIII) - (25.98*IX)$$

	I	II	II/III	III	IV	V	VI	VII	VIII	IX
Arvicola sapidus	0	0	0	0	0.5	0	0.5	0	0	0
Arvicola terrestris	0	0	0	0	0.25	0	0.25	0.25	0.25	0
Microtus agrestis	0	0	0	0	0	0	0.5	0	0.5	0
Microtus arvalis	0	0	0	0	0	0	1	0	0	0
Iberomys cabrerae	0	0	0	0	1	0	0	0	0	0
Chionomys nivalis	0	0	0	0	0.25	0	0.25	0	0.25	0.25
M. (T.) duodecimcostatus	0	0	0	0	1	0	0	0	0	0
Pliomys lenki (=coronensis)	0	0	0	0.2	0.2	0	0.2	0.2	0.2	0
Apodemus sylvaticus	0	0	0	0	0.5	0	0.5	0	0	0
Eliomys quercinus	0	0	0	0	0.5	0	0.5	0	0	0
Microtus oeconomus	0	0	0	0	0	0	0.333	0	0.333	0.333
Microtus gregalis	0	0	0	0	0	0	0	0.333	0.333	0.333
Glis glis	0	0	0	0	0	0	1	0	0	0
Spermophilus citellus	0	0	0	0	0.333	0	0.333	0.333	0	0
Sciurus vulgaris	0	0	0	0	0.333	0	0.333	0	0.333	0

Table 2.7 Distribution of each species into climatic zones according to the Bioclimatic Model method.

10.3 Oxygen isotope estimations

The reconstruction of past air temperatures from the oxygen isotope composition of rodent teeth is a two-step procedure involving two linear equations: 1) the measured $\delta^{18}O_p$ values of the fossil rodent teeth allow for the estimation of the $\delta^{18}O$ values of local meteoric water ($\delta^{18}O_{mw}$) and, 2) the calculated $\delta^{18}O_{mw}$ values can be used to estimate past air temperatures. Several equations are available both for step 1 (D'Angela and Longinelli, 1990; Lindars et al., 2001; Luz and Kolodny, 1985; Navarro et al., 2004; Royer et al., 2013a) and step 2 (e.g., Amiot et al., 2004; Bernard et al., 2009; Dansgaard, 1964; Pryor et al., 2014; von Grafenstein et al., 1996). This thesis has developed a three-step method for the reconstruction of MAT from $\delta^{18}O_p$ adapted for rodent teeth accumulated in the Iberian Peninsula, which is extensively developed in Chapter 5.

11. Present-day data sources

As has been previously discussed, most of the applied methodologies rely on the actualistic principle and, thus, present-day data sources are required.

- Ethology and biogeographical distribution of each taxon, considered in the general environmental interpretation of the species and in the habitat(s) definition (Habitat Weighting Method), come from Palomo et al. (2007). The Iberian species' present-day distribution maps (10x10 km UTM square grid) used in the MER method are also obtained from Palomo et al. (2007).

- The climatic conditions of the intersecting area are evaluated via the MER method using current climatic maps from AEMET & IMP (2011) to infer the MAT and MAP of the past for the Abric Romaní sequence. MER reconstruction of Xaragalls, Teixoneres, and Arbreda caves are not developed in this thesis and therefore use data from previous publications (López-García et al., 2015, 2012a, 2012b). All these studies estimate the past climatic conditions from Font-Tullot (2000) maps of Spain. Also, the first reconstruction of past climate in level O from Abric Romaní used this data source (Chapter 3). This reconstruction is after review during the analysis of the entire sequence (Chapter 5). Though current AEMET & IMP (2011) climatic maps provide more precise data and are therefore generally preferred, it has been confirmed that only small discrepancies can expected in the final estimations, and that previous estimations are maintained for Xaragalls, Teixoneres, and Arbreda sites (Fig. 2.3).

- The present-day mean annual temperatures and precipitations used to estimate average differences in past climatic data from the four site areas were taken from Climate-Data.org (https://es.climate-data.org/). These data are based on a climatic model using extended world climate data collected between 1982 and 2012 from the OpenStreetMap project. Some previous research on the studied sites followed Ninyerola et al. (2003) or Font-Tullot (2000), which are also studies which use 30-years of climatic records from Spanish meteorological stations. The last source presents notable changes in current climatic estimations derived from Climate-data.org, due to the absence of meteorological stations near the studied sites. For this reason, the same source-data is always employed (Climate-data.org) to avoid these problems and standardized relative temperatures, allowing for a higher-resolution comparison.

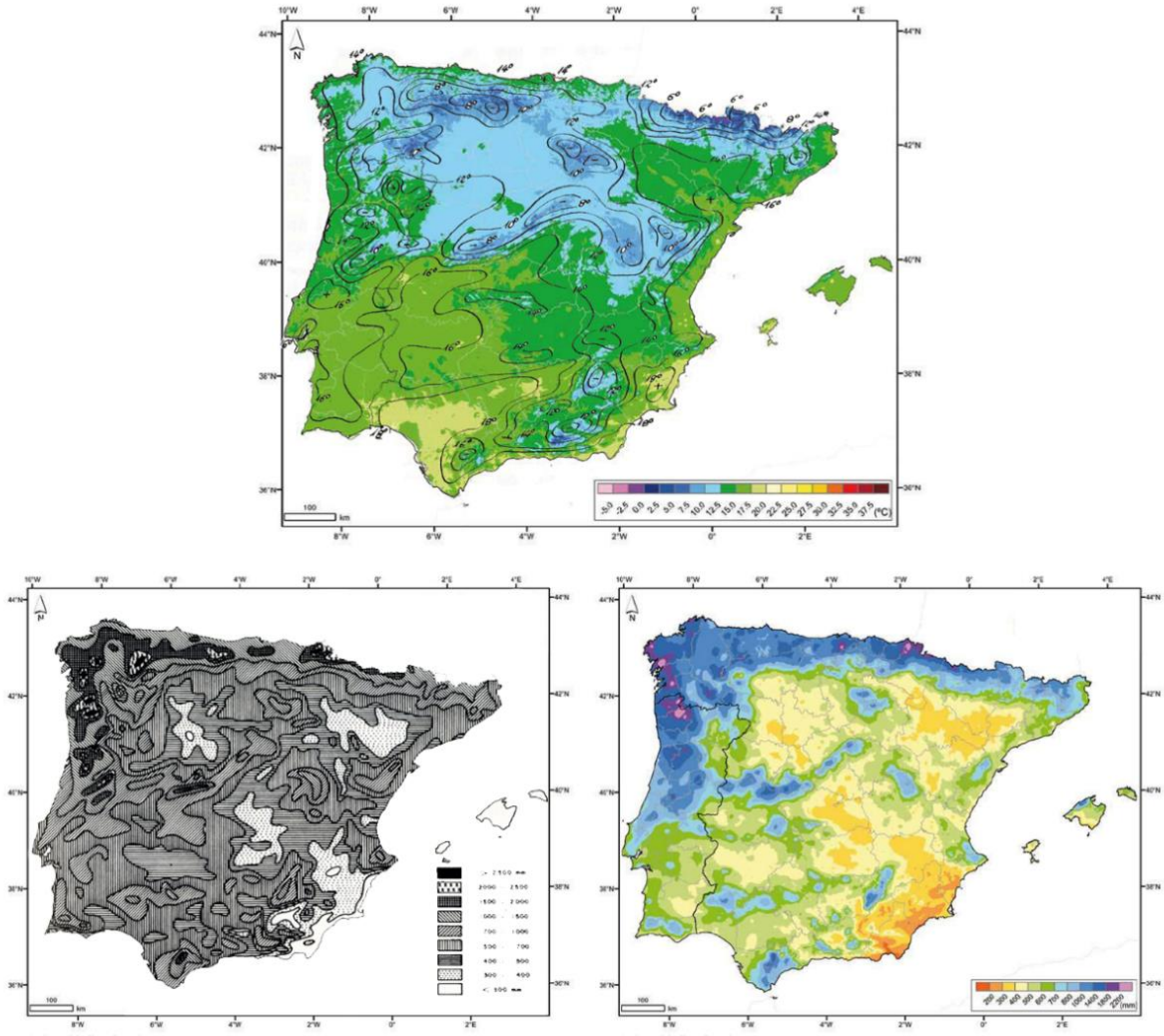

Figure 2.3 Comparison of Font-Tullot (2000) and AEMET & IMP (2011) data-source. Above: both mean annual temperatures estimations are superimposed; areas by a black line were established by Font-Tullot (2000) and color coding is related to AEMET & IMP (2011). Below: mean annual precipitations areas established by Font-Tullot (2000) on the left and AEMET & IMP (2011) on the right.

- Current oxygen isotopic composition of meteoric waters ($\delta^{18}O_{mw}$) in the localities where the modern samples were taken and for the studied sites were obtained using the Online Isotopes in Precipitation Calculator (OIPC; Bowen, 2017). This online software employs an algorithm based on datasets collected by the Global Network for Isotopes in Precipitation (GNIP), which is operated by the International Atomic Energy Agency and the World Meteorological Organization (IAEA/WMO, 2018).

12. Statistics calculations

A great part of the interpretations in this thesis are based on basic descriptive methods and data distribution measurements (mean, median, range, standard deviation, standard error, boxplot, and jitter plot). Normality tests (Shapiro-Wilk) and inferential tests of variance (*F*-test, Student's *t*-test, Levene's test and One-way ANOVA test) are applied to oxygen isotopic results of each fossil deposit analyzed (Chapters 5, 7-9). In some cases, multivariable statistics such as Principal

Components Analysis and Cluster Analysis are considered (Chapter 3). In Chapter 5, ordinary least squares (OLS) regressions are used to explore the relationship between oxygen isotope compositions and air temperatures. Uncertainties in temperature calculations were determined by applying error propagations according to the method developed by Pryor et al. (2014). All statistical analyses were performed with Microsoft Excel, R v3.3.2 (R Core Team 2016), and the Paleontological Statistics program (PAST 3.20; Hammer et al., 2001).

Chapter 3.
Palaeoecological implications of rodents as proxies for the Late Pleistocene – Holocene environmental and climatic changes in northeastern Iberia

ABSTRACT

Rodents are among the most useful proxies for reconstructing the ecology and environment of the Quaternary. The present paper focuses on a series of fossil rodent assemblages from northeastern Iberia of the Late Pleistocene (ca. 128-11.7 ka BP) and the beginning of the Holocene (< 11.7 ka BP). Descriptive and multivariate statistical methods have been applied to expand what is known about the species involved and their palaeoecological implications. The results show the importance of the three predominant species: Microtus arvalis, Microtus agrestis and Apodemus sylvaticus. A transition in the ecological conditions is shown in the studied area during the course of this interval: from open environments and cooler climatic conditions to more forested landscapes and temperate conditions. The beginning of the Late Pleistocene and the Holocene share similarities, and both differ clearly from the end of the Late Pleistocene, showing the singular nature of the environmental conditions of Marine Isotope Stage 2 in the northeastern sector of the Iberian Peninsula.

1. Introduction

The Late Pleistocene (128 – 11.7 ka BP) is an interval characterized by high climate instability, which alternates cold and warm phases and isolated climatic episodes (such as Heinrich Events or Dansgaard-Oeschger events) (Sánchez Goñi & d'Errico, 2005). Theses fluctuations are likely to have had impacts on flora, fauna and human societies. The transition from the Latest Pleistocene to the Holocene, characterized by a sharp increase in temperatures occurring around 11,700 years ago, also constituted an environmental break with major consequences (Bradley, 2008).

Different proxies (such as Greenland ice cores, marine pollen cores or continental records) have increased what is known of the Quaternary environment. In the continental domain, the temporal discontinuity of sedimentary records limits the reconstruction of reliable climatic parameters. Many proxies have been developed in order to quantify climatic parameters, on the basis either of palaeobiological approaches or geochemical methods. Over the last two decades, multidisciplinary approaches have been developed in order to improve the reconstruction of continental climate models and understand the responses of living organisms to climatic changes (Sánchez Goñi & d'Errico, 2005; Sánchez-Goñi et al., 2008). For the Iberian Peninsula, climatic particularities have been discussed that differed from the dynamics of the rest of Europe on account of geographical situation and as a consequence of the condition of southern Europe as particularities that can also be found in the Italian Peninsula and the Balkans (Fletcher et al., 2010; Harrison & Sánchez-Goñi, 2010).

Rodents are one of the most noteworthy groups of mammals in the European Quaternary, and they have become one of the most useful tools for reconstructing the ecology and environment of the Quaternary. Species from this order tend to undergo an accelerated evolution and are generally characterized by short life spans (Van Dam et al., 2006), a close relationship with their environment and strict ecological requirements. These factors make them extremely good markers for studies that focus on evolution, biochronology and particularly for inferring a record of their local living environments. Moreover, their widely ranging geographical distribution and the high presence of their remains in Quaternary sedimentary deposits makes it possible to apply multiple statistical approaches and quantitative methods (Alcalde & Galobart, 2002; Chaline, 1988;

López-García, 2011). In the present study the statistical analysis of rodent assemblages from Late Pleistocene (128-11.7 ka BP) and Holocene (<11.7 ka BP) sites from the northeastern Iberian Peninsula increases what is known of the species in question during this time frame, taking into account the specific palaeoecological implications of the assemblages with the aim of understanding the environmental evolution of this region. On the basis of this methodology our aim is to ascertain the differences and similarities between these sites/levels depending on the occurrence of species and also establish which species assemblages are the most common and which are the dominant ones.

2. Materials and methods

2.1 Data matrix

The data matrix employed corresponds to specimens recovered from 37 levels from 12 archaeological sites from the northeast of the Iberian Peninsula, chronologically located in the Late Pleistocene and the beginning of the Holocene. For each species, the minimum number of individuals (MNI) has been taken into account. Only levels with an MNI greater than or equal to 15 have been included in these analyses. This MNI limit has been decided as the optimal point to remove the assemblages with low individuals but not loss to much levels from this region (Fig. 3.1; Table 3.1) (Appendix 2.1.A).

Corrections have been applied to the data matrix in order to simplify the interpretation and reduce the dispersion of the results. Firstly, the specimens of *Microtus arvalis* and *Microtus agrestis* are integrated into a single group because it is common, especially in older publications, not to differentiate between these two species (identified as *Microtus arvalis–agrestis*). In order not to overlook the importance of the presence of these two species, the adopted solution is to put these categories into a single group. As regards the ecological restrictions on the two species, both are mid-European species associated with cool climates, high altitudes and open landscapes; they only differ in their preference for moisture (Palomo et al., 2007; Sans-Fuentes & Ventura, 2000).

Secondly, all specimens identified as *Arvicola* sp. in previous publications (Alcalde, 1986) have been interpreted as belonging to the species *Arvicola sapidus,* because this is the only species from this genus present during this interval in the northeast of Iberia (López-García, 2011). The only example of *Arvicola terrestris*, the other extant species from this genus, is located in Cova d'Olopte B (Villalta, 1972), and this is probably misidentified, also corresponding to *A. sapidus*, a species widely extended in Catalonia during the Late Pleistocene – Holocene. Finally, the specimens identified as *Terricola* sp. have been considered to be *Microtus (Terricola) duodecimcostatus.* The other known species of this genus that is close morphologically, *Microtus (T.) gerbei*, is not an abundant species in the region and is commonly associated with cooling temperatures (Palomo et al., 2007). The reason for this grouping is not to lose sight of the importance of *M. (T.) duodecimcostatus* as a result of fragmentation of the information associated with this species, which is dominant in some assemblages.

2.2 Classification of levels

The 37 studied levels have been grouped, in accordance with their chronology, in three time intervals:

- **Early Late Pleistocene (ELP).** This includes all archaeological levels from ca. 128 to 40 ka BP, generally related to the Middle Palaeolithic and consequently to *Homo neanderthalensis*

activity. Since in the northeast of Iberia there are only a few Middle Palaeolithic sites with chronologies older than 60 ka BP, the greater part of the assemblages belong to MIS 3 (ca. 60-30 ka BP). Thirteen levels of five different fossil sites are included: Levels III and II from Teixoneres cave (López-García et al., 2012b); Levels O, N and E from Abric Romaní (Fernández-García, 2014; López-García, 2011); Levels I, V and III from Cova del Gegant (López-García et al., 2012c); Levels C8, C7, C6 and C4 from Xaragalls Cave (López-García et al., 2012a) and Level I from Arbreda cave (Alcalde, 1986; López-García, 2011). This group represents a total of 946 individuals.

- **Latest Late Pleistocene (LLP).** This comprises all archaeological levels from ca. 40 to 11.7 ka BP, commonly related to the Upper Palaeolithic and the presence of Anatomically Modern Humans. This time interval is equivalent to end of MIS 3 and the complete MIS 2 (ca. 30-14 ka BP). Twelve levels from four different fossil sites are included: Levels I, H, G, F, E, D, C, B and A from Arbreda cave (Alcalde, 1986; López-García, 2011); the assemblage from Galls Carboners cave (López-García et al., 2014b); Levels 3 and 2 from Toll cave (Fernández-García & López-García, 2013) and Level CE15 from Cova Colomera (López-García et al., 2010). This group represents a total of 1455 individuals.

- **Holocene (HOL).** Groups all archaeological sites recent than 11.7 ka BP, including Epipalaeolithic, Neolithic, Chalcolithic and Bronze Age sites. All these levels belong to MIS 1. Twelve levels from four different fossil sites are included: Level CE13-14, CE12, EE1 and A. sup. from Cova Colomera (López-García et al., 2010); the assemblage from Cingle Vermell (Alcalde, 1986); Level 6, 5, 4 and 3 from Cova del Frare (Alcalde, 1986) and Level III, II and I from Cova 120 (Alcalde, 1986). This group represents a total of 666 individuals.

2.3 Multivariable Statistical methodology

To provide a better understanding of such a large corpus of data, multivariate statistical methods have been applied, allowing us to reduce the number of variables involved in order to facilitate our ecological interpretations. Methods of multivariate analysis without previous assumptions of dependence and independence have been selected, with the aim of defining coherent patterns in space and time (Shennan, 1997). The original data correspond to absolute frequency variables, so the most recommended multivariate statistics proxy is correspondence analysis (López-Roldan & Lozares-Colina, 2000). However, this method has been shown to have limitations for the studied data, such as its low representativeness and the low explanatory capacity of its results. Consequently, other methods have been applied.

On the one hand, a principal component analysis (PCA) has been applied. This analysis has been performed after the transformation of the data from absolute frequency variables to ratio variables, replacing the original values by percentages. This data for which the sum over the variables is 100% is equivalent to compositional data (Baxter, 2003). The PCA makes it possible to analyse the sample in standardized form and yields advantages in interpretation by placing the different variables on a coordinate axis, distinguishing different components (the resulting variables) that indicate the weight of each original variable in the graphical representation obtained (Jolliffe, 2002). The covariance matrix has been used, because it proves to be the most appropriate to increase the total variance obtained in the first, second and third components (Shennan, 1997; López-Roldan & Lozares-Colina, 2000).

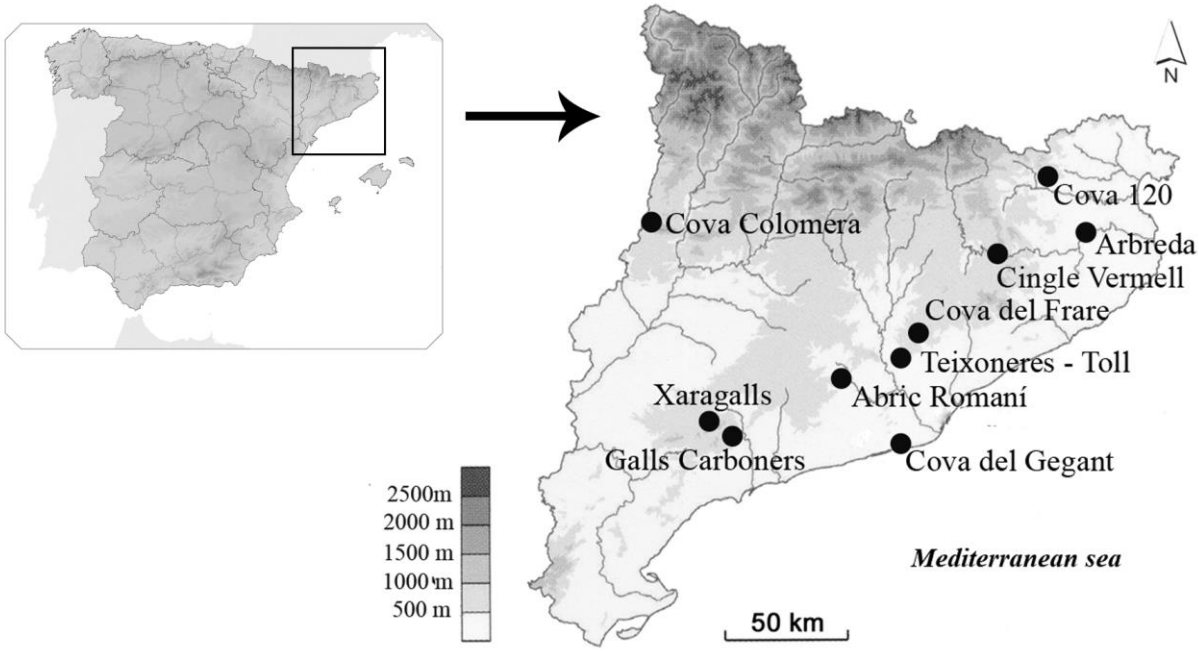

Sites	Levels	Chronology
Teixoneres cave	III, II	90-30 ka BP
Abric Romaní rockshelter	O, N, E	55-49 ka BP
Cova del Gegant (old levels)	I	128-40 ka BP
Cova del Gegant (new levels)	V, III	55.7-49.3 ka cal BP
Xaragalls cave	C8, C7, C6, C4	45-13 ka BP
Arbreda cave	I, H, G, F, E, D, C, B, A	40-18.8 ka BP
Galls Carboners cave	Capa 100	31.17-31.38 ka cal BP
Toll cave	3, 2	<35 - >13 ka
Cova Colomera	CE15, CE13-14, CE12, EE1, A. sup	13-3.5 ka BP
Cingle Vermell		9.76 ±0.16 ka BP
Cova del Frare	6, 5, 4, 3	6.3-3.9 ka BP
Cova 120	III, II, I	4.27-3.1 ka BP

Figure 3.1 Location of Late Pleistocene – Holocene archaeological sites included from the northeast of the Iberian Peninsula, and table showing the site and the corresponding levels, with their general chronology.

On the other hand, for a better and more visual compression of the data, a cluster analysis has been applied. Behind this method lies the idea that objects can be similar to one another at different levels; accordingly, the results can be represented in the form of a dendrogram, where the hierarchical relationships can be detected (Shennan, 1997). In the both cluster analyses presented, the original values have also been transformed into ratio variables. The first one have included the same data than the PCA; whereas in the second, the levels have been group in the three time intervals distinguished, including totals. A Euclidean Index is selected for grouping the data in both; this index is recommended for quantitative measures and ratio variables. The "paired group linkage" has been applied in all cases. For all the statistical approaches the Paleontological Statistics program has been used (PAST3) (Hammer et al., 2001).

		Arvicola sapidus	*Chionomys nivalis*	*Microtus arvalis-agrestis*	*M. (Terricola) duodecimcostatus*	*Microtus (Terricola) gerbei*	*Microtus oeconomus*	*Iberomys cabrerae*	*Clethrionomys glareolus*	*Pliomys lenki*	*Apodemus sylvaticus*	*Mus musculus*	*Eliomys quercinus*	*Glis glis*	*Hystrix* sp.
Early Late Pleistocene (128 - 40 ka BP)	**Teixoneres - Level III**	3	1	35	35	1	0	2	0	1	75	0	11	7	0
	Teixoneres - Level II	2	8	100	9	0	0	0	0	1	19	0	8	0	0
	Abric Romaní - Level O	55	0	55	25	0	0	45	0	0	69	0	8	0	0
	Abric Romaní - Level N	3	0	0	1	0	0	8	0	0	3	0	0	0	0
	Abric Romaní - Level E	3	0	3	4	1	0	0	0	0	5	0	1	0	0
	Cova del Gegant - Level I	0	0	5	5	2	0	4	0	0	24		4	0	2
	Cova del Gegant - Level V	0	0	0	1	0	0	5	0	0	1	0	17	0	0
	Cova del Gegant - Level III	0	0	1	0	0	0	3	0	0	3	0	11	0	0
	Xaragalls - C8	0	0	1	4	0	0	2	0	0	18	0	2	0	0
	Xaragalls - C7	0	0	2	0	0	0	1	0	0	33	0	3	0	0
	Xaragalls - C6	1	1	4	7	0	0	3	0	0	69	0	6	0	0
	Xaragalls - C4	0	2	6	2	0	0	1	0	0	14	0	3	0	0
	Arbreda - Level I	5	7	30	4	0	0	0	0	0	12	0	7	0	0
Latest Late Pleistocene (40-11 ka BP)	**Arbreda - Level H**	4	0	95	12	0	0	0	0	0	3	0	2	0	0
	Arbreda - Level G	0	0	41	7	0	1	0	0	0	3	0	3	1	0
	Arbreda - Level F	2	0	89	2	0	0	0	0	0	7	0	6	0	0
	Arbreda - Level E	6	0	98	1	0	1	0	0	0	6	0	4	0	0
	Arbreda - Level D	16	0	192	4	0	0	0	0	0	7	0	9	0	0
	Arbreda - Level C	13	0	248	0	0	2	0	0	0	5	0	8	0	0
	Arbreda - Level B	2	0	61	0	0	0	0	0	0	3	0	3	0	0
	Arbreda - Level A	6	0	125	60	0	0	2	0	0	22	0	15	0	0
	Galls Carboners	0	9	3	0	0	0	0	0	0	9	0	33	0	0
	Toll - Level 3	0	1	16	19	0	0	1	0	0	1	0	2	1	0
	Toll - Level 2	0	0	3	61	2	0	3	0	0	2	0	0	0	0
	Colomera - Level CE15	0	34	33	4	0	0	0	0	0	12	0	5	0	0
Holocene (<11 ka BP)	**Colomera - Level CE13 -14**	0	24	11	5	0	0	1	0	0	36	0	4	0	0
	Colomera - Level CE12	0	11	11	4	0	0	2	0	0	32	0	6	0	0
	Colomera - Level EE1	0	6	8	1	0	0	1	0	0	22	0	4	0	0
	Colomera - Level A sup.	0	0	0	6	0	0	1	0	0	32	0	9	0	0
	Cingle Vermell	3	0	6	2	0	0	1	1	0	37	0	3	0	0
	Cova del Frare - Level 6	0	0	0	16	0	0	0	0	0	8	0	0	0	0
	Cova del Frare - Level 5	0	0	0	33	0	0	8	0	0	29	0	2	0	0
	Cova del Frare - Level 4	0	0	0	25	0	0	9	1	0	19	0	3	1	0
	Cova del Frare - Level 3	0	0	0	5	0	0	2	0	0	8	0	1	1	0
	Cova 120 - Level III	0	0	3	6	0	0	0	0	0	49	0	2	0	0
	Cova 120 - Level II	0	3	4	11	0	0	11	0	0	70	2	6	7	0
	Cova 120 - Level I	1	0	1	0	0	0	1	0	0	18	6	3	1	0
	Early Late Pleistocene	72	19	242	97	4	0	74	0	2	345	0	81	7	2
	Latest Late Pleistocene	49	44	1004	170	2	4	6	0	0	80	0	90	2	0
	Holocene	4	44	44	114	0	0	37	2	0	360	8	43	10	0
	Total MNI	125	107	1290	381	6	4	117	2	2	785	8	214	19	2

Table 3.1 Data matrix for the occurrence of species in Late Pleistocene – Holocene archaeological levels in the northeastern of Iberia. The occurrence of the species is expressed as the minimum number of individuals (MNI).

3. Results

3.1 Previous data

A preliminary view of the occurrence of species in different levels from the Late Pleistocene – Holocene epoch clearly shows the dominance of some taxa over other, more poorly represented taxa. The most abundant taxa, listed in increasing order, are: the group of the common vole and the field vole (*Microtus arvalis-agrestis*), the wood mouse (*Apodemus sylvaticus*), the Mediterranean pine vole (*M. (T.) duodecimcostatus*), Cabrera's vole (*Iberomys cabrerae*), the garden dormouse (*Eliomys quercinus*), the European snow vole (*Chionomys nivalis*) and the southwestern water vole (*Arvicola sapidus*). However, in many cases their dominance do not extend for long intervals of time and are restricted to the singularities of certain sites (Table 3.1). The important presence of *M. arvalis-agrestis* is clear, but it combines an abundant presence in some levels with being very scarce in others. Meanwhile, *A. sylvaticus* is dominant in some levels but always at lower rates than in intervals of *M. arvalis-agrestis* dominance (Table 3.1; Fig. 3.2).

Leaving aside the peculiarities of each site and taking into account the species representativeness during the different time intervals, various trends have been observed (Fig. 3.3). Notable changes in species abundance are observed for certain intervals, particularly regarding the presence of these two dominant species. During the early Late Pleistocene both species show a roughly equal representation: *A. sylvaticus* (36.5%) and *M. arvalis-agrestis* (25.6%). However, with the arrival of the latest Late Pleistocene a significant shift is detected, involving a remarkable decrease in *A. sylvaticus* (5.5%) and the almost complete dominance of *M. arvalis-agrestis* (69%). In the

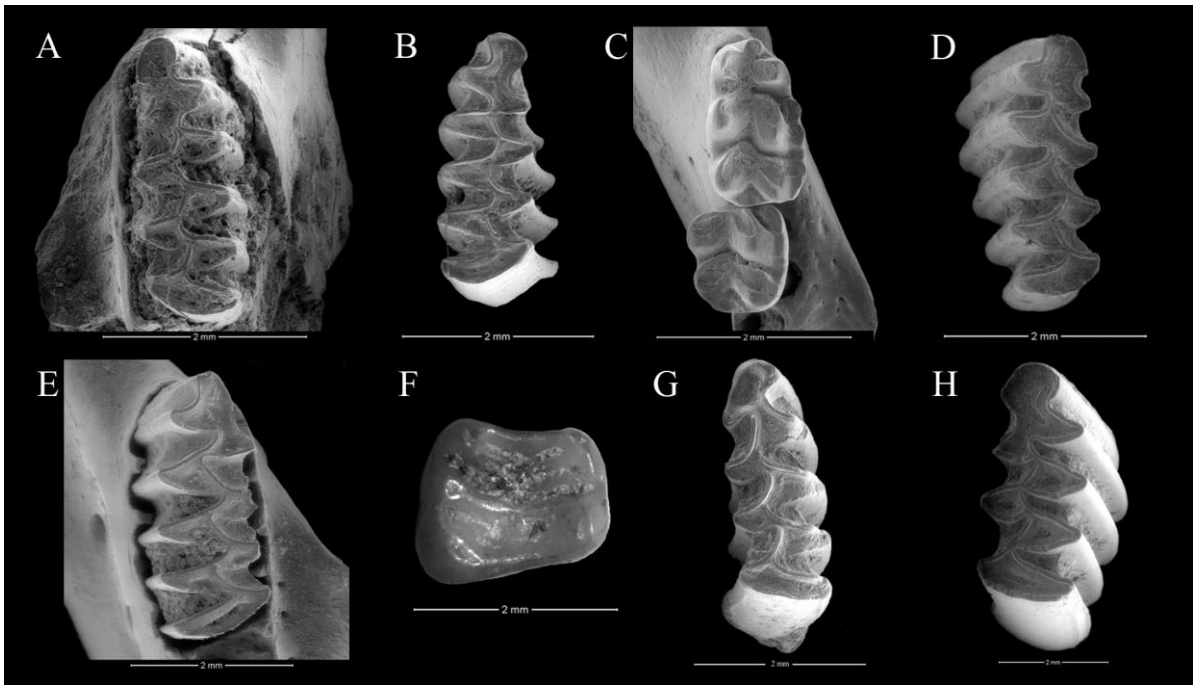

Figure 3.2 Most common rodent species from northeastern Iberia during the Late Pleistocene – Holocene: A. left m1 of *Microtus arvalis* (Toll cave); B. right m1 of *Microtus agrestis* (Cova del Gegant); C. right m1 and m2 of *Apodemus sylvaticus* (Toll cave); D. right m1 of *Microtus (Terricola) duodecimcostatus* (Cova del Gegant); E. right m1 of *Iberomys cabrerae* (Abric Romaní); F. right m2 of *Eliomys quercinus* (Toll cave); G. left m1 of *Chionomys nivalis* (Toll cave); H. left m1 of *Arvicola sapidus* (Toll cave). Occlusal view: scale 2mm.

Holocene, by contrast, the opposite situation occurs: *A. sylvaticus* undergoes a revival (54%) and *M. arvalis-agrestis* loses in importance (6.6%). The other species barely exceed 1% in any of the intervals considered, except for *M. (T.) duodecimcostatus*, *E. quercinus*, *C. nivalis*, *A. sapidus* and *I. cabrerae*, which are better represented but remain more or less constant in the different intervals.

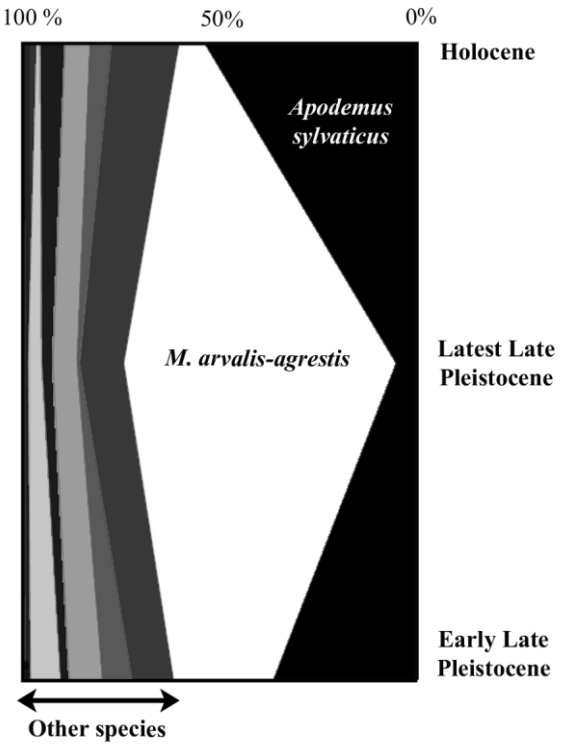

Figure 3.3 Relative frequency of Late Pleistocene – Holocene rodent species in northeastern Iberia throughout the three chronological periods differentiated. From left to right: non-significant species (*Microtus (Terricola) gerbei*, *Microtus oeconomus*, *Clethrionomys glareolus*, *Pliomys lenki*, *Mus musculus*, *Glis glis*, *Hystrix* sp., *Spermophilus citellus*, *Sciurus vulgaris*); *Arvicola sapidus*; *Chionomys nivalis*; *Eliomys quercinus*; *Iberomys cabrerae*; *Microtus (Terricola) duodecimcostatus*; *Microtus arvalis-agrestis*; *Apodemus sylvaticus*.

3.2 Multivariate statistics

3.2.1 Principal component analysis

Interesting results were obtained when principal component analysis was applied (Fig. 3.4). Considering the eigenvalues attributed to each of the components (Appendix 2.1.B), the first three should be included. The scree plot clearly shows that Component 4 is not relevant (PC4, less than 5% of variance). In contrast, the first three principal components present high representativeness, summarizing more than 90% of the variance of the studied sample (PC1, 55.6%; PC2, 19.4%; PC3, 15.5%).

PC1 arranges the archaeological levels in relation to high values of MNI of two main groups of species (Fig. 3.4A): *M. arvalis-agrestis* for positive values of this axis and *A. sylvaticus* for negative values. The *M. arvalis-agrestis* group of species can be related with open environments, low humidity rates and cold temperatures, whereas the second is adapted to forest environments in a temperate climate without major climatic constraints (Palomo et al., 2007). Nevertheless, it is also remarkable the importance of *M. (T.) duodecimcostatus*, *E. quercinus* and *I. cabrerae* for negative values. *M. (T.) duodecimcostatus* and *I. cabrerae* are species typical of Mediterranean areas, while *E. quercinus* is a generalist species but usually related to forest cover (Sans-Fuentes & Ventura, 2000; Purroy & Varela, 2003; Palomo et al., 2007). From a palaeoenvironmental point of view, a distribution of sites along the PC1 can be inferred between a more open and possibly colder climate, represented by "the *M. agrestis-arvalis* tendency", to forested areas and more temperate climate, represented by "the *A. sylvaticus* tendency". Accordingly, the simplest interpretation for the distribution of levels on the graph would be a gradient from more closed environments (negative values on PC1 axis) to more open environments (positive values of PC1 axis), with the climatic implications that this might entail.

In addition, positive PC2 values are determined by the occurrence of *M. (T.) duodecimcostatus* and secondly by *I. cabrerae.* Both are commonly associated with Mediterranean conditions and

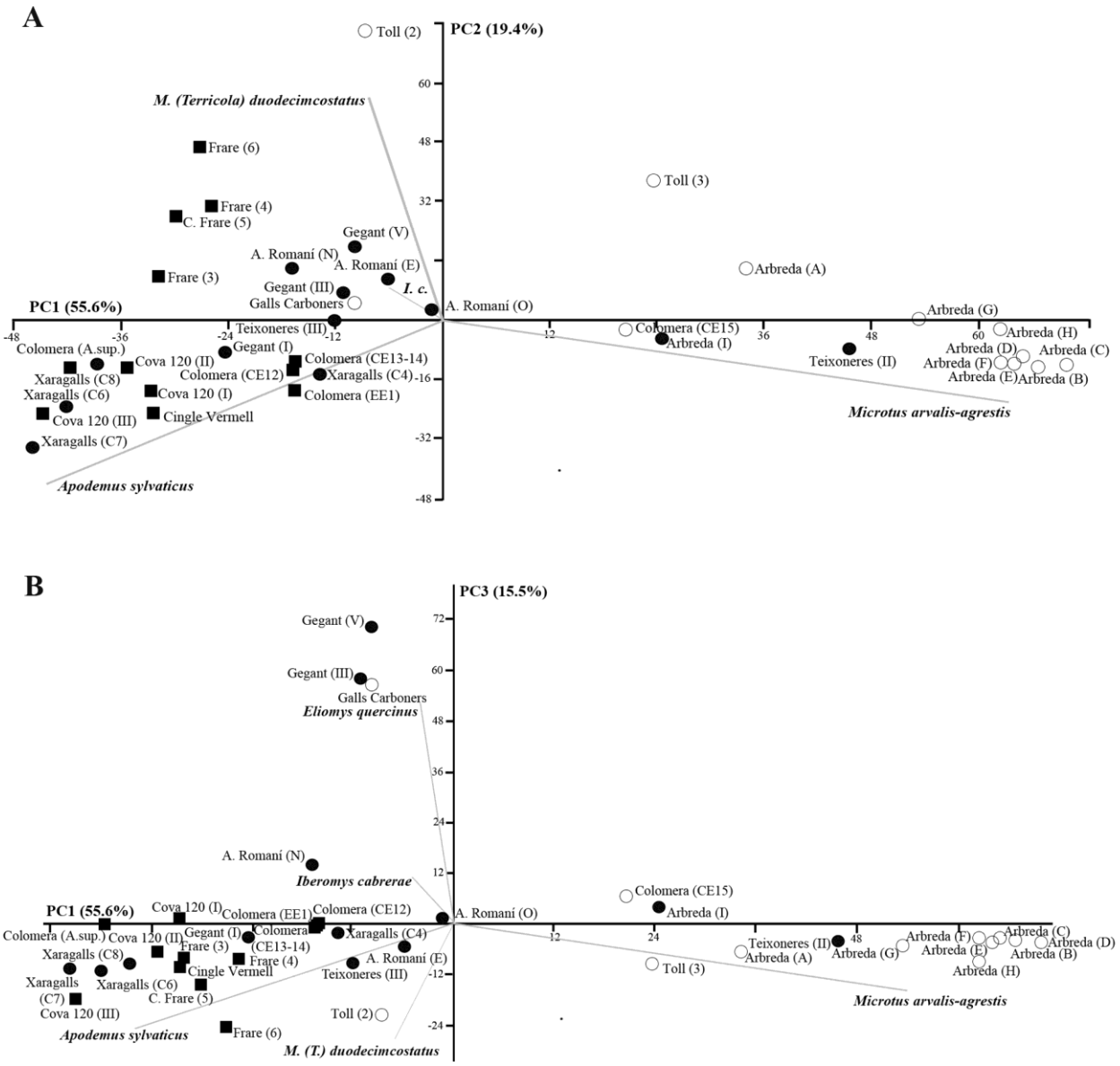

Figure 3.4 Principal component analysis of Late Pleistocene – Holocene levels from northeastern Iberia according to rodent species occurrence. A. Graphical representation of components 1 (x) and 2 (y); B. Graphical representation of components 1 (x) and 3 (y). Early Late Pleistocene levels in black dots, Latest Late Pleistocene levels in white dots, and Holocene levels in squares.

related forest or wet grassland habitats (Sans-Fuentes & Ventura, 2000; Palomo et al., 2007). On the other hand, negative values depend on *A. sylvaticus* and *M. arvalis-agrestis* and in lesser proportion on *C. nivalis*. The latter three are mid-European species nowadays living in areas at notable altitudes, with cold temperatures and lower rainfall; by contrast, *A. sylvaticus* is a generalist species, related to the forest and not restricted by altitudinal factors (Palomo et al., 2007; Purroy & Varela, 2003; Sans-Fuentes & Ventura, 200). In this sense, it proves difficult to develop a palaeoecological interpretation for PC2. Nevertheless, the contrast between PC1 and PC2 suggests a classification of assemblages in terms of the three most dominant species (*M. arvalis-*

agrestis, *A. sylvaticus* and *M. (T.) duodecimcostatus*) in the northeast of the Iberian Peninsula during the Late Pleistocene and Early Holocene.

As regards the three above-defined time intervals, it can be observed that the closest associations over time within each time interval tend to appear together on the graph. Specifically, LLP levels appear separated from the rest of the associations and concentrated together in relation to *M. arvalis-agrestis*. Moreover, ELP and HOL levels are grouped together, their distribution depends on the dominance of *A. sylvaticus* or *T. duodecimcostatus*, showing no particularly distinctive patterns between these two time intervals. In complementary form, the ELP and HOL samples tend to appear far away from *M. arvalis-agrestis*, and the LLP ones from *A. sylvaticus*, showing the respective low presence of these species. This demonstrates the great similarity of these two climatic phases (ELP and HOL), or rather the high particularity of LLP.

On the one hand, all the LLP levels from Arbreda cave and Level CE15 from Cova Colomera are grouped together in the "*M. arvalis-agrestis* tendency". The location of some LLP levels shows that, in spite of the above-noted clear bipolarization between the two main groups of species, there are other determinant taxa during this interval, such as the Mediterranean pine vole (*M. (T.) duodecimcostatus*). The high presence of this taxon is evident in levels from Toll cave and is the reason about its position in the graph. The only incoherent level is Galls Carboners cave assemblage, which appears somewhat distant, because is the oldest site from the LLP samples and is affected by the Mediterranean influence on its location.

On the other hand, among the ELP and HOL levels, two levels appear closer to the LLP group: Level I from Arbreda cave and Level II from Teixoneres cave. These correspond to the latest and earliest levels, respectively, among the ELP assemblages. The reasons could be related both to chronological and geographical influences. The former could be interpreted as a marker for a progressive trend on decrease of temperatures and changing conditions associated with the beginning of the LLP and the resulting glacial acceleration. Level II from Teixoneres cave has been linked in previous publications (López-García et al., 2014c) with Heinrich Event 2 or 3, a cooling episode that led to a high presence of mid-European species such as *M. arvalis* and *M. agrestis*. This phenomenon is also found in Levels O and E of the Abric Romaní rock-shelter, previously associated with cold episodes: Stadial 17-15 and Heinrich Event 5, respectively (Fernández-García, 2014; López-García, 2011).

By combining PC1 and PC3, we can observe small differences in the association of levels (Fig. 3.4B). Positive values for PC3 are related with the occurrence of *E. quercinus* and, less importantly, with *C. nivalis* and *I. cabrerae*, while negative values are defined by the proportionally greater occurrence of *M. (T.) duodecimcostatus*, *A. sylvaticus* and *M. arvalis-agrestis.* As occurred in the PC2, this makes an ecological interpretation somewhat more complex, but a chronological trend is conserved, clustering LLP closer to *M. arvalis-agrestis* and the rest (ELP and HOL) closer to *A. sylvaticus*. The only exceptions are the Galls Carboners assemblage and levels III and V from Cova del Gegant, a result of the tendency established by the predominance of *E. quercinus* in these samples, which is a particularity of these locations. However, the chronological distribution detected by the combination of PC1 and PC2 is in general terms maintained in the combination of PC1 and PC3, revealing the great influence of the *M. arvalis-agrestis* and *A. sylvaticus* bipolarization shown by PC1.

3.2.2 Cluster analysis

The results obtained by the cluster analysis of the total occurrences of species by time intervals are congruent with those obtained through the PCA (Fig. 3.5). Certainly, the divergence of the assemblages from the LLP from the other two time intervals can be appreciated, with the ELP and the HOL assemblages appearing closer to each other (Fig. 3.5B). This phenomenon can be observed clearly if the relative presence of the species by interval is tested, but also if we cluster their occurrence by isolated levels (Fig. 3.5A). The clustering level analysis shows only three possible outliers. The possible reasons for this anomaly have already been explained for the PCA. In the case of Level 2 from Toll cave (LLP), the high presence of *M. (T.) duodecimcostatus* would be determinant in its association.

Once again, the trend showed is probably related to the high occurrence of mid-European species during the LLP, while in the other two-time intervals the dominant species are those common in forest environments and more temperate environments or climates with a Mediterranean influence. If we pay attention to how the graph shows the association of species (Fig. 3.5B), *M. arvalis-agrestis* is clearly far from the rest, as is *A. sylvaticus*. *M. (T.) duodecimcostatus* is also somewhat further away from the rest but to a lower degree. These relations demonstrate the singular character of these three species, which are commonly more abundant in northeastern assemblages, as has been observed by means of the PCA. The rest of the species appear much more clustered, with only *E. quercinus, A. sapidus, I. cabrerae* and *C. nivalis* showing a certain distance from the rest (but always within this group of unrepresentative species).

4. Discussion

There are some species that dominate in specific archaeological records as a result of the precise conditions of each site, including parameters such as the altitude, the proximity to the coast or to river courses. In the light of the results obtained in this study, however, it seems consistent to interpret an ecological trend reflected in the rodent associations, a trend that is relatively independent of the precise conditions of the archaeological sites in the northeast of Iberia. In short, one can observe a gradient in the environmental conditions running from open spaces such as meadows or grasslands and linked to the presence of *M. arvalis-agrestis,* to more wooded areas or areas with greater vegetation cover associated with *A. sylvaticus*. Nonetheless, the particularities of the Iberian Peninsula make some Mediterranean species (such as *M. (T.) duodecimcostatus* and *I. cabrerae*) or woodland species (such as *E. quercinus*) crucial in the interpretation of the environment (Palomo et al., 2007; Purroy & Varela, 2003). The continuous transitions in the ecological conditions between open and cooling environments and more forested and temperate ones constitute a common tendency in the western Mediterranean during the Late Pleistocene cycles (Harrison & Sánchez-Goñi, 2010). Overall, the Late Pleistocene is in general terms considered colder than the Holocene because of the alternation of glacial and interglacial cycles, whereas the Holocene constitutes an interval of climatic recovery, identified as the last interglacial before the present (Uriarte, 2003). However, we can see a greater proximity in the overall association of species during the HOL and ELP than during the LLP. The singularity of the LLP can be observed in its fauna composition characterized by species related with mid-European requirements and open environments (*M. arvalis, M. agrestis* and *C. nivalis*).

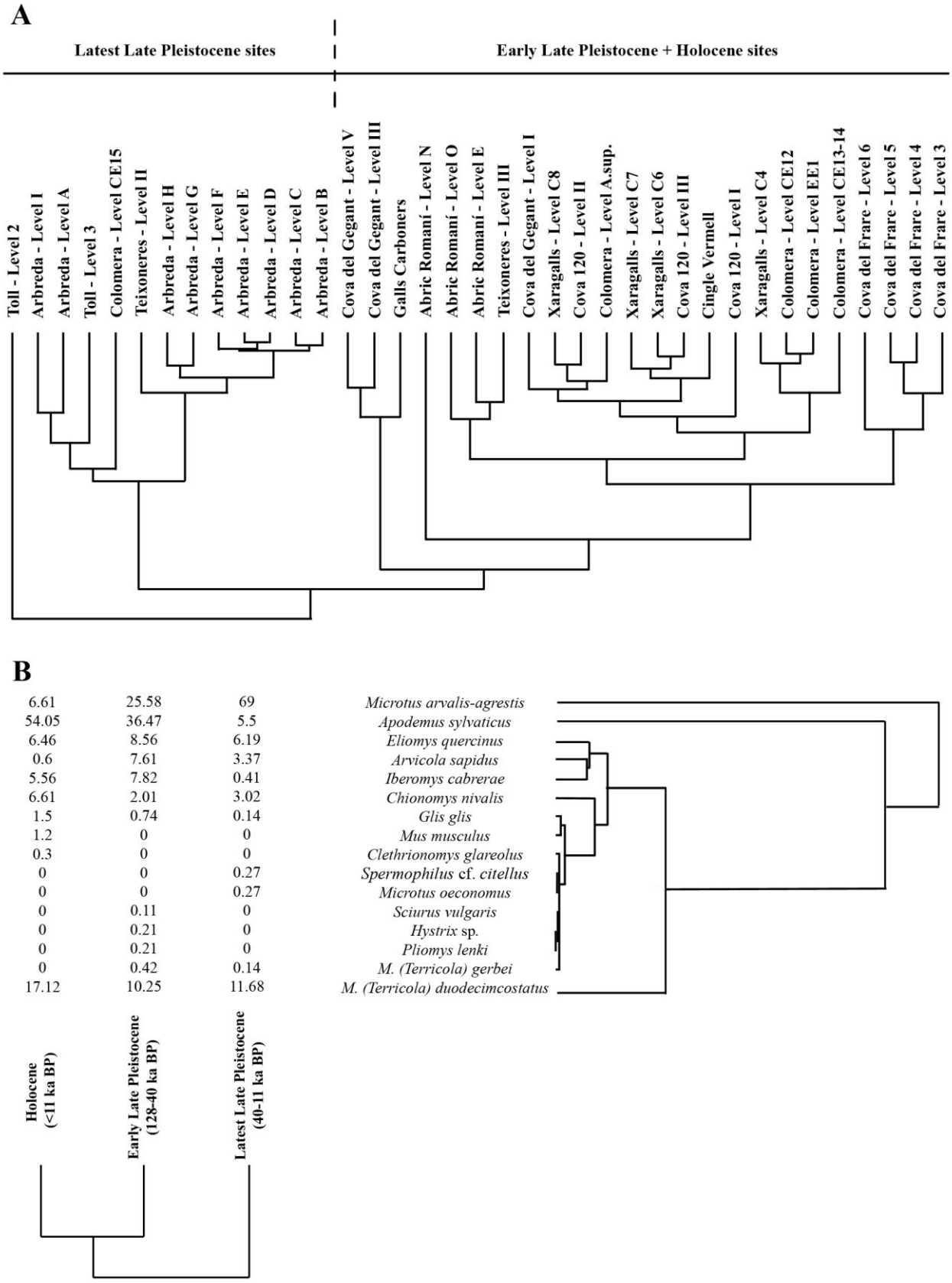

Figure 3.5 Late Pleistocene – Holocene species occurrence in northeastern Iberia by cluster analysis in different levels (A) and associated by chronological periods (B) (on the top right, the species groups and, on the lower left margin, the periods grouped).

By contrast, the ELP (Middle Palaeolithic) assemblages are not as different from the HOL ones as might have been expected, presenting similar proportions of woodland species (*A. sylvaticus*) and Mediterranean species (*M. (T.) duodecimcostatus* and *I. cabrerae*). This can be understood in terms of climate issues related with MIS 2 and the Last Glacial Maximum (LGM), which testifies to the largest drop in temperature experienced during this time interval and the subsequent reduction of wood cover (Sánchez-Goñi & d'Errico, 2005). However, it should be borne in mind that this phenomenon occurs in lower intensity in Iberia than in the rest of Europe, where the conditions of aridity in cold moments are more pronounced, as reflected in faunal communities and other proxies (Fletcher & Sánchez-Goñi, 2008; Sommer & Nadachowski, 2006). The maintenance of woodland cover remains a constant in Iberia in spite of the intervals of instability.

4.1 Early Late Pleistocene environment (128-40 ka BP)

During MIS 4, solar insolation was minimal, initiating a global cold period. Long-term pollen records obtained from French lacustrine deposits, such as La Grande Pile and the Velay Maars (Guiot et al., 1992), indicate the predominance of boreal forests during MIS 4, declining at the end of MIS 4 with the expansion of steppe–tundra vegetation (Fletcher et al., 2010; Sánchez-Goñi et al., 2008). According to pollen analysis, MIS 3 is characterized in southern Europe by a dynamic that alternates between phases of forest development and the expansion of semi-arid areas in accordance with the warming and cooling, respectively, of the sea-surface temperatures (Fletcher et al., 2010; Harrison & Sánchez-Goñi, 2010). However, various proxies, including pollen and small mammals, have shown that this alternation of dryness and wetness and the consequent reduction-extension of forest are not straightforward.

There are many Middle Palaeolithic sites located in the northeast of Iberia during MIS 3. Some of them present interesting climatic reconstructions based on small mammals, such as Level II from Teixoneres cave (60-30 ka BP), Level IV from Cova del Gegant (60 ±3.8 ka BP), Level O from Abric Romaní (54.24 ±0.42 ka BP), Level C8 from Xaragalls cave (> 43.5 ka BP), Level I from Arbreda cave (40 – 32 ka BP) and Galls Carboners (31.38 – 31.17 ka BP) (Fernández-García, 2014; López-García, 2011; López-García et al., 2012a; 2012b; 2012c; 2014b). As has previously been reported by López-García et al. (2014c), small-mammal proxies show lower mean annual temperatures and higher precipitation levels throughout this period in this region (Fernández-García, 2014). Coexistence is also observed between temperate and cold rodent species, which underwent changes in proportion depending on the stadial-interstadial fluctuations. Moreover, Mediterranean species (*M. (T.) duodecimcostatus* or *I. cabrerae*) are always present in the assemblages. However, the predominance of typical woodland species (*A. sylvaticus* and *E. quercinus*) in MIS 3 assemblages becomes a defining characteristic of the environment conditions, independent of whether it was a stadial or interstadial phase. These two latter trends are probably related with the clustering of the ELP sites with HOL assemblages in the statistical proxy in this paper.

This is coherent with palynological studies that have suggested that southern Europe (below 40°N) never underwent a complete loss of woodland, even in stadials or Heinrich Events (Fletcher et al., 2010). During interstadials the forest recovered extremely quickly, though depending on regional climatic conditions (Fletcher et al., 2010; Sánchez-Goñi & d'Errico,

2005). The Mediterranean coast was where the forest development was most pronounced, as a result of the influence of the Mediterranean climate and the smaller effect of North Atlantic fluctuations (Fletcher et al., 2010; Harrison & Sánchez-Goñi, 2010). In fact, important differences from the rodent communities of southwestern France can be noted. The typical rodent species in sedimentary sequences from MIS 4 and MIS 3 in these areas are *M. arvalis, Microtus gregalis* and *Dicrostonyx torquatus* (Chaline, 1972; Marquet, 1993; Royer et al., 2013; Villa et al., 2010). These three species today live in open habitats (tundras, forested tundras or steppes) and have a distribution that is latitude-dependent (MacDonald & Barrett, 2008). Their presence thus argues in favour of a very cold and arid environment, different from that detected for the northeast of Iberia during this interval.

4.2 Latest Late Pleistocene (40 – 14.7 ka BP)

The LLP is basically represented by the end of MIS 3, the complete MIS 2 and the beginning of MIS 1 (ca. 14.7 ka BP) (Lisiecki & Raymo, 2005). These stages are highlighted in all geological sources as the most intense glacial phases, characterized by rapid and major climatic changes (Vermeersch, 2005), and ranging chronologically from ca. 27 to 11.7 ka BP. MIS 2 contains two Heinrich Events (H2 and H1), dated respectively to ca. 24 ka BP (H2) and to 16 ka BP (Oldest Dryas or H1), and also the Last Glacial Maximum (LGM) (ca. 22-19 ka BP), the moment of maximum cold in the Northern Hemisphere which represents the time of maximum extension of ice sheets at the polar caps (Fletcher & Sánchez-Goñi, 2008). This singularity of the LLP (Upper Palaeolithic) can be observed beyond the changes in the fauna composition and is clear in our statistical proxy, associated with an important increase in the species related with mid-European requirements and open environments (*M. arvalis, M. agrestis* and *C. nivalis*) and a lower representation of woodland species (*A. sylvaticus*).

According to the available data, the rodent species present in the northeastern Iberian Peninsula during the LLP were predominantly mid-European taxa with an ecological preference for cold environmental conditions (*M. arvalis* and *M. agrestis*), humid meadows (*M. agrestis* and *M. (T.) gerbei*) and, to a lesser extent, open forests (*A. sylvaticus* and *E. quercinus*) (Alcalde, 1986; López-García, 2011). Assemblages with such characteristics have been described in Levels C4-C1 of Cova dels Xaragalls (48.2-13.7 ka BP) (López-García et al., 2012a), Level III of Balma de la Griera (21.2 ka BP) (Nadal, 2000) and the oldest levels of Arbreda cave (39.9-17.3 ka BP) (Alcalde, 1986; López-García, 2011). LLP levels from Arbreda cave (39.9-17.32 ka BP) present a clear predominance of rodent species associated with open humid conditions (*M. arvalis*, *M. agrestis* and *M. (T.) duodecimcostatus*), whereas species associated with forest conditions are present in much lower proportions (*A. sylvaticus*, *G. glis* and *E. quercinus*). The association is also characterized by a strong representation of mid-European species (*M. arvalis* and *M. agrestis*), meaning cold conditions and open landscapes (Alcalde & Brunet-Lecomte, 1985; Alcalde, 1986). This great relative abundance of *M. arvalis* and *M. agrestis* is a common trend in other sites in Iberia (López-García, 2011). Additionally, it has been detected in some southern French sequences, accompanied by a high presence of *Microtus gregalis*, as at Tailles-des-Coteaux (Jeannet, 2011; Royer at al., 2014), and is also common in the LLP sites of the Italian Peninsula, such as Grotta della Serratura, Cava Filo, Grotta de la Ferrovia, Grotta Paglicci, Riparo Tagliente and Grotta del Romito (Bertolini et al., 1996; Berto, 2013; López-García et al., 2014a).

However, mention should be made of the Galls Carboners (López-Garcia et al., 2014b) assemblage, which is located somewhat further away from the rest of the LLP levels in our PCA proxy. Associated with Heinrich Event 3, this level is at a distance from the rest of the sites as a result of the high presence of *E. quercinus*, a generalist species that is nonetheless linked with woodland cover, and the scarce representation of *M. arvalis-agrestis* group. This site provides an example of the particularities of small-mammal proxies in the Iberian Peninsula. Firstly, it warns us that there are other species, generally less abundant than *A. sylvaticus*, which should also be taken into account in the definition of open *vs*. closed landscape changes; in other words, that we cannot reduce the northeastern Iberian scenario to the bipolarization between *M. arvalis-agrestis* and *A. sylvaticus*. In this case, *E. quercinus* is the predominant species, indicating the importance of woodland cover, as well as *C. nivalis,* a species that is scarcely present in the northeastern Iberian Peninsula but is extremely indicative of cool periods (nowadays being restricted to the Pyrenean region) (Palomo et al., 2007; Pérez-Aranda, 2009). Secondly, it warns us that, within the cool and open environmental tendency of the LLP, some Iberian sites were exceptions to the global European pattern, showing the importance of a Mediterranean influence, also influenced by their geographical location. This finds expression in the maintenance of woodland cover even in the coldest episodes, such as Heinrich Event 3 or the LGM.

In fact, the Iberian Peninsula enjoyed a milder climate than the rest of Europe and served as a refugium for certain mid-European species (Sommer & Nadachowski, 2006), such as *C. nivalis* or *M. oeconomus.* Marine cores close to the coast of Iberia Peninsula reveal that during the LGM the Iberian Peninsula was characterized by conditions that were slightly more humid than in the rest of Europe (Fletcher & Sánchez-Goñi, 2008; Kageyama et al., 2005; Sánchez-Goñi & D'Errico, 2005). The study of pollen fluctuations has established that the climate was cold and wet during the LGM (Kageyama et al., 2005), while the analysis of lakes has shown a greater degree of humidity than in other areas of Europe during the same interval. The study of small-mammal faunas from Iberia has also suggested a predominance of woodland during this time interval, with small-mammal species indicating an environment with a high level of humidity. This has been shown by small-mammal studies from four Iberian sites dated to the LGM: El Mirón Cave (Ramales de Victoria, Cantabria), Valdavara-1 (Becerreá, Lugo), El Portalón (Sierra de Atapuerca, Burgos) and Sala de las Chimeneas (Maltravieso, Cáceres) (Bañuls-Cardona et al., 2014; Cuenca-Bescós et al., 2009; López-García et al., 2011; 2012b). In general, these sites show a combination of species associated with mid-European requirements (*M. arvalis, M. agrestis, M. oeconomus* and *C. nivalis*) and species associated with Mediterranean climatic conditions (*I. cabrerae* and *M. (T.) duodecimcostatus*). As regards the landscape, there is a high presence of species associated with open woodland areas and wet environments. In short, it is suggested that the climate was harsher than nowadays during the LLP, though not as rigorous as elsewhere in Europe, with mean annual temperatures lower than at present and an environment dominated by wet open meadows (with species associated with humidity: *A. terrestris* and *M. agrestis*). However, it is also considered a more humid period than in the rest of Europe with higher precipitation levels than nowadays.

4.3 Pleistocene – Holocene transition (<14.7 ka BP)

This glacial maximum phase is followed by the Late Glacial (corresponding to the beginning of MIS 1),

which precedes the Holocene and ranges chronologically from ca. 14.7 to 11.7 ka BP (Bradley & England, 2007; Lisiecki & Raymo, 2005; Walker et al., 2009). The Younger Dryas–Holocene transition is dated to ca. 10-11 ka BP, and is characterized by a sharp increase in temperatures and precipitation, constituting a definitive break from Pleistocene climatic dynamics and leading to the climatic improvement related to the Holocene, an overall stable period from the thermal point of view (Bradley & England, 2007; Walker et al., 2009). Many studies demonstrate a clear change in the landscape composition of the Iberian Peninsula during this period, which culminated in the current composition of the flora and fauna. In the Iberian Peninsula a variety of pollen and anthracological sequences reveal this sudden rupture, with the majority agreeing that there was a change in landscape composition marked in most places by the substitution of certain taxa by others (Carrión et al., 2010; Fernández et al., 2007; Gil García et al., 2002). There is clear increase in thermophilous plant species indicative of a warm climate and in species associated with vegetation cover, with a greater expansion of forests to the detriment of open spaces (Burjachs & Renault-Miskovsky, 1992; Carrión et al., 2010).

This change is also manifest in the small-vertebrate associations from the northeast of the Iberian Peninsula. The general pattern observed throughout rodent communities is a sharp increase in taxa with warmer requirements or a Mediterranean character (*M. (T.) duodecimcostatus* and *I. cabrerae*) and others linked to forest habitats (*A. sylvaticus* and *E. quercinus*), together with a decrease in mid-European species with cold requirements and open habitat preferences (*M. arvalis, M. agrestis* and *C. nivalis*). This transition is detected in several localities, such as Toll Cave (35-13 ka BP), Balma de la Griera (21.25 ±0.35 ka BP), Cova Colomera (13-3ka BP), Cingle Vermell (9.76 ±0.16 ka BP) and Cova de la Guineu (9.8 ±0.8 ka BP) (Alcalde, 1986; Alcalde & Brunet-Lecomte, 1985; Fernández-García & López-García, 2013; López-García, 2011; López-García et al., 2010a). The greater or lesser descent in mid-European species depends on the particular characteristics of the sites in question (latitude, altitude, proximity to coast); sites of mid-European influence and at high altitude will preserve adequate conditions for the preservation of some of these specimens, as at Cova Colomera (López-García et al., 2010a).

The Pleistocene-Holocene faunal transition can also be detected in other small-mammal associations from Iberia. There is a break in the faunal assemblage at the cave of El Mirador in Burgos (López-García et al., 2008), where this transition is marked by the disappearance of micromammal species such as *C. nivalis* and *M. oeconomus*, taxa with mid-European requirements and nowadays only found at higher altitudes. It is also in evidence at El Mirón in Cantabria (Cuenca-Bescós et al., 2009). This transition is also present in other southern European localities; a turning point is detected in faunal assemblages from this period in southern Italy. There, the general trend is the replacement of *M. arvalis* and *M. agrestis* by a strictly Mediterranean species, *M. (T.) savii.* This phenomenon is observed in Grotta de la Serratura, Riparo Salvini, Grotta Paglicci, Caballo Cave and Grotta delle Mura (Bertolini et al., 1996; Berto, 2013). However, in Grotta del Romito (Calabria) this substitution is related with the dominance of a glirid species, *Glis glis,* associated with woodland formations (López-García et al., 2014a). However, both species indicate a climatic improvement, with an increase in forest cover.

5. Conclusions

Both descriptive statistical methods and more complex statistical methods bring to light that there are three dominant species during the studied chronology: *Microtus arvalis, Microtus agrestis* and *Apodemus sylvaticus*. *M. arvalis* and *M. agrestis* are species associated with mid-European requirements that were especially dominant at the end of the Late Pleistocene (ca. 40-11.7 ka BP), whereas *A. sylvaticus*, a generalist species but mainly associated with wooded areas and temperate environments, was dominant at the beginning of the Late Pleistocene (ca. 128-30 ka BP) and regained its importance with the arrival of the Holocene (<11.7 ka BP). Accordingly, this bipolarization between *M. arvalis-agrestis* and *A. sylvaticus* could be interpreted as a transition in the ecological conditions at the different sites between open, cooling environments and more forested and temperate ones. Nevertheless, there are other species that seem determinant to evaluate the faunal dynamics of this time interval (*M. (T.) duodecimcostatus, Eliomys quercinus* and *Iberomys cabrerae*). The results also show that the beginning of the Late Pleistocene and the Holocene have similarities in common and differ clearly from the end of the Late Pleistocene, demonstrating the singular nature of the environment associated with the extreme environmental conditions of MIS 2 and the Late Glacial Maximum in the northeast of the Iberian Peninsula. Other palaeoenvironmental proxies and small-mammal studies from Iberia and southern Europe confirm the singular nature of the latest Late Pleistocene and the general increase in woodland cover with the arrival of the Holocene period.

References

Alcalde, G., 1986. Les faunes de rongeurs du Pléistocène supérieur et de l'Holocène de Catalogne (Espagne) et leurs significations paléoécologiques et paléoclimatiques. École pratique des Hautes études-Sciences de la Vie et de la Terre IIIème section, Paris, 114p. Doctoral thesis (inedit).

Alcalde, G., Brunet-Lecomte, P., 1985. Contribució al coneixement del medi i el clima durant el Pleistocè superior i l'Holocè a Catalunya, amb l'aplicació de l'ànalisis factorial de correspondencies a les associacions de rosegadors. Paleontologia i Evolució 19, 49-55.

Alcalde, G., Galobart, A., 2002. Els petits mamífers del Plistocè superior. In: Maroto, J., Ramió, S., Galobart, A. (Eds.), Els vertebrats fossils del Pla de l'Estany. Quaderns. Centre d'Estudis Comarcals de Banyoles 23, 141-154.

Arribas, O., 2004. Fauna y paisaje de los Pirineos en la Era Glaciar. Lynx, Barcelona, 540p.

Bañuls-Cardona, S., López-García, J.M., Blain, H.-A., Lozano-Fernández, I., Cuenca-Bescós, G., 2014. The end of the Last Glacial Maximum in the Iberian Peninsula characterized by the small-mammal assemblages. Journal of Iberian Geology 40(1), 19-27.

Baxter, M., 2003. Statistics in Archaeology. Arnold Publishers, London, 292p.

Berto, C., 2013. Distribuzione ed evoluzione delle associazioni a piccoli mammiferi nella penisola italiana durante il Pleistocene superiore. Università degli Studi di Ferrara, Ferrara, 157p. Doctoral thesis (inedit).

Bertolini, M., Fedozzi, S., Martini, F., Sala, B., 1996. Late glacial and Holocene climatic oscillations inferred from the variations in the micromammal associations at Grotta della Serratura (Marina di Camerota, Salerno, S Italy). Il Quaternario 9 (2), 561–566.

Bradley, R.S., England, J.H., 2008. The Younger Dryas and the Sea if Ancient Ice. Quaternary Research 70, 1-10.

Burjachs, F., Renault-Miskovsky, J., 1992. Paléonvironnement et paléoclimatologie de la Catalogne durant près de 30,000 ans (du Würmien ancien au début de l'Holòcene) d'après la Palynologie du site de L'Arbreda (Gérone, Catalogne). Quaternaire 3(2), 75-85.

Carrión, J.S., Fernández, S., González-Sampériz, P., Gil-Romera, G., Badal. E., Carrión-Marco, Y., López-Merino, L., López-Sáez, J.A., Fierro, E., Burjachs, F., 2010. Expected trends and surprises in the Lateglacial and Holocene vegetation history of the Iberian Peninsula and Balearic Islands. Review of Palaeobotany and Palynology 162, 458-475.

Chaline, J., 1988. Paleocronòmetres, paleotermòmetres i paleoindicadors dels entorns prehistòrics, els rosegadors irremplaçables. Cota Zero 4, 61-64.

Cuenca-Bescós, G., Straus, L.G., González Morales, M., García Pimineta, J.C., 2009. The reconstruction of past environments through small mammals: From the Mousterian to Bronze Age in El Mirón cave. Journal of Archaeological Science. 36, 947–955.

Fernández, S., Fuentes, N., Carrión, J.S., González-Sampériz, P., Montoya, E., Gil, G., Vega-Toscano, G., Riquelme, J.A., 2007. The Holocene and Upper Pleistocene pollen sequence of Carihuela Cave, Southern Spain. Geobios 40, 75–90.

Fernández-García, M., 2014. Análisis paleoecológico en relación a las ocupaciones humanas del Nivel O del Abric Romaní (Capellades, Barcelona) mediante el estudio de los micromamíferos y sus mecanismos de acumulación. Universitat Rovira i Virgili, Tarragona, 179p. Master Thesis (inedit).

Fernández-García, M., López-García, J.M., 2013. Palaeoecology and biochronology based on the rodent analysis from the Late Pleistocene/Holocene of Toll Cave (Moià, Barcelona). Spanish Journal of Palaeontology 28 (2), 227-238.

Fletcher, W.J., Sánchez-Goñi, M.F., Allen, J.R.M., Cheddadi, R., Combourieu-Nebout, N., Huntley, B., Lawson, I., Londeix, L., Magri, D., Margari, V., Müller, U.C., Naughton, F., Novenko, E., Roucoux, K., Tzedakis, P.C., 2010. Millennian-scale variability during the last glacial in vegetation records from Europe. Quaternary Science Reviews 29, 2839-2864.

Fletcher, W.J., Sánchez-Goñi, M.F., 2008. Orbital and sub-orbital-scale climate impacts on vegetation of the western Mediterranean basin over the last 48.000 yr. Quaternary Research 70, 451-464.

Gil García, M.J., Dorado, M., Valdeolmillos, A., Ruiz-Zapata, M.B., 2002. Late-glacial and Holocene palaeoclimatic record from Sierra de Cebollera (northern Iberian Range, Spain). Quaternary International 93–94, 13–18.

Hammer, Ø., Harper, D.A.T., Ryan, P.D., 2001. PAST: Paleontological statistics software package for education and data analysis. Palaeontologia Electronica 4(1), 1-9.

Harrison, S.P., Sánchez-Goñi, M.F., 2010. Global patterns of vegetation response to millennnial-scale variability and rapid climate change during the last glacial period. Quaternary Science Reviews, 29, 2957-2980.

Jeannet, M., 2011. La grotte du Taillis des Coteaux à Antigny (Vienne). Taphonomie et Paléo-environnement selon les microvertébrés. Bilan scientifique, 304–313.

Jolliffe, I. T., 2002. Principal Component Analysis. Second Edition. Springer Text in Statistics. Springer, New York, 372p.

Kageyama, M., Combourieu Nebout, N., Sepulchre, P., Peyron, O., Krinner, G., Ramstein, G., Cazet, J.-P. (2005) The Last Glacial Maximum and Heinrich Event 1 in terms of climate and vegetation around the Alborán sea: a preliminary model-data comparison. C. R. Geosciences 337, 983-992.

Lisiecki, L.E., Raymo, M.E., 2005. A Pliocene–Pleistocene stack of 57 globally distributed benthic $\delta^{18}O$ records. Paleoceanography 20, PA 1003.

López-García, J.M., 2011. Los micromamíferos del Pleistoceno superior de la Península Ibérica. Evolución de la diversidad taxonómica y cambios paleoambientales y paleoclimáticos. Editorial Académica Española, Saarbrücken, 368p.

López-García, J.M., Cuenca-Bescós, G., Rosell-Ardèvol, J., 2008. Resultados del estudio de microvertebrados del Neolítico de la Cueva del Mirador (Ibeas de Juarros, Sierra de Atapuerca, Burgos). In: Hernández-Pérez, M.S., Soler-Díaz, J.A., López-Padilla, J.A. (Eds.), Actas IV Congreso del Neolítico Peninsular. Museo Arqueológico de Alicante, pp. 338-344.

López-García, J.M., Blain, H.A., Allúe, E., Bañuls, S., Bargalló, A., Martín, P., Morales, J.I., Pedro, M., Rodríguez, A., Solé, A., Oms, F.X., 2010a. First fossil evidence of an "interglacial refugium" in the Pyrenean region. Naturwissenschaften 97, 753-761.

López-García, J.M., Blain, H.A., Cuenca-Bescós, G., Ruiz-Zapata, M.F., Dorado-Valiño, M., Gil-García, M.J., Valdeolmillos, A., Ortega, A.I., Carretero, J.M., Arsuaga, J.L., Bermúdez de Castro, J.M., Carbonell, E., 2010b. Palaeoenvironmental and paleoclimatic reconstruction of the Latest Pleistocene of Portalón site, Sierra de Atapuerca, northwestern Spain. Palaeogeography, Palaeoclimatology, Palaeoecology 292, 453-464.

López-García, J.M., Blain, H.A., Cuenca-Bescós, G., Alonso, C., Alonso, S., Vaquero, M., 2011. Small vertebrates (Amphibia, Squamata, Mammalia) from the late Pleistocene-Holocene of the Valdavara-1 cave. Geobios 44, 253-269.

López-García, J.M., Blain, H.-A., Bennàsar, M., Euba, I., Bañuls, S., Bischoff, J., López-Ortega, E., Saladié, P., Uzquiano, P., Vallverdú, P., 2012a. A multiproxy reconstruction of the palaeoenvironment and paleoclimate of the Late Pleistocene in northeastern Iberia: Cova dels Xaragalls, Vimbodí-Poblet, Paratge Natural de Poblet, Catalonia. Boreas 41, 235-249.

López-García, J.M., Blain, H.-A., Burjachs, F., Ballesteros, A., Allue, E., Cuevas-Ruiz, G. E., Rivals, F., Blasco, R., Morales, J.I., Hidalgo, A. R., Carbonell, E., Serrat, E., Rosell, J., 2012b. A multidisciplinary approach to reconstructing the southwestern European Neanderthals: the contribution of Teixoneres cave (Moià, Barcelona). Quaternary Science Reviews 43, 33-44.

López-García, J.M., Blain, H.-A., Sanz, M., Daura, J., 2012c. A coastal reservoir of terrestrial resources for Neanderthal populations in north-eastern Iberia: palaeoenvironmental data inferred from the small-vertebrate assemblage of Cova del Gegant, Sitges, Barcelona. Journal of Quaternary Science 27(1), 105-113.

López-García, J.M., Berto, C., Colamussi, V., Dalla Valle, C., Lo Vetro, D., Luzi, E., Malavasi, G., Martini, F., Sala, B. 2014a. Palaeoenvironmental and palaeoclimatic reconstruction of the latest Pleistocene-Holocene sequence from Grotta del Romito (Calabria, southern Italy) using the small-mammal assemblages. Palaeogeography, Palaeoclimatology, Palaeoecology 409, 169-179.

López-García, J., Blain, H.A., Bennàsar, M., Alcover, J.A., Bañuls-Cardona, S., Fernández-García, M., Fontanals, M., Martín, P., Morales, J.I., Muñoz, L., Pedro, M., Vergés, J.M., 2014b. Climate and landscape during Heinrich Event 3 in south-western Europe: the small-vertebrate association from Galls Carboners cave (Mont-ral, Tarragona, north-eastern Iberia). Journal of Quaternary Science 29(2), 130-140.

López-García, J., Blain, H.A., Bennàsar, M., Fernández-García, M., 2014c. Environmental and climatic context of Neanderthal occupation in southwestern Europe during MIS3 inferred from the small-vertebrate assemblages. Quaternary International 326-327, 319-328.

López-Roldan, P., Lozares-Colina, C. 2000. Anàlisis multivariable de dades estadístiques. Universitat Autònoma de Barcelona, Bellaterra, 198p.

MacDonald, D., Barrett, P., 2008. Guía de campo de los mamíferos de España y de Europa. Barcelona: Ediciones Omega, 365p.

Nadal, J., 2000. La fauna mamífera al Garraf i els seus voltants a través del registre arqueològic. III Trobada d'estudiosos del Garraf 30, 165-170.

Palomo, L.J., Gisbert, J., Blanco, C., 2007. Atlas y libro rojo de los mamíferos terrestres de España. Dirección General para la Biodiversidad -SECEM-SECEMU, Madrid, 588p.

Pérez-Aranda, D., 2009. Biología, ecología, genética y conservación del topillo nival ("Chionomys nivalis") en Peñalara y en Sierra Nevada. Universidad Complutense de Madrid, Madrid, 382. Doctoral thesis (inedit).

Purroy, F. J., Varela, J.M., 2003. Mamíferos de España. Península, Baleares y Canarias. Lynx, Barcelona, 165p.

Royer, A., Lécuyer, C., Montuire, S., Escarguel, G., Fourel, F., Mann, A., Maureille, B., 2013. Late Pleistocene (MIS 3-4) climate inferred from micromammal communities and $\delta^{18}O$ of rodents from Les Pradelles, France. Quaternary Research 80, 113–124.

Royer, A., Lécuyer, C., Montuire, S., Primault, J., Foruel, F., Jeannet, M., 2014. Summer air temperature, reconstruction from the last glacial stage based on rodents from the site Taillis-des-Coteaux (Vienne), Western France. Quaternary Research 82, 420-429.

Sánchez-Goñi, M. F., D'Errico, F., 2005. La historia de la vegetación y el clima del último ciclo climático (OIS5-OIS1, 140.000-10.000 años BP) en la Península Ibérica y su posible impacto sobre los grupos paleolíticos. Museo de Altamira. Monografías 20, 115-129.

Sánchez-Goñi, M. F., Landais, A., Fletcher, W.J., Naughton, F., Desprat, S., Duprat, J., 2008. Contrasting impacts of Dansgaard-Oeschger event over a western Europe latitudinal transect modulated by orbital parameters. Quaternary Science Reviews 27, 1136-1151.

Sans-Fuentes, M.A., Ventura, J., 2000. Distribution patterns of the small mammals (Insectivora and Rodentia) in a transitional zone between the Eurosiberian and the Mediterranean regions. Journal of Biogeography 27, 755-764.

Shennan, S. 1997. Quantifying Archaeology. Edinburgh University Press, Edinburgh, 433p.

Sommer, R.S., Nadachowski, A., 2006. Glacial refugia of mammals in Europe: evidence from fossil records. Mammal Review 36, 251-265.

Uriate, A., 2003. Historia del clima de la Tierra. Servicio Central de Publicaciones del Gobierno Vasco, Vitoria-Gasteiz, 311p.

Van Dam, J. A., Aziz, H. A., Sierra, M. Á. Á., Hilgen, F. J., van den Hoek Ostende, L. W., Lourens, L. J., Mein, P., van der Meulen, Albert J., Pelaez-Campomanes, P., 2006. Long-period astronomical forcing of mammal turnover. Nature 443(7112), 687-691.

Vermeersch, P.M., 2005. European population changes during the Marine Isotope Stage 2 and 3. Quaternary International 137, 77–85.

Villalta, J.F., 1972. Presencia de la Marmota y otros elementos de la fauna esteparia en el Pleistocena catalán. Acta Geológica Hispánica 7(6), 170-173.

Walker, M., Johnsen, S., Rasmussen, S.O., Popp, T., Steffensen, J.-P., Gibbard, P., Hoek, W., Lowe, J., Andrews, J., Björck, S., Cwynar, Les C., Hughen, K., Kershaw, P., Kromer, B., Litt, T., Lowe, D. J., Nakagawa, T., Newham, R., Schwander, J.,

2009. Formal definition and dating of the GSSP (Global Stratotype Section and Point) for the base of the Holocene using the Greenland NGRIP ice core, and selected auxiliary records. Journal of Quaternary Science 24(1), 3-17.

Chapter 4.
Paleoenvironmental context of Neanderthal occupations in northeastern Iberia: the small-mammal assemblage from Abric Romaní (Capellades, Barcelona, Spain)

ABSTRACT

The Abric Romaní site (Capellades, Barcelona, Spain) constitutes a key site for understanding the latest Neanderthal occupations in Western Europe. Here we present a comprehensive systematic and taphonomic analysis of a small-mammal assemblage from Level O of the Abric Romaní site, with the aim of reconstructing the paleoecological context in which the Neanderthals lived. The assemblage, which probably dates from a stadial episode between Interstadial 15 and Interstadial 14, contains fifteen small mammal species, including species uncommon for the northeast of Iberia, such as Sciurus vulgaris, Nyctalus lasiopterus and Pipistrellus pipistrellus. Taphonomic studies suggest a predatory origin for the assemblage, probably related to Strix aluco, and paleoecological inferences suggest lower temperatures (-3/-4 °C) and higher rainfall (+70/+170 mm) than at present and a landscape dominated by an open forest with watercourses. The new data improve our knowledge of trends associated with Marine Isotope Stage 3 that affected Neanderthal populations in the Iberian Peninsula, showing that the Neanderthals were well adapted to cooler and wetter conditions across Iberia.

1. Introduction

Given the close relationship between hunter-gatherer societies and the prevailing climate and environment, knowledge of the ecological landscapes in the vicinity of occupations is essential to reach a better understanding of evolutionary processes. The changing paleoenvironmental conditions that occurred during the Middle Paleolithic tend to be related with Neanderthal dynamics and their extinction (Baena et al., 2012; D'Errico and Sánchez Goñi, 2003; Leroyer and Leroi-Gourhan, 1983; Mellars, 1998; Sánchez Goñi and D'Errico, 2005; Sepulchre et al., 2007; Zilhão, 2000). Neanderthals inhabited Europe for more than 100,000 years (from Marine Isotope Stages, [MIS] 6/5 to 3/2) and are usually associated with the Mousterian technocomplexes. The end of the Mousterian occurred at ca. 40 ka across Europe. The late survival of Neanderthals in southern Iberia is suggested at sites such as Gorham's Cave (Gibraltar), although this hypothesis has recently been challenged (Finlayson et al., 2006; Higham et al., 2014; Wood et al., 2014). Northern Iberia also contains some late Mousterian sites, such as El Esquilleu, Cova Gran, Abric Romaní and L'Arbreda cave (Martínez-Moreno et al., 2010; Camps and Higham, 2012; Maroto et al., 2012; Vaquero and Carbonell, 2012; Wood et al., 2014). Some authors have connected these relict populations with the favorable environmental conditions associated with peninsulas and the preservation of larger open woodland areas than in the rest of Europe (Burjachs and Julià, 1994; Zilhão, 2000; Finlayson et al., 2006; Finlayson and Carrión, 2007; Fletcher et al., 2010; López-García et al., 2014b).

The Abric Romaní rock-shelter is a key site for understanding the last Neanderthal populations and their relationships with the paleoenvironment of southwestern Europe. In this paper, we analyze the paleoenvironment of Level O, the richest level for both archaeological and paleontological remains, undertaking the first complete analysis of the small-mammal assemblage, and considering the implications of these environmental conditions for Neanderthal occupations. A combination of paleontological approaches, including the taxonomic identification of small-mammal bone remains and their taphonomic characterization, is used to identify the origin of the assemblage and post-depositional processes. The analysis also takes into account other paleoenvironmental

proxies for the Middle Paleolithic Abric Romaní sequence (from B to O; ca. 70-30 ka) and the paleoenvironmental context of the Iberian Peninsula, especially the northeastern part, during MIS 3.

2. Site description

The Abric Romaní archaeological site is a rock-shelter in the Quaternary travertine formation known as "Cinglera del Capelló", located on the west bank of the Anoia River, near the town of Capellades (Barcelona, Spain). Its coordinates are 41° 32' N and 1° 41' E and its altitude is 280 m.a.s.l. (Fig. 4.1A). The deposit was discovered in 1909 by Amador Romaní and the present excavations started in 1983 (Bartrolí et al., 1995; Carbonell et al., 1996, 1994). The exposed section is made up of a minimum thickness of 17 m of well-stratified travertine sediments. At present, sixteen levels have been excavated completely (labeled from A to P), most of them belonging to the Middle Paleolithic, with the exception of the uppermost Level A, which has been attributed to the Protoaurignacian (Carbonell et al., 1996; Giralt and Julià, 1996; Vaquero and Carbonell, 2012; Vaquero et al., 2013) (Fig. 4.1B). The Mousterian lithics, the faunal remains derived from butchering activities and the combustion structures preserved in the succession of layers indicate that Neanderthals occupied this site at different periods during MIS 4 and MIS 3. Dates obtained by U-series and ^{14}C AMS provide calendar ages from ca. 40 ka (Level A) to ca. 70 ka (from the base sediments) (Bischoff et al., 1988). However, new data from Sharp et al. (2016) have suggested that carbonate tufas extend at least 30 m beneath the current base of the excavation, reaching ~ 110 ka at the base of the core, with a possible human occupation as old as ~ 100 ka. The sequence can be considered a natural sequence punctuated by short periods of human occupation using the rock-shelter as a residential camp-site (Vaquero et al., 2013). The sedimentary rate is estimated to be approximately 0.46 mm/yr (Bischoff et al., 1988; Vaquero et al., 2013). Palynological analyses indicate a succession of five different climatic phases, between the final phase of MIS 4 and the Hengelo Interstadial (Burjachs and Julià, 1994). The pollen analysis is complemented by analyses of charcoals, phytoliths, herpetofauna, small mammals and ungulate tooth wear (Allué et al., 2017; Burjachs et al., 2012; Vaquero et al., 2013). The milder conditions documented at the bottom of the sequence progressed towards the interstadial climate in evidence in the topmost levels through cycles of warmer and colder events.

Archaeological Level O comprises poorly stratified sand and fine gravel with a weathered surface (Fig. 4.1C, 4.1D). These finer-grained deposits lie above a basal succession composed of gravel, blocks and megablocks originating from the fall of travertine rocks from the cliff above the rock-shelter (Vallverdú et al., 2012). The underlying and overlying travertine layers have been U-series dated to 54.24 ±0.42 ka and 54.60 ±0.40 ka, respectively (Bischoff et al., 1988). The excavated surface covers most of the originally occupied surface with an area of 271 m^2, and more than 40,000 archaeological remains have been reported, including lithic artifacts, faunal remains, charcoal, wood negatives and combustion structures have been reported. Malacofauna and small-mammal remains have also been recovered (Vallverdú et al., 2012; Chacón et al., 2013). Previous zooarchaeological and taphonomic analyses suggest that Neanderthals were the principal accumulator of large-mammal carcasses, with a small degree of intervention by carnivores and a humid fossilization microenvironment (Gabucio et al., 2018, 2012). Level O exhibits an elaborate technology based on the use of the Levallois flaking method, showing a marked technological

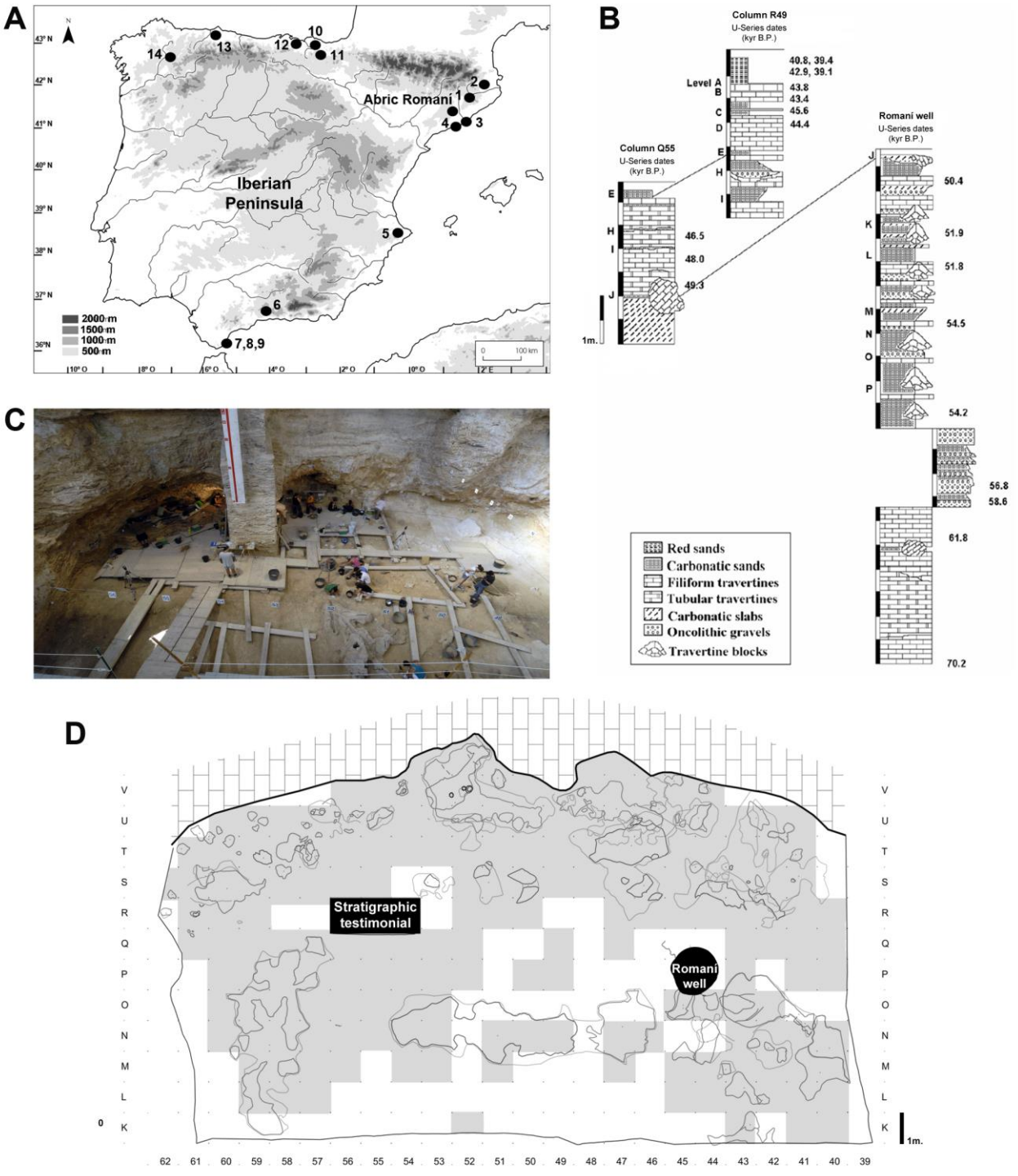

Figure 4.1 (A) Location of the Abric Romaní site in Iberia and the locations of other Middle Paleolithic sites: 1, Teixoneres cave; 2, Arbreda cave; 3, Cova del Gegant; 4, Cova del Coll Verdaguer; 5, El Salt; 6, Zafarraya cave; 7, Vanguard cave; 8, Gorham's cave; 9, Ibex cave; 10, Askondo; 11, Lezetxiki II; 12, El Mirón; 13, Cueva del Conde; 14, Cova Eirós (Barroso et al., 2014; Daura et al., 2017; Fagoaga et al., 2017; Finlayson et al., 2016; García-Ibaibarriaga, 2015; López-García, 2011; López-García et al., 2011b, 2011c, 2012b, 2012c, 2014b, 2015; Murelaga et al., 2012; Rey-Rodríguez et al., 2016; Talamo et al., 2016); (B) Stratigraphy of Abric Romaní with U/Th dates (Bischoff et al., 1988); (C) Level O surface in the excavation campaign of 2010; (D) Level O surface. Lines indicate areas with combustion structures; brick pattern corresponds to rock-shelter wall; in gray, areas included in the small-mammal taphonomic sample of this study.

difference with respect to the overlying levels, in which discoid knapping is dominant (Chacón et al., 2013; Bargalló, 2014; Bargalló et al., 2016; Picin and Carbonell, 2016). This technological shift is associated with a different use of the space in the settlement and could be related to a modification in the mobility patterns of the Neanderthals (Chacón et al., 2013; Picin and Carbonell, 2016). The paleoenvironmental conditions of Level O fall within the framework of pollen zone 3 (56.8–49.5 ka) (from Level O to J), characterized by short and abrupt oscillations within warmer and wetter episodes at intervals of about 10 kyr (Burjachs and Julià, 1994; Burjachs et al., 2012; López-García et al., 2014b). Previous works have included preliminary small-mammal analyses of Level O when fieldwork on this level was still in progress (Burjachs et al., 2012; Fernández-García et al., 2016; López-García, 2011, 2008; López-García et al., 2009; López-García and Cuenca-Bescós, 2010; López García, 2007).

3 Materials and methods

3.1 Recovery and taxonomic study of the material

The small mammal remains included in this analysis consist mainly of isolated teeth and disarticulated bones obtained from a random sediment sampling of the 271 m^2 surface of Level O, which take place over the course of eight excavation seasons (2004-2011). The remains were collected by washing and sieving the sediment, with two superimposed meshes of 5 mm and 1 mm, and selected by the subsequent sorting. The taxonomic identification is based on various reference criteria (Bab et al., 2007; Chaline, 1972; Cuenca-Bescós et al., 2014; Gosàlbez, 1987; López-García, 2011; Menu and Popelard, 1987; Nadachowski, 1982; Sevilla, 1988) and on a comparison with the reference collections of the *Institut Català de Paleoecologia Humana i Evolució Social (IPHES)* and the *Università degli Studi di Ferrara (UNIFE)*. Specific identifications are based mainly on the best diagnostic elements: isolated teeth for Murinae, Glirinae and Sciuridae; first lower molars (m1) for Arvicolinae; mandible, maxilla and isolated teeth for Chiroptera and Soricomorpha; and mandible, isolated teeth and postcranial material for Talpidae. The remains were counted (NISP) and grouped using the minimum number of individuals (MNI) method, determined by counting the most highly represented diagnostic element, taking into account laterality, for each species.

3.2 Taphonomic analysis

The taphonomic study is based on the observation and description of the superficial alterations of skeletal elements (Andrews, 1990; Fernández-Jalvo et al., 2016), differentiating between alterations caused by predation (biostratinomic origin) and post-depositional alterations (biostratinomic or fossil diagenetic origin). According to Andrews (1990) and Fernandez-Jalvo and Andrews (1992), taphonomic effects of predation can be detected through the skeletal representation, breakages and, particularly, features of digestion. To determine the skeletal representation and the proportions of elements present, all the elements of the sample are considered (Andrews, 1990; Fernández-Jalvo and Andrews, 1992).

To evaluate the patterns of breakage and digestion, only incisors, molars and femora are included. For each skeletal element, the number of complete elements is compared to the number of fractured elements (Andrews, 1990; Fernández-Jalvo and Andrews, 1992). Nevertheless, the most important indicator in determining a predatory origin is the corrosion marks produced by gastric juices during digestion, which is the only type of alteration that cannot be confused with other agents. Digestion is a directional and progressive process (Fernández-Jalvo et al., 2016, 2014). In the

present analysis, the proportion of fossil bones affected together with the degree of alteration is considered, distinguishing between light, moderate, heavy and extreme digestion (Fernández-Jalvo and Andrews, 1992; Fernández-Jalvo et al., 2016). The obtained results are compared with indices obtained for current reference predation collections developed by Andrews (1990). After the accumulation of the small mammal assemblage, post-depositional taphonomic processes occurred, including effects associated with roots, water abrasion, cementation, combustion, manganese oxide pigmentation and weathering (Fernández-López, 2000). To identify and characterize these alterations, we used the criteria published by Shipman et al. (1984), Andrews and Cook (1985), Andrews (1990), Fernández-Jalvo (1992), Lyman (1994), Bennàsar (2010), Fernández-López (2000) and Cáceres (2002), among others. Our analysis evaluates molars, incisors and femora in terms of the absence/presence of these alterations and, in some cases, their degree and location.

3.3 Paleoenvironmental and paleoclimatic reconstruction

To reconstruct the ecological conditions prevalent during the deposition of Level O, several methodologies are used. Firstly, to assess the homogeneity of the environment, the species evenness and diversity is calculated (Margalef, 1974), using Paleontological Statistics (PAST) software (Hammer et al., 2001). Williams et al. (2002) associated a highly even community with complex and heterogeneous vegetation. The evenness of a community can be represented by Simpson's Diversity Index ($1 - \Sigma((n_i/n)^2)$, where n_i is the number of individuals of taxon *i*). This, allows us to quantify how equal communities are through numerical representation (between 0 and 1). A larger difference in species within communities results in a higher value for the evenness index (Simpson, 1949).

Climatic conditions prevailing during the formation of the assemblage are inferred by quantitative and qualitative methods. The quantitative method involves the chorotypes previously established for small-mammal faunas in Catalonia by López et al. (2006) and Sans-Fuentes and Ventura (2000), assigning each taxon to one chorotype according to its current climatic requirements and geographical distribution. The chorotypes differentiated are as follows: *chorotype 1* includes species with mid-European requirements; *chorotype 2* includes mid-European species tolerant of Mediterranean conditions; *chorotype 3* includes Mediterranean species; *chorotype 4* includes generalist species with a broad distribution (*Eliomys quercinus*, *Apodemus sylvaticus* and *Sciurus vulgaris*) or species with a particular habitat (such as *Arvicola sapidus, Pipistrellus pipistrellus* and *Nyctalus lasiopterus*), which in general provide little climatic information (Table 4.1) (Fernández-García and López-García, 2013).

The qualitative Mutual Ecogeographic Range (MER) method is used for a similar purpose. This method determines in which present geographical regions a given fossil species assemblage would be located through the intersection obtained from the overlap of the current distributions of each species, obtained from Palomo et al. (2007). The current climatic conditions of the intersecting area (Font-Tullot, 2000) are used to infer the past temperatures and precipitation levels, including the mean annual temperature (MAT), the mean temperature of the coldest month (MTC), the mean temperature of the warmest month (MTW), the mean annual precipitation (MAP), the mean precipitation of the winter months (DJF) and the mean precipitation of the summer months (JJA).

	Recount			Chorotypes				Habitat				
Taxon	**NISP (n)**	**MNI (n)**	**MNI (%)**	**C1**	**C2**	**C3**	**C4**	**OD**	**OH**	**WO**	**R**	**WA**
Microtus agrestis	47	25	8.8		x				0.5	0.5		
Microtus arvalis	54	30	10.56	x				0.5		0.5		
Iberomys cabrerae	87	45	15.85			x			0.5	0.5		
M. (Terricola) duodecimcostatus	46	25	8.8			x			0.25	0.5	0.25	
Arvicola sapidus	284	55	19.37				x					1
Apodemus sylvaticus	327	69	24.3				x			1		
Eliomys quercinus	55	8	2.82				x			0.5	0.5	
Sciurus vulgaris	10	2	0.7				x			1		
Rodentia indet.	1195											
Crocidura russula	17	3	1.06			x		0.5		0.5		
Sorex gr. *araneus-coronatus*	3	2	0.7	x					0.5	0.5		
Sorex minutus	1	1	0.35		x				0.5	0.5		
Neomys gr. *fodiens-anomalus*	10	2	0.7	x					0.25			0.75
Talpa europaea	31	7	2.46		x				0.75	0.25		
Soricidae indet.	10	7	2.46									
Pipistrellus pipistrellus	1	1	0.35				x			0.5	0.5	
Nyctalus lasiopterus	6	1	0.35				x			1		
Chiroptera indet.	1	1	0.35									
Indet.	481											
Total	2666	284	100									

Table 4.1 Number of identified specimens (NISP), minimum number of individuals (MNI) and the MNI as a percentage of the total for the small-mammal assemblage of Level O of Abric Romaní.C1, chorotype 1; C2, chorotype 2; C3, chorotype 3; C4, chorotype 4; OD, open dry; OH, open humid; WO, woodland; R, rocky; WA, water.

Careful attention is paid to ensure that the real current distribution of each species corresponds to the potential ecological distribution and has not been strongly affected by other limiting or perturbing parameters (such as human impact or predation). Accordingly, *Iberomys cabrerae* is excluded because its current distribution is conditioned by anthropic factors. The little-known and generally fragmentary distribution of bat species precludes this order of mammals (Palomo et al., 2007). This method has already been applied to assemblages containing extant reptile and amphibian taxa (Blain et al., 2009, 2016) and to Late Pleistocene small-mammal assemblages (López-García, 2011). The results of our analysis were compared to the present climatic conditions for the Capellades region provided by Ninyerola et al. (2003).

Finally, the landscape is reconstructed using the Habitat Weighting Method, employed by Evans et al. (1981) and Andrews (2006). This method is based on the distribution of each taxon in the habitat(s) in which it is currently present on the Iberian Peninsula (Palomo et al., 2007), considering five main habitat types: open dry, open humid, woodland, rocky and water (López-García et al., 2011a). Each species is given a maximum score of 1.00, which is divided among the habitat types according to its habitat preferences (Table 4.1).

4. Results and discussion

4.1 Origin of the small-mammal assemblage

The taphonomic analysis includes 2,268 elements (MNI: 160). The differential anatomical representation (the relative abundance and the proportional elements representation), the high presence of fragmentation, and especially the detection of digestion marks on the analyzed elements indicate that a considerable portion of

the small-mammal accumulation in Level O is associated with predation (Table 4.2; Fig. 4.2). The breakage rates and the proportional skeletal representation are not coherent with the expected pattern for any of the predators considered by Andrews (1990) and are probably related with post-depositional agents, as is common in archaeological contexts. Indeed, only 6% of the molars and 2% of the incisors were found *in situ.* These results reinforce the importance of digestion marks, such as the only diagnostic alteration, over other proxies in the determination of predation (Bennàsar, 2010; Bennàsar et al., 2016; Fernández-Jalvo, 1992; Fernández-Jalvo et al., 2016, 2014; López-García et al., 2014a). At least 40% of the elements exhibit digestion marks, demonstrating the predatory origin of the assemblage: 40% of incisors, 32% of molars and 89% of femora. The predominant digestion marks are light in degree (27%), but a significant presence of moderate (10%) and some heavy digestion marks (2.3%) are also observed.

Digestion is progressive, sequential and dependent on several parameters, such as digestion time, predator age or even the position in the predator's stomach (Andrews, 1990; Duke et al., 1975; Fernández-Jalvo et al., 2016, 2014). The homogeneity observed in the assemblage, considering the progressive proportion of degrees of digestion, is indicative of a single predator and rules out mixtures of different predator types (Bennàsar, 2010).

The percentage of small-mammal incisors, molars and femora showing digestion marks and the degree of alteration point to the presence of a category 3 predator as defined by Andrews (1990), capable of intermediate modification. Candidates include two different nocturnal raptors: the tawny owl (*Strix aluco*) or the Eurasian eagle-owl (*Bubo bubo*) (Andrews, 1990; Fernández-Jalvo and Andrews, 1992). Both are currently present in the Anoia region (Jiménez, 2003) and have been common in Iberia since the Early Pleistocene (Arribas, 2004). It is difficult to differentiate between the accumulations produced by these two avian predators, although there are small differences. In general terms, *S. aluco* tends to produce concentrations with higher rates of breakage, higher percentages of digested elements and a higher number of strongly digested teeth than *B. bubo*, which rarely produces alterations exceeding the moderate degree (Andrews, 1990; Fernández-Jalvo and Andrews, 1992; López-García et al., 2014a). For these reasons, *S. aluco* is considered the probable accumulator of the small-mammal remains from Level O. Additionally, the general range and size of the species in the fossil assemblage are coherent with the modern tawny owl diet (Olsson, 1979; Andrews, 1990; Kowalski, 1995; Palomo et al., 2007).

The tawny owl is a strongly territorial and sedentary raptor that remains year round in the nesting territory, which is restricted in size (8-75 ha). This owl nests in rocky soil, in rock crevices or in tree holes (Mikkola, 1983; Andrews, 1990; Svensson, 2010). The hunting behavior of this predator involves no preferential criteria in selecting taxa, as it is an extremely opportunistic feeder. It adjusts its behavior to the environment and its diet to whatever is available in its particular hunting territory. Usually, its hunting range is restricted to less than 1 km from the nest (Andrews, 1990; König et al., 1999; Mikkola, 1983; Svensson, 2010). Consequently, its prey assemblage is extremely diverse (coherent with the high diversity detected in the studied assemblage) and constitutes a good record of the nearby ecosystem inhabited by this predator. The enlarged sample of the present work provides enough remains to undertake a complete

Recount		
NISP (n)	2268	
MNI (n)	160	
Skeletal representation		
Relative Abundance Index (%)	29.1	
SD of Relative Abundance Index	24.9	
Proportional representation indexes		
Postcranial/Cranial Index	0.69	
Humerus+Femur/Maxilla+Mandible Index	0.03	
Radius+Tibia/Humerus+Femur Index	0.78	
Isolated molars/ Empty Alveolus Index	1.47	
Breakage		
Incisors fracture (%)	67.3	
Molars fracture (%)	41	
Femora fracture (%)	96.5	
Digestion	**(n)**	**(%)**
Total of digested elements	401	39.3
Light degree	277	27
Moderate degree	101	10
Heavy degree	23	2.3
Extreme degree	0	0
Digested incisors	151	40.5
Light degree	115	31
Moderate degree	30	8
Heavy degree	6	1.5
Extreme degree	0	0
Digested molars	191	33
Light degree	119	20.5
Moderate degree	55	9.5
Heavy degree	17	3
Extreme degree	0	0
Digested femora	59	89.4
Light degree	43	65.2
Moderate degree	16	24.2
Heavy degree	0	0
Extreme degree	0	0
Post-depositional agents	**(n)**	**(%)**
Cracking for humidity and temperature changes	332	79.6-25
Desquamation	92	6.9
Manganese oxide pigmentation	625	47.1
Plant Activity	600	45.2
Cementation	175	13.2
Burned	192	14.5
Water abrasion	73	5.5
Weathering	3	0.2

Table 4.2 Synthesis of taphonomic analysis, including number of items (number of identified specimens; minimum number of individuals), alterations caused by predation (skeletal representation, proportional representation indexes, breakage and digestion) and post-depositional alterations. The Relative Abundance Index compare the number of skeletal elements recovered with the expected number of each element multiplied by MNI; the proportion postcranial/cranial ratio relates the number of postcranial elements (humerus, radius, ulna, femur and tibia) to cranial ones (mandible, maxillae and isolated molars). Digestion and post-depositional analysis are performed on incisors, molars and femurs (NISP: 1,327).

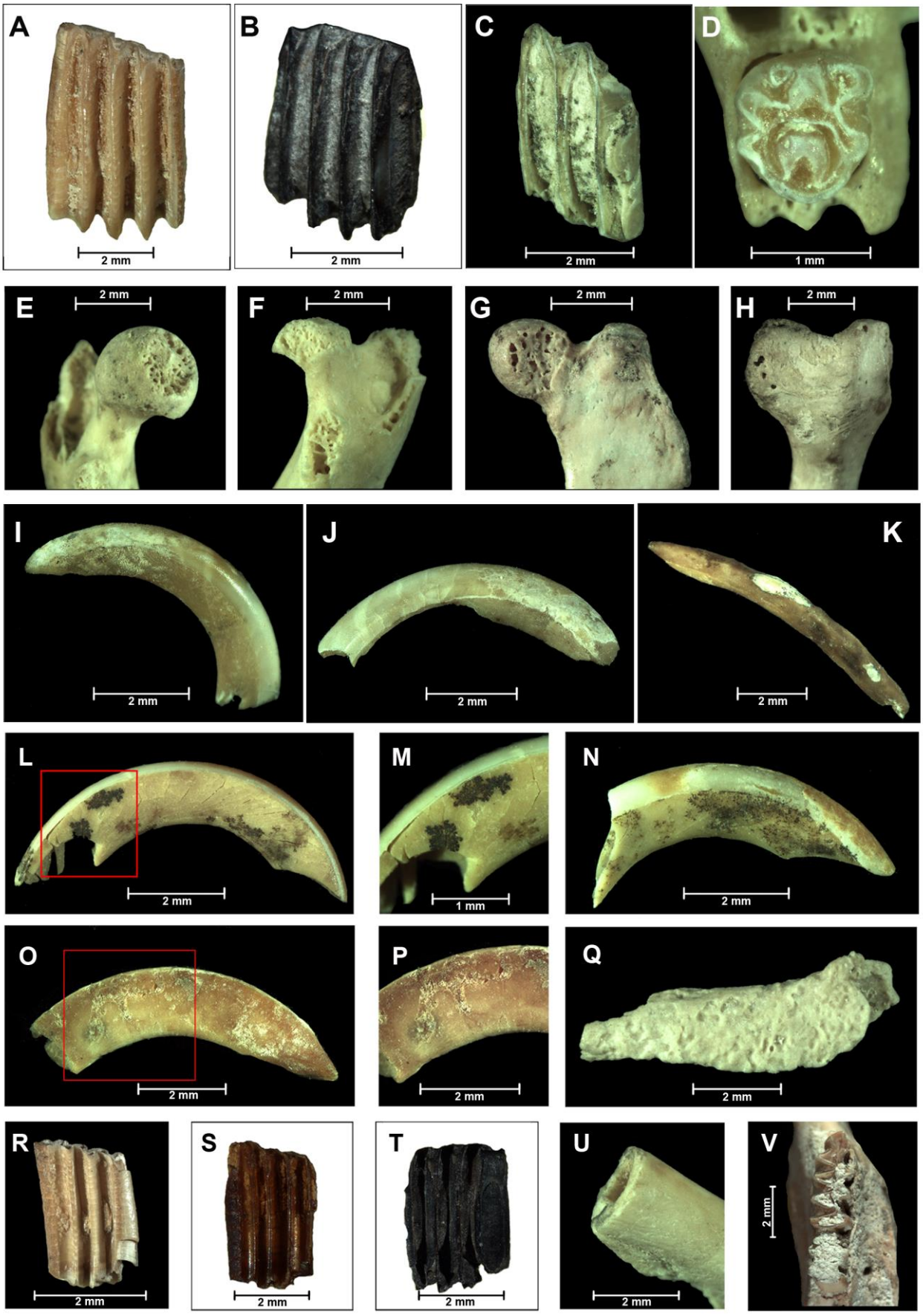

(Figure captation on next page)

Figure 4.2 Taphonomic features associated with the small-mammal remains from Level O. (A) right m1 Arvicola sapidus with light digestion; (B) left m1 Iberomys cabrerae with moderate digestion; (C) upper molar Arvicolinae with heavy digestion; (D) right M2 Apodemus sylvaticus with moderate digestion; (E) proximal epiphysis of a rodent left femur with light digestion; (F) proximal epiphysis of a rodent right femur with moderate digestion; (G) proximal epiphysis of Talpa europaea left femur with light digestion; (H) distal epiphysis of Talpa europaea left femur with light digestion; (I) rodent upper incisor with light digestion; (J) rodent upper incisor with moderate digestion; (K) rodent lower incisor with heavy digestion; (L) rodent upper incisor with dispersed manganese oxide pigmentation; (M) detail of manganese oxide pigmentation; (N) rodent upper incisor with dispersed manganese oxide pigmentation; (O) rodent upper incisor with chemical corrosion associated with roots; (P) detail of chemical corrosion; (Q) rodent left femur with generalized root corrosion; (R) left m1 Arvicola sapidus with cracking due to changes in humidity; (S) left m1 Iberomys cabrerae, burned (Grade 2); (T) Arvicolinae molar, burned (Grade 3); (U) rodent right femur with rounded breaking edge; (V) right mandible Arvicola sapidus with cement concretion.

taphonomic analysis and rule out preliminary attribution to a Category 1 predator (such as *Asio otus* or *Tyto alba*) (López-García et al., 2014b). Even though the tawny owl inflicts major digestion damage on the remains, it is also an eclectic predator and, like *Asio otus* and *Tyto alba*, is not likely to have produce a significant representation bias in the fossil assemblage. Therefore, the fossil assemblage from Level O is assumed to preserve consistent relative species abundances from the past environment of the Abric Romaní region and can be used to develop paleoecological interpretations.

4.2 Post-depositional processes and taphonomic history

After the deposition of pellets by the predator, post-depositional agents will affect the small-mammal remains (Fernández-López, 2000) (Fig. 4.3). The most common effects detected in Level O are related to changes in temperature and humidity (striations, 79.6%; fissures, 68.6%; cracks, 25%), the presence of water (manganese oxide, 47.1%; abrasion, 5.5%), plant activity (chemical corrosion, 45.2%) and the use of fire at the site (burned bones, 14.5%) (Table 4.2). To a lesser degree, cementation is also observed (13.2%). None of the alterations shows a taxonomic or anatomical preference, and the alterations are homogeneously distributed across the surface of the level. All the post-depositional alterations are coherent with a fossiliferous rock-shelter environment (Fernández-Jalvo, 1992) that combines open-environment agents (such as plant activity) with common karst agents characterized by humidity patterns (for instance, manganese oxide precipitation).

Some of the alterations suggest an important presence of water, related to a wet environment (evidenced by chemical corrosion), abrupt humidity changes (evidenced by cementation and fissures) or flooding (evidenced by manganese oxide). Marín-Arroyo et al. (2014) also associated manganese oxide with a high proportion of abandoned organic matter produced by intensive human occupations. According to Gabucio et al. (2012), this site can be described as a humid fossiliferous microenvironment, characterized by wet conditions and the reactivation of water flows and flooding, which is consistent with the underground streams responsible for the formation of the travertine rock-shelter (Vallverdú et al., 2012). The high rates of breakage, previously noted as incoherent with any of the predation patterns defined by Andrews (1990) (Table 4.2), are probably related to changes in the humidity level and possibly trampling and sediment compaction. Chemical corrosion, evidence of plant activity, is probably associated with mosses (Gabucio et al., 2012; 2018; Vallverdú et al., 2012; Vaquero et al., 2013). Even though water was present, no transport is detected, due to the low presence of abrasion modifications (with consistently low degrees of polishing and rounding) (Cáceres, 2002). Nevertheless, differential dynamic transport could be related to the low weight and density of small-mammal

remains (Korth, 1979; Fernández-Jalvo and Andrews, 2003). In any case, all the taphonomic evidence confirms an *in situ* accumulation of remains, ruling out considerable transport dynamics. Therefore, *S. aluco* likely established its roost in one of the fissures of the rock-shelter, leaving the pellets in the substrate (Olsson, 1979; Svensson, 2010). Moreover, the absence of desquamation and weathering rules out long and continuous exposure to meteorological agents (Fernández-Jalvo et al., 2002), coherent with the site conditions and with the inferred rapid burial dynamics (Bischoff et al., 1988; Vaquero et al., 2013; Sharp et al., 2016).

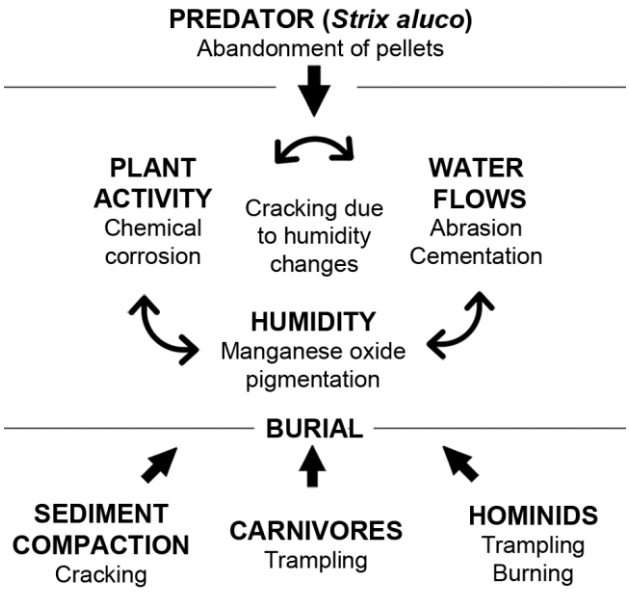

Figure 4.3 Simplified taphonomic sequence to explain the formation of the Level O small mammal assemblage

In comparison with previous zooarchaeological studies (Gabucio et al., 2012; 2018), with the exception of anthropic, carnivore and rodent modifications, all the alterations observed in the large-mammal assemblage are present in the small-mammal assemblage. This confirms the *in situ* nature of the whole deposit. A comparison in spatial terms (Bargalló et al., 2016; Gabucio et al., 2014; 2018) shows homogeneity between small- and large-mammal remains in the spatial distribution of alterations, indicating a unitary taphonomic pattern, with only a few differences probably related to short-distance water transport. In any case, post-depositional alterations have not caused considerable damage to the assemblage as a whole.

4.3 Identified species of small mammals

Level O presents the richest small-mammal assemblage in the whole archaeological sequence (López-García, 2011; Burjachs et al., 2012). From the number of identified specimens (NISP) of 2,666, 990 elements have been identified at the species level, representing 284 individuals (MNI) that belong to 15 different taxa: five insectivores (*Crocidura* cf. *russula, Sorex* gr. *araneus-coronatus, Sorex minutus, Neomys* gr. *fodiens-anomalus* and *Talpa europaea*); two chiropters (*Pipistrellus pipistrellus* and *Nyctalus lasiopterus*) and eight rodents (*Apodemus sylvaticus, Arvicola sapidus, Iberomys cabrerae, Microtus (Terricola) duodecimcostatus*, *Microtus agrestis, Microtus arvalis, Eliomys quercinus* and *Sciurus vulgaris*) (Table 4.1; Fig. 4.4). With respect to preliminary published works (López-García et al., 2014b), the present study has incorporated 2,451 remains, at least 175 individuals, and found four new taxa not previously identified in Level O: *P. pipistrellus, S. vulgaris, N.* gr. *fodiens-anomalus* and *S. minutus.* The latter three are identified for the first time in the Abric Romaní sequence.

The wood mouse (*A. sylvaticus*) is the most abundant taxon in Level O (24%). This species is a generalist but is usually associated with forested environments in a temperate climate without major climatic constraints (Palomo et al., 2007). Consequently, this species is currently highly

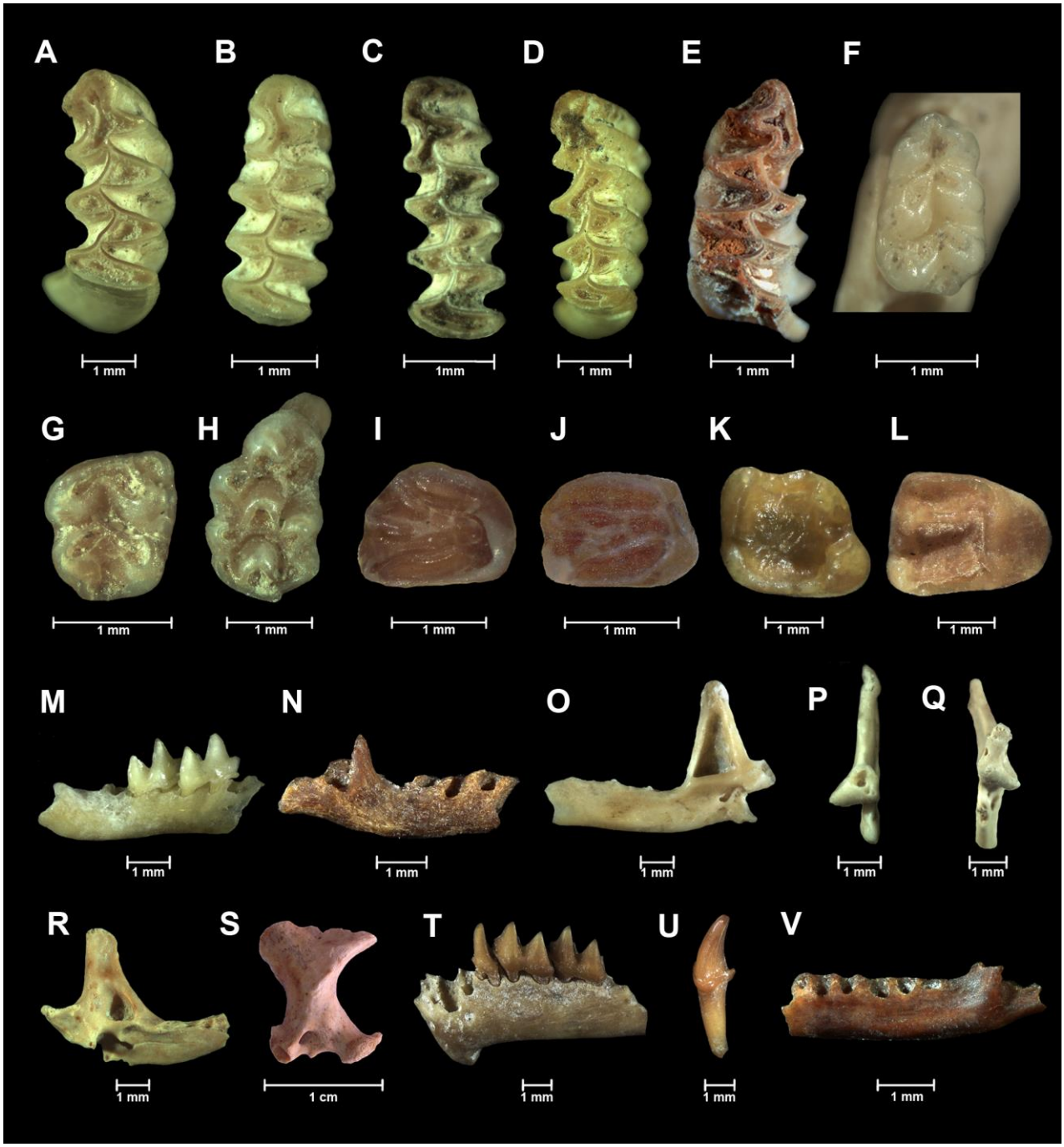

Figure 4.4 Small-mammal species identified in Level O of Abric Romaní. (A) left m1 *Arvicola sapidus* (occlusal view); (B) left m1 *Microtus arvalis* (occlusal view); (C) left m1 *Microtus agrestis* (occlusal view); (D) left m1 *Microtus (Terricola) duodecimcostatus* (occlusal view); (E) right m1 *Iberomys cabrerae* (occlusal view); (F) left m1 *Apodemus sylvaticus* (occlusal view); (G) right m2 *Apodemus sylvaticus* (occlusal view); (H) left M1 *Apodemus sylvaticus* (occlusal view); (I) left m1-m2 *Eliomys quercinus* (occlusal view); (J) right M1-M2 *Eliomys quercinus* (occlusal view); (K) right m1 *Sciurus vulgaris* (occlusal view); (L) right M1 *Sciurus vulgaris* (occlusal view); (M) right mandible *Crocidura russula* (buccal view); (N) right mandible *Sorex minutus* (buccal view); (O) right mandible *Sorex* gr. *araneus-coronatus* (lingual view); (P) right mandible *Sorex* gr. *araneus-coronatus* (posterior view); (Q) left mandible *Neomys* gr. *fodiens-anomalus* (posterior view); (R) left mandible *Neomys* gr. *fodiens-anomalus* (lingual view); (S) left humerus *Talpa europaea;* (T) left mandible *Nyctalus lasiopterus* (buccal view); (U) left Ci *Nyctalus lasiopterus* (buccal view); (V) left mandible *Pipistrellus pipistrellus* (buccal view).

widespread on the Iberian Peninsula, and its occurrence in the Late Pleistocene sites of northeastern Iberia is common (Palomo et al., 2007; Fernández-García et al., 2016). The second most frequent species (19%), the southwestern water vole or *A. sapidus*, is an endemic Gallaic-Iberian species that occurs only in freshwater habitats, without specific climatic restrictions (Louarn and Quéré, 2003; Palomo et al., 2007). Cabrera's vole (*I. cabrerae*; 15%) and the Mediterranean pine vole (*M. (T.) duodecimcostatus*; 8%) are endemic Iberian species with typically Mediterranean requirements. Representing lower proportions of the assemblage, both the common vole (*M. arvalis*; 10%) and the field vole (*M. agrestis*; 8%) are associated with open environments, low humidity and cold temperatures. Currently, they are present in the mountainous regions in the north and the center of the Iberian Peninsula (Palomo et al., 2007; Fernández-García et al., 2016).

All the species from Level O are common in the Late Pleistocene Iberian sites (Sesé, 1994; Cuenca-Bescós et al., 2010; López-García, 2011; Fernández-García et al., 2016), with the exception of the chiropters and the red squirrel (*S. vulgaris*). Level O of Abric Romaní includes one of the most ancient records of *I. cabrerae* in northeastern Iberia (López-García, 2011). *N. lasiopterus* and *P. pipistrellus* are unusual taxa in Late Pleistocene sites. *N. lasiopterus* has been recorded in Cueva del Agua (Sevilla, 1988) and Cova dels Xaragalls (López-García et al., 2012a), being the specimen from Level O the second oldest in Catalonia (López-García, 2011; López-García et al., 2009). *P. pipistrellus* is only recorded in other levels of Abric Romaní, in Cova Colomera (López-García et al., 2010) and in Cueva del Agua (Sevilla, 1988). The occurrence of *S. vulgaris*, as ascertained in Abric Romaní (Fernández-García et al., 2016), is also rare in the Pleistocene of the Iberian Peninsula. Although nowadays it is common in the north, it is strange to find this species in fossil deposits prior to Holocene (López-García, 2011; Sesé, 2011). Its presence in northern Iberia is only recorded in Cova del Coll Verdaguer (Daura et al., 2017) and in old excavations at Cova del Gegant (Estévez, 1980), however it has not been detected in the subsequent revisions of the small-mammal assemblage of Cova del Gegant (López-García et al., 2012c, 2008).

4.4 Paleoenvironmental reconstruction

Level O possesses a high species richness and diversity. Fifteen small-mammal taxa are recorded in the assemblage, and the Simpson's Diversity Index is 0.84, indicating that the species are approximately numerically equal and that no one species dominates the assemblage. From a paleoecological perspective, this may be related to stable environmental conditions and heterogeneous vegetation (woodland) capable of sustaining such diversity (Margalef, 1974); evenness is usually coherent with a high presence of forest species (Williams et al., 2002). Comparison of our results with the species currently present in the site area (Gosàlbez, 1987; Jiménez and Tomás, 2009; Palomo et al., 2007) reveals a slight decrease in the diversity and several faunal replacements, as well as the disappearance of mid-European species such as *M. agrestis* and *M. arvalis*.

The small-mammal chorotype distribution in Level O indicates a preponderance of generalist taxa or taxa without particular climatic requirements (chorotype 4: 49.3%) (Fig. 4.5), as evidenced by the high proportion of *A. sylvaticus* and *A. sapidus*. Nevertheless, the similar proportion of Mediterranean (chorotype 3: 26.4%) and mid-European species (chorotype 1 and 2: 24.3%) is remarkable. Concurrently, the Mutual

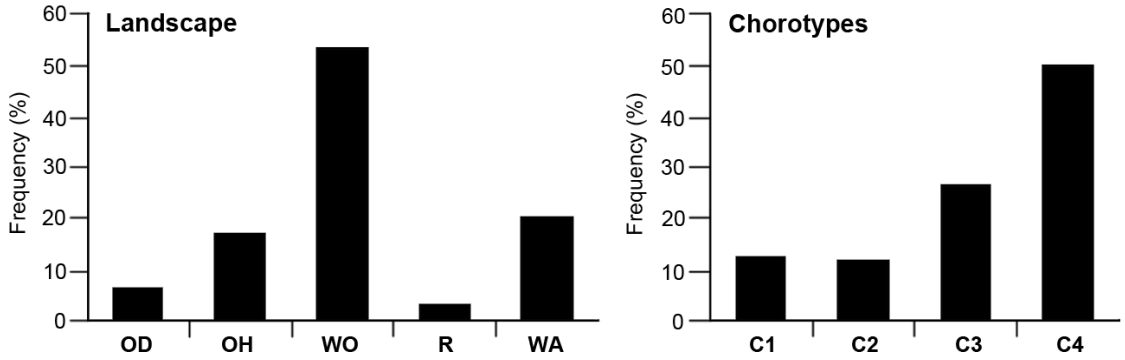

Figure 4.5 Distribution by chorotype and landscape preferences of the small mammals from Level O of Abric Romaní. C1, chorotype 1 (mid-European species); C2, chorotype 2 (mid-European species tolerant of Mediterranean conditions); C3, chorotype 3 (Mediterranean species); C4, chorotype 4 (generalist species or species with a particular habitat, which provide little climatic information); OD, open dry (meadows with seasonal change); OH, open humid (evergreen meadows with dense pastures and suitable topsoils); WO, woodland (mature forest including woodland margins and forest patches, with moderate ground cover); R, rocky (areas with suitable rocky or stony substratum); WA, water (areas along streams, lakes and ponds).

	MAT	MTC	MTW	MAP	DJF	JJA
30TDG38	11	4	19	1000	129	138
30TXN14	11	4	21	1000	204	131
30TVN74	11	3	18	1000	204	131
30TVN85	11	3	18	1000	204	131
30TVN33	12	3	18	700	136	71
30TVN46	12	2	17	700	256	102
30TVN12	12	5	17	700	136	71
Mean	**11.4**	**3.4**	**18.3**	**871**	**181**	**111**
Max	12	5	21	1000	256	138
Min	11	2	17	700	129	71
SD	±0.53	±0.97	±1.38	±160	±48	±29
Current data	**14-15**	**5-6**	**21-22**	**700-800**	**100-120**	**100-120**

Table 4.3 Reconstruction of the temperature and precipitation of Level O of Abric Romaní, using the Mutual Ecogeographic Range based on 10 x10 km UTM squares with equivalent species presence, and modern climatic data of the site. The 10 x 10 km UTM square names (e.g., 30TDG38) are taken from http://www.aitorgaston.com/utm10.php. Mean, average values obtained; Max, maximum values obtained; Min, minimum values obtained; SD, standard deviation; MAT, mean annual temperature; MTC, mean temperature of coldest month; MTW, mean temperature of warmest month; MAP, mean annual precipitation; DJF, mean precipitation of winter months; JJA, mean precipitation of summer months. Temperature data in degrees centigrade (ºC) and precipitation data in millimeters (mm).

Ecogeographic Range (MER), connects this assemblage with seven geographical points (10x10 km UTM) located in the northern Iberian region: five in the Cantabrian area (30TVN12; 30TVN33; 30TVN46; 30TVN74; 30TVN85), one in the Ebro Valley (30TVN14), and one in the Catalan Pre-Pyrenees (30TDG38). The present climatic data for these regions, when compared with current climatic information for Capellades (Ninyerola et al., 2003), show lower temperatures (MAT between -3 and -4 °C; MTC between -2 and -3 °C; MTW between -3 and -4 °C). However, the annual precipitation levels are only slightly higher than at present for Capellades (MAP: between +70 and

+170 mm), and the winter precipitation is also slightly higher (DJF: between +60 and +80 mm) (Table 4.3). Notable differences are detected between this reconstruction and previous paleotemperature estimations for Level O (Burjachs et al., 2012; López-García, 2011; López-García et al., 2014b), such as an increase of +2.5 °C in the MAT and a decrease of -100 mm in the MAP. This is related to new identified species, warning us of the effect that a larger small-mammal sampling can have in drawing paleoenvironmental inferences. For the habitat reconstruction, the Habitat Weighting Method indicated that the area surrounding the site featured an extended open-woodland environment, as confirmed by the presence of forest dwellers (52%) (*A. sylvaticus*, *S. vulgaris* and *N. lasiopterus*) and open-environment taxa (18%) (*M. arvalis, M. agrestis* and *T. europaea*). The existence of stable watercourses close to the rock-shelter is confirmed by water-dependent specimens (20%) (*A. sapidus* and *N.* gr. *fodiens-anomalus*) recovered from Level O (Fig. 4.5). The presence of water is likely related to the Anoia River, which flows at the foot of the site, and to the hydrologic dynamics (i.e., water streams) directly associated with the formation of the site (Vallverdú et al., 2012). The landscape reconstruction undertaken in the present study differs substantially from previous reconstructions (Burjachs et al., 2012; López-García, 2011), underling the importance of forest at the expense of open spaces (wet and dry) and the aquatic component. The ecological behavior of the predator responsible for the small-mammal assemblage, *Strix aluco,* coincides with this habitat. In fact, the tawny owl is considered the most common woodland owl in Europe (Mikkola, 1983; Andrews, 1990); it is usually found in deciduous and mixed forests with forest clearings (Jutglar and Masó, 1999; König et al., 1999; Mikkola, 1983; Svensson, 2010). Presently, it is widely distributed on the Iberian Peninsula. It is considered a Palearctic species, and its distribution in the past was likely similar to its present distribution but reaching more southern latitudes during cold periods (Arribas, 2004).

MIS 3 is characterized by large climatic oscillations within a cool general context. After the cold episodes, large and rapid temperature increases occurred, followed by a progressive cooling (Arrizabalaga, 2004; Harrison and Sanchez Goñi, 2010). The lower temperature estimates (MAT: -4/-3 °C; MTC: -2/-3 °C) and the large differences between winter and summer temperatures (a difference of 15 °C between MTC and MTW), which are features more common for Atlantic areas than for the Mediterranean coast (Fletcher et al., 2010), relate Level O with a cool period. Moreover, the presence of some species that currently inhabit high latitudes (*S.* gr. *araneus-coronatus*, *T. europaea*, *M. arvalis*, *M. agrestis* and *Rana temporaria*) (Burjachs et al., 2012; López-García et al., 2014b; Sans-Fuentes and Ventura, 2000) and the equal proportion of Mediterranean and mid-European taxa are common features in Iberia during cold episodes (Sommer and Nadachowski, 2006). Considering the chronology of Level O (54.24 ±0.42 ka; 54.60 ±0.40 ka) (Bischoff et al., 1988; Vaquero et al., 2013), it could be related with a stadial episode, probably between IS15 (55.8 ±1.2 ka b2k) and IS14 (54.2 ±1.2 ka b2k) (Svensson et al., 2008; López-García et al., 2014b), enclosing previous correlations based on archaeobotanical analysis (Burjachs et al., 2012). The high levels of precipitation and the forested habitat indicate humid conditions for this cool period. The correlation agrees with the palynological and anthracological studies (Burjachs and Julià, 1994; Burjachs et al., 2012), which characterize this phase as generally cool, interrupted by short, hot, wet episodes. Both proxies reflect equivalent landscapes and humid environments for the level, with the arboreal taxa (*Artemisia,* Poaceae and *Pinus*) representing between 62-81% of the total pollen in the palynological studies.

Finally, it is interesting to observe the climatic conditions of Level O whitin the Abric Romaní sequence (Table 4.4.). According to previous small-mammal data from the site (Burjachs et al., 2012; López-García et al., 2014), all the levels present lower temperatures than currently (-2.5 ºC and -4.7 ºC), but not all of them are more humid than at present (between -160 mm and +170 mm). Level O is the most humid level but not the coldest, which is Level E (-3.3 ºC to -4.3 ºC), correlated with Heinrich Event 5 by López-García et al. (2014b). Regarding the landscape, species associated with woodland are always present. This is also confirmed by the pollen and charcoal analyses, which indicate that arboreal coverage was maintained throughout the sequence, with just brief decreases (Burjachs et al., 2012; Vaquero et al., 2013; Allué et al., 2017). Instead of the differential occupational pattern detected for Level O in relation to the upper levels (Gabucio and Bargallo, 2012; Chacón et al., 2013; Picin and Carbonell, 2016), major changes are not detected in the environment by small-mammal analysis. Even so, it has been shown that when the sample size is increased for a particular level, the estimations of the climatic parameters may well differ; accordingly, paleotemperature reconstructions of these levels should be taken with caution, since the MNI is low throughout the sequence (MNI=16-39), with the sole exception of Level O.

4.5 Environmental aspects of the Neanderthal occupations in Iberia during MIS 3

Middle Paleolithic sites with a significant human presence are scarce in Iberia almost until the arrival of MIS 3. This period is related to globally warm conditions characterized by extended forest cover and interrupted by semiarid and cool phases (Burjachs and Julià, 1994; D'Errico and Sánchez Goñi, 2003; Sánchez Goñi and D'Errico, 2005; Sánchez Goñi et al., 2008; Fletcher et al., 2010). There are many Middle Paleolithic sites located in the northeast of Iberia during MIS 3. In some cases, complete climatic reconstructions have been based on small mammals, such as level III (45,870-44,840 cal yr B.P.) and II (44,210-33,060 cal yr B.P.) of Teixoneres cave, level IV of Cova del Gegant (60,000 ±3800 cal yr B.P.) and level I of Arbreda cave (45,840-41,410 cal yr B.P.) (López-García, 2011; López-García et al., 2015, 2014b, 2012b, 2012c; Talamo et al., 2016) (Fig. 4.1A; Fig. 4.6). Irrespective of whether they shown a stadial or an interstadial correlation, all these assemblages indicate a cold (6-10 ºC) and humid climate (870-1500 mm precipitation) related to major presence of forest (always greater than 60%). The temperatures are

Level	Chronology (ka BP)	Climatic Event	MAT (ºC)	MAP (mm)
D	49-44.9	Interstadial 12**	-3.3/-4.3	-160/-60
E	49	Heinrich Event 5*	-3.7/-4.7	-48/+48
J	51-49		-3.4/-4.4	-160/-60
N	54.6	Interstadial 16**	-2.5/-3.5	-130/-30
O	54.2	Stadial 17-15	-3/-4	+70/+170

Table 4.4 Mean annual temperature (MAT) and mean annual precipitation (MAP) estimates corrected for Abric Romaní levels with high MNI content (López-García et al., 2014b). Level O data belong to the estimates in this study. (*) López-García et al., 2014b; (**) Burjachs et al., 2012. To allow comparison with previous small-mammal studies (López-García, 2011; López-García et al., 2014b), some corrections are applied to the temperature and precipitation estimates related to the climatic source (this work uses Ninyerola et al. (2003) rather than Font-Tullot (2000) employed in previous works).

lower than at present (between -9.1 and -5.3 °C) and the precipitation levels are higher (between +692 and +349 mm). Level O fits within this general climatic context.

This is in accordance with the climatic pattern that López-García et al. (2014b) associated with Neanderthals in northeastern Iberia during MIS 3, based on lower temperatures and higher precipitations than at present and a major presence of an open woodland habitat. In all these Middle Paleolithic sites, temperatures oscillated but the precipitation levels and woodland estimates were always high. This is evidenced by assemblages with oscillations in the balance of Mediterranean and mid-European taxa but the continuous presence of woodland dwellers. This scheme seems to become a little more complex when other MIS 3 archaeological sites with small-vertebrate studies from throughout Iberia are considered. The considerable environmental differences among the different regions of the Iberian Peninsula, with a mix of Atlantic, Mediterranean and continental influences, have to be taken into account. Some archaeological sites exhibit diverse dynamics, such as El Mirón cave, Zafarraya and Ibex cave (Barroso et al., 2014; Finlayson et al., 2016), but the overall trend seems to fit well with the northeastern pattern of lower temperatures than at present and the major presence of the forest biotope integrated within mosaic environments with high levels of humidity. This pattern is recorded at Lezetxiki II, Askondo, Cueva del Conde, Vanguard cave and Gorham's cave (López-García et al., 2011b, 2011c; Murelaga et al., 2012; Blain et al., 2013; Garcia-Ibaibarriaga, 2015; Finlayson et al., 2016). Similar environmental characteristics are also in evidence in level 3 of Cova Eirós (Rey-Rodríguez et al., 2016), subunit Xb of El Salt (Fagoaga et al., 2018) and Cova del Coll Verdaguer (Daura et al., 2017), three sites with

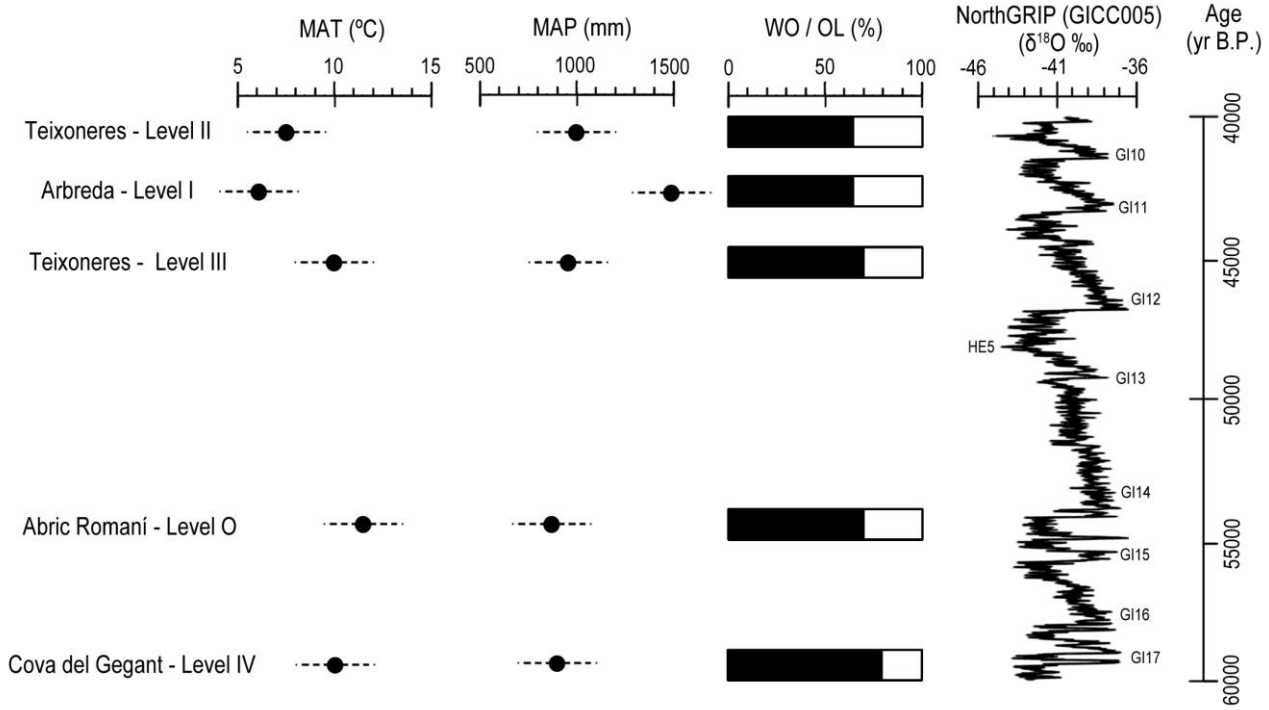

Figure 4.6 Mean annual temperature (MAT) and mean annual precipitation (MAP) estimates and woodland (WO) vs. open landscape (OL) proportions from five northeastern Iberian sites, provided by previous small vertebrate studies (López-García, 2011; López-García et al., 2015, 2014b, 2012b, 2012c; Talamo et al., 2016). The assemblages are correlated with the NorthGRIP δ18O curve, published by Svensson et al. (2008).

chronologies close to Level O but geographically and climatically different.

This general situation is coherent with palynological studies that have suggested that southern Europe (below 40°N) never experienced a complete loss of woodland, even in stadials or Heinrich Events (Fletcher et al., 2010; Harrison and Sanchez Goñi, 2010), making Iberia an optimal region for human occupation. The maintenance of woodland cover or at least mosaic landscapes preserves the ecological quality of the surrounding area. Indeed, the Neanderthal occupations at Abric Romaní are probably more closely related to the conditions of ecological and faunal diversity that an open woodland landscape allows, than to any specific climatic condition. Also, it is well-known that fuel wood for fire production played an important role in Neanderthal settlements, as occurs in Abric Romaní (Vallverdú et al., 2012; Allué et al., 2017). Bearing in mind other Iberian Middle Paleolithic sites, our results suggest that the climate instability of MIS 3 within the cool global context had no real impact on the Neanderthal populations that occupied the northeastern part of the Iberian Peninsula at the time, remaining unclear what effects this instability could have exerted on their shifts in adaptive behavior that are evidenced in the Abric Romaní sequence. In environmental terms and in accordance with previous studies of the Late Pleistocene in the northeastern Iberia, a general preference for woodland landscapes is confirmed, probably in relation with Neanderthal habits of adaptation.

5. Conclusions

Level O represents the richest level in small-mammal remains from the Abric Romaní rock-shelter, a fundamental archaeological site for the understanding of the last Neanderthals occupations in Iberia. A detailed study of this assemblage reveals that:

- The origin of the assemblage is related to the activity of the tawny owl (*Strix aluco*), and post-depositional alterations indicate a fossiliferous microenvironment of relative environmental humidity and occasional water flows. Both taphonomic analyses confirm the reliability of the assemblage for paleoecological reconstructions.
- During the deposition of this level, the region of Capellades was colder (MAT: -3/-4 °C) and slightly wetter (MAP: +70/+170 mm; DJF: +60/+80 mm) than at present and featured semi-open woodland with a watercourse in the vicinity of the site. Futher, the equal proportion of Mediterranean and mid-European species and the chronology of the level suggest a correlation with a cool climatic phase, probably between interstadials IS15 and IS14.
- Considering the Abric Romaní sequence and other Iberian MIS3 sites, it is suggested that these hominid groups were well adapted to the instability of this period. It is not clear what direct impact the climate had on their adaptive shifts on a local scale, as occurred in Abric Romaní. However, a general preference for occupying forest biotopes is detected.

References

Allué, E., Solé, A., Burguet-Coca, A., 2017. Fuel exploitation among Neanderthals based on the anthracological record from Abric Romaní (Capellades, NE Spain). Quat. Int. 431, 6–15.

Andrews, P., 2006. Taphonomic effects of faunal impoverishment and faunal mixing. Palaeogeogr. Palaeoclimatol. Palaeoecol. 241, 572–589.

Andrews, P., 1990. Owls, Caves and Fossils. Predation, preservation and accumulation of small mammal bones in caves, with an analysis of the Pleistocene Cave Faunas from Westbury-sub-Mendip, Somerset, UK. The University of Chicago, Chicago.

Andrews, P., Cook, J., 1985. Natural modifications to bones in temperate setting. Man 20, 675–691.

Arribas, Ó., 2004. Fauna y paisaje de los Pirineos en la Era Glaciar. Lynx, Barcelona.

Arrizabalaga, Á., 2004. Paleoclimatología y cronología del Würm reciente: un intento de síntesis. Zephyrus 57, 27–53.

Bab, I., Hajbi-Yonissi, C., Gabet, Y., Müller, R., 2007. Micro-Tomographic Atlas of the Mouse Skeleton. Springer, New York.

Baena, J., Carrión, E., Cuartero, F., Fluck, H., 2012. A chronicle of crisis: the Late Mousterian in north Iberia (Cueva del Esquilleu, Cantabria, Spain). Quat. Int. 247, 199–211.

Bargalló, A., 2014. Technological Analysis of Neanderthal settlement of the level O Abric Romaní (Barcelona, Spain). Universitat Rovira i Virgili. Doctoral thesis (inedit).

Bargalló, A., Gabucio, M.J., Rivals, F., 2016. Puzzling out a palimpsest: Testing an interdisciplinary study in level O of Abric Romaní. Quat. Int. 417, 51–65.

Barroso, C., Caparrós, M., Barsky, D., Moigne, A.-M., Monclova, A., 2014. Cueva del Boquete de Zafarraya : Un yacimiento de neandertales en el sur Iberia, in: Sala Ramos, R. (Ed.), Los Cazadores Recolectores Del Pleistoceno y Del Holoceno En Iberia y El Estrecho de Gibraltar: Estado Actual Del Conocimiento Del Registro Arqueológico. Universidad de Burgos, Burgos, pp. 463–472.

Bartrolí, R., Cebria, A., Muro, I., Riu-Barrera, E., Vaquero, M., 1995. A frec de ciencia. L'Atles d'Amador Romaní i Guerra. Ajuntament de Capellades, Capellades (Barcelona).

Bennàsar, M., 2010. Tafonomía de micromamíferos del Pleistoceno Inferior de la Sierra de Atapuerca (Burgos): Sima del Elefante y Gran Dolina. Universitat Rovira i Virgili (Tarragona). Doctoral thesis (inedit).

Bennàsar, M., Cáceres, I., Cuenca-Bescós, G., 2016. Paleoecological and microenvironmental aspects of the first European hominids inferred from the taphonomy of small mammals (Sima del Elefante, Sierra de Atapuerca, Spain). Comptes rendus Palevol 15, 635–646.

Bischoff, J.L., Julia, R., Mora, R., 1988. Uranium-series dating of the Mousterian occupation at Abric Romani, Spain. Nature 332, 68–70.

Blain, H.-A., Bailon, S., Cuenca-Bescós, G., Arsuaga, J.L., Bermúdez de Castro, J.M., Carbonell, E., 2009. Long-term climate record inferred from early-middle Pleistocene amphibian and squamate reptile assemblages at the Gran Dolina Cave, Atapuerca, Spain. J. Hum. Evol. 56, 55–65.

Blain, H.-A., Gleed-Owen, C.P., López-García, J.M., Carrión, J.S., Jennings, R., Finlayson, G., Finlayson, C., Giles-Pacheco, F., 2013. Climatic conditions for the last Neanderthals: Herpetofaunal record of Gorham's Cave, Gibraltar. J. Hum. Evol. 64, 289–299

Blain, H.A., Lozano-Fernández, I., Agustí, J., Bailon, S., Menéndez Granda, L., Espígares Ortiz, M.P., Ros-Montoya, S., Jiménez Arenas, J.M., Toro-Moyano, I., Martínez-Navarro, B., Sala, R., 2016. Refining upon the climatic background of the Early Pleistocene hominid settlement in western Europe: Barranco León and Fuente Nueva-3 (Guadix-Baza Basin, SE Spain). Quat. Sci. Rev. 144, 132–144.

Burjachs, F., Julià, R., 1994. Abrupt Climatic Changes during the Last Glaciation Based on Pollen Analysis of the Abric Romani, Catalonia, Spain. Quat. Res. 42, 308-315.

Burjachs, F., López-García, J.M., Allué, E., Blain, H.-A., Rivals, F., Bennàsar, M., Expósito, I., 2012. Palaeoecology of Neanderthals during Dansgaard–Oeschger cycles in northeastern Iberia (Abric Romaní): From regional to global scale. Quat. Int. 247, 26–37.

Cáceres, I., 2002. Tafonomía de yacimientos antrópicos en karst. Complejo Galería (Sierra de Atapuerca, Burgos), Vanguard Cave (Gibraltar) y Abric Romaní (Capellades, Barcelona). Univeristat Rovira i Virgili. Doctoral thesis (inedit).

Camps, M., Higham, T., 2012. Chronology of the Middle to Upper Palaeolithic transition at Abric Romaní, Catalunya. J. Hum. Evol. 62, 89–103.

Carbonell, E., Cebrià, A., Allué, E., Cáceres, I., Castro, Z., Díaz, R., Esteban, M., Ollé, A., Pastó, I., Rodríguez, X.P., Rosell, J., Sala, R., Vallverdú, J., Vaquero, M., Vergés, J.M., 1996. Behavioural and organizational complexity in the Middle Palaeolithic from the Abric Romaní, in: Carbonell, E., Vaquero, M. (Eds.), The Last Neandertals, the First Anatomically Modern Humans. Cultural Change and Human Evolution: The Crisis at 40 Ka BP. Universitat de Tarragona, Tarragona, pp. 385–434.

Carbonell, E., Giralt, S., Vaquero, M., 1994. Abric Romani (Capellades, Barcelone, Espagne): une importante séquence anthropisée au Pléistocène supérieur. Bull. la Société Préhistorique Française 91, 47–55.

Chacón, M.G., Bargalló, A., Gómez, B., Picin, A., Vaquero, M., Carbonell, E., 2013. Continuity or discontinuity of neanderthal technological behaviours During MIS 3: level M and level O of the Abric Romani site (Capellades, Spain), in: Pleistocene

Foragers on the Iberian Peninsula: Their Culture and Environment. Festschrift in Honour of Gerd-Christian Weniger for his sixtieth birthday. Wissenschaftliche Schriften des Neanderthal Museums 7, 55–84.

Chaline, J., 1972. Les rongeurs du Pléistocène moyen et supérieur de France. Éditions du Centre National de la Recherche Scientifique, Paris.

Cuenca-Bescós, G., López-García, J.M., Galindo-Pellicena, M.A., García-Perea, R., Gisbert, J., Rofes, J., Ventura, J., 2014. Pleistocene history of Iberomys, an endangered endemic rodent from southwestern Europe. Integr. Zool. 9, 481–497.

Cuenca-Bescós, G., Rofes, J., López-García, J.M., Blain, H.-A., De Marfá, R.J., Galindo-Pellicena, M.A., Bennásar-Serra, M.L., Melero-Rubio, M., Arsuaga, J.L., Bermúdez de Castro, J.M., Carbonell, E., 2010. Biochronology of Spanish Quaternary small vertebrate faunas. Quat. Int. 212, 109–119.

D'Errico, F., Sánchez Goñi, M.F., 2003. Neandertal extinction and the millennial scale climatic variability of OIS 3. Quat. Sci. Rev. 22, 769–788.

Daura, J., Sanz, M., Allué, E., Vaquero, M., López-García, J.M., Sánchez-Marco, A., Domènech, R., Martinell, J., Carrión, J.S., Ortiz, J.E., Torres, T., Arnold, L.J., Benson, A., Hoffmann, D.L., Skinner, A.R., Julià, R., 2017. Palaeoenvironments of the last Neanderthals in SW Europe (MIS 3): Cova del Coll Verdaguer (Barcelona, NE of Iberian Peninsula). Quat. Sci. Rev. 177, 34–56.

Duke, G.E., Jeers, A.A., Loft, G., Evanson, O.A., 1975. Gastric digestion in some systems. Comp. Biochem. Physiol. 50, 649–656.

Estévez, J., 1980. El aprovechamiento de los recursos faunísticos: Aproximación a la economía en el Paleolítico catalán. Cypsela 3, 9–30.

Evans, E.M.N., Van Couvering, J.A.H., Andrews, P., 1981. Palaeoecology of Miocene sites in Western Kenya. J. Hum. Evol. 10, 99–116.

Fagoaga, A., Ruiz-Sánchez, F.J., Laplana, C., Blain, H.-A., Marquina, R., Marin-Monfort, M.D., Galván, B., 2017. Palaeoecological implications of Neanderthal occupation at Unit Xb of El Salt (Alcoi, eastern Spain) during MIS 3 using small mammals proxy. Quat. Int. 1–12.

Fernández-García, M., López-García, J.M., 2013. Palaeoecology and biochronology based on the rodents analysis from the Late Pleistocene/Holocene of Toll Cave (Moià, Barcelona). Spanish J. Palaeontol. 28, 227–238.

Fernández-García, M., López-García, J.M., Lorenzo, C., 2016. Palaeoecological implications of rodents as proxies for the Late Pleistocene–Holocene environmental and climatic changes in northeastern Iberia. Comptes Rendus Palevol 15, 707–719.

Fernández-Jalvo, Y., 1992. Tafonomía de microvertebrados del complejo cárstico de Atapuerca (Burgos). Universidad Complutense de Madrid. Doctoral thesis (inedit).

Fernández-Jalvo, Y., Andrews, P., 2003. Experimental Effects of Water Abrasion on Bone Fragments. J. Taphon. 1, 147–164.

Fernández-Jalvo, Y., Andrews, P., 1992. Small mammal taphonomy of Gran Dolina, Atapuerca (Burgos), Spain. J. Archaeol. Sci. 19, 407–428.

Fernández-Jalvo, Y., Andrews, P., Denys, C., Sesé, C., Stoetzel, E., Marin-Monfort, D., Pesquero, D., 2016. Taphonomy for taxonomists: Implications of predation in small mammal studies. Quat. Sci. Rev. 139, 138–157.

Fernández-Jalvo, Y., Andrews, P., Sevilla, P., Requejo, V., 2014. Digestion versus abrasion features in rodent bones. Lethaia 47, 323–336.

Fernández-Jalvo, Y., Sánchez-Chillón, B., Andrews, P., Fernández-López, S., Alcalá Martínez, L., 2002. Morphological taphonomic transformations of fossil bones in continental environments, and repercussions on their chemical composition. Archaeometry 44, 353–361.

Fernández-López, S., 2000. Temas de tafonomía. Universidad Complutense de Madrid, Madrid.

Finlayson, C., Carrión, J.S., 2007. Rapid ecological turnover and its impact on Neanderthal and other human populations. Trends Ecol. Evol. 22, 213–222.

Finlayson, C., Finlayson, S., Giles, F., Giles, F., Rodriguez, J., 2016. Using birds as indicators of Neanderthal environmental quality: Gibraltar and Zafarraya compared 421, 32–45.

Finlayson, C., Giles Pacheco, F., Rodríguez-Vidal, J., Fa, D.A., María Gutierrez López, J., Santiago Pérez, A., Finlayson, G., Allué, E., Baena, J., Cáceres, I., Carrión, J.S., Fernández-Jalvo, Y., Gleed-Owen, C.P., Jimenez Espejo, F.J., López, P., Antonio López Sáez, J., Antonio Riquelme Cantal, J., Sánchez Marco, A., Giles Guzman, F., Brown, K., Fuentes, N., Valarino, C.A., Villalpando, A., Stringer, C.B., Martinez Ruiz, F., Sakamoto, T., 2006. Late survival of Neanderthals at the southernmost extreme of Europe. Nature 443, 850–853.

Fletcher, W.J., Sánchez Goñi, M.F., Allen, J.R.M., Cheddadi, R., Combourieu-Nebout, N., Huntley, B., Lawson, I., Londeix, L., Magri, D., Margari, V., Müller, U.C., Naughton, F., Novenko, E., Roucoux, K., Tzedakis, P.C., 2010. Millennial-scale variability during the last glacial in vegetation records from Europe. Quat. Sci. Rev. 29, 2839–2864.

Font-Tullot, I., 2000. Climatología de España y Portugal. Universidad de Salamanca, Salamanca.

Gabucio, M.J., Bargallo, A., 2012. Neanderthal subsistence change around 55 kyr. Actas das IV Jornadas Jovens em Investig. Archeol. - JIA 2011 vol. II, 193–200.

Gabucio, M.J., Cáceres, I., Rivals, F., Bargalló, A., Saladié, P., Vallverdú, J., Vaquero, M., Carbonell, E., 2018. Unraveling a Neanderthal palimpsest from a zooarcheological and taphonomic perspective. Archaeol. Anthropol. Sci. 10, 197–222.

Gabucio, M.J., Cáceres, I., Rosell, J., 2012. Evaluating post-depositional processes in level O of the Abric Romaní archaeological site. Neues Jahrb. für Geol. und Paläontologie - Abhandlungen 265, 147–163.

Gabucio, M.J., Cáceres, I., Rosell, J., Saladié, P., Vallverdú, J., 2014. From small bone fragments to Neanderthal activity areas: The case of Level O of the Abric Romaní (Capellades, Barcelona, Spain). Quat. Int. 330, 36–51.

Garcia-Ibaibarriaga, N., 2015. Los microvertebrados en el registro arqueo-paleontológico del País Vasco: Cambios climáticos y evolución paleoambiental durante el Pleistoceno Superior. Universidad del País Vasco. Doctoral thesis (inedit).

Giralt, S., Julià, R., 1996. The sedimentary record of the Middle/Upper Paleolithic transition in the Capellades area (NE Spain), in: Carbonell, E., Vaquero, M. (Eds.), The Last Neanderthals, the First Anatomically Modern Humans: Cultural Change and Human Evolution: The Crisis at 40 Ka BP. Universitat de Tarragona, Tarragona, pp. 356–376.

Gosàlbez, J., 1987. Insectívors i rosegadors de Catalunya. Metodologia d'estudi i catàleg faunístic. Ketres Editora, Barcelona.

Hammer, Ø., Harper, D.A.T., Ryan, P.D., 2001. Paleontological statistics software package for education and data analysis. Palaeontol. Electron. 4, 9–18.

Harrison, S.P., Sanchez Goñi, M.F., 2010. Global patterns of vegetation response to millennial-scale variability and rapid climate change during the last glacial period. Quat. Sci. Rev. 29, 2957–2980.

Higham, T., Douka, K., Wood, R., Ramsey, C.B., Brock, F., Basell, L., Camps, M., Arrizabalaga, A., Baena, J., Barroso-Ruíz, C., Bergman, C., Boitard, C., Boscato, P., Caparrós, M., Conard, N.J., Draily, C., Froment, A., Galván, B., Gambassini, P., Garcia-Moreno, A., Grimaldi, S., Haesaerts, P., Holt, B., Iriarte-Chiapusso, M.-J., Jelinek, A., Jordá Pardo, J.F., Maíllo-Fernández, J.-M., Marom, A., Maroto, J., Menéndez, M., Metz, L., Morin, E., Moroni, A., Negrino, F., Panagopoulou, E., Peresani, M., Pirson, S., de la Rasilla, M., Riel-Salvatore, J., Ronchitelli, A., Santamaria, D., Semal, P., Slimak, L., Soler, J., Soler, N., Villaluenga, A., Pinhasi, R., Jacobi, R., 2014. The timing and spatiotemporal patterning of Neanderthal disappearance. Nature 512, 306–309.

Jiménez, C., 2003. Guía dels ocells de Vilanova del Camí. Ajuntament de Vilanova del Camí, Vilanova del Camí (Barcelona).

Jiménez, C., Tomás, M., 2009. Mamífers de Vilanova del Camí. Ajuntament de Vilanova del Camí, Vilanova del Camí (Barcelona).

Jutglar, F., Masó, A., 1999. Aves de la Península Ibérica. Guía de campo. Planeta, Barcelona.

König, C., Weick, F., Becking, J.H., 1999. Owls. A guide to the owls of the world. Pica press, New Haven.

Korth, W.W., 1979. Taphonomy of microvertebrate fossil assemblages. Ann. Carnegie Museum 48, 235–285.

Kowalski, K., 1995. Taphonomy of bats (Chiroptera). Geobios 18, 251–256.

Leroyer, C., Leroi-Gourhan, A., 1983. Problèmes de chronologie. Le Castelperronien et l'Aurignacien. Bullétin la Société Préhistorique française 80, 41–44.

López-García, J.M., 2011. Los micromamíferos del Pleistoceno superior de la Península Ibérica. Evolución de la diversidad taxonómica y cambios paleoambientales y paleoclimáticos. Ed. Académica Española, Saarbrücken.

López-García, J.M., 2008. Late Pleistocene small mammals from Abric Romaní (Barcelona, Spain). Ann. dell'Università degli Stud. di Ferrara vol.spec., 105–110.

López-García, J.M., Blain, H.-A., Bennàsar, M., Alcover, J.A., Bañuls-Cardona, S., Fernández-García, M., Fontanals, M., Martín, P., Morales, J.I., Muñoz, L., Pedro, M., Vergés, J.M., 2014a. Climate and landscape during Heinrich Event 3 in south-western Europe: The small-vertebrate association from Galls Carboners cave (Mont-ral, Tarragona, north-eastern Iberia). J. Quat. Sci. 29, 130–140.

López-García, J.M., Blain, H.-A., Bennàsar, M., Euba, I., Bañuls, S., Bischoff, J., López-Ortega, E., Saladié, P., Uzquiano, P., Vallverdú, J., 2012a. A multiproxy reconstruction of the palaeoenvironment and palaeoclimate of the Late Pleistocene in northeastern Iberia: Cova dels Xaragalls, Vimbodí-Poblet, Paratge Natural de Poblet, Catalonia. Boreas 41, 235–249.

López-García, J.M., Blain, H.-A., Burjachs, F., Ballesteros, A., Allué, E., Cuevas-Ruiz, G.E., Rivals, F., Blasco, R., Morales, J.I., Hidalgo, A.R., Carbonell, E., Serrat, D., Rosell, J., 2012b. A multidisciplinary approach to reconstructing the chronology and

environment of southwestern European Neanderthals: the contribution of Teixoneres cave (Moià, Barcelona, Spain). Quat. Sci. Rev. 43, 33–44.

López-García, J.M., Blain, H.-A., Cuenca-Bescós, G., Alonso, C., Alonso, S., Vaquero, M., 2011a. Small vertebrates (Amphibia, Squamata, Mammalia) from the late Pleistocene-Holocene of the Valdavara-1 cave (Galicia, northwestern Spain). Geobios 44, 253–269.

López-García, J.M., Blain, H.-A., Cuenca-Bescós, G., Arsuaga, J.L., 2008. Chronological, environmental, and climatic precisions on the Neanderthal site of the Cova del Gegant (Sitges, Barcelona, Spain). J. Hum. Evol. 55, 1151–1155.

López-García, J.M., Blain, H.A., Allué, E., Bañuls, S., Bargalló, A., Martín, P., Morales, J.I., Pedro, M., Rodríguez, A., Solé, A., Oms, F.X., 2010. First fossil evidence of an "interglacial refugium" in the pyrenean region. Naturwissenschaften 97, 753–761.

López-García, J.M., Blain, H.A., Bennàsar, M., Fernández-García, M., 2014b. Environmental and climatic context of neanderthal occupation in southwestern Europe during MIS3 inferred from the small-vertebrate assemblages. Quat. Int. 326–327, 319–328.

López-García, J.M., Blain, H.A., Sanz, M., Daura, J., 2012c. A coastal reservoir of terrestrial resources for neanderthal populations in north-eastern Iberia: Palaeoenvironmental data inferred from the small-vertebrate assemblage of Cova del Gegant, Sitges, Barcelona. J. Quat. Sci. 27, 105–113.

López-García, J.M., Cuenca-Bescós, G., 2010. Évolution climatique durant le Pléistocène Supérieur en Catalogne (nord-est de l'Espagne) d'après l'étude des micromammifères. Quaternaire 21, 249–258.

López-García, J.M., Cuenca-Bescós, G., Blain, H.-A., Álvarez-Lao, D., Uzquiano, P., Adán, G., Arbizu, M., Arsuaga, J.L., 2011b. Palaeoenvironment and palaeoclimate of the Mousterian–Aurignacian transition in northern Iberia: The small-vertebrate assemblage from Cueva del Conde (Santo Adriano, Asturias). J. Hum. Evol. 61, 108–116.

López-García, J.M., Cuenca-Bescós, G., Finlayson, C., Brown, K., Pacheco, F.G., 2011c. Palaeoenvironmental and palaeoclimatic proxies of the Gorham's cave small mammal sequence, Gibraltar, southern Iberia. Quat. Int. 243, 137–142.

López-García, J.M., Sevilla, P., Cuenca-Bescós, G., 2009. New evidence for the greater noctule bat (Nyctalus lasiopterus) in the Late Pleistocene of western Europe. Comptes Rendus Palevol 8, 551–558.

López-García, J.M., Soler, N., Maroto, J., Soler, J., Alcalde, G., Galobart, A., Bennàsar, M., Burjachs, F., 2015. Palaeoenvironmental and palaeoclimatic reconstruction of the Latest Pleistocene of L'Arbreda Cave (Serinyà, Girona, northeastern Iberia) inferred from the small-mammal (insectivore and rodent) assemblages. Palaeogeogr. Palaeoclimatol. Palaeoecol. 435, 244–253.

López García, J.M., 2007. Primeros datos sobre los microvertebrados del Pleistoceno Superior del Abric Romaní (Capellades, Barcelona), in: Cambra-Moo, O. et al. (Ed.), Cantera Paleontológica. Diputación Provincial de Cuenca, Cuenca, pp. 235–245.

López, M., López-Fuster, M.J., Palazón, S., Ruiz-Olmo, J., Ventura, J., 2006. Els mamífers, in: La Fauna Vertebrada a Les Terres de Lleida. Universitat de Lleida, Lleida, pp. 230–262.

Louarn, H.L., Quéré, J.-P., 2003. Les Rongeurs de France. Faunistique et biologie. Institut National de la Recherche Agronomique, Paris.

Lyman, R.L., 1994. Vertebrate Taphonomy. Cambridge University Press, Cambridge.

Margalef, R., 1974. Ecología. Omega, Barcelona.

Marín-Arroyo, A.B., Landete-Ruiz, M.D., Seva-Román, R., Lewis, M.D., 2014. Manganese coating of the Tabun faunal assemblage: Implications for modern human behaviour in the Levantine Middle Palaeolithic. Quat. Int. 330, 10–18.

Maroto, J., Vaquero, M., Arrizabalaga, Á., Baena, J., Baquedano, E., Jordá, J., Julià, R., Montes, R., Van Der Plicht, J., Rasines, P., Wood, R., 2012. Current issues in late Middle Palaeolithic chronology: New assessments from Northern Iberia. Quat. Int. 247, 15–25.

Martínez-Moreno, J., Mora, R., de la Torre, I., 2010. The Middle-to-Upper Palaeolithic transition in Cova Gran (Catalunya, Spain) and the extinction of Neanderthals in the Iberian Peninsula. J. Hum. Evol. 58, 211–226.

Mellars, P., 1998. The Neanderthal Legacy: an archaeological perspective from Western Europe. Princeton University Press, Princeton (NY).

Menu, H., Popelard, J.B., 1987. Utilisation des caracteres dentaires pour la determination des vespertilionines de l'ouest europeen. Butlletin la Coord. ouest pour l'étude la Prot. des chauves-souris 4, 11–88.

Mikkola, H., 1983. Owls of Europe. Buteo Books, Sussex.

Murelaga, X., Bailón, S., Rofes, J., García-Ibaibarriaga, N., 2012. Estudio arqueozoológico de los macromamíferos del yacimiento de Askondo (Mañaria, Bizkaia), in: Garate, D., Rios-Garaizar, J. (Eds.), La Cueva de Askondo (Mañaria): Arte Parietal y Ocupación Humana Durante La Prehistoria. Kobie. Bizkaiko Arkeologi Indusketak 2, Bilbao, 65–70.

Nadachowski, A., 1982. Late Quaternary rodents of Poland with special reference to morphotype dentition analysis of voles. Polska Academia Nauk, Panstwowe Wydawnictwo Naukowe, Krakow.

Ninyerola, M., Pons, X., Roure, J.M., Martín-Vide, J., Raso-Nadal, J.M., Clavero, P., 2003. Atles Climátics de Catalunya. Generalitat de Catalunya (Departament de Medi Ambient), Barcelona.

Olsson, V., 1979. Studies on a population of Eagle owls in southeast Sweden. Viltrevy 11, 1–99.

Palomo, L.J., Gisbert, J., Blanco, C., 2007. Atlas y libro rojo de los mamíferos terrestres de España. Organismo Autónomo Parques Nacionales, Madrid.

Picin, A., Carbonell, E., 2016. Neanderthal mobility and technological change in the northeastern of the Iberian Peninsula: The patterns of chert exploitation at the Abric Romaní rock-shelter. Comptes Rendus Palevol 15, 581–594.

Rey-Rodríguez, I., López-García, J.-M., Bennàsar, M., Bañuls-Cardona, S., Blain, H.-A., Blanco-Lapaz, Á., Rodríguez-Álvarez, X.-P., de Lombera-Hermida, A., Díaz-Rodríguez, M., Ameijenda-Iglesias, A., Agustí, J., Fábregas-Valcarce, R., 2016. Last Neanderthals and first Anatomically Modern Humans in the NW Iberian Peninsula: Climatic and environmental conditions inferred from the Cova Eirós small-vertebrate assemblage during MIS 3. Quat. Sci. Rev. 151, 185–197.

Sánchez Goñi, M.F., D'Errico, F., 2005. La historia de la vegetación y el clima del último ciclo climático (OIS5-OIS1, 140.000-10.000 años BP) en la Península Ibérica y su posible impacto sobre los grupos paleolíticos. Monogr. - Mus. Altamira 20, 115–129.

Sánchez Goñi, M.F., Landais, A., Fletcher, W.J., Naughton, F., Desprat, S., Duprat, J., 2008. Contrasting impacts of Dansgaard-Oeschger events over a western European latitudinal transect modulated by orbital parameters. Quat. Sci. Rev. 27, 1136–1151.

Sans-Fuentes, M.A., Ventura, J., 2000. Distribution patterns of the small mammals (Insectivora and Rodentia) in a transitional zone between the Eurosiberian and the Mediterranean regions. J. Biogeogr. 27, 755–764.

Sepulchre, P., Ramstein, G., Kageyama, M., Vanhaeren, M., Krinner, G., Sánchez-Goñi, M.F., d'Errico, F., 2007. H4 abrupt event and late Neanderthal presence in Iberia. Earth Planet. Sci. Lett. 258, 283–292.

Sesé, C., 2011. Micromamíferos (Erinaceomorfos y Roedores) del final del Pleistoceno Superior y primera parte del Holoceno de Cova Fosca (Alto Maestrazgo , Castellón): Reconstrucción paleoambiental del entorno del yacimiento 20, 119–137.

Sesé, C., 1994. Paleoclimatical interpretation of the quaternary small mammals of Spain. Geobios 27, 753–767.

Sevilla, P., 1988. Estudio paleontológico de los Quirópteros del Cuaternario español. Paleontol. i Evol. 22, 113–233.

Sharp, W.D., Mertz-Kraus, R., Vallverdu, J., Vaquero, M., Burjachs, F., Carbonell, E., Bischoff, J.L., 2016. Archeological deposits at Abric Romaní extend to 110 ka : U-series dating of a newly cored, 30 meter-thick section. J. Archaeol. Sci. Reports 5, 400–406.

Shipman, P., Foster, G., Schoeninger, M., 1984. Burnt Bones and Teeth: an Experimental-Study of Color, Morphology, Crystal-Structure and Shrinkage. J. Archaeol. Sci. 11, 307–325.

Simpson, E.H., 1949. Measurement of Diversity. Nature 163, 688.

Sommer, R.S., Nadachowski, A., 2006. Glacial refugia of mammals in Europe: Evidence from fossil records. Mamm. Rev. 36, 251–265.

Svensson, A., Andersen, K.K., Bigler, M., Clausen, H.B., Davies, D.D.S.M., Johnsen, S.J., 2008. A 60000 year Greenland stratigraphie ice core chronology. Clim. Past 4, 47–57.

Svensson, L., 2010. Guía de aves. España, Europa y región mediterránea. Omega, Barcelona.

Talamo, S., Blasco, R., Rivals, F., Picin, A., Chacón, M.G., Iriarte, E., López-García, J.M., Blain, H.-A., Arilla, M., Rufà, A., Sánchez-Hernández, C., Andrés, M., Camarós, E., Ballesteros, A., Cebrià, A., Rosell, J., Hublin, J.-J., 2016. The Radiocarbon Approach to Neanderthals in a Carnivore Den Site: a Well-Defined Chronology for Teixoneres Cave (Moià, Barcelona, Spain). Radiocarbon 58, 247–256.

Vallverdú, J., Alonso, S., Bargalló, A., Bartrolí, R., Campeny, G., Carrancho, Á., Expósito, I., Fontanals, M., Gabucio, J., Gómez, B., Prats, J.M., Sañudo, P., Solé, À., Vilalta, J., Carbonell, E., 2012. Combustion structures of archaeological level O and mousterian activity areas with use of fire at the Abric Romaní rockshelter (NE Iberian Peninsula). Quat. Int. 247, 313–324.

Vaquero, M., Allué, E., Bischoff, J.L., Burjachs, F., Vallverdú, J., 2013. Environmental, depositional and cultural changes in the Upper Pleistocene and Early Holocene: The Cinglera del Capelló sequence (Capellades, Spain). Quaternaire 24, 49–64.

Vaquero, M., Carbonell, E., 2012. Some clarifications on the Middle-Upper Paleolithic transition in Abric Romaní: Reply to Camps and Higham (2012). J. Hum. Evol. 63, 711–717.

Williams, S.E., Marsh, H., Winter, J., 2002. Spatial scale, species diversity, and habitat structure: small mammals in Australian tropical rain forest. Ecology 83, 1317–1329.

Wood, R.E., Arrizabalaga, A., Camps, M., Fallon, S., Iriarte-Chiapusso, M.J., Jones, R., Maroto, J., De la Rasilla, M., Santamaría, D., Soler, J., Soler, N., Villaluenga, A., Higham, T.F.G., 2014. The chronology of the earliest Upper Palaeolithic in northern Iberia: New insights from L'Arbreda, Labeko Koba and La Viña. J. Hum. Evol. 69, 91–109.

Zilhão, J., 2000. The Ebro Frontier: A Model for the Late Extinction of Iberian Neanderthals, in: Stringer, C.B., Barton, R.N.E., Finlayson, C. (Eds.), Neanderthals on the Edge: 150th Anniversary Conference of the Forbes' Quarry Discovery, Gibraltar. Oxbow Books, Oxford, pp. 111–121.

Chapter 5.
Unravelling the oxygen isotope signal ($\delta^{18}O$) from rodent teeth in northeastern Iberia, and the implications for past climate reconstructions

ABSTRACT

Small mammals, especially rodents, constitute valuable proxies for continental Quaternary environments at a regional and local scale. Recent studies have demonstrated the relation between the stable oxygen isotope composition of the biogenic phosphate from rodent teeth ($\delta^{18}O_p$) and the oxygen isotope composition of meteoric waters ($\delta^{18}O_{mw}$), which is related to past air temperatures at mid and high latitudes. This work explores the $\delta^{18}O_p$ of rodent tooth enamel (from Murinae and Arvicolinae subfamilies) to investigate the palaeoenvironmental conditions in northeastern Iberia during Marine Isotope Stage 3 (MIS 3; ca. 60-30 ka). Fourteen new $\delta^{18}O_p$ analyses from modern samples in conjunction with forty-six $\delta^{18}O_p$ analyses previously published are used to decipher the isotope record of present-day rodent teeth in this region. This work shows that two main factors should be considered in Iberian palaeoenvironmental reconstructions: the singular nature of Iberian $\delta^{18}O_{mw}$ records and the preferential moment of the year during which the accumulation of small mammals can potentially be produced. Methodological proposals are made with a view to ensuring the correct interpretation of the $\delta^{18}O_p$ of small mammals in reconstructing past air temperatures. This methodology is applied to the MIS 3 sequence of the Cova dels Xaragalls site (Vimbodí-Poblet, Tarragona, Spain), where fifty-one $\delta^{18}O$ analyses were performed on wood mouse (Apodemus sylvaticus) lower incisors. A spring-summer accumulation of small mammals is suggested for the layers at Cova dels Xaragalls. In agreement with previous environmental studies of the site, variations in the $\delta^{18}O_p$ values suggest slight fluctuations in the climatic conditions throughout the sequence, which are related to the MIS 3 stadial-interstadial alternations within a globally stable climatic period cooler than that prevailing nowadays.

1. Introduction

The Iberian Peninsula is characterized by unique environmental conditions. Located at medium latitude, this peninsula with an area of 582,000 km^2 and an average altitude of 660 m constitutes the southwestern extremity of the Eurasian continent, while it is partially isolated from the rest of the continent by the Pyrenean Mountains. Today, Iberia enjoys temperate climatic conditions, which nonetheless vary spatially due to the proximity of the Atlantic Ocean, the Mediterranean Sea and the Pyrenean Mountains. The specific orography of the Iberian Peninsula adds more complexity by structuring the climate and the landscape, with the Central Meseta located at high altitude (660 m), surrounded by several ranges such as the Sierra Nevada and the Cantabrian Mountains. The Galician-Cantabrian and Pyrenean mountain systems shelter the rest of the peninsula from the Atlantic Ocean and the continental cold air masses coming from the northwest and the northeast, respectively.

The Late Pleistocene glacial regime and the subsequent glacial-interglacial fluctuations had an impact both on flora and fauna, including human populations throughout western Europe and the Iberian Peninsula (Uriarte, 2003; Arrizabalaga, 2004). In southern Europe, Marine Isotope Stage 3 (MIS 3; ca. 60-30 ka) was characterized by climate dynamics that alternated between warming and cooling periods in sea-surface temperatures, which on the continent generated phases of forest development and expansion of semi-arid areas, respectively (Fletcher et al., 2010; Harrison and Sanchez Goñi, 2010). However, pollen and small-mammal studies have shown that these alternations are not detected straightforwardly in regional and local contexts, thus suggesting that

Iberia never underwent a complete loss of woodland, even during stadial periods or Heinrich events (Fletcher et al., 2010; López-García et al., 2014). Small-vertebrate assemblages, which reflect local environments, reveal cooler and wetter conditions for the MIS 3. The coexistence of cold and temperate species has been observed to vary with stadial and interstadial fluctuations, although the major presence of woodland-dwelling species has been systematically observed (Fernández-García et al., 2016; López-García et al., 2014). Insofar as it is located at a low latitude, the Iberian Peninsula served as a macro-refugium for many floral and faunal species during stadial periods, sheltering them from rigorous climates until more favourable environmental conditions allowed their geographic radiation (Hewitt, 2000; Sommer and Nadachowski, 2006).

To obtain a complete view of past changes in climate and biodiversity, it is necessary to increase the continental palaeoenvironmental record, which is underrepresented compared to marine and ice-core proxies. Geochemical approaches based on stable oxygen isotope compositions ($\delta^{18}O$) constitute a promising tool for obtaining high-resolution environmental records from regional and local contexts. Isotope compositions measured from bone and tooth fossil remains from mammals can permit the quantification of climatic parameters, due to the interdependence of climatic variables such as air temperatures, the oxygen isotope composition of meteoric waters ($\delta^{18}O_{mw}$) and the oxygen isotope composition of body tissues (Dansgaard, 1964; Kolodny et al., 1983; Longinelli, 1984; Longinelli and Nuti, 1973; Luz et al., 1984; Rozanski et al., 1993). These isotopic data can be combined with palaeoecological data inferred from vertebrate assemblages in order to obtain a coherent and refined picture of continental palaeoenvironments (e.g. Freudenthal et al., 2014; Royer et al., 2013b, 2014). Advances in chemical techniques and analytical methodologies now offer an opportunity to perform geochemical analyses on small-mammal teeth, which are particularly relevant in documenting high-resolution climatic changes at a regional or a local scale (e.g. Barham et al., 2017; Freudenthal et al., 2014; García-Alix, 2015; Grimes et al., 2003; Héran et al., 2010; Jeffrey et al., 2015; Leichliter et al., 2017; Lindars et al., 2001; Navarro et al., 2004).

Nonetheless, interpreting the oxygen isotope composition of small-mammal skeletal apatite is not straightforward, and several questions concerning its application to the fossil record have recently been raised (Jeffrey et al., 2015; Royer et al., 2014, 2013a, 2013b). The question of prey-predator interactions is considered to be of paramount importance in deciphering the isotopic signal recorded in accumulated fossil rodent remains, especially for regions with a specific climatic mode such as the Iberian Peninsula. The main purpose of this work is thus to develop an isotopic framework for environmental and climatic reconstructions for the Iberian Peninsula, based on the oxygen isotope composition of phosphate ($\delta^{18}O_p$) from present-day rodent teeth recovered from pellets. A first step aims to assess the specific role of the climatic context of the Iberian Peninsula, whilst a second one seeks to achieve a better understanding of $\delta^{18}O$ from small-mammal teeth, focusing on the origin of the remains and their period of production. A refinement of the interpretation of the $\delta^{18}O_p$ of fossil rodent tooth phosphate in terms of palaeotemperature reconstructions is finally applied to Cova dels Xaragalls assemblage. This Iberian Late Pleistocene sedimentary sequence, rich in small-vertebrate remains, thus offers the opportunity to reconstruct climate parameters in a continental environment contemporaneous with MIS 3.

2. Cova dels Xaragalls (Tarragona, Spain)

Cova dels Xaragalls is located in Poblet Forest in the municipality of Vimbodí-Poblet (Tarragona), on the right bank of the River Sec at 590 m a.s.l. (Fig. 5.1A). It is a fossiliferous cave of karstic origin composed of Mesozoic limestones. The site can be separated into two main areas: at the entrance there is an Holocene deposit, and at the end of the cave system, in the "Sala Gran" gallery, there is a Pleistocene sequence (Fig. 5.1B). The fossil remains analysed in this work were recovered from the Pleistocene deposit of "Sala Gran" during the excavations started in 2008 (López-García et al., 2012). The sedimentary matrix that contains the small-vertebrate fossils is mainly composed of the mechanical fragmentation of the walls and ceiling and of sediments that entered the cave through fissure openings. Two sedimentary units were defined in the stratigraphic sequence of "Sala Gran". Unit 2, containing layers C8-C5, is composed of gravel and limestone rocks with a clastic support. Unit 1, comprising layers C4-C1, is composed of gravel and blocks with a clastic support, poorly organized and with a structure filled with red sandy clays and fossil remains. Three radiometric datings are available for the site: one charcoal dating from layer C6 by the ^{14}C method recorded an outside range result interpreted as an age older than 43,500 years BP; one charcoal dating from layer C4 by the ^{14}C AMS method gives an age of 45,120-48,240 cal. years BP; and a stalagmite plate from layer C1 dated by the U/Th method yields an age of 13,723 ± 99 years (Vallverdú et al., 2012) (Fig. 5.1C).

Colder and wetter periods compared to present-day conditions have been reconstructed using both small vertebrates and charcoal from the site (López-García et al., 2012). Indeed, the regular presence of woodland-dwelling species, including the notable abundance of the wood mouse (*Apodemus sylvaticus*), throughout the sequence attests that the surrounding landscape was regularly constituted by open-forest formations. Although the wood mouse is a generalist species capable of inhabiting forested to shrubby areas, but also crops, meadows, heaths or boundaries, this species has a clear preference for low-altitude areas with good tree cover, under the influence of a Mediterranean climate, in which it can collect diverse foods (Palomo et al., 2007; Sánchez-González et al., 2016; IUCN, 2018). Layers C8 and C5 correspond to warmer environmental conditions with open dry meadows by contrast with layers C4 and C3, which are more humid and cooler with landscape openings. The origin of the small-vertebrate remains recovered from the whole sequence seems to be related mainly to the activity of a single predator. No major changes in the proportion of digested elements were observed throughout the sequence, this proportion being close to that of a nocturnal bird of prey such as the little owl (*Athene noctua*) (López-García et al., 2012). This sedentary predator is an opportunistic hunter that yields a faithful record of the prey originally present in its ecosystem (Andrews, 1990). Thus, changes in both the small-vertebrate compositions and in the relative abundance of *A. sylvaticus* can be interpreted as real changes in local ecosystem conditions. According to charcoal studies of this sedimentary sequence, the forest was less taxon-diverse than the current Poblet Forest, with a clear predominance of *Pinus*-type *sylvestris*, confirming the harsher conditions during the stage under study. For this sequence, correlations with global climatic fluctuations have been proposed, relating layer C8 to Interstadial 15 or 16 (ca. 56-59 ka), layer C5 to Interstadial 13 or 14 (ca. 50-55 ka) and layers C4-C3 to Heinrich Event 5 (ca. 47 ka) (López-García et al., 2012).

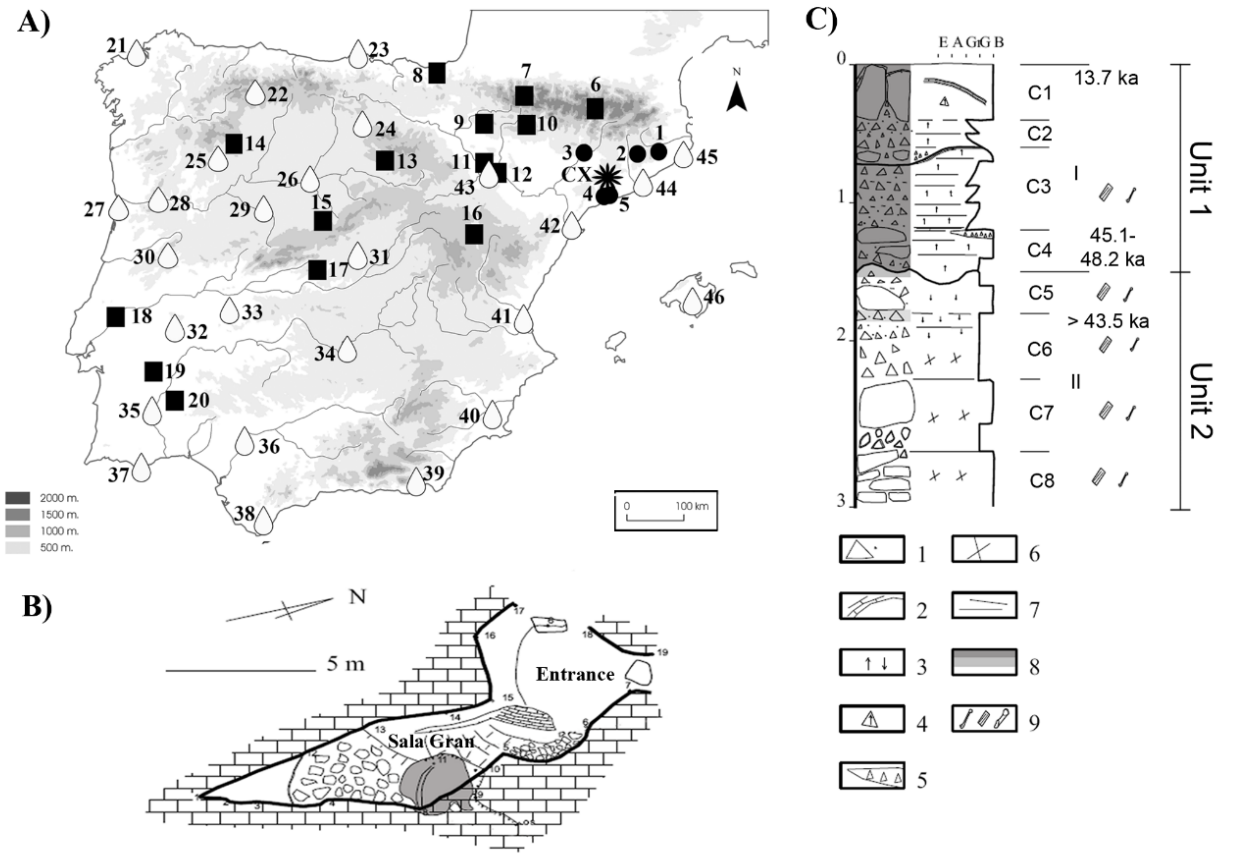

Figure 5.1 A) Map showing the location of Cova dels Xaragalls (CX), Iberian localities where present-day oxygen isotope analyses have been performed (black dots, this work; black squares, Royer et al. (2013a)) and IAEA/WMO stations (light grey drops; IAEA/WMO, 2018); 1, Serinyà; 2, Moià; 3, Balaguer; 4, Prades; 5, El Catllar; 6, Espot; 7, Basarán; 8, Berastegui; 9, Uncastillo; 10, Lárrede; 11, Sobradiel; 12, Zaragoza; 13, Palacios de la Sierra; 14, Cernadilla; 15; Yanguas de Eresma; 16, Caminreal; 17, San Martín de Valdeiglesias; 18, Tomar; 19, Redondeo; 20, Amareleja; 21, La Coruña; 22, León (Virgen del Camino); 23, Santander; 24, Burgos (Villafría); 25, Braganza; 26; Valladolid; 27, Porto; 28, Vila Real; 29, Salamanca (Matacán); 30, Penhas Douras; 31, Madrid (Retiro); 32, Porto Alegre; 33, Cáceres (Trujillo); 34, Cuidad Real; 35, Beja; 36, Sevilla (Morón Base); 37, Faro; 38, Gibraltar; 39, Almería airport; 40, Murcia; 41, Valencia; 42, Tortosa; 43, Zaragoza airport; 44, Barcelona; 45, Girona airport; 46, Palma de Mallorca. B) Topographical map of the Sala Gran of Cova dels Xaragalls; in grey the studied section. C) Stratigraphy of the sampled section in the Sala Gran of Cova dels Xaragalls. 1: angular limestone, gravel and stones; 2: stalagmite; 3: normal and reverse gradation; 4: vertical clasts; 5: channel field with gravel; 6: massive internal stratification; 7: horizontal stratification; 8: filled structure, half-filled and open; 9: bones and charcoals.

3. Material and methods

3.1 Recovery of the small-mammal remains

3.1.1 Modern samples from northeastern Iberia

Fourteen lower incisors from present-day rodents were collected from pellets to analyse their oxygen isotope composition. These pellets were collected from five different sites located in northeastern Iberia (Fig. 5.1A, 2; Table 5.1): Serinyà (Girona), Moià (Barcelona), Prades (Tarragona), Balaguer (Lleida) and El Catllar (Tarragona). The sites are distributed within the same latitudinal range (from parallel 41°N to 42°N) but at different altitudes ranging from 188 m a.s.l. at Serinyà to 1000 m a.s.l. at Moià (Fig. 5.1A; Table 5.1). Northeastern Iberia is mostly assigned to the

Mediterranean climate mode. The region is further divided into several microclimates resulting from local factors, such as continentality or orography. The five selected localities correspond to different climate subtypes (Font-Tullot, 2000; Meteocat, 2018).

The teeth recovered belong to three extant species of the Muroidea superfamily: the wood mouse (*Apodemus sylvaticus*), the Mediterranean pine vole (*Microtus (Terricola) duodecimcostatus*) and the house mouse (*Mus musculus*). The teeth were extracted from owl pellets from nest or roosting sites (Fig. 5.2). However, pellets can be preserved over several months depending on their exposure to weather conditions. The pellets from Moià, Prades and Serinyà were recovered in August-September in fresh or semi-dry states. These pellets were produced by either the barn owl (*Tyto alba*) or the tawny owl (*Strix aluco*). Both are opportunistic hunters, sedentary and highly territorial species, nesting in tree holes, cliffs or buildings that are reused year after year. Their hunting area ranges from 3 to 10 km^2 for *T. alba* and is lower than 3 km^2 for *S. aluco* (Mikkola, 1983; Yalden, 2009; UICN, 2018).

3.1.2 Fossil samples from Cova dels Xaragalls

The rodent remains from Cova dels Xaragalls were collected by water-screening using superimposed 5 and 0.5 mm mesh sieves and then sorted at the Institut Català de Paleoecologia Humana i Evolució Social (Tarragona). The specific attribution of the remains and the taphonomic study were performed by López-García et al. (2012a). Oxygen isotope compositions were measured on 46 teeth from layers C8 to C4. To avoid possible interspecies variability, *A. sylvaticus* fossil incisors were preferentially selected, with 44 incisors representing at least 29 individuals (Fig. 5.2). One tooth from *Microtus arvalis* and one tooth from *Eliomys quercinus* were also included (Table 5.2). Taking into account previous works (Gehler et al., 2012; Lindars et al., 2001; Navarro et al., 2004; Royer et al., 2013a), a minimum number of five to ten samples was selected from each layer in order to gather a representative range of samples.

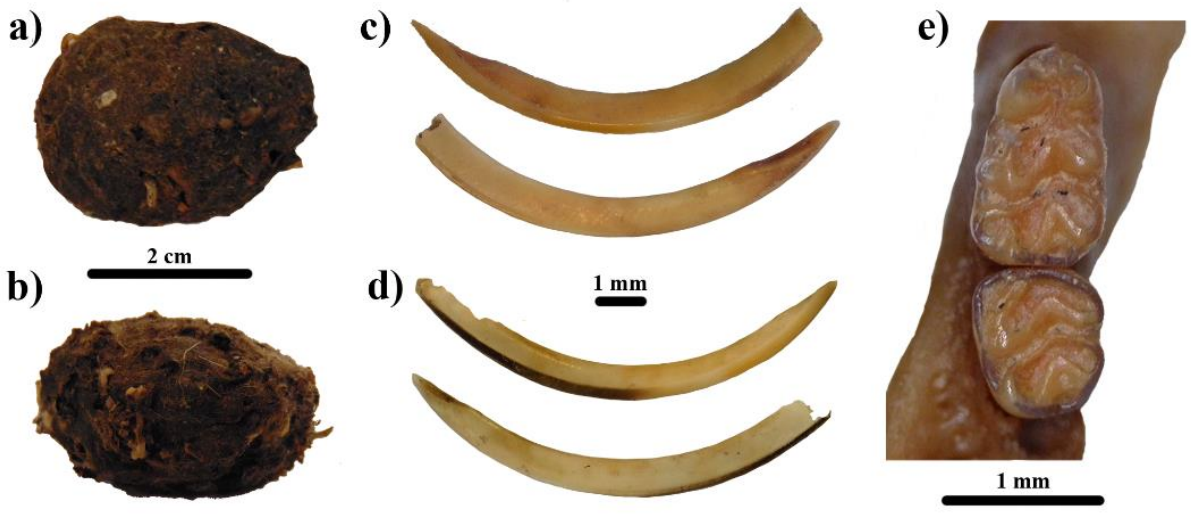

Figure 5.2 a) *Tyto alba* pellet from Serinyà (Girona); b) *Tyto alba* pellet from Moià (Barcelona); c) left lower incisor of *Apodemus sylvaticus* from Cova dels Xaragalls, in labial and lingual view; d) right lower incisor of *Apodemus sylvaticus* from a pellet from Serinyà, in labial and lingual view; e) left mandible with m1 and m2 of *Apodemus sylvaticus* from Cova dels Xaragalls, in occlusal view.

Sample	Location	Coordinates	Altitude (m)	Climatic subtype	MAT (ºC)	MAP (mm)	Predator	Recovering	Taxon	Laterality	$\delta^{18}O_p$ (‰V-SMOW)	S.D.
MA-3	Serinyà	42º 10' 7'' N; 2º 47' 42'' E	188	Northern pre-littoral	14.8	733	*Tyto alba*	August-September	*M. (T.) duodecimcostatus*	left	18.8	0.4
MA-1	Serinyà	42º 10' 7'' N; 2º 47' 42'' E	188	Northern pre-littoral	14.8	733	*Tyto alba*	August-September	*A. sylvaticus*	right	19.0	0.1
MA-2	Serinyà	42º 10' 7'' N; 2º 47' 42'' E	188	Northern pre-littoral	14.8	733	*Tyto alba*	August-September	*A. sylvaticus*	left	19.5	0.3
MA-12	Moià	41º 48' 51'' N; 2º 11' 54'' E	1000	Continetal sub-humit	12.3	749	*Tyto alba*	Unknown	*Microtus (T.) duodecimcostatus*	right	16.1	0.4
MA-4	Moià	41º 48' 51'' N; 2º 11' 54'' E	1000	Continetal sub-humit	12.3	749	*Tyto alba*	End of August	*Microtus (T.) duodecimcostatus*	left	18.6	0.4
MA-6	Moià	41º 48' 51'' N; 2º 11' 54'' E	1000	Continetal sub-humit	12.3	749	*Tyto alba*	End of August	*M. musculus*	right	19.2	0.3
MA-5	Moià	41º 48' 51'' N; 2º 11' 54'' E	1000	Continetal sub-humit	12.3	749	*Tyto alba*	End of August	*M. musculus*	left	19.5	0.3
MA-14	Balaguer	41º 45' 21'' N; 0º 47' 25'' E	200	Continental dry	14.3	501	*Tyto alba*	Unknown	*M. (T.) duodecimcostatus*	right	17.4	0.3
MA-13	Balaguer	41º 45' 21'' N; 0º 47' 25'' E	200	Continental dry	14.3	501	*Tyto alba*	Unknown	*M. (T.) duodecimcostatus*	left	18.9	0.1
MA-9	Prades	41º 18' 35'' N; 0º 59' 19'' E	990	South pre-littoral	12.6	728	*Strix aluco*	September	*A. sylvaticus*	left	18.3	0.4
MA-10	Prades	41º 18' 35'' N; 0º 59' 19'' E	990	South pre-littoral	12.6	728	*Strix aluco*	September	*A. sylvaticus*	left	19.5	0.6
MA-11	Prades	41º 18' 35'' N; 0º 59' 19'' E	990	South pre-littoral	12.6	728	*Strix aluco*	September	*A. sylvaticus*	right	20.2	0.4
MA-7	El Catllar	41º 11' 5" N; 1º 20' 14" E	110	Southern littoral	15.9	562	*Tyto alba*	Unknown	*Mus musculus*	right	18.2	0.2
MA-8	El Catllar	41º 11' 5" N; 1º 20' 14" E	110	Southern littoral	15.9	562	*Tyto alba*	Unknown	*Mus musculus*	left	18.8	0.4

Table 5.1 Oxygen isotope composition of tooth enamel phosphate ($\delta^{18}O_p$; ‰ V-SMOW) from present-day rodent lower incisors. The table includes information about the pellet, the location where it was recovered and identified taxa. The conversion to the oxygen isotope composition of meteoric waters ($\delta^{18}O_{mw}$; ‰ V-SMOW) follows the Royer et al. (2013a) oxygen isotope fractionation equation. SD, Standard Deviation.

Sample	Level	Taxa	Laterality	Location	$\delta^{18}O_p$ (‰ V-SMOW)	SD	$\delta^{18}O_{mw}$ (‰ V-SMOW)
CX45	C4	*Apodemus* cf. *sylvaticus*	right	isolated	**16.6**	0.2	**-6.8**
CX42	C4	*Apodemus* cf. *sylvaticus*	right	isolated	**17.7**	0.5	**-5.8**
CX44	C4	*Apodemus* cf. *sylvaticus*	left	isolated	**17.9**	0.2	**-5.7**
XG4B-5	C4	*Apodemus sylvativus*	right	*in situ*	**17.9**	0.2	**-5.7**
CX46	C4	*Microtus arvalis*	right	*in situ*	**18.2**	0.5	**-5.4**
CX41	C4	*Apodemus* cf. *sylvaticus*	right	isolated	**18.4**	0.4	**-5.3**
XG4-2a	C4	*Apodemus sylvativus*	left	*in situ*	**18.5**	0.5	**-5.2**
XG4-3a	C4	*Apodemus sylvativus*	right	*in situ*	**19.8**	0.3	**-4.1**
XG4B-4	C4	*Apodemus sylvativus*	left	*in situ*	**20.8**	0.3	**-3.2**
CX43	C4	*Apodemus* cf. *sylvaticus*	right	isolated	**21.4**	0.5	**-2.8**
XG4-1a	C4	*Apodemus sylvativus*	left	*in situ*	**22.2**	0.1	**-2.1**
XG5-3	C5	*Apodemus sylvativus*	left	*in situ*	**16.3**	0.3	**-7.0**
XG5-4	C5	*Apodemus sylvativus*	right	*in situ*	**17.4**	0.3	**-6.1**
CX52	C5	*Apodemus sylvativus*	left	*in situ*	**17.5**	0.3	**-6.0**
CX54	C5	*Apodemus* cf. *sylvaticus*	left	isolated	**17.6**	0.3	**-5.9**
CX53	C5	*Apodemus* cf. *sylvaticus*	left	isolated	**19.0**	0.9	**-4.7**
XG5-1	C5	*Apodemus sylvativus*	left	*in situ*	**19.6**	0.3	**-4.3**
XG5-2	C5	*Apodemus sylvativus*	left	*in situ*	**19.7**	0.4	**-4.2**
CX51	C5	*Eliomys quercinus*	right	*in situ*	**19.8**	0.3	**-4.1**
CX55	C5	*Apodemus* cf. *sylvaticus*	right	isolated	**19.9**	0.1	**-4.0**
XG5-5	C5	*Apodemus sylvativus*	right	*in situ*	**20.4**	0.3	**-3.6**
XG6-4	C6	*Apodemus sylvativus*	right	*in situ*	**16.0**	0.4	**-7.3**
XG6-3	C6	*Apodemus sylvativus*	left	*in situ*	**17.0**	0.2	**-6.4**
XG6-2	C6	*Apodemus sylvativus*	left	*in situ*	**17.1**	0.5	**-6.3**
XG6-1	C6	*Apodemus sylvativus*	left	*in situ*	**17.3**	0.3	**-6.2**
CX64	C6	*Apodemus sylvativus*	right	*in situ*	**17.8**	0.4	**-5.8**
CX65	C6	*Apodemus* cf. *sylvaticus*	left	*in situ*	**19.3**	0.4	**-4.5**
CX62	C6	*Apodemus* cf. *sylvaticus*	left	*in situ*	**19.6**	0.5	**-4.3**
CX63	C6	*Apodemus* cf. *sylvaticus*	left	*in situ*	**19.6**	0.2	**-4.2**
CX61	C6	*Apodemus* cf. *sylvaticus*	right	*in situ*	**20.2**	0.4	**-3.8**
XG6-5	C6	*Apodemus sylvativus*	right	*in situ*	**23.2**	0.6	**-1.3**
XG7-3b	C7	*Apodemus sylvativus*	left	*in situ*	**14.6**	0.2	**-8.4**
XG7-4a	C7	*Apodemus sylvativus*	right	*in situ*	**17.0**	0.3	**-6.4**
CX71	C7	*Apodemus sylvativus*	right	*in situ*	**17.2**	0.2	**-6.2**
XG7-1b	C7	*Apodemus sylvativus*	right	*in situ*	**17.4**	0.8	**-6.0**
CX72	C7	*Apodemus* cf. *sylvaticus*	right	isolated	**18.0**	0.3	**-5.6**
CX73	C7	*Apodemus* cf. *sylvaticus*	left	isolated	**18.3**	0.2	**-5.4**
XG7-5a	C7	*Apodemus sylvativus*	left	*in situ*	**20.0**	0.3	**-3.9**
XG7-2b	C7	*Apodemus sylvativus*	right	*in situ*	**20.3**	0.4	**-3.7**
CX75	C7	*Apodemus* cf. *sylvaticus*	left	isolated	**20.6**	0.1	**-3.4**
CX74	C7	*Apodemus* cf. *sylvaticus*	left	isolated	**21.5**	0.4	**-2.7**
CX80	C8	*Apodemus* cf. *sylvaticus*	left	isolated	**17.9**	0.1	**-5.6**
CX81	C8	*Apodemus* cf. *sylvaticus*	right	isolated	**18.2**	0.3	**-5.4**
CX84	C8	*Apodemus* cf. *sylvaticus*	left	isolated	**18.6**	0.4	**-5.1**
CX83	C8	*Apodemus* cf. *sylvaticus*	left	isolated	**18.7**	0.4	**-5.0**
CX82	C8	*Apodemus* cf. *sylvaticus*	left	isolated	**19.3**	0.3	**-4.5**

Table 5.2 Oxygen isotope composition of tooth enamel phosphate (δ18Op; ‰ V-SMOW) from rodent lower incisors from Cova dels Xaragalls. The table includes the stratigraphic layer, identified taxa and the conversion to the oxygen isotope composition of meteoric waters (δ18Omw; ‰ V-SMOW) following the Royer et al. (2013a) oxygen isotope fractionation equation. SD, Standard Deviation.

3.2 Sampling procedure for oxygen isotope analysis

For each rodent sample, only lower incisor enamel was sampled, as the mineral fraction is greater in tooth enamel than in dentine or bones, favouring a better preservation of the original isotopic composition (Barham et al., 2017; Kolodny et al., 1983; Lécuyer et al., 1999; Lee-Thorp and van der Merwe, 1991; Zazzo et al., 2004). Unbroken and well-preserved lower incisors were preferentially selected, whereas remains with physical damage such as soil or root corrosion, manganese oxide, fissures and cracks, cementation or water abrasion, which could facilitate diagenetic alteration of the oxygen isotopic system, were systematically avoided (Andrews, 1990; Barham et al., 2017; Royer et al., 2014). In addition, all rodent remains showing clear evidence of digestion were discarded due to the possible modification of the original oxygen isotope composition that may result from the chemically and enzymatically digestive environment (Barham et al., 2017), and *in situ* incisors were preferred because they were likely to be more protected from chemical exchanges with sedimentary matrices (Royer et al., 2013b). Only adult specimens were selected, to avoid the possible damping of the oxygen isotope composition associated with the immature teeth of juvenile individuals, where the mineralization process is incomplete (Blumenthal et al., 2014; Passey and Cerling, 2002). Regarding diagenetic considerations, the phosphate radical (PO_4^{3-}) constitutes the major source of oxygen in biogenic apatite, and the phosphorus-oxygen bond is stronger than the carbon-oxygen one (CO_3^{2-}) and less prone to geochemical and biological alteration (Clementz, 2012; Grimes et al., 2008; Lécuyer et al., 1999; Lindars et al., 2001). Pristine oxygen isotope compositions can thus be preserved at geological timescales even though the diagenetic alteration of biogenic apatites cannot be excluded in some cases, such as the processes of dissolution and recrystallization induced by microbial activity (Blake et al., 1997; Zazzo et al., 2004). On the basis of phosphate chemical yields measured during the wet chemistry procedure, clustered phosphorus pentoxide (P_2O_5) contents close to 40 wt% indicate that the original stoichiometry of the teeth was most likely preserved (Héran et al., 2010; Lécuyer, 2004; Navarro et al., 2004; Royer et al., 2013b).

3.3 Analytical techniques

The rodent teeth were cleaned with double-deionized water (DDW) in an ultrasonic bath to remove any trace of sediment matrix. Then, the basal part of the enamel was discarded while the remaining part was gently crushed in an agate mortar. Enamel fragments were separated from dentine by hand-picking under a binocular microscope. The enamel tooth samples were treated following the wet chemistry procedure described by Crowson et al. (1991) and slightly modified by Lécuyer et al. (1993) and adapted for small-sample weights (1-3 mg of apatite) by Bernard et al. (2009), Fourel et al. (2011) and Lécuyer et al. (2007). This protocol is based on the isolation of phosphate ions (PO_4^{3-}) from apatite as silver phosphate (Ag_3PO_4) crystals using acid dissolution and anion-exchange resin. For each sample, around 3 mg of enamel powder was dissolved in 1ml of hydrofluoric acid (2M HF) overnight. Calcium fluoride (CaF_2) residue was separated by centrifugation and the solution was neutralized by adding 1 ml of potassium hydroxide (2M KOH); then 1.5 ml of Amberlite™ anion-exchange resin was added to the solution to separate the PO_4^{3-} ions. After 24 hours, the solution was removed, and the resin was eluted with 6 ml of ammonium nitrate (0.1M NH_4NO_3). After 4 hours, 0.1 ml of ammonium hydroxide (NH_4OH) and 3 ml of an ammoniacal solution of silver nitrate ($AgNO_3$) were added and the samples were placed in a thermostated bath at 70 °C for 6 hours,

enabling the precipitation of Ag_3PO_4 crystals. Four standard samples of natural phosphorite (NBS120c) were included during the wet chemistry of each series of 10 samples to ensure that no isotopic fractionation occurred during the wet chemistry.

Oxygen isotope compositions were measured using a high-temperature elemental analyser (EA)-pyrolysis (Py) interfaced in continuous flow (CF) mode to an isotopic ratio mass spectrometer (IRMS) (EA-Py-CF-IRMS technique performed at UMR 5276 LGL; Fourel et al., 2011; Lécuyer et al., 2007). For each sample, five aliquots of 300 µg of Ag_3PO_4 were mixed with 300 µg of pure powder graphite loaded in silver foil capsules. Pyrolysis was performed at 1,450 °C using a varioPYROcube™ elemental analyser and the isotopic ratio mass spectrometer Isoprime™. Measurements were calibrated with the standard samples of NBS120c phosphorite, whose value was fixed at 21.7‰ (V-SMOW; Lécuyer et al., 1993), and NBS127 barium sulphate with a value of 9.3‰ (V-SMOW; Hut, 1987). The average standard deviation for the Cova dels Xaragalls samples is 0.34 ± 0.04‰ (n=48) and 0.33 ± 0.07‰ (n=14) for the modern samples. Aliquots of silver phosphate were analysed several times a day in order to account for possible instrumental drift.

3.4 Oxygen isotope compositions of modern meteoric waters ($\delta^{18}O_{mw}$)

Present-day $\delta^{18}O_{mw}$ values for the localities where the modern samples were taken and for the Cova dels Xaragalls area (Vimbodí) were obtained using the Online Isotopes in Precipitation Calculator (OIPC; Bowen, 2017). This online software employs an algorithm based on datasets collected by the Global Network for Isotopes in Precipitation (GNIP), operated by the International Atomic Energy Agency and the World Meteorological Organization (IAEA/WMO, 2018) (Appendix 2.2.A, 2.2.C). Using the same approach as Fricke and O'Neil (1999) and Bernard et al. (2009), we calculated seasonal $\delta^{18}O_{mw}/T_{air}$ regressions using a sub-dataset of the IAEA-GNIP/ISOHIS dataset (2018) restricted to the Iberian Peninsula (Appendix 2.2.B). This sub-dataset comprises $\delta^{18}O_{mw}$ values obtained from 26 localities throughout the Iberian Peninsula ranging from 5 to 1380 m a.s.l. The current-temperature data for the Cova dels Xaragalls area are from Climate-Data.org (https://es.climate-data.org/) based on a climatic model using extended world climate data collected between 1982 and 2012 from the OpenStreetMap project.

3.5 Mutual ecogeographic range method and bioclimatic model

The mean annual temperatures (MAT) calculated from the $\delta^{18}O_p$ values of rodent teeth are compared with those derived from two alternative and independent palaeoenvironmental methods. The first, called the mutual ecogeographic range (MER) method, determines the present-day geographical region in which a given fossil species assemblage would be located through the intersection obtained from the overlap of the current distributions of each species (Blain et al., 2009, 2016; López-García, 2011). The current climatic conditions of the intersecting area are used to infer the MAT. The MER estimations presented in this work have already been published by López-García et al. (2012). The second method, called the bioclimatic model (BM), is based on the adscription of small-mammal species to ten different climatic zones (Hernández Fernández, 2001; Hernández Fernández et al., 2007). This allows the calculation first of the Climatic Restriction Index ($CRI_i=1/n$, where i is the climatic zone inhabited by the species and n is the number of climatic zones the species inhabit) and then the Bioclimatic Component ($BC_i=(\Sigma CRI_i)100/S$, where S is the number of species). From the BC it

is possible to calculate the MAT by means of a multiple linear regression developed specifically for the order Rodentia (Hernández Fernández, 2001; Hernández Fernández et al., 2007).

3.6 Statistical calculations

Ordinary least squares (OLS) regression was used to examine the relationship between the mean annual $\delta^{18}O_{mw}$ values and the mean March-June $\delta^{18}O_{mw}$ values from 26 Iberian localities. OLS was also used to examine the relationship between the mean annual $\delta^{18}O_{mw}$ values and the monthly mean air temperatures (Appendix 2.2.B; 2.2.C). The equations calculated by the OLS regression model were further used for calculations using transposed fits (Skrzypek et al., 2016). Uncertainties in temperature calculations were determined by applying error propagations according to the method developed by Pryor et al. (2014). Statistical analyses were performed with R v3.3.2 (R Core Team 2016) and the Paleontological Statistics program (PAST3; Hammer et al., 2001).

4. Results and discussion

The reconstruction of past air temperatures from the oxygen isotope composition of rodent teeth is a two-step procedure: 1) the measured $\delta^{18}O_p$ values of the fossil rodent teeth allow the estimation of the $\delta^{18}O$ values of local meteoric water ($\delta^{18}O_{mw}$) and, 2) the calculated $\delta^{18}O_{mw}$ values can be used to estimate past air temperatures. Since pioneering works (Longinelli, 1984; Luz et al., 1984; Luz and Kolodny, 1985), many studies have explored the complex relationship between the oxygen isotope composition of vertebrate phosphatic tissues and body water, itself related to the oxygen isotope composition of ingested water, which ultimately derives from meteoric water. The oxygen isotope composition of body water is species-dependent, being controlled by both input and output oxygen fluxes as well as physiological factors such as basal metabolism and body temperature (Lindars et al., 2001; Longinelli, 1984; Luz et al., 1984; Podlesak et al., 2008). Over the last two decades, distinct species-dependent oxygen isotope fractionation equations relating $\delta^{18}O_p$ and $\delta^{18}O_{mw}$ have thus been experimentally determined (e.g. for rodents, D'Angela and Longinelli, 1990; Lindars et al., 2001; Luz and Kolodny, 1985; Navarro et al., 2004). Recently, using a large dataset which extends from 38°N to 65°N in Europe, Royer et al. (2013a) proposed a robust linear oxygen isotope fractionation equation for Muroidea teeth between the $\delta^{18}O_p$ values and $\delta^{18}O_{mw}$ values:

$$\delta^{18}O_p = 1.21\ (\pm 0.20) \times \delta^{18}O_{mw} + 24.76\ (\pm 2.70) \qquad (1)$$

Equation (1) is used in this study to estimate the $\delta^{18}O_{mw}$ contemporaneous with MIS 3 in the Iberian Peninsula.

At mid and high-latitudes, mean annual $\delta^{18}O_{mw}$ values are linearly related to the mean air temperatures at regional and global scales (Dansgaard, 1964; Rozanski et al., 1993). The $\delta^{18}O_{mw}$ values are mainly controlled by the water vapour source, the trajectories of humid air masses, seasonal variations of precipitation and the ambient air during the process of condensation. During the warm season the $\delta^{18}O_{mw}$ values increase, whereas they decrease during the cold season. At a regional scale such as in Europe, a "continental effect" is observed, with decreasing $\delta^{18}O_{mw}$ values landward, and an "altitude effect", with $\delta^{18}O_{mw}$ values decreasing with increasing altitude, in response to the gradual removal of moisture from uplifted air masses with a preferential removal of the heavy isotope ^{18}O during condensation. Several equations have been proposed for estimating past temperatures from $\delta^{18}O_{mw}$ at mid and high latitudes (e.g. Bernard et al., 2009; García-Alix, 2015; Lécuyer, 2014; Pryor et al., 2014; Rozanski et al., 1993; von Grafenstein et

al., 1996). These equations are based on data related to different geographic scales, which can result in sizable differences in the estimations for air temperatures (Daux et al., 2005) when applied to specific regions such as the Iberian Peninsula.

4.1 Oxygen isotope composition of meteoric water in the Iberian Peninsula

Previous isotopic studies have underlined the particular climate mode of the Mediterranean Basin (Dansgaard, 1964; Gat et al., 2003; Gat and Carmi, 1970; Hartman et al., 2015; Lécuyer, 2014; Lécuyer et al., 2018). Nonetheless, the Iberian Peninsula cannot simply be equated with any other Mediterranean region. Indeed, it is a complex territory in terms of climate due to its latitude range, its location between Atlantic and African-Mediterranean influences and its particularly complex orography, thus incorporating all the features of a small-scale continent (Font-Tullot, 2000). Indeed, Iberia plays a major role as a centre of secondary action in the mechanism of the general circulation of the atmosphere (Font-Tullot, 2000).

This peculiar climatic mode is reflected by the $\delta^{18}O_{mw}$ values for the Iberian Peninsula. The current seasonal variation in the $\delta^{18}O_{mw}$ values observed in the Iberian Peninsula (OIPC data; Bowen, 2017; Appendix 2.2.A; Fig. 5.3A) follows the isotopic pattern of mid and high latitudes (Dansgaard, 1964; Gat, 1980; Rozanski et al., 1993) with an increase in $\delta^{18}O_{mw}$ values in summer and a decrease in winter. Nonetheless, sizable differences between Iberia and higher-latitude localities, such as southwestern France, can be seen in the annual ranges of the $\delta^{18}O_{mw}$ values, with higher seasonal differences observed in Iberia (6.8-8.9‰) than in southern France (3.7-5‰). The differences between these two regions correspond to the presence of lower $\delta^{18}O_{mw}$ values in the Iberian Peninsula for the colder season in conjunction with notably higher $\delta^{18}O_{mw}$ for the warmer season. This phenomenon may be related to the motion of humid air masses that occurs in Iberia (Gat et al., 2003). During summer, most of the Iberian Peninsula (with the exception of the Cantabrian to Atlantic seaboards) is under the influence of the continental tropical air mass from North Africa, which imposes hot and arid summers (Font-Tullot, 2000). Before reaching Iberia, the continental tropical air mass from North Africa becomes more and more heavily charged with moisture during its transport over the Mediterranean Sea and is enriched by the heavy isotope 18O. Likewise, the complex Iberian orography characterized by remarkable altitudes causes large seasonal climatic amplitudes, which may be reflected in large annual ranges of $\delta^{18}O_{mw}$. However, even though altitude may influence the oxygen isotope composition of meteoric water, it is clearly not the dominant parameter explaining the range of $\delta^{18}O_{mw}$ values in Iberia (Fig. 5.3A).

Considering the singular climate mode of the Iberian Peninsula, a specific linear regression is therefore established between the mean annual $\delta^{18}O_{mw}$ values and the mean annual air temperatures. The linear regression of the GNIP data provides the following equation (Fig. 5.4A; Appendix 2.2.B):

$$\text{MAT (°C)} = 2.38(\pm 0.10) \times \delta^{18}O_{mw} + 28.19(\pm 0.58)$$
$$\text{with } R^2 = 0.65 \ (n = 304; p<0.0001; S_{y/x} = 3.6) \quad (2)$$

4.2 Oxygen isotope composition of present-day rodents from the Iberian Peninsula

4.2.1 $\delta^{18}O_p$ intra-pellet variability

A key factor in understanding the isotopic variability recorded in rodent teeth is the formation of rodent accumulations (e.g. Royer et al., 2013a, b). In cases where the accumulations are produced by predators such as owls, one sampling

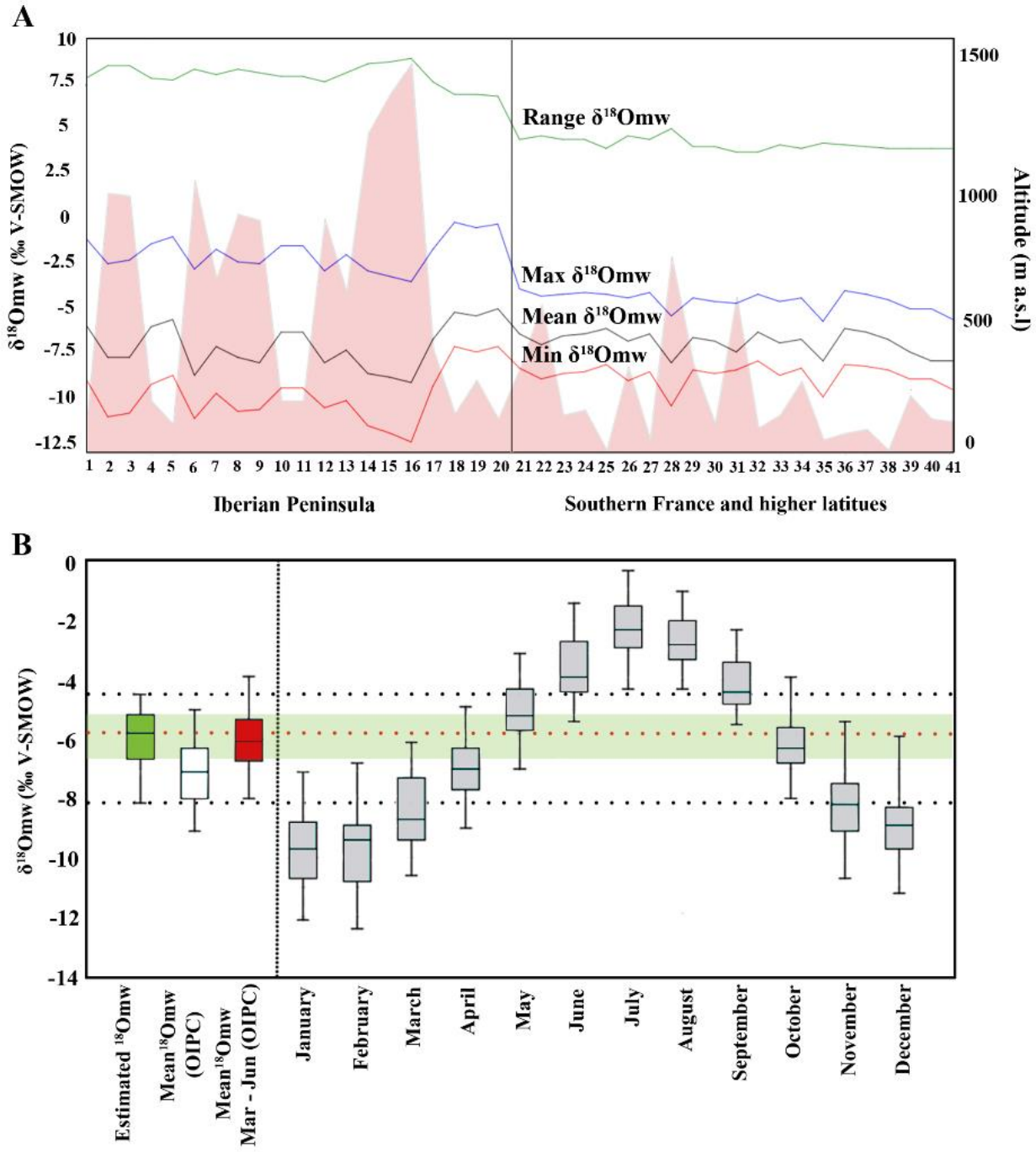

Figure 5.3 A) Oxygen isotope composition (‰ V-SMOW) of meteoric waters (δ18Omw) from localities in the Iberian Peninsula, southern France and other localities from higher latitudes (numbers 1 to 20 and 21 to 41, respectively; detailed information available in Appendix 2.2.A), using data from OIPC software (Bowen, 2017). The red, black, blue and green curves represent respectively the minimum, the maximum, the mean annual and the range of δ18Omw values (‰ V-SMOW) for each locality. The altitude is indicated in light red (m above sea level) for each locality. B) Box plot representation of the oxygen isotope composition (‰ V-SMOW) of meteoric waters (δ18Omw) estimated.

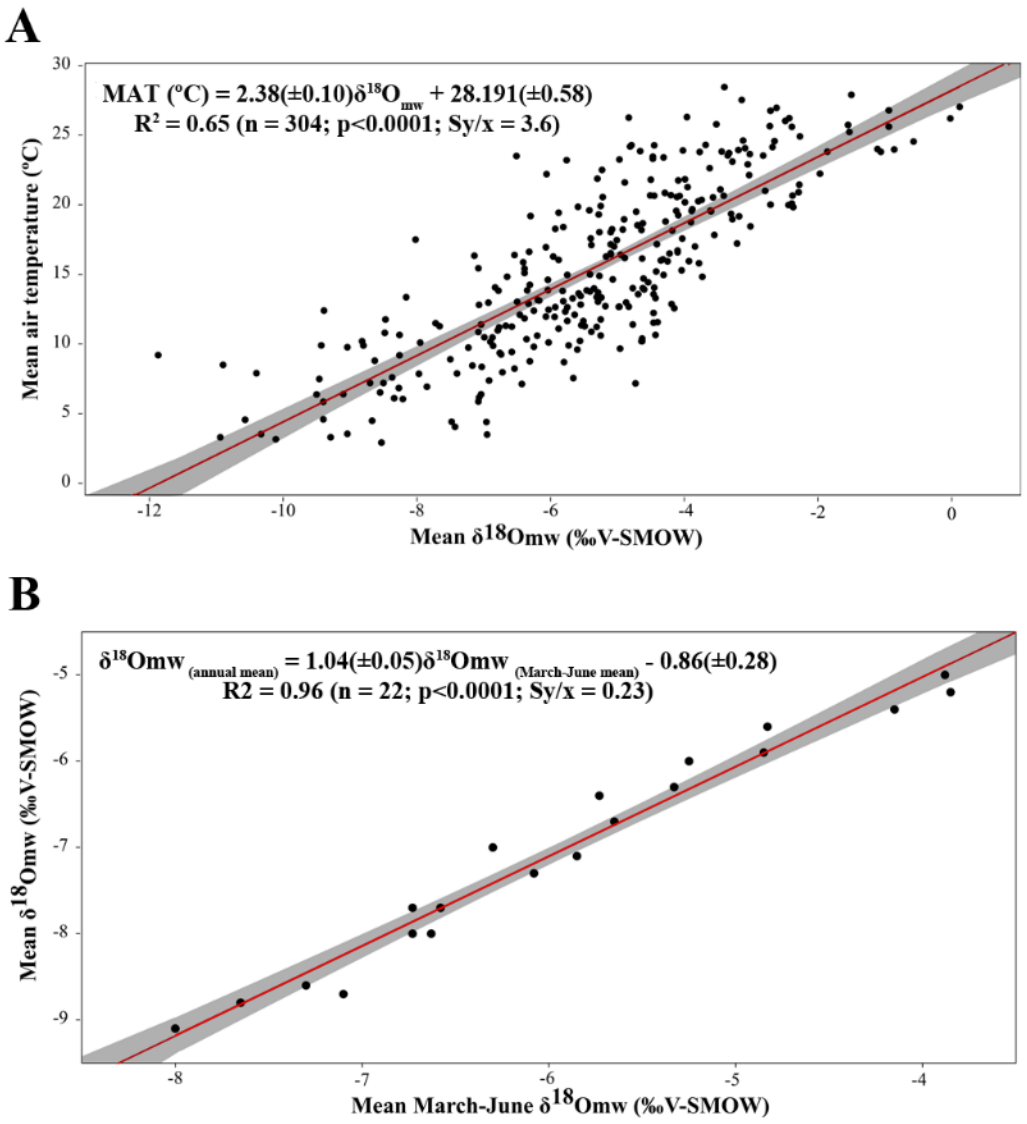

Figure 5.4 Proposed corrections for palaeotemperature reconstruction in northeastern Iberia. A) Linear regression model (OLS equation) relating monthly mean $\delta^{18}O_{mw}$ values and monthly mean air temperatures, from available dataset for Iberia from the Global Network of Isotopes in Precipitation, operated by the International Atomic Energy Agency and the World Meteorological Organization (IAEA/WMO, 2018); B) Linear regression model (OLS equation) between current mean annual $\delta^{18}O_{mw}$ and mean March-June $\delta^{18}O_{mw}$ values from Iberian localities included in this study, using data from OIPC software (Bowen, 2017). In light grey, uncertainty with 95% confidence interval. Extended information in Appendix 2.2.B and 2.2.C, respectively.

bias may be related to the hunting territories, which vary among predators as a function of the local orography. The $\delta^{18}O_p$ values measured in fourteen modern rodents collected in Northeastern Iberia range from 16.1‰ to 20.2‰ (Table 5.1; Appendix 2.2.A). Despite the limited number of specimens, the variations in the $\delta^{18}O_p$ values between different incisors within each pellet are relatively low, with differences between the minimum and maximum $\delta^{18}O_p$ values ranging from 0.5 to 1.9‰. The intra-pellet variation of $\delta^{18}O_p$ is lower than 1‰ in the case of Serinyà (0.7‰), El Catllar (0.5‰) and Moià (0.9‰). In the case of Moià, it should be noted that an extra specimen collected outside of the pellet shows a distinct value lower by 2‰. The higher variability in the

pellets from Prades (1.9‰) and Balaguer (1.5‰) could be related to the complex orography in the surrounding region, as a result of which the activity of the predator may cover a large altitude range (from 200 to 1000 m a.s.l.) within a rather restricted area. The predator thus has access to prey that are more isotopically variable due to the altitude effect. From the intra-pellet ranges observed in this work, we calculated an average range of 1.1±0.5‰ (SD = 0.5‰). Barham et al. (2017) observed greater intra-specific variability (up to 2‰) for $\delta^{18}O_p$ values among individuals from equal laboratory conditions, warning of greater variation in natural conditions. However, the isotopic ranges in the current study are bracketed by the minimum (0.2‰) and the maximum (5.2%) values measured by Royer et al. (2013a) on pellets, with a mean value of 2.9 ±1.1‰ (SD = 1.6‰).

4.2.2 Recording time of rodent lower incisors

Various factors lead rodent tooth phosphate to record a $\delta^{18}O_{mw}$ value that corresponds to a short time interval of less than a season (Royer et al., 2013a). Small-sized animals, such as the great majority of present-day rodents, have a rapid water turnover (according to Podlesak et al. (2008) woodrats reach isotopic equilibrium two weeks after a change of drinking water), and their teeth are mineralized in a brief time interval, a few days after their birth (Blumenthal et al., 2014; Hillson, 2005). Furthermore, rodent incisors are characterized by their continuous growth throughout the life of the individual, offering opportunities to provide a record of the last moments before the individual's death. The growth time of the incisor is species-dependent, mainly in relation to their size and body weight. The renewal time for the lower incisors is generally around 30-60 days (Coady et al., 1967; Klevezal, 2010; Klevezal et al., 1990), whereas the murine species of the genus *Apodemus* tend more towards 50-60 days (Klevezal, 2010). In the case of the murids, on the basis of the thickness the dentin increments, Klevezal (2010) has noted that the daily growth rate of the incisor may also vary according to the diet and especially according to the season and the age of the specimen. The gestation period of *A. sylvaticus* extends over 20-30 days, and weaning takes place between 13 and 21 days after birth, when the development of the incisors starts (Sánchez-González et al., 2016; Palomo et al., 2007). Thus, the $\delta^{18}O_p$ recovered from a murid lower incisor contains integrated oxygen isotope information from the last two months of the individual's life and avoids any weaning effect as recorded in rooted adult molars (Gehler et al., 2012, 2011; Jeffrey et al., 2015; Royer et al., 2013a). Indeed, pellets from Moià, Prades and Serinyà were recovered between the end of August and the beginning of September. The $\delta^{18}O_{mw}$ values estimated from the $\delta^{18}O_p$ values of the rodent incisors recovered from these pellets match those documented by the IAEA/WMO stations for the April-May (Serinyà) and May-June (Moià and Prades) periods.

4.2.3 Preferential moment of rodent accumulation reflected by $\delta^{18}O$

The mean $\delta^{18}O_p$ value calculated for the fourteen new present-day samples is 18.7±0.5‰, which is higher than most values recorded at higher latitudes, but in accordance with other Iberian and Mediterranean localities previously published (Royer et al., 2013a) (Fig. 5.1A; Appendix 2.2.A). By combining these fourteen $\delta^{18}O_p$ values with fifteen previously published by Royer et al. (2013a) from Iberian locations (Fig. 5.1A), we obtained a set of $\delta^{18}O_p$ values ranging from 13.1‰ to 22.2‰, with a mean value of 17.7±0.6‰ (SD = 1.9‰). When these $\delta^{18}O_p$ values are converted into $\delta^{18}O_{mw}$ values using equation (1) and then compared to current $\delta^{18}O_{mw}$ data (OIPC data; Bowen, 2017), they are seen mainly to match the spring and the beginning of

summer (between March and June) or the autumn (between September and November), thus characterized by more contrasting isotopic compositions than for higher latitudes such as southwestern France (Fig. 5.3B). The mean $\delta^{18}O_{mw}$ values estimated from present-day Iberian samples are closer to the mean value corresponding to the March-June time span, being slightly higher (by + 1.1‰) than the expected mean $\delta^{18}O_{mw}$ values (IAEA/WMO) corresponding to the March-May interval in each location (Fig. 5.3B). This slight overestimation of $\delta^{18}O_{mw}$ values translates into overestimated annual air temperatures (by + 2.6 ‰). As previously noted, the Iberian Peninsula is characterized by a large seasonal amplitude of $\delta^{18}O_{mw}$ values, and the March-June period is one of the most variable in $\delta^{18}O_{mw}$ values (Fig. 3A). Indeed, the variation is around 5‰ between March and June, whereas it only reaches 2 to 3‰ at higher latitudes such as southwestern France.

Predator-prey interactions and ethological factors should also be considered. Generally, rodents show greater outdoor activity from spring to autumn, whereas their activity is less in winter, with their population increasing during spring-summer (Le Louarn and Quéré, 2003). For northern latitudes and higher altitudes, the reproductive activity of the wood mouse mainly occurs between spring and summer and ceases during winter. By contrast, in Mediterranean areas such as northeastern and southern Spain, or in areas with a Mediterranean influence (such as Portugal), the pattern of reproductive activity is reversed, starting in autumn and ending in spring, with summer always being the rest period (Fons and Saint Girons, 1993; Moreno and Kufner, 1988; Rosário and Mathias, 2004; Sans-Coma and Gosalbez, 1976; Sunyer et al., 2016). The great variability in the reproductive cycles of *A. sylvaticus* is related to its great capacity to adapt to the availability of food and thus to local climatic and environmental conditions (Fons and Saint Girons, 1993). In the Mediterranean Basin, high temperatures coupled with low summer rainfall, sometimes generating drought periods, may explain the absence of reproduction in summer and the occurrence of population peaks in spring (Moreno and Kufner, 1988; Rosário and Mathias, 2004). Summer is considered a period of stress for this species living in Mediterranean environments, as also expressed by a low survival rate (Rosário and Mathias, 2004).

At the same time, the observed oxygen isotopic variations in rodent teeth can be partly explained by the period of prey capture, which is responsible for the record of specific time intervals (Royer et al., 2013a, 2013b). At mid and high latitudes, the dynamic and structure of raptor populations (breeding, density, natality and migration) are affected by rodent abundances in spring-summer (Norrdahl and Korpima, 2002; Salamolard et al., 2000). The success of the predator population depends to a large extent on the abundance of its prey during the breeding season. This phase is the optimal period for predator hunting activity. For instance, Sundell et al. (2004) have shown that the success of avian predators at high latitudes (60°N) is strongly correlated with the abundance of rodents, showing a seasonal numerical response. In addition, birds of prey tend to improve their hunting efficiency during the breeding season, to meet the energy requirements for feeding their young. In the Iberian Peninsula, the most common rodent predators, owls (*Tyto alba, Athene noctua, Otus scops, Asio otus, Bubo bubo, Asio flammeus, Strix aluco*), usually have their reproduction and breeding period between spring and the beginning of summer (Manzanares, 2012) (Appendix 2.2.D). Consequently, the probability of rodent capture by owls is highest during this period.

It is therefore considered that rodent $\delta^{18}O_p$ values mainly reflect the $\delta^{18}O_{mw}$ values of the March-June period in Iberian Peninsula localities (Fig. 5.3B). We propose a linear regression based on OIPC data (Bowen, 2017) between the $\delta^{18}O_{mw}$ values of the March-June period and the mean annual $\delta^{18}O_{mw}$ values. This can be applied to Iberian rodent populations to calculate the mean annual $\delta^{18}O_{mw}$ values in the fossil record (Fig. 5.4B):

$$\delta^{18}O_{mw\ (annual\ mean)} = 1.04(\pm0.05) \times \delta^{18}O_{mw\ (March\text{-}June\ mean)} - 0.86(\pm0.28),$$
$$\text{with } R^2 = 0.96\ (n = 22;\ p<0.0001;\ S_{y/x} = 0.23) \quad (3)$$

4.4 Application to fossil rodent teeth: from $\delta^{18}O_p$ values to temperatures in the Iberian Peninsula

In the Iberian Peninsula, as indicated earlier the period of maximal rodent density and predator activity mainly corresponds to the spring-summer months. We suggest that a similar line of argument could be applied to rodent fossil assemblages sampled from Late Pleistocene deposits from Iberia. To this end, we recommend using median $\delta^{18}O$ values, which are less subject to extreme values. Furthermore, we consider the variability of the $\delta^{18}O_p$ values obtained from several teeth per level as an indicator of intra-level distribution to evaluate inter-annual climate instability. This variability can be restrained (<4‰) or very substantial (>8‰). In the case of positive asymmetry in the frequency distribution of $\delta^{18}O_p$ values, a bias due to a warm and arid period can be surmised, whereas a negative asymmetrical distribution of values could be related to individual captures during the winter period (Royer et al., 2013b, 2014). Consequently, confidence in the interpretation of such data is intrinsically limited as these two cases could also result from a seasonal effect alone. Complexity is also added by the structure of fossil deposits, where the isotopic composition of rodent teeth could reflect either a unique short event or long periods of accumulation (from a couple of years to thousands of years) yet distinguishing between these two possibilities is highly challenging.

Estimations of palaeotemperatures usually require a two-step procedure involving two linear equations: 1) from $\delta^{18}O_p$ to $\delta^{18}O_{mw}$; 2) from $\delta^{18}O_{mw}$ to air temperatures. Considering the possible seasonality of the rodent assemblages and the regional peculiarities of the Iberian Peninsula, the following three-step strategy is proposed for the reconstruction of estimated palaeotemperatures from rodent tooth $\delta^{18}O_p$ accumulated in the Iberian Peninsula:

1. Estimation of $\delta^{18}O_{mw}$ from $\delta^{18}O_p$, employing the linear oxygen isotope fractionation equation determined by Royer et al. (2013a) (1), using the median $\delta^{18}O_p$ value from a given level.
2. When the rodent isotopic record is preferentially biased towards air temperatures of the spring-summer months, we also recommend an additional equation (3) that can be applied to $\delta^{18}O_{mw}$ for the March-June period in order to obtain the corresponding mean annual $\delta^{18}O_{mw}$ (3).
3. Estimation of air temperatures from $\delta^{18}O_{mw}$, using the linear regression model specific to Iberia developed in this work, relating the mean annual $\delta^{18}O_{mw}$ and the mean annual air temperatures (2).

Nonetheless, one additional correction should be performed before $\delta^{18}O_{mw}$ values can be quantitatively estimated, related to the ice volume effect. During glacial periods, the oxygen isotope composition of seawater changes in response to the fluctuations in the volume of continental ice. Any change in the seawater oxygen composition is passed on to the surface hydrological cycle at a globe scale, which includes the oxygen isotope

composition of meteoric waters. For instance, the global seawater $\delta^{18}O$ value increased by 1.0 ±0.1‰ during the Last Glacial Maximum, whereas during MIS 3 the sea level was around 50 m below the present-day sea level. This sea level fluctuation may have contributed to an increase in the global $\delta^{18}O_{mw}$ value by +0.6‰, resulting in a bias in calculated air temperatures of +1 °C (see Schrag et al., 2002).

4.5 Palaeoenvironmental and palaeoclimatic reconstruction of Cova dels Xaragalls

The oxygen isotope composition of the rodent incisor enamel from the different studied layers of Cova dels Xaragalls ranges from 14.6‰ to 23.2‰, representing a range of variation of 8.6‰ (Fig. 5.5; Table 5.3). The mean $\delta^{18}O_p$ values are nearly constant over the sequence, varying between 18.4‰ (layer C7) and 19.0‰ (layer C4). The median $\delta^{18}O_p$ values present slight oscillations, extending from 18.2‰ (layer C7) to 19.3‰ (layer C5), but staying largely similar, with the mean $\delta^{18}O_p$ never exceeding more than 0.6‰ the median $\delta^{18}O_p$ value. The oxygen isotope compositions of *M. arvalis* (18.2‰, layer C4) and *E. quercinus* (19.8‰; layer C5) keep within the general range obtained from *A. sylvaticus* measurements and have no influence either on the mean or median values. All sedimentary layers show a normal distribution of data (Shapiro-Wilk test, p-value>0.01). Sizeable intra-level variations are observed, which range from 1.4‰ to 7.2‰. Layers C8 and C5 are characterized by the lowest intra-level amplitude (1.4‰ and 4.1‰, respectively), lower standard deviations (0.5‰ and 1.4‰, respectively) and the highest medians (18.6‰ and 19.3‰, respectively). By contrast, layers C7, C6 and C4 show a higher amplitude of $\delta^{18}O_p$ values (6.9‰, 7.2‰ and 5.6‰, respectively), higher standard deviations (2.1‰, 2.1‰ and 1.8‰, respectively) and lower medians (18.2‰, 18.5‰ and 18.4‰, respectively).

The low to medium $\delta^{18}O_{mw}$ intra-level amplitudes recorded in the Cova dels Xaragalls fossil deposits, which range from 1.1 to 5.9‰ (Table 5.3), are lower than the current seasonal amplitude for $\delta^{18}O_{mw}$ values at Vimbodí-Poblet (8.5‰; OIPC data) and the average seasonal amplitude of $\delta^{18}O_{mw}$ values for Iberia (8‰; OIPC data; Fig. 5.3a). These patterns suggest that small-mammal remains were most likely accumulated during a preferential period of the year, which would have probably been during the warm season. Taphonomic analyses suggest that the predator responsible for the rodent accumulation throughout the Cova dels Xaragalls sequence is *Athene noctua* (López-García et al., 2012). This nocturnal bird of prey feeds mainly on insects, but also on small mammals, frogs and birds. It is a sedentary species that inhabits restricted territories (around 0.8 km^2), and within the Iberian Peninsula it breeds from April to May, in tree holes or rock fissures (Andrews, 1990; Manzanares, 2012; Mikkola, 1983; UICN, 2018). At higher altitudes, this species is known to hunt small mammals preferentially during winter (Andrews, 1990; Delibes et al., 1983). However, some studies have quantified high rates of small-mammal consumption during both spring and autumn in Mediterranean areas (e.g. Sekour et al., 2011).

The high variation in $\delta^{18}O_p$ values observed within the layers could be related to a higher seasonal amplitude or to climatic fluctuations. Combining median data with ranges and standard deviations and taking into account previous environmental data inferred from the small-vertebrate and charcoal studies of the site (López-García et al., 2012; Vallverdú et al., 2012), it is noticeable that layers C6, C7 and C4 show a degree of climatic variation in comparison to layers C8 and C5, which seem relatively more stable (Table 5.3; Fig. 5.5). Layers C6 and C4 show very high $\delta^{18}O_p$ values (>22‰), which could be related to water ^{18}O

enrichment due to arid events (Jeffrey et al., 2015; Royer et al., 2013b). By contrast, low $\delta^{18}O_p$ values such as those from layer C7 (<15‰) could be related to the predation of specimens in the cold season or in an exceptionally cold spring. The different altitudes at which the predator may have been hunting may also explain a part of these variations. Indeed, Cova dels Xaragalls is surrounded by a mountainous environment with highly variable altitudes at a kilometre scale. López-García et al. (2012) indicate an inverse relationship between the temperatures and the amount of precipitation, with the warmest layers being the driest (C5 and C8) and the coldest layers being the wettest (C3-C4 and C6). These pluviometric changes could have magnified the variability in the oxygen isotope composition of layers C4 and C6. However, the global picture of slight inter-level variation, both for means and medians, indicates rather stable climatic conditions throughout the sequence, an interpretation which supports the results from previous studies based on small-mammal assemblages and charcoal.

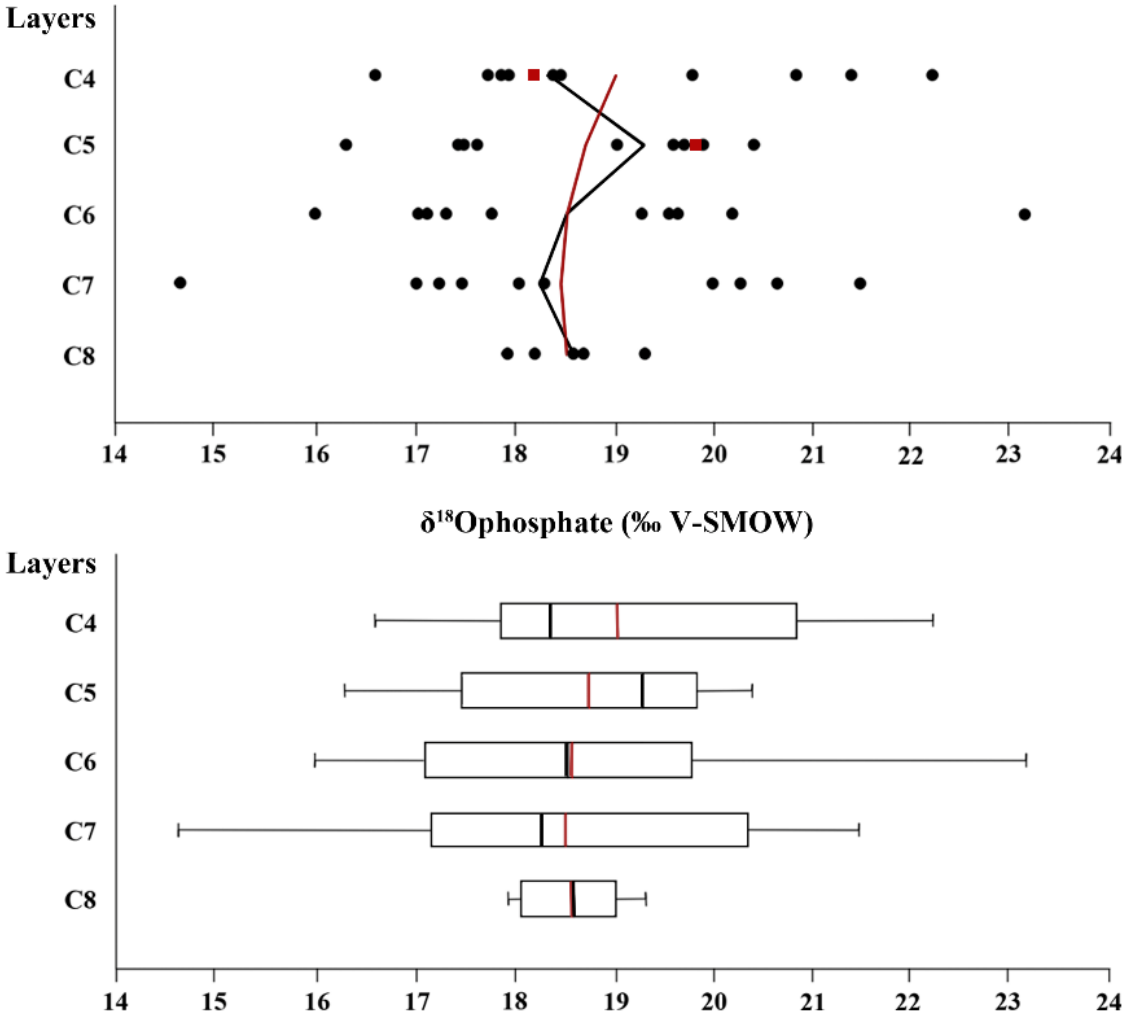

Figure 5.5 Oxygen isotope composition (‰ V-SMOW) of rodent incisor enamel from the Cova dels Xaragalls samples. Above, distribution of $\delta^{18}O$ values per layer, with mean (red) and median (black) curves. Red squares illustrate the *Microtus arvalis* (C4) and *Eliomys quercinus* (C5) samples; black points identify the *Apodemus sylvaticus* samples. Bellow, box plots of the oxygen isotope composition (‰ V-SMOW) of rodent incisor enamel by layer with mean (red) and median (black) indicated; the bars cover the full extension of the values; the boxes extend from the 1st to 3rd quartile.

	Levels	C4	C5	C6	C7	C8
	n	11	10	10	10	5
$\delta^{18}O_p$	Min	16.6	16.3	16.0	14.6	17.9
	Max	22.2	20.4	23.2	21.5	19.3
	Mean	19.0	18.7	18.6	18.4	18.5
	Median	18.4	19.3	18.5	18.2	18.6
	Range	5.6	4.1	7.2	6.9	1.4
	SD	1.8	1.4	2.1	2.1	0.5
$\delta^{18}O_{mw}$	Min	-6.8	-7.0	-7.3	-8.4	-5.6
	Max	-2.1	-3.6	-1.3	-2.7	-4.5
	Mean	-4.8	-5.0	-5.1	-5.3	-5.1
	Median	-5.3	-4.5	-5.2	-5.5	-5.1
	Range	4.7	3.4	5.9	5.7	1.1
MAT	$\delta^{18}O_{mw}$ - seasonality correction	-6.3	-5.6	-6.2	-6.5	-6.2
	$\delta^{18}O_{mw}$ - sea level correction	-6.9	-6.2	-6.8	-7.1	-6.8
	MAT (ºC)	11.7	13.6	12.0	11.2	12.1
	SD	1.3	1.4	1.3	1.3	1.8
	Error margin	2.5	2.7	2.6	2.6	3.5

Table 5.3 Minimum, maximum, mean, median, standard deviation and range of oxygen isotope composition of incisor enamel phosphate ($\delta^{18}O_p$; ‰ V-SMOW) from fossil rodents recovered from Cova dels Xaragalls; conversion to the oxygen isotope composition of meteoric waters ($\delta^{18}O_{mw}$; ‰ V-SMOW), including minimum, maximum, mean, median and range; and, mean annual temperature estimations (MAT; º C), including seasonality and sea-level corrections of $\delta^{18}O_{mw}$. SD, Standard Deviation.

For each sedimentary level, mean annual temperatures (MAT) were calculated based on median $\delta^{18}O_p$ values and following the protocol previously proposed in section 4.4 using equations (1), (2) and (3). The estimated MATs vary between 11.2 ±2.6 ºC and 13.6 ±2.7 ºC (Table 5.3; Fig. 5.6). These temperatures are slightly lower than the current MAT recorded at Vimbodí-Poblet (13.6 ºC; Climate-Data.org), with the difference ranging from -2.4 ºC (C7) to -1.5 ºC (C8), except for layer C5, which recorded air temperatures comparable to present-day temperatures. The MAT temporal trend calculated from the $\delta^{18}O_p$ record is reasonably similar to that obtained by the mutual ecogeographic range (López-García et al., 2012) and bioclimatic model reconstruction methods (Fig. 5.6) (Appendix 2.2.E and 2.2.F). However, an offset of a few degrees is observed between the three methods, remaining small enough to fall within the confidence interval.

Previous anthracological studies performed at Cova dels Xaragalls have revealed a low variability of taxa, which is related to the predominance of *Pinus*-type *sylvestris* throughout the sequence (more than 75%). This is a common feature of Late Pleistocene vegetation formations in northeastern Iberia due to the harsher conditions, suggesting that Cova dels Xaragalls had a cooler climate than at present and a landscape dominated by open forests (López-García et al., 2012). Nevertheless, the presence of more than 50% *A. sylvaticus*, which is mainly associated with forests or forest margins, is uncommon during cold climate stages because species more associated with open landscapes are usually found (Appendix 2.2.G). The location of Cova dels Xaragalls within Poblet Forest may have provided a suitable environment for species with generalist requirements, protected by low-altitude woodland formations and buffered climatic conditions. Recent morphological and

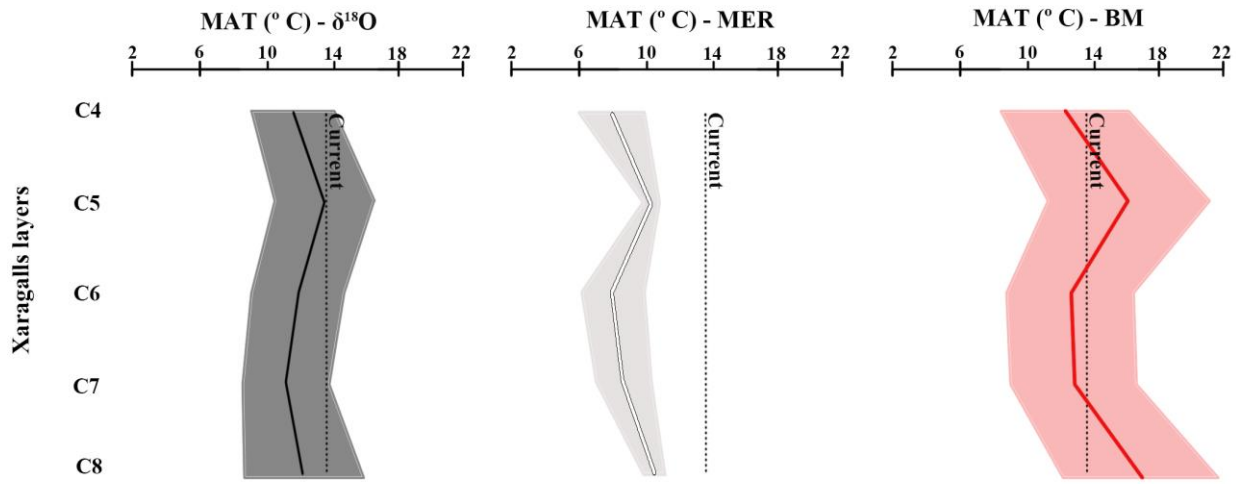

Figure 5.6 Mean annual temperature (MAT; ºC) reconstructed for the Cova dels Xaragalls layers using the oxygen isotope composition ($\delta^{18}O$) of rodent incisor enamel, the mutual ecogeographic range (MER) method and the bioclimatic model (BM). Dashed lines correspond to the current MAT at Vimbodí, and the shaded fringes to the error associated with each method

morphometric studies performed on *M. agrestis* and *M. arvalis* remains sampled from levels C4-C6 have pointed to a possible increase in humidity levels, which in a Mediterranean context can be related to an extension of forest cover (Luzi, 2018). A correlation between layer C5 and interstadial phase IS13 or 14 (ca. 50-55 ka) has previously been suggested by López-García et al. (2012), despite the fact that the biodiversity recorded in this level was not reliable due to the low abundance of individuals. Nonetheless, oxygen isotope compositions of rodent teeth from layer C5 are relatively high with a small standard deviation, reflecting a MAT comparable to the present (13.6 °C). This observation thus confirms the temporal trends inferred from the MER and BM models. It also agrees with the documented faunal biodiversity in the interstadial context that prevailed during the deposition of layer C5. Even though the climatic conditions recorded throughout the sedimentary sequence seem to be slightly cooler than nowadays, our study raises the possibility that warm air temperatures close to Holocene conditions could have occurred during MIS 3 in the northeast of Iberia.

5. Conclusions

Oxygen isotope compositions were measured in rodent teeth accumulated in modern pellet samples from five different sites located in northeastern Iberia and complemented with previously published $\delta^{18}O$ results from rodent teeth from the Iberian Peninsula. Narrow intra-pellet variability is observed for the $\delta^{18}O$ values of modern rodent tooth enamel. The peculiar orography and climatic mode of the Iberian Peninsula are emphasized by this study, which documents low $\delta^{18}O_p$ values and a high annual amplitude of $\delta^{18}O_{mw}$ in comparison to higher latitudes. On the basis of recent $\delta^{18}O_{mw}$ values extracted from IAEA/WMO databases, the oxygen isotope composition of contemporaneous Iberian rodent tooth samples reflects spring and early summer $\delta^{18}O_{mw}$ values. Consequently, the estimated mean $\delta^{18}O_{mw}$ values are closer to the March-June mean $\delta^{18}O_{mw}$ value than to the expected March-May mean $\delta^{18}O_{mw}$ value. The most likely cause is a preferential accumulation of rodent remains during this period associated with optimal predation activity. This interpretation is

supported by ethological studies that suggest a higher probability of prey capture by owls from Iberia during the spring-summer time interval as a consequence of the rising number of murid specimens. The oxygen isotope compositions recorded in present-day rodent tooth samples correspond to $\delta^{18}O_{mw}$ values contemporaneous with the two months that elapse before the deposition of the pellets by the predator. This is coincident with histological studies of genus *Apodemus*, which completes the renewal of its lower incisors in about two months.

The results obtained for the $\delta^{18}O$ values of rodent tooth enamel from modern pellet samples indicated that the interpretation of $\delta^{18}O_p$ is not simple. In fossil sites, where the phenomenon of the palimpsest is common, the $\delta^{18}O$ variations can be related both to intra-annual and to inter-annual changes in air temperature. Whenever possible, it is necessary to ascertain whether $\delta^{18}O_p$ intra-level variations are more related to the seasonality of samples or to climatic fluctuations. In addition, for Iberian palaeoenvironmental reconstructions based on $\delta^{18}O_p$, singular $\delta^{18}O_{mw}$ seasonal amplitudes and the preferential formation of rodent accumulations in the warm season could lead to an overestimation of the annual $\delta^{18}O_{mw}$ values and consequently of the mean annual air temperatures. In consequence, this work has proposed two solutions for calculating mean annual temperatures: the development of a specific $\delta^{18}O_{mw}/T_{air}$ regression equation designed for the Iberian environmental context (2) and a regression equation that relates the March-June $\delta^{18}O_{mw}$ to the mean annual $\delta^{18}O_{mw}$ in order to correct the seasonal bias recorded in rodent tooth apatite resulting from the probable preferential accumulation of rodent remains in the warm season (3).

Finally, the rodent incisor enamel sampled from layers C8 to C4 in Cova dels Xaragalls is characterized by low to medium $\delta^{18}O_p$ intra-level variations, suggesting that the small-mammal remains were preferentially accumulated during the warm season. The inter-level variations observed in C7, C6 and C4 could be related to high seasonal amplitude or high-frequency climatic fluctuations. However, the $\delta^{18}O_p$ variations suggest rather steady-state climatic conditions throughout the sequence with mean annual temperatures lower than current ones (-2.4°C to -1.5°C), except for layer C5, which records similar mean annual temperatures to those at present (13.6 ±2.7 °C). This observation supports the correlation between layer C5 and interstadial phase IS13 or 14 (ca. 50-55 ka). Comparison with different models of palaeotemperature reconstruction for the deposit at Cova dels Xaragalls demonstrates homogeneity in the climatic signal.

References

Andrews, P., 1990. Owls, Caves and Fossils. Predation, preservation and accumulation of small mammal bones in caves, with an analysis of the Pleistocene Cave Faunas from Westbury-sub-Mendip, Somerset, UK. The University of Chicago, Chicago.

Arrizabalaga, Á., 2004. Paleoclimatología y cronología del Würm reciente: un intento de síntesis. Zephyrus 57, 27–53.

Barham, M., Blyth, A.J., Wallwork, M.D., Joachimski, M.M., Martin, L., Evans, N.J., Laming, B., McDonald, B.J., 2017. Digesting the data - Effects of predator ingestion on the oxygen isotopic signature of micro-mammal teeth. Quat. Sci. Rev. 176, 71–84.

Bernard, A., Daux, V., Lécuyer, C., Brugal, J., Genty, D., Wainer, K., Gardien, V., Fourel, F., Jaubert, J., 2009. Pleistocene seasonal temperature variations recorded in the $\delta^{18}O$ of *Bison priscus* teeth. Earth Planet. Sci. Lett. 283, 133–143.

Blain, H.-A., Bailon, S., Cuenca-Bescós, G., Arsuaga, J.L., Bermúdez de Castro, J.M., Carbonell, E., 2009. Long-term climate record inferred from early-middle Pleistocene amphibian and squamate reptile assemblages at the Gran Dolina Cave, Atapuerca, Spain. J. Hum. Evol. 56, 55–65.

Blain, H.A., Lozano-Fernández, I., Agustí, J., Bailon, S., Menéndez Granda, L., Espígares Ortiz, M.P., Ros-Montoya, S., Jiménez Arenas, J.M., Toro-Moyano, I., Martínez-Navarro, B., Sala, R., 2016. Refining upon the climatic background of the Early Pleistocene hominid settlement in western Europe: Barranco León and Fuente Nueva-3 (Guadix-Baza Basin, SE Spain). Quat. Sci. Rev. 144, 132–144.

Blake, R.E., Neil, R.O., Garcia, G.A., 1997. Oxygen isotope systematics of biologically mediated reactions of phosphate: I. Microbial degradation of organophosphorus compounds. Geochim. Cosmochim. Acta 61, 4411–4422.

Blumenthal, S.A., Cerling, T.E., Chritz, K.L., Bromage, T.G., Kozdon, R., Valley, J.W., 2014. Stable isotope time-series in mammalian teeth: In situ $\delta^{18}O$ from the innermost enamel layer. Geochim. Cosmochim. Acta 124, 223–236.

Bowen, G.J., 2017. The Online Isotopes in Precipitation Calculator, Version 3.1 (4/2017): http://waterisotopes.org.

Clementz, M.T., 2012. New insight from old bones: stable isotope analysis of fossil mammals. J. Mammal. 93, 368–380.

Climate-Data.org, 2018. https://es.climate-data.org/

Coady, J.M., Toto, P.D., Santangelo, M.V., 1967. Histology of the Mouse Incisor. J. Dent. Res. 46, 384–388.

Crowson, R.A., Showers, W.J., Wright, E.K., Hoering, T.C., 1991. Preparation of Phosphate Samples for Oxygen Isotope Analysis. Anal. Chem. 63, 2397–2400.

D'Angela, D., Longinelli, A., 1990. Oxygen isotopes in living mammal's bone phosphate: Further results. Chem. Geol. 86, 75–82.

Dansgaard, W., 1964. Stable isotopes in precipitation. Tellus XVI, 436–468.

Fernández-García, M., López-García, J.M., Lorenzo, C., 2016. Palaeoecological implications of rodents as proxies for the Late Pleistocene–Holocene environmental and climatic changes in northeastern Iberia. Comptes Rendus Palevol 15, 707–719.

Fletcher, W.J., Sánchez Goñi, M.F., Allen, J.R.M., Cheddadi, R., Combourieu-Nebout, N., Huntley, B., Lawson, I., Londeix, L., Magri, D., Margari, V., Müller, U.C., Naughton, F., Novenko, E., Roucoux, K., Tzedakis, P.C., 2010. Millennial-scale variability during the last glacial in vegetation records from Europe. Quat. Sci. Rev. 29, 2839–2864.

Fons, R., Saint Girons, M.C., 1993. Le cycle sexuel chez le mulot sylvestre, Apodemus sylvaticus (L., 1758), (Muridae) en region mediterraneenne. Z. Säugertierkd. 58, 38–47.

Font-Tullot, I., 2000. Climatología de España y Portugal. Universidad de Salamanca, Salamanca.

Fourel, F., Martineau, F., Lécuyer, C., Kupka, H.J., Lange, L., Ojeimi, C., Seed, M., 2011. $^{18}O/^{16}O$ ratio measurements of inorganic and organic materials by elemental analysis–pyrolysis–isotope ratio mass spectrometry continuous-flow techniques. Rapid Commun. Mass Spectrom. 25, 2691–2696.

Freudenthal, M., García-Alix, A., Rios, M., Ruiz-Sánchez, F., Martín-Suárez, E., Delgado, A., 2014. Review of paleo-humidity parameters in fossil rodents (Mammalia): Isotopic vs. tooth morphology approach. Palaeogeogr. Palaeoclimatol. Palaeoecol. 395, 122–130.

García-Alix, A., 2015. A multiproxy approach for the reconstruction of ancient continental environments. The case of the Mio–Pliocene deposits of the Granada Basin (southern Iberian Peninsula). Glob. Planet. Change 131, 1–10.

Gat, J.R., 1980. The relationship between surface and subsurface waters: water quality aspects in areas of low precipitation. Hydrol. Sci. des Sci. Hydrol. 25, 257–267.

Gat, J.R., Carmi, I., 1970. Evolution of the Isotopic Composition of Atmospheric Waters im the Mediterranean Sea Area. J. Geophys. Res. 75, 3039–3048.

Gat, J.R., Klein, B., Kushnir, Y., Roether, W., Wernli, H., Yam, R., Shemesh, A., Klein, B., Kushnir, Y., Roether, W., Wernli, H., Yam, R., Shemesh, A., 2003. Isotope composition of air moisture over the Mediterranean Sea: an index of the air-sea interaction pattern. Chem. Phys. Meteorol. 55, 953–965.

Gehler, A., Tütken, T., Pack, A., 2012. Oxygen and Carbon Isotope Variations in a Modern Rodent Community - Implications for Palaeoenvironmental Reconstructions. PLoS One 7, 16–27.

Gehler, A., Tütken, T., Pack, A., 2011. Triple oxygen isotope analysis of bioapatite as tracer for diagenetic alteration of bones and teeth. Palaeogeogr. Palaeoclimatol. Palaeoecol. 310, 84–91.

Grimes, S.T., Collinson, M.E., Hooker, J.J., Mattey, D.P., 2008. Is small beautiful? A review of the advantages and limitations of using small mammal teeth and the direct laser fluorination analysis technique in the isotope reconstruction of past continental climate change. Palaeogeogr. Palaeoclimatol. Palaeoecol. 266, 39–50.

Grimes, S.T., Mattey, D.P., Hooker, J.J., Collinson, M.E., 2003. Palaeogene palaeoclimate reconstruction using oxygen isotopes from land and freshwater organisms: the use of multiple palaeoproxies. Geochim. Cosmochim. Acta 67, 4033–4047.

Hammer, Ø., Harper, D.A.T., Ryan, P.D., 2001. Paleontological statistics software package for education and data analysis. Palaeontol. Electron. 4, 9–18.

Harrison, S.P., Sanchez Goñi, M.F., 2010. Global patterns of vegetation response to millennial-scale variability and rapid climate change during the last glacial period. Quat. Sci. Rev. 29, 2957–2980.

Hartman, G., Hovers, E., Hublin, J.-J., Richards, M., 2015. Isotopic evidence for Last Glacial climatic impacts on Neanderthal gazelle hunting territories at Amud Cave, Israel. J. Hum. Evol. 84, 71–82.

Héran, M.A., Lécuyer, C., Legendre, S., 2010. Cenozoic long-term terrestrial climatic evolution in Germany tracked by $\delta^{18}O$ of rodent tooth phosphate. Palaeogeogr. Palaeoclimatol. Palaeoecol. 285, 331–342.

Hernández Fernández, M., 2001. Bioclimatic discriminant capacity of terrestrial mammal faunas. Glob. Ecol. Biogeogr. 10, 189–204.

Hernández Fernández, M., Álvarez Sierra, M.Á., Peláez-Campomanes, P., 2007. Bioclimatic analysis of rodent palaeofaunas reveals severe climatic changes in Southwestern Europe during the Plio-Pleistocene. Palaeogeogr. Palaeoclimatol. Palaeoecol. 251, 500–526.

Hewitt, G.M., 2000. The genetic legacy of the Quarternary ice ages. Nature 405, 907–913.

Hillson, S., 2005. Teeth. Cambridge University Press, New York.

Hut, G., 1987. Consultants' group meeting on stable isotope reference samples for geochemical and hydrological investigations, 16-18 Sep. 1985, Report to the Director General. International Atomic Energy Agency, Vienna.

IAEA/WMO, 2018. Global Network of Isotopes in Precipitation. The GNIP Database. Accessible at WISER (Water Isotope System for Data Analysis, Visualization and Electronic Retrieval): https://nucleus.iaea.org/wiser.

IUCN, 2018. The IUCN Red List of Threatened Species. Version 2017-3: www.iucnredlist.org.

Jeffrey, A., Denys, C., Stoetzel, E., Lee-Thorp, J. a., 2015. Influences on the stable oxygen and carbon isotopes in gerbillid rodent teeth in semi-arid and arid environments: Implications for past climate and environmental reconstruction. Earth Planet. Sci. Lett. 428, 84–96.

Klevezal, G.A., 2010. Dynamics of Incisor Growth and Daily Increments on the Incisor Surface in Three Species of Small Rodents. Biol. Butlletin 37, 836–845.

Klevezal, G.A., Pucek, M., Sukhovskaja, L.I., 1990. Incisor growth in voles. Acta Theriol. 35 (3-4), 331–344.

Kolodny, Y., Luz, B., Navon, O., 1983. Oxygen isotope variations in phosphate of biogenic apatites, I. Fish bone apatite rechecking the rules of the game. Earth Planet. Sci. Lett. 64, 398–404.

Le Louarn, H., Quéré, J.P., 2003. Les Rongeurs de France. Faunistique et biologie. Editions d'Institut National de la Recherche Agronomique, Paris.

Lécuyer, C., 2014. Water on Earth. John Wiley & Sons Inc, London, UK and New York.

Lécuyer, C., 2004. Oxygen Isotope Analysis of Phosphate, in: Groot, P.A. de (Ed.), Handbook of Stable Isotope Analytical Techniques. Elsevier B.V., pp. 482–499.

Lécuyer, C., Atrops, F., Amiot, R., Angst, D., Daux, V., Flandrois, J., Fourel, F., Rey, K., Royer, A., Seris, M., Touzeau, A., Rousseau, D.D., 2018. Tsunami sedimentary deposits of Crete records climate during the 'Minoan Warming Period' (≈3350 yr BP). The Holocene in press, 1–16.

Lécuyer, C., Fourel, F., Martineau, F., Amiot, R., Bernard, A., Daux, V., Escarguel, G., Morrison, J., 2007. High-precision determination of $^{18}O/^{16}O$ ratios of silver phosphate by EA-pyrolysis-IRMS continuous flow technique. J. Mass Spectrom. 42, 36–41.

Lécuyer, C., Grandjean, P., O'Neil, J.R., Cappetta, H., Martineau, F., 1993. Thermal excursions in the ocean at the Cretaceous-Tertiary boundary (northern Morocco): $\delta^{18}O$ record of phosphatic fish debris. Palaeogeogr. Palaeoclimatol. Palaeoecol. 105, 235–243.

Lécuyer, C., Grandjean, P., Sheppard, S.M.F., 1999. Oxygen isotope exchange between dissolved phosphate and water at temperatures ≤135°C: Inorganic versus biological fractionations. Geochim. Cosmochim. Acta 63, 855–862.

Lee-Thorp, J. a., van der Merwe, N.J., 1991. Aspects of the chemistry of modern and fossil biological apatites. J. Archaeol. Sci. 18, 343–354.

Leichliter, J., Sandberg, P., Passey, B., Codron, D., Avenant, N.L., Paine, O.C.C., Codron, J., de Ruiter, D., Sponheimer, M., 2017. Stable carbon isotope ecology of small mammals from the Sterkfontein Valley: Implications for habitat reconstruction. Palaeogeogr. Palaeoclimatol. Palaeoecol. 485, 57–67.

Lindars, E.S., Grimes, S.T., Mattey, D.P., Collinson, M.E., Hooker, J.J., Jones, T.P., 2001. Phosphate $\delta^{18}O$ determination of modern rodent teeth by direct laser fluorination: An appraisal of methodology and potential application to palaeoclimate reconstruction. Geochim. Cosmochim. Acta 65, 2535–2548.

Longinelli, A., 1984. Oxygen isotopes in mammal bone phosphate: A new tool for paleohydrological and paleoclimatological research? Geochim. Cosmochim. Acta 48, 385–390.

Longinelli, A., Nuti, S., 1973. Oxygen isotope measurements of phosphate from fish teeth and bones. Earth Planet. Sci. Lett. 20, 337–340.

López-García, J.M., 2011. Los micromamíferos del Pleistoceno superior de la Península Ibérica. Evolución de la diversidad taxonómica y cambios paleoambientales y paleoclimáticos. Ed. Académica Española, Saarbrücken.

López-García, J.M., Blain, H.-A., Bennàsar, M., Euba, I., Bañuls, S., Bischoff, J., López-Ortega, E., Saladié, P., Uzquiano, P., Vallverdú, J., 2012. A multiproxy reconstruction of the palaeoenvironment and palaeoclimate of the Late Pleistocene in northeastern Iberia: Cova dels Xaragalls, Vimbodí-Poblet, Paratge Natural de Poblet, Catalonia. Boreas 41, 235–249.

López-García, J.M., Blain, H.A., Bennàsar, M., Fernández-García, M., 2014. Environmental and climatic context of neanderthal occupation in southwestern Europe during MIS3 inferred from the small-vertebrate assemblages. Quat. Int. 326–327, 319–328.

Luz, B., Kolodny, Y., 1985. Oxygen isotope variations in phosphate of biogenic apatites, IV. Mammal teeth and bones. Earth Planet. Sci. Lett. 75, 29–36.

Luz, B., Kolodny, Y., Horowitz, M., 1984. Fractionation of oxygen isotopes between mammalian. Geochim. Cosmochim. Acta 48, 1689–1693.

Luzi, E. (2018) Morphological and morphometric variations in Middle and Late Pleistocene in *Microtus arvalis* and *Microtus agrestis* populations: chronological insight, evolutionary trends and paleoclimatic and palaeoenvironmental inferences. Universitat Rovira i Virgili, Tarragona. Pp. 316. Doctoral thesis (inedit).

Manzanares, A., 2012. Aves rapaces de la Península Ibérica, Baleares y Canarias. Ediciones Omega, Barcelona.

Meteocat, 2018. http://www.meteo.cat/wpweb/climatologia/el-clima-ahir/el-clima-de-catalunya

Mikkola, H., 1983. Owls of Europe. Buteo Books, Sussex.

Montuire, S., Navarro, N., Le, C., Langlois, C., Lécuyer, C., Montuire, S., Langlois, C., Martineau, F., 2004. Oxygen isotope compositions of phosphate from arvicoline teeth and Quaternary climatic changes, Gigny, French Jura. Quat. Res. 62, 172–182.

Moreno, S., Kufner, M.B., 1988. Seasonal Patterns in the Wood Mouse Population in Mediterranean Scrubland. Acta Theriol. (Warsz). 33, 79–85.

Norrdahl, K., Korpima, E., 2002. Seasonal changes in the numerical responses of predators to cyclic vole populations. Ecography (Cop.). 25, 428–438.

Palomo, L.J., Gisbert, J., Blanco, C., 2007. Atlas y libro rojo de los mamíferos terrestres de España. Organismo Autónomo Parques Nacionales, Madrid.

Passey, B.H., Cerling, T.E., 2002. Tooth enamel mineralization in ungulates: Implications for recovering a primary isotopic time-series. Geochim. Cosmochim. Acta 66, 3225–3234.

Podlesak, D.W., Torregrossa, A., Ehleringer, J.R., Dearing, M.D., Passey, B.H., Cerling, T.E., 2008. Turnover of oxygen and hydrogen isotopes in the body water, CO2, hair, and enamel of a small mammal. Geochim. Cosmochim. Acta 72, 19–35.

Pryor, A.J.E., Stevens, R.E., Connell, T.C.O., Lister, J.R., 2014. Quantification and propagation of errors when converting vertebrate biomineral oxygen isotope data to temperature for palaeoclimate reconstruction. Palaeogeogr. Palaeoclimatol. Palaeoecol. 412, 99–107.

Rosário, I.T., Mathias, M.L., 2004. Annual weight variation and reproductive cycle of the wood mouse (*Apodemus sylvaticus*) in a Mediterranean environment. Mammalia 68, 133–140.

Royer, A., Lécuyer, C., Montuire, S., Amiot, R., Legendre, S., Cuenca-Bescós, G., Jeannet, M., Martineau, F., 2013a. What does the oxygen isotope composition of rodent teeth record? Earth Planet. Sci. Lett. 361, 258–271.

Royer, A., Lécuyer, C., Montuire, S., Escarguel, G., Fourel, F., Mann, A., Maureille, B., 2013b. Late Pleistocene (MIS 3-4) climate inferred from micromammal communities and $\delta^{18}O$ of rodents from Les Pradelles, France. Quat. Res. 80, 113–124.

Royer, A., Lécuyer, C., Montuire, S., Primault, J., Fourel, F., Jeannet, M., 2014. Summer air temperature, reconstructions from the last glacial stage based on rodents from the site Taillis-des-Coteaux (Vienne), Western France. Quat. Res. 82, 420–429.

Rozanski, K., Araguás-Araguás, L., Gonfiantini, R., 1993. Isotopic Patterns in Modern Global Precipitation, in: Swart, P.K., Lohman, K.C., McKenzie, J., Savin, S. (Eds.), Climate Change in Continental Isotopic Records. Washington, pp. 1–36.

Salamolard, M., Butet, A., Leroux, A., Bretagnolle, V., 2000. Responses of an avian predator to variations in prey density at a temperature latitude. Ecology 81, 2428–2441.

Sans-Coma, V., Gosalbez, J., 1976. Sobre la reproducción de Apodemus sylvaticus L, 1758 en el nordeste ibérico. Miscelánea Zoológica III, 227–233.

Schrag, D.P., Adkins, J.F., Mcintyre, K., Alexander, J.L., Hodell, A., Charles, C.D., Mcmanus, J.F., 2002. The oxygen isotopic composition of seawater during the Last Glacial Maximum. Quat. Sci. Rev. 21, 331–342.

Sekour, M., Beddiaf, R., Souttou, K., Denys, C., Doumandji, S., Guezoul, O., 2011. Variation saisonnière du régime alimentaire de la Chouette chevêche (*Athene noctua*) (Scopoli, 1769) dans l' extrême Sud-Est du Sahara algérien (Djanet , Algérie). Rev. d'Écologie (La Terre la Vie) 66, 79–91.

Skrzypek, G., Sadler, R., Wi, A., 2016. Reassessment of recommendations for processing mammal phosphate $\delta^{18}O$ data for paleotemperature reconstruction. Palaeogeogr. Palaeoclimatol. Palaeoecol. 446, 162–167.

Sommer, R.S., Nadachowski, A., 2006. Glacial refugia of mammals in Europe: Evidence from fossil records. Mamm. Rev. 36, 251–265.

Sundell, J., Huitu, O., Henttonen, H., Kaikusalos, A., Korpimäki, E., Pietiäinen, H., Saurola, P., Hanski, I., 2004. Large-scale spatial dynamics of vole populations in Finland revealed by the breeding success of vole-eating avian predators. J. Anim. Ecol. 73, 167–178.

Sunyer, P., Muñoz, A., Mazerolle, M.J., Bonal, R., Espelta, J.M., 2016. Wood mouse population dynamics: Interplay among seed abundance seasonality, shrub cover and wild boar interference. Mamm. Biol. 81, 372–379.

Uriarte, A. (2003) Historia del clima de la Tierra. Vitoria-Gasteiz: Servicio Central de Publicaciones del Gobierno Vasco.

Vallverdú, J., López-García, J.M., Blain, H.-A., Saladíe, P., Uzquiano, P., Bischoff, J., Vaquero, M., 2012. El Pleistocè de la cova dels Xaragalls, in: III Jornades Del Bosc de Poblet i les Muntanyes de Prades. pp. 241–250.

von Grafenstein, U., Erlenkeuser, H., Müller, J., Trimborn, P., Alefs, J., 1996. A 200 year mid-European air temperature record preserved in lake sediments: An extension of the $\delta^{18}O_p$-air temperature relation into the past. Geochim. Cosmochim. Acta 60, 4025–4036.

Yalden, D.W., 2009. Dietary separation of owls in the Peak District. Bird Study 32, 122–131.

Zazzo, A., Lécuyer, C., Mariotti, A., 2004. Experimentally-controlled carbon and oxygen isotope exchange between bioapatites and water under inorganic and microbially-mediated conditions. Geochim. Cosmochim. Acta 68, 1–12.

Chapter 6.
Combined palaeoecological methods using small-mammal assemblages to decipher environmental context of a long-term Neanderthal settlement in northeastern Iberia

ABSTRACT

Recurrent long- and short-term Neanderthal occupations occurred in the Abric Romaní rock shelter (Capellades, Barcelona, Spain) for more than 20,000 years. This provides a unique opportunity to enhance our understanding of the evolution of behavioral strategies of these human groups. The site has a long and high-resolution sequence with 17 levels completely excavated, 14 of which are presented in this work, from D to Q; ca. 40-60 ka. These levels have generated extensive research concerning Neanderthals' hunting, lithic production, and fire technology. The ecological framework in which these populations established repeated occupations is essential in order to understand their adaptative behavior. In this chapter is presented the evolution of palaeoenvironment under which these populations lived using different methods of palaeoecological reconstruction from small-mammal remains along the entire sequence. The study is completed with taphonomic analyses that locate the origin of their accumulation in the action of owls (Category 2-3). Among post-depositional agents, plant activity, cracking, and manganese oxide precipitations are common; describing a humid fossiliferous microenvironment where intense human occupation occurred. To reconstruct the palaeotemperature, oxygen isotope analyses were performed on rodent incisors from the richest levels (D, E, N and O). The medium to low intra-level ranges of oxygen isotopic values indicate a preferential accumulation moment of small mammals, which is likely related to spring-summer predator activity. The species of small-mammal most commonly identified through the sequence are Arvicola sapidus, Apodemus sylvaticus and Iberomys cabrerae. Throughout the sequence, the landscape evolution is marked by an extended forestall cover and abundant water resources. Climatic conditions were globally cooler and slightly wetter than present, but rather stable across the sequence. The greater relative presence of Mid-European small-mammal species and the estimated lower palaeotemperatures correspond to relatively cooler episodes, such as stadial events, in levels E and O. However, certain discrepancies in palaeotemperature estimations are detected between oxygen isotopic analyses and other methods based on species occurrence. Both pollen and anthracological studies with micro-wear and stable isotope analyses in large mammals allow for an extensive discussion of ecological evolution across the sequence from an interdisciplinary approach.

1. Introduction

The Abric Romaní sequence constitutes a methodological challenge for testing and comparing different environmental proxies, not only because several studies have focused on the environmental features of this rock-shelter, including charcoal, pollen or dental wear analyses studies (e.g., Allué et al., 2017; Burjachs et al., 2012; Burjachs and Julià, 1996, 1994; López-García, 2011; López-García et al., 2014; Vaquero et al., 2013), but also because the different aspects of human behavior have been studied in each of its levels through analysis of lithic and large mammal assemblages or combustion structures (Allué et al., 2017; Bargalló et al., 2016; Fernández-Laso et al., 2010; Gabucio et al., 2017; Gómez de Soler, 2016; Marín et al., 2017a; Romagnoli et al., 2018; Vallverdú et al., 2012; Vaquero et al., 2012; among others). Thus, the high-resolution stratigraphy, complemented with different dating methods, and the exceptional preservation of materials at this site, provide detailed knowledge of subsistence strategies of groups of Neanderthals well-settled in this region. The aim of this chapter is to understand the environmental evolution surrounding the subsistence of these populations. To understand the landscape and climate

evolution of this region and achieve a complete environmental reconstruction, all available small-mammal assemblage data (historical and new) regarding the origin and post-depositional processes of the assemblages are presented, as well as oxygen isotope composition analyses on murid teeth to facilitate past temperature estimations.

2. The Abric Romaní sequence

The Abric Romaní archaeological site is a rock-shelter in the Quaternary travertine cliff formation known as "Cinglera del Capelló", near the town of Capellades (Barcelona, Spain). The coordinates are 41°32'N and 1°41'30"E and the altitude is 280 m a.s.l. (Fig. 6.1A). The site is located 70 m above a narrow gorge of the Anoia river. This gorge constitutes a strategic passage between inland mountains and the coastal plain, offering a wide variety of resources to the prehistoric groups who made use of the area (Carbonell et al., 1996; Fernández-Laso et al., 2010; Vallverdú et al., 2012). Ongoing excavations started in 1983, since then the full extent of the rock-shelter surface (around 250-300 m^2) has been excavated (Bartrolí et al., 1995; Carbonell et al., 1996, 1994; Chacón et al., 2013). The stratigraphy is made up of 20 m of well-stratified travertine sediments. Seventeen levels (labeled from A to Q) have been excavated completely to date. These belong to the Middle Palaeolithic, only except for the uppermost Level A, which has been attributed to the Proto-Aurignacian (Carbonell et al., 1996; Giralt and Julià, 1996; Vaquero and Carbonell, 2012; Vaquero et al., 2013) (Fig. 6.1B). Dates obtained by U-series and ^{14}C AMS provide a chronological range from ca. 70 ka (from the base of the sequence) to ca. 40 ka (Level A) (Bischoff et al., 1994, 1988). The travertine formation is associated with a waterfall system that was intermittently active during the Pleistocene and connected regional aquifer springs with the Anoia river. Rock fragmentation and alluvial and biochemical sedimentary processes have generated beds of consolidated stones, gravel, calcarenites and calcilutites interleaved with sandy and well-delimited thin archaeological levels (Bischoff et al., 1988; Vaquero et al., 2013).

The different archaeological levels of the Abric Romaní sequence are the result of the accumulation of an unknown number of occupational events. Different occupation models have been proposed, distinguishing between long-term and short-term (and/or non-residential) occupations events (Chacón et al., 2013; Vallerdú et al., 2005; Vallverdú et al., 2010; Vaquero et al., 2012). Lithic assemblages are typical of Middle Palaeolithic sites and are mainly composed of flakes, whereas cores and retouched flakes are scarce (Bargalló, 2014; Chacón et al., 2007; Chacón and Fernández-Laso, 2007; Picin et al., 2014; Vaquero, 2008; Vaquero et al., 2001). The predominant raw material is flint from regional areas (10-30 km), but other common raw materials (such as quartz and limestone) are from a local source (Gómez de Soler, 2016, 2007; Morant and García-Antón, 2000; Picin and Carbonell, 2016; Vaquero et al., 2012). Faunal remains are abundant in all levels and a total of thirteen taxa have been identified. Herbivores are predominant, with reed deer (*Cervus elaphus*) and horse (*Equus ferus*) being the most abundant species. Remains of aurochs (*Bos primigenius*) and chamois (*Rupicapra pyrenaica*) are also common. In addition, scarce remains of rhinoceros (*Stephanorhinus* cf. *hemitoechus*) and proboscidean have been documented. The faunal record is the result of Neanderthal activities, who had primary access to animal carcasses. Carnivores are present but rare (Cáceres et al., 1998; Chacón and Fernández-Laso, 2007; Fernández-Laso et al., 2010; Gabucio et al., 2018, 2017, 2014, Marín et al., 2017a, 2017b, Rosell et

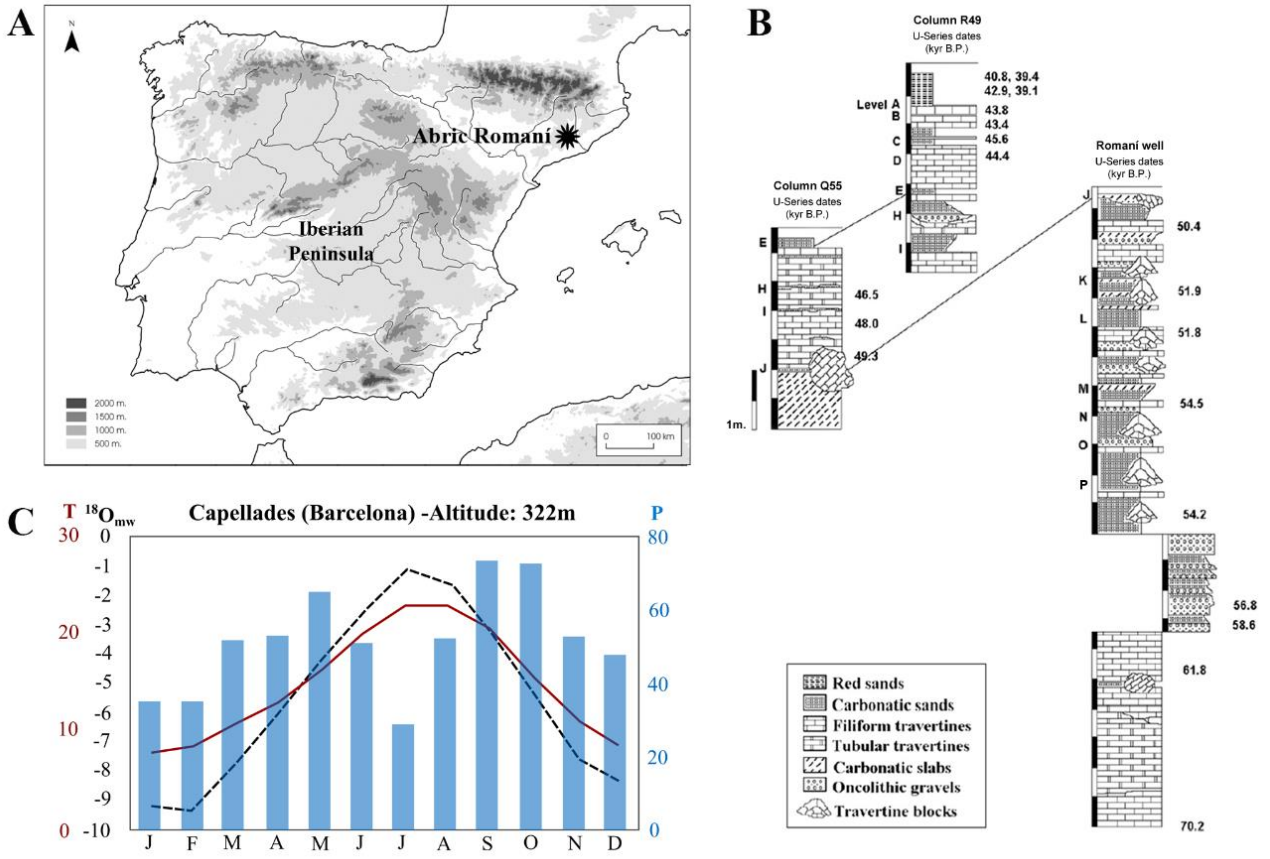

Figure 6.1 (A) Location of the Abric Romaní site in Iberia; (B) Stratigraphy of Abric Romaní with U/Th dates (Bischoff et al., 1988); (C) Current monthly temperatures (red line; T; in ºC) and precipitations (bars; P; in mm)(Climate-data.org) and present-day oxygen isotope composition of meteoric waters (dash black; $\delta^{18}O_{mw}$; in ‰ V-SMOW) (Bowen, 2017) of Capellades.

al., 2012b, 2012a). Hearths and wood imprints have been documented at all archaeological levels. Hearths are normally reused, especially during long-term occupations (Allué et al., 2017, 2012; Carbonell et al., 1996; Carbonell and Castro-Curel, 1992; Carrancho et al., 2016; Castro-Curel and Carbonell, 1995; Solé et al., 2013; Vallverdú et al., 2012; Vaquero and Pasto, 2001). It has also been possible to differentiate between domestic areas where specific activities were performed, such as sleeping areas, cleaning zones or animal processing areas (Bargalló et al., 2016; Cabanes et al., 2007; Carbonell, 2012; Carrancho et al., 2016; Chacón et al., 2007; Vallverdú et al., 2012; Vaquero, 2008; Vaquero and Pasto, 2001).

Abric Romaní's sequence has provided several environmental proxy-data through floral and faunal records with different resolution degrees. The sequence extends from Marine Isotope Stage (MIS) 4 to the first part of the MIS 3, including the Dansgaard-Oeschger (D-O) cycles (from 19 to 12) and the Heinrich Events (HE) 6 and 5 (Burjachs et al., 2012). Initial pollen analyses differentiated five different climatic phases associated with five palynological phases between the final phase of MIS 5 and the Hengelo Interstadial (Burjachs and Julià, 1996, 1994). Pollen analyses and the anthracological record confirm the importance of the montane pine forest growing near the site and indicate that *Pinus* dominated throughout the

entire sequence (Allué et al., 2012; Burjachs et al., 2012; Burjachs and Allué, 2003; Burjachs and Julià, 1994). Indeed, hearths from site yielded large amounts of charcoals, and in all layers *Pinus* type *sylvestris* dominated (Allué et al., 2017). However, minor secondary vegetation formations of Mediterranean and mid-European character also appeared. Along the sequence are expansions and contractions of pine trees and related thermophilous taxa (such as cf. *Juniperus, Quercus* or *Olea*), depending on whether the climatic pulsation resulted in wet and warm or cold and arid episodes (Burjachs et al., 2012). Dental wear analyses on ungulates have confirmed the presence of various biotopes near the site, in both closed and open habitats, where these animals were hunted. Micro and macro faunal remains confirm the presence of open forest landscapes, according to animal adaptations to different biota. Previous small-mammal studies (Allué et al., 2012; Burjachs et al., 2012; Fernández-García et al., 2016; López-García, 2011, 2008; López-García et al., 2009; López-García and Cuenca-Bescós, 2010; López García, 2007) point to assemblages dominated by open forests dwellers and species requiring relatively humid environments, some related to stable water sources. The remains of amphibians and squamate reptiles are scarce at the site (only *Bufo bufo, Bufo calamita, Rana temporaria, Lacertidae* indet., *Anguis fragilis*, and *Vipera aspis* were identified), and their presence is related to a colder and more humid climate and a wet and cold forest environment. Derived preliminary palaeoclimatic estimations denote mean annual temperatures notably lower, and mean annual precipitations higher, than present-day in this area. According to pollen analysis, moments when open-landscapes species occurred are related to stadial phases, which complemented with previous past temperatures estimations based on small vertebrates studies, has led to different climatic correlations by Burjachs et al. (2012), Fernández-García et al. (2018), López-García (2011) and López-García et al. (2014) (Table 6.1) (see Chapter 4).

Capellades is located in an area currently included in the continental sub-humid Mediterranean climate (Servei Meteorològic de Catalunya, 2018). The climate is generally warm and temperate (mean annual temperatures around 14 °C), but with dry summers (21-23 °C) and cool winters (7-8 °C), with a consequent thermic annual oscillation of 15 °C. The mean annual rainfall is between 550 and 650 mm. The wet seasons are spring and autumn, while winter and summer are drier (Climate-data.org; Servei Meteorològic de Catalunya, 2018). Average monthly temperatures are coherent with monthly oxygen isotope compositions of meteoric water estimated for the area (OIPC data, Bowen, 2017; climate-data.org) (Fig. 6.1C).

3. Material and methods

3.1 Recovering, sampling and identification

The small mammal remains included in this analysis consist mainly of isolated teeth and disarticulated bones recovered from sediment samplings from the completely excavated surface, recovered during excavation seasons between 1990 and 2017. Remains were collected by washing and sieving the sediment, with two superimposed meshes of 5 mm and 0.5 mm and subsequently selected by hand-picking. The sampling strategy consisted of a random selection of 1x1m squares dispersed over each level at the site. From a total of 7333 remains, a minimum of 500 individuals have been identified, including 22 taxa identified at the species level (Fig. 6.2; Table 6.2). Remains were observed under light microscopes (Exacta-Optech LFZ 10x-90x; Olympus SZ-PT 18x-50x). Reference criteria for taxonomic identification are detailed in Chapter 2, Chapter 4 and Appendix 1. All the remains

	Age (ka BP)	Pollen (Burjachs and Julià, 1994; 1996)	Multidisciplanar approach: pollen, charcoals, use wear and small vertebrates (Burjachs et al., 2012)	Sedimentary analyses (Vaquero et al., 2013)	Small vertebrates (López-García et al., 2014)	Charcoals (Allué et al., 2017)
Level D	Plat. Sup.: 44.4 (U-series) / Plat. Inf.:44.9 ±2.5 (U-series) / 40.6 ±0.9 (^{14}C AMS)	Palynological Phase 5 (G-A): Warm with arboreal taxa increment. Expansion of pioneer taxa (*Junisperus*, *Pinus*) and mesotermophilous taxa (*Quercus*, *Olea-Phyllyrea*). Decrease of Asteraceae and *Artemisia*	Correlation with GI 12. Cool interstadial. Extension of pioneer trees (Cupressaceae and *Pinus*) and increase of termophilous taxa (*Quercus* spp. and *Olea-Phillyrea*). Small-mammal estimations (MAT=-5.7/-5.4 ºC; MAP=+150/+60 mm)	Capelló V sequence - Romaní sedimentary unit 1 (D-B): Thick tufas and speleothems in the base indicate a warm and wet period, correlated with an ending Bond cylce.	Cool and less wet intestadial. MAT=-5.4 ºC; MAP=+60 mm	Dominance of *Pinus* type *sylvestris*. Most taxa-diverse level, with mesothermophilous taxa *(Acer, Vitis, Quercus* spp., *Olea, Hedera*)
Level E	43.2 ±1.1 (^{14}C AMS)			Capelló VI sequence - Romaní sedimentary unit 2 (E-J): Sedimenary facies indicate interstadial conditions were dominant. Harsh conditions only in top of unit 2, irregular bed of red sands related to aeolian activity, absence of dripping and abrupt lithological change. The end of this stage is correlated with HE5.	Correlation with HE5. Mid-European species present (*Rana temporaria, Microtus arvalis, Microtus agrestis*). MAT=-5.7 ºC; MAP=+148 mm	Dominance of *Pinus* type *sylvestris*. Presence of *Rhamnus cathartica/saxatilis*
Level J	Plat. Sup.: 49.3 ±1.6 (U-series) / Plat. Inf.: 50.4 ±1.6 (U-series) / 47 ±2.1 (14C AMS)	Palynological Phase 3 (O-J): Cold phase interrupted by warm and humid events. Dominance of *Artemisia,* Asteraceae, Poaceae and *Pinus*. Considerable oscillations in pollen curves and ocurrence of mesotermophilous taxa (*Quercus* spp., *Olea-Phyllyrea*, *Rhamnus*).	Correlation with HE5 (Ja-H). Cold phase with aridity peaks, intermidiated phase of pine forest spreading. Forest steppe with grassland and xerophytic steppe elements (Asteraceae, Poaceae, *Artemisia*). Abundance of *Bufo calamita*.		Cool and less wet period. MAT=-5.4 ºC; MAP=+60 mm	Dominance of *Pinus* type *sylvestris*. Presence of *Populus/Salix*
			Correlation with D-O14 (M-J). Pine forest development and warm temperate taxa. Usewear analysis on ungulates indicate patchy landscape. Small-mammal estimations (MAT=-5.4 ºC; MAP=+60 mm)			Dominance of *Pinus* type *sylvestris*
Level K	Plat. Sup.: 50 ±1.6 / Plat. Inf: 51.9 ±9 (U-series)			Capelló sequence VII- Romaní sedimentary unit 4 and 3 (K-O): abrupt changes from Mediterranean-type temperate groves to arid steppe. Tufa points a trasition from the base of unit 3, a interstadial stage with low seasonality in dripping activities, to the higher seasonality in rainfall in top of the unit. Correlation D-O17 to D-O14.	No data.	Dominance of *Pinus* type *sylvestris*
Level N	54.9 ±0.1 / 55.1 ±0.1 (U-series)		Correlation with GI16. Pollen records maintenance of pine forest with warm temperate taxa. Anthracology confirms predominance of pine grooves as firewoods. Small-mammal estimations (MAT=-4.6 ºC; MAP=+75 mm)		Cool and less wet period with lower summer temperatures. MAT=-4.5 ºC; MAP=+76 mm	Dominance of *Pinus* type *sylvestris*. Presence of *Populus/Salix*
Level O	Plat. Sup.: 54.2 ±0.4 / Plat. Inf.: 54.6 ±0.4 (U-series)		Correlation with GS17. Open forest, grassland and xerophytic steppe elements. Small-mammal estimations (MAT=-7.5 ºC; MAP=+350 mm)		Cold and wet period between GI14 and GI17. Mid-European taxa (*Rana temporaria, Sorex, Talpa, Microtus arvalis* and *Microtus agrestis)*. MAT=-7.5 ºC; MAP=+349 mm.	Dominance of *Pinus* type *sylvestris*. Presence of *Junisperus, Prunus* and *Sambucus*.

Table 6.1 Summary of palaeoenvironmental studies performed on the Abric Romaní sequence through different proxies. Dating information from Bischoff et al. (1988), Carbonell et al. (1994) and Sharp et al. (2016).

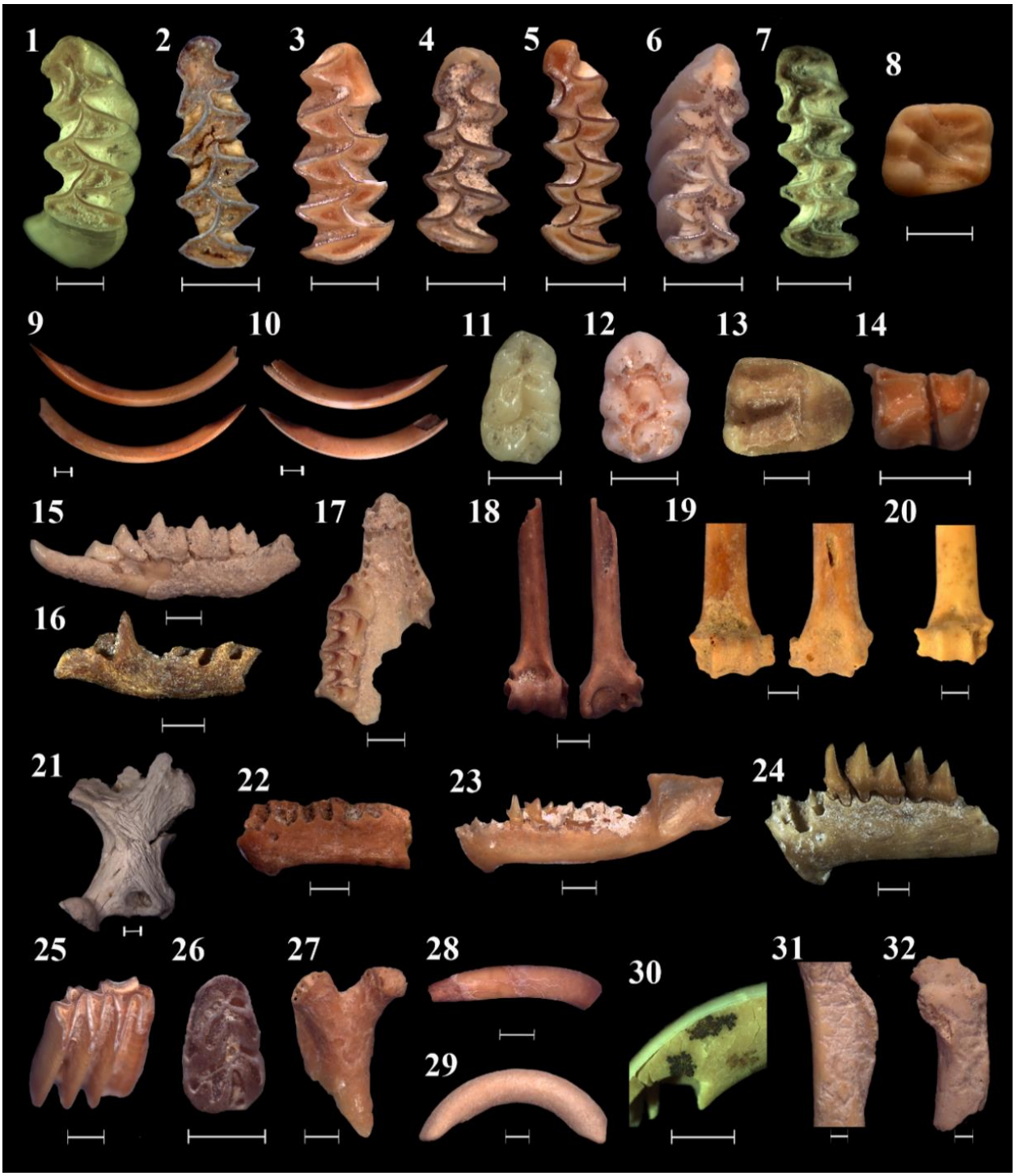

Figure 6.2 Small mammals of the Abric Romaní sequence and some associated taphonomic features. 1) left m1 of *Arvicola sapidus* from level O, occlusal view; 2) left m1 of *Microtus (Terricola) gerbei* from level Q, occlusal view; 3) right m1 of *Iberomys cabrerae* from level Q, occlusal view; 4) left m1 of *Chionomys nivalis* from level E, occlusal view; 5) left m1 of *Microtus arvalis* of level H, occlusal view; 6) right m1 of *M. (T.) duodecimcostatus* from level N, occlusal view, with manganese oxide pigmentation; 7) left m1 of *M. agrestis* from level O, occlusal view; 8) left m2 of *Eliomys quercinus* from level N, occlusal view; 9) left lower incisor of Arvicolinae from level D, in labial and lingual view, used in biochemical analysis; 10) right lower incisor of *Apodemus* cf. *sylvaticus* from level D, in labial and lingual, used in biochemical analysis; 11) left m1 of *A. sylvaticus* from level O, occlusal view; 12) right M1 of *A. sylvaticus* of level N, occlusal view; 13) right M1 of *Sciurus vulgaris* from level O, occlusal view; 14) right m2 of *Myotis* sp. from level N, occlusal view; 15) left mandible of *Crocidura russula* from level E, labial view, with travertine cementation; 16) right mandible of *Sorex minutus* from level O, labial view, burned; 17) maxilla of *Sorex* gr. *araneus-coronatus* from level E, occlusal view; 18) right humerus of *Pipistrellus pipistrellus* burned from level N;

(figure captation continues in the next page)

19) left humerus of *Myotis* gr. *myotis-blythii* from level D; 20) right humerus of *Plecotus* gr. *auritus-austriacus* from level E; 21) right humerus of *Talpa europaea* calcinated from level N; 22) left mandible of *Miniopterus* cf. *schreibersii* from level N, in labial view; 23) left mandible of *P. pipistrellus* from level N, in labial view; 24) left mandible of *Nyctalus lasiopterus* from level O, in labial view; 25) Arvicolinae molar with moderate digestion, level N; 26) left m1 of *A. sylvaticus* burned and with heavy digestion, level E; 27) right rodent femur with heavy digestion, level N; 28) rodent incisor with intra-mandibular digestion, level E; 29) rodent incisor completely covered by travertine patina and rounded, level E; 30) detail of dispersed manganese oxide pigmentation in a rodent incisor, level O; 31) rodent femur with generalized root corrosion, level J; 32) rodent femur with root corrosion, after round, level P. Scale 1 mm.

	Recount	*Crocidura russula*	*Sorex* gr. *araneus-coronatus*	*Sorex minutus*	*Neomys* gr. *fodiens-anomalus*	*Talpa europaea*	Soricidae indet.	*Myotis* sp.	*Myotis* gr. *myotis-blythii*	*Miniopterus* cf. *schreibersii*	*Plecotus* gr. *auritus-austriacus*	*Pipistrellus* sp.	*Pipistrellus pipistrellus*	*Nyctalus lasiopterus*	Chiroptera indet.	*Arvicola sapidus*	*Microtus arvalis*	*Microtus agrestis*	*Iberomys cabrerae*	*Chionomys nivalis*	*M. (Terricola) duodecimcostatus*	*M. (Terricola) gerbei*	*Apodemus sylvaticus*	*Eliomys quercinus*	*Sciurus vulgaris*	Rodentia indet.	Taxonomically indet.	Total
D	**NR (n)**	3					2		3						7	35	3	4	14		6		74	14		410	344	**919**
	MNI (n)	2							2		2					11	1	2	11		4		15	2				**52**
	MNI (%)	**4**							**4**		**4**					**21**	**2**	**4**	**21**		**8**		**29**	**4**				100
E	**NR (n)**	2	1				4				8	1			5	19	7	4	1	1	16		75	17		744	385	**1290**
	MNI (n)	1	1								2	1				3	6	4	1	1	1		23	3				**47**
	MNI (%)	**2.1**	**2.1**								**4.3**	**2.1**				**6.4**	**12.8**	**8.5**	**2.1**	**2.1**	**2.1**		**48.9**	**6.4**				100
F	**NR (n)**															2										4	8	**14**
	MNI (n)															1												**1**
	MNI (%)															**100**												100
H	**NR (n)**															11	2	1								57	4	**75**
	MNI (n)															2	2	1										**5**
	MNI (%)															**40**	**40**	**20**										100
I	**NR (n)**	1					1									15	1	2					2			21	26	**69**
	MNI (n)	1														3	1	1					1					**7**
	MNI (%)	**14.3**														**42.9**	**14.3**	**14.3**					**14.3**					100
J	**NR (n)**					2	6									74	4	2	5				6	2		309	175	**585**
	MNI (n)					1										7	3	1	3				2	1				**18**
	MNI (%)					**5.6**										**38.9**	**16.7**	**5.6**	**16.7**				**11.1**	**5.6**				100
K	**NR (n)**						1									210	2	1	3		4					110	81	**412**
	MNI (n)															11	1	1	2		3							**18**
	MNI (%)															**61.1**	**5.6**	**5.6**	**11.1**		**16.7**							100
L	**NR (n)**															26			1		2		2			22	2	**55**
	MNI (n)															4			1		1		1					**7**
	MNI (%)															**57.1**			**14.3**		**14.3**		**14.3**					100
M	**NR (n)**					21										21			1							19	17	**79**
	MNI (n)					2										2			1									**5**
	MNI (%)					**40**										**40**			**20**									100
N	**NR (n)**					7	5	1		1			7		4	54		1	11		10		41	12		543	126	**823**
	MNI (n)					3		1		1			2			6		1	6		9		8	2				**39**
	MNI (%)					**7.7**		**2.6**		**2.6**			**5.1**			**15.4**		**2.6**	**15.4**		**23.1**		**20.5**	**5.1**				100
O	**NR (n)**	9	3	1	10	31	12						1	2	1	266	54	45	87		46		310	55	10	1193	481	**2617**
	MNI (n)	3	2	1	2	7							1	1		55	30	25	45		25		69	8	2			**276**
	MNI (%)	**1.1**	**0.7**	**0.4**	**0.7**	**2.5**							**0.4**	**0.4**		**19.9**	**10.9**	**9.1**	**16.3**		**9.1**		**25.0**	**2.9**	**0.7**			100
P	**NR (n)**						2									59					1		7			91	26	**186**
	MNI (n)															8					1		2					**11**
	MNI (%)															**72.7**					**9.1**		**18.2**					100
Q	**NR (n)**					4	4								1	12			12		1	2	2		1	126	44	**209**
	MNI (n)					1										2			6		1	1	2		1			**14**
	MNI (%)					**7.1**										**14.3**			**42.9**		**7.1**	**7.1**	**14.3**		**7.1**			100

Table 6.2 Number of remains (NR), minimum number of individuals (MNI) and the MNI as a percentage of the total for the small-mammal assemblage Abric Romaní sequence.

recovered were counted (NR), differentiating the number of identified specimens (NISP) and grouped using the minimum number of individuals (MNI) method, which involves counting the most highly represented diagnostic element while considering laterality for each species.

3.2 Taphonomic analysis

This taphonomic study is based on the observation and description of the superficial alterations of skeletal elements (Andrews, 1990; Fernández-Jalvo et al., 2016), including the differentiation between predation and post-depositional alterations (for a detailed explanation of the taphonomic analyses see Chapter 2 and Chapter 4). All recovered remains from each level were included in the analysis, except in levels O and D. These levels present a high amount of small-mammal material available, thus, samples dispersed over the complete level surface were randomly selected. This study considers three main aspects of detected predation effects (Andrews, 1990; Fernández-Jalvo et al., 2016; Fernández-Jalvo and Andrews, 1992): anatomical representation, breakage, and corrosion by digestion. Results are compared with indices from current predation reference collections developed by Andrews (1990) and recent revision studies (e.g., Fernández-Jalvo et al., 2016). Incisors, molars, and femora of rodents, talpids, soricids, and chiropters were inspected for markers of breakage and digestion; however, only rodents were included in final analyses due to low sample sizes for other groups. Post-depositional alterations were also evaluated in molars, incisors, and femora of all orders in terms of the absence/presence of these alterations and, in some cases, their degree and location. A complete taphonomic analysis of level O was completed by Fernandez-Garcia et al. (2018), which related the origin of the small-mammal assemblage to the activity of the tawny owl (*Strix aluco*). The authors found that post-depositional alterations indicated a fossiliferous microenvironment of relative environmental humidity and occasional water flows. Additionally, some preliminary taphonomic comments focused on digestion were done for other levels of this sequence (Allué et al., 2012; Burjachs et al., 2012; López-García et al., 2014), but the present work constitutes the first complete taphonomic analysis of levels N, K, J, E and D.

3.3 Palaeoenvironmental reconstruction

To reconstruct the ecological conditions during the deposition of Abric Romaní, several methodologies were used. First, the species evenness and diversity were evaluated (Margalef, 1974) using Simpson's Diversity Index (Simpson, 1949), via Paleontological Statistics (PAST) software (Hammer et al., 2001). Second, landscape reconstructions were made based on the Habitat Weighting Method, a quantitative method developed by Evans et al. (1981) and Andrews (2006). This method is based on the distribution of each taxon in the habitat(s) in which it is currently present on the Iberian Peninsula (Palomo et al., 2007). Finally, species occurrence is evaluated under chorotype classification previously established for present-day small-mammal faunas in Catalonia by López et al. (2006) and Sans-Fuentes and Ventura (2000). Detailed information of these methods of palaeoenvironmetal reconstruction and species classification employed in this work according to chorotypes and weighting habitat detailed in Chapter 2 and 4.

3.4 Oxygen isotope analysis on rodent teeth

Oxygen isotope compositions were measured on 38 teeth from levels O, N, E and D. To avoid potential issues of interspecific variability, *Apodemus sylvaticus* remains were preferentially selected, with 34 incisors from at least 21 individuals (Fig. 6.2; Table 6.3). Four incisors from the subfamily Arvicolinae, from a minimum of four individuals, were also included. Eight to ten samples were selected from each layer in order to gather a representative range of samples (Lindars et al., 2001; Navarro et al., 2004; Royer et al., 2013a).

Level	Taxon	Remain	Laterality	Location	$\delta^{18}O_p$ (‰ V-SMOW)	SD	$\delta^{18}O_{mw}$ (‰ V-SMOW)
D	*Apodemus* cf. *sylvaticus*	Lower incisor	right	*in situ*	**21.1**	0.2	**-3.0**
D	*Apodemus* cf. *sylvaticus*	Lower incisor	left	isolated	**19.2**	0.5	**-4.6**
D	*Apodemus* cf. *sylvaticus*	Lower incisor	left	*in situ*	**18.8**	0.1	**-4.9**
D	*Apodemus* cf. *sylvaticus*	Lower incisor	right	isolated	**18.8**	0.4	**-5.0**
D	Arvicolinae	Lower incisor	right	*in situ*	**18.7**	0.3	**-5.0**
D	Arvicolinae	Lower incisor	left	isolated	**18.0**	0.5	**-5.6**
D	*Apodemus* cf. *sylvaticus*	Lower incisor	left	isolated	**18.0**	0.3	**-5.6**
D	*Apodemus* cf. *sylvaticus*	Lower incisor	left	isolated	**17.4**	0.1	**-6.0**
D	*Apodemus* cf. *sylvaticus*	Lower incisor	left	isolated	**17.3**	0.3	**-6.1**
D	*Apodemus* cf. *sylvaticus*	Lower incisor	right	isolated	**17.1**	0.8	**-6.3**
E	*Apodemus* cf. *sylvaticus*	Lower incisor	left	isolated	**23.5**	0.1	**-1.0**
E	*Apodemus* cf. *sylvaticus*	Lower incisor	left	isolated	**20.2**	0.5	**-3.8**
E	*Apodemus* cf. *sylvaticus*	Lower incisor	right	isolated	**19.8**	0.3	**-4.1**
E	*Apodemus sylvaticus*	Lower incisor	left	*in situ*	**19.2**	0.4	**-4.6**
E	*Apodemus sylvaticus*	Lower incisor	right	*in situ*	**19.0**	0.4	**-4.7**
E	*Apodemus sylvaticus*	Lower incisor	left	*in situ*	**18.8**	0.7	**-4.9**
E	Arvicolinae	Lower incisor	right	*in situ*	**18.2**	0.2	**-5.4**
E	Arvicolinae	Lower incisor	right	isolated	**17.9**	0.1	**-5.7**
E	*Apodemus sylvaticus*	Lower incisor	left	*in situ*	**17.8**	0.2	**-5.8**
E	*Apodemus sylvaticus*	Lower incisor	right	*in situ*	**16.8**	0.3	**-6.6**
N	*Apodemus* cf. *sylvaticus*	Lower incisor	left	isolated	**21.4**	0.5	**-2.8**
N	*Apodemus* cf. *sylvaticus*	Lower incisor	left	isolated	**20.7**	0.6	**-3.4**
N	*Apodemus* cf. *sylvaticus*	Lower incisor	right	isolated	**20.1**	0.7	**-3.9**
N	*Apodemus* cf. *sylvaticus*	Lower incisor	right	isolated	**18.9**	0.1	**-4.8**
N	*Apodemus* cf. *sylvaticus*	Lower incisor	right	isolated	**17.5**	0.3	**-6.0**
N	*Apodemus* cf. *sylvaticus*	Lower incisor	right	isolated	**17.2**	0.8	**-6.3**
N	*Apodemus* cf. *sylvaticus*	Lower incisor	right	isolated	**17.0**	0.7	**-6.4**
N	*Apodemus* cf. *sylvaticus*	Lower incisor	left	isolated	**15.7**	0.3	**-7.5**
O	*Apodemus* cf. *sylvaticus*	Upper incisor	left	isolated	**21.4**	0.6	**-2.8**
O	*Apodemus* cf. *sylvaticus*	Lower incisor	right	isolated	**20.9**	0.6	**-3.2**
O	*Apodemus* cf. *sylvaticus*	Lower incisor	left	isolated	**20.5**	0.2	**-3.5**
O	*Apodemus* cf. *sylvaticus*	Lower incisor	right	isolated	**19.7**	0.4	**-4.2**
O	*Apodemus* cf. *sylvaticus*	Lower incisor	left	isolated	**19.1**	0.1	**-4.7**
O	*Apodemus* cf. *sylvaticus*	Upper incisor	left	isolated	**18.8**	0.3	**-4.9**
O	*Apodemus* cf. *sylvaticus*	Lower incisor	left	isolated	**18.8**	0.6	**-4.9**
O	*Apodemus* cf. *sylvaticus*	Lower incisor	right	isolated	**18.4**	0.1	**-5.2**
O	*Apodemus sylvaticus*	Lower incisor	left	*in situ*	**18.2**	0.3	**-5.4**
O	*Apodemus* cf. *sylvaticus*	Lower incisor	right	isolated	**16.7**	0.2	**-6.7**

Table 6.3 Oxygen isotope composition of tooth enamel phosphate ($\delta^{18}O_p$; ‰ V-SMOW) from rodent lower incisors from Abric Romaní. The table includes the stratigraphic layer, identified taxa and the conversion to the oxygen isotope composition of meteoric waters ($\delta^{18}O_{mw}$; ‰ V-SMOW) following the Royer et al. (2013a) oxygen isotope fractionation equation. SD, Standard Deviation.

The enamel tooth samples were treated following the wet chemistry procedure described by Crowson et al. (1991) that was subsequently slightly modified by Lécuyer et al. (1993) and adapted for small-sample weights (1-3 mg of apatite) by Bernard et al. (2009), Fourel et al. (2011), and Lécuyer et al. (2007). For detailed information about sampling criteria and wet-

chemistry protocol see Chapter 2 and Chapter 5. Based on phosphate chemical yields measured during the wet chemistry procedure, clustered phosphorus pentoxide (P_2O_5) contents close to 40 wt% indicate that the original stoichiometry of the teeth was most likely preserved. Oxygen isotope compositions were measured using a high-temperature elemental analyser (EA)-pyrolysis (Py) interfaced in continuous flow (CF) mode to an isotopic ratio mass spectrometer (IRMS) (EA-Py-CF-IRMS technique performed at UMR 5276 LGL; Fourel et al., 2011; Lécuyer et al., 2007). The average standard deviation for the Abric Romaní sequence samples is 0.36 ± 0.07‰ (n=48).

3.5 Palaeotemperatures estimations

Mean annual temperatures (MAT) were calculated from oxygen isotope compositions ($\delta^{18}O$) of levels O, N, E and D. This work follows the methodology detailed in Chapter 5 for palaeotemperature estimation, including the three-step strategy proposed by Fernández-García et al. (under review) for $\delta^{18}O_p$ from rodent teeth accumulated in the Iberian Peninsula, which considers the seasonality of the rodent assemblages in the warmest season and the regional peculiarities of the Iberian Peninsula. In parallel, past temperatures and precipitations were estimated by two independent qualitative palaeoenvironmental methods: the mutual ecogeographic range (MER) method (Blain et al., 2009, 2016; López-García, 2011; see Chapter 2 and 4) and the bioclimatic model (BM) method (Hernández Fernández, 2001; Hernández Fernández et al., 2007; see Chapter 2). Using MER, Iberian species distribution maps (10x10 km UTM square grid) were obtained from Palomo et al. (2007). The current climatic conditions of the intersecting area (AEMET & IMP, 2011) were used to infer the MAT and mean annual precipitations (MAP). *Iberomys cabrerae* and bat species were excluded in this analysis due to anthropic-conditionate distribution and little-known and fragmentary distributions, respectively. Using the BM, present-day $\delta^{18}O_{mw}$ values for the Abric Romaní area were obtained using the Online Isotopes in Precipitation Calculator (OIPC; Bowen, 2017) (Fig. 6.1C). This online software employs an algorithm based on datasets collected by the Global Network for Isotopes in Precipitation (GNIP), operated by the International Atomic Energy Agency and the World Meteorological Organization (IAEA/WMO, 2018). The current-temperature data for the Abric Romaní area are from Climate-Data.org (https://es.climate-data.org/).

4. Results and discussion

4.1 Origin of small-mammal accumulation in the Abric Romaní

Fragmentary and uneven representation of remains were detected along the sequence. Some levels contained a low number of remains and, consequently, individuals (Table 6.2). Levels poorest in small-mammal remains (such as F, H, I, L, M, P and Q) cannot be explained by intensive destructive activity of predators such as small carnivores because a preliminary analysis did not detect notable digestion of them. The small mammals' absence is most likely attributable to external factors, such as absence of or lower frequentation by owls to the site, or post-depositional processes. As such, NR (>400) and MNI (>15) were only high enough to perform reliable taphonomic interpretations of levels O, N, K, J, E, and D. The taphonomic analysis includes 6,517 remains; in each subunit, between 80 and 85% of total remains was anatomically identified. The most abundant small-mammal assemblages are found at levels O, D and E. Low sample sizes at levels K and J necessitate more conservative interpretations. Rodents are the most represented order, with an abundance between 82% (level N)

and 96% (level O). Among rodents, remains comprise mostly arvicolins and murins and, occasionally, glirids and sciurids. A minimum of 27 individuals from the Soricidae and Talpidae families were recovered in total, with relative abundances ranging from 2.5% (level O; MNI=7) to 7.7% (level N; MNI=3). Similarly, remains from the family Chiroptera were only recovered from levels O, N, E and D, with a total minimum number of 13 individuals and with a relative abundance between 0.8% (level O; MNI=2) and 10.3% (level N; MNI=4) (Table 6.2).

The levels with better relative presence of skeleton elements are J and E, with total relative abundance of elements up to 60%; on the contrary, level O presents the major disequilibrium between identified individuals and preserved remains of these individuals (29.6%) (Table 6.4; Appendix 2.3.A). As indicated by indices comparing cranial and postcranial elements, postcranial bones are better represented in levels J and E, but almost at equilibrium. On the contrary, levels O, N, K and D show a high representation of cranial elements. However, this cranial disequilibrium is only related to better preservation of dental elements. Incisors are the best represented elements in all assemblages, and in some cases surpass the number of individuals indicated by molars alone. Proximal elements are more abundant than distal ones (between 50 and 80%). Indeed, humeri and femora are better preserved than mandibles and maxillae (>100%, except in level K). The proportion between isolated teeth and empty alveoli highlights the destruction of mandibles and maxillae (>150%), only expect for level K. Crania and, particularly, maxillae are the least abundant elements in all levels (<18%) (Appendix 2.3.A). In addition, a disproportion between incisors and molars is detected in all levels, with the former clearly overrepresented, indicating a significant loss of molars. Molars of arvicolids are more easily detached from their alveoli than the incisors, and breakage of loose teeth is usually greater than molars preserved *in situ*. However, this discrepancy may also be explained by collecting bias (Andrews, 1990; Fernández-Jalvo, 1992). Most recovered teeth in these assemblages are isolated. In levels O and N, less than 6% of molars and 2% of incisors were found in their alveolar place. At the other levels these values ranged between 24% to 30% for molars and 13% and 20% for incisors. The molars preserved *in situ* were most commonly those of murids, which have rhizodont teeth. At all studied levels, total breakage was 45% for incisors and >90% for femora. Molar breakage was more variable, with the highest rates being present at levels O and N (>40%) to the lowest rates at <13% in levels K, E, and D. Breakage and anatomical representation rates are not coincident with any predator profile (Andrews, 1990), even sometimes showing values included in Categories 4 and 5 of predators (Fig. 6.3). This discrepancy with modern collections is common in archaeological contexts where palimpsests and long-term post-depositional processes have occurred.

Digestion observed in these levels ranged between 8.4% at level J to 39.6% at level O (Table 6.4). Different degrees of digestion from light to heavy were observed, but extreme digestion was not detected in the sequence. Remains without digestion marks predominate the sample, while the most frequent degree of digestion is categorized as "light," with no evidence of extreme digestion. Based on these factors, and despite the fragmentation rates at some levels, the potential presence of predators in Cateogry 4-5 (Andrews, 1990), such as diurnal raptors or small carnivores, can be excluded (Fig. 6.3) (Andrews, 1990; Comay and Dayan, 2018; Fernández-Jalvo and Andrews, 1992; Lloveras et al., 2012, 2008a,

	O		N		K		J		E		D	
Recount												
NR (n)	2268		827		419		667		1390		946	
NISP (n)	1874		712		363		589		1131		781	
Rodentia NISP (n)	1676		629		279		366		825		483	
Rodentia MNI (n)	149		32		18		17		42		33	
Skeletal representation												
Relative Abundance Index (%)	29.6		54.6		38.3		67.7		61.9		42.8	
SD of Relative Abundance Index	26.6		64.8		27.2		31		29.1		19	
Proportional representation indeces												
Postcranial/Cranial Index	70		90		50		130		130		90	
Humerus+Femur/Maxilla+Mandible Index	120		200		60		150		130		100	
Radius+Tibia/Humerus+Femur Index	80		60		80		80		70		50	
Isolated teeth/Empty Alveolus Index	260		450		170		200		240		180	
Breakage												
Incisors fracture (%)	67.3		68.2		47.8		62.5		48.7		59.4	
Molars fracture (%)	41.3		50.5		9.2		23.7		12.6		12.9	
Femora fracture (%)	98.2		100		100		90.9		93.3		100	
Digestion	**n**	**%**	**n**	**%**	**n**	**%**	**n**	**%**	**n**	**%**	**n**	**%**
Total of digested elements	399	**39.6**	152	**37.5**	14	**8.4**	60	**31.9**	113	**25.9**	46	**17**
Light degree	275	27.3	121	29.9	8	4.8	33	17.6	64	14.6	32	11.8
Moderate degree	101	10	27	7	5	3	17	9	28	6	8	3
Heavy degree	23	2.3	4	1	1	0.6	10	5.3	21	4.8	6	2.2
Extreme degree	0	0	0	0	0	0	0	0	0	0	0	0
Digested incisors	151	**40.5**	109	**50.2**	4	**8.3**	18	**35.3**	45	**28.3**	11	**13.8**
Light degree	115	30.8	93	42.9	1	2.1	11	21.6	29	18.2	9	11.3
Moderate degree	30	8	14	6.5	2	4.2	4	7.8	10	6.3	2	2.5
Heavy degree	6	1.6	2	0.9	1	2.1	3	5.9	6	3.8	0	0
Extreme degree	0	0	0	0	0	0	0	0	0	0	0	0
Digested molars	191	**33.4**	33	**19.6**	9	**8.1**	29	**26.4**	51	**22.1**	23	**14.4**
Light degree	119	20.8	20	11.9	7	6.3	12	10.9	22	9.5	12	7.5
Moderate degree	55	9.6	12	7.1	2	1.8	10	9.1	14	6.1	6	3.8
Heavy degree	17	3	1	1	0	0	7	6	15	6	5	3
Extreme degree	0	0	0	0	0	0	0	0	0	0	0	0
Digested femora	57	**90.5**	10	**50**	1	**12.5**	13	**48.1**	17	**36.2**	12	**38.7**
Light degree	41	65.1	8	40	0	0.0	10	37	13	27.7	11	35.5
Moderate degree	16	25.4	1	5	1	12.5	3	11.1	4	8.5	0	0
Heavy degree	0	0	1	5	0	0	0	0	0	0	1	3
Extreme degree	0	0	0	0	0	0	0	0	0	0	0	0
Post-depositional agents	**n**	**%**	**n**	**%**	**n**	**%**	**n**	**%**	**n**	**%**	**n**	**%**
Cracking for humidity and temperature changes	910	**69**	238	**46.5**	28	**14.4**	64	**27.5**	114	**21.8**	50	**15.3**
Desquamation	92	**6.9**	3	**0.6**	0	**0**	0	**0**	0	**0**	0	**0**
Cementation	175	**13.2**	15	**2.9**	26	**13.3**	13	**5.6**	49	**9.4**	11	**3.4**
Manganese oxide pigmentation	621	**46.8**	159	**31.1**	21	**10.8**	70	**30**	233	**44.6**	61	**18.7**
Plant Activity	600	**45.2**	138	**27.0**	44	**22.6**	130	**55.8**	134	**25.7**	126	**38.5**
Water abrasion	73	**5.5**	8	**1.6**	1	**0.5**	4	**1.7**	8	**1.5**	2	**0.6**
Burned	192	**14.5**	32	**6.3**	0	**0**	6	**2.6**	60	**11.5**	9	**2.8**
Weathering	3	**0.2**	0	**0**	0	**0**	0	**0**	0	**0**	0	**0**

Table 6.4 Summary of taphonomic variables analyzed, including recounts (NR, number of remains; NISP, number of identified specimens; MNI, minimum number of individuals of order Rodentia considered in skeletal representation), alterations caused by predation (skeletal representation, proportional representation indexes, breakage and digestion) and post-depositional alterations. Discrepancies with Table 6.2 are explained due to elements in NR and NISP here are considered independent regardless of whether they are *in situ* or isolated (e.g. each tooth on a mandible is counted here as a single remain).

2008b; Terry, 2007). Two different trends can be distinguished. In levels O and N, at least 35% of the elements exhibit digestion marks: 40-50% of incisors, 19-33% of molars and 50-90% of femora. The predominant digestion marks are light in degree (27-30%), but a significant presence of moderate (7-10%) and some heavy digestion marks (1-2%) are also observed. Otherwise, in levels E and D digestion affects less than 25% of remains: 14-22% of incisors, 14-28% of molars and 36-38% of femora. The degree and the percentage of affected remains are similar to those in levels O and N but demonstrate a decrease in remains with evidence of light digestion (12-15%). Level J demonstrates an intermediate position between these two types of assemblages (32% of total elements with digestion); whereas level K has a markedly lower number of affected remains (8%) and some unusual digestion percentages, probably due to the sampling bias. Some digestion was detected in soricid remains from levels N and O level and in chiropters from level N. Though the presence of these species is scarce, their teeth are more resistant to digestive corrosion (Fernández-Jalvo, 1992; Fernández-Jalvo et al., 2016; Moya-Costa et al., 2018), and so it is most likely that soricids, talpids and bats were occasionaly preyed upon by same predator that accumulated the rodents (Fernández-Jalvo and Andrews, 1992; Kowalski, 1995). Lagomorph, amphibian, reptile and avian remains were also occasionally detected at some of these levels (Burjachs et al., 2012; Gabucio et al., 2014), but the taphonomic study of these remains is under development.

Based on the alterations caused by digestion, the origin of the small-mammal assemblages is most likely related to predator activity. Level O small-mammal remains were already related by Fernández-García et al. (2018) to the action of nocturnal bird of prey in the intermediate category of modification (Category 3 considering digestion; Andrews, 1990), most likely the tawny owl (*Strix aluco*). The high rates of breakages, the proportion of digested dental elements and the presence of some strongly digested teeth in level N point to the same kind of predator, and fit with the expected values for the tawny owl (Andrews, 1990; Andrews and Fernández-Jalvo, 2018; Comay and Dayan, 2018; Fernández-Jalvo et al., 2016; Fernández-Jalvo and Andrews, 1992) (Fig. 6.3). The homogeneity observed in levels O and N, considering the progressive proportion of digestion degrees and the coherence between proportion and degrees of digestion between skeleton elements, indicates that these are most likely due to a single predator type (Bennàsar, 2010; Bennàsar et al., 2016).

This is not evident in upper levels; remains from levels J, D and E seem to fit with a predator that produces a lower degree of modification (Table 6.4; Fig. 6.3). The quantity of remains digested is incompatible with the heavy degrees of digestion reached and equal ratios of digested molars and incisors are rare. The general digestion trend is similar to those at levels O and N, but the amount of digested remains is much lower, especially for incisors. Whereas some indices of anatomical representation, proportions of digested incisors and the detection of some incisors retained during digestion point to a Category 2 predator (such as *Asio otus* or *Nyctea scandiaca*), the proportion of digested molars and the degrees of digestion attained suggest a Category 3 predator (such as *Bubo bubo* or *Strix aluco*). These discrepancies suggest that the most plausible hypothesis is that these small-mammal assemblages are the result of a mixture of light and intermediate modification predators. It is possible that the actions of *Strix aluco*, detected in levels O and N, continue in upper levels, but the intervention of another predator type that inflicts less damage on bones obscures the proportion of digested elements. *Asio otus* is a good candidate, as it tends to inflict light

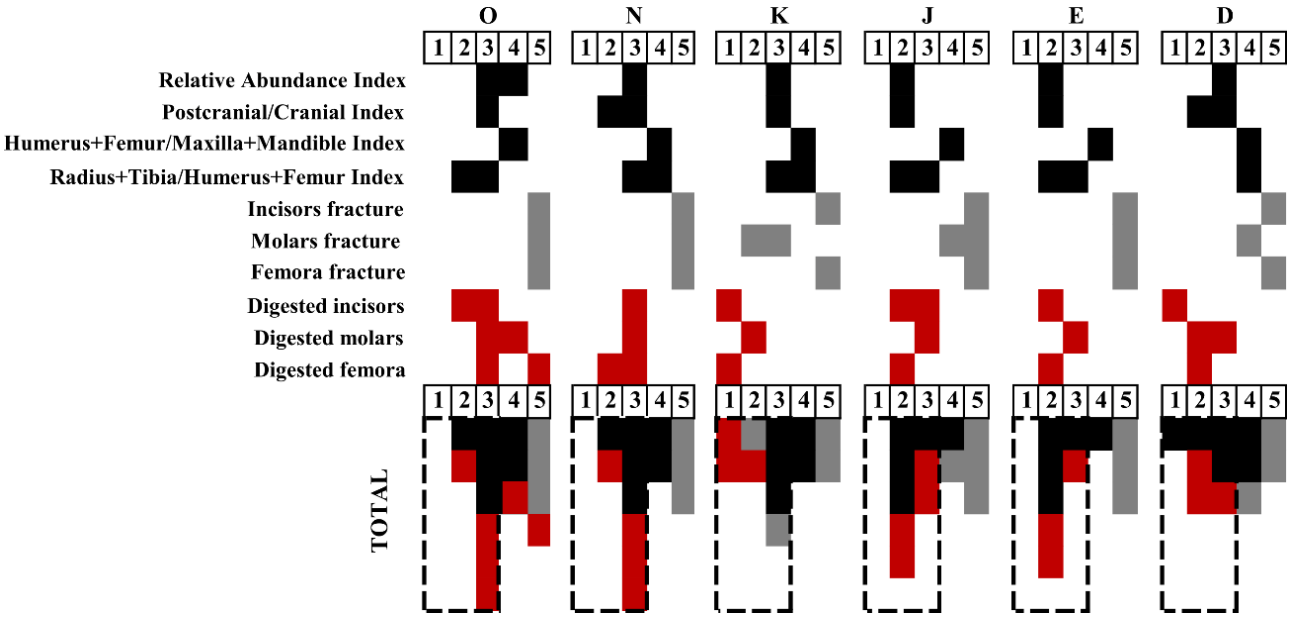

Figure 6.3 Predator categories obtained for the different taphonomic variables considered in analyzed levels. Each taphonomic variable is assigned to a category (from 1 to 5) according to Andrews (1990) classification and Fernández-Jalvo & Andrews (2016) revision. Black squares, postrcranial representation indexes; grey squares, breakage; red squares, digestion. Each level total is the sum of each category squares.

modification on dental remains, but higher than other owls of this category. It is also characteristic the retention of incisors inside mandibles during digestion, detected in some incisors of level E. Nevertheless, the action of an unknown predator with an usually high degree of digestion of molars cannot be rejected, since in current reference data some species of predators are absent or little-known (Denys, 2011; Terry, 2007). The discrepancies detected in level K are probably due to the scarce number of recovered remains. The large sample presented in this work provides enough remains to rule out the preliminary attribution to Category 1 predators (such as *Asio otus* or *Tyto alba*) as the main small-mammal accumulator (Allué et al., 2012; Burjachs et al., 2012; López-García et al., 2014) in any of the studied levels, at least in exclusivity, but confirms the presence of nocturnal birds of prey in the rock-shelter.

The tawny owl (*Strix aluco*) is a sedentary predator and strongly territorial. It usually places its nest in tree holes, cliffs, or rocky walls, which are reused year after year. It is an opportunistic hunter, including in its diet whatever is available in its hunting territory (usually an area between 1 and 3 km^2). It is a typical generalist and opportunistic species, being very adapt to different food sources and environmental conditions. Its prey assemblages are highly diverse and reflect the local ecological variability of its nesting area. Forest and semi-open forest are its preferential habitats, but it can also be found in riversides and open landscapes near forests or in rocky areas (Andrews and Fernández-Jalvo, 2018; Arribas, 2004; Manzanares, 2012; Mikkola, 1983; Obuch, 2011; Svensson, 2010; Yalden, 1985). The presence of this species has been confirmed in Iberia since the Early Pleistocene (Arribas, 2004) and it is currently present in Anoia region (Jiménez, 2003). Alternatively, the action of an unidentified owl in the light category of modification (probably Category 2 considering digestion; Andrews, 1990), depending on the species, could distort the original ecological signal of its local environment

through bias in its prey assemblages. For example, one known predator of this category is the long-eared owl (*Asio otus*). This species has been present in Iberia since the Middle Pleistocene, most likely with a similar, or perhaps more southern, distribution than today (Arribas, 1999; Manzanares, 2012). The long-eared owl inhabits boreal and temperate forests and Mediterranean and steppe areas of Eurasia (Mikkola, 1983; IUCN, 2018). Caution should be taken in ecological interpretations deduced from prey assemblages of this owl, since it is considered a selective hunter of voles and other small mammals in open country habitats, and thus does not provide a complete picture of its ecological niche (Andrews, 1990; Yalden, 1985).

4.2 Taphonomy history of small-mammal remains in Abric Romaní

Post-depositional agents have also been evaluated (Table 6.4; Appendix 2.3.A). Chemical corrosion related to plant activity is usually the main agent in all levels, often with a scattered distribution over the remains, affecting between 22.6% (level K) and 37.3% (level D), with an exceptional rate of 55.8% in level J. Cracking and manganese oxide pigmentation are also common (14.4-68.6% and 10.8-46.8%, respectively). Cracking results quantification is related to fissures in the remains, but we can detect slight striations in most of them. Precipitation of manganese oxides is common, but it appears in an isolated way, except in levels O, J, and E. Remains affected by cementation, sometimes as a fine carbonated patina, extends between 2.9% (level N) and 13.3% (level K). Abrasion is present in all analyzed levels, but in a low percentage (from 0.5% to 5.5%) and never exceeding mild degrees of polishing and rounding (P1 and R1, according to the classification of Cáceres (2002)). Some burning remains related to indirect human activity were found (from 2.6% to 14.5%), except in level K. The degrees of burning extend from weak color alterations to carbonization (levels O, N, E and D) and calcination (levels O and N) states. Other alterations such as dissolution, desquamation, or weathering are rare or absent. None of the alterations shows a taxonomic or anatomical preference. No particular spatial distribution of alterations is detected across level surfaces, however in levels N, E, and D most of the small-mammal accumulation occurs next to shelter walls or even in rock fissures.

In general, close microenvironmental conditions are identified through the post-depositional alterations observed in all studied levels. All levels show grooves and chemical corrosions produced by roots and mosses related to an open microenvironment, alterations caused by water (such as manganese oxide coatings) and changes in humidity and dryness (cementation and cracking), although with varying degrees of modification. In some cases, as in level J, manganese oxide is inside fissures and below chemical corrosions produced by roots, indicating the order of the post-depositional processes: humidity changes for water activation, followed by subsequent flooding and matter decomposition and posterior mosses activity. This is consistent with a fossiliferous rock-shelter context (Fernández-Jalvo, 1992) and the depositional fossiliferous microenvironment previously described for level O from Abric Romaní (Fernández-García et al., 2018); this is characterized by wet conditions and weak water flows and flooding, which is expected for this kind of travertine formation (Fernández-García et al., 2018; Gabucio et al., 2012; Vallverdú et al., 2012). A different pattern for small-mammal assemblages from levels E and D was not detected, despite their different sedimentary conditions that are closer to a cave environment (Vallverdú et al., 2005; Vaquero et al., 2013). Otherwise, levels K and D show a lower presence of remains with

manganese oxide coating (10.8% and 18.7%, respectively; mainly with isolated distribution), and fewer remains affected by cracking (14.4% and 15.3%, respectively) and water abrasion (0.5% and 0.6%, respectively). This could indicate less humidity and stagnant water during their deposition, and consequently fewer humidity and temperature change effects. However, manganese oxide has also been related to intense human activity due to the abundant presence of organic matter (Marín-Arroyo et al., 2014). Indeed, these levels are related to short-term human occupation (Marín et al., 2017a). In contrast, levels O and E present the highest presence of manganese oxide pigmentation (46.8% and 44.6%, respectively) and burning (14.5% and 11.5%). Notable fragmentation is also detected in these levels. In a lower proportion, level N also shows this trend (cracking: 46.5%; manganese oxide: 31.1%; burning: 6.3%). These levels are related to more intense human activity or to long-term human occupations (Gabucio et al., 2014; Marín et al., 2017a).

The absence of notable abrasion alterations, desquamation, and weathering, and the consistence in taphonomic patterns with large mammal remains, mainly accumulated by hominins in all levels (Fernández-Laso et al., 2010; Gabucio et al., 2017, 2014, Marín et al., 2017a, 2017b; Modolo and Rosell, 2017), do not support the presence of re-sedimentation processes and fixed *in situ* production and rapid burial of the remains (Fernández-García et al., 2018). It is probable that the identified small-mammal accumulators, nocturnal birds of prey, established their roosts or nests directly on rock outcrops or crevices that were part of Abric Romaní rock-shelter (Andrews, 1990; Mikkola, 1983). The high breakage rates, cracking, molar and maxillary losses, and the predominance of isolated teeth point to high-destructive post-depositional agents, especially for levels O and N. Frequently, manganese oxide precipitation coexists with cracking and covers bone fissures, indicating that some fragmentation occurred previously. One of the most common causes of high breakage is trampling by other animals, including birds of prey at their nesting sites (Andrews, 1990; Andrews et al., 2016; Lloveras and Moreno-García, 2009). Moreover, large-mammal remains taphonomic data point to a good state of bone preservation and no differential conservation with regards to bone density. However, the level of fragmentation is always high, suggesting that bone destruction can be explained by intensive human occupations and the processing of large-mammal carcasses (Fernández-Laso et al., 2010; Gabucio et al., 2012). Thus, the fragmentation and the subsequent isolated teeth recovered in small-mammal remains are probably the consequence of a combination of predator activity and post-depositional agents such as humidity changes, water courses or sediment compaction, but also intense human activities (such as trampling or even undirected burning).

4.3 Palaeoecological reconstruction: species occurrence, chorotypes, and landscape

In the whole sequence of Abric Romaní, 22 different taxa have been identified, consisting of shrews, moles, bats, voles, mice, dormice and squirrels (Table 6.2; Fig. 6.2). Among the Eulipotyphla, five different species were identified: the white-toothed shrew (*Crocidura russula*; levels O, I, E-D), the Eurasian pygmy shrew (*Sorex minutus*; level O), the common shrew or the crowned shrew (*Sorex* gr. *araneus-coronatus*; levels O and E), the Eurasian water shrew or Southern water shrew (*Neomys* gr. *fodiens-anomalus*; level O) and the common mole (*Talpa europaea*; levels Q, O-M and J). The few remains of bats were related to five species or groups of

species: the greater mouse-eared bat or the lesser mouse-eared bat (*Myotis* gr. *myotis-blythii*; level D), the greater noctule bat (*Nyctalus lasiopterus*, level O), the common pipistrelle (*Pipistrellus pipistrellus*; levels O and N), the common bent-wing bat (*Miniopterus schreibersii*; level N) and the brown long-eared bat or the gray long-eared bat (*Plecotus* gr. *auritus-austriacus*; levels E and D). In some cases, bat remains could only be identified at the genus level: *Myotis* sp. (level N) and *Pipistrellus* sp. (level E). The identified rodent species are the southwestern water vole (*Arvicola sapidus*; levels Q-D), the common vole (*Microtus arvalis*; levels O, K-H and E-D), the field vole (*Microtus agrestis*; levels O-N, K-H and E-D), the Cabrera's vole (*Iberomys cabrerae*; levels Q, O-J and E-D), the European snow vole (*Chionomys nivalis*; level E), the Mediterranean pine vole (*Microtus (Terricola) duodecimcostatus*; levels Q-N, L-K and E-D), the Pyrenean pine vole (*Microtus (Terricola) gerbei*; level Q), the wood-mouse (*Apodemus sylvaticus*; levels Q-N, L, J-I and E-D), the garden dormouse (*Eliomys quercinus*, levels O-N, J and E-D) and the red-squirrel (*Sciurus vulgaris*; levels Q and O). With respect to preliminary works (Burjachs et al., 2012; López-García, 2011; López-García et al., 2014), the current research has incorporated 7,199 remains and at least 427 individuals. This is especially relevant for levels D, E, K and N. Levels F, H, P and Q have been analyzed for the first time. The enlarged sample allows for the identification of species not previously record in some of the levels, and even species not previously detected in the sequence, such as *C. nivalis*, *M.* gr. *myotis-blythii* and *P. auritus-austriacus*. Nevertheless, given the fragmentary representation of remains along the sequence, only levels O, N, K, J, E and D are considered reliable for palaeoecological reconstructions.

The species with major relative abundance in the sequence are *A. sapidus, I. cabrerae* and *A. sylvaticus*. In some levels there is also an abundance of *M. (T.) duodecimcostatus, M. arvalis, M. agrestis* and *Talpa europaea.* The presence of *A. sapidus*, a species commonly found near water courses, is continuous throughout the sequence, even in more impoverished levels. The *A. sylvaticus*, mainly a generalist species, but with preference for forested covertures (Blanco, 1998; Palomo et al., 2007), is present in all studied levels, except level K, with variations in its relative presence. Co-occurrence between *I. cabrerae* and the *M. (T.) duodecimcostatus*, typical Mediterranean species, with *M. arvalis* and *M. agrestis*, mid-European species which preferred open environments and wetter and cooler climate, is frequent (Blanco, 1998; Palomo et al., 2007; Sans-Fuentes and Ventura, 2000). The occasional occurrences of *T. europaea* indicate the presence of moist soils, which are necessary for burrowing (Blanco, 1998; Palomo et al., 2007). The richest levels in small-mammal remains D, E, N and O, but also J and K, scored >0.6 beyond the Simpson's Diversity Index, indicating that the species are approximately numerically equal and that no single species dominates the assemblage (Appendix 2.3.B). Level O, the richest level of the sequence (Fernández-García et al., 2018), presents the highest level of species evenness (15 small-mammal species) and diversity (Simpson's Diversity Index record 0.84). This level's high diversity of species is consistent with an opportunistic-type predator, such as the tawny owl suggested by the taphonomic analyses for some levels (Obuch, 2011). Level K presents the lowest species diversity, due to the notable dominance of the water vole (>60%) and the low number of individuals recovered.

Regarding chorotype classification, generalist species are predominant in all studied levels (>45%) (Fig. 6.4). Unfortunately, these species provide little information about climate evolution.

However, slight fluctuations between Mediterranean and mid-European species occur throughout the sequence, except at level O, which has a balanced relative abundance between both groups. A notable increase of Mediterranean species and concomitant decrease of mid-European was detected in level N, K and D. The opposite situation is recorded in levels E and J.

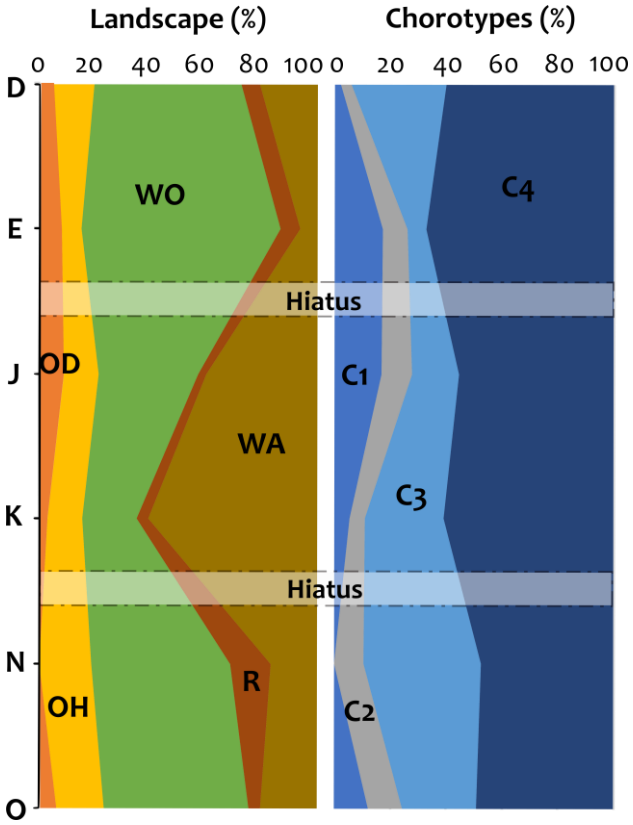

Figure 6.4 Palaeoenvironmental reconstruction based on small mammal assemblages of Abric Romaní, considering chorotypes classification and landscape components. C1, chorotype 1; C2, chorotype 2; C3, chorotype 3; C4, chorotype 4; OD, open dry; OH, open humid; WO, woodland; R, rocky; WA, water.

Regarding landscape evolution, the woodland component is the most notable, supporting the idea of a stable forest at Abric Romaní. Only levels J and K point some forest retreatment (<40%), however this phenomenon is only related to an increase open field component in level J. Otherwise, the forest environment is noticeable in level E (>70%). The water component is also constant, and its fluctuations are closely related to the abundance of the water vole, indicating the existence of water courses next to the site throughout the sequence. Finally, the open humid component points to humid meadows surrounding the site and enclosing the patchy landscape previously described (Burjachs et al., 2012); this area is composed mainly of open woodland, meadows, and water sources, which are optimal for human subsistence. In addition to earlier reported small-mammal results, the existence of open forest in the areas surrounding the rock-shelter is further supported by the identification of the tawny owl in the lower levels, and its possible contribution to upper ones (Arribas, 2004; Domingo de Pedro, 2011; Manzanares, 2012).

4.4 Climatic reconstruction and palaeotemperature estimations from Abric Romaní

Only the richest levels in remains (O, N, E, and D) were used for palaeoclimatic reconstructions (MNI>35; NISP>800) (Table 6.2). The oxygen isotope composition of the rodent incisor enamel from the different studied levels of Abric Romaní range from 15.7‰ to 23.5‰, representing a range of variation of 7.8‰ (Fig. 6.5; Table 6.3; Table 6.5). Both mean and median $\delta^{18}O_p$ values are very similar between different levels, varying between 18.4‰ (level D) and 19.3‰ (level O) and between 18.2‰ (level N) and 18.6‰ (level O), respectively. The mean $\delta^{18}O_p$ never exceeds more than 0.4‰ of the median $\delta^{18}O_p$ value, demonstrating a homogenous distribution of data within each level. The oxygen isotope compositions of Arvicolinae remains included in level D and E are within the general range obtained from *A. sylvaticus* measurements, and have no influence on either the mean or median values. All sedimentary layers show a normal distribution of data (Shapiro-Wilk test, p-value>0.01). Little intra-level variations are observed, ranging from 4‰ (level D) to 6.7‰ (level E). The ranges observed in levels D and E are highly

skewed by one value each: 21.1‰ and 23.5‰, respectively. When these values are excluded, the major amplitude is consistent with that of level N (5.7‰; SD: 2).

4.4.1. Seasonality of small-mammal accumulation

The sequence seems generally homogenous, with no big difference in means and medians along the sequence (<1‰). No significant differences were found between $\delta^{18}O$ means of any studied level (ANOVA sample test; p>0.01). The low to medium $\delta^{18}O_{mw}$ amplitudes recorded at all levels are lower than the current seasonal amplitude for $\delta^{18}O_{mw}$ values at Capellades (7.8‰; OIPC data; Bowen, 2017) (Fig. 6.1C; Table 6.5) and the average seasonal amplitude of $\delta^{18}O_{mw}$ values for Iberia (8‰; OIPC data; Bowen, 2017; Fernández-García et al., under review). Indeed, excluding $\delta^{18}O_p$ values from D and E results in ranges are even lower. These patterns suggest that analyzed rodent remains most likely accumulated during a preferential period of the year, which could correspond to the warmest season. Given the higher number of murid specimens and the observed oxygen isotope composition of contemporaneous Iberian rodent tooth samples, the warm season may have resulted in a higher probability of prey capture by owls (Chaline, 1974; Lagos, 2019; Manzanares, 2012; Norrdahl and Korpima, 2002; Royer et al., 2013b, 2013a; Salamolard et al., 2000) (see Chapter 5 for a detailed discussion). Mean and medians $\delta^{18}O_{mw}$ fossil values are higher (from -4.5‰ to -5.2‰ and from -4.8‰ to -5.4‰, respectively) than current mean $\delta^{18}O_{mw}$ values on Capellades (-5.9‰; OIPC data; Bowen, 2017), reinforcing this hypothesis. The record $\delta^{18}O_p$ values in all levels do not record predation of specimens in the cold season due to an absence of low $\delta^{18}O_p$ values (<15‰). The minimum $\delta^{18}O_p$ values from level N express in $\delta^{18}O_{mw}$ are equivalent to -7.5‰ (Table 6.3; 6.5), not reaching present-day winter $\delta^{18}O_{mw}$ (-8.3‰ and -9.3‰; OIPC data; Bowen, 2017; Fig. 6.1C). The maximum values recorded from level D ($\delta^{18}O_p$=21.1‰;$\delta^{18}O_{mw}$=-3‰) and specially from level E ($\delta^{18}O_p$=23.5‰; $\delta^{18}O_{mw}$=-1‰) correspond to extreme present-day summer values in the site region (Fig. 6.1C) and might be related to aridity peaks during

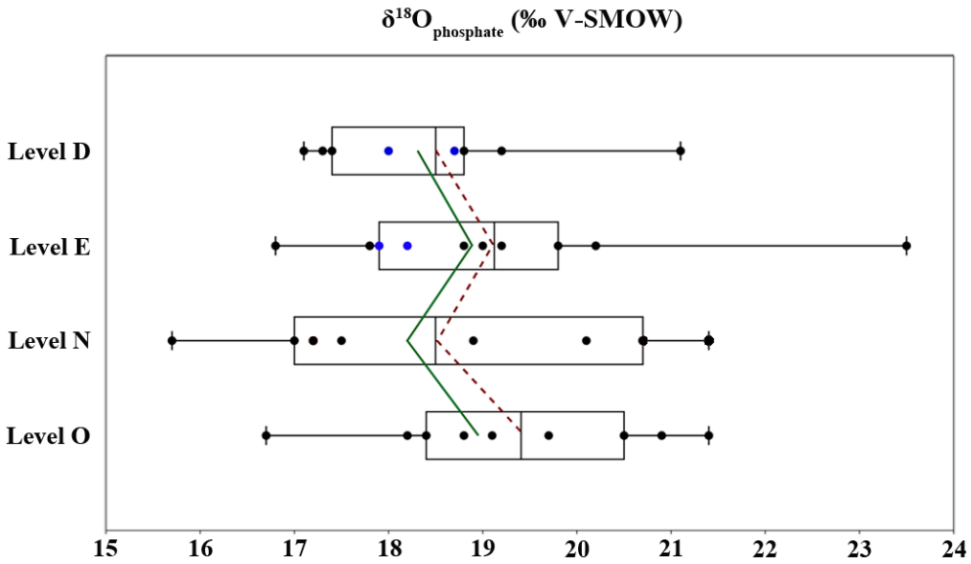

Figure 6.5 Oxygen isotope composition (‰ V-SMOW) of rodent incisor enamel from the Abric Romaní samples. Box plots and distribution of $\delta^{18}O$ values per layer, with mean (green line) and median (red dashed line) curves. Box plots' bars cover the full extension of the values; the boxes extend from the 1st to 3rd quartile. Black points illustrate *Apodemus sylvaticus* and blue points Arvicolinae samples.

	Levels	D	E	N	O
	n	10	10	8	10
$\delta^{18}O_p$	Min	17.1	16.8	15.7	16.7
	Max	21.1	23.5	21.4	21.4
	Mean	18.4	19.1	18.6	19.3
	Median	18.4	18.9	18.2	19.0
	Range	4.0	6.7	5.7	4.7
	SD	1.2	1.8	2.0	1.4
$\delta^{18}O_{mw}$	Min	-6.3	-6.6	-7.5	-6.7
	Max	-3.0	-1.0	-2.8	-2.8
	Mean	-5.2	-4.7	-5.1	-4.6
	Median	-5.3	-4.8	-5.4	-4.8
	Range	3.3	5.5	4.7	3.9
MAT	$\delta^{18}O_{mw}$ - seasonality correction	-6.4	-5.9	-6.5	-5.9
	$\delta^{18}O_{mw}$ - sea level correction	-7.0	-6.5	-7.1	-6.5
	MAT (ºC)	11.6	12.7	11.3	12.8
	SD	1.3	1.4	1.5	1.4
	Error margin	2.6	2.7	2.9	2.7

Table 6.5 Minimum, maximum, mean, median, standard deviation, and range of oxygen isotope composition of incisor enamel phosphate ($\delta^{18}O_p$; ‰ V-SMOW) from fossil rodents recovered from Abric Romaní samples; conversion to the oxygen isotope composition of meteoric waters ($\delta^{18}O_{mw}$; ‰ V-SMOW), including minimum, maximum, mean, median and range; and, mean annual temperature estimations (MAT; º C), including seasonality and sea-level corrections of $\delta^{18}O_{mw}$. SD, standard deviation.

the deposition of the level (Jeffrey et al., 2015; Royer et al., 2013b).

Taphonomic analyses have suggested that the predator *Strix aluco* is most likely responsible for the rodent accumulation in levels N and O, whereas in upper levels a combined accumulation from the same kind of predator and an unidentified lighter modificatory predator is the most parsimonious hypothesis. Today, the tawny owl breeds between February and April in the Iberian Peninsula. Incubation lasts about a month, and offspring can fly after about five weeks. This supports the hypothesis of preferential accumulation in the warmest months (Manzanares, 2012). Although this species hunts small mammals throughout the year, some studies show an intensification of this activity in the breeding season and the incorporation of high rates of insects in early summer as well (Andrews and Fernández-Jalvo, 2018; Chaline, 1974; Southern, 1954; Yalden, 1985). Southern (1954) and Andrews and Fernández-Jalvo (2018) note that small-mammal accumulation in pellets decreases in early summer'. Southern (1954) suggested that this is mainly related to the ground vegetation growth in England forests, which can hinder hunting. However, both studies specify that each season's weather would be determinant (temperature and rainfall); thus, the seasonal evolution of the landscape is expected to be quite different in Mediterranean areas. The simultaneous occupation of the shelter by raptors and humans could be controversial. Using a combination of zooarchaeological analyses of large-mammal remains, seasonality of human occupations was evaluated on levels M, L, K and J (Fernández-Laso et al., 2010; Rosell et al., 2012b). A clear profile was not detected for these occupations, and the seasonality of ungulates

occurred at different periods of the year within each level: spring (cervids and aurochs in level L), spring and early summer (horses and aurochs in level J), summer (cervids and aurochs in level K) or autumn (cervids in level M and red deer in level J). Seasonality has not been researched in currently studied levels, so it is difficult to confirm whether human settlement and frequentation by owls occurred simultaneously at the rock shelter.

4.4.2. Palaeotemperature reconstruction

MATs were calculated based on median $\delta^{18}O_p$ of each sedimentary level. The estimated MATs vary between 12.8 ±2.7 °C (level O) and 11.3 ±2.9 °C (level N) (Table 6.5; Fig. 6.6). These temperatures are lower than the current MAT recorded at Capellades (14.8 °C; Climate-Data.org; Fig. 6.1C), with the difference ranging from -3.5 °C to -2 °C. Interlevel MAT differences are small (≤1.5 °C). Therefore, from the perspective of oxygen isotope compositions, a homogenous and temperate climate without notable changes is supported. The MATs calculated from the $\delta^{18}O_p$ are compared with two other methods of palaeoclimatic reconstruction usually used for small-mammal assemblages: the bioclimatic model (BM) and the mutual ecogeographic range (MER) (Appendix 2.3.C and 2.3.D). The three methods indicate that temperatures were lower than present-day, but the magnitude of these differences depends on the method; with differences ranging from 2.2 °C to 3 °C between methods for each of the levels. The BM method tends to produce the highest temperatures (-0.5 °C and -2.1 °C than present-day), whereas MER estimations produce lower temperatures (-2.6 to -5.1 °C than present-day). $\delta^{18}O$ estimations produce an intermediate position between both methods. Results are in accordance

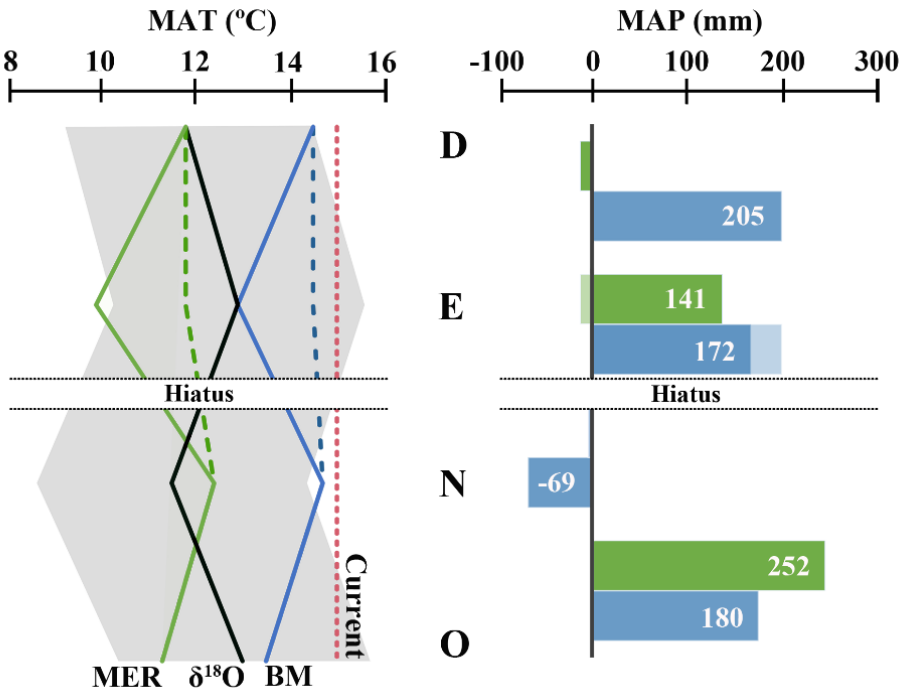

Figure 6.6 Mean Annual Temperature (MAT) and Mean Annual Precipitation (MAP) estimations for levels O, N, E and D, considering the oxygen isotope compositions ($\delta^{18}O$) of rodent phosphates samples (error associated in shaded fringe), the bioclimatic model (BM) and mutual ecogeographical range (MER) methods. Current MAT corresponds to red dashed lines (14.8 ºC; Climate-data.org) in Capellades; green and blue dashed lines illustrated MAT estimations of level E not considering *Chionomys nivalis*; past MAPs are represented with respect to present-day MAP in Capellades (619 mm; Climate-data.org)

with BM temperatures in levels O and E (~13 °C and 12.7 °C, respectively), whereas MER temperatures are underestimated (11.1 °C and 9.2 °C, respectively). In levels N and D, $\delta^{18}O$ results correlate with MER temperatures (~12 °C and 11.6 °C, respectively) and BM calculations are overestimated, with recorded air temperatures comparable to present-day temperatures (-0.3 °C and -0.4 °C, respectively). Nevertheless, these offsets remain small enough to fall within the confidence interval of $\delta^{18}O$ estimations (a completed discussion of methods discrepancies in presented Chapter 9).

MAPs obtained by BM method are higher (between +172/+205 mm) than present-day (619 mm; Climate-Data.org), except for level E (-69 mm) (Fig. 6.6); whereas MER method reports MAPs equal to present-day for levels N (-4 mm) and D (-13 mm), but higher for levels O (+252 mm) and E (+141 mm). These estimations are notably different than previous climatic estimations based on small vertebrates, which showed lower MATs (between -4.6 and -7.5 °C) and higher MAPs (between +60 and +349 mm) than this area in present-day (Burjachs et al., 2012; López-García, 2011; López-García et al., 2017). These differences are explained by the larger sample present in this work and the subsequent incorporation of new species. In addition, previous estimations consider climatic data from meteorological station of Barcelona airport, which is located at 93 m a.s.l. (Font-Tullot, 2000).

4.5 Combined palaeoecological approaches to reconstructing the palaeoenvironmental conditions of the Abric Romaní sequence during MIS 3

Besides extensive dating, the high-resolution stratigraphy of Abric Romaní gives us the opportunity to tentatively relate environmental evolution at the site with global climatic oscillations manifested in the Northern Hemisphere. Nevertheless, continuous stadial-interstadial oscillations are the main characteristic denoted by Greenland ice cores contemporaneous to deposition of levels N-O, and even to level J (Fig. 6.7). Rasmussen et al. (2014) identified the beginning of the MIS 3, specifically the interval between 68 and 48 ka b2k, as the most marked change in the expression of centennial-to-millennial-scale variability. This period is characterized by a change from stable and mainly cold climate (GS19 and GS18), through a high oscillating period between GI17 to GI15, which was followed by 6,000 years of a predominantly mild climate (GI14 to GI12). The deposition of levels O and N, regarding its chronology, occurred during D-O 14 (ca. 54-49 ka b2K) or, most likely, during D-O 15 (ca. 54-55 b2K) in relation to Greenland ice cores (Svensson et al., 2008). Level O has been identified as cool phase tentatively related to GS15, for its lower temperatures, seasonal temperature variation and equal proportions of mid-European and Mediterranean species (Fernández-García et al., 2018; see Chapter 4 for a detailed discussion). In spite of being considered a cool event (between -1.5 to -3.7 °C with respect to present-day), precipitations are high (between +180 and +252 with respect to present-day), forest dwellers are dominant (such as *A. sylvaticus, E. quercinus*, *S. vulgaris* or *N. lasipterus*), high species richness is recorded, and Mediterranean species are common (*I. cabrerae*, *M. (T.) duodecimcostatus* and *C. russula*).

Compared to level O, the upper level N presents equal small-mammal species diversity but an increase in Mediterranean species (42% vs. 26%) with a concomitant reduction in mid-European ones (11% vs. 24%) (Fig. 6.4; 6.7). Indeed, *M. agrestis* is not identified in this level (Table 6.2). Otherwise, no notable differences in the landscape component are detected, maintaining species with

preference for open forest environments (*A. sylvaticus*, *E. quercinus* and *P. pipistrellus*). The predator identified as the main author of the assemblage, *Strix aluco*, is a good indication that forest surrounded the site. Because this research has shown that the type of predator is the same in both levels, a different ecological signal is not expected to be related with bias in their accumulation. This level was related to an interstadial phase (Burjachs et al., 2012; López-García et al., 2014) based on increments in *Pinus* forest associated with warm temperate taxa and reinforced by previous palaeotemperatures estimations based on small-vertebrate studies (Table 6.1). Considering the BM and MER methods used in this work, a climatic improvement is estimated between level O and level N (BM=+1.2 °C; MER=+1.1 °C), but oxygen isotope compositions point to the opposite situation (-1.5 °C) (Fig. 6.6). Moreover, the biggest range in $\delta^{18}O_p$ values is found at this level (Fig. 6.5; Table 6.5). Is not simple to correlated small mammals and other environmental data during the defined as Palynological Phase 3 in Abric Romaní. This phase is located between 57 and 50 ka, characterized by remarkable oscillation of arboreal pollen and mesothermophilous species, but interstadial conditions prevailed (Burjachs et al., 2012; Burjachs and Julià, 1996, 1994; Vaquero et al., 2013) (Table 6.1; Fig. 6.7). These oscillations are consistent with the unstable scenario indicated by Greenland ice cores (Rasmussen et al., 2014; Svensson et al., 2008; Wolff et al., 2010) and Iberian marine pollen cores (Fletcher et al., 2010; Fletcher and Sánchez-Goñi, 2008) from this period. Oxygen compositions of level N could fit a stadial-interstadial scenario which is inconsistent with the original climatic signal interpretation.

Higher up in the stratigraphy, regarding species' relative abundance in relation with upper and lower levels, a decrease in species with preferences for the forest is documented (20-36%) in levels K-J, along with an increase in species of mid-European requirements from level K to level J (Fig. 6.4; 6.7). The deposition of these levels occurs between D-O 14 (ca. 54-49) and D-O 13 (ca. 49-46 ka b2k). Both levels occur at the end of the previously mentioned Palynological Phase 3, and are characterized by continuous oscillations between cool-dry and warm-humid episodes (Burjachs and Julià, 1996, 1994) (Table 6.1; Fig. 6.7). Burjachs et al. (2012) correlated these levels with D-O 14, but sublevel Ja and level H with HE5 (related to GS13), due to the detection of a cold phase with aridity peaks based on the reduction of thermophilous taxa and a decrease in arboreal pollen, but with an intermediated phase of open pine forest expansion. Environmental deterioration of level J pointed by small-mammal assemblages can tentatively agree with this correlation with the GS13 event, however in the light of the scarce small-mammal remains (Table 6.2), cautious interpretation is recommended. Among large mammals, the presence of *Stephanorhinus hemiteoechus* in both levels and the appearance of *Rupicapra pyrenaica* for the first time in the sequence during level J formation reinforces the idea of the opening landscape trend (Cáceres et al., 1998; Rosell et al., 2012a). Indeed, the diversity of dietary behavior under dental wear analyses of level J and M reveals the presence of various habitats in the surrounding areas of the site (Burjachs et al., 2012).

At the top of the sequence, levels E-D are contemporaneous with D-O 12 (ca. 46-43 ka b2K) or to D-O 11 (ca.43-41 ka b2K). Climate fluctuations documented during this period have been highlighted in some studies, which have linked GS12 and GS11 with the initial fragmentation of Neanderthal populations by the cooling and arid conditions of these stadials (e.g., Staubwasser et al., 2018; Wolf et al., 2018). Nevertheless, D-O 12 is

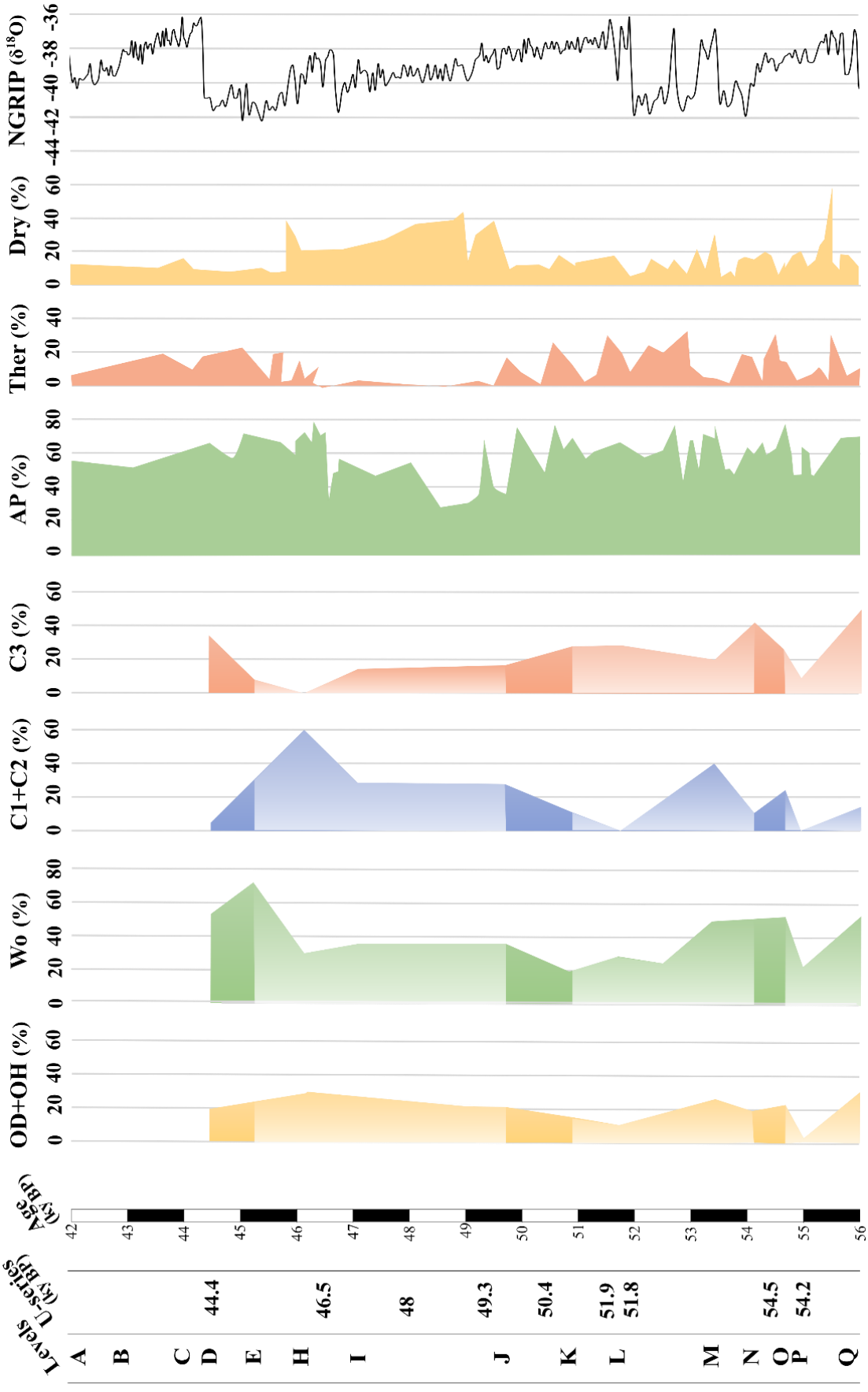

Figure 6.7 Comparison of ecological methods apply to Abric Romaní sequence. Species abundances obtained through small mammal studies: OD+OH, open dry and open humid; Wo, woodland; C1+C2, chorotypes 1 and 2 (mid-European species); C3, chorotype 3 (Mediterranean species). Light areas are related to levels with poor small-mammal remains and, thus, dubious. Pollen curves from Burjachs et al. (2012): AP, Arboreal pollen, including *Pinus*; Ther, Thermophilous pollen taxa; Dry, dry pollen taxa. Isotopic curve NGRIP (NGRIP, 2004; Svensson et al., 2008).

characterized by strong forest developments with temperate elements in southernmost European latitudes, based on marine pollen records (Fletcher et al., 2010; Genty et al., 2010; Sánchez Goñi et al., 2008). This research has recorded a significant proportion of forestall component in both levels, especially in level E, where the highest relative presence of *A. sylvaticus* is observed (~50%; normally 15-20%); this explains the relatively lower species diversity in this level (Table 6.2; Fig. 6.4; 6.7). The presence of this species is accompanied by an equally important presence of species with mid-European requirements (26%; *M. arvalis*, *M. agrestis* and *C. nivalis*) in level E. In contrast, level D reports an increase of Mediterranean species (34%; highest presence of *I. cabrerae*) and decrease of mid-European ones (6%).

Both levels were initially associated with the Palynological Phase 5 (46-41 ka BP), a warm phase with forest expansion, along with the upper levels of the sequence (G-A) (Burjachs and Julià, 1996, 1994) (Table 6.1). Charcoal studies from the site reveal the singularity of level D: like the rest of the sequence, montane *Pinus* is the most abundant here (74%), but this level shows more taxonomic diversity, which is primarily related to the spread of genus *Quercus* and other mesothermophilus taxa (Allué et al., 2017; Burjachs et al., 2012). Nevertheless, levels E-D were considered the coolest interstadial of the sequence by Burjachs et al. (2012). This led Vaquero et al. (2013) and López-García et al. (2014) to correlate level E with HE5 based on abrupt sedimentary changes and, considering previous small-mammal estimations, low winter temperatures and an abundance of mid-European species. However, previous small-mammal analyses relied on a small number of remains. Based on the present results, level E presents lower MAT than level D, given both BM (-1.6 °C respect to level D) and MER (-1.9 °C respect to level D) (Fig. 6.6). However, oxygen isotope compositions do not agree, indicating only ~1 °C of difference in the opposite direction and both levels' $\delta^{18}O_p$ values distribution are homogenous (Fig. 6.5). Indeed, it is difficult to use MER palaoeotemperature reconstruction as a criterion for this correlation, since the exclusion of a single taxon from this qualitative analysis, in this case *Chionomys nivalis*, could indicate a temperature estimation equivalent to that of level D (in Fig. 6.6, MATs not considering this species for level E are in dashed line). A similar problem occurs with the BM method. Moreover, the main predator at these levels is not well-identified and hunting predator preferences could result in an unknown bias in the final relative species abundance (Andrews, 1990; Scott et al., 1996). However, this research supports a slight climatic deterioration in level E, related to an aridity event, expressed by the highest oxygen isotope value inside level E (Fig. 6.5); this is further supported by the prevalence of *Bufo calamita* (Burjachs et al., 2012; López-García et al., 2014), the aeolic sedimentary facies (Vaquero et al., 2013), the increase of mid-European species (López-García et al., 2014; this work), and major development of steppe forest (Burjachs et al., 2012) (Table 6.1). It can also explain the recovery of a *Mammuthus primigenius* remain in this level (Rosell et al., 2012b).

5. Conclusions

- A total of 7,333 remains were recovered from the entire sequence, which correspond to at least 500 individuals belonging to 22 different taxa. Fragmentary and uneven representation of remains is detected along the sequence; only the use of levels N, O, K, J, E and D (NR>400; MNI>15) is recommended for reliable palaeoecological reconstructions.
- The small-mammals origin at Abric Romaní is related to owl predation activities. The type of predator is not the same along the sequence:

remains at lower levels (O-N) are most likely the result of an intermediate modification predator (probably *Strix aluco*) whereas those found at upper levels (J-E) are prey assemblages deposited by a mixture of light and intermediate modification predators. The small sample size of remains in level K does not permit the identification of the predator. Species diversity and richness point to an opportunistic predator, that draws a complete ecological picture of the past; but caution in the interpretation of upper levels is needed since a selective predator may have also contributed to the assemblage.

- Among post-depositional agents, plant activity, cracking, and manganese oxide precipitations are common, describing a humid fossiliferous microenvironment, where intense human occupation occurred.
- Both the results presented in this study and those previously found using pollen and anthracological analyses support the idea of a predominance of the forest biotope around the rock-shelter. Only slight changes in the landscape occurred, with a continuous presence of relatively humid open forest and active watercourses next to the rock shelter, punctuated by expansions of meadows.
- Recorded low ranges of values from oxygen isotope analyses suggest that rodent accumulations are mainly related to the warmer season when predators are more actively hunting. Amplitudes and means in $\delta^{18}O_p$ values indicate climatic homogeneity across lower and upper levels.
- The relative abundances of small-mammal species, particularly with regard to the presence of Mediterranean versus mid-European species, seems to be in agreement with palynological estimations and other environmental proxies of the site. Few changes in small-mammal communities, together with palynological and charcoal fluctuation from the site, indicate that levels O and E were slightly cooler, which could be related to stadial moments. The isotopic signal for these levels is not fully coincident, probably related to increments in the mean annual precipitations, which can hide changes in temperatures, or to stadial-interstadial interactions.
- Lowest temperatures ($\delta^{18}O$: -3.5/-2 °C; MER: -5.1/-2.6 °C; BM: - 2.1/+0.3 °C) and slightly higher or equal precipitation levels (MER: -13/+252 mm; BM: -69/+205 mm) than present-day are estimated for levels O, N, D and E from Abric Romaní. This work adjusts previous palaeotemperatures estimations, increasing previous MATs calculations and reducing MAPs estimations.
- Despite the fluctuations described, mainly among Mediterranean versus mid-European species, this work reports weak climatic changes between levels. In terms of palaeotemperatures, differences are <2.5 °C, with independence of the method applied. Oxygen isotope compositions of analyzed rodent teeth show little variation between levels, with both mean and median variations being less than 1‰, with equivalent small ranges of $\delta^{18}O_p$ values. In comparing $\delta^{18}O_p$, the most and the least variable level only differed by 2.7‰, even when considering the possible maximum outlier of level E. Thus, globally milder and more stable conditions are expected to have occurred during the period of the deposition of these levels.

References

AEMET & IMP, 2011, Atlas climático ibérico. Temperatura del aire y precipitación (1971-2000). Agencia Española de Meteorología & Instituto de Meteorología de Portugal. Pp., 79.

Allué, E., Burjachs, F., García, A., López-García, J.M., Bennàsar, M., Rivals, F., Blain, H.-A., Expósito, I., Martinell, J., 2012. Neanderthal Landscapes and Their Home Environment: Flora and Fauna Records from Level J, in: Carbonell i Roura, E. (Ed.), High Resolution Archaeology and Neanderthal Behavior. Vertebrate Paleobiology and Paleoanthropology. Springer, Dordrecht, pp. 135–157.

Allué, E., Solé, A., Burguet-Coca, A., 2017. Fuel exploitation among Neanderthals based on the anthracological record from Abric Romaní (Capellades, NE Spain). Quat. Int. 431, 6–15.

Andrews, P., 2006. Taphonomic effects of faunal impoverishment and faunal mixing. Palaeogeogr. Palaeoclimatol. Palaeoecol. 241, 572–589.

Andrews, P., 1990. Owls, Caves and Fossils. Predation, preservation and accumulation of small mammal bones in caves, with an analysis of the Pleistocene Cave Faunas from Westbury-sub-Mendip, Somerset, UK. The University of Chicago, Chicago.

Andrews, P., Andrews, S.H., King, T., Fernández-Jalvo, Y., Nieto-Díaz, M., 2016. Paleoecology of Azokh 1, in: Fernandez-Jalvo, Y., Yepiskoposyan, L., Andrews, P. (Eds.), Azokh Cave and the Transcaucasian Corridor. Springer, New York, pp. 305–320.

Andrews, P., Fernández-Jalvo, Y., 2018. Seasonal variation in prey composition and digestion in small mammal predator assemblages. Int. J. Osteoarchaeol. 1–14.

Arribas, a, 1999. On the Ecological Connection Between Sabre-tooths and Hominids: Faunal Dispersal Events in the Lower Pleistocene and a Review of the Evidence for the First Human Arrival in Europe. J. Archaeol. Sci. 26, 571–585.

Arribas, Ó., 2004. Fauna y paisaje de los Pirineos en la Era Glaciar. Lynx, Barcelona.

Bargalló, A., 2014. Technological Analysis of Neanderthal settlement of the level O Abric Romaní (Barcelona, Spain). Universitat Rovira i Virgili. Doctoral thesis (inedit).

Bargalló, A., Gabucio, M.J., Rivals, F., 2016. Puzzling out a palimpsest: Testing an interdisciplinary study in level O of Abric Romaní. Quat. Int. 417, 51–65.

Bartrolí, R., Cebria, A., Muro, I., Riu-Barrera, E., Vaquero, M., 1995. A frec de ciencia. L'Atles d'Amador Romaní i Guerra. Ajuntament de Capellades, Capellades (Barcelona).

Bennàsar, M., 2010. Tafonomía de micromamíferos del Pleistoceno Inferior de la Sierra de Atapuerca (Burgos): Sima del Elefante y Gran Dolina. Universitat Rovira i Virgili (Tarragona). Doctoral thesis (inedit).

Bennàsar, M., Cáceres, I., Cuenca-Bescós, G., 2016. Paleoecological and microenvironmental aspects of the first European hominids inferred from the taphonomy of small mammals (Sima del Elefante, Sierra de Atapuerca, Spain). Comptes Rendus Palevol 15, 635–646.

Bernard, A., Daux, V., Lécuyer, C., Brugal, J., Genty, D., Wainer, K., Gardien, V., Fourel, F., Jaubert, J., 2009. Pleistocene seasonal temperature variations recorded in the $\delta^{18}O$ of *Bison priscus* teeth. Earth Planet. Sci. Lett. 283, 133–143.

Bischoff, J.L., Julia, R., Mora, R., 1988. Uranium-series dating of the Mousterian occupation at Abric Romani, Spain. Nature 332, 68-70.

Bischoff, J.L., Ludwig, K., Garcia, J.F., Carbonell, E., Vaquero, M., Stafford, T.W., Jull, A.J.T., 1994. Dating of the Basal Aurignacian Sandwich at Abric Romaní (Catalunya, Spain) by Radiocarbon and Uranium-Series. J. Archaeol. Sci 21, 541-551.

Blain, H.-A., Bailon, S., Cuenca-Bescós, G., Arsuaga, J.L., Bermúdez de Castro, J.M., Carbonell, E., 2009. Long-term climate record inferred from early-middle Pleistocene amphibian and squamate reptile assemblages at the Gran Dolina Cave, Atapuerca, Spain. J. Hum. Evol. 56, 55–65.

Blain, H.A., Lozano-Fernández, I., Agustí, J., Bailon, S., Menéndez Granda, L., Espígares Ortiz, M.P., Ros-Montoya, S., Jiménez Arenas, J.M., Toro-Moyano, I., Martínez-Navarro, B., Sala, R., 2016. Refining upon the climatic background of the Early Pleistocene hominid settlement in western Europe: Barranco León and Fuente Nueva-3 (Guadix-Baza Basin, SE Spain). Quat. Sci. Rev. 144, 132–144.

Blanco, J.C., 1998. Mamíferos de España. Vol II. Cetáceos, Artiodáctilos, Roedores y Lagomorfos de la península Ibérica, Baleares y Canarias. Planeta, Barcelona.

Bowen, G.J., 2017. The Online Isotopes in Precipitation Calculator, Version 3.1 (4/2017): http://waterisotopes.org

Burjachs, F., Allué, E., 2003. Paleoclimatic evolution during the last glacial cycle at the NE of the Iberian Peninsula, in: Ruiz, M.B., Dorado, M., Valdeolmillos, A., Gil, M.J., Bardají, T., de Bustamante, I., Martínez, I. (Eds.), Quaternary Climatic Changes and Environmental Crises in the Mediterranean Region. Universidad de Alcalá, Ministerios de Ciencia y Tecnologia, INQUA, Alcalá de Henares (Madrid), pp. 191–200.

Burjachs, F., Julià, R., 1996. Palaeonvironmental evolution during the Middle-Upper Palaeolithic transition in the NE of the Iberian Peninsula, in: Carbonell, E., Vaquero, M. (Eds.), The Last Neandertals, the First Anatomically Modern Humans. Cultural Change and Human Evolution: The Crisis at 40 Ka BP. Gràfiques Lluc, Igualada (Barcelona), pp. 377–383.

Burjachs, F., Julià, R., 1994. Abrupt Climatic Changes during the Last Glaciation Based on Pollen Analysis of the Abric Romani, Catalonia, Spain. Quat. Res. 42, 308-315.

Burjachs, F., López-García, J.M., Allué, E., Blain, H.-A., Rivals, F., Bennàsar, M., Expósito, I., 2012. Palaeoecology of Neanderthals during Dansgaard–Oeschger cycles in northeastern Iberia (Abric Romaní): From regional to global scale. Quat. Int. 247, 26–37.

Cabanes, D., Allué, E., Vallverdú, J., Cáceres, I., Vaquero, M., Pastó, I., 2007. Hearth structure and function at level J (50kyr , bp) from Abric Romaní (Capellades , Spain): phytolith, charcoal, bones and stone-tools, in: International Meeting on Phytolith

Research; Plants, People and Places; Recent Studies in Phytolith Analysis. Oxbow Books, Cambridge, pp. 98–106.
Cáceres, I., 2002. Tafonomía de yacimientos antrópicos en karst. Complejo Galería (Sierra de Atapuerca, Burgos), Vanguard Cave (Gibraltar) y Abric Romaní (Capellades, Barcelona). Univeristat Rovira i Virgili. Doctoral thesis (inedit).
Cáceres, I., Rosell, J., Huguet, R., 1998. Sequence d'utilisation de la biomasse animale dans le gisement de l'Abric Romani (Barcelone, Espagne). Quaternaire 9, 379–383.
Carbonell, E., 2012. High Resolution Archaeology and Neanderthal Behavior. Time and Space in Level J of Abric Romaní (Capellades, Spain). Springer, New York & London.
Carbonell, E., Castro-Curel, Z., 1992. Palaeolithic wooden artefacts from the Abric Romani (Capellades, Barcelona, Spain). J. Archaeol. Sci. 19, 707–719.
Carbonell, E., Cebrià, A., Allué, E., Cáceres, I., Castro, Z., Díaz, R., Esteban, M., Ollé, A., Pastó, I., Rodríguez, X.P., Rosell, J., Sala, R., Vallverdú, J., Vaquero, M., Vergés, J.M., 1996. Behavioural and organizational complexity in the Middle Palaeolithic from the Abric Romaní, in: Carbonell, E., Vaquero, M. (Eds.), The Last Neandertals, the First Anatomically Modern Humans. Cultural Change and Human Evolution: The Crisis at 40 Ka BP. Universitat de Tarragona, Tarragona, pp. 385–434.
Carbonell, E., Giralt, S., Vaquero, M., 1994. Abric Romani (Capellades, Barcelone, Espagne): une importante séquence anthropisée au Pléistocène supérieur. Bull. la Société Préhistorique Française 91, 47–55.
Carrancho, Á., Villalaín, J.J., Vallverdú, J., Carbonell, E., 2016. Is it possible to identify temporal differences among combustion features in Middle Palaeolithic palimpsests? The archaeomagnetic evidence: A case study from level O at the Abric Romaní rock-shelter (Capellades, Spain). Quat. Int. 417, 39–50.
Castro-Curel, Z., Carbonell, E., 1995. Wood Pseudomorphs From Level I at Abric Romani, Barcelona, Spain. J. F. Archaeol. 22, 376–384.
Chacón, M.G., Bargalló, A., Gómez, B., Picin, A., Vaquero, M., Carbonell, E., 2013. Continuity or discontinuity of neanderthal technological behaviours During MIS 3: level M and level O of the Abric Romani site (Capellades, Spain), in: Pleistocene Foragers on the Iberian Peninsula: Their Culture and Environment. Festschrift in Honour of Gerd-Christian Weniger for his sixtieth birthday. Wissenschaftliche Schriften des Neanderthal Museums 7, pp. 55–84.
Chacón, M.G., Fernández-Laso, M.C., 2007. Modelos de ocupación durante el Paleolítico medio: El nivel K del Abric Romaní (Capellades, Barcelona, España). Complutum 18, 47–60.
Chacón, M.G., Fernández-Laso, M.C., García-Antón, M.D., Allué, E., 2007. Level K and L from Abric Romaní (Barcelona, Spain): procurement resources and territory management. Proc. XV World UISPP Congr. Lisbon 5, 187–197.
Chaline, J., 1974. Les proies des rapaces. Doin Éditeurs, Paris.
Climate-Data.org, 2018. https://es.climate-data.org/
Comay, O., Dayan, T., 2018. Taphonomic signatures of owls: New insights into micromammal assemblages. Palaeogeogr. Palaeoclimatol. Palaeoecol. 492, 81–91.
Crowson, R.A., Showers, W.J., Wright, E.K., Hoering, T.C., 1991. Preparation of Phosphate Samples for Oxygen Isotope Analysis. Anal. Chem. 63, 2397–2400.
Denys, C., 2011. Des referentiels en Taphonomie des petits vertebres: Bilan et perspectives, in: Laroulandie, V., Mallye, J.-B., Denys, C. (Eds.), Taphonomie Des Petits Vertébrés: Référentiels et Transferts Aux Fossiles. British Archaeological Reports, International Series 2269, Oxford, pp. 7–22.
Domingo de Pedro, M., 2011. Rapinyaires a Catalunya. Cossetània Edicions.
Evans, E.M.N., Van Couvering, J. a. H., Andrews, P., 1981. Palaeoecology of Miocene sites in Western Kenya. J. Hum. Evol. 10, 99–116.
Fernández-García, M., López-García, J.M., Bennàsar, M., Gabucio, M.J., Bargalló, A., Gema Chacón, M., Saladié, P., Vallverdú, J., Vaquero, M., Carbonell, E., 2018. Paleoenvironmental context of Neanderthal occupations in northeastern Iberia: The small-mammal assemblage from Abric Romaní (Capellades, Barcelona, Spain). Palaeogeogr. Palaeoclimatol. Palaeoecol. 506, 154–167.
Fernández-García, M., López-García, J.M., Lorenzo, C., 2016. Palaeoecological implications of rodents as proxies for the Late Pleistocene–Holocene environmental and climatic changes in northeastern Iberia. Comptes Rendus Palevol 15, 707–719.
Fernández-García, M., Royer, A., López-García, J.M., Bennàsar, M., Goedert, J., Fourel, F., Julien, M.A., Bañuls-Cardona, S., Rodríguez-Hidalgo, A., Vallverdú, J., Lécuyer, C. Unravelling the oxygen isotope signal ($\delta^{18}O$) from rodent teeth in northeastern Iberia, and the implications for past climate reconstructions. Quaternary Science Reviews (under review).
Fernández-Jalvo, Y., 1992. Tafonomía de microvertebrados del complejo cárstico de Atapuerca (Burgos). Universidad Complutense de Madrid. Doctoral thesis (inedit).
Fernández-Jalvo, Y., Andrews, P., 1992. Small mammal taphonomy of Gran Dolina, Atapuerca (Burgos), Spain. J. Archaeol. Sci. 19, 407–428.
Fernández-Jalvo, Y., Andrews, P., Denys, C., Sesé, C., Stoetzel, E., Marin-Monfort, D., Pesquero, D., 2016. Taphonomy for taxonomists: Implications of predation in small mammal studies. Quat. Sci. Rev. 139, 138–157.
Fernández-Laso, M.C., Rivals, F., Rosell, J., 2010. Intra-site changes in seasonality and their consequences on the faunal assemblages from Abric Romaní (Middle Palaeolithic, Spain). Quaternaire 21, 155–163.
Fletcher, W.J., Sánchez-Goñi, M.F., 2008. Orbital- and sub-orbital-scale climate impacts on vegetation of the western Mediterranean basin over the last 48,000 yr. Quat. Res. 70, 451–464.
Fletcher, W.J., Sánchez Goñi, M.F., Allen, J.R.M., Cheddadi, R., Combourieu-Nebout, N., Huntley, B., Lawson, I., Londeix, L., Magri, D., Margari, V., Müller, U.C., Naughton, F., Novenko, E., Roucoux, K., Tzedakis, P.C., 2010. Millennial-scale variability during the last glacial in vegetation records from Europe. Quat. Sci. Rev. 29, 2839–2864.
Font-Tullot, I., 2000. Climatología de España y Portugal. Universidad de Salamanca, Salamanca.

Fourel, F., Martineau, F., Lécuyer, C., Kupka, H.-J., Lange, L., Ojeimi, C., Seed, M., 2011. $^{18}O/^{16}O$ ratio measurements of inorganic and organic materials by elemental analysis–pyrolysis–isotope ratio mass spectrometry continuous-flow techniques. Rapid Commun. Mass Spectrom. 25, 2691–2696.

Gabucio, M.J., Cáceres, I., Rivals, F., Bargalló, A., Saladié, P., Vallverdú, J., Vaquero, M., Carbonell, E., 2018. Unraveling a Neanderthal palimpsest from a zooarcheological and taphonomic perspective. Archaeol. Anthropol. Sci. 10, 197–222.

Gabucio, M.J., Cáceres, I., Rosell, J., 2012. Evaluating post-depositional processes in level O of the Abric Romaní archaeological site. Neues Jahrb. für Geol. und Paläontologie - Abhandlungen 265, 147–163.

Gabucio, M.J., Cáceres, I., Rosell, J., Saladié, P., Vallverdú, J., 2014. From small bone fragments to Neanderthal activity areas: The case of Level O of the Abric Romaní (Capellades, Barcelona, Spain). Quat. Int. 330, 36–51.

Gabucio, M.J., Fernández-Laso, M.C., Rosell, J., 2017. Turning a rock shelter into a home. Neanderthal use of space in Abric Romaní levels M and O. Hist. Biol. 30, 743–766.

Genty, D., Combourieu-nebout, N., Peyron, O., Blamart, D., Wainer, K., Mansuri, F., Ghaleb, B., Isabello, L., Dormoy, I., Grafenstein, U. Von, Bonelli, S., Landais, A., Brauer, A., 2010. Isotopic characterization of rapid climatic events during OIS3 and OIS4 in Villars Cave stalagmites (SW-France) and correlation with Atlantic and Mediterranean pollen records. Quat. Sci. Rev. 29, 2799–2820.

Giralt, S., Julià, R., 1996. The sedimentary record of the Middle/Upper Paleolithic transition in the Capellades area (NE Spain), in: Carbonell, E., Vaquero, M. (Eds.), The Last Neanderthals, the First Anatomically Modern Humans: Cultural Change and Human Evolution: The Crisis at 40 Ka BP. Universitat de Tarragona, Tarragona, pp. 356–376.

Gómez de Soler, B., 2016. Procedencia del aprovisionamiento lítico durante el Paleolítico Medio en el yacimiento del Abric Romaní (Capellades, Barcelona). Niveles M, Oa y P. Universitat Rovira i Virgili, Tarragona.

Gómez de Soler, B., 2007. Áreas de captación y estrategías de aprovisionamiento de rocas silíceas en el nivel L del Abric Romaní (Capellades, Barcelona). Universitat Rovira i Virgili, Tarragona. Doctoral thesis (inedit).

Hernández Fernández, M., 2001. Bioclimatic discriminant capacity of terrestrial mammal faunas. Glob. Ecol. Biogeogr. 10, 189–204.

Hernández Fernández, M., Álvarez Sierra, M.Á., Peláez-Campomanes, P., 2007. Bioclimatic analysis of rodent palaeofaunas reveals severe climatic changes in Southwestern Europe during the Plio-Pleistocene. Palaeogeogr. Palaeoclimatol. Palaeoecol. 251, 500–526.

IAEA/WMO, 2018. Global Network of Isotopes in Precipitation. The GNIP Database. Accessible at WISER (Water Isotope System for Data Analysis, Visualization and Electronic Retrieval): https://nucleus.iaea.org/wiser.

IUCN, 2018. The IUCN Red List of Threatened Species. Version 2017-3: www.iucnredlist.org.

Jeffrey, A., Denys, C., Stoetzel, E., Lee-Thorp, J. a., 2015. Influences on the stable oxygen and carbon isotopes in gerbillid rodent teeth in semi-arid and arid environments: Implications for past climate and environmental reconstruction. Earth Planet. Sci. Lett. 428, 84–96.

Jiménez, C., 2003. Guía dels ocells de Vilanova del Camí. Ajuntament de Vilanova del Camí, Vilanova del Camí (Barcelona).

Kowalski, K., 1995. Taphonomy of bats (Chiroptera). Geobios 18, 251–256.

Lagos, P., 2019. Predation and Its Effects on Individuals: From Individual to Species. Encyclopedia of Ecology 2, 365-368.

Lécuyer, C., Fourel, F., Martineau, F., Amiot, R., Bernard, A., Daux, V., Escarguel, G., Morrison, J., 2007. High-precision determination of $^{18}O/^{16}O$ ratios of silver phosphate by EA-pyrolysis-IRMS continuous flow technique. J. Mass Spectrom. 42, 36–41.

Lécuyer, C., Grandjean, P., O'Neil, J.R., Cappetta, H., Martineau, F., 1993. Thermal excursions in the ocean at the Cretaceous-Tertiary boundary (northern Morocco): $\delta^{18}O$ record of phosphatic fish debris. Palaeogeogr. Palaeoclimatol. Palaeoecol. 105, 235–243.

Lindars, E.S., Grimes, S.T., Mattey, D.P., Collinson, M.E., Hooker, J.J., Jones, T.P., 2001. Phosphate $\delta^{18}O$ determination of modern rodent teeth by direct laser fluorination: An appraisal of methodology and potential application to palaeoclimate reconstruction. Geochim. Cosmochim. Acta 65, 2535–2548.

Lloveras, L., Moreno-García, M., 2009. Butchery, cooking and human consumption marks on Rabbit (*Oryctolagus cuniculus*) bones: an axperimental study. J. Taphon. 7, 179–201.

Lloveras, L., Moreno-Garcia, M., Nadal, J., 2008a. Taphonomic study of leporid remains accumulated by the Spanish Imperial Eagle (*Aquila adalberti*). Geobios 41, 91–100.

Lloveras, L., Moreno-García, M., Nadal, J., 2012. Feeding the Foxes: An Experimental Study to Assess Their Taphonomic Signature on Leporid Remains. Int. J. Osteoarchaeol. 22, 577–590.

Lloveras, L., Moreno-García, M., Nadal, J., 2008b. Taphonomic analysis of leporid remains obtained from modern Iberian lynx (*Lynx pardinus*) scats. J. Archaeol. Sci. 35, 1–13.

López-García, J.M., 2011. Los micromamíferos del Pleistoceno superior de la Península Ibérica. Evolución de la diversidad taxonómica y cambios paleoambientales y paleoclimáticos. Ed. Académica Española, Saarbrücken.

López-García, J.M., 2008. Late Pleistocene small mammals from Abric Romaní (Barcelona, Spain). Ann. dell'Università degli Stud. di Ferrara vol.spec., 105–110.

López-García, J.M., Blain, H.-A., Lozano-Fernández, I., Luzi, E., Folie, A., 2017. Environmental and climatic reconstruction of MIS 3 in northwestern Europe using the small-mammal assemblage from Caverne Marie-Jeanne (Hastière-Lavaux, Belgium). Palaeogeogr. Palaeoclimatol. Palaeoecol. 485, 622–631.

López-García, J.M., Blain, H.A., Bennàsar, M., Fernández-García, M., 2014. Environmental and climatic context of neanderthal occupation in southwestern Europe during MIS3 inferred from the small-vertebrate assemblages. Quat. Int. 326–327, 319–328.

López-García, J.M., Cuenca-Bescós, G., 2010. Évolution climatique durant le Pléistocène Supérieur en Catalogne (nord-est de l'Espagne) d'après l'étude des micromammifères. Quaternaire 21, 249–258.

López-García, J.M., Sevilla, P., Cuenca-Bescós, G., 2009. New evidence for the greater noctule bat (*Nyctalus lasiopterus*) in the Late Pleistocene of western Europe. Comptes Rendus Palevol 8, 551–558.

López García, J.M., 2007. Primeros datos sobre los microvertebrados del Pleistoceno Superior del Abric Romaní (Capellades, Barcelona), in: Cambra-Moo, O. et al. (Ed.), Cantera Paleontológica. Diputación Provincial de Cuenca, Cuenca, pp. 235–245.

López, M., López-Fuster, M.J., Palazón, S., Ruiz-Olmo, J., Ventura, J., 2006. Els mamífers, in: La Fauna Vertebrada a Les Terres de Lleida. Universitat de Lleida, Lleida, pp. 230–262.

Manzanares, A., 2012. Aves rapaces de la Península Ibérica, Baleares y Canarias. Ediciones Omega, Barcelona.

Margalef, R., 1974. Ecología. Omega, Barcelona.

Marín-Arroyo, A.B., Landete-Ruiz, M.D., Seva-Román, R., Lewis, M.D., 2014. Manganese coating of the Tabun faunal assemblage: Implications for modern human behaviour in the Levantine Middle Palaeolithic. Quat. Int. 330, 10–18.

Marín, J., Saladié, P., Rodríguez-Hidalgo, A., Carbonell, E., 2017a. Neanderthal hunting strategies inferred from mortality profiles within the Abric Romaní sequence. PLoS One 12, 1–42.

Marín, J., Saladié, P., Rodríguez-Hidalgo, A., Carbonell, E., 2017b. Ungulate carcass transport stratigies at the Middle Paleolithic site of Abric Romaní (Capellades, Spain). Comptes Rendus Palevol 16, 103–121.

Mikkola, H., 1983. Owls of Europe. Buteo Books, Sussex.

Modolo, M., Rosell, J., 2017. Reconstructing occupational models: Bone refits in Level I of Abric Romaní. Quat. Int. 435, 180–194.

Montuire, S., Navarro, N., Le, C., Langlois, C., Lécuyer, C., Montuire, S., Langlois, C., Martineau, F., 2004. Oxygen isotope compositions of phosphate from arvicoline teeth and Quaternary climatic changes, Gigny, French Jura. Quat. Res. 62, 172–182.

Morant, N., García-Antón, M.D., 2000. Estudio de las materias primas líticas del nivel I del Abric Romaní., in: Paleolítico Da Península Ibérica. Actas Do 30 Congresso Do Arqueologia Peninsular.

Moya-Costa, R., Cuenca-Bescós, G., Bauluz, B., Rofes, J., 2018. Structure and composition of tooth enamel in quaternary soricines (Mammalia). Quat. Int. 481, 52–60.

Norrdahl, K., Korpima, E., 2002. Seasonal changes in the numerical responses of predators to cyclic vole populations. Ecography (Cop.). 25, 428–438.

Obuch, J., 2011. Spatial and temporal diversity of the diet of the tawny owl (*Strix aluco*). Slovak Raptor J. 5, 1–120.

Palomo, L.J., Gisbert, J., Blanco, C., 2007. Atlas y libro rojo de los mamíferos terrestres de España. Organismo Autónomo Parques Nacionales, Madrid.

Picin, A., Carbonell, E., 2016. Neanderthal mobility and technological change in the northeastern of the Iberian Peninsula: The patterns of chert exploitation at the Abric Romaní rock-shelter. Comptes Rendus Palevol 15, 581–594.

Picin, A., Vaquero, M., Weniger, G.C., Carbonell, E., 2014. Flake morphologies and patterns of core configuration at the Abric Romaní rock-shelter: A geometric morphometric approach. Quat. Int. 350, 84–93.

Rasmussen, S.O., Bigler, M., Blockley, S.P., Blunier, T., Buchardt, S.L., Clausen, H.B., Cvijanovic, I., Dahl-Jensen, D., Johnsen, S.J., Fischer, H., Gkinis, V., Guillevic, M., Hoek, W.Z., Lowe, J.J., Pedro, J.B., Popp, T., Seierstad, I.K., Steffensen, J.P., Svensson, A.M., Vallelonga, P., Vinther, B.M., Walker, M.J.C., Wheatley, J.J., Winstrup, M., 2014. A stratigraphic framework for abrupt climatic changes during the Last Glacial period based on three synchronized Greenland ice-core records: Refining and extending the INTIMATE event stratigraphy. Quat. Sci. Rev. 106, 14–28.

Romagnoli, F., Gómez de Soler, B., Bargalló, A., Chacón, M.G., Vaquero, M., 2018. Here and now or a previously planned strategy? Rethinking the concept of ramification for micro-production in expedient contexts: Implications for Neanderthal socio-economic behaviour. Quat. Int. 474, 168–181.

Rosell, J., Blasco, R., Fernández-Laso, M.C., Vaquero, M., Carbonell, E., 2012a. Connecting areas: Faunal refits as a diagnostic element to identify synchronicity in the Abric Romaní archaeological assemblages. Quat. Int. 252, 56–67.

Rosell, J., Cáceres, I., Blasco, R., Bennàsar, M., Bravo, P., Campeny, G., Esteban-Nadal, M., Fernández-Laso, M.C., Gabucio, M.J., Huguet, R., Ibáñez, N., Martín, P., Rivals, F., Rodríguez-Hidalgo, A., Saladié, P., 2012b. A zooarchaeological contribution to establish occupational patterns at Level J of Abric Romaní (Barcelona, Spain). Quat. Int. 247, 69–84.

Royer, A., Lécuyer, C., Montuire, S., Amiot, R., Legendre, S., Cuenca-Bescós, G., Jeannet, M., Martineau, F., 2013a. What does the oxygen isotope composition of rodent teeth record? Earth Planet. Sci. Lett. 361, 258–271.

Royer, A., Lécuyer, C., Montuire, S., Escarguel, G., Fourel, F., Mann, A., Maureille, B., 2013b. Late Pleistocene (MIS 3-4) climate inferred from micromammal communities and $\delta^{18}O$ of rodents from Les Pradelles, France. Quat. Res. 80, 113–124.

Salamolard, M., Butet, A., Leroux, A., Bretagnolle, V., 2000. Responses of an avian predator to variations in prey density at a temperature latitude. Ecology 81, 2428–2441.

Sánchez Goñi, M.F., Landais, A., Fletcher, W.J., Naughton, F., Desprat, S., Duprat, J., 2008. Contrasting impacts of Dansgaard-Oeschger events over a western European latitudinal transect modulated by orbital parameters. Quat. Sci. Rev. 27, 1136–1151.

Sans-Fuentes, M. a., Ventura, J., 2000. Distribution patterns of the small mammals (Insectivora and Rodentia) in a transitional zone between the Eurosiberian and the Mediterranean regions. J. Biogeogr. 27, 755–764.

Scott, L., Fernandez-Jalvo, Y., Denys, C., 1996. Owl pellets, pollen and the palaeoenvironment. S. Afr. J. Sci. 92, 223–224.

Servei Meteorològic de Catalunya, 2018. Climatologies Comarcals & Anuari de dades meteorològiques.

Solé, A., Allué, E., Carbonell, E., 2013. Hearth-related wood remains from Abric Romaní layer M (Capellades, Spain). J. Anthropol. Res. 69, 535–559.

Southern, H.N., 1954. Tawny owl and their prey. Int. J. Avian Sci. 96, 384–410.

Staubwasser, M., Drăgușin, V., Onac, B.P., Assonov, S., Ersek, V., Hoffmann, D.L., Veres, D., 2018. Impact of climate change on the transition of Neanderthals to modern humans in Europe. Proc. Natl. Acad. Sci. 115, 9116–9121.

Svensson, A., Andersen, K.K., Bigler, M., Clausen, H.B., Davies, D.D.S.M., Johnsen, S.J., 2008. A 60000 year Greenland stratigraphie ice core chronology. Clim. Past 4, 47–57.

Svensson, L., 2010. Guía de aves. España, Europa y región mediterránea. Omega, Barcelona.

Terry, R.C., 2007. Inferring predator identity from skeletal damage of small-mammal prey remains. Evol. Ecol. Res. 9, 199–219.

Vallerdú, J., Allué, E., Bischoff, J.L., Cáceres, I., Carbonell, E., Cebrià, A., García-Antón, D., Huguet, R., Ibáñez, N., Martínez, K., Pastó, I., Rosell, J., Saladíe, P., Vaquero, M., 2005. Short human occupations in the Middle Palaeolithic level I of the Abric Romaní rock-shelter (Capellades, Barcelona, Spain). J. Hum. Evol. 48, 157–174.

Vallverdú, J., Alonso, S., Bargalló, A., Bartrolí, R., Campeny, G., Carrancho, Á., Expósito, I., Fontanals, M., Gabucio, J., Gómez, B., Prats, J.M., Sañudo, P., Solé, À., Vilalta, J., Carbonell, E., 2012. Combustion structures of archaeological level O and mousterian activity areas with use of fire at the Abric Romaní rockshelter (NE Iberian Peninsula). Quat. Int. 247, 313–324.

Vallverdú, J., Vaquero, M., Cáceres, I., Allué, E., Rosell, J., Saladié, P., Chacón, G., Ollé, A., Canals, A., Sala, R., Courty, M. A., Carbonell, E., 2010. Sleeping Activity Area within the Site Structure of Archaic Human Groups. Curr. Anthropol. 51, 137–145.

Vallverdú, J., Vaquero, M., Courty, M.-A., Carbonell, E., 2005. Procesos sedimentarios rápidos y ocupaciones humanas poco frecuentes. La sección del Pleistoceno Superior de la Coveta Nord del Abric Romaní (Capellades, Comarca de l'Anoia, Barcelona), in: Santonja, M., Peréz-González, A., Machado, M.L. (Eds.), Geoarqueología y Patrimonio En La Península Ibérica y El Entorno Mediterráneo. IV Reunión Nacional de Geoarqueología. Septiembre 2002. Ed. Adema, Almazán (Soria), pp. 319–331.

Vaquero, M., 2008. The history of stones: behavioural inferences and temporal resolution of an archaeological assemblage from the Middle Palaeolithic. J. Archaeol. Sci. 35, 3178–3185.

Vaquero, M., Allué, E., Bischoff, J.L., Burjachs, F., Vallverdú, J., 2013. Environmental, depositional and cultural changes in the Upper Pleistocene and Early Holocene: The Cinglera del Capelló sequence (Capellades, Spain). Quaternaire 24, 49–64.

Vaquero, M., Carbonell, E., 2012. Some clarifications on the Middle-Upper Paleolithic transition in Abric Romaní: Reply to Camps and Higham (2012). J. Hum. Evol. 63, 711–717.

Vaquero, M., Chacón, M.G., García-Antón, M.D., Gómez de Soler, B., Martínez, K., Cuartero, F., 2012. Time and space in the formation of lithic assemblages: The example of Abric Romaní Level J. Quat. Int. 247, 162–181.

Vaquero, M., Pasto, I., 2001. The Definition of Spatial Units in Middle Palaeolithic Sites: The Hearth-Related Assemblages. J. Archaeol. Sci. 28, 1209–1220.

Vaquero, M., Vallverdú, J., Rosell, J., Pastó, I., Allué, E., 2001. Neanderthal Behavior at the Middle Palaeolithic Site of Abric Romaní, Capellades, Spain. J. F. Archaeol. 28, 93–114.

Wolf, D., Kolb, T., Alcaraz-Castaño, M., Heinrich, S., Baumgart, P., Calvo, R., Sánchez, J., Ryborz, K., Schäfer, I., Bliedtner, M., Zech, R., Zöller, L., Faust, D., 2018. Climate deteriorations and Neanderthal demise in interior Iberia. Sci. Rep. 8, 1–10.

Wolff, E.W., Chappellaz, J., Blunier, T., Rasmussen, S.O., Svensson, A., 2010. Millennial-scale variability during the last glacial: The ice core record. Quat. Sci. Rev. 29, 2828–2838.

Yalden, D.W., 1985. Dietary separation of owls in the Peak District. Bird Study 32, 122–131.

Chapter 7.
Palaeoecological reconstruction of Teixoneres site (Moià, Barcelona) based on small mammals: origin of the assemblage and palaeoclimatic inferences

ABSTRACT

Short-term but repeated occupations of Neanderthal groups occurred in Teixoneres cave (Moià, Barcelona) in alternation with hyaenas, bears and raptors. This fossiliferous deposit was formed during Marine Isotope Stage 3 (MIS 3; 60-30 ka) and consists of two main units (III and II) where abundant small-mammal remains have accumulated. The general palaeoenvironment during human-carnivore occupations has previously been presented, but this work focuses on the origin of small-mammal faunas that provide ecological information, and on the site's taphonomic history until it was recovered thousands of years later. In addition, alternative palaeoclimatic data are provided through oxygen isotope analyses on rodent teeth from all subunits (IIIb, IIIa, IIb and IIa), which are compared with independent methods of palaeotemperature estimations. As has been previously observed with leporids and bird remains, raptors are considered the major source of small-mammal remains found in the sequence. The most likely accumulator of small mammals for lower subunits (IIIb and IIIa) is the eagle owl (Bubo bubo). Its activity likely contributed to unit II as well, but discrepancies detected could indicate mixed assemblages to which different owls also contributed. Occasional inputs by carnivores are also identified in subunit IIIb. The post-depositional alterations are mainly related to a wet fossiliferous environment and important breakage rates are detected. The medium to low amplitudes of $\delta^{18}O$ values point to a preferential accumulation of rodents around the spring months, in accordance with previous seasonality inferences for leporids, birds, and ungulates of the sequence. According to $\delta^{18}O$ estimation of temperatures, cooler conditions than present-day (between -1.6 °C and -0.5 °C) are recorded along the sequence, but they are globally homogenous (<1 °C). Only slight changes are observed between lower unit III and II, showing climatic instability and slightly cooler temperatures in the former. This variation could be related to palimpsests of stadial-interstadial events. Complementary methods of climatic reconstruction also explain higher precipitation rates for the site than present-day levels (between + 44 mm and +682 mm).

1. Introduction

Neanderthal groups recurrently occupied Teixoneres cave (Moià, Barcelona) during the Marine Isotopic Stage 3 (MIS 3). Carnivores such as hyenas, bears, and other small mammals, and birds of prey, both nocturnal and diurnal, also frequented the cave and played an active role in the development of this sequence. These occupational dynamics were interrupted by short and sporadic Neanderthal settlements (Rosell et al., 2008, 2010a, 2010b, 2017; Rufà et al., 2014, 2016; Sánchez-Hernández et al., 2014, 2016). Owls which probably roosted inside the cave over decades and centuries are preliminarily assumed to be the main agent involved in the large number of small mammals (insectivores, bats and rodents) trapped in Teixoneres cave sediments. However, until now any complete taphonomic analysis was performed on this group and only some preliminary comments were made (López-García et al., 2012b, 2014). Accurate ecological inferences based on small mammals require a complete knowledge of the agent involved in their accumulation, especially for deposits to which carnivores have frequently contributed, as is the case of Teixoneres cave (see synthesis in Rosell et al., 2017). In this chapter taphonomic analyses of small-mammal samples recovered from the four subunits differentiated in the site (IIIb, IIIa, IIb and IIa) are presented. Apart from the identification of the main taphonomic agent involved in their accumulation, post-depositional alterations complemented the history of these small-mammal remains until they were

recovered. A multidisclipinary team working at the site has recently provided extensive data concerning problems that can affect small-mammal communities, such as the origin of small prey (leporids and birds), the seasonality of the production of these remains, and the evaluation of time periods of human occupations, that should be addressed (Rosell et al., 2017; Rufà et al., 2014, 2016; Sánchez-Hernández et al. , 2014, 2016).

Recent excavations in unit III have also provided interesting findings with ecological implications, such as the occasional presence of the woolly mammoth and the woolly rhinoceros, two cold-adapted fauna infrequent in Iberia (Álvarez-Lao et al., 2017). Moreover, previous absolute datings (Tissoux et al., 2006) and relative chronology inferred from small vertebrate faunas (López-García et al., 2012b) have been recently adjusted thorough new ^{14}C datings (Talamo et al., 2016) (note that dating provide in Chapter 3 correspond to old published data). These new findings, in addition to expanding archaeo-palaeontological material during the ongoing excavations, allows us to reconsider the initial palaeoenvironmental reconstruction based on small vertebrates. This work complements previous reconstructions by using 40 oxygen isotope analysis ($\delta^{18}O$) on rodent incisors from subunit IIIb to IIa. The relationship between $\delta^{18}O$ preserved in mammal body tissues with $\delta^{18}O$ of meteoric waters and mean annual temperatures, allows us to quantify the intensity of the climatic changes through the sequence (see Chapter 2 and 4). Thus, considering all the recent research on the site, this work aims to reevaluate the ecological conditions during this sequence formation, unravelling the origins of the small-mammal remains and post-depositional processes. In addition, it presents an attempt to estimate palaeotemperatures, based on the oxygen isotope analysis of rodent remains, and a comparison with independent methods for the estimation of climatic parameters.

2. Teixoneres cave

Teixoneres cave is located 5 km east of the village of Moià (Barcelona, Spain) (Fig. 7.1A) and belongs to the karstic system called Toll Caves, which forms a course of galleries more than 2 km long. The karst's coordinates are 2°09'02"E and 41°48'25"N at 760 m a.s.l.. This complex was formed by the drainage system of Torrent Mal, which modelled the Neogene limestone (called Collsuspina Formation) and configures the present-day endokarstic landscape (Rosell et al., 2008). Several archaeological deposits from different chronologies are contained within this complex of caves, of which Teixoneres Cave and Toll Cave are the most representative sites (Rosell et al., 2014). The site is located in the highlands between the two main rivers the Llobregat and the Ter, connecting the central region of Catalonia with the Mediterranean coast (Rosell et al., 2017). Toll Caves were discovered in the 1950s by a local speleological group. Afterward, several interventions were carried out by different research teams until the 1990s, bringing to light an important Holocene sequence and Late Pleistocene palaeontological record. Since 2003, systematic excavations are undergone annually under the direction of a multidisciplinary team of the *Institut Català de Paleoecologia Humana i Evolució Social* (IPHES), applying the extension method of fieldwork that involves the extension of the whole surface of the site (Rosell et al., 2008, 2010a, 2010b, 2014).

Teixoneres cave is composed of three main chambers (X, Y, and Z) that together form a 30 m length U-shape, with two access points from chambers X and Z (Fig. 7.2). Chamber X is the bigger gallery, which is long and filled with a 6 m-

thick sediment package containing nine archaeo-palaeontological units, including two speleothems (unit I and IV) (Rosell et al., 2008, 2010a). The dates of unit I (ca. 14-16 ka) and unit IV (ca. 100.3 ±6.1 ka) have been obtained through U-series dating of stalagmite layers (Fig. 7.1B) (Tissoux et al., 2006), providing minimum and maximum ages for intermediate units II and III. Relative dating was inferred from biochronology based on small-mammal communities, indicating a range from 90 to 60 ka for unit III and 60 to 30 ka for unit II (López-García et al., 2012b). Recently, ^{14}C dating adjust the chronology of unit III, from >51,000 ^{14}C BP to 44,210 cal BP, and unit II, which extends between 44,210 and 33,060 cal BP (Talamo et al., 2016). This chapter focuses on these two units (II and III) of Chamber X, which have been the focus of recent excavations (Rosell et al., 2008, 2010a; Rufà et al., 2016). Both are units comprising sandy lutites and limestone blocks. A distinction between two archaeo-stratigraphic subunits (IIa and IIb) has been drawn due to the presence of large limestone blocks at the base of IIa. In turn, at least two different subunits (IIIa and IIIb) can be appreciated in unit III. They can be distinguished by an increased presence of reddish clays in IIIb, limestone blocks at the base of IIIa, and the intensification of archaeological material in IIIb. The sediment comes from allochthonous colluvial clays and silts, which entered the cave through the main entrance and a chimney located at the northeast side of the cave. Those sediments imbricate at the center of the main gallery. An autochthonous component is formed by limestone blocks falling from the walls and the roof of the cave.

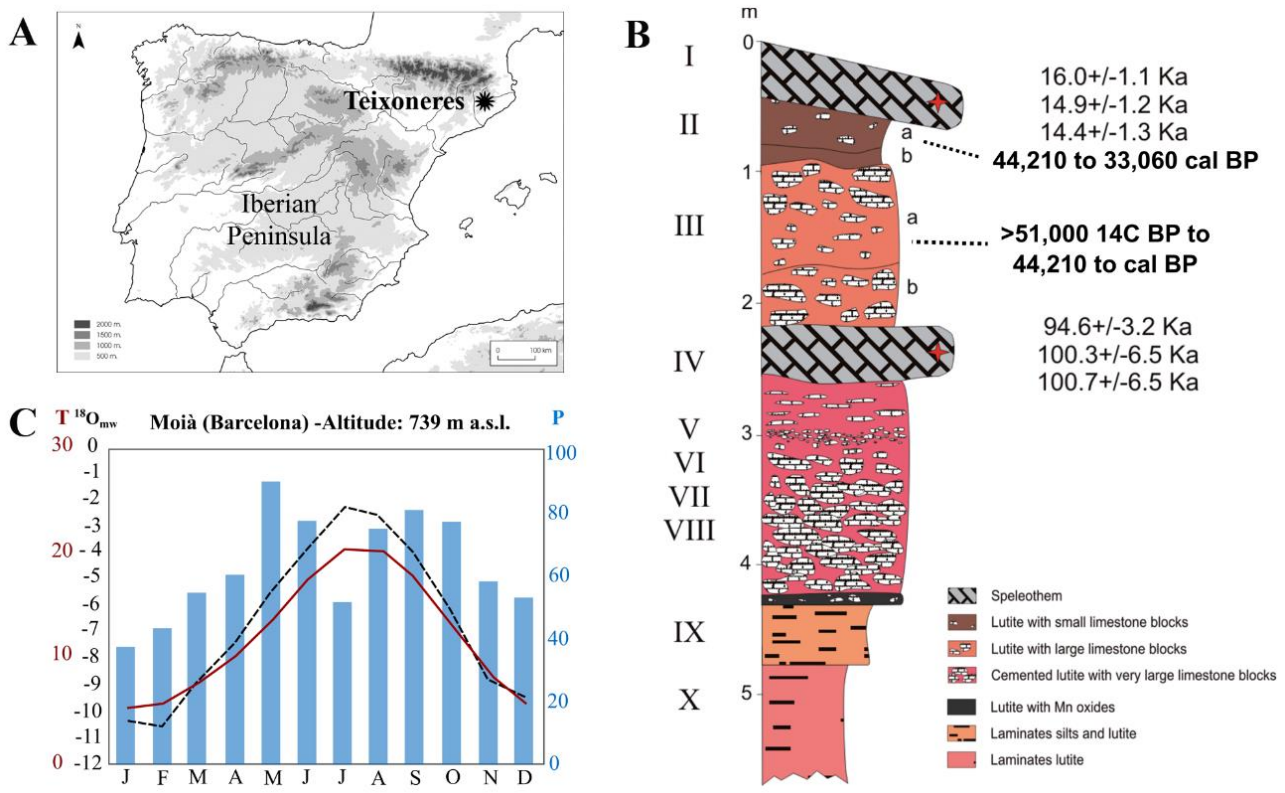

Figure 7.1 (A) Location of the Teixoneres cave in Iberia; (B) Stratigraphy of the fossiliferous sequence and U-series (Tissoux et al., 2006) and radiocarbon dates Teixoneres cave (Talamo et al., 2016); (C) Current monthly temperatures (red line; T; in ºC) and precipitations (bars; P; in mm)(Climate-data.org) and present-day oxygen isotope composition of meteoric waters (dash black; $\delta^{18}Omw$; in ‰ V-SMOW) (Bowen, 2017) of Moià.

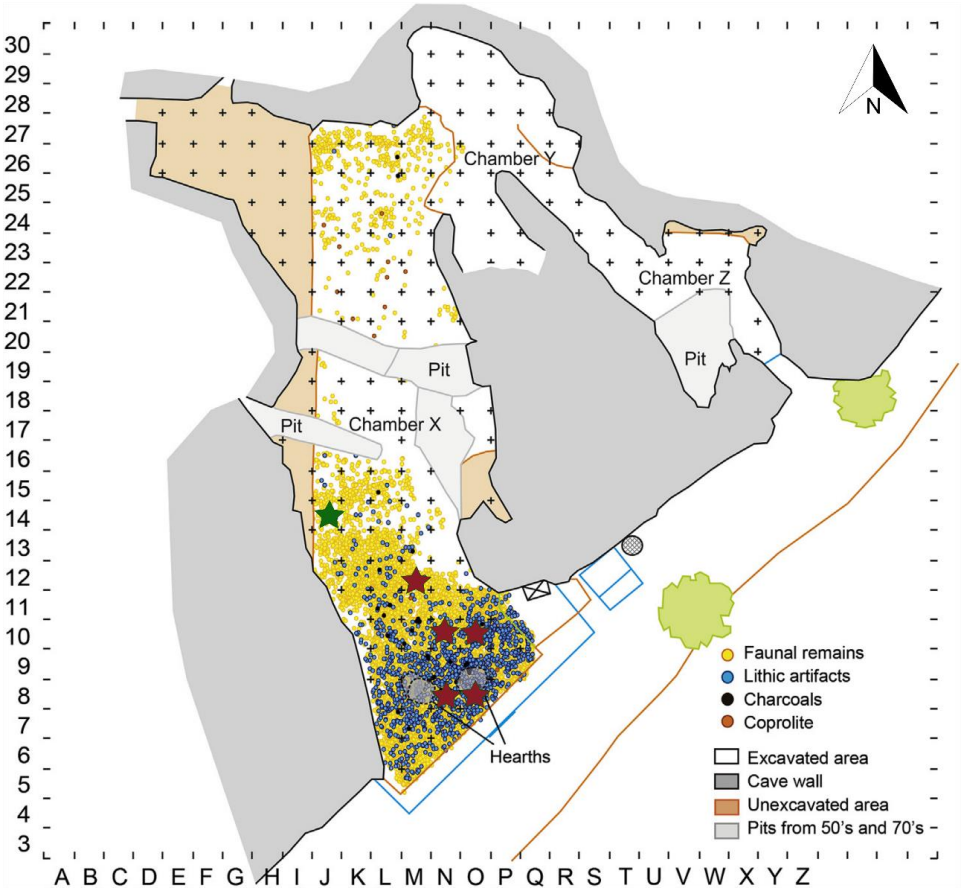

Figure 7.2 Ground plan of unit III of Teixoneres cave showing the 3D-position of the recovered items: lithics (blue), faunal remains (yellow), charcoals (black) and coprolites (brown). Squares sampled for taphonomic analyses of small mammals correspond to red (unit III) and green (unit II) stars. Drawing modified from Rosell et al. (2017).

Most previous work has concluded that there were short-term human occupations of the cave, alternated with use by carnivorous predators, ruling out temporal contact between them (Bustos-Pérez et al., 2017; Rosell et al., 2010a, 2010b, 2014, 2017; Rufà et al., 2014, 2016; Sánchez-Hernández et al., 2014, 2016). Moreover, a bimodal spatial distribution is observed, which human groups tend to concentrate their activities at the entrance of the cave, whereas carnivores and other predators preferentially use the inner areas (Fig. 7.2). Among large mammals, a wide diversity of species was recorded in the cave, where both herbivores (*Equus ferus*, *Equus hydruntinus*, *Cervus elaphus*, *Capreolus capreolus, Bos primigenius, Sus scrofa, Capra pyrenaica,* and *Rupicapra rupicapra*) and carnivores (*Ursus spelaeus, Crocuta crocuta, Canis lupus, Vulpes vulpes, Lynx spelaea*, *Meles meles*) are frequent. Medium-sized animals were also identified as tortoise (*Testudo hermanni*), leporids (*Oryctolagus cuniculus* and *Lepus* sp.), and birds (Corvidae, Phasianidae, Strigidae and Columbidae) (Rosell et al., 2010a, 2010b; Rosell et al., 2008; Rufà et al., 2016, 2014). Recently, the presence of two cold-adapted species has been recorded, *Mammuthus primigenius* and *Coelodonta antiquitatis* (Álvarez-Lao et al., 2017). Both hominin and carnivore activities were documented in larger fauna. Human butchering activities, mainly in ungulates, was confirmed from the detection of cut marks, fresh fractures, and burning (Rosell et al., 2008, 2010a, 2010b). Leporids from unit III and

birds from the four subunits (IIIb-IIa), seem to be the result of input from mixed sources to which mammalian carnivores and nocturnal raptors contributed to different degrees (Rufà et al., 2014, 2016). Birds do not seem to be part of the Neanderthals' diet at Teixoneres cave, not even as an opportunistic resource. However, sporadic consumption of leporids by humans was detected. The presence of Neanderthal groups is confirmed at the site by the discovery of Mousterian lithic tools. Raw materials have a local or semi-local origin (<15 km) and consist mainly of quartz, followed by chert, agates, and limestones. Both expedient knapping and hierarchical strategies are documented. Reduction sequences are highly fragmented, consisting in flakes and final products, with some retouched tools (mainly scrapers) that have been link to short-term occupation patterns (Bustos-Pérez et al., 2017; Rosell et al., 2010a, 2010b; Talamo et al., 2016). Some combustion structures by means of sediment areas with rubefaction or hearths were detected mainly at the entrance in unit III (Rosell et al., 2010a, 2014).

Different approaches to reconstructing the palaeoecological conditions of Teixoneres cave were taken. The specific attribution of the small-vertebrate remains (amphibians, squamates reptiles and small mammals) was performed by López-García et al. (2012, 2014). Small-vertebrate assemblages abundances underline a clear predominance of the forest component (>60%), especially in unit III, and cooler and wetter conditions in the region than present-day. These data, in combination with pollen, charcoal, and large-mammal dental wear analyses, describe an open forest landscape, with temperate and humid conditions during the formation of unit III, and cooler and drier conditions during the formation of unit II. Palynological data confirm a landscape dominated by woodlands and some open areas, showing high proportions of arboreal pollen (>50%). Woodlands are composed of pines and oaks (*Quercus* sp.) with herbaceous taxa such as Poaceae, Chenopodicea and Astareceae; whereas semi-open landscape is confirmed by the presence of heliophilous taxa (such as Cupressaceae or Cistaceae). Charcoal remains are scarce in the cave, but four taxa are recorded (*Buxus sempervirens*, *Pinus pinea/pinaster* type, *Pinus sylvestris* type and *Quercus* sp.). Luzi et al. (2017) studied the morphological and morphometric variation of first lower molars of two vole species abundant at the site, *Microtus agrestis* and *Microtus arvalis*, and concluded that the former decreased from subunit IIIa to IIb. In contrast, *M. arvalis* increased from IIIa to IIb. The authors related these changes to better water management given the reduction in humidity from lower to upper units.

The Moià region is included in the continental Mediterranean climate, in the boundary between the humid and sub-humid areas inside Catalonian climatic subdivisions (Servei Meteorològic de Catalunya, 2018). The climate is generally wet and temperate (mean annual temperatures around 12 °C), but with hot summers (18-21 °C) and cold winters (5-6 °C), with a consequent thermic annual oscillation around 15° C. Mean annual rainfall is between 700 and 800 mm. Precipitation is abundant throughout the year, with autumn and spring being the wettest period and winters being slightly drier (Climate-data.org; Servei Meteorològic de Catalunya, 2018). There is a consistent correspondence between average monthly temperatures and monthly oxygen isotope compositions of meteoric water estimated for the area (OIPC data, Bowen, 2017; Climate-Data.org, 2018) (Fig. 7.1C).

3. Remarks on materials and methods

The small-mammal remains included in this analysis consist mainly of isolated teeth and disarticulated bones recovered from sediment samplings (organized in depth-range of 5-10 cm) from the entire excavated surface of Chamber X (divided in 1x1 m squares), completed during excavation seasons from 2008 to 2016. The remains were collected by washing and sieving the sediment, with two superimposed meshes of 5 mm and 0.5 mm, and selected by subsequent sorting. This work has followed the same methods explained in Chapter 2 and Chapter 4 regarding taphonomic analysis, oxygen isotope analysis, and palaeotemperatures reconstruction. However, some remarks should be noted.

Due to the high amount of small-mammal material available at the site, during the taphonomic study specific areas (1 m^2) were selected from units III and II of Chamber X. Additionally, subunit divisions were considered (IIIb, IIIa, IIb, IIa) to get more accurate data (Fig. 7.2). For unit II, square J14 was selected, which corresponds with the area of the site where small-mammal remains were most abundant. Not enough material was available in unit III and a random selection that included squares N8, O8, N10, O10 and M12 was chosen from the exterior part of the cave, where the human occupations were more intense. Remains were observed under light microscopes (Exacta-Optech LFZ 10x-90x; Olympus SZ-PT 18x-50x). The identified remains were counted (NISP) and grouped using the minimum number of individuals (MNI) method, determined by counting the most highly represented diagnostic element, considering laterality. Dental remains were considered independent whether they are *in situ* or isolated (e.g. each molar on a mandible is a count as a single remain). The MNI was adapted according to the taphonomic sampling performed by considering the minimum number of elements (MNE) of each subunit. The taphonomic analysis included all rodent elements in anatomical representation (recount and indexes) and incisors, molars, femora, and humeri of rodents were included in analyses of breakage and digestion. Postcranial digestion is only considered for the proximal epiphyses of femora and the distal epiphyses of humeri. The analyses of soricids, talpids, and chiropters were also considered in the final interpretation. Post-depostional damage was evaluated in incisors, molars, femora, and humeri without considering taxonomical attribution.

Oxygen isotope compositions were measured on 40 teeth from subunits IIIb, IIIa, IIb and IIa. To avoid possible interspecific variability, *Apodemus sylvaticus* fossil incisors were preferentially selected, with thirty-four incisors corresponding to at least twenty-two individuals (Table 7.1). However, well-preserved incisors were not always available, and so four teeth of the subfamily Arvicolinae in subunit IIb (n=1) and IIa (n=3) and two teeth of the species *Eliomys quercinus* in subunit IIIb and IIa were included. In total, ten samples from each subunit were selected in order to gather a representative range of samples (Gehler et al., 2012; Lindars et al., 2001; Navarro et al., 2004; Royer et al., 2013a). The wet-chemistry and the mass spectrometer measurements were developed in the Laboratoire de Géologie of Université Claude Bernard (Lyon, France), following the sampling criteria and analytical techniques explained in Chapter 2 and Chapter 5. Based on phosphate chemical yields measured during the wet chemistry procedure, clustered phosphorus pentoxide (P_2O_5) contents close to 40 wt% indicate that the original stoichiometry of the teeth was most likely preserved. The average

Sample	Subunit	Taxon	Laterality	Location	$\delta^{18}O_p$ (‰ V-SMOW)	SD	$\delta^{18}O_{mw}$ (‰ V-SMOW)
TX430	IIa	Arvicolinae	right	isolated	20.4	0.2	-3.6
TX431	IIa	*Apodemus* cf. *sylvaticus*	right	isolated	19.0	0.2	-4.8
TX429	IIa	*Apodemus* cf. *sylvaticus*	left	isolated	18.9	0.1	-4.9
TX433	IIa	Arvicolinae	left	*in situ*	18.8	0.3	-4.9
TX432	IIa	*Apodemus* cf. *sylvaticus*	right	isolated	18.7	0.4	-5.0
TX355	IIa	*Apodemus* cf. *sylvaticus*	left	isolated	18.2	0.5	-5.4
TX348	IIa	*Eliomys quercinus*	left	*in situ*	18.0	0.3	-5.6
TX164	IIa	*Apodemus* cf. *sylvaticus*	right	isolated	17.8	0.4	-5.7
TX163	IIa	*Apodemus* cf. *sylvaticus*	left	isolated	17.3	0.3	-6.2
TX356	IIa	Arvicolinae	left	isolated	16.6	0.3	-6.7
TXB161	IIb	*Apodemus* cf. *sylvaticus*	left	isolated	20.3	0.2	-3.7
TXB160	IIb	Arvicolinae	right	isolated	19.3	0.4	-4.5
TXB377	IIb	*Apodemus* cf. *sylvaticus*	right	isolated	19.3	0.3	-4.5
TXB385	IIb	*Apodemus* cf. *sylvaticus*	left	isolated	19.2	0.3	-4.6
TXB381	IIb	*Apodemus sylvaticus*	right	*in situ*	18.3	0.2	-5.3
TXB387	IIb	*Apodemus* cf. *sylvaticus*	left	*in situ*	18.1	0.1	-5.5
TXB383	IIb	*Apodemus* cf. *sylvaticus*	right	isolated	18.0	0.3	-5.6
TXB378	IIb	*Apodemus* cf. *sylvaticus*	left	isolated	18.0	0.5	-5.6
TXB382	IIb	*Apodemus* cf. *sylvaticus*	left	isolated	17.9	0.3	-5.7
TXB376	IIb	*Apodemus* cf. *sylvaticus*	left	isolated	16.8	0.3	-6.6
TX3816	IIIa	*Apodemus* cf. *sylvaticus*	left	*in situ*	19.5	0.2	-4.3
TX3814	IIIa	*Apodemus* cf. *sylvaticus*	right	isolated	19.1	0.3	-4.7
TX3145	IIIa	*Apodemus* cf. *sylvaticus*	right	isolated	18.7	0.4	-5.0
TX3813	IIIa	*Apodemus* cf. *sylvaticus*	left	*in situ*	18.3	0.2	-5.4
TX3815	IIIa	*Apodemus* cf. *sylvaticus*	right	*in situ*	18.1	0.2	-5.5
TX38111	IIIa	*Apodemus sylvaticus*	right	*in situ*	17.7	0.3	-5.9
TX3820	IIIa	*Apodemus* cf. *sylvaticus*	right	*in situ*	16.7	0.3	-6.7
TX3819	IIIa	*Apodemus* cf. *sylvaticus*	right	isolated	16.7	0.3	-6.7
TX3818	IIIa	*Apodemus* cf. *sylvaticus*	right	*in situ*	16.5	0.3	-6.8
TX3823	IIIa	*Apodemus* cf. *sylvaticus*	right	isolated	15.5	0.3	-7.7
T3B525	IIIb	*Apodemus* cf. *sylvaticus*	right	isolated	21.3	0.4	-2.9
T3B1000	IIIb	*Apodemus sylvaticus*	left	*in situ*	20.3	0.3	-3.7
T3B421	IIIb	*Apodemus sylvaticus*	left	*in situ*	18.9	0.2	-4.8
T3B424	IIIb	*Apodemus* cf. *sylvaticus*	right	isolated	18.6	0.5	-5.1
T3B524	IIIb	*Eliomys* cf. *quercinus*	left	*in situ*	18.2	0.4	-5.5
T3B423	IIIb	*Apodemus* cf. *sylvaticus*	left	isolated	17.7	0.5	-5.8
T3B432	IIIb	*Apodemus sylvaticus*	left	*in situ*	17.6	0.5	-6.0
T3B435	IIIb	*Apodemus sylvaticus*	left	*in situ*	17.4	0.4	-6.1
T3B492	IIIb	*Apodemus sylvaticus*	right	*in situ*	16.1	0.3	-7.1
T3B2000	IIIb	*Apodemus* cf. *sylvaticus*	right	isolated	16.0	0.4	-7.2

Table 7.1 Oxygen isotope composition of tooth enamel phosphate ($\delta^{18}O_p$; ‰ V-SMOW) from rodent lower incisors from Teixoneres cave (levels II-IIIb). The table includes the stratigraphic layer, identified taxa, and the conversion to the oxygen isotope composition of meteoric waters ($\delta^{18}O_{mw}$; ‰ V-SMOW) following the Royer et al. (2013a) oxygen isotope fractionation equation. SD, Standard Deviation.

standard deviation of oxygen isotope compositions for the Teixoneres samples is 0.31 ±0.03‰ (n=40). Oxygen isotope analysis on present-day material of the Moià area are also included. The remains came from one pellet produced by a barn-owl (*Tyto alba*), recovered 7.7 km from Teixoneres cave at 1000 m a.s.l (Table 7.2; Fernández-García et al., under review; Chapter 5). These remains consist of three lower incisors from *M. (T.) duodecimcostatus* and *M. musculus*. The

	MA-12	MA-4	MA-6	MA-5
Origin	Scattered pellets	Pellet		
State	Disgregated	Semidry		
Recovering	Unknown	End of August		
Taxon	*M. (T.) duodecimcostatus*	*M. (T.) duodecimcostatus*	*M. musculus*	*M. musculus*
Laterality	right	left	right	left
$\delta^{18}O_p$ (‰V-SMOW)	16.1	18.6	19.2	19.5
SD	0.4	0.4	0.3	0.3
$\delta^{18}O_{mw}$ (‰ V-SMOW)	-7.2	-5.1	-4.6	-4.4

Table 7.2 Oxygen isotope composition of tooth enamel phosphate ($\delta^{18}O_p$; ‰ V-SMOW) from rodent lower incisors from a modern pellet of Moià. The table includes the procedence of remains, identified taxa and the conversion to the oxygen isotope composition of meteoric waters ($\delta^{18}O_{mw}$; ‰ V-SMOW) following the Royer et al. (2013a) oxygen isotope fractionation equation. SD, Standard Deviation.

pellet was recovered at the end of August, just on the foot of the owl's nest, where a big accumulation of scattered pellets was conserved. From this amount of vertebrate material, one lower incisor of *M. (T.) duodecimcostatus* was also included for oxygen isotopes analysis. The season in which this last element was produced is unknown.

Mean annual temperatures (MAT) were calculated from oxygen isotope compositions ($\delta^{18}O$) of each subunit, following the three-step strategy proposed for $\delta^{18}O_p$ from rodent teeth accumulated in the Iberian Peninsula (Chapter 5). In parallel, the past temperatures (MAT) and precipitations (mean annual precipitations; MAP) are compared with two qualitative and independent palaeoenvironmental methods: the mutual ecogeographic range (MER) and the bioclimatic model (BM). The former was previously calculated for the Teixoneres site by López-García et al. (2014; 2012), but this work applies BM for the first time (detailed explanation of these methods can be found in Chapters 2 and 5). The current temperature data of Teixoneres area (Moià) are taken from Climate-Data.org (https://es.climate-data.org/). Note that this supposed some differences with previous MER estimations when they are expressed in comparative terms, due to use in the previous study (López-García et al., 2014, 2012a) of climatic data from the meteorological station of Barcelona airport, which is located at 83 m a.s.l. (Font-Tullot, 2000). Present-day $\delta^{18}O_{mw}$ values for Teixoneres area were obtained using the Online Isotopes in Precipitation Calculator (OIPC; Bowen, 2017).

4. Results and discussion

4.1 Origin of small mammals and post-depositional alterations

The taphonomic analysis was completed on 2,642 remains; in each subunit, between 70% and 85% of total remains was anatomically identified (Table 7.3; Fig. 7.3; 7.4). The most frequent taxonomic group is the order Rodentia (NISP= 1,536; 58%), with a minimum number of 98 individuals. Chiropters (NISP=163; 6%), talpids (NISP=11; 0.5%), and soricids (NISP=37; 1.4%) were also identified, but in lower proportions (Appendix 2.4.A). Better relative abundances of skeleton elements have been recorded from unit III (around 55%), whereas unit II shows a major disequilibrium between identified individuals and preserved remains of these individuals (IIb=29%; IIa=42%). However, all subunits shared similar general characteristics

regarding skeletal part conservation. According to indexes comparing cranial and postcranial elements, these are almost in equilibrium, with the former slightly better represented than the latter. However, this better cranial conservation is mainly related to better preservation of dental elements (molars and incisors), as is shown by the predominance of humeri and femora as compared to maxillae and mandibles. Indeed, incisors are the best-represented elements in all assemblages. Breakage of mandibles and maxillae can be deduced, considering a notable disproportion between isolated teeth and empty alveolus, especially for lower subunits (between 205% and 297%). Proximal elements (humeri and femora) are more abundant than distal ones (between 50% to 70%). Most recovered teeth in these assemblages are isolated. For all analyzed subunits, less than 8% of incisors were found in their alveolar place. *In situ* molars ranged between 10.5% (subunit IIb) to 21% (subunit IIIb), mainly because of murid specimens, which have rhizodont teeth which avoid easy detachment from their alveoli. Molar breakage is low, around 15-20% in subunits IIIb and IIb, and 8-10% in subunits IIIa and IIa. Breakage is nonexistent among *in situ* molars. On the contrary, total breakage in incisors is around 65% for unit III and around 45% for unit II. Some incisors preserved in their alveolar place are also incomplete (between 20% and 27%). The overrepresentation of incisors previously reported for unit III may be related to these elevated breakage rates. All humeri and femora found in the sample were broken.

Digestion percentages ranged between 31% from subunit IIb and 43% from subunit IIa; subunits IIIb and IIIa had an almost equal proportion of total elements digested (Table 7.3; Fig. 7.3). Different degrees of digestion are observed from light to heavy, except for subunit IIIb where extreme degrees are also observed. At least 35% of the elements in unit III exhibit digestion marks, which show a practically equal pattern in the digestion of molars (50%) and incisors (around 25%). Unit II is not far from these estimations, but there is a certain disturbance within their subunits, as both present an equivalent number of digested molars and incisors: around 30% in subunit IIb and around 40% in subunit IIa. Considering present-day referential data (Andrews, 1990; Fernández-Jalvo et al., 2016), molars are expected to be less digested than incisors. The most likely explanation is the higher presence of arvicolids in these subunits, in opposition to unit III where the abundance of Murinae is important. Light digestion is easier to detect in Arvicolinae molars due to their pointed edges covered by enamel, whereas it is difficult to detect digestion in molars of Murinae until moderate degrees are reached (Fernández-Jalvo et al., 2016). Postcranial digestion accounts for around 40% of the elements, except for subunit IIIb where this percentage is reduced to less than 30%. Occasionally, intra-mandibular digestion of incisors, characterized by relatively strong digestion located only on the tip of the teeth, was identified in all subunits. Digestion was occasionally detected in bats (subunit IIb and IIIb) and also in soricids (IIIb), in whom extreme degrees of digestion are reached. Bat remains were preliminarily considered a result of both predation and *in situ* death, because the species has been recorded to frequently inhabit caves (Kowalski, 1995; López-García et al., 2012b; Palomo et al., 2007).

More than 30% of elements in each subunit were affected by digestion, and skeleton parts spectra are fragmentary, confirming that predation was the main cause of small-mammal accumulation. Breakage and proportional representation indexes are not coincident with any predator pattern

	IIIb		IIIa		IIb		IIa	
Recount								
NR (n)	782		988		388		484	
NISP (n)	573		791		323		402	
Rodent MNI (n)	22		31		23		22	
Skeletal representation								
Relative Abundance Index (%)	58.5		62.1		33.6		47	
SD of Relative Abundance Index	42.2		42.2		14.9		47	
Proportional representation indexes								
Postcranial/Cranial Index	90		90		80		90	
Humerus+Femur/Maxilla+Mandible Index	120		110		100		120	
Radius+Tibia/Humerus+Femur Index	70		50		50		50	
Isolated teeth/Empty Alveolus Index	205		297		154		121	
Breakage								
Incisors fracture (%)	68.1		68		45.8		42	
Molars fracture (%)	11.7		8.3		17.1		6.9	
Postcranial fracture (%)	100		100		100		100	
Digestion	**n**	**%**	**n**	**%**	**n**	**%**	**n**	**%**
Total digested elements	93	**35.6**	134	**36.3**	48	**31.4**	78	**43.3**
Light degree	63	24.1	105	28.5	36	23.5	56	31.1
Moderate degree	17	7	22	6	10	7	15	8
Heavy degree	9	3.4	7	1.9	2	1.3	7	3.9
Extreme degree	4	2	0	0	0	0	0	0
Digested incisors	49	**49.5**	76	**50**	16	**31.4**	21	**43.8**
Light degree	32	32.3	61	40.1	11	21.6	14	29.2
Moderate degree	12	12.1	13	8.6	3	5.9	5	10.4
Heavy degree	3	3	2	1.3	2	3.9	2	4.2
Extreme degree	2	2	0	0	0	0	0	0
Digested molars	36	**26.9**	39	**22.5**	23	**29.5**	44	**44.4**
Light degree	25	18.7	29	16.8	16	20.5	29	29.3
Moderate degree	3	2.2	5	2.9	7	9	10	10.1
Heavy degree	6	4	5	3	0	0	5	5
Extreme degree	2	1	0	0	0	0	0	0
Digested postcrania	8	**28.6**	19	**43.2**	9	**37.5**	13	**39.4**
Light degree	6	21.4	15	34.1	9	37.5	13	39.4
Moderate degree	2	7.1	4	9.1	0	0	0	0
Heavy degree	0	0	0	0	0	0	0	0
Extreme degree	0	0	0	0	0	0	0	0
Post-depositional agents	**n**	**%**	**n**	**%**	**n**	**%**	**n**	**%**
Estriations	295	**79.1**	381	**79**	167	**79.5**	171	**77.4**
Fissures	104	**27.9**	141	**29.3**	34	**16.2**	46	**20.8**
Cracks	33	**8.8**	56	**11.6**	10	**4.8**	4	**1.8**
Cementation	20	**5.4**	57	**11.8**	2	**1**	3	**1.4**
Manganese oxide pigmentation	175	**46.9**	177	**36.7**	121	**57.6**	108	**48.9**
Chemical corrosion - Plant Activity	126	**33.8**	105	**21.8**	34	**16.2**	35	**15.8**
Burning	7	**1.9**	2	**0.4**	2	**1**	0	**0**

Table 7.3 Summary of taphonomic variables analyzed, including recounts (NR, number of remains; NISP, number of identified specimens; MNI, minimum number of individuals of order Rodentia considered in skeletal representation), alterations caused by predation (skeletal representation, proportional representation indexes, breakage and digestion), and post-depositional alterations.

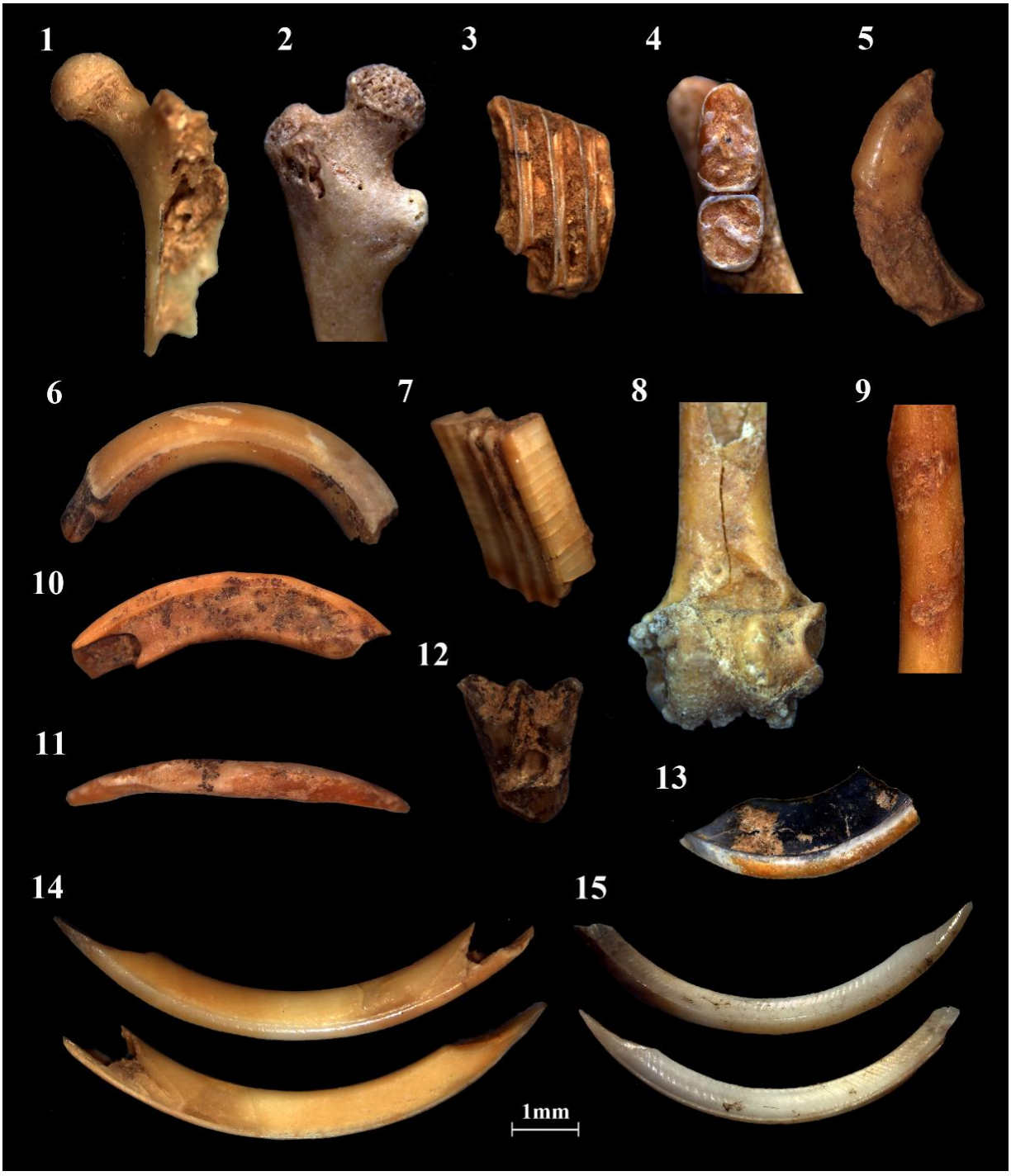

Figure 7.3 Some taphonomic features detected on small-mammal remains from Teixoneres cave and oxygen isotope samples. 1) left femur proximal epiphysis of a rodent with light digestion (subunit IIIa); 2) left femur proximal epiphysis of a rodent with moderate digestion (IIIa); 3) Arvicolinae molar with heavy digestion (IIIa), in lateral view; 4) right first and second lower molars of *Apodemus sylvaticus* with extreme digestion (IIIb), in occlusal view; 5) rodent upper incisor with light digestion (on the tip) and root damage (on the posterior part) (IIIa), in lateral view; 6) rodent upper incisor with light intra-mandibular digestion, with scattered manganese oxide pigmentation on dentine and root imprints in enamel (IIIa); 7) Arvicolinae molar with fissures related to humidity changes (IIIa); 8) right humerus distal epiphysis of *Myotis myotis-blythii* with cementation (IIIb); 9) roots imprints on a rodent femur shaft (IIIb); 10) rodent upper incisor with extreme digestion (IIIb), in lateral view; 11) rodent lower incisor with heavy (IIIb), in occlusal view; 12) right upper molar of *Myotis myotis-blythii* with widespread manganese oxide pigmentation (IIIa), in occlusal view; 13) burned rodent upper incisor (IIIa), in lateral view; 14) left lower incisor fossil of *Apodemus sylvaticus* (level IIIa), in labial and lingual view; 15) modern right lower incisor modern of *Mus musculus* (origin: *Tyto alba* pellet), in labial and lingual view. 14) and 15) are included in biochemical analysis. Scale 1 mm.

(Andrews, 1990), even sometimes showing values included in Categories 4 and 5 of predators. It is common for indexes in archaeological contexts to differ from those from modern collections, because palimpsets and long-term post-depositional processes can occur. The overrepresentation of teeth, specially incisors, in most of the cases isolated and the high rates of breakage attained by incisors and femora denoted important destruction of small-mammal remains. Some of the hypotheses suggested for the breakage and anatomical profile biases rely on post-depositional agents, such as trampling, weathering, burning or scavenging of carnivores (Rufà et al., 2014, 2016). Considering slow rates of sedimentation in Teixoneres cave, these post-mortem alterations could be more common than in other fossiliferous contexts. The predominance of remains without digestion marks, light alterations being the most frequent degree of digestion, low frequency of heavy digestions, and the absence of extreme digestion (except in subunit IIIb) throughout the sequence point to nocturnal raptors as the main agent. They do not support the possibility of intervention by predators included in Category 4-5 (Andrews, 1990), such as diurnal raptors or small carnivores, which was suggested by fragmentation rates (Andrews, 1990; Comay and Dayan, 2018; Fernández-Jalvo and Andrews, 1992; Lloveras et al., 2008a, 2008b, 2012; Terry, 2007). The occasional extreme digestions recorded in subunit IIIb (2% of rodents, but also detected in some Soricidae remains) are not consistent with owls and are probably a consequence of punctual intervention of small carnivores in the cave.

Globally, progressive proportion of degrees of digestion across each anatomical element and the correlation between proportion and degrees of digestion between skeleton elements analyzed, could indicate that a single type of predator is the most likely cause (Bennàsar, 2010; Bennàsar et al., 2016). This pattern is clear for unit III, but less so for unit II, for which some clarifications should be made. Digestion remains percentages and degree of digestion attained, besides medium-high relative abundance of elements and molar breakage recorded by small mammals analyzed at all subunits, fit with an intermediate modification predator (Andrews, 1990) such as *Bubo bubo* or *Strix aluco*. Distinguishing between these two owls, *B. bubo* and *S. aluco*, is not simple, as both inflict similar damage on small-mammal remains. Subunits IIIa and IIIb, that provide similar digestion results in each skeletal element, present some characteristics that are more consistent with patterns expected from *B. bubo* than those of *S. aluco*. This owl tends to produce higher relative abundances of elements (around 60%), a low incidence of heavy digestion (which would be even lower in unit III if carnivores had contributed) and medium-sized prey such as leporids (some of which have been already related to this predator in unit III, Rufà et al., 2014)(Andrews, 1990; Bennàsar et al., 2016; Fernández-Jalvo, 1992).

The interpretation of results from unit II is more complex. Considering the scarcity of remains with moderate and heavy digestion, diurnal raptors and carnivores can be ruled out as the main cause (Andrews, 1990). In unit III as well, the main action of a predator of intermediate modification has been confirmed, but high rates of digested molars relative to digested incisors indicate that it is a different predator than *B. bubo*. Based on present-day reference collections (Andrews, 1990; Fernández-Jalvo et al., 2016), none of the nocturnal bird of prey inflicted equal damage to molars and incisors. The presence of this equal damage in these subunits is most likely attributed a combination of nocturnal birds of prey, who

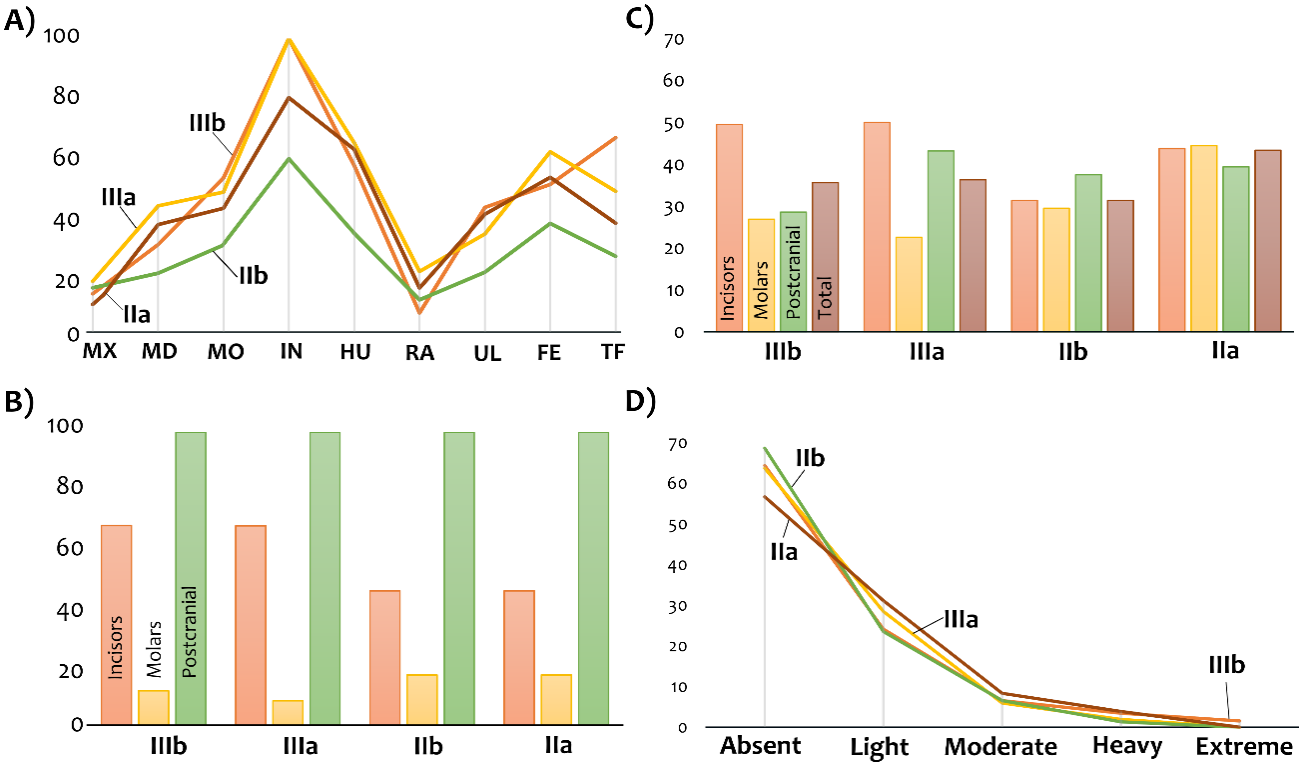

Figure 7.4 Taphonomic variables related to predation observed on rodents from subunits IIIb-IIa. (A) Skeletal profile based on relative abundances of maxillae (MX), mandibles (MD), molars (MO), incisors (IN), humeri (HU), radii (RA), ulnae (UL), femora (FE), and tibia-fibule (TF); (B) Breakage rates; (C) Digestion percentatges; (D) Total degree reached.

produce low to intermediate modification. This altered final percentages of digested remains and reduce relative abundances (<50%). It is possible that *B. bubo* continued to contribute to unit II, but other predator inputs obscure results. In addition, low quantity of remains involved in the analysis of these subunits and higher presence of Arvicolinae subfamily should also be considered. The enlarged sample presented in this work provides enough remains to rule out preliminary attribution to a Category 1 predators (such as *Tyto alba*) as the main small-mammal accumulator (López-García et al., 2012b, 2014) in any of the subunits, at least in exclusivity, but confirms that birds of prey primarily contributed to the remains in the cave.

Previous studies on small-prey remains from the site also demonstrated a high degree of breakage of leporids in unit III (>80%) and birds for the full sequence (>70%). Anatomical profiles of leporids demonstrated proportions closer to accumulations produced by diurnal raptors or mammal carnivores (such as foxes, lynx or wolves) (Rufà et al., 2014, 2016). However, as well as it is observed in small mammals included in this work, the percentages of digested remains (9% in leporids, 19-35% in birds) and the predominance of light degrees of digestion and, in the case of birds also anatomical representation, are unlike patterns established for small carnivores. This suggests the assemblages were mainly produced by nocturnal raptors. In both cases, similarity with digestion patterns of *Bubo bubo* was suggested. Anecdotally, one remain of *Bubo bubo* was recovered in subunit IIa and Strigidae family remains were found in subunits IIIa, IIb and IIa (Rufà et al., 2016). However, a low percentage of modifications by carnivores in some avian remains

(pits, punctures, scores, and chewing) was also found throughout the sequence, with percentages being higher in subunits IIIa and IIa (25%) than in subunits IIIb and IIb (<15%). Small carnivores' alternations were also detected in leporid accumulations from unit III (16%), as were low percentages of heavy and extreme digestion, which were related mainly to the action of foxes (*Vulpes vulpes*). In the case of small mammals analyzed here, the intervention of carnivores through digestion traces has been only detected in subunit IIIb. However, it cannot be rejected that their action increment breakage rates and bias anatomical profiles in this subunit and in the rest of the sequence.

In summary, results indicate that the small-mammal assemblages of Teixoneres cave were mainly produced by nocturnal raptors and, at least for unit III, most likely by the eagle owl, whose nest or roosting site might have been located near or even inside the cave. This species has been present in the Iberian Peninsula since the Lower Pleistocene and has been the sole species of genus *Bubo* since the Middle Pleistocene. It is assumed that their past distribution was similar to the present but was probably more southern during stadials periods (Arribas, 2004). The eagle owl is a sedentary species that usually nests in cave entrances, cliffs ledges, or rock crevices, using same place for several years (Andrews, 1990; IUCN, 2018; Manzanares, 2012; Mikkola, 1983). It is an opportunistic hunter, including in its diet whatever is available in its hunting territory, which normally extends to around 10 km^2. It feeds mostly on mammals, but its prey assemblages are highly diverse and reflect the local ecological variability of its nesting area, and include reptiles, amphibians, fish and larger insects. This owl species is the largest in Iberia (2-4 kg) and, thus, tends to include larger prey in its diet, frequently consuming leporids and birds (such as herons and buzzards) (Andrews, 1990; IUCN, 2018; Manzanares, 2012; Olsson, 1979). It is a valid predator for palaeoecological reconstructions, since it generates representative and coherent accumulations from the ecosystem that it exploits (Andrews, 1990). In addition, it provides some environmental information itself, because it has a preference by wooded habitats despite being found in a wide range of environments (IUCN, 2018; Mikkola, 1983).

4.2 Post-depostional alterations

After this small mammal deposition on the substrate of the cavity, post-depositional alterations occurred (Table 7.3; Fig. 7.2; Appendix 2.4.A). A common pattern was detected in the post-depositional history of small-mammal remains along the sequence. Most of the analyzed remains show striations (>75%), fissures (15-30%), and cracks (2-12%) most likely related to humidity changes. Between 37% (subunit IIIa) and 58% (subunit IIb) of the remains are affected by manganese oxide pigmentation, mainly with an isolated distribution. Another common alteration is chemical corrosion, which affected more of the lower subunits (from 34% to 22%) than upper ones (around 16%). This alteration is mainly related to the presence of roots given the location of round and wide grooves in both bone and tooth surfaces. Occasionally, remains from subunits IIIb and IIIa were covered by isolated cementations (5% and 12%, respectively), being rare in unit II (<2%). Therefore, all features recorded indicated a wet fossiliferous environment where humidity levels underwent some fluctuation, in keeping with cave taphonomic patterns. Finally, few remains in subunit IIIb (n=7), IIIa (n=2) and IIb (n=2) were burned but reached carbonization and calcination degrees. Presence of hearths was confirmed at the site, mainly in the entrance of the cave in unit III. In

unit II, sediment alterations in form of rubefactions were related to thermal exposure (Rosell et al., 2010a, 2014). Small mammals trapped in the substrate would have been affected by unintentional thermal alterations as a consequence of the surrounding combustion activities.

None of the analyzed remains show dissolutions, desquamations, or alterations related to weathering, trampling, or water abrasion. The absence of rounding and polish produced by water abrasion supports the idea that small-mammal remains were not affected by water streams active in the surroundings of the site, as was previously inferred for the cavity, due to the absence of round-angle gravel accumulation (Rosell et al., 2010a). Considering the frequency of manganese oxide coating, however, punctual events of flooding cannot be rejected. Taphonomic analysis on birds revealed some cases of weathering and trampling (Rufà et al., 2016). In the last case, it should be clarified that an absence small-mammal remains can be conditional, in that is not easy to detect trampling in them without the help of scanning electron microscopes. The absence of weathering is common in cave deposits where light was limited. This may confirm the *in situ* deposition of the small-mammal assemblages and the potentially faster burial of small-mammals remains than was expected for larger remains and considering the slow-sedimentation rates defined by this cavity (Rosell et al., 2010a, 2010b; Rufà et al., 2016). As was previously observed, the anatomical profiles and breakage rates obtained in each subunit differ from those produced by owls. Post-depositional modifications should be considered as a possible cause of these fractures. Considering the absence of trampling and weathering among small mammals and a low incidence of this damage in medium-size vertebrates (Rufà et al., 2014, 2016), is not simple to relate these agents as the main cause of higher fragmentation rates. Sediment compactions could also play a role in this sense. In addition, occasionally manganese oxide pigmentation covered fissures of analyzed remains, indicating that this damage occurred before.

4.3 Oxygen isotope compositions of rodent remains

The oxygen isotope composition of the rodent incisor enamel from the Teixoneres sequence ranges from 15.5‰ to 21.3‰, representing a range of variation of 5.8‰ (SD=1.3) (Fig. 7.5; Table 7.1; Table 7.4). Both mean and median $\delta^{18}O_p$ values show little variation among different subunits, ranging between 17.7‰ (subunit IIIa) and 18.5‰ (subunit IIb) and between 17.9‰ (subunit IIIa) and 18.5‰ (subunit IIa), respectively. Differences in mean and median $\delta^{18}O_p$ values are around 0.1-0.3‰, showing a homogenous distribution of data inside each subunit and validating the use of both means and medians values. The oxygen isotope compositions of remains from the subfamilies Glirinae and Arvicolinae included in subunits IIa and IIb, are consistent with the general $\delta^{18}O_p$ range obtained from Murinae remains and have no influence either on the mean or median values. However, in subunit IIa two of the three values related to Arvicolinae correspond to extreme $\delta^{18}O_p$ values incrementing the intra-level range. If these samples are not considered, no differences are noticed in average measurements, but the amplitude of this subunit is largely reduced (1.7; SD=0.6). All sedimentary layers show a normal distribution of data (Shapiro-Wilk test, p-value>0.01).

The low $\delta^{18}O_{mw}$ amplitudes recorded inside each subunit of Teixoneres cave are lower than the current seasonal amplitude of $\delta^{18}O_{mw}$ values at

Moià (8.3‰; OIPC data; Bowen, 2017) (Fig. 7.1C; Table 7.4) and the average seasonal amplitude of $\delta^{18}O_{mw}$ values for Iberia (8‰; Bowen, 2017; Fernández-García et al., under review). This suggests that analyzed rodent remains most likely accumulated during a preferential period of the year, which may have corresponded either to spring-summer or autumn months. Considering present-day $\delta^{18}O_{mw}$ record at Moià (Bowen, 2017), fossil $\delta^{18}O_{mw}$ values would be placed between April-June (from -7.3‰ to -3.8‰) or September-November (from -4.2‰ to -8.8‰). However, during the warm season there is a higher probability of prey capture by owls from Iberia, as indicated by the higher number of murid specimens and the observed oxygen isotope composition of contemporaneous Iberian rodent tooth samples (Chaline, 1974; Lagos, 2019; Manzanares, 2012; Norrdahl and Korpima, 2002; Royer et al., 2013a, 2013b; Salamolard et al., 2000; Fernández-García et al., under review). Mean and median $\delta^{18}O_{mw}$ fossil values are notably higher (from -5.2‰ to -5.9‰) than current mean annual $\delta^{18}O_{mw}$ values on Moià (-7.3‰; Bowen, 2017), reinforcing this hypothesis. The minimum value from the sequence, in subunit IIIa, expressed in $\delta^{18}O_{mw}$ equivalent to -7.7‰ (Table 7.2), not reaching present-day winter $\delta^{18}O_{mw}$ (from -8.8‰ to -10.5‰; Bowen, 2017; Fig. 7.1C). In contrast, the maximum $\delta^{18}O_p$ value record in the subunit IIIb ($\delta^{18}O_p$=21.3‰; $\delta^{18}O_{mw}$=-2.9‰), corresponds with present-day summer oxygen compositions (from -2.6‰ to -3.8‰; Bowen, 2017; Fig. 7.1C). Thus, recorded $\delta^{18}O$ values in all subunits do not indicate predation of specimens in the cold season and coincide between lower mean-medias and higher ranges-SDs in unit III. This could be either a consequence of instability (if samples are produced in the same period), stadial-interstadial conditions (if mixed faunal communities occurred), or changes in seasonality patterns of the predator.

The eagle owl (*Bubo bubo*) has been identified in this work as the main cause of small mammals in Teixoneres sequence at least in unit III, in keeping with results obtained for birds and leporids (Rufà et al., 2014, 2016). Today, it breeds between January and March in the Iberian Peninsula, incubation lasts about five weeks, and the offspring can fly about two months after

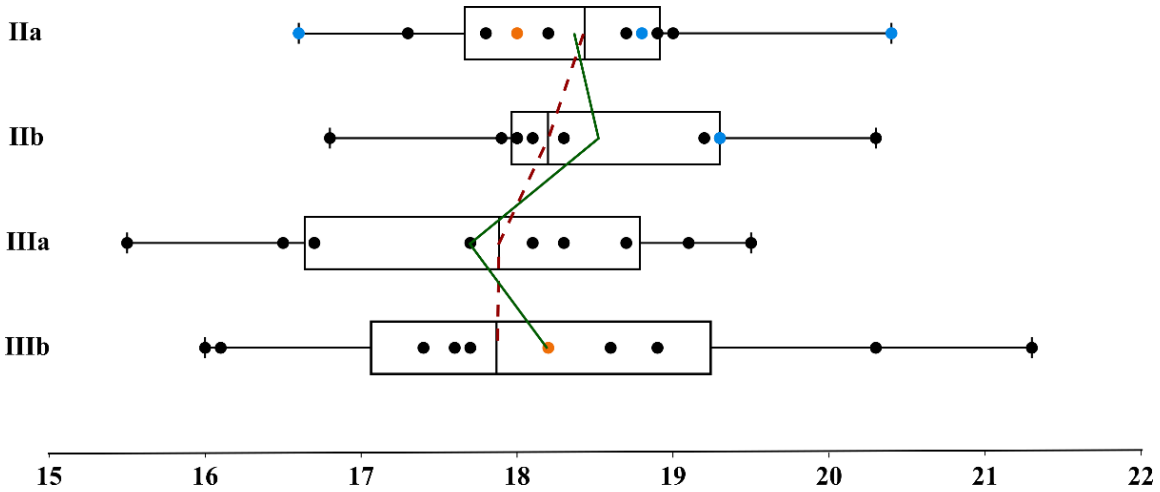

Figure 7.5 Oxygen isotope composition (‰ V-SMOW) of rodent incisor enamel from the Teixoneres samples. Box plots and distribution of $\delta^{18}O$ values per subunit, with mean (green line) and median (red dashed line) curves. Box plots' bars cover the full extension of the values; boxes extend from the 1st to 3rd quartile. Black points, *Apodemus sylvaticus*; blue points, Arvicolinae; yellow points, *Eliomys quercinus*.

	Levels	IIa	IIb	IIIa	IIIb	Pellet
	n	10	10	10	10	3
$\delta^{18}O_p$	Min	16.6	16.8	15.5	16.0	19.0
	Max	20.4	20.3	19.5	21.3	19.5
	Mean	18.4	18.5	17.7	18.2	19.1
	Median	18.5	18.2	17.9	18.0	19.2
	Range	3.8	3.5	4.0	5.2	0.5
	SD	1.0	1.0	1.3	1.7	0.3
$\delta^{18}O_{mw}$	Min	-6.7	-6.6	-7.7	-7.2	-4.8
	Max	-3.6	-3.7	-4.3	-2.9	-4.3
	Mean	-5.3	-5.2	-5.9	-5.4	-4.7
	Median	-5.2	-5.4	-5.7	-5.6	-4.6
	Range	3.2	2.9	3.3	4.3	0.4
MAT	$\delta^{18}O_{mw}$ - seasonality correction	-6.3	-6.5	-6.7	-6.7	x
	$\delta^{18}O_{mw}$ - sea level correction	-6.9	-7.1	-7.3	-7.3	x
	MAT (ºC)	11.8	11.3	10.7	10.8	17.3
	SD	1.3	1.3	1.3	1.3	2.3
	Error margin	2.6	2.6	2.6	2.6	4.5

Table 7.4 Minimum, maximum, mean, median, standard deviation and range of oxygen isotope composition of incisor enamel phosphate ($\delta^{18}O_p$; ‰ V-SMOW) from fossil rodents recovered from Teixoneres cave samples; conversion to the oxygen isotope composition of meteoric waters ($\delta^{18}O_{mw}$; ‰ V-SMOW), including minimum, maximum, mean, median, and range; mean annual temperature estimations (MAT; º C), including seasonality and sea-level corrections of $\delta^{18}O_{mw}$. Present-day samples from Moià are also incorporated to calculate their average temperature, without applying corrections.

coinciding with their breeding period. Some recent studies on Teixoneres cave help to infer the seasonality of human and carnivore/raptors occupations. Taphonomic studies on avian remains provide some inferences for the seasonality of the accumulation of these remains. The presence of few medullary bones among avian remains (*Pica pica* in level IIa and *Pyrrhocorax* spp. in level IIIb), tentatively suggest that some of these bones were accumulated in spring, if breeding periods of these species are considered (Rufà et al., 2016).

Zooarchaeological and taphonomic analyses reflect that presence of carnivores (mainly cave bear and hyena) alternated with Neanderthal occupations, and the evidence associated with humans and carnivores does not usually overlap temporally (Rosell et al., 2010a, 2010b, 2017). With regard to carnivores, bears are known to use the cave mainly for hibernation during winter months, but patterns of hyaenas and small carnivores are unkown (Rosell et al., 2017). From a combination of tooth microwear and dental eruption patterns in ungulates (cervids and equids) from the site, Sánchez-Hernández et al. (2014, 2016) suggested that there were repeated short-term hominin occupations at the site within the same season of the year, probably summer for subunit IIa, autumn and early winter for subunit IIb and two different seasons, summer and winter, in subunit IIIb; in subunit IIIa, repeated and short occupations in all seasons is suggested, but equids were hunted mainly during late spring and summer. These periods of frequentation of the cave may be related to an abundance of to cervids and equids in the territory (Rosell et al., 2017; Sánchez-

Hernández et al., 2014, 2016). Based on these interpretations of short-term human occupations and the preferential use of the cave by owls in spring, in addition to noted carnivore dynamics, in general no coexistence between humans and owls and/or carnivores is supported. This reinforces the absence of temporal contact between them underlined by previous taphonomic and zooarchaeological studies, which demonstrate long periods without human occupation of the site (Rosell et al., 2010a, 2010b, 2017; Rufà et al., 2014, 2016; Sánchez-Hernández et al., 2014).

4.4 Past temperatures reconstruction

Mean annual temperature (MAT) was calculated based on median $\delta^{18}O_p$ of each sedimentary subunit (Fig. 7.6). The estimated MATs vary between 10.7 ±2.6 °C (subunit IIIa) and 11.8 ±2.6 °C (subunit IIa). These temperatures are lower than the current MAT recorded at Moià (12.3 °C; Climate-Data.org; Fig. 7.1C), with differences ranging from -0.5 °C to -1.6 °C. Along the sequence MAT differences are small (≤1.1 °C). Therefore, based on oxygen isotope compositions, a homogenous and milder climate without notable changes is underscored; however, a slight increase in temperatures from lower subunits (10.8-10.7 °C) to upper ones (11.3-11.8 °C) has been detected.

Additionally, oxygen isotope composition of the remains recovered in one present-day pellet from the Teixoneres region were also measured. $\delta^{18}O_p$ values extend from 19‰ to 19.5‰ (-4.4‰ to -4.8‰; in $\delta^{18}O_{mw}$) and the incisor from scattered pellet accumulations were recorded at 16.1‰ ($\delta^{18}O_{mw}$=-7.2‰). Considering $\delta^{18}O_{mw}$ of the place of recovery (at 1000 m a.s.l.; OIPC data; Bowen, 2017), the pellet records could be coincident with May-June (-5.4/-4.2‰) or with September (-4.5‰). The pellet was recovered in August in a semi-dry state. Thus, the most plausible explanation is that this pellet was produced in July, having recorded information about May-July, given the growth rate of lower incisors of *Apodemus* and *Microtus* genus -

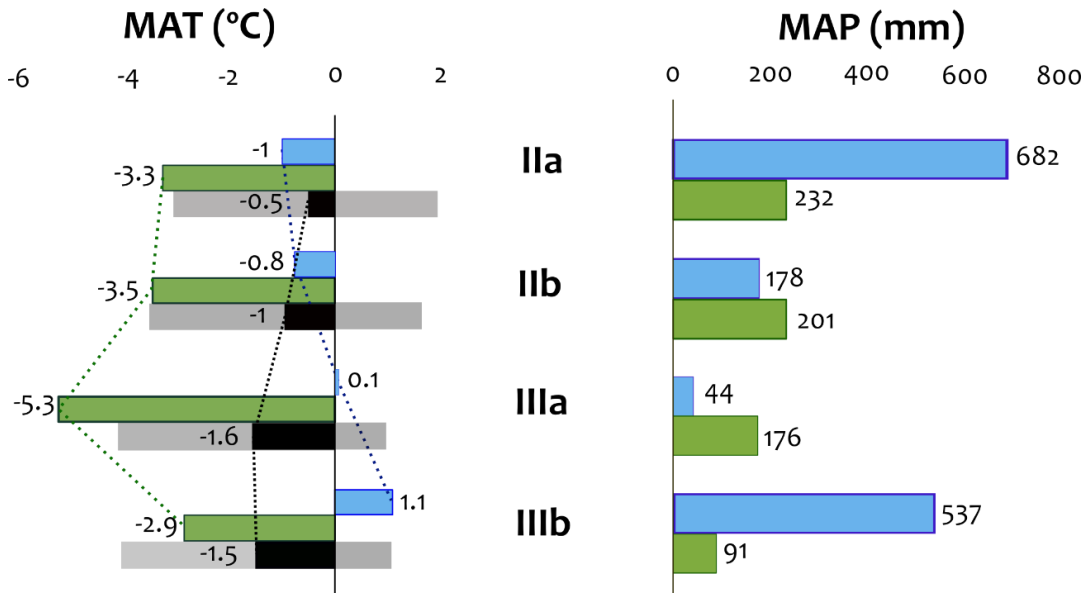

Figure 7.6 Mean annual temperature (MAT) and mean annual precipitation (MAP) estimations for the Teixoneres cave sequence with respect to present-day climate in Moià (MAT= 12.3 °C; MAP= 749 mm; Climate-data.org), considering the bioclimatic model (in blue) and mutual ecogeographical range (in green) methods, and the oxygen isotope compositions (in black) of rodent phosphates samples (error is presented in grey fringe).

(between one and two months) (Klevezal, 2010; Klevezal et al., 1990; Royer et al., 2013a; Fernández García et al., under review). The remain recovered out of the pellet can be related either with March-April (-8.8/-7.3‰) or with October-November (-6.4/-8.8‰). Results of modern complete pellet are included in Table 7.4. The mean $\delta^{18}O_{mw}$ value of the pellet (-4.6‰) equals an average temperature (without applying unnecessary seasonality and sea level corrections) of 17.3 °C, close to the current mean temperature recorded for June. This mean temperature is notably higher than the fossil samples of Teixoneres cave and is generally consistent with temperature and $\delta^{18}O_{mw}$ annual variations for the region.

The MATs calculated from the $\delta^{18}O_p$ of Teixoneres samples are compared with two other methods of palaeoclimatic reconstruction usually used for small-mammal assemblages: the bioclimatic model (BM) and the mutual ecogeographic range (MER) (Fig. 7.6; Appendix 2.4.C and 2.4.D). The BM method tends to provide the highest temperatures (between +1.1 °C and -0.8 °C than present-day), whereas MER estimations always provide lower temperatures (between -3.3 °C and -5.3 °C than present-day). $\delta^{18}O$ estimations offer an intermediate position between both methods, recording similar trends as MER temperature reconstructions, but with an import lag (+1.4/+3.7 °C). Both methods confirm lower MATs than present-day in Moià. This trend is more evident when mean oxygen isotope values of each level are considered (Table 7.4). On the contrary, the BM method provides MATs comparable to present-day temperatures for subunits IIIb and IIIa (+1.1/+0.1 °C, respectively), consequently supporting trends opposing those previously explained, with lower subunits being slightly warmer than upper subunits (from -0.8 to -1 °C). Despite these differences, BM and MER method estimations fall within the confidence interval of $\delta^{18}O$ estimations (a completed discussion of methods discrepancies in presented Chapter 9). Both MER and BM methods record mean annual precipitations (MAP) higher than present-day in Moià (749 mm; Climate-Data.org) but differ in the magnitude of this estimation (+44/+682 mm and +91/+232 mm, respectively). Whereas MER records only slight pluviometry changes along the sequence, increasing from lower to upper subunits, BM denotes high precipitation regimes for subunit IIa and IIIb, which were reduced during subunits IIIa-IIb formation.

4.5 Teixoneres sequence and Neanderthals ecological context

Short-term Neanderthal occupations occurred in Teixoneres cave, in alternation with carnivore and raptor activities in the site. Competition and cohabitation theories between carnivores/raptors and humans have been highly discussed (e.g. Rosell et al., 2010a, 2010b, 2017). Climatic conditions should play an important role in the subsistence strategies and mobility patterns of these humans' populations and their migration routes. New radiometric dating in Teixoneres cave (Talamo et al., 2016) allows for a correlation between global-climatic data and the contemporaneous deposition of these units and for the evaluation of how these fluctuations are reflected in this local context. MIS 3 (ca. 60-30 ka) is a period characterized by a continuous oscillation of climatic events, including strong and brief cold episodes, such as stadials and Heinrich Events (e.g., Fletcher et al., 2010; Rasmussen et al., 2014; Sánchez Goñi et al., 2008; Wolff et al., 2010). This research shows that climatic conditions were generally cooler and always wetter than present-day, but a climatically homogenous sequence should be noted given oxygen isotope differences of less than 1 °C between subunits. Nevertheless,

slight differences are found between lower subunits (unit III) and upper subunits (unit II). Owls are considered responsible for the most small-mammal inputs, so taphonomic causes are primarily rejected as an explanation for these inconsistencies, considering the opportunist behavior of the main accumulator, the eagle owl. Despite some easily detectable inputs from small mammal carnivores, subunits can faithfully represent the ecological conditions of the past.

According to oxygen isotope analysis on rodent incisors, subunits IIIb and IIIa have higher amplitudes and dispersion of $\delta^{18}O$ values and lower $\delta^{18}O$ averages values (Table 7.5). This indicates there were cooler conditions there than in upper subunits, and slight climatic instability. MATs estimated by $\delta^{18}O$ median values are the lowest of the sequence (IIIb=10.8 ±2.6 °C; IIIa= 10.7 ±2.6 °C), in agreement with MER, which describes notably lower MAT for subunit IIIa (7 °C), but not for subunit IIIb (9.4 °C). The BM method proposed MATs equal to present-day in the region for both subunits (12.4-13.4 °C). Moreover, unit III is drier than II based on MAPs obtained by MER method (from 840 to 980 mm), whereas results from the BM method point to lower precipitations from subunit IIIa to IIb. Thus, some discrepancies are found between methods and with previous environmental studies, which correlated unit III with an interstadial period and indicated that conditions were relatively temperate and humid (López-García et al., 2012). Relative species abundances of small mammals are also not fully in keeping with what would be expected for cooler and drier conditions. In unit III, the presence of the Mediterranean species, *Microtus (T.) duodecimcostatus,* is higher (12-14%), lower in subunit IIb (2.3%), and disappears in upper subunit IIa. Relative abundance of *A. sylvaticus,* a generalist species with a preference for woodland environments, is remarkably high for subunit IIIb (41%) (Appendix 2.4.B).

Recent studies on this unit can provide some insight. Occurrence of *Mammuthus primigenius* (0.7%) and *Coelodonta antiquitatis* (0.1%) are clear indicators of a cold and arid environment (Álvarez-Lao et al., 2017). Regarding large mammals, unit III assemblage reflects a faunal mixture in which temperate ungulate species are predominant and cold-adapted taxa are very scarce, which is common in other Iberian assemblages with these species' presence. This suggests that cold-adapted taxa only reached the Peninsula occasionally, during the coldest episodes of the Pleistocene. Some cold-dependent species also appear among small mammals of subunit IIIa (*Chionomys nivalis, M. (T.) gerbei* and *Sorex coronatus*) (Appendix 2.4.B). Considering the slow sedimentation rates of Teixoneres cave (Rosell et al., 2010a, 2010b) and the complex formation of unit III that implies mixed contributions by predators inhabiting the cave in different periods, the most plausible explanation is that the palimpsest nature of these subunits (Rosell et al., 2017) is the result of overlap among different climatic events, precluding the isolation of different stadial and interstadial events. Depending on the exact origin of the sample, results can highly vary. Detailed spatial distribution of remains, horizontal and vertical, might enable the deciphering of climatic events, especially for subunit IIIb, where small-mammal remains are very abundant. In sum, climatic conditions during the deposition of unit III were cooler than present-day. However, contradictory data were recovered in particular for subunit IIIa, due to a probable mix of species dependent on either temperate or cold conditions. This points to the recording of a cold event deposition in agreement with the occurrence of the woolly mammoth and the woolly rhinoceros, but that

Unit	Subunits	Pollen & Charcoals (López-García et al., 2012)	Large mammals (Álvarez-Lao et al., 2017)	Small vertebrates (López-García et al., 2012)	Oxygen isotopes analysis (This work)	Small mammals' predator (This work)	Past temperatures (This work & López-García et al., 2012)	Past precipitations (This work & López-García et al., 2012)
II (ca.33-44 ka)	IIa	Open woodland and meadows. Dry conditions in relation to steppe taxon *Artemisia* (IIa). *Pinus*, *Quercus* and angiosperm charcoals.	Abundant temperate-adapted species (mainly *Cervus elaphus* followed by equids), presence of *Coelodonta antiquitatis* and higher presence of *Rupicapra-Capra pyrenaica* and *Sus scrofa*. Open forest and rocky landscape.	Abundant Mid-European species (*Microtus agrestis*, *Microtus arvalis*) , scarce presence of forest-dwellers (*Apodemus sylvaticus*) and absence of Mediterranean species. Cooler and drier phase related to stadial. Open woodland.	Homogenous, low amplitude and the highest median. Stable period.	Nocturnal raptors - Digestion=43%	BM=11.3 °C / MER=9 °C/ $\delta^{18}O$=11.8 °C	BM=1431 mm/ MER=981 mm
	IIb			Abundant Mid-European species (*M. arvalis, M. agrestis, M. (Terricola) gerbei, Chionomys nivalis*) , scarce presence of forest-dwellers (*A. sylvaticus*) and scarce Mediterranean species (*M. (T.) duodecimcostatus*). Cooler and drier phase related to stadial. Open woodland, increase in dry meadows and rocky areas.	Homogenous, the lowest amplitude and high median. Stable period.	Nocturnal raptors - Digestion=31%	BM=11.5 °C / MER=8.8 °C/ $\delta^{18}O$=11.3 °C	BM=927 mm/ MER=950 mm
III (ca. 44-51 ka)	IIIa	Open woodland and meadows. Relative moisture, due to high representation of *Corylus* and Pteridophyta spores. *Buxus* charcoals.	Abundant temperate-adapted species (maily *Cervus elaphus* and some equids) but scarce cold-adapted species (*Mammuthus primigenius* and *Coelodonta antiquitatis*). Open forested landscape.	Mediterranean species (*M. (Terricola) duodecimcostatus, Iberomys cabrerae*), Mid-European species (*M. arvalis, M. agrestis, C. nivalis, M. (T.) gerbei*) and forest-dwellers (*A. sylvaticus*). Temperate and humid phase related to interstadial. Open woodland but increase in humid meadows and water component.	Heterogenous, medium amplitude, the lowest median. Unstable.	*Bubo bubo* - Digestion=36%	BM=12.4 °C / MER=7 °C/ $\delta^{18}O$=10.7 °C	BM=793 mm/ MER=925 mm
	IIIb			Abundant presence of forest-dwellers (*A. sylvaticus*), presence of Mediterranean (*M. (T.) duodecimcostatus*) and Mid-European (*M. arvalis, M. agrestis*) species. Temperate and humid phase related to interstadial. Open woodland.	Heterogenous, low median and the largest amplitude. Unstable.	*Bubo bubo* + Carnivores occasional inputs - Digestion=36%	BM=13.4 °C / MER=9.4 °C/ $\delta^{18}O$=10.8 °C	BM=1286 mm/ MER=840 mm

Table 7.5 Previous palaeoenvironmental approaches to Teixoneres sequence and results from this work. Mean annual temperature and mean annual precipitation estimations are included, according to Bioclimatic Model method (BM), Mutual Ecogeographic Range method (MER) and oxygen isotope compositions ($\delta^{18}O$).

under current small mammal analysis is not possible to isolated, giving a general faunal spectrum that seems globally temperate.

Contrary to unit III, oxygen isotope compositions of the upper subunits (IIb-IIa) show higher means and medians (18.4-18.5‰ and 18.2-18.5‰, respectively), lower intra-level amplitude (3.5-3.8‰), and lower standard deviations (1-1.1‰) (Table 7.5). According to $\delta^{18}O$ estimations, MATs are slightly higher than for unit III (IIb=11.3 ±2.6 °C; IIa= 11.8 ±2.6 °C), but differences between both units are tiny (+0.5/+1 °C), with both units being cooler than current conditions. In this case, both MER and BM methods coincide in inferring cooler (MATs from –3.3 to -3.5 °C and from -0.8 to -0.1 °C, respectively) and wetter (MAPs from +178 to +682 mm) conditions than present-day in the region. According to previously recorded small-mammal relative abundances (Appendix 2.4.B), a progressive decrease in woodland-dwelling species (*A. sylvaticus, Eliomys quercinus* and *Glis glis*) in favor of open-environment species with mid-European requirements (*M. arvalis* and *M. agrestis*) can be noticed between unit III and II (López-García et al., 2012b). In parallel, there is an increase in mid-European species (*M. arvalis* and *M. agrestis*) and decrease of Mediterranean species (mainly *M. (T.) duodecimcostatus*). Moreover, in subunit IIb other cold-dependent species occurred (*C. nivalis, Neomys fodiens* and *S. coronatus*). Cooler and drier conditions detected by López-García et al. (2012, 2014) in unit II were tentatively associated with cold events, such as Heinrich Event peaks of MIS 3, which is consistent with the punctual occurrence of *C. antiquitatis* in this level (1.5%) (Álvarez-Lao et al., 2017). Considering new radiometric dating of this unit (ca. 33-44) (Talamo et al., 2016), in case this correlation was accepted, should correspond to HE4 (Hemming, 2004). However, given new results, this climatic adscription with an exceptional cold and dry event cannot be fully supported. In addition, the occurrence of the thermophilous snake *Malpolon monspessulanus* in subunit IIb suggests MATs over 10 °C, and the presence of *Salamandra salamandra* indicates conditions during the deposition of subunits IIa and IIb were not very dry (López-García et al., 2012b). It should be considered that unit II has been affected by the loss of materials from former excavations. Thus, less material is available and complete faunal spectra may be highly biased, especially in subunit IIa.

5. Conclusions

- Analyzed small mammals accumulated in the cave mainly due to predation by nocturnal raptors (digestion=31-43%). In coincidence with taphonomic analyses on bird and leporid remains, the main action corresponds to the eagle owl (*Bubo bubo*), at least in unit III. *Bubo bubo*-type predators probably maintained their roosting or nesting place in Teixoneres cave during the formation of unit II, but other owls may have contributed with small mammals's inputs as well. Consistent with small-prey studies, the punctual intervention of mammal carnivores was detected in subunit IIIb.
- Among post-depositional agents, plant activity, cracking, and manganese oxide coating are common, indicating a wet fossiliferous microenvironment with humidity fluctuations, where abundant breakage rates are observed. Some burned remains have been detected in relation to unintentional burning. Water abrasion, weathering, and trampling were not detected along the sequence.
- The medium to low intra-level ranges of oxygen isotopic values indicate a preferential accumulation moment of rodents, probably during the spring season. This period of

frequentation by owls is in accordance with previous seasonality inferences based on some medullary bones of birds, which share a common origin with small mammals, and results generally differed from use-wear and dental eruption analyses on ungulates, mainly related to hominin contributions to the cave.

- According to $\delta^{18}O$ estimations of temperatures, slightly cooler climatic conditions than present were recorded (-1.6/-0.5 °C). The observed trend is globally in agreement with MER estimations, which recorded colder MATs (-2.9/-5.3 °C), but differ in unit III with BM, which recorded MATs similar to present-day levels (+0.1/+1.1 °C). Both methods calculated wetter conditions than present-day (+ 44 mm/+682 mm).
- However, oxygen isotope compositions of analyzed rodent teeth underscore the presence of rather stable climatic conditions across the sequence, with little variation between subunits, including those expressed in MAT (<1 °C). Only slight changes are observed between lower unit III and II, showing the former higher $\delta^{18}O$ amplitudes and lower median $\delta^{18}O$ values, which may tentatively be related to some climatically instability and slightly cooler temperatures. This trend is not fully in agreement with previous environmental interpretations based on small-mammal relative abundances, but may be in keeping with the occasional occurrence of cold-dependent large and small mammal species. These inconsistencies between methods could point to a palimpsest where stadial and interstadial events overlapped, especially in subunit IIIa.

References

Álvarez-Lao, D.J., Rivals, F., Sánchez-Hernández, C., Blasco, R., Rosell, J., 2017. Ungulates from Teixoneres Cave (Moià, Barcelona, Spain): Presence of cold-adapted elements in NE Iberia during the MIS 3. Palaeogeogr. Palaeoclimatol. Palaeoecol. 466, 287–302.

Andrews, P., 1990. Owls, Caves and Fossils. Predation, preservation and accumulation of small mammal bones in caves, with an analysis of the Pleistocene Cave Faunas from Westbury-sub-Mendip, Somerset, UK. The University of Chicago, Chicago.

Arribas, Ó., 2004. Fauna y paisaje de los Pirineos en la Era Glaciar. Lynx, Barcelona.

Bennàsar, M., 2010. Tafonomía de micromamíferos del Pleistoceno Inferior de la Sierra de Atapuerca (Burgos): Sima del Elefante y Gran Dolina. Universitat Rovira i Virgili (Tarragona). Doctoral thesis (inedit).

Bennàsar, M., Cáceres, I., Cuenca-Bescós, G., 2016. Paleoecological and microenvironmental aspects of the first European hominids inferred from the taphonomy of small mammals (Sima del Elefante, Sierra de Atapuerca, Spain). Comptes Rendus Palevol 15, 635–646.

Bowen, G.J., 2017. The Online Isotopes in Precipitation Calculator, Version 3.1 (4/2017) [WWW Document]. URL http://waterisotopes.org

Bustos-Pérez, G., Chacón, M.G., Rivals, F., Blasco, R., Rosell, J., 2017. Quantitative and qualitative analysis for the study of Middle Paleolithic retouched artifacts: Unit III of Teixoneres cave (Barcelona, Spain). J. Archaeol. Sci. Reports 12, 658–672.

Chaline, J., 1974. Les proies des rapaces. Doin Éditeurs, Paris.

Climate-Data.org [WWW Document], 2018. URL https://es.climate-data.org/

Comay, O., Dayan, T., 2018. Taphonomic signatures of owls: New insights into micromammal assemblages. Palaeogeogr. Palaeoclimatol. Palaeoecol. 492, 81–91.

Fernández-Jalvo, Y., 1992. Tafonomía de microvertebrados del complejo cárstico de Atapuerca (Burgos). Universidad Complutense de Madrid. Doctoral thesis (inedit).

Fernández-Jalvo, Y., Andrews, P., 1992. Small mammal taphonomy of Gran Dolina, Atapuerca (Burgos), Spain. J. Archaeol. Sci. 19, 407–428.

Fernández-Jalvo, Y., Andrews, P., Denys, C., Sesé, C., Stoetzel, E., Marin-Monfort, D., Pesquero, D., 2016. Taphonomy for taxonomists: Implications of predation in small mammal studies. Quat. Sci. Rev. 139, 138–157.

Fletcher, W.J., Sánchez Goñi, M.F., Allen, J.R.M., Cheddadi, R., Combourieu-Nebout, N., Huntley, B., Lawson, I., Londeix, L., Magri, D., Margari, V., Müller, U.C., Naughton, F., Novenko, E., Roucoux, K., Tzedakis, P.C., 2010. Millennial-scale variability during the last glacial in vegetation records from Europe. Quat. Sci. Rev. 29, 2839–2864.

Font-Tullot, I., 2000. Climatología de España y Portugal. Universidad de Salamanca, Salamanca.

Gehler, A., Tütken, T., Pack, A., 2012. Oxygen and Carbon Isotope Variations in a Modern Rodent Community - Implications for Palaeoenvironmental Reconstructions. PLoS One 7, 16–27.

Hemming, S.R., 2004. Heinrich events: Massive late Pleistocene detritus layers of the North Atlantic and their global climate imprint. Rev. Geophys. 42, RG1005.

IUCN, 2018. The IUCN Red List of Threatened Species [WWW Document]. Version 2018-2. URL www.iucnredlist.org

Klevezal, G.A., 2010. Dynamics of Incisor Growth and Daily Increments on the Incisor Surface in Three Species of Small Rodents. Biol. Butlletin 37, 836–845.

Klevezal, G.A., Pucek, M., Sukhovskaja, L.I., 1990. Incisor growth in voles. Acta Theriol. 35 (3-4), 331–344.

Kowalski, K., 1995. Taphonomy of bats (Chiroptera). Geobios 18, 251–256.

Lagos, P., 2019. Predation and Its Effects on Individuals: From Individual to Species. Encyclopedia of Ecology 2, 365-368.

Lindars, E.S., Grimes, S.T., Mattey, D.P., Collinson, M.E., Hooker, J.J., Jones, T.P., 2001. Phosphate $\delta^{18}O$ determination of modern rodent teeth by direct laser fluorination: An appraisal of methodology and potential application to palaeoclimate reconstruction. Geochim. Cosmochim. Acta 65, 2535–2548.

Lloveras, L., Moreno-Garcia, M., Nadal, J., 2008a. Taphonomic study of leporid remains accumulated by the Spanish Imperial Eagle (*Aquila adalberti*). Geobios 41, 91–100.

Lloveras, L., Moreno-García, M., Nadal, J., 2012. Feeding the Foxes: An Experimental Study to Assess Their Taphonomic Signature on Leporid Remains. Int. J. Osteoarchaeol. 22, 577–590.

Lloveras, L., Moreno-García, M., Nadal, J., 2008b. Taphonomic analysis of leporid remains obtained from modern Iberian lynx (*Lynx pardinus*) scats. J. Archaeol. Sci. 35, 1–13.

López-García, J.M., Blain, H.-A., Bennàsar, M., Euba, I., Bañuls, S., Bischoff, J., López-Ortega, E., Saladié, P., Uzquiano, P., Vallverdú, J., 2012a. A multiproxy reconstruction of the palaeoenvironment and palaeoclimate of the Late Pleistocene in northeastern Iberia: Cova dels Xaragalls, Vimbodí-Poblet, Paratge Natural de Poblet, Catalonia. Boreas 41, 235–249.

López-García, J.M., Blain, H.-A., Burjachs, F., Ballesteros, A., Allué, E., Cuevas-Ruiz, G.E., Rivals, F., Blasco, R., Morales, J.I., Hidalgo, A.R., Carbonell, E., Serrat, D., Rosell, J., 2012b. A multidisciplinary approach to reconstructing the chronology and environment of southwestern European Neanderthals: the contribution of Teixoneres cave (Moià, Barcelona, Spain). Quat. Sci. Rev. 43, 33–44.

López-García, J.M., Blain, H.A., Bennàsar, M., Fernández-García, M., 2014. Environmental and climatic context of neanderthal occupation in southwestern Europe during MIS3 inferred from the small-vertebrate assemblages. Quat. Int. 326–327, 319–328.

Luzi, E., López-García, J.M., Blasco, R., Rivals, F., Rosell, J., 2017. Variations in *Microtus arvalis* and *Microtus agrestis* (Arvicolinae, Rodentia) Dental Morphologies in an Archaeological Context: the Case of Teixoneres Cave (Late Pleistocene, North-Eastern Iberia). J. Mamm. Evol. 24, 495–503.

Manzanares, A., 2012. Aves rapaces de la Península Ibérica, Baleares y Canarias. Ediciones Omega, Barcelona.

Mikkola, H., 1983. Owls of Europe. Buteo Books, Sussex.

Navarro, N., Lécuyer, C., Montuire, S., Langlois, C., Martineau, F., 2004. Oxygen isotope compositions of phosphate from arvicoline teeth and Quaternary climatic changes, Gigny, French Jura. Quat. Res. 62, 172–182.

Norrdahl, K., Korpima, E., 2002. Seasonal changes in the numerical responses of predators to cyclic vole populations. Ecography 25, 428–438.

Olsson, V., 1979. Studies on a population of Eagle owls in southeast Sweden. Viltrevy 11, 1–99.

Palomo, L.J., Gisbert, J., Blanco, C., 2007. Atlas y libro rojo de los mamíferos terrestres de España. Organismo Autónomo Parques Nacionales, Madrid.

Rasmussen, S.O., Bigler, M., Blockley, S.P., Blunier, T., Buchardt, S.L., Clausen, H.B., Cvijanovic, I., Dahl-Jensen, D., Johnsen, S.J., Fischer, H., Gkinis, V., Guillevic, M., Hoek, W.Z., Lowe, J.J., Pedro, J.B., Popp, T., Seierstad, I.K., Steffensen, J.P., Svensson, A.M., Vallelonga, P., Vinther, B.M., Walker, M.J.C., Wheatley, J.J., Winstrup, M., 2014. A stratigraphic framework for abrupt climatic changes during the Last Glacial period based on three synchronized Greenland ice-core records: Refining and extending the INTIMATE event stratigraphy. Quat. Sci. Rev. 106, 14–28.

Rosell, J., Blasco, R., Cebrià, A., Chacón, M.G., Menéndez, L., Morales, J.I., Rodríguez, A., 2008. Mossegades i Levallois: les noves intervencionsa la Cova de les Teixoneres (Moià, Bages). Trib. d'Arqueologia 29–43.

Rosell, J., Blasco, R., Rivals, F., Cebrià, A., Morales, J.I., Rodríguez-Hidalgo, A., Serrat, D., Carbonell, E., 2010a. Las ocupaciones en la Cova de les Texoneres (Moià, Barcelona): relaciones espaciales y grado de competencia entre hienas, osos y neandertales durante el Pleistoceno superior. Zo. Arqueol. 13, 392–403.

Rosell, J., Blasco, R., Rivals, F., Chacón, M.G., Menéndez, L., Morales, J.I., Rodríguez-Hidalgo, A., Cebrià, A., Carbonell, E., Serrat, D., 2010b. A stop along the way: The role of neanderthal groups at level III of Teixoneres cave (Moià, Barcelona, Spain). Quaternaire 21, 139–154.

Rosell, J., Blasco, R., Rivals, F., Chacón, M.G., Arilla, M., Camarós, E., Rufà, A., Sánchez-Hernández, C., Picin, A., Andrés, M., Blain, H.A., López-García, J.M., Iriarte, E., Cebrià, A., 2017. A resilient landscape at Teixoneres Cave (MIS 3; Moià, Barcelona, Spain): The Neanderthals as disrupting agent. Quat. Int. 435, 195–210.

Rosell, J., Blasco, R., Rivals, F., Chacón, M.G., Blain, H.-A., López-García, J.M., Picin, A., Camarós, E., Rufà, A., Sanchéz, C., Gómez, G., Arilla, M., Gómez de Soler, B., Bustos, G., Iriarte, E., Cebrià, A., 2014. Cova del Toll y Cova de les Teixoneres Moià, Barcelona, in: Sala, R. (Ed.), Pleistocene and Holocene Hunter-Gatherers in Iberia and Gibraltar Strait: The Current Archaeological Record. Universidad de Burgos & Fundación Atapuerca, Burgos, pp. 302–307.

Royer, A., Lécuyer, C., Montuire, S., Amiot, R., Legendre, S., Cuenca-Bescós, G., Jeannet, M., Martineau, F., 2013a. What does the oxygen isotope composition of rodent teeth record? Earth Planet. Sci. Lett. 361, 258–271.

Royer, A., Lécuyer, C., Montuire, S., Escarguel, G., Fourel, F., Mann, A., Maureille, B., 2013b. Late Pleistocene (MIS 3-4) climate inferred from micromammal communities and $\delta^{18}O$ of rodents from Les Pradelles, France. Quat. Res. 80, 113–124.

Rufà, A., Blasco, R., Rivals, F., Rosell, J., 2016. Who eats whom? Taphonomic analysis of the avian record from the Middle Paleolithic site of Teixoneres Cave (Moià, Barcelona, Spain). Quat. Int. 421, 103–115.

Rufà, A., Blasco, R., Rivals, F., Rosell, J., 2014. Leporids as a potential resource for predators (hominins, mammalian carnivores, raptors): An example of mixed contribution from level III of Teixoneres Cave (MIS 3, Barcelona, Spain). Comptes Rendus Palevol 13, 665–680.

Salamolard, M., Butet, A., Leroux, A., Bretagnolle, V., 2000. Responses of an avian predator to variations in prey density at a temperature latitude. Ecology 81, 2428–2441.

Sánchez-Hernández, C., Rivals, F., Blasco, R., Rosell, J., 2016. Tale of two timescales: Combining tooth wear methods with different temporal resolutions to detect seasonality of Palaeolithic hominin occupational patterns. J. Archaeol. Sci. Reports 6, 790–797.

Sánchez-Hernández, C., Rivals, F., Blasco, R., Rosell, J., 2014. Short, but repeated Neanderthal visits to Teixoneres Cave (MIS 3, Barcelona, Spain): A combined analysis of tooth microwear patterns and seasonality. J. Archaeol. Sci. 49, 317–325.

Sánchez Goñi, M.F., Landais, A., Fletcher, W.J., Naughton, F., Desprat, S., Duprat, J., 2008. Contrasting impacts of Dansgaard-Oeschger events over a western European latitudinal transect modulated by orbital parameters. Quat. Sci. Rev. 27, 1136–1151.

Servei Meteorològic de Catalunya, 2018. Climatologies Comarcals & Anuari de dades meteorològiques.

Talamo, S., Blasco, R., Rivals, F., Picin, A., Chacón, M.G., Iriarte, E., López-García, J.M., Blain, H.-A., Arilla, M., Rufà, A., Sánchez-Hernández, C., Andrés, M., Camarós, E., Ballesteros, A., Cebrià, A., Rosell, J., Hublin, J.-J., 2016. The Radiocarbon Approach to Neanderthals in a Carnivore Den Site: a Well-Defined Chronology for Teixoneres Cave (Moià, Barcelona, Spain). Radiocarbon 58, 247–256.

Terry, R.C., 2007. Inferring predator identity from skeletal damage of small-mammal prey remains. Evol. Ecol. Res. 9, 199–219.

Tissoux, H., Falgueres, C., Bahain, J.J., Rosell I Ardevol, J., Cebria, A., Carbonell, E., Serrat, D., 2006. Datation par les séries de l'uranium des occupations moustériennes de la grotte des Teixoneres (Moia, province de Barcelone, Espagne). Quaternaire 17, 27–33.

Wolff, E.W., Chappellaz, J., Blunier, T., Rasmussen, S.O., Svensson, A., 2010. Millennial-scale variability during the last glacial: The ice core record. Quat. Sci. Rev. 29, 2828–2838.

Chapter 8.
Latest Pleistocene in northeastern Iberia: oxygen isotope analysis and palaeoenvironment inferences from rodent assemblages of Arbreda cave (Serinyà, Girona)

ABSTRACT

Arbreda cave (Serinyà, Girona) constitutes one of the most complete terrestrial records with small-mammal studies and human occupations during the latest Pleistocene in northeastern Iberia. Both Neanderthal (levels N to I) and Anatomically Modern Human (levels H to A) occupations have been recorded in its fossiliferous deposits. The substitution between these two populations occurred at the latest stages of the Marine Isotopic Stage 3 (MIS 3; 60-30 ka) in this region. The end of MIS 3 and the beginning of MIS 2 (ca. 30-11.7 ka) is explored through oxygen isotope analysis on rodent teeth from levels H to D (ca. 40-20 ka BP), with the aim of reconstructing palaeoclimatic conditions during the arrival of Anatomically Modern Humans in Iberia. From the biochemical perspective, during this period palaeotemperature records were notably lower (from -5 to -1 °C) than today in the region. These estimations are globally in agreement with other methods of palaeotemperature calculations, which also estimate mean annual precipitations as being higher (from +30 to +767 mm) than present-day. An important climatic shift is identified between level H (ca. 31-36 ka BP) and level G (ca. 32-33 ka BP), with a mean annual temperature drop (– 4.5 °C from H to G) that is progressively recovered from levels F to D. Using both quantitative and qualitative methods, small mammals show there were relatively cold conditions in level G. Though some inconsistencies are detected with respect to interpretations of previous palynological studies of level G, the general climatic evolution of the sequence is consistent with previous environmental studies. These results reinforce the particular climatic conditions of the end of the MIS 3 in Iberia. It can be ascertained that Anatomically Modern Humans were fully adapted to their environment since its arrival.

1. Introduction

Arbreda cave (Serinyà, Girona, Northeastern Iberia) is one of the most continuous, long, and well-dated terrestrial sequences from northeastern Iberia, containing archaeo-palaeontological deposits that extend from the Mousterian to the Early Holocene period. Neanderthal (levels N to I) and Anatomically Modern Human (AMH) (levels H to A) occupations have been recorded, thus providing information about prehistoric hominin occupations in this region and the ecological conditions that surrounded this cave. Moreover, the Middle-Upper Palaeolithic transition appears within the sequence, usually assumed to be the substitution of Neanderthals by AMH. This has been deduced by the presence of tool-kits associated with each population (Mousterian/Aurignacian). Climatic causes are one of the most extended topics for explaining this human shift (e.g., Baena et al., 2012; D'Errico and Sánchez Goñi, 2003; Finlayson et al., 2004; Sepulchre et al., 2007; Zilhão, 2000). Arbreda cave sequence offers the opportunity to increase our knowledge about the environmental conditions to which both human groups, Neanderthals and AMH, were adapted.

In this work, the end of the Marine Isotope Stage (MIS) 3 and the beginning of MIS 2 is explored through rodent assemblages. Previous small-mammal studies have not denoted important climatic changes between these two marine isotopic stages in this local context, but some fluctuations related to stadial-interstadial alternations were described (López-García, 2011; López-García et al., 2014, 2015; López-García and Cuenca-Bescós, 2010). The objective is to test, through oxygen isotope analysis, how important and how progressive these climatic fluctuations were from levels H to D (ca. 40-20 ka BP). The common kestrel (*Falco tinnunculus*) was identified

as the main accumulator of small-mammal assemblages from levels H to E (López-García et al., 2015). This diurnal bird of prey could impose some bias in the species spectra and the relative abundances of small mammals in these levels. Biochemical analyses offer the opportunity to test, from a quantitative point of view, if the changes observed are reliable, or if other factors are interfering with our ecological interpretations. If changes in MIS 3-2 period are significant, oxygen isotope records in rodent teeth should reflect this shift. In addition, this work compares the results with two independent methods of palaeoclimatic reconstruction based on small mammals and with other environmental proxies performed on the site.

2. Arbreda cave

Arbreda cave is located at geographical coordinates 42° 9' 38" N and 2° 44' 49" E and at 206 m a.s.l. (Fig. 8.1A). The site is one of the Reclau Caves (Serinyà, Girona), where more than fourteen caves have been discovered, such as Mollet, Mollet III, En Pau, Cau del Roure, and Reclau Viver (Maroto et al., 1996, 2012a; Soler et al., 2013, 2014; Soler and Soler, 2016). They are located between the west margin of the Pla d'Usall and the Serinyadell river valley. Pla d'Usall is within the Banyoles-Besalú Basin, bounded by Eocene and Neogene reliefs and filled with Plio-Pleistocene sediments (Soler et al., 2014). Arbreda cave was originally a travertine cascade shelter, formed around 190-250 ka, that collapsed and adopted the current cave morphology, prior to sediment deposition from the end of the Middle Pleistocene to the Early Holocene (Soler et al., 2014). Karstification processes, secondary travertine deposits, and recrystallization have remodeled the original geomorphology of Reclau Caves, and roof collapses and detrital sediment inputs have filled the cavities (Kehl et al., 2014; Soler et al., 2014). The first archaeological interventions in Arbreda cave were coordinated by Josep Maria Corominas, starting in 1972 with a 9-m-deep survey that revealed the prehistoric sequence of the site, followed by secondary surveys. Research directed by Narcís Soler has continued from 1975 until today, and the archaeological surface has been enlarged (Maroto et al., 1996; Soler et al., 2014).

In the Pleistocene stratigraphy, which covers more than 12 m of depth, fourteen archaeo-palaeontological levels have been partially excavated, from levels N to A, covered by the Holocenic Terra Rossa level (Fig. 8.1B) (Maroto et al., 1996; Soler et al., 2014; Soler and Soler, 2016). Several ^{14}C datings have been performed along the sequence (Table 8.1) (López-García et al., 2015; Maroto et al., 2012b, 1996; Soler et al., 2014; Wood et al., 2014). Neanderthal occupations are documented from levels N to I, based on the recovery of Mousterian tools (mainly retouched flakes configured with local raw materials) (Higham et al., 2014; Maroto et al., 1996; Soler and Soler, 2016). During this period, Arbreda probably served as den cave for ursid hibernation in alternation with human occupation. The occasional presence of other carnivores, such as *Crocuta crocuta* and *Canis lupus*, has also been recorded (Lloveras et al., 2010; Maroto et al., 1996; Rufí et al., 2018). Neanderthal groups were replaced by AMH groups on level H, as deduced from the cultural change indicated by the appearance of lithic assemblages attributed to the Archaic Aurignacian. These are associated with bone tools, the exploitation of allochthonous raw materials, and systematic small-prey consumption (Galobart et al., 1996; Lloveras et al., 2016; Maroto et al., 1996, 2012b; Soler and Soler, 2016; Wood et al., 2014). Carnivore frequentation of the site is reduced beginning at this level (Estévez, 1980;

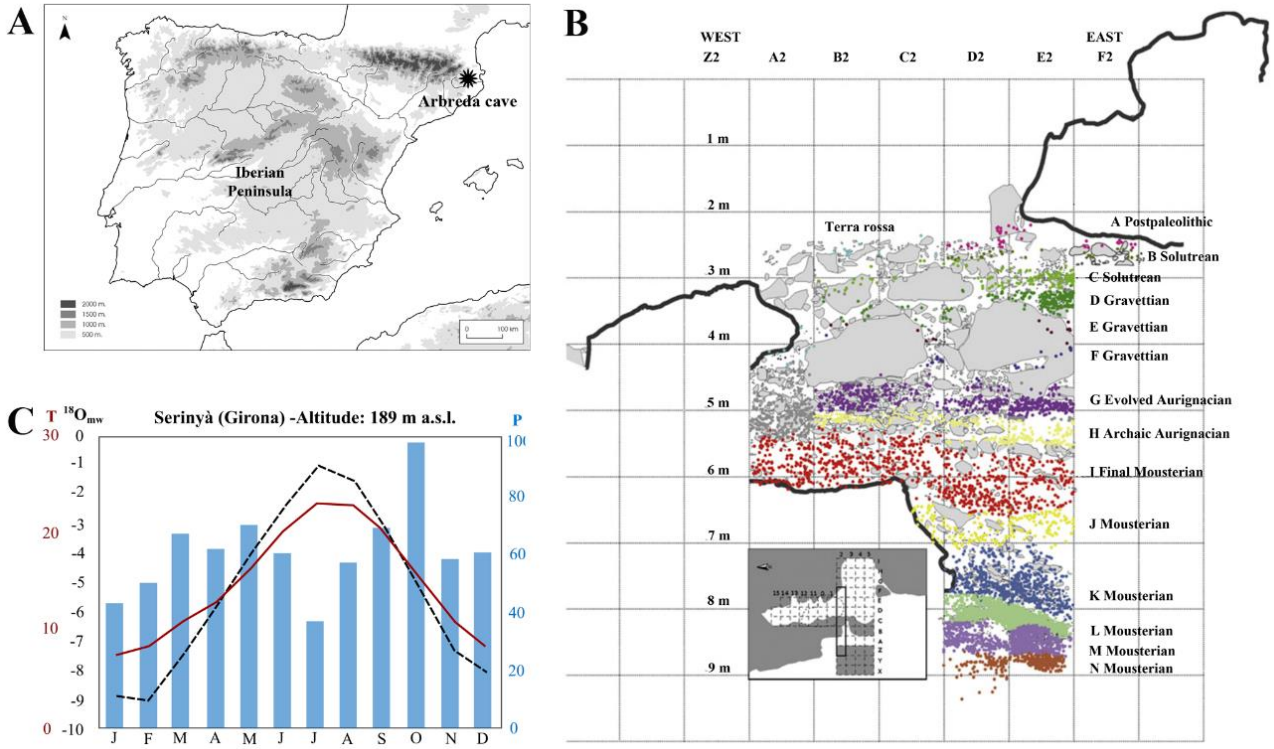

Figure 8.1 (A) Location of the Arbreda cave in Iberia; (B) Stratigraphic section of Arbreda cave (Soler et al., 2014); (C) Current monthly temperatures (red line; T; in ºC), precipitations (bars; P; in mm) (Climate-data.org), and present-day oxygen isotope composition of meteoric waters (dash black; $\delta^{18}O_{mw}$; in ‰ V-SMOW) (Bowen, 2017) of Serinyà.

Galobart et al., 1996; Lloveras et al., 2016; Maroto et al., 1996). Human groups occupied the cave in the subsequent levels associated with different cultural attributions: Gravettian (from levels F to D) and Solutrean (from levels C to B) (Soler et al., 2014; Soler and Soler, 2016). Some human remains have been recovered: two molars of *Homo neanderthalensis* (level N), a premolar of *Homo neanderthalensis* (level J), and a molar germ of AMH (level G) (Rufí et al., 2018; Soler et al., 2014; Soler and Soler, 2016).

Previous palaeoenvironmental reconstruction based small mammals and archaeobotanical studies were undergone from level I and the top of the sequence (Table 8.1). Palynological studies described open and herbaceous vegetation with steppic characters, with the emergence of *Pinus* and Cupressaceae, but detected short periods of climatic ameliorations related to interstadials and characterized by the sporadic extension of mesothermophilous and thermophilous vegetal associations (Burjachs and Renault-Miskovsky, 1992). According to changes detected by palynological diagrams, eleven pollen zones were differentiated inside the sequence. Anthracological analyses point to a predominance of *Pinus sylvestris* throughout the Pleistocene sequence (Ros, 1987). Regarding small-mammal studies of the sequence, the first approaches focused mainly on the taxonomic identification of the recovered remains (Alcalde, 1986; Alcalde and Brunet-Lecomte, 2002; Alcalde and Galobart, 2002; Estévez, 1987; Galobart et al., 1996). Small mammal assemblages of Arbreda cave are characterized by a predominance of species adapted to open-wet -

Levels	^{14}C Datings (ka BP)	^{14}C Datings (ka cal. BP)	Cultural adscription	Pollen zones (PZ) (Burjachs and Renault-Mikovski, 1992)	Small mammal's predator (López-García et al., 2015)	Small mammals (López-García et al., 2015)
Terra Rossa			Neolithic	PZ11 - warm-humid phase	*Strix aluco* / *Bubo bubo* - Digestion=28%	Warm and humid phase at the beginning of the Holocene Preboreal/Boreal period
A			Post-Solutrean or Post-Paleolithic	PZ10 - warm-humid phase	*Strix aluco* / *Bubo bubo* - Digestion=21%	Milder and humid conditions probably related with the Bölling/Allerod interstadial
B	(**)18.9±0.1	22.9 - 22.4	Solutrean	PZ9 - cold-humid phase PZ8 - temperate-humid phase	*Strix aluco* / *Bubo bubo* - Digestion=28%	Cold but relatively humid conditions associated with Last Glacial Maximum
C	(**)19.5±0.8	23.6 - 22.9	Solutrean	PZ7 - cold and dry phase	*Strix aluco* / *Bubo bubo* - Digestion=22%	
D	(**)22.7±0.1	27.7 - 27	Gravettian	PZ6 - cold and dry phase	*Strix aluco* / *Bubo bubo* - Digestion=23%	
E	(*)25.8±0.2; 26.1±0.2;(**)24.8±0.2 ; 25.2±0.1	31.1 - 30.4	Gravettian	PZ5 - cold and dry phase	*Falco tinnunculus* - (Digestion=28%)	
F	(*)28.3±0.3; (**)28.3±0.3	33.3 - 31.8	Gravettian		*Falco tinnunculus* - Digestion=34%	
G	(*)32.1±0.5; 32.3±0.5; 32.8±0.5	38.2 - 35.6	Evolved Aurignacian	PZ4 - temperate-humid phase PZ3 - cool-humit phase PZ2 - cold-dry phase	*Falco tinnunculus* - Digestion=37%	
H	(*)31.9±0.5; 33.8±0.5; 34.8±0.8; 35.9±0.7; 35.9±0.9; 35.7±0.7; 36±0.7	41.6 - 38.3	Archaic Aurignacian		*Falco tinnunculus* - Digestion=45%	Milder and relatively dry respect level I, related to GI10
I	(*)32.1±0.5; 32.3±0.5; 37.3±0.8; 39.2±1; 44±1.9; (***)38.4±0.4	45.8 - 41.4	Final Mousterian	PZ1 - alternation of temperate-humid phases with a cold-dry phase	*Strix aluco* / *Bubo bubo* - Digestion=19%	Cold and humid phase between GI12 and GI10

Table 8.1 Summary of palaeoenvironmental studies performed on Arbreda cave upper levels through different proxies. ^{14}C dating information from (*) Wood et al., 2014; (**) Soler et al., 2014; (***) Maroto et al., 2012b. Calibration of ^{14}C dating were obtained using the Oxcal 4.1.7 software (López-García et al., 2015). GI, Greenland Interstadial.

environments (*Microtus (Terricola) duodecimcostus*, *M. arvalis, M. agrestis*) and the presence of species with mid-European requirements (*M. arvalis* and *M. agrestis* and, occasionally, *M. gregalis, M. (T.) gerbei* and *Spermophilous* cf. *citellus*), which fluctuate in their relative presence through the sequence (López-García, 2011; López-García et al., 2014, 2015) (Appendix 2.5.A).

Taphonomic analysis was performed from level I to Terra Rossa (López-García et al., 2015), and demonstrated that the small-mammal accumulation was associated with predation (Table 8.1). The main agent identified for level I and for levels D to A is a predator with an intermediate capacity for modification, such as the tawny-owl (*Strix aluco*) or the eagle owl (*Bubo bubo*). Both are opportunistic owls that can reliably reflect the ecological community at the time of level formation (Andrews, 1990; López-García et al., 2015). Otherwise, the common kestrel (*Falco tinnunculus*) is the most likely cause of small-mammal assemblages from levels H to F. Their diurnal and moderately selective habits can result in some bias as compared to the original community of small mammals during the deposition of these levels (Andrews, 1990; López-García et al., 2015). Identified predators are in agreement with the defined open or semi-open palaeoecological conditions that prevailed in the area of Arbreda Cave (IUCN, 2018; López-García et al., 2015; Manzanares, 2012). High abundances of bat remains (mostly *Myotis myotis-blythii*) in the entire sequence are related to thanatocenosis from colonies of this species inside Arbreda cave (López-García, 2011; López-García et al., 2014, 2015). A review of non-flying small mammals (insectivores and rodents), which considered global consistency with palynological studies in the site, led to the tentative correlation of some levels with global-climatic fluctuations recorded in Greenland ice cores and from sea-surface temperatures of the Alboran Sea (Table 8.1) (López-García et al., 2015).

The Serinyà region is currently included in the pre-littoral north Mediterranean climate within Catalonian climatic subdivisions (Servei Meteorològic de Catalunya, 2018). The climate is generally wet and temperate (mean annual temperatures around 14-15 °C), but with hot summers (20-23 °C) and cool winters (7-8 °C), with a consequent thermic annual oscillation of 16° C. The mean annual rainfall is between 700 and 900 mm and precipitation is abundant throughout the year. Autumn is the wettest period, and summer is slightly drier (Climate-data.org; Servei Meteorològic de Catalunya, 2018). There is a consistent correspondence between average monthly temperatures and monthly oxygen isotope compositions of meteoric water estimated for the area (OIPC data, Bowen, 2017; climate-data.org) (Fig. 8.1C).

3. Synthesis of methods

The small mammal remains from Arbreda cave were recovered during excavation seasons from sediment samplings that extended along the entire excavated surface. The remains were collected by washing and sieving the sediment, using 0.5 mm mesh screens, and selected by subsequent sorting during field seasons at the site. Oxygen isotope compositions were measured on 49 teeth from levels H-D (MNI=36) (Table 8.2). Nine to ten samples were selected from each level in order to gather a representative range of samples (Lindars et al., 2001; Montuire et al., 2004; Royer et al., 2013a). To avoid possible interspecies variability with respect to previous oxygen isotope analysis (Chapters 5-7), *Apodemus sylvaticus* fossil incisors were preferred, with twenty-three incisors

corresponding at least to sixteen individuals (Fig. 8.2). However, the low presence of this species, especially in the upper levels, made it difficult to find well-preserved Murinae remains, which necessitated the inclusion of other taxa in better conditions: two *Eliomys quercinus* (MNI=2; levels H and D); five *Microtus arvalis* (MNI= 3; levels G, E, and D); two *M. agrestis* (MNI=2; levels E and D); one *M. arvalis-agrestis* (level D); and two *M. (T.) duodecimcostatus* (MNI=2; levels G and F). Fourteen medium-sized incisors from the subfamily Arvicolinae, related to a minimum of ten individuals, were also included in levels E, F, and H. The wet-chemistry and the mass spectrometer measurements were developed in the Laboratoire de Géologie of Université Claude Bernard (Lyon, France). For detailed information about sampling criteria and analytical techniques see Chapter 2 and Chapter 5. On the basis of phosphate chemical yields measured during the wet chemistry procedure, clustered phosphorus pentoxide (P2O5) contents close to 40 wt% indicate that the original stoichiometry of the teeth was most likely preserved. The average standard deviation of oxygen isotope compositions for the Arbreda samples is 0.28 ±0.03‰ (n=49).

Oxygen isotope analysis on present-day material of the Serinyà area were also performed (Table 8.2). The remains came from a pellet produced by a barn-owl (*Tyto alba)*, which was recovered less than 5 km from Arbreda cave, at 188 m a.s.l (see Fernández-García et al., under review; Chapter 5). The pellet was recovered in a fresh state at the beginning of September, just next to the bird's nesting place, where a large accumulation of pellets was conserved. The remains analyzed consist of three lower incisors, two of *A. sylvaticus* and one of *M. (T.) duodecimcostatus*.

Mean annual temperature (MAT) was calculated from oxygen isotope compositions ($\delta^{18}O$) of each level, following the three-step strategy proposed for $\delta^{18}O_p$ from rodent teeth accumulated in the Iberian Peninsula (Chapter 5). In parallel, the MATs were compared with two qualitative and independent palaeoenvironmental methods: the mutual ecogeographic range (MER) and the bioclimatic model (BM). In addition, these methods allow for the calculation of mean annual precipitation (MAP). The former was previously calculated for Arbreda levels by López-García et al. (2015), but this work applies the BM method for the first time (detailed explanation of these methods can be found in Chapters 2, 4 and 5). The current temperature data of the Arbreda area (Serinyà) come from Climate-Data.org (https://es.climate-data.org/). Present-day values of oxygen isotope compositions of meteoric waters ($\delta^{18}O_{mw}$) for the Arbreda area were obtained using the Online Isotopes in Precipitation Calculator (OIPC; Bowen, 2017).

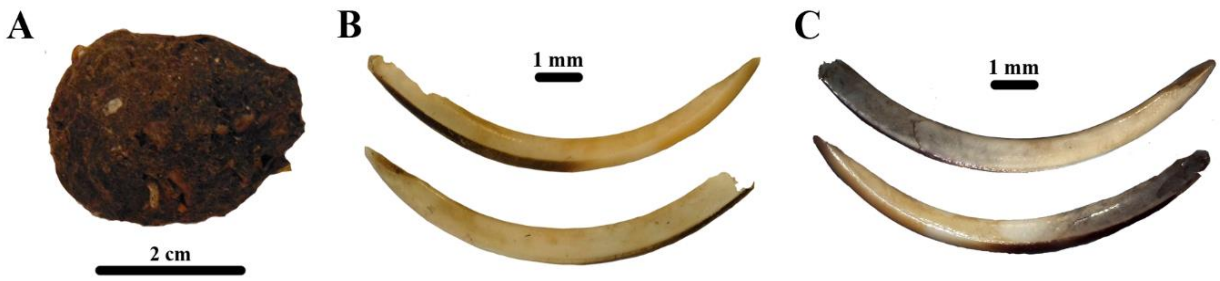

Figure 8.2 (A) Tawny-owl (*Tyto alba*) current pellet from Serinyà; (B) right lower incisor of *Apodemus sylvaticus*, in labial and lingual view; (C) left lower incisor of *Apodemus sylvaticus*, in labial and lingual view. (B) and (C) were recovered from the pellet (A) and used in biochemical analysis.

Sample	Level	Taxon	Remain	Laterality	Location	$\delta^{18}O_p$ (‰ V-SMOW)	SD	$\delta^{18}O_{mw}$ (‰ V-SMOW)
ARBD78	D	*Microtus agrestis*	Lower incisor	left	*in situ*	**20.2**	0.5	**-3.8**
ARBD82	D	*Microtus arvalis-agrestis*	Lower incisor	left	*in situ*	**19.9**	0.3	**-4.0**
ARBD79	D	*Microtus arvalis*	Lower incisor	left	*in situ*	**19.1**	0.4	**-4.6**
ARBD80	D	*Microtus arvalis*	Lower incisor	right	*in situ*	**19.0**	0.2	**-4.8**
ARBD73	D	*Apodemus* cf. *sylvaticus*	Lower incisor	left	isolated	**18.9**	0.2	**-4.8**
ARBD76	D	*Apodemus* cf. *sylvaticus*	Lower incisor	left	isolated	**17.5**	0.3	**-6.0**
ARBD74	D	*Apodemus* cf. *sylvaticus*	Lower incisor	left	isolated	**17.4**	0.2	**-6.1**
ARBD72	D	*Eliomys quercinus*	Upper incisor	right	*in situ*	**17.4**	0.3	**-6.1**
ARBD75	D	*Apodemus sylvaticus*	Lower incisor	left	*in situ*	**17.2**	0.4	**-6.2**
ARBE18	E	Arvicolinae	Lower incisor	left	isolated	**20.8**	0.3	**-3.2**
ARBE16	E	Arvicolinae	Lower incisor	left	isolated	**19.8**	0.3	**-4.1**
ARBE12	E	*Microtus arvalis*	Lower incisor	right	*in situ*	**19.4**	0.3	**-4.4**
ARBE15	E	Arvicolinae	Lower incisor	left	isolated	**19.0**	0.3	**-4.7**
ARBE52	E	*Apodemus* cf. *sylvaticus*	Upper incisor	left	isolated	**18.7**	0.6	**-5.0**
ARBE58	E	*Microtus arvalis*	Lower incisor	left	*in situ*	**18.7**	0.4	**-5.0**
ARBE40	E	Arvicolinae	Lower incisor	left	isolated	**18.2**	0.6	**-5.4**
ARBE65	E	*Microtus agrestis*	Lower incisor	left	*in situ*	**17.0**	0.3	**-6.4**
ARBE17	E	*Apodemus* cf. *sylvaticus*	Upper incisor	right	isolated	**16.9**	0.3	**-6.5**
ARBE14	E	Arvicolinae	Lower incisor	right	isolated	**14.2**	0.4	**-8.7**
ARBF57	F	Arvicolinae	Lower incisor	right	*in situ*	**20.9**	0.2	**-3.2**
ARBF49	F	*Apodemus* cf. *sylvaticus*	Lower incisor	left	isolated	**20.5**	0.3	**-3.5**
ARBF21	F	*Apodemus* cf. *sylvaticus*	Lower incisor	left	isolated	**20.2**	0.1	**-3.7**
ARBF24	F	Arvicolinae	Lower incisor	left	isolated	**19.7**	0.4	**-4.2**
ARBF54	F	*Apodemus* cf. *sylvaticus*	Lower incisor	left	isolated	**18.7**	0.4	**-5.0**
ARBF4	F	Arvicolinae	Lower incisor	left	isolated	**18.1**	0.1	**-5.5**
ARBF22	F	Arvicolinae	Lower incisor	right	isolated	**17.4**	0.4	**-6.1**
ARBF55	F	Arvicolinae	Lower incisor	left	*in situ*	**17.4**	0.1	**-6.1**
ARBF13	F	*M. (T.) duodecimcostatus*	Lower incisor	right	*in situ*	**16.9**	0.2	**-6.5**
ARBF23	F	Arvicolinae	Lower incisor	left	isolated	**15.3**	0.2	**-7.9**
AG27	G	*Apodemus* cf. *sylvaticus*	Lower incisor	left	isolated	**23.2**	0.5	**-1.3**
AG1	G	*Apodemus* cf. *sylvaticus*	Lower incisor	left	isolated	**21.0**	0.3	**-3.1**
AG26	G	*Microtus arvalis*	Lower incisor	right	*in situ*	**20.6**	0.3	**-3.5**
AG37	G	*Apodemus sylvaticus*	Lower incisor	right	*in situ*	**18.6**	0.2	**-5.1**
AG8	G	*Apodemus* cf. *sylvaticus*	Lower incisor	left	isolated	**17.9**	0.3	**-5.7**
AG3	G	*M. (T.) duodecimcostatus*	Lower incisor	left	*in situ*	**16.6**	0.3	**-6.8**
AG10	G	*Apodemus sylvaticus*	Lower incisor	right	*in situ*	**16.3**	0.2	**-7.0**
AG39	G	*Apodemus* cf. *sylvaticus*	Lower incisor	left	isolated	**16.0**	0.2	**-7.3**
AG7	G	*Apodemus* cf. *sylvaticus*	Lower incisor	right	isolated	**15.9**	0.2	**-7.3**
AG2	G	*Apodemus* cf. *sylvaticus*	Lower incisor	right	isolated	**15.6**	0.3	**-7.6**
AH20	H	Arvicolinae	Lower incisor	right	*in situ*	**21.5**	0.3	**-2.7**
AH36	H	*Apodemus* cf. *sylvaticus*	Lower incisor	left	isolated	**21.3**	0.2	**-2.8**
AH32	H	Arvicolinae	Lower incisor	left	isolated	**20.5**	0.1	**-3.5**
AH31	H	*Apodemus* cf. *sylvaticus*	Lower incisor	right	isolated	**20.0**	0.1	**-3.9**
AH69	H	*Eliomys quercinus*	Lower incisor	right	*in situ*	**19.7**	0.3	**-4.2**
AH64	H	*Apodemus* cf. *sylvaticus*	Lower incisor	right	isolated	**19.2**	0.2	**-4.6**
AH9	H	*Apodemus* cf. *sylvaticus*	Lower incisor	left	isolated	**17.9**	0.1	**-5.7**
AH19	H	*Apodemus* cf. *sylvaticus*	Lower incisor	left	isolated	**17.7**	0.2	**-5.8**
AH29	H	*Apodemus* cf. *sylvaticus*	Lower incisor	left	isolated	**16.7**	0.1	**-6.7**
AH34	H	Arvicolinae	Lower incisor	left	isolated	**16.2**	0.4	**-7.1**
MA-3		*M. (T.) duodecimcostatus*	Lower incisor	left	*in situ*	**18.8**	0.4	**-4.9**
MA-1		*Apodemus sylvaticus*	Lower incisor	right	*in situ*	**19.0**	0.1	**-4.8**
MA-2		*Apodemus sylvaticus*	Lower incisor	left	*in situ*	**19.5**	0.3	**-4.4**

Table 8.2 Oxygen isotope composition of tooth enamel phosphate ($\delta^{18}O_p$; ‰ V-SMOW) from rodent incisors of Arbreda cave (levels D-H). The table includes the stratigraphic layer, identified taxa, and the conversion to the oxygen isotope composition of meteoric waters ($\delta^{18}O_{mw}$; ‰ V-SMOW) following the Royer et al. (2013a) oxygen isotope fractionation equation. Rodent lower incisors coming from a modern pellet of *Tyto alba* are also included. SD, Standard Deviation.

4. Results and discussion

4.1 Oxygen isotope compositions of rodent remains

The oxygen isotope composition of the rodent incisor enamel ($\delta^{18}O_p$) from the different analyzed levels of Arbreda cave range from 14.2‰ to 23.2‰, with a range of variation of 9‰ (SD=1.9) (Fig. 8.3; Table 8.2; 8.3). This large range, however, is highly affected by some extreme and isolated values ("outliers") present in levels G, F, and E. When these values are excluded the total range is reduced to 6‰ (SD=1.7). The mean values of $\delta^{18}O_p$ show a limited variation along the sequence (<1‰), ranging between 18.2‰ (level G) and 19.1‰ (level H). The median $\delta^{18}O_p$ values increase the magnitude of these oscillations (>2‰), extending from 17.2‰ (level G) to 19.4‰ (level H), but stay largely similar. Mean $\delta^{18}O_p$ value never differs more than 1‰ from the median $\delta^{18}O_p$ value, showing a limited influence of extreme values and a homogenous distribution of data within each level. All sedimentary layers show a normal distribution of data (Shapiro-Wilk test; p-value>0.01).

Arvicolinae species and *Eliomys quercinus* samples were included within analyzed levels (Table 8.2; Fig. 8.3; 8.4). *E. quercinus* samples (in levels H and D) keep within the general range obtained from each level's measurements and have no influence either on the mean or median values. However, differences between 1-2‰ are detected in some levels' average estimations if Murinae and Arvicolinae are analyzed separately. Nevertheless, no specific trends are detected for each subfamily, considering that average estimations vary due to external factors unrelated to the taxonomy and physiology of each species. The causes may simply be due to a disproportionate number of remains of each genus within a given level or just different periods of deposition of remains.

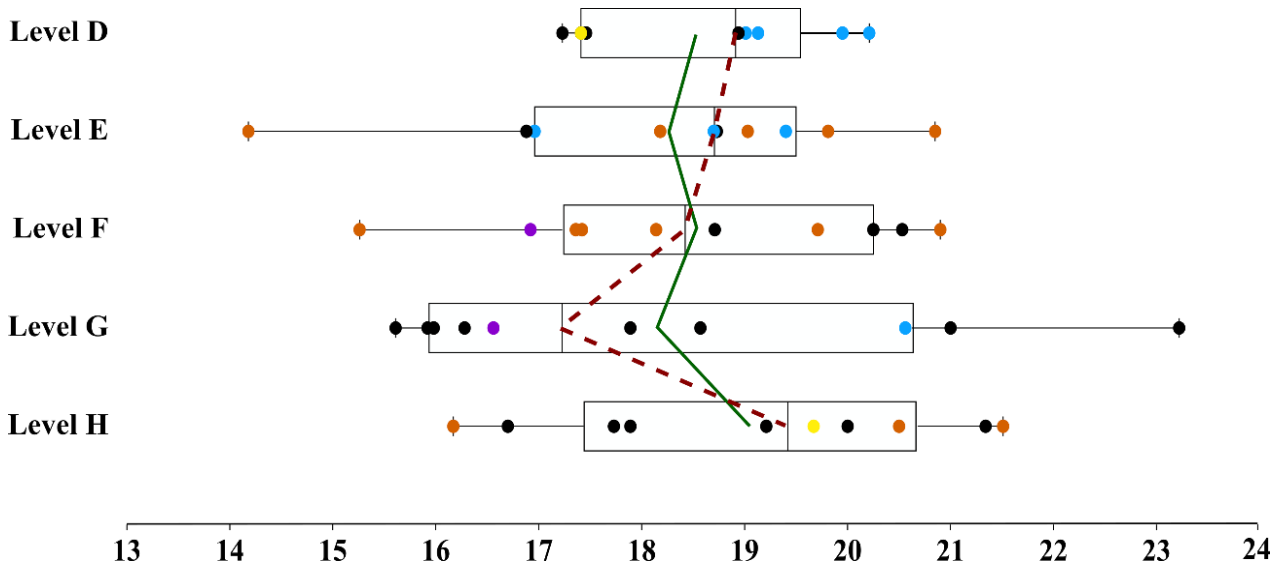

Figure 8.3 Oxygen isotope composition (‰ V-SMOW) of rodent incisor enamel from the Arbreda samples. Box plots and distribution of $\delta^{18}O$ values per layer, with mean (green line) and median (red dashed line) curves. Box plot bars cover the full extension of the values; the boxes extend from the 1st to 3rd quartile. Black points, *Apodemus sylvaticus*; yellow points, *Eliomys quercinus*; blue points, *Microtus arvalis-agrestis*; orange points, Arvicolinae; lilac points, *M. (Terricola) duodecimcostatus*.

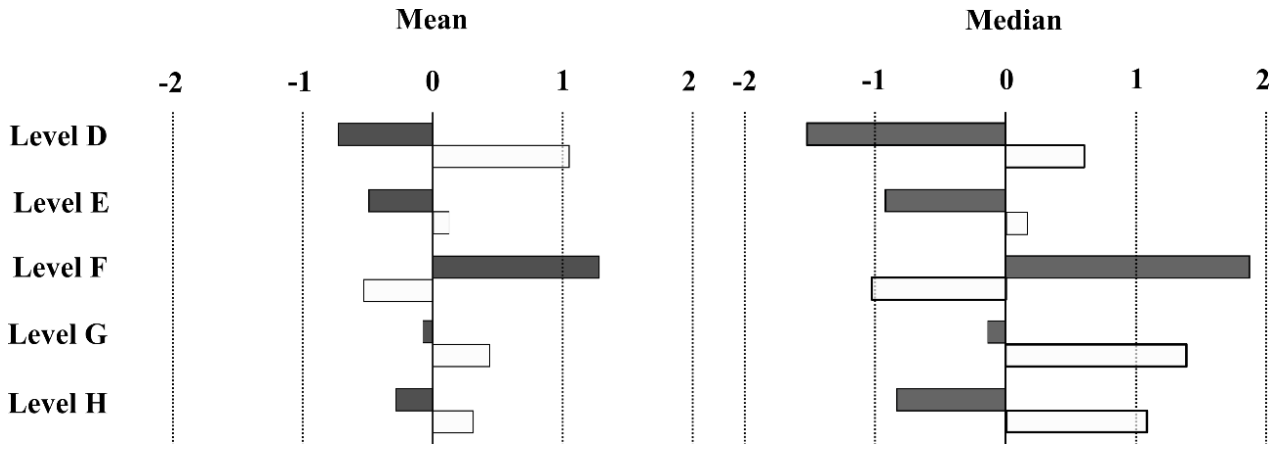

Figure 8.4 Comparison between Murinae (black) and Arvicolinae (white) average oxygen isotope compositions (‰ V-SMOW) with respect to estimated total mean and median for each level.

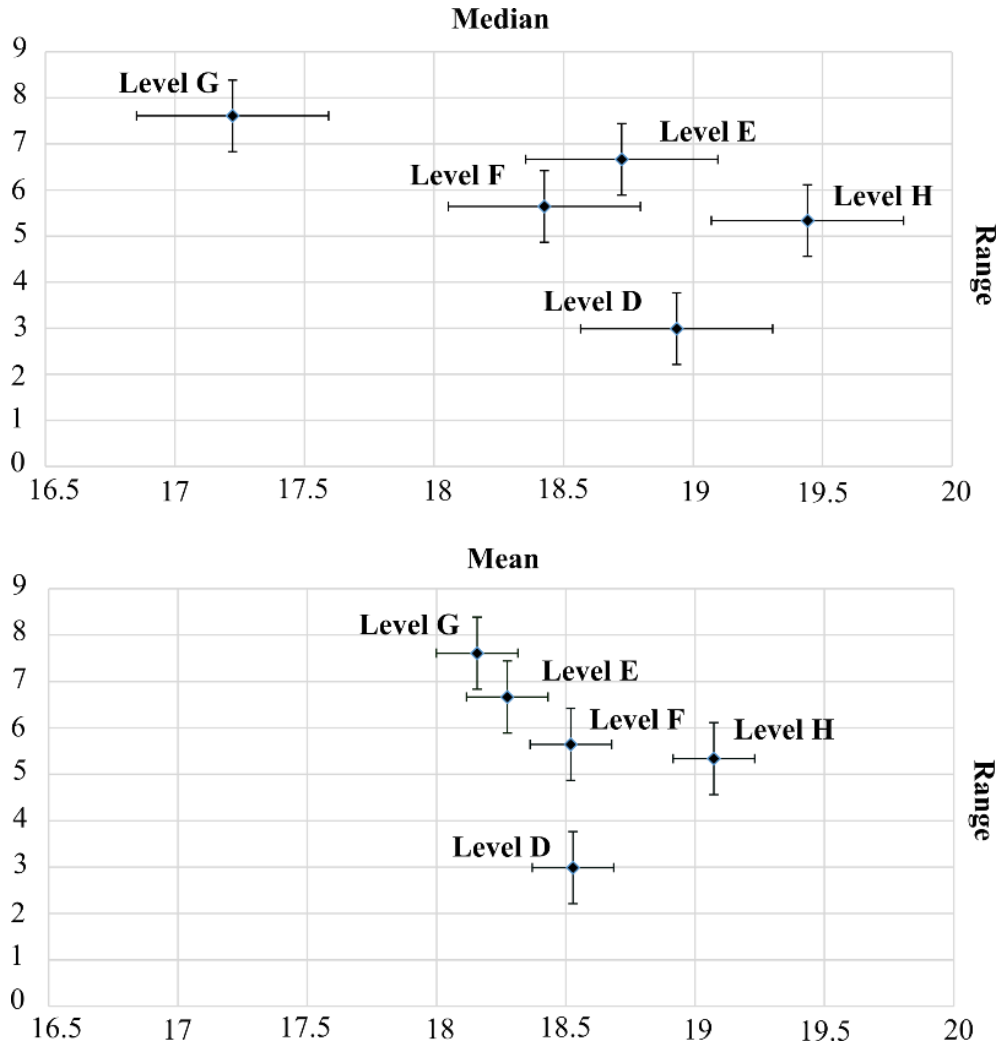

Figure 8.5 Oxygen isotope composition of incisor enamel phosphate ($\delta^{18}O_p$; ‰ V-SMOW) of Arbreda samples on rodent incisors, crossing range and median values (A) and range and mean values (B) of each analyzed level

Sizeable intra-level variations are observed, which range from 3‰ (level D) to 7.6‰ (level G) (Fig. 8.3; Table 8.3). Globally an inverse relationship between average $\delta^{18}O_p$ values and amplitude of $\delta^{18}O_p$ ranges between levels is observed: when the range increases, the mean and the median $\delta^{18}O$ values decrease (Fig. 8.5). Levels H and D are characterized by the lowest intra-level amplitude (5.3‰ and 3‰, respectively) and the highest medians (19.4‰ and 19‰, respectively). By contrast, levels G, F, and E show a higher amplitude of $\delta^{18}O_p$ values (7.6‰, 5.6‰ and 6.7‰, respectively) and lower medians (17.2‰, 18.4‰ and 18.7‰, respectively). However, the $\delta^{18}O_p$ ranges observed in levels G, F, and E are highly affected by only one extreme value: 23.2‰, 14.2‰ and 15.3‰, respectively. No significant differences were found between $\delta^{18}O$ means of any studied level (ANOVA sample test; $p>0.01$; Levene's test; $p>0.01$). Low to medium $\delta^{18}O_{mw}$ amplitudes recorded in the Arbreda sequence (between 1.5‰ and 5.3‰) are lower than the current seasonal amplitude for $\delta^{18}O_{mw}$ values at Serinyà (7.8‰; Bowen, 2017) (Fig. 8.1C; 8.3; Table 8.3) and the average seasonal amplitude of $\delta^{18}O_{mw}$ values for Iberia (8‰; Bowen, 2017; Fernández-García et al., under review). This suggests that analyzed rodent remains most likely accumulated during a preferential period of the year, which might correspond to spring-summer or autumn months. Considering present-day $\delta^{18}O_{mw}$ recorded at Serinyà (Bowen, 2017), fossil $\delta^{18}O_{mw}$ values (in $\delta^{18}O_{mw}$, from -8.7‰ to -1.3‰) can occur throughout the year (from -1.1‰ in July to -8.9‰ in February), but the majority of fossil $\delta^{18}O_{mw}$ values would have occurred on March-June (from -7.3‰ to -2.4‰; range: 4.9‰) or September-November (from -3‰ to -7.2‰; range: 4.2‰). During the warm season there is a higher probability of prey capture by owls in Iberia, as indicated by the rising number of murid specimens and the observed oxygen isotope composition of contemporaneous Iberian rodent tooth samples (Chaline, 1974; Lagos, 2019; Manzanares, 2012; Norrdahl and Korpima, 2002; Royer et al., 2013b, 2013a; Salamolard et al., 2000 (see Chapter 5). In keeping with this hypothesis, all levels report mean and median $\delta^{18}O_{mw}$ values (from -4.4‰ to -5.5‰) higher than current mean annual $\delta^{18}O_{mw}$ values on Serinyà (-5.9‰; Bowen, 2017), except for level G, which has a $\delta^{18}O_{mw}$ median value of -6.2‰.

Taphonomic analyses have suggested that the probable predator responsible for the rodent accumulation for levels H to C is *Falco tinnunculus*. This diurnal bird of prey is migratory, but currently acts as a sedentary species in the Iberian Peninsula, residing there all year. Migrant populations from northern latitudes leave their breeding grounds since August-October to occupy sub-Saharan Africa until February-April, depending on food availability (IUCN, 2018; Manzanares, 2012). This predator is an opportunistic forager but is characterized by its preference for small mammals in north and central Europe (IUCN, 2018; Mikkola, 1983). This preference is less marked in the Mediterranean, where it preferentially hunts the energetically most advantageous prey: either small mammals, birds, or insects (Costantini et al., 2005; Manzanares, 2012; Orihuela-Torres et al., 2017; Souttou et al., 2007). In Iberia, the breeding season generally takes place between April and June (Manzanares, 2012). Incubation lasts around four weeks and the offspring can fly about a month after hatching (Manzanares, 2012). Otherwise, the small-mammal assemblage of the upper level where oxygen isotopes were analyzed, level D, might be related to *S. aluco* or *B. bubo*. Both are sedentary and opportunistic predators (Andrews, 1990; Fernández-Jalvo et al., 2016; IUCN, 2018). Today in Iberia, the former breeds between January and March, whereas the latter starts its breeding season slightly later, between February

and April (Manzanares, 2012) (detailed information about *Strix aluco* can be found in Chapter 6, and about *Bubo bubo* in Chapter 7). Thus, predators related to small-mammal accumulation along the sequence could be in keeping with a preferential accumulation during spring and early-summer months, considering that their foraging habits are usually increment, coinciding with their breeding period. If the hypothesis that samples occurred in the same time period is validated, lower mean-medias and higher ranges-SDs may mainly be the consequence of climatic fluctuations and, occasionally, out-season samples.

Indeed, outside the main range of $\delta^{18}O_{mw}$ fossil values, related to this preferential season of accumulation, there are some particular cases, such as the aforementioned three isolated values in level G (-1.3‰), F (-7.9‰) and E (-8.7‰), and the three lowest values of level G that extend from -7.3‰ to -7.6‰ (Table 8.2; Fig. 8.3). The minimum $\delta^{18}O_{mw}$ values from levels F and E can be found within present-day $\delta^{18}O_{mw}$ winter values (from -7.9‰ to -8.9‰), maximum $\delta^{18}O_{mw}$ value of level G can be recorded today between July and August ($\delta^{18}O_{mw}$=-1.1‰/-1.5‰) and the lowest values of level G might correspond to the end or begging of winter (Bowen, 2017; Fig. 8.1C). Thus, these out-of-range values leave open two possibilities: 1) these $\delta^{18}O_{mw}$ values are related to production outside the preferential moment of accumulation, during summer or winter; or, 2) the records are produced during the preferential season and are indicative of cooler/hotter conditions, or even aridity in the case of upper values (see Jeffrey et al., 2015; Royer et al., 2013b). In the specific case of level G, it can be

	Levels	D	E	F	G	H	Pellet
	n	9	10	10	10	10	3
$\delta^{18}O_p$	Min	17.2	14.2	15.3	15.6	16.2	18.8
	Max	20.2	20.9	20.9	23.2	21.5	19.5
	Mean	18.5	18.3	18.5	18.2	19.1	19.1
	Median	18.9	18.7	18.4	17.2	19.4	19.3
	Range	3.0	6.7	5.6	7.6	5.3	0.7
	SD	1.2	1.9	1.8	2.6	1.9	0.4
$\delta^{18}O_{mw}$	Min	-6.2	-8.7	-7.9	-7.6	-7.1	-4.9
	Max	-3.8	-3.2	-3.2	-1.3	-2.7	-4.3
	Mean	-5.2	-5.4	-5.2	-5.5	-4.7	-4.7
	Median	-4.8	-5.0	-5.2	-6.2	-4.4	-4.6
	Range	2.5	5.5	4.7	6.3	4.4	0.6
MAT	$\delta^{18}O_{mw}$ - seasonality correction	-5.9	-6.0	-6.3	-7.3	-5.4	x
	$\delta^{18}O_{mw}$ - sea level correction	-6.5	-6.6	-6.9	-7.9	-6.0	x
	MAT (ºC)	12.8	12.4	11.8	9.3	13.8	16.9
	SD	1.4	1.3	1.3	1.3	1.4	2.3
	Error margin	2.8	2.6	2.6	2.6	2.7	4.5

Table 8.3 Minimum, maximum, mean, median, standard deviation, and range of oxygen isotope composition of incisor enamel phosphate ($\delta^{18}O_p$; ‰ V-SMOW) from fossil rodents recovered from Arbreda cave samples; conversion to the oxygen isotope composition of meteoric waters ($\delta^{18}O_{mw}$; ‰ V-SMOW), including minimum, maximum, mean, median, and range, and mean annual temperature estimations (MAT; º C), including seasonality and sea-level corrections of $\delta^{18}O_{mw}$. Present-day pellet samples from Serinyà are also incorporated to calculate their average temperature, without applying corrections.

also argued that remains were accumulated throughout the year, because values obtained extend through a year's range.

Present-day oxygen isotope composition of incisors preserved in a barn owl pellet that come from the area surrounding Arbreda cave (Chapter 5) were also analyzed (Table 8.2; 8.3; Fig. 8.2). Pellet $\delta^{18}O_p$ values extended from 18.8‰ to 19.5‰ (-4.9‰ to -4.3‰; in $\delta^{18}O_{mw}$). Based on current $\delta^{18}O_{mw}$ values in the area (Bowen, 2017) (Fig. 8.1C), the pellet records are coincident with April-May (-5.8‰/-3.9‰) or September-October (-3‰/-5‰). These results show some inconsistency with expected current $\delta^{18}O_{mw}$ values, considering that the pellet was recovered between August and September. The different altitudes at which the predator may have been hunting could explain this discrepancy, because $\delta^{18}O_{mw}$ values are lower in the highlands during summer. Not far from the owl's nest and within its hunting area range (3-10 km^2), altitudes between 500-700 m a.s.l. can easily be reached, precluding altitude from being an extra factor to be considered in out-of-range $\delta^{18}O$ values.

4.2 Past climatic reconstruction of Arbreda sequence

Mean annual temperature (MAT) was calculated based on median $\delta^{18}O_p$ of each sedimentary level. The estimated MATs vary between 9.3 ±2.6 °C (level G) and 13.8 ±2.7 °C (level H) (Table 8.3; Fig. 8.6). These temperatures are lower than the current MAT recorded at Serinyà (14.8 °C; Climate-Data.org, 2018; Fig. 8.1C), with differences ranging from -5.5 °C to -1 °C. An important climatic shift (-4.5 °C) was detected between levels H (13.8 °C) and G (9.3 °C) with a progressive recovering of temperatures from levels F (11.8 °C) to D (12.8 °C). Results of present-day pellets sampled are included in Table 8.3. The mean $\delta^{18}O_{mw}$ value of the pellet (-4.6‰) is equivalent to an average temperature (without applying unnecessary seasonality and sea level corrections) of 16.9 °C, close to the current mean temperatures of May or October. This mean temperature is higher than fossil samples from Arbreda cave.

MATs and mean annual precipitation (MAP) were estimated with MER for all excavated levels of the sequence (from I to Terra Rossa) by López-García et al., (2015) (Appendix 2.5.B). This work incorporates the BM method of estimation for these levels (Appendix 2.5.C). Both methods show colder temperatures than present-day along the sequence; however, the magnitude of these differences depends on the method, with differences from 0.7 °C to 5.8 °C between methods for each of the levels. The BM method tends to estimate the highest temperatures (from -2 °C to -5.1 °C, in relation to present-day), whereas MER estimations always give lower temperatures (-4.7 to -8.8 °C, in relation to present-day). The MAT temporal trend calculated from the $\delta^{18}O_p$ record in levels H-D is reasonably similar to that obtained by MER (López-García et al., 2015) and BM reconstruction methods (Fig. 8.6). However, an offset of a few degrees is observed among the three methods (between 1 °C and 4 °C with BM and between 0.6 °C and 5.4 °C with MER), but in most cases remains small enough to be included within the confidence interval (a complete discussion of methods discrepancies in presented Chapter 9). This work underscores the singularity of level G and the climatic shift between levels G and H.

Both MER and BM methods record MAPs higher than present-day Serinyà (733 mm; Climate-Data.org) but differ in the magnitude of this estimation (+30/+767 mm and +30/+467 mm, respectively); this excludes level E that, considering MER reconstruction, recorded an

annual pluviometry comparable to present-day (-19 mm) (Fig. 8.6). Under MER reconstruction, highest MAPs are record from levels I (1500 mm) and F (1200 mm) and the lowest from the aforementioned level E (714 mm). The other levels (H-G and D-Terra Rossa) fluctuated between 927 and 967 mm. According to the BM method, the driest level was D (763 mm) followed by levels H-G and C-A (849-991 mm); the wettest phases correspond to levels I, F-E, and Terra Rossa (>1000 mm). There is not a clear relationship between pluviometry regime oscillation during the formation of levels H and D and the variations in oxygen isotope results.

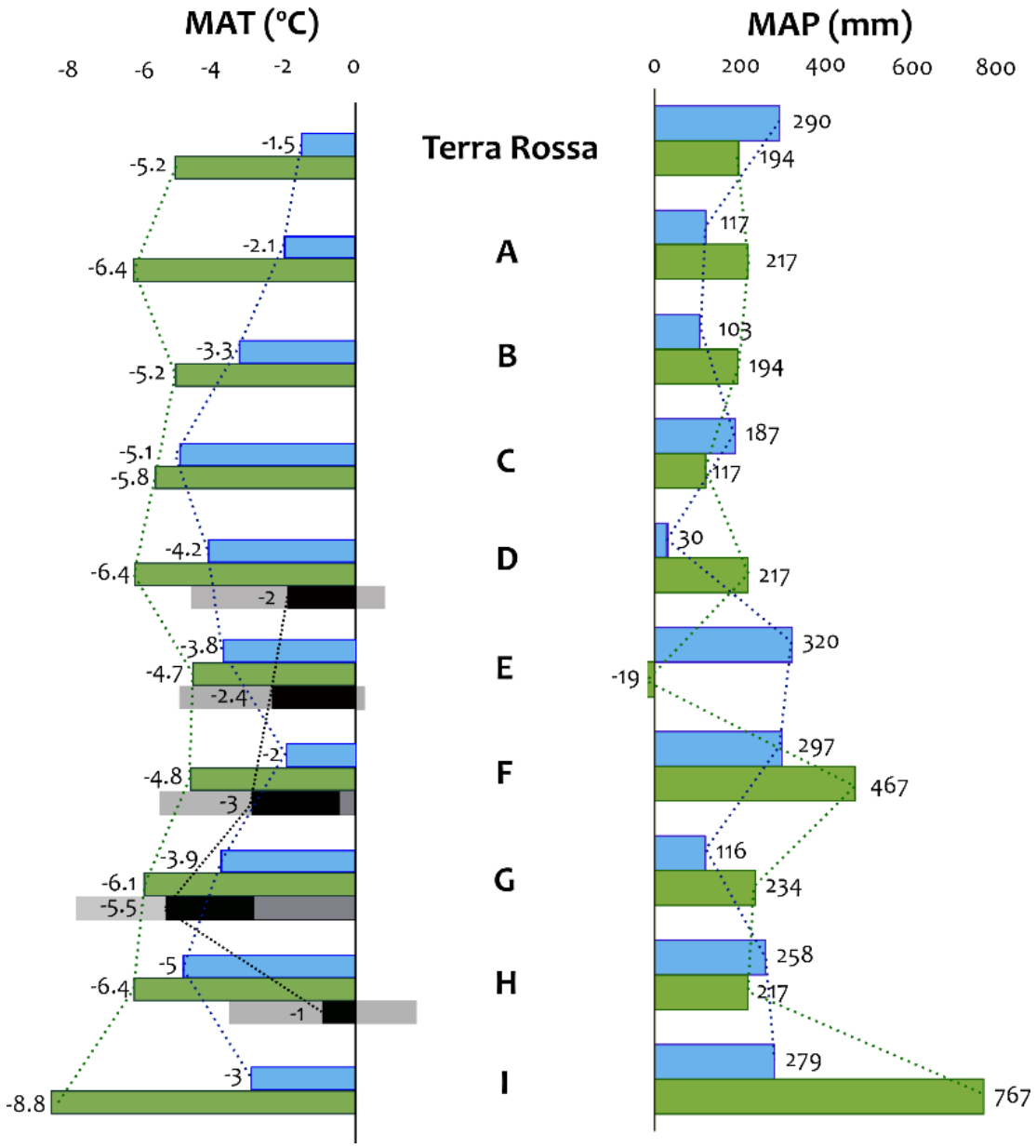

Figure 8.6 Mean annual temperature (MAT) and mean annual precipitation (MAP) estimations for Arbreda cave sequence with respect to present-day climate in Serinyà (MAT= 14.8 ºC; MAP= 733 mm; Climate-data.org), considering the bioclimatic model (in blue) and mutual ecogeographical range (in green) methods and, for levels H-D, the oxygen isotope compositions (in black) of rodent phosphate samples (error presented in grey fringe).

4.3 Latest Pleistocene environment recorded in Arbreda cave

Environmental reconstructions of the site based on small vertebrates, pollen, and charcoals have until now focused on the most-excavated levels, from level I to Terra Rossa (mainly Burjachs and Renault-Miskovsky, 1992; López García et al., 2015; Ros, 1987) (Table 8.1). The last Neanderthal occupations in the Arbreda cave, related to Final Mousterian, are found in Level I (dating from 31.9 ±0.5 ka BP to 36 ±0.7 ka BP; Wood et al., 2014). These occupations are considered short and in alternation with carnivores (Lloveras et al., 2010; Maroto et al., 1996; Rufí et al., 2018; Soler et al., 2014). This level corresponds to the latest stages of the MIS 3 and was correlated to an stadial period (probably between GI12 and GI10) based on low temperatures (MAT=-8.8 °C, with respect to the present-day MER estimation), high presence of Mid-European species (*M. arvalis, M. agrestis, C. nivalis or M. (T.) gerbei*), and low percentages (<10%) of arboreal pollen (Burjachs and Renault-Miskovsky, 1992; López-García et al., 2015) (Table 8.4). However, the BM method notably reduced this MAT estimation (-3 °C) (Fig. 8.6). Both methods are in agreement for precipitation rates, showing level I as one of the wettest periods of the sequence (MAP between 1000 and 1500 mm). Indeed, excluding level A, the highest abundances of woodland dweller rodent species was recorded in this level, representing *A. sylvaticus* and *E. quercinus* >35%, and the lowest relative abundances of *M. arvalis* and *M. agrestis* species (around 40%) adapted to open meadows (Fernández-García et al., 2016; López-García et al., 2014, 2015).

The transition between levels I and H has generated great deal of scientific discussion (e.g., Higham et al., 2014; Maroto et al., 2012b, 1996; Wood et al., 2014; Zilhão, 2000; Zilhao and D'Errico, 1999), due to testifies substitution of Neanderthals by AMH (see Maroto et al., 1996; Soler et al., 2014; Soler and Soler, 2016). Previous environmental studies, however, do not point to the important climatic shift within the Mousterian-Aurignacian transition, even more a general climatic and environmental improvement is noticed, with a temperature increase (Table 8.1). López-García et al. (2015) relate level H to the GI10 and describe it as milder and relatively dry with respect to level I. However, dating of this level is not clear at all, with recent ^{14}C re-datings ranging from 32.1 ±0.5 ka BP to 44.4 ka BP (Maroto et al., 2012b; Wood et al., 2014). Oxygen isotope analysis of this level emphasizes these mild and favorable conditions. Level H presents the highest mean and median $\delta^{18}O_p$ values (19.1‰/19.4‰) and medium range (5.3‰) consistent with accumulation mainly produced in the warm season that preserved stable conditions (Fig. 8.3; 8.5; Table 8.3). None $\delta^{18}O_{mw}$ value correspond to current $\delta^{18}O_{mw}$ winter values. This is traduced in the highest MAT estimation (13.8 ±2.7 °C;-1 °C with respect to present-day MAT), but is notably higher than the estimate using MER and BM methods (-6.4 °C and -5 °C, respectively) (Fig. 8.6). Results from MER and BM methods indicate it was a wet phase (MAP around 950-1000 mm), but moderate in relation to other levels of the sequence. Nevertheless, the presence of some rodent species with woodland preferences, as *E. quercinus* and *A. sylvaticus*, is reduced at this level, ranging between 4% and 14% until the deposition of level A. On the contrary, *M. arvalis* and *M. agrestis* increase in relative abundance from <40% in level I to >65% from level H, progressively increasing their dominance until level A (Fernández-García et al., 2016; López-García et al., 2014, 2015). Small mammals are probably correlated with some of the temperate and humid

Levels	Pollen zones (PZ) (Burjachs and Renault-Mikovski, 1992)	Small mammals (López-García et al., 2015)	Oxygen isotope analysis (This work)	Past temperatures (This work & López-García et al., 2015)	Past precipitation (This work & López-García et al., 2015)
Terra Rossa	PZ11 - warm-humid phase	Warm and humid phase at the beginning of the Holocene Preboreal/Boreal period		BM=13.3 °C / MER=9.6 °C	BM=1023 mm/ MER=927 mm
A	PZ10 - warm-humid phase	Milder and humid conditions probably related with the Bölling/Allerod interstadial		BM=12.7 °C / MER=8.4 °C	BM=850 mm/ MER=950 mm
B	PZ9 - cold-humid phase PZ8 - temperate-humid phase	Cold but relatively humid conditions associated with Last Glacial Maximum		BM=11.5 °C / MER=9 °C	BM=836 mm/ MER=927 mm
C	PZ7 - cold and dry phase			BM=9.7 °C / MER=9 °C	BM=920 mm/ MER=850 mm
D	PZ6 - cold and dry phase		The lowest amplitude and high median. Temperate and stable period.	BM=10.6 °C / MER=8.4 °C/ $\delta^{18}O$=	BM=763 mm/ MER=950 mm
E	PZ5 - cold and dry phase		Low-medium amplitude and low median, but globally stable period.	BM=10.6 °C / MER=8.4 °C/ $\delta^{18}O$=12.8°C	BM=1053 mm/ MER=714 mm
F			Low-medium amplitude and low median, but globally stable period.	BM=12.8 °C / MER=10 °C/ $\delta^{18}O$=11.8 °C	BM=1030 mm/ MER=1200 mm
G	PZ4 - temperate-humid phase PZ3 - cool-humit phase PZ2 - cold-dry phase		The most heterogenous level, the lowest median and the largest amplitude. Instability related to rigorous climatic conditions.	BM=10.9 °C / MER=8.7 °C/ $\delta^{18}O$=9.3 °C	BM=849 mm/ MER=967 mm
H		Milder and relatively dry with respect to level I, related to GI10	The highest median and medium amplitude. Warm and stable.	BM=9.8 °C / MER=8.4 °C/ $\delta^{18}O$=13.8 °C	BM=991 mm/ MER=950 mm
I	PZ1 - alternation of temperate-humid phases with a cold-dry phase	Cold and humid phase between GI12 and GI10		BM=11.8 °C / MER=6 °C	BM=1012 mm/ MER=1500 mm

Table 8.4 Previous palaeoenvironmental approaches to the Arbreda sequence and results from this work. Mean annual temperature and mean annual precipitation estimations are included, based on the bioclimatic model method (BM), mutual ecogeographic range method (MER), and oxygen isotope compositions ($\delta^{18}O$).

phases recorded in palynological studies (Burjachs and Renault-Miskovsky, 1992).

Above, level G (ca. 32 ka BP; Wood et al., 2014) is characterized by intensive human occupation in the cave related to the Evolved Aurignacian. During this period the cave was mostly a human settlement with short periods of abandonment, during which small carnivores probably used the site (Lloveras et al., 2016; Soler et al., 2014). From the perspective of biochemical analyses, this level is the most heterogenous of the sequence. This level includes the maximum $\delta^{18}O_p$ value of the sequence (23.2‰) and three $\delta^{18}O_p$ lower values out of the common ranges of the sequence (<15‰). These are related to hotter/cooler warmer seasons, to the production of rodent remains in summer/winter season, or to bigger seasonality amplitudes of small-mammal accumulation (Fig. 8.3). Inside Arbreda cave, level G has the largest range (7.6‰) and the largest SD (2.6) in relation to the lowest mean and, especially, median $\delta^{18}O_p$ values (18.2‰ and 17.2‰, respectively) (Fig. 8.5; Table 8.3). Thus, this level is mainly indicative of climatic instability and demonstrates the lowest MAT of the sequence (9.3 ±2.6 °C) with a difference of -4.5 °C with respect to temperate level H (Fig. 8.6). Although MER and BM point to cold conditions in this level (MAT between -6.1 °C and -3.9 °C) this deterioration is not fully supported in comparison to upper level F and lower level H. However, some small mammal qualitative data provided some corroboration, as the low presence of typical Mediterranean small mammal species and increasing abundances of species with mid-European and open-environment requirements

(*M. arvalis, M. agrestis, C. nivalis*) and the occurrence of some cold species currently present in Central Eurasia (as *M. oeconomus*). Level G, as well as the aforementioned level H, is a wet period (MAP between 850 and 1000 m) but drier than level I and upper levels, representing in H-G levels a decrease in humidity, probably accompanied with a reduction of surrounding forested area. Accordingly, *M. arvalis* and *M. agrestis* experienced a higher relative abundance (>70%), to the detriment of *A. sylvaticus* and *E. quercinus* (~14%) (López-García et al., 2015).

The Aurignacian period is followed by levels related to the Gravettian (from F to D), that show irregular intensity of human occupations: abundant lithic and faunal assemblages are recovered from level E, but are scarce during F and D (Soler et al., 2014; Soler and Soler, 2016). The chronology of these levels extends between ca. 28 to 22 ka BP (Soler et al., 2014; Wood et al., 2014). In view of oxygen isotope compositions recorded from rodent incisors, these levels are globally homogenous and stable (Fig. 8.5). Larger $\delta^{18}O_p$ ranges from levels E and F are highly biased by a minimum and isolated value (15.3‰ and 14.2‰, respectively), probably related to samples produced during winter (Fig. 8.3). If these values are excluded, ranges are reduced to 4‰, close to the range in level D (3‰), the lowest of the sequence. Median $\delta^{18}O$ values increase along these levels and, consequently, palaeotemperature estimations show a progressive amelioration from level F (MAP=11.8 ±2.6 °C) to D (MAP=12.8 ±2.6 °C). In accordance with MER and BM reconstruction, though, MATs are still notably lower than present-day conditions (from – 3 °C to – 2 °C), but an important offset of degrees is observed among methods (detailed discussion of palaeotemperatures estimations methods in Chapter 9) (Table 8.3; Fig. 8.6). BM and MER also demonstrate discrepancies between MAP estimations in magnitude and general trend. Level F is one of the wettest periods based on both BM and MER (>1000 mm), so an increase in humidity with respect H-G is presumed. After, level E according to BM it the wettest phase of the sequence (1053 mm); on the opposite, under MER analysis it could be the driest phase (714 mm). Moderate precipitation is estimated for level D, which slightly differs between MER (950 mm) and BM (763 mm). In light of small-mammal abundances (López-García et al., 2015), cool and dry climate and open landscape conditions are underscored by the significant predominance of *M. arvalis* and *M. agrestis* (>80%). Palynological and anthracological analyses suggest a landscape dominated by prairies, where genus *Artemisia* and Asteraceae dominated, with few river pine forest and riverbank trees (Burjachs and Renault-Miskovsky, 1992; Ros, 1987).

In summary, these results highlight the singular climatic conditions of the latest stages of MIS 3 to which AMH should have adapted upon their arrival. Globally colder and wetter conditions than present-day are recorded along the sequence. Biochemical analyses highlight a climatic shift between levels H and G (- 4.5 °C). On the one hand, temperate conditions detected in level H (MAT=13.8±2.7 °C) confirm interstadial conditions previously inferred for this deposit. Considering current results, it is not possible to support an environmental hypothesis for Neanderthal population fragmentation, because this climatic shift occurred after their occupations ended inside Arbreda cave. Independently, it can be inferred that the first AMH occupation is coincident with a temperate period/event, probably related to interstadial conditions. On the other hand, a climatic deterioration is contemporaneous with the deposition of level G, which coincides with the

latest stages of the MIS 3. Both quantitative methods and oxygen isotope results are in keeping with qualitative analyses based on the relative abundance of small mammals that highlighted the dominance of species with Mid-European and open-environment requirements in this level. However, palynological and anthracological studies point to a relatively warm climate with thermophilic plant species, suggesting a greater extension of the forests that was related to interstadial conditions (Burjachs and Renault-Miskovsky, 1992; Ros, 1987; Soler et al., 2014). Palynological analyses described one cool-humid phase (PZ3) for the top of this level, which could be related to the results described here. Inconsistencies between palaeoenvironmetal proxies might be explained by a different origin of the samples and/or different climatic scales used for each method (different hypothesis of methods discrepancies are discussed in Chapter 9). Considering these results, level G could correspond to a notably cold period (MAT=9.3 ±2.6 °C), probably related to a stadial period. Level G record intense human occupation by Aurignacian groups, demonstrating to be well-adapted to climatic cold periods.

5. Conclusions

- The mean values of $\delta^{18}O_p$ show limited variation along the sequence (<1‰), but median $\delta^{18}O_p$ values increase the magnitude of this oscillations (>2‰). Sizeable intra-level $\delta^{18}O_p$ fluctuations are observed between levels H and D, with the lowest amplitude (5.3‰/3‰) and the highest medians (19.4‰/19‰) and levels G, F, and E, with higher amplitudes (7.6‰/5.6‰/6.7) and lower medians (17.2‰/18.4‰/18.7‰).
- No specific pattern is observed for any taxonomic group in the obtained oxygen isotope composition results. The average differences observed are consequences of external factors, related to characteristics of the data-set.
- The medium ranges $\delta^{18}O_{mw}$ calculated for each level (between 3‰ and 7.6‰) point to a preferential accumulation moment of small-mammal remains in the cave. Considering the higher median $\delta^{18}O_{mw}$ (-4.4‰ to -5.2‰) with respect to present-day mean annual $\delta^{18}O_{mw}$ (7.8‰), they were most likely produced during the warmer season (spring and early summer). This period is equivalent to present-day nesting-breeding seasons of the predators identified as causes of the accumulation (*Falco tinnunculus* and *Bubo bubo*/*Strix aluco*).
- Some singular $\delta^{18}O_{mw}$ values are detected in levels G (-1.3‰; -7.3‰ to -7.6‰), F (-7.9‰) and E (-8.7‰), related to current $\delta^{18}O_{mw}$ summer or winter conditions. That could indicate that there was accumulation during these periods or that there were climatic oscillations during the warmer season.
- The oxygen isotope palaeotemperature estimations denote cooler (from -1 to -5.5 °C) conditions than today for levels H-D, close to results using BM and MER methods of climatic reconstruction (-2 °C to -5 °C and -3.9 to -6.4, respectively). Results using BM and MER methods also suggest a wetter environment (+30 mm to +320 mm and +217 mm to + 467 mm, respectively), except for in level E, according to MER analysis. Lower temperatures and higher precipitation rates are also observed before (level I) and after (level C-Terra Rossa).
- Biochemical analyses highlight a climatic shift between levels H and G (- 4.5 °C). Temperate conditions detected in level H (MAT=13.8 ±2.7 °C) confirm interstadial conditions previously inferred for this deposit and indicate climatic deterioration within level G that coincides with the Evolved Aurginacian occupations of the cave.

Considering the results presented here, level G corresponds to a notably cold moment (MAT=9.3 - 2.6 °C), probably related to a stadial moment.

References

Alcalde, G., 1986. Les faunes de rongeurs du Pléistocène supérieur et de l'Holocène de Catalogne (Espagne) et leurs significations paléoécologiques et paléoclimatiques. Hautes études-Sciences de la Vie et de la Terre IIIème section (Paris). Doctoral thesis.

Alcalde, G., Brunet-Lecomte, P., 2002. Contribució al coneixement del medi i el clima durant el Plesitocè superior i l'Holocè a Catalunya, amb l'aplicació de l'ànalisis factorial de correspondencies a les associacions de rosegadors. Paleontol. i Evol. 19, 49–55.

Alcalde, G., Galobart, À., 2002. Els petits mamífers del Pleistocè superior. Els Vertebr. Foss. del Pla l'Estany. Quad. 23. 23, 141–154.

Andrews, P., 1990. Owls, Caves and Fossils. Predation, preservation and accumulation of small mammal bones in caves, with an analysis of the Pleistocene Cave Faunas from Westbury-sub-Mendip, Somerset, UK. The University of Chicago, Chicago.

Baena, J., Carrión, E., Cuartero, F., Fluck, H., 2012. A chronicle of crisis: The Late Mousterian in north Iberia (Cueva del Esquilleu, Cantabria, Spain). Quat. Int. 247, 199–211.

Bowen, G.J., 2017. The Online Isotopes in Precipitation Calculator, Version 3.1 (4/2017) [WWW Document]. URL http://waterisotopes.org

Burjachs, F., Renault-Miskovsky, J., 1992. Paléoenvironnement et paléoclimatologie de la Catalogne durant près de 30,000 ans (du Würmien ancien au début de l'Holocène) d'après la Palynologie du site de l'Arbreda (Gérone, Catalogne). Quaternaire 3, 75–85.

Chaline, J., 1974. Les proies des rapaces. Doin Éditeurs, Paris.

Climate-Data.org [WWW Document], 2018. URL https://es.climate-data.org/

Costantini, D., Casagrande, S., Di Lieto, G., Fanfani, A., Dell'Omo, G., 2005. Consistent differences in feeding habits between neighbouring breeding kestrels. Behaviour 142, 1409–1421.

D'Errico, F., Sánchez Goñi, M.F., 2003. Neandertal extinction and the millennial scale climatic variability of OIS 3. Quat. Sci. Rev. 22, 769–788.

Estévez, J., 1987. La fauna de l'Arbreda (sector Alfa) en el conjunt de faunes del Plistocè Superior. Cypsela 6, 73–87.

Estévez, J., 1980. El aprovechamiento de los recursos faunísticos: Aproximación a la economía en el Paleolítico catalán. Cypsela 3, 9–30.

Fernández-García, M., López-García, J.M., Lorenzo, C., 2016. Palaeoecological implications of rodents as proxies for the Late Pleistocene–Holocene environmental and climatic changes in northeastern Iberia. Comptes Rendus Palevol 15, 707–719.

Fernández-Jalvo, Y., Andrews, P., Denys, C., Sesé, C., Stoetzel, E., Marin-Monfort, D., Pesquero, D., 2016. Taphonomy for taxonomists: Implications of predation in small mammal studies. Quat. Sci. Rev. 139, 138–157.

Finlayson, C., Fa, D.A., Finlayson, G., Pacheco, F.G., Vidal, J.R., 2004. Did the moderns kill off the Neanderthals? A reply to F. d'Errico and Sánchez Goñi. Quat. Sci. Rev. 23, 1205–1209.

Galobart, À., Maroto, J., Ros, X., 1996. Las faunas cuaternarias de mamíferos de la cuenca de Banyoles-Besalú (Girona). Rev. Española Paleontología nº ext., 248-255.

Higham, T., Douka, K., Wood, R., Ramsey, C.B., Brock, F., Basell, L., Camps, M., Arrizabalaga, A., Baena, J., Barroso-Ruíz, C., Bergman, C., Boitard, C., Boscato, P., Caparrós, M., Conard, N.J., Draily, C., Froment, A., Galván, B., Gambassini, P., Garcia-Moreno, A., Grimaldi, S., Haesaerts, P., Holt, B., Iriarte-Chiapusso, M.-J., Jelinek, A., Jordá Pardo, J.F., Maíllo-Fernández, J.-M., Marom, A., Maroto, J., Menéndez, M., Metz, L., Morin, E., Moroni, A., Negrino, F., Panagopoulou, E., Peresani, M., Pirson, S., de la Rasilla, M., Riel-Salvatore, J., Ronchitelli, A., Santamaria, D., Semal, P., Slimak, L., Soler, J., Soler, N., Villaluenga, A., Pinhasi, R., Jacobi, R., 2014. The timing and spatiotemporal patterning of Neanderthal disappearance. Nature 512, 306–309.

IUCN, 2018. The IUCN Red List of Threatened Species [WWW Document]. Version 2018-2. URL www.iucnredlist.org

Jeffrey, A., Denys, C., Stoetzel, E., Lee-Thorp, J. a., 2015. Influences on the stable oxygen and carbon isotopes in gerbillid rodent teeth in semi-arid and arid environments: Implications for past climate and environmental reconstruction. Earth Planet. Sci. Lett. 428, 84–96.

Kehl, M., Eckmeier, E., Franz, S.O., Lehmkuhl, F., Soler, J., Soler, N., Reicherter, K., Weniger, G.C., 2014. Sediment sequence and site formation processes at the Arbreda Cave, NE Iberian Peninsula, and implications on human occupation and climate change during the Last Glacial. Clim. Past 10, 1673–1692.

Lagos, P., 2019. Predation and Its Effects on Individuals: From Individual to Species. Encyclopedia of Ecology 2, 365-368.

Lindars, E.S., Grimes, S.T., Mattey, D.P., Collinson, M.E., Hooker, J.J., Jones, T.P., 2001. Phosphate $\delta^{18}O$ determination of modern rodent teeth by direct laser fluorination: An appraisal of methodology and potential application to palaeoclimate reconstruction. Geochim. Cosmochim. Acta 65, 2535–2548.

Lloveras, L., Maroto, J., Soler, J., Thomas, R., Moreno-García, M., Nadal, J., Soler, N., 2016. The role of small prey in human subsistence strategies from Early Upper Palaeolithic sites in Iberia: the rabbits from the Evolved Aurignacian level of Arbreda Cave. J. Quat. Sci. 31, 458–471.

Lloveras, L., Moreno-García, M., Nadal, J., Maroto, J., Soler, J., Soler, N., 2010. The application of actualistic studies to assess the taphonomic origin of Musterian rabbit accumulations from Arbreda Cave (North-East Iberia). Archaeofauna 19, 99–119.

López-García, J.M., 2011. Los micromamíferos del Pleistoceno superior de la Península Ibérica. Evolución de la diversidad taxonómica y cambios paleoambientales y paleoclimáticos. Ed. Académica Española, Saarbrücken.

López-García, J.M., Blain, H.A., Bennàsar, M., Fernández-García, M., 2014. Environmental and climatic context of neanderthal occupation in southwestern Europe during MIS3 inferred from the small-vertebrate assemblages. Quat. Int. 326–327, 319–328.

López-García, J.M., Cuenca-Bescós, G., 2010. Évolution climatique durant le Pléistocène Supérieur en Catalogne (nord-est de l'Espagne) d'après l'étude des micromammifères. Quaternaire 21, 249–258.

López-García, J.M., Soler, N., Maroto, J., Soler, J., Alcalde, G., Galobart, A., Bennàsar, M., Burjachs, F., 2015. Palaeoenvironmental and palaeoclimatic reconstruction of the Latest Pleistocene of L'Arbreda Cave (Serinyà, Girona, northeastern Iberia) inferred from the small-mammal (insectivore and rodent) assemblages. Palaeogeogr. Palaeoclimatol. Palaeoecol. 435, 244–253.

López García, J.M., Berto, C., Luzi, E., Dalla Valle, C., Bañuls Cardona, S., Sala, B., 2015. The genus *Iberomys* (Chaline,1972) (Rodentia, Arvicolinae, Mammalia) in the Pleistocene of Italy. Ital. J. Geosci. 134, 1–33.

Manzanares, A., 2012. Aves rapaces de la Península Ibérica, Baleares y Canarias. Ediciones Omega, Barcelona.

Maroto, J., Julià, R., López-García, J.M., Blain, H.-A., 2012a. Chronological and environmental context of the Middle Pleistocene human tooth from Mollet Cave (Serinyà, NE Iberian Peninsula). J. Hum. Evol. Evol. 62, 655–63.

Maroto, J., Soler, N., Fullola, J.M., 1996. Cultural change between Middle and Upper Paleolithic in Catalonia, in: Carbonell, E., Vaquero, M. (Eds.), The Last Neanderthals, the First Anatomically Modern Humans: Cultural Change and Human Evolution: The Crisis at 40 Ka BP. Gràfiques Lluc, pp. 219–250.

Maroto, J., Vaquero, M., Arrizabalaga, Á., Baena, J., Baquedano, E., Jordá, J., Julià, R., Montes, R., Van Der Plicht, J., Rasines, P., Wood, R., 2012b. Current issues in late Middle Palaeolithic chronology: New assessments from Northern Iberia. Quat. Int. 247, 15–25.

Mikkola, H., 1983. Owls of Europe. Buteo Books, Sussex.

Montuire, S., Navarro, N., Le, C., Langlois, C., Lécuyer, C., Montuire, S., Langlois, C., Martineau, F., 2004. Oxygen isotope compositions of phosphate from arvicoline teeth and Quaternary climatic changes, Gigny, French Jura. Quat. Res. 62, 172–182.

Norrdahl, K., Korpima, E., 2002. Seasonal changes in the numerical responses of predators to cyclic vole populations. Ecography 25, 428–438.

Orihuela-Torres, A., Perales, P., Rosado, D., Pérez-García, J.M., 2017. Feeding ecology of the Common Kestrel Falco tinnunculus in the south of Alicante (SE Spain). Rev. Catalana d'Ornitologia 33, 10–16.

Ros, M.T., 1987. Anàlisi antracològica de la cova de l'Arbreda. Cypsela VI, 67–71.

Royer, A., Lécuyer, C., Montuire, S., Amiot, R., Legendre, S., Cuenca-Bescós, G., Jeannet, M., Martineau, F., 2013a. What does the oxygen isotope composition of rodent teeth record? Earth Planet. Sci. Lett. 361, 258–271.

Royer, A., Lécuyer, C., Montuire, S., Escarguel, G., Fourel, F., Mann, A., Maureille, B., 2013b. Late Pleistocene (MIS 3-4) climate inferred from micromammal communities and $\delta^{18}O$ of rodents from Les Pradelles, France. Quat. Res. 80, 113–124.

Rufí, I., Solés, A., Soler, J., Soler, N., 2018. A mammoth (Mammuthus primigenius Blumenbach 1799, Proboscidea) calf tooth from the Mousterian of Arbreda Cave (Serinyà, NE Iberian Peninsula). Estud. Geológicos 74, e079.

Salamolard, M., Butet, A., Leroux, A., Bretagnolle, V., 2000. Responses of an avian predator to variations in prey density at a temperature latitude. Ecology 81, 2428–2441.

Sepulchre, P., Ramstein, G., Kageyama, M., Vanhaeren, M., Krinner, G., Sánchez-Goñi, M.F., d'Errico, F., 2007. H4 abrupt event and late Neanderthal presence in Iberia. Earth Planet. Sci. Lett. 258, 283–292.

Servei Meteorològic de Catalunya, 2018. Climatologies Comarcals & Anuari de dades meteorològiques.

Soler, J., Soler, N., Agustí, B., Bolus, M., 2013. The Gravettian calvaria from Mollet III cave (Serinyà, Northeastern Iberian Peninsula). J. Hum. Evol. 65, 322–329.

Soler, J., Soler, N., Solés, A., Niell, X., 2014. Arbreda cave from the Middle Paleolithic to the Neolithic, in: Sala, R. (Ed.) Los cazadores recolectores del Pleistoceno y del Holoceno en Iberia y el Estrecho de Gibraltar: Estado actual del conocimiento del registro arqueológico. Universidad de Burgos & Fundación Atapuerca, Burgos, pp. 266–276.

Soler, N., Soler, J., 2016. The first *Homo sapiens* in Catalonia, hunters and gatherers from the old Upper Palaeolithic. Catalan Historical Review 9, 9–23.

Souttou, K., Baziz, B., Doumandji, S., Denys, C., 2007. Prey selection in the common kestrel, *Falco tinnunculus* (Aves, Falconidae) in the Algiers suburbs (Algeria). Folia Zool. 56, 405–415.

Wood, R.E., Arrizabalaga, A., Camps, M., Fallon, S., Iriarte-Chiapusso, M.J., Jones, R., Maroto, J., De la Rasilla, M., Santamaría, D., Soler, J., Soler, N., Villaluenga, A., Higham, T.F.G., 2014. The chronology of the earliest Upper Palaeolithic in northern Iberia: New insights from L'Arbreda, Labeko Koba and La Viña. J. Hum. Evol. 69, 91–109.

Zilhão, J., 2000. The Ebro Frontier: A Model for the Late Extinction of Iberian Neanderthals, in: Stringer, C.B., Barton, R.N.E., Finlayson, C. (Eds.), Neanderthals on the Edge: 150th Anniversary Conference of the Forbes' Quarry Discovery, Gibraltar. Oxbow Books, Oxford, pp. 111–121.

Zilhao, J., D'Errico, F., 1999. The chronology and taphonomy of the earliest Aurignacian and its implications for the understanding of Neandertal extinction. J. World Prehistory 13, 1–68

Chapter 9.
General discussion

The preceding chapters have already presented brief discussions on the particular problems detected for each site or question. The aim of this chapter is to summarize and discuss cross-curricular problems observed in previous chapters through a holistic interpretation. In order to facilitate its reading as an independent chapter, brief explanations of results and questions previously addressed are included, but for broader interpretations readings of the preceding chapters are recommended. The discussion focuses on five aspects: 1) the implications that spatial and, especially, temporal factors have in the meaning of oxygen isotope compositions recorded by rodent teeth that mainly rely on predator-prey interactions; 2) a comparison of the methods employed in this thesis for palaeoclimatic reconstruction and a reflection on their implications and limits; 3) the environmental conditions estimated by oxygen isotope composition and other ecological methods during the MIS 3 in northeastern Iberia; 4) the singularities of northeastern Iberia as compared to Eurasian environmental conditions, and; 5) the implications that the defined palaeoenvironment have for Neanderthal populations.

1. Oxygen isotope meaning, predator-prey interactions, and seasonality

1.1. Oxygen isotope meaning

At mid and high-latitudes, mean annual values of oxygen isotope composition of meteoric waters ($\delta^{18}O_{mw}$) are linearly related to mean air temperatures at regional and global scales (Dansgaard, 1964; Rozanski et al., 1993). Thus, oxygen isotope compositions recorded from the phosphate of rodent teeth ($\delta^{18}O_p$), obtained by the animal through drinking meteoric waters, are expected to potentially reflect the air temperatures of its specific temporal and spatial context (D'Angela and Longinelli, 1990; Longinelli, 1984; Royer et al., 2013a). Unlike large mammals, whose $\delta^{18}O$ analyses are normally based on sequential sampling (e.g., Knockaert et al., 2018; Tornero et al., 2017), the small size of rodents' bones and teeth prevents to know the trend of $\delta^{18}O$ along a determinate temporal period for the same specimen. For rodents, combining different incisors is needed to obtain an approximate range and mean of $\delta^{18}O_p$ values (Gehler et al., 2012; Peneycad et al., 2019; Royer et al., 2013a). This could lead to the recording of important variability in $\delta^{18}O_p$ values that need to be decoded to obtain accurate environmental information. Several factors can influence variability in oxygen isotope compositions recorded from the phosphate of rodent teeth ($\delta^{18}O_p$), apart from air temperature and precipitation. These variations could appear between different species, but also within the same population in a small area or even in the individual itself (Barham et al., 2017; Gehler et al., 2012; Jeffrey et al., 2015; Peneycad et al., 2019; Royer et al., 2013a, 2014).

Intra-population variation in $\delta^{18}O_p$ obtained from present-day rodent teeth were reported (Barham et al., 2017; Gehler et al., 2012; Peneycad et al., 2019; Royer et al., 2013a). This variability can be mainly explained by spatial and temporal parameters of the $\delta^{18}O$ composition of the drinking water ingested by rodents within a population (Royer et al., 2013a). In the case of rodents recovered from pellets, this variability is intrinsically related to the specific place and moment of rodent specimen capture by the predator. The time period or season relative to $\delta^{18}O_p$ values of a particular specimen are one aspect that has only been preliminarily discussed in previous studies of $\delta^{18}O$ in small mammal body tissue (Lindars et al., 2001; Navarro et al., 2004; Peneycad et al., 2019; Royer et al., 2013b, 2014). Some of these studies (e.g., Peneycad et al., 2019) failed to not consider the exact season or month when these remains were accumulated. Although intra-population variations

are known with independence of the water ingested by the individuals (Barham et al., 2017), not considering the month of deposition has probably led to misunderstandings of the biochemical information provided by these teeth.

Understanding the time lapse measured from $\delta^{18}O$ of rodent teeth is essential to interpret the data in environmental terms. Rodents have incisors that grow continuously throughout the life of the individual (Hillson, 2005). The growth area, located in the basal part of the incisor, produces odontoblasts that form a dentine ring. The dentine ring moves continuously and gradually in the apical direction and compensates for the wear of the apical surface of the incisor (Klevezal et al., 1990). That the growth rate of the incisor varies between rodent species, mainly because of their size and body weight, must be considered. As explained in Chapter 5, it has generally been observed that the time of renewal of the lower incisors of voles extends between 30 and 60 days (Coady et al., 1967; Klevezal, 2010; Klevezal et al., 1990), whereas the lower incisors of the genus *Apodemus* extend around 50-60 days (Klevezal, 2010). If the growth time of lower incisors of the genus *Apodemus*, mainly used in this work, is around two months, it is expected that their incisors normally record $\delta^{18}O$ information around the individual's last two months of life.

Otherwise, temporal variations in $\delta^{18}O_p$ are expected, considering the annual fluctuations of $\delta^{18}O$ of meteoric waters that a rodent will acquire through drinking or eating. These fluctuations are mainly related to seasonal variations in air temperatures and precipitation throughout the year (Dansgaard, 1964; Rozanski et al., 1993). During the warm season, an enrichment in $\delta^{18}O_{mw}$ is usually recorded (Bowen, 2017). Surprisingly, results obtained through isotope oxygen analyses presented in this work, both from modern samples coming from pellets and Late Pleistocene samples recovered in archaeo-palaeontological sites, show little and medium ranges of $\delta^{18}O_p$ (1.4-7.6‰), equivalent to restricted ranges of $\delta^{18}O_{mw}$ (1.1-6.3‰), that can provide some insights for these considerations from the past (Fig. 9.1A). The variability of Iberian oxygen isotope compositions is extensively explained in Chapter 5 and in the specific chapters on each site (Chapters 5-8). In summary, for all analyzed samples, modern or fossil, recorded values are within the present-day annual variability of $\delta^{18}O_{mw}$. Moreover, when intra-level or intra-site ranges of $\delta^{18}O_{mw}$ values are considered, the ranges are always lower than the annual $\delta^{18}O_{mw}$ amplitudes recorded in present-day in their specific area of recovery. They are also lower than the current annual amplitude of $\delta^{18}O_{mw}$ values estimated in the Iberian Peninsula (between 7 and 9‰ depending on location; OIPC data from Bowen (2017)). Based on the OIPC information, it seems that oxygen isotope compositions presented in this work reproduced variability of $\delta^{18}O_{mw}$ from a period shorter than the variability expected for a year (Fig. 9.1B). Furthermore, the recorded fossil mean and median $\delta^{18}O_{mw}$ values for each sedimentary unit are higher with respect to current annual $\delta^{18}O_{mw}$ means in the recovery localities (between +0.5‰ to +2‰), except in level G from Arbreda cave.

Yet why are sedimentary units analyzed in this research so homogeneous? Among oxygen isotope analyses developed from fossil samples here, wood mouse (*Apodemus sylvaticus*) lower incisors were preferentially selected whenever possible to avoid interspecific variability. The oxygen isotope composition of body water is species-dependent, being controlled by both input and output oxygen fluxes as well as physiological

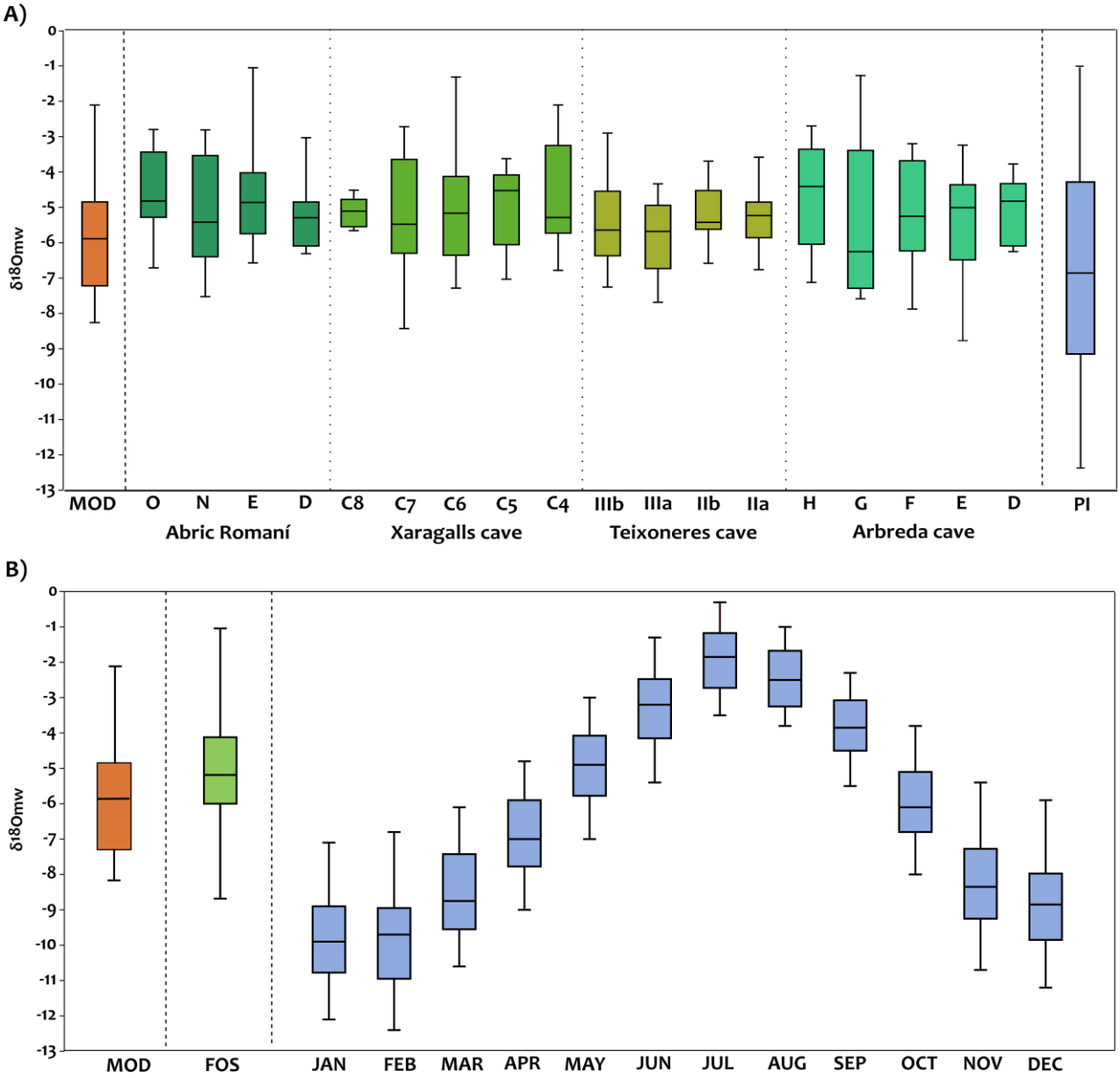

Figure 9.1 Oxygen isotope composition of meteoric waters ($\delta^{18}O_{mw}$; ‰ V-SMOW) represented in box plots, comparing $\delta^{18}O_{mw}$ estimated from the oxygen isotope composition of phosphate from present-day Iberian rodent teeth (MOD; orange box plots in (A) and (B)) and from rodent incisors coming from fossil deposits analyzed in this thesis (FOS; green box plots in (A), summarized in (B)) and $\delta^{18}O_{mw}$ of localities where analyses were performed (PI; blue box plots by months in (B), summarized in (A)) obtained from OIPC data (Bowen, 2017). Box plots' bars cover the full extension of the values; the boxes extend from the 1st to 3rd quartile and median is indicated by the black line.

factors such as basal metabolic rate and body temperature (Lindars et al., 2001; Longinelli, 1984; Luz et al., 1984; Podlesak et al., 2008). Thus, it is possible that some diet habits or physiology of the wood mouse species might generate an alteration of $\delta^{18}O$ values with respect to other species that could bias the results, as was observed by Royer et al. (2013b) in the water vole (*Arvicola sapidus*). Nevertheless, species other than *A. sylvaticus* have been included in some sedimentary units (such as *Eliomys quercinus* and *Microtus arvalis*). These species reported $\delta^{18}O_p$ values that appear well-integrated within samples of Murinae and have no influence on either mean or median $\delta^{18}O_p$ values

(Chapters 5-8). In Arbreda cave the lower abundances of murine remains necessitated the inclusion of many vole incisors of different species (such as *Microtus agrestis, Microtus arvalis* and *Microtus (Terricola) duodecimcostatus*). Differences between 1-2‰ are detected in some levels' average estimations if Murinae and Arvicolinae are analyzed separately, as is discussed in chapter 8 (see Fig. 8.4 in this chapter). However, none directional trend is detected between both subfamilies $\delta^{18}O_p$ signatures, allowing to tentatively reject enrichment or depletion in $\delta^{18}O_p$ values as consequence of physiology or dietary habits of the wood mouse.

1.2. Predator-prey interactions and seasonality

Under the principle of actualism, ethological and physiological studies of the biological entities involved (predator and prey) shed some light. It is not simple to make assumptions of predator-prey interactions in the past due to a constant coevolution that occurs between prey, which develop adaptive strategies to avoid being hunted, and predators, which improve their hunting efficiency (Lagos, 2019; Sundell et al., 2004). Owls are mainly responsible for small mammal inputs in fossil deposits (e.g., Andrews, 1990; Denys and Patou-Mathis, 2004; Desclaux et al., 2011; Fernández-Jalvo et al., 2016). Indeed, in the Pleistocene sequences analyzed in this work and in previous studies, accumulation mainly by nocturnal birds of prey has been confirmed: the little owl (*Athene noctua*) in Xaragalls cave, the tawny owl (*Strix aluco*) in Abric Romaní rock-shelter, and the eagle owl (*Bubo bubo*) in Teixoneres cave (Chapters 4-8; López-García et al., 2015, 2012a). The only exception is that accumulation at some levels of Arbreda cave were attributed to the common kestrel (*Falco tinnunculus*) (López-García et al., 2015). Modern samples analyzed in this work were extracted from barn owl (*Tyto alba*) and tawny owl pellets.

The breeding season of these owl species in present-day Iberia extends between spring and early summer (IUCN, 2018; Manzanares, 2012). The breeding season of many species of avian predators is highly dependent on the abundance of small mammals because many of them are small mammal specialists, dependent on the availability of these prey for survival and especially for breeding success (Mikkola, 1983; Norrdahl and Korpima, 2002; Sundell et al., 2004). When small mammal populations decline locally to low numbers, migratory avian predators specializing in small mammals may seek better hunting grounds, while resident predators respond primarily by altering their breeding efforts. Resident avian predators may even skip breeding if densities of small mammals are very low (Mikkola, 1983; Sundell et al., 2004). Indeed, some studies at mid and high latitudes have demonstrated that raptor populations show seasonal numerical responses (breeding, density, natality, and migration) to spring-summer rodent abundances (Norrdahl and Korpima, 2002; Salamolard et al., 2000; Sundell et al., 2004). Thus, this phase is the optimal period of predator hunting activities and therefore the probability of catchments by owls is high during spring-summer.

In this line of argument, rodent species globally engage in greater outdoor activity from spring to fall during winter and populations increase during spring-summer (Le Louarn and Quéré, 2003; Sundell et al., 2004). In higher latitudes, the wood mouse reproduces between spring and summer and ceases this activity in winter. On the contrary, in Mediterranean areas (such as northeastern and southern Spain, Corsica, or North Africa) and areas with Mediterranean climate influence (such as Portugal), reproductive activity is reversed,

starting in autumn and ending in spring, with summer always being the rest period (Fons and Saint Girons, 1993; Moreno and Kufner, 1988; Rosário and Mathias, 2004; Sans-Coma and Gosalbez, 1976; Sunyer et al., 2016). The main factor influencing population demography is reproduction, and usually the highest densities are produced before the non-reproductive period. Therefore, the displacement of the wood mouse's reproductive activity in Iberia implies a displacement of population densities with respect to the European trend: advancing the highest abundances in spring, being at higher latitudes between summer and autumn (Rosário and Mathias, 2004; Sans-Coma and Gosalbez, 1976). The great variability in the reproductive cycles of *A. sylvaticus* is related to its capacity for adaptation, as it adopts a strategic response according to the availability of food, which is in turn related to climatic and environmental conditions in each region (Fons and Saint Girons, 1993). In Mediterranean areas, hot and arid summers, even with drought episodes, may be a time of stress for this species, highly reducing its survival success (Moreno and Kufner, 1988; Rosário and Mathias, 2004).

Therefore, according to current ethological information, the highest abundances of rodents and the optimal period for owl hunting could correspond to the spring and early summer months. Considering the low variability recorded by $\delta^{18}O$ in each sedimentary unit, never surpassing the current annual $\delta^{18}O_{mw}$ variability and higher mean $\delta^{18}O_{mw}$ than present-day within each location, the most plausible hypothesis points to a preferential accumulation period by owls around the spring and early summer months. These months will be recorded by $\delta^{18}O_p$ from rodent incisors with higher probability than other extreme seasons, such as midsummer or midwinter. Thus, in archaeological and palaeontological sites, where contexts of palimpsests occur, a detailed evaluation of $\delta^{18}O_p$ values inside each level (intra-level) and between levels of a specific site (inter-level) is essential for reaching reliable interpretations in order to differentiate whether variations are mainly related to seasonal changes derived from predator behaviors or to climatic instability (Royer et al., 2014, 2013b) (Fig. 9.1A). Really low amplitudes ($\delta^{18}O_p$<4‰ ≈ $\delta^{18}O_{mw}$<3‰), as suggested by Royer et al. (2014, 2013b), can easily confirm preferential accumulation of samples related to predator inputs during a time shorter than a year, that according to previous discussion could most likely correspond to spring-early summer. From the analyzed series, only layer C8 of Xaragalls cave fits well with this scenario. On the contrary, high amplitudes surpassing the current annual range of $\delta^{18}O_{mw}$ variation (above 8‰ in Iberian locations included in these analyses) could indicate a higher annual amplitude of $\delta^{18}O_{mw}$ in the past. In this scenario, it is probable that values throughout the year have been recorded from frequent predator contributions and, thus, median $\delta^{18}O$ values can be easily related to mean annual $\delta^{18}O$ values. In addition, $\delta^{18}O_{mw}$ outside of the current annual variability could suggest some climatic instability, either related to cold or aridity (Jeffrey et al., 2015; Royer et al., 2013b). None of the assemblages analyzed in this work fit with this situation.

More problematic are medium $\delta^{18}O$ ranges, which occurred in most of the Late Pleistocene assemblages analyzed in this work. Two interpretative hypotheses are possible: 1) variations in the seasonality patterns of the predator were recorded, and the possibility of recording $\delta^{18}O_p$ values produced during different parts of the year cannot be rejected, obscuring the differentiation of changes related to the environment; or, 2) there is a preferential period of accumulation and, therefore, $\delta^{18}O_p$ values are

mainly accumulated by the predator in a specific season; if inter-level variations occurred this could lead to the detection of inter-annual climate instability. It is complex to deal with this differentiation, but some advice can be followed. Throughout the $\delta^{18}O$ results obtained in the Late Pleistocene sequences, it has been observed that median values are normally more informative than means and allow the effect of extreme values in a given assemblage to be minimized. In addition, ranges and standard deviations, as measurements by which to consider the internal variability of $\delta^{18}O$, seem to be a more powerful tool for determining accumulation type than a simple translation of median $\delta^{18}O$ from phosphate values to air temperatures. Preliminarily, the combination of medians and ranges may give us clues about the greater or lesser climatic stability of a certain fossil deposit.

In this work, different tendencies are observed among the sedimentary units analyzed using oxygen isotope studies. Two main types of deposits can be distinguished from the point of view of the intra-level variability of $^{18}O_p$ values: more heterogeneous levels with greater amplitudes (>4‰) and more homogeneous levels with reduced ranges (<4‰). Among the most heterogeneous levels (>6‰), sedimentary units with relatively low medians are detected (<18.5‰), with the most singular case being level G of Arbreda cave (ARB-G) and, to a lesser extent, layers C6 and C7 of Xaragalls cave (CX-C6; CX-C7). Other levels with medium ranges (6-4‰) also show relatively low medians, such as subunit IIIb of Teixoneres cave (TX-IIIb), level N of Abric Romaní (AR-N) and TX-IIIa. On the contrary, among the homogenous levels (range>4‰), some presented relatively high medians (>18.5‰), such as CX-C5, CX-C8, ARB-D and TX-IIa. These situations have been considered significant in the internal analysis of the sequences, however from a global perspective the observed variability is quite reduced. Here, it has been useful to compare $\delta^{18}O_{mw}$ obtained in a specific fossil assemblage with the present-day annual $\delta^{18}O_{mw}$ variability of the location where the samples were produced. As was previously explained, all levels recorded lower ranges of $\delta^{18}O_{mw}$ than annual $\delta^{18}O_{mw}$ variability and higher median $\delta^{18}O_{mw}$ values than present-day in each location of recovery, suggesting preferential accumulation in all the fossil deposits and in some cases attributing this variation of $\delta^{18}O$ ranges to changes in climatic conditions.

Indeed, it is necessary to consider the dataset in its entirety and adapt to the characteristics of each level. Only with a detailed observation of intra-level and inter-level variations, will it be possible to detect singular data. As has been described, rodents will register a relatively short period of time, shorter than a season, and there is enough evidence to hypothesize about a preferential accumulation and subsequent $\delta^{18}O$ values preferably related to spring-summer months. However, that does not exclude that we could occasionally have obtained specimens predated in the other seasons. There are some values that surpass the common range of $\delta^{18}O_p$ values, showing very high $\delta^{18}O_p$ values (>22‰) that appear isolated, in CX-C4 (22.2‰), CX-C6 (23.2‰), AR-E (23.5‰) and ARB-G (23.2‰). These values surpass any $\delta^{18}O_p$ signature previously recorded in current samples on rodent teeth (Royer et al., 2013a). Only *Arvicola sapidus* present-day rodent teeth of Almaraleja (South Portugal) present comparable signatures. If these values are transformed to $\delta^{18}O_{mw}$ and compared with annual $\delta^{18}O_{mw}$ variability in their recovery localities, they might correspond to summer values. Thus, the simplest explanation is that they are remains recorded out of the main season of accumulation of the assemblage, or that they could be related to water ^{18}O enrichment due to arid events (Jeffrey et al.,

2015; Royer et al., 2013b). If we transform these values in temperature through the Iberian equation proposed in this work (Chapter 5), without applying a seasonality correction, a value between 23 °C and 25 °C is obtained. Those summer temperatures would be higher than current summer temperatures in any of the recovery sites (Climate-Data.org, 2018).

By contrast, low and isolated $\delta^{18}O_p$ values such as those from levels CX-C7 (14.6‰), ARB-E (14.2‰) and ARB-F (15.3‰) could be related to the predation of specimens in the cold season. If these values are transformed to $\delta^{18}O_{mw}$ and compared with annual $\delta^{18}O_{mw}$ variability in their recovery localities, they might correspond to present-day winter values. Thus, the most parsimonious interpretation for these minimal $\delta^{18}O_p$ values (<15.5‰) is that they reflect specimens accumulated in the cold season, because they appear isolated from the rest of the $\delta^{18}O_p$ values of their sedimentary unit. Alternatively, they might correspond to an exceptionally cold spring, keeping in mind that the temperature estimates can be biased by the presence of different sources of ingested waters, such as snow melting during the spring season (Royer et al., 2013b). If we transform these values into temperatures, values between 6 °C and 8 °C are obtained, which are lower than current winter temperatures in both Arbreda cave and Xaragalls cave (Climate-Data.org, 2018). Other low $\delta^{18}O_p$ values are recorded in CX-C6, AR-N, TX-IIIa, TX-IIIb and, especially, ARB-G, but they are only slightly isolated from the variability of the rodent samples of their sedimentary unit. From a global view, these values are suspected to be related to cooler springs. However, the different altitudes at which the predator could have been hunting might also explain some of this variation. Each individual in a population will consume meteoric water coming from different sources, which would present small changes in their $\delta^{18}O$ values related to different degrees of evaporative enrichment (Peneycad et al., 2019; Royer et al., 2013a). $\delta^{18}O_{mw}$ values tend to decrease when altitude increases, as a consequence of the gradual removal of moisture from uplifted air masses with a preferential removal of the heavy isotope ^{18}O during condensation (Dansgaard, 1964; Rozanski et al., 1993). Thus, the capture of rodents from different localities would lead to differences in $\delta^{18}O_p$ values being recorded from the incisors of these individuals. Considering the altitude (between 206 and 760 m a.s.l.) and the orography of the study sites, which are surrounded by a mountainous environment with highly variable altitudes at a kilometre scale, the different altitude ranges at which the predator may have been hunting could also explain a some of this variation. Indeed, this problem was suggested for some of the pellet samples analyzed in this work (Chapter 5).

2. Methods for palaeotemperature and palaeoprecipitation reconstructions from rodent assemblages

The qualitative analysis of faunal communities to establish environmental inferences is extended between palaeontological and palaeecological works that focused on small mammals (e.g, Bañuls Cardona et al., 2012; Cuenca-Bescós et al., 2009; Garcia-Ibaibarriaga et al., 2015; López-García, 2011; among many other). Changes in the species spectra recovered from each sedimentary unit are usually employed to infer climatic and environmental shifts (e.g., Chaline, 2005; Cuenca-Bescós et al., 2010, 2016; Sesé, 1994). A wide range of qualitative and quantitative methods are used to detect environmental trends through species classifications according to chorotypes (López et al., 2006; Sans-Fuentes and Ventura, 2000), preferred species habitat (Cuenca-Bescós et al.,

2005, 2009), or the weighted habitat method (Andrews, 2006; Evans et al., 1981; López-García et al., 2010). When the aim is the quantification of these environmental changes in climatic terms, tools to transform qualitative data into standard metadata (such as temperatures or precipitation) are required and allow easier comparisons between fossil deposits and present-day climatic conditions. Several methods can be employed for the estimation of past climatic parameters, such as the mean annual temperature (MAT) and the mean annual precipitation (MAP). In combination with $\delta^{18}O$ analyses, this work has focused on two methods commonly used in Iberia for reconstructed MATs and MAPs with small-mammal assemblages: the bioclimatic model (BM) (Hernández Fernández, 2001; Hernández Fernández et al., 2007) and the mutual ecogeographic range (MER) (Blain et al., 2009, 2016; López-García, 2011).

The three methods are applied to most of the small-mammal sedimentary units of the four Late Pleistocene sequences analyzed (Xaragalls, Arbreda, Abric Romaní and Teixoneres) and agreement between methods is highly variable (Table 9.1). Different situations are observed: 1) Xaragalls cave presents reasonably similar climatic signals among the three methods, with lower MATs on layers C7-C6 and C4 and higher on layers C8 and C5. However an offset of a few degrees is observed between methods; with respect $\delta^{18}O$ calculations, BM results are overestimated (between +0.5 and +4.7 °C) and MER results underestimated (between -1.6 and –4 °C); 2) In Arbreda cave there is also global agreement among the methods in the estimation of cooler palaeotemperatures than present-day for all levels and comparable climatic evolution; however, offsets are notable between methods (from -5.4 to + 1.6 °C); 3) In Abric Romaní, the three methods show lower MATs than present-day, but the magnitude of differences can vary between 2.2 and 3 °C depending on the method considered. Whereas there is an agreement in MER and BM methods on the climatic trend along the sequence, $\delta^{18}O$ estimations follow the opposite pattern, but provide intermediate degrees between BM and MER proxies; 4) In Teixoneres cave, $\delta^{18}O$ estimations also acquire an intermediate position between both methods, recording lower MATs in agreement with MER temperatures reconstruction and similar climatic trend, but with an import lag (+1.4/+3.7 °C). On the contrary, BM method present some discrepancies, showing MATs to be comparable to present-day temperatures for unit III, and the opposite trend as compared to MER and $\delta^{18}O$ estimations.

Despite these differences among sites, some patterns can be observed among the sedimentary units analyzed using the three methods. MATs of these sequences, when estimated by $\delta^{18}O$, fluctuated between 9.3 °C and 13.8 °C. If MATs are considered in relation to present-day data, temperatures are lower than today (-5.5 °C to -0.5 °C). This excludes layer C5 of Xaragalls cave, which presents air temperatures comparable to present-day in the site region. Results using the MER method are in agreement with previously reported colder conditions and mostly provide the lowest MATs estimations (from -6.4 °C in ARB-H cave to -2.6 °C in AR-N), whereas BM frequently reports colder temperatures (from -5 °C in ARB-H to -0.3 °C in AR-N), though it sometimes reports MATs higher than present-day (TX-IIIa, TX-IIIb, CX-C5 and CX-C8). Thus, MER estimations on MAT are usually underestimated with respect $\delta^{18}O$ calculations (-4.4 °C to –0.6 °C, except for AR-N and AR-D), where the BM method, with some exceptions, tends to overestimate temperatures (-4 °C to +4.7 °C). Frequently, estimations based on oxygen isotope compositions tend to occupy an intermediate position between both methods, although they

		BM	Difference	MER	Difference	$\delta^{18}O$	Difference	Present-day
Xaragalls cave	C4	12.2	-1.4	8.0	-5.6	11.7	-1.9	13.6
	C5	16.2	2.6	10.4	-3.2	13.6	0.0	
	C6	12.7	-0.9	8.0	-5.6	12.0	-1.6	
	C7	12.9	-0.7	8.7	-4.9	11.2	-2.4	
	C8	16.8	3.2	10.5	-3.1	12.1	-1.5	
Arbreda cave	D	10.6	-4.2	8.4	-6.4	12.8	-2.0	14.8
	E	11.0	-3.8	10.1	-4.7	12.4	-2.4	
	F	12.8	-2.0	10.0	-4.8	11.8	-3.0	
	G	10.9	-3.9	8.7	-6.1	9.3	-5.5	
	H	9.8	-5.0	8.4	-6.4	13.8	-1.0	
Abric Romaní rockshelter	D	14.3	-0.5	11.6	-3.2	11.6	-3.2	14.8
	E	12.7	-2.1	9.7	-5.1	12.7	-2.1	
	N	14.5	-0.3	12.2	-2.6	11.3	-3.5	
	O	13.3	-1.5	11.1	-3.7	12.8	-2.0	
Teixoneres cave	IIA	11.3	-1.0	9.0	-3.3	11.8	-0.5	12.3
	IIB	11.5	-0.8	8.8	-3.5	11.3	-1.0	
	IIIA	12.4	0.1	7.0	-5.3	10.7	-1.6	
	IIIB	13.4	1.1	9.4	-2.9	10.8	-1.5	

Table 9.1 Mean annual temperature (MAT; expressed in ºC) estimations obtained in the sedimentary units analyzed in this thesis using three different methods: the Bioclimatic Model (BM), the Mutual Ecogeographical Range (MER) and oxygen isotope compositions ($\delta^{18}O$). Next to each estimation, the relative MAT with respect present-day data provided by Climate-Data.org (2018). The range of colors goes from light to dark in relation to the values of MAT obtained with each approach, from low to high.

		BM	Difference	MER	Difference	Present-day	BM vs. MER
Arbreda cave	D	763	30	950	217	733	-187
	E	1053	320	714	-19		339
	F	1030	297	1200	467		-170
	G	849	116	967	234		-118
	H	991	258	950	217		41
Abric Romaní rockshelter	D	824	205	606	-13	619	218
	E	791	172	760	141		31
	N	550	-69	615	-4		-65
	O	799	180	871	252		-72
Teixoneres cave	IIA	1431	682	981	232	749	450
	IIB	927	178	950	201		-23
	IIIA	793	44	925	176		-132
	IIIB	1286	537	840	91		446

Table 9.2 Mean annual precipitation (MAP; expressed in mm) estimations obtained in the sedimentary units analyzed in this thesis using the Bioclimatic Model (BM) and the Mutual Ecogeographical Range (MER). Next to each estimation, the relative MAP with respect to present-day data provided by Climate-Data.org (2018). The range of colors goes from light to dark in relation to the values of MAP obtained with each approach, from low to high. On the right is the offset between both methods.

are occasionally in agreement with some estimations either of BM (e.g. AR-E) or MER (e.g. AR-D) methods. In most cases, MER and BM offsets remain small enough to fall within the margin of error in $\delta^{18}O$ estimations. These offsets and high variability are also observed between mean annual precipitations (MAP) estimated by MER and BM methods, but not do not follow a clear pattern in this case (Table 9.2). However, both agree in the definition of MAPs globally higher than nowadays, considering BM between +682 mm and -69 mm and, according to MER, between +467 mm and -19 mm.

The discrepancies between relative abundances of small mammals, climatic estimations done by MER and BM and $\delta^{18}O$ analysis observed in the Late Pleistocene sequences analyzed can be explained by several factors (Table 9.3). Firstly, the different nature of the data should be considered. MER and BM methods are based on the actualism principle, which assumes that present-day species ecological requirements are equivalent to those of the past. They are also qualitative methods, and thus rely on the occurrence of species independent of their relative abundance (Blain et al., 2009, 2016; Hernández Fernández, 2001; Hernández Fernández et al., 2007). The presence or absence of a single species in MER and BM can highly alter the final palaeotemperature estimation. This risk increases when faunal assemblages are fragmentary or poor in remains, as in Abric Romaní assemblages. As an example, the relatively lower MATs recorded by BM and MER methods in levelsO and E on this site are mainly affected by the presence of vole species *Chionomys nivalis* and *Microtus arvalis*, respectively. Level E has the same species as level D, but a single *Chionomys nivalis* remain produced a MAT change of -1.6 °C using BM and -1.9 °C using MER (see Fig. 6.6 in Chapter 6). The same occurs between the association of levels N and O, the only qualitative difference being the presence of *Microtus arvalis* in level O which resulted in a change of -1.2 °C.

Both methods rely on present-day species distributions in the interpretation of the fossil fauna association, in the case of MER is considered where current distribution of recovered species in a given sedimentary unit intersected nowadays. But is possible that these species associations did not occur equally in the past (Lyman, 2017). Though some species are extensively known to have fragmented current distribution due to anthropic factors and are usually excluded from MER, such as *Iberomys cabrerae* (e.g. in Bañuls Cardona et al., 2012; Fernández-García et al., 2018; López-García, 2011), it is not easy to calibrate the effects that anthropic pressure can have on the current species distributions. Some limiting parameters could be urban development or human impact on landscape, or even predation or competition with other species (Blain et al., 2016; López-García et al., 2012a; Lyman, 2017). Thus, environmental factors will probably not be the unique aspect that determined the preferred habitat of extant small-mammal species. Moreover, some species with mid-European requirements in present-day Iberia inhabit very restricted areas, such as *Chionomys nivalis* or *Microtus (Terricola) gerbei* (Blanco, 1998; Palomo et al., 2007). When this kind of species occurs in a given assemblage and the MER method is applied, the areas of intersection tend to be limited to few points spread mainly in the highlands. These methods rarely consider the margins of error associated with estimations and usually only standard deviation is provided. For example, considering the MER method, levels E and O presented the fewest intersection points (5 and 7 respectively, compared to 110 for level D and 166 for level N), with a subsequently higher margin of error (3.2 °C and 1.8 °C, respectively, as opposed to 0.3 °C in levels D and N). In that case, the standard

deviations of oxygen isotope calculations are always lower ($\delta^{18}O_p$=1.2-2‰; MAT=1.3-1.5 ºC) than those from MER (1.6-2.6 ºC).

Thus, oxygen isotopic analysis gives us the opportunity to discuss if, from a geochemical point of view, these estimations are supported. This method allows us to obtain quantifiable parameters based in the geochemical properties of vertebrate tissues, which are less susceptible to taphonomic and archaeological biases that may occur. However, a wide-range of elections that the research must consider could also affect the final results. As has been explained (Chapter 5), the estimations of palaeotemperatures require at least two steps of calculations that involve two linear equations: 1) transformation of $^{18}O_p$ values into $^{18}O_{mw}$ and, 2) transformation of $^{18}O_{mw}$ into air temperatures. The selected regression for both steps and the interference of these two equations (each with its intercept, correlation line, and associated error) can highly affect final reconstructions of temperatures (Pryor et al., 2014). These relationships rely also on the actualism principle, assuming that they are also valid for the past. Through present-day observations, several equations have been developed for both steps. Indeed, during MIS 3, the variation in the ice volume supposed that the sea level was around 50 m below the present-day sea level and may have contributed to a change in the $\delta^{18}O_{mw}$ around the +0.6‰, resulting in a bias of calculated air temperatures of +1 ºC (Schrag et al., 2002). It is known that the relation between $^{18}O_p$ and $^{18}O_{mw}$ is species-dependent, mainly related to the origin of water inputs and physiological aspects (Lindars et al., 2001; Longinelli, 1984; Luz et al., 1984; Podlesak et al., 2008). Thus, for step (1) different regression equations are available, mainly based on phosphates, that differed in the taxonomic group (from mammal class to family level) and body tissues (bones and teeth together or exclusively teeth) considered (e.g. for rodents, D'Angela and Longinelli, 1990; Lindars et al., 2001; Luz and Kolodny, 1985; Navarro et al., 2004). This work has selected the linear oxygen fractionation equation of Royer et al. (2013a) due to the large dataset focused on tooth remains of extant species in Iberia that was used. Moreover, variability in the $^{18}O_p$ results has tried to be reduce under decisions as employed same skeleton elements (lower incisors) and same species (*A. sylvaticus*), whenever it was possible.

Regarding step (2), several linear equations are also available that varied mainly according to geographical scale or time scale of the data-set considered (e.g. Bernard et al., 2009; García-Alix, 2015; Lécuyer, 2014; Pryor et al., 2014; Rozanski et al., 1993; von Grafenstein et al., 1996), which can result in sizable differences in the estimations for air temperatures when applied to specific regions such as the Iberian Peninsula. Previous studies similar to this one (Navarro et al., 2004; Royer et al., 2013a, 2014) recommended von Grafenstein et al. (1996) for mean annual air temperature estimations ($\delta^{18}O_{mw}$ = 0.58(±0.11) T – 14.48) and Bernard et al., (2009) for summer mean air temperature calculations (T = 1.06(±0.07) $\delta^{18}O_{mw}$ + 24.1(±0.7). These equations are not applicable to our results, due to higher mean annual air temperatures or notably colder summer mean summer temperatures than nowadays would be obtained in present-day. In order to avoid these problems, this thesis has adapted methodological proceedings specifically to the context of our samples, as detailed in Chapter 5. This protocol proposed two solutions for calculating mean annual temperatures: 1) a specific $\delta^{18}O_{mw}/T_{air}$ regression equation designed for the Iberian environmental context according to monthly climatic data-sets provided by IAEA/WMO stations; 2) and a regression equation that relates the March-June $\delta^{18}O_{mw}$ to the mean annual $\delta^{18}O_{mw}$ in

order to correct the seasonal bias recorded in rodent tooth apatite resulting from the probable preferential accumulation of rodent remains in the warm season. Sea level correction (+0.6‰) is also considered in MAT estimations.

In parallel, some previous work on small mammals has indicated a complex relationship between $\delta^{18}O$ and moisture. In northwestern Africa, the $\delta^{18}O$ of gerbil tooth apatite is strongly correlated with mean annual precipitation (MAP) below 600 mm, but above 600 mm the teeth reflect the oxygen isotope composition of local meteoric water instead (Jeffrey et al., 2015); whereas in western France at a site contemporaneous with MIS 3, Les Pradelles, $\delta^{18}O_p$ enrichments are related to aridity events (Royer et al., 2014). Thus, influential changes in precipitation regimes along the sequence can have consequences. Some sites analyzed in this work might demonstrate a relationship with pluviometric changes. In Abric Romaní, slight increases of temperatures in level E and O, based on $\delta^{18}O$ estimations, are coincident with moments of higher precipitations, whereas the lowest MATs were recorded in the driest phases, levels D and N (Table 9.2). This fact allows us to hypothesize about the influence that changes in pluviometry range could have on reported $\delta^{18}O$ values, but the magnitude of these precipitation changes seems weak and the pattern of association unclear.

	Mutual Ecogeographic Range & Bioclimatic Model	**Oxygen isotope compositions**
Actualistic assumptions	Assume that present-day distribution and/or climatic requirements of taxa can be extrapoled to the past	Assumes that the present-day relationship between $\delta^{18}O_p$-$\delta^{18}O_{mw}$-MAT was the same past
	Current anthropic pressures in extant species distribution is difficult to control	Regression equation selected to transform $\delta^{18}O_P$ into $\delta^{18}O_{mw}$ and $\delta^{18}O_{mw}$ into MAT will influcence the climatic estimations
Sampling	Fragmentary and poor assemblages will not reflected the complete faunal spectra	The exact point where the samples are taken, the number of samples and the taxa selected will influence the results
Taphonomy	Bias derived from predator hunting preferences can affect final species representation	Seasonality of predator contributions is need for faithfull interpretation of data
	Bias derived from predator or post-depositional alterations can affect final species spectra	Predator chemical action and other diagenetic agents can alterated the phosphate preservation
Archae-palaeontological palimpsets	Stadial-interstadial fluctuations can produce mixed faunal assemblages between cold- or hot-dependent species accumulated in different periods	Stadial-interstadial fluctuations can provide different $\delta^{18}O$ signals if samples are produced in different climatic episodes
Other	Margin errors are rarely considered in these estimations	Amount of precipitation can have a uncontrolled influence on the $\delta^{18}O$ signal

Table 9.3 Summary of main limitations of methods of palaeotemperature estimations that should be considered in the final environmental interpretation of a given archaeo-palaeontological assemblage.

Nevertheless, a fossil always has a taphonomic history that will affect its characteristics either in preservation or in ecological terms. For this reason, taphonomic analyses should be considered for any of the three methods used. In the case of BM and MER methods, the primary hypothesis for explaining inconsistencies should rely on possible bias in small-mammal species composition inflicted by predators in some levels as a consequence of their hunting preferences (see Andrews, 2006, 1990; Fernández-Jalvo et al., 2016; Scott et al., 1996). As has been previously explained, the presence or absence of a single taxon can have big influences in the final estimations from these methods. Thus, these methods could be especially sensitive to effects that small-mammal predators can inflict on the final faunal spectra, producing the absence of prey not located in its preferential hunting environments. In this sense, identification of the main predator of the accumulation, besides species diversity and richness, can be helpful to also reveal if the accumulator is an opportunist predator, which can help draw a complete ecological picture. Indeed, high species diversity, and digestion patterns of remains that are commonly associated with owls, are found in most of the sedimentary units analyzed in this thesis. It was suggested a accumulation by predators with opportunist habits (*Strix aluco, Bubo bubo, Athene noctua*), which draw a complete ecological picture (Andrews, 1990; Fernández-Jalvo et al., 2016). However, caution is recommended in levels E-H of Arbreda cave, related to accumulation by *Falco tinnunculus*. The main predator can also have consequences that should be considered using oxygen isotope analysis on small mammals. As explained in the first section of this chapter, the seasonality of predator inputs and even the different altitudes at which the predator may have been hunting can affect the final interpretation of $\delta^{18}O$ amplitudes in a given assemblage. Moreover, unknown diagenetic processes or chemical alteration during predator digestion can affect the conservation of $\delta^{18}O$ in the enamel of rodent teeth (Barham et al., 2017; Blake et al., 1997; Zazzo et al., 2004).

The palimpsest conditions inherent in archaeological levels, and stadial and interstadial fluctuations experienced during MIS 3, do not allow for the rejection of stadial-interstadial scenarios. These can lead to contradictory results either to BM and MER methods due to mixed faunal assemblages coming from different environmental conditions (Andrews, 2006; Lyman, 1994), or in oxygen isotopes compositions conditionate by different time lapse record on exact point of sampling. A pool of rodent teeth records a short period of time but is accumulated over an unknown number of years. Consequently, in the case of high inter-annual climatic variability, isotopic variability and mean can be difficult to interpret (Royer et al., 2013b). This was suggested as an explanation for level N of the Abric Romaní site, with a higher $\delta^{18}O$ amplitude and a lower median $\delta^{18}O$ value than other levels of the sequence, whereas BM and MER methods, in addition to anthracological and palynological studies, indicated interstadial conditions (Burjachs et al., 2012; Burjachs and Julià, 1994, 1996; Vaquero et al., 2013). Discrepancies between disciplines and methods led to the consideration of this possibility for unit III of Teixoneres as well. In addition, the sampling criteria can alter results, such as the exact point where samples are taken and how many specimens are included from each assemblage. Taking into account previous research (Gehler et al., 2012; Lindars et al., 2001; Navarro et al., 2004; Royer et al., 2013a), a minimum of four to ten teeth were selected from each sedimentary unit in order to gather a representative range of samples. The minimum number of samples needed to obtain an accurate

population mean $\delta^{18}O$ at ≥90% confidence has recently been confirmed by Peneycad et al. (2019), who recommend ≥7 teeth. Moreover, based on this thesis, it is highly recommended that samples found in a similar location and depth are chosen, to avoid external conditionings.

Finally, a reflection is presented on the importance of the source used for: 1) extrapolating climatic conditions from present-day to the past, and, 2) comparing past climatic results obtained with present-day data. The data sources variated in its application and this has implications for the final interpretation, not only in absolute numbers but also even in detected trends. For example, is not the same to compare present-day temperatures from a site located at an altitude of 500 m a.s.l employing Font-Tullot (2000) if the closest meteorological station is at sea level (as in Teixoneres and Abric Romaní sites) or to use Climate-data.org which employed a climatic model for responding to approximate coordinates, thus considering associated altitude. These uncertainties are also present in this thesis (Table 9.4). The data-source employed in level O of Abric Romaní to deduce past temperatures was Font-Tullot (2000) and the present-day temperatures come from Ninyerola et al. (2003) in Chapter 3. In Chapter 5, an attempt to standardize was made employing AEMET and IMP (2011) for past estimations, and Climate-Data.org for current temperatures, including level O. Fortunately, AEMET & IMP (2011) and Font-Tullot (2000) provided close climatic information and were designed with the same primary data and differences are generally low (<1 °C). AEMET & IMP (2011) provides more precise results, considering small local climate variabilities not included in Font-Tullot (2000). For this reason, in the case of Arbreda, Teixoneres, and Xaragalls, MER reconstruction of previous publications (López-García et al., 2012a, 2012b, 2015) is assumed produce non-significant error, but temperatures relative to present-day are recalculated considering Climate-data.org to obtain the most accurate approach which considers orography, which is sometimes not provided by closest meteorological stations.

In summary, palaeotemperature reconstructions require some protocol or convention about the data source to avoid tedious comparisons of past climatic conditions between sites. At minimum, it is necessary to always express the source data and the primary data, including temperature estimates in absolute values (e.g., MAT_{levelO}= 11.1 °C) and present-day temperatures considered (e.g., $MAT_{Capellades}$=14.8 °C). A comparison between assemblages or methods will not be possible if this relation is not considered. Caution is recommended in comparing relative temperatures (e.g., level O is -3.7 °C with respect to present-day MAT) if the data source differ. For example, in the case of Abric Romaní notable changes in estimated temperatures can be seen between previous works (Burjachs et al., 2012; López-García et al., 2014), corrected present-day estimations of level O (Chapter 4), and final estimations proposed (Chapter 6) (Table 9.4).

Palaeotemperature reconstruction will always be an extra tool of analysis for climatic interpretation. As discussed, this kind of analysis has important inherent limitations that should be considered in the final interpretation of a given fossil deposit. Frequently, global trend observed in the sequence and the differences between levels are more informative than the absolute degree obtained. Discrepancies between methods might sometimes also provide information, as in the case of unit III of Teixoneres and level N of Abric Romaní, where these inconsistencies allowed for the

	MAT - Previous works			MAT - Chapter 3			MAT-Chapter 6		
	Present-day	MER	Difference	Present-day	MER	Difference	Present-day	MER	Difference
D		11.1	-5.4		11.1	-3.4		11.6	-3.2
E		10.8	-5.7		10.8	-2		9.7	-5.2
J	16.5	11.1	-5.4	14.5	11.1	-3.4	14.8	11.1	-3.7
N		11.9	-4.5		11.9	-2.6		12.2	-2.6
O		9	-7.5		11.4	-3.1		11.1	-3.7

Table 9.4 Comparison of mean annual temperature (MAT) reconstruction of Abric Romaní levels. First estimations were performed by Burjachs et al., 2012 and employed climatic maps and meteorological station information provided by Font-Tullot (2000); in Chapter 3, level O estimations were obtained from climatic maps from Font-Tullot (2000) and present-day temperatures from Ninyerola et al. (2003); in Chapter 6, climatic maps are from AEMET & IMP (2011) and present-day temperatures from Climate-Data.org (2018). In yellow, samples increased by this work.

consideration of a palimpsest between stadial-interstadial events. Moreover, none of the three methods of palaeotemperature reconstruction should be used alone, because a comparison with external approaches is required, such as in relative abundances of taxa and general faunal spectra. Multidisciplinary environmental approaches that consider different disciplines from palaeo-archaeobotanic remains (such as pollen, charcoals, phytholits), taphonomy of large and medium mammals, use-wear analyses on teeth and sedimentological analyses, among others, are fully recommended and probably the best way to faithfully approach past climatic conditions.

3. Palaeoenvironment of Late Pleistocene and MIS3 in northeastern Iberia

Throughout this thesis, four Late Pleistocene sequences from the Northeast of the Iberian Peninsula have been analyzed in climatic and environmental terms: Abric Romaní rock-shelter (levels O-N (55.1-54.2 ka) and D-E (44.9-43.2 ka)); Barcelona, Spain), Teixoneres cave (units IIIb-IIa; >51 14C ka BP-33 ka cal. BP; Barcelona, Spain), Xaragalls cave (levels C8-C4; >45.1 - 45.1 ka BP; Tarragona, Spain), and Arbreda cave (levels H-D; 41.6-27 ka cal. BP; Girona, Spain). The four sequences are contemporaneous with Marine Isotopic Stage 3 (MIS 3; ca. 60-30 ka) and present small-vertebrate assemblages were mainly accumulated by owls, which reflected local environments, allowing for the potential reconstruction of past ecological conditions that surrounded these sites, from a local to regional scale. In Iberia, this stage was defined as a global warm period characterized by climate dynamics that alternated between warming and cooling phases reflected in sea-surface temperatures, which on the continent generated phases of forest development and expansion of semi-arid areas, respectively (D'Errico and Sánchez Goñi, 2003; Fletcher et al., 2010; Sánchez Goñi et al., 2008; Sánchez Goñi and D'Errico, 2005).

These four palaeontological and/or archaeological sequences have undergone biochemical analysis, giving us the opportunity to reconstruct the palaeotemperatures of MIS 3 from an independent method to species spectra recovered in each fossiliferous deposit. The four sequences analyzed have generally recorded palaeoetemperatures lower than present-day (from -5.5 to – 0.5 °C), except for layer C5 of Xaragalls cave, which recorded temperatures comparable to today's (Fig. 9.2). The MAT reconstruction extended between 9.3 °C and 13.8 °C when estimated by $\delta^{18}O$, and between 7 °C and 16.8 °C when all methods are taken together. According to MER and BM

methods the mean annual precipitation (MAP) was globally higher than present-day in each region (from +682 mm to -69 mm), than in absolute terms supposed precipitation between 550 mm to 1430 mm.

3.1. Palaeoenvironment in the studied sites

The complete Abric Romaní sequence has been analyzed, but given the fragmentary representation of small-mammal remains along the sequence, only levels O, N, E, and D (ca. 55-43 ka) are considered reliable for biochemical considerations. All methods of palaeotemperature estimations agree in estimating lower temperatures at these levels than present-day (from -5.1 to -0.3 °C), though there is some offset between methods. According to oxygen isotope compositions, MATs were between -2 and -3.5 °C lower than present-day (14.8 °C). Higher levels of precipitation are recorded for analyzed levels (from -69 to + 252 mm) in comparision to present-day in Capellades (619 mm), especially at levels O and E, but slight discrepancies are found in level D. Little changes in small-mammal communities, with equal proportions between mid-European and Mediterranean species, together with palynological and charcoal fluctuation from the site, allow us to consider levels O and E as slightly cooler, which could be related to stadial periods (Burjachs et al., 2012; Fernández-García et al., 2018; López-García et al., 2014b; Vaquero et al., 2013). Comparison between lower (O-N, ca. 54-55 ka) and upper (E-D, ca.43-45 ka) levels of the Abric Romaní sequence report equivalent climatic conditions (differences <1.5 °C), reflecting only small climatic fluctuations primarly reflected in faunal composition, but not in the recorded isotopic signatures or their palaeotemperature estimations. This is probably related to increments in the mean annual precipitation, which can hide changes in temperatures, or to stadial-interstadial scenarios.

Considering the oxygen isotope results from Xaragalls cave, a palaeontological site with chronology contemporaneous with Abric Romaní (López-García et al., 2012a), generally cooler but also most stable conditions are reported (Fernández-García et al., under review). This is consistent with colder and wetter conditions as compared to present-day, as described by both small vertebrates and charcoal from the site (López-García et al., 2012a). Layers C8 to C4 are characterized by low to medium $\delta^{18}O$ amplitudes related to preferential accumulation in the warm season, but higher variations in $\delta^{18}O$ values detected in layers in C7, C6 and C4 could be related to high-frequency climatic fluctuations, similar to other methods of palaeotemperature reconstruction. These environmental fluctuations are in agreement with changes in small-mammal communities that indicated a humid and cooler environment with landscape openings for these units (López-García et al., 2012a). However, the $\delta^{18}O_p$ median variations suggest rather steady-state climatic conditions throughout the sequence with mean annual temperatures lower than current ones (-2.4 °C to -1.5 °C). This excludes layer C5, which was previously correlated to interstadial phase IS13 or 14 (ca. 50-55 ka), which records similar mean annual temperatures to those at present (13.6 ±2.7 °C).

According to $\delta^{18}O$ estimation of temperatures obtained for Teixoneres, slightly cooler climatic conditions than present are recorded (-1.6/-0.5 °C, with respect to present-day MAT=14.8 °C) in agreement with results from the MER method, but different from results using BM. Notably wetter conditions are defined at this site (from +43 to + 681 mm) in comparison to current MAP (749 mm) but the magnitude and the trend varies between

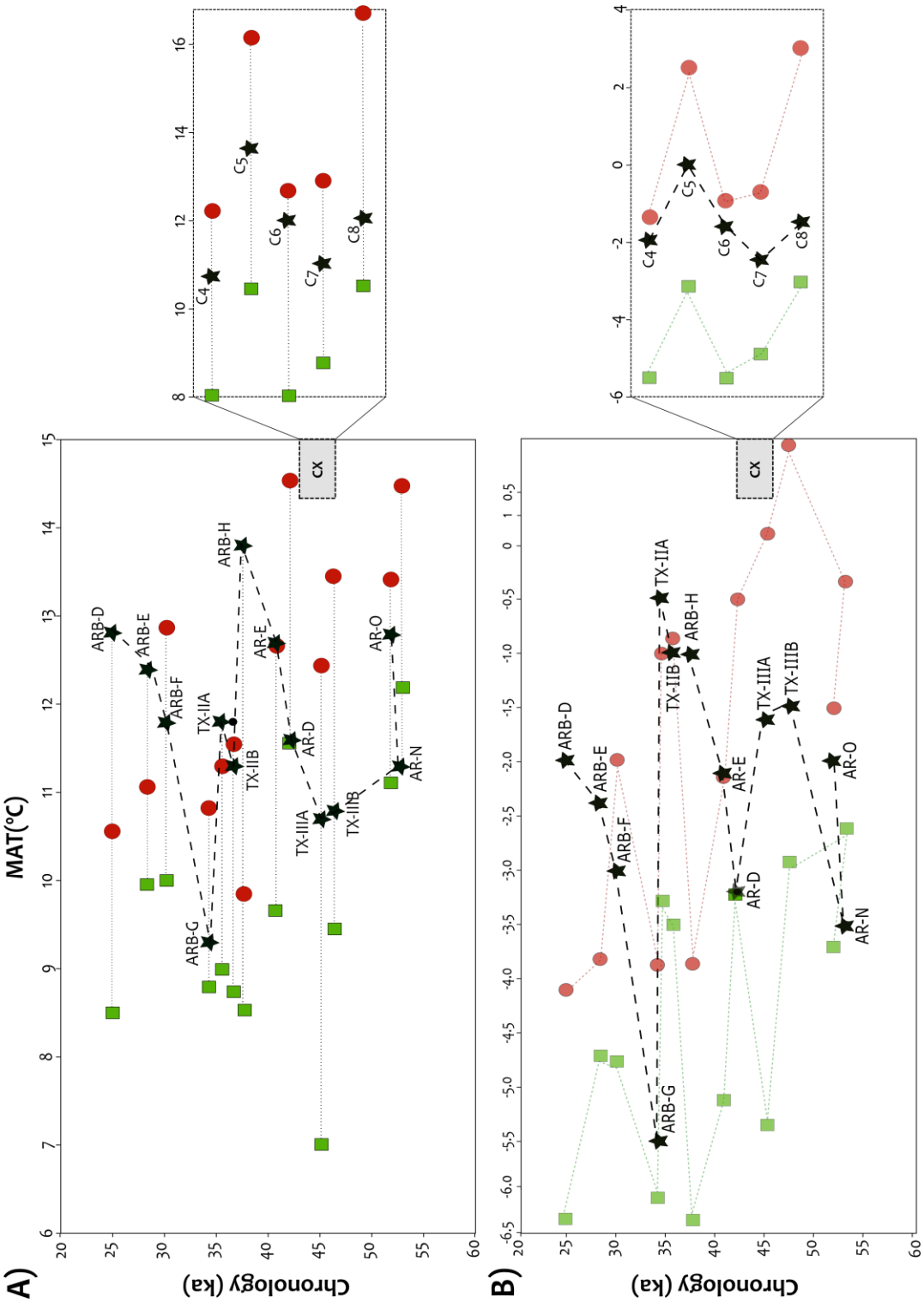

Figure 9.2 Mean annual temperature (MAT) estimations of Abric Romaní (AR), Xaragalls (CX), Teixoneres (TX) and Arbreda (ARB) through oxygen isotope compositions from rodent incisors (black stars), but also included estimations of Bioclimatic Model (red dots) and Mutual Ecogeographic Range (green squares). (A) Absolute MAT estimations and (B) relative to current MAT of each site. The chronology provide for the sites is based on U-Series or 14C calibrated datings

BM and MER. According to biochemical analyses, Teixoneres cave represents the most homogenous sequence, with little $\delta^{18}O$ variation between subunits (<1 ºC when expressed in MAT). Unit III shows slightly higher $\delta^{18}O$ amplitudes and lower median $\delta^{18}O$ values than unit II and is tentatively related to some climatically instability and slightly cool temperatures. This could be consistent with the occasional occurrence of cold-dependent large and small mammals (Álvarez-Lao et al., 2017; López-García et al., 2012b), but is not consistent with previous environmental interpretations based on small-mammal relative abundances. These discrepancies between methods could point to a palimpsest where stadial and interstadial events overlapped, especially in subunit IIIa.

The latest stages of the MIS 3 are recorded in Arbreda cave, which is the only sequences that records lower temperatures than present-day with regardless of the methods for palaeotemperature estimation used. Using oxygen isotope analysis, temperatures at levels H-D are between -1 ºC and -5.5 ºC lower than present-day (14.8 ºC). Sizable intra-level $\delta^{18}O_p$ fluctuations are observed, mainly in levels G, F, and E, with higher amplitude and lower medians in relation to levels H and D. Moreover, this sequence presented the level with highest $\delta^{18}O$ median in level H (38.3-41.6 ka cal. BP) but also the level with highest variation in $\delta^{18}O$ values and lowest median $\delta^{18}O$, level G (35.6-38.2 ka cal. BP). That indicates a drop in -4.5 ºC between both levels and progressive recovering of temperatures along the sequence. Small-mammal assemblages are related to interstadial conditions in level H and relatively cold conditions in level G. Globally colder conditions are maintained according to BM and MER methods throughout all the sequence with the constant presence of mid-European species (López-García et al., 2012a). Both methods also estimate a globally wetter environment (+30 mm to + 467 mm).

3.2. Late Pleistocene in Northeastern Iberia

The third chapter of this thesis (Fernández-García et al., 2016) draws a general picture of the rodent relative abundances in northeastern Iberia from the Late Pleistocene (ca. 128-11.7 ka) to the Holocene (<11.7 ka), providing the regional clues that allow us to differentiate types of rodent assemblages primarily as a consequence of environmental factors. Local factors, such as continentality, altitude, or proximity to water courses, will have an influence on faunal communities. However, the dominant relative presence of three species (*Microtus arvalis, Microtus agrestis* and *Apodemus sylvaticus*) was critical to chronological discrimination between the sites. *M. arvalis* and *M. agrestis,* which are species associated with mid-European requirements, open environments, and cool temperatures, were especially dominant at the end of the Late Pleistocene (ca. 40-11.7 ka BP). Conversely, *A. sylvaticus*, a generalist species mainly associated with wooded areas and temperate environments without major climatic constraints, was dominant at the beginning of the Late Pleistocene (ca. 128-40 ka BP) and regained its importance with the arrival of the Holocene (<11.7 ka BP).

In this multifactorial analysis, some of the levels of Abric Romaní (O, N and E) were included, but previous to revisions done in chapters 4 and 6. These rodent assemblages were located in the middle range of influence between forest species (*Apodemus sylvaticus*, *Eliomys quercinus*) and Mediterranean species (mainly *Iberomys cabrerae* and *Microtus (T.) duodecimcostatus*), even though the influence of the wood mouse is slightly attenuated in front of other MIS 3 assemblages and coexistence with mid-European species is detected. However, the wood mouse appeared closer to other MIS 3 assemblages related to

milder environments than to the latest stages of MIS 3, represented by Arbreda levels. Level N of this site differs from other MIS 3 assemblages by the major occurrence of Mediterranean taxa (*Iberomys cabrerae* and *M. (T.) duodecimcostatus*), which have been increased through the sampling presented in Chapter 6, and practical absence of *M. arvalis* and *M. agrestis*. An equivalent situation is observed for level D, but A. *sylvaticus* abundance is reduced from E to D. Despite oxygen isotopic results, and considering new identifications, these faunal assemblages differ from those of levels O and E, where a slightly greater presence of mid-European taxa is recorded. This is in keeping with with BM and MER estimations of palaeotemperatures and fits well with previous studies on pollen, charcoals, and sediments (Allué et al., 2017; Burjachs et al., 2012; Burjachs and Julià, 1996; López-García et al., 2014b; Vaquero et al., 2013). Regarding Xaragalls cave, layers C6-C7, related to cool phases, and layer C8, related to warmer phases, appear equally group by the relative high presence of the wood mouse. Layer C4 appears slightly separate but group among MIS 3 and MIS 1 assemblages and influence by *A. sylvaticus* dominance. This underlines maintenance of the open forest landscape, with independence of climatic fluctuations.

Some inconsistencies were found in Teixoneres cave (Chapter 7) between palaeotemperatures estimations and small mammal abundances. According to Chapter 3, when small-mammal communities of unit III are compared with assemblages of northeastern Iberia, they appear well-integrated with other MIS 3 archaeological sites, influenced by *A. sylvaticus* and *M. (T.) duodecimcostatus*, mainly in subunit IIIb. On the contrary, when unit II small-mammal communities are compared with other contemporaneous assemblages of northeastern Iberia, they appear highly differentiated and similar to latest MIS 3 assemblages, as Arbreda cave. That is affected by the abundances of *M. arvalis-agrestis,* especially in unit IIa, and the low presence of *A. sylvaticus* (López-García et al., 2012b). But some cold-dependent species appear also among small mammals of subunit IIIa (*Chionomys nivalis, M. (T.) gerbei* and *Sorex coronatus*). This approach is not entirely reliable, since the slow sedimentation rates of the deposit (Rosell et al., 2010a, 2010b, 2017) could generate important palimpsests that preclude the isolation of different climatic phases, and required at least subunit differentiation, as this work has underscored. Finally, levels H-B of Arbreda cave are clearly differentiated from the oldest sequences due to the higher relative presence of mid-European rodent species (mainly *M. arvalis* and *M. agrestis*). Apart from their more recent chronology, the geographical location of this site, which is northern, cooler and wetter than other MIS 3 sequences, will have influence in the species spectra. However, level I and A slightly differed from the rest of levels clearly cluster, probably because they frame the moments before and after climatic worsening or declining forest, recorded through all methods of palaeoclimatic methods (López-García et al., 2015). From this point of view, no major changes in rodent communities is detected between levels H and G, although a noticeable drop in temperatures is inferred from biochemical analyses.

3.3 The MIS 3 in the Iberian Peninsula

The climatic evolution in northeast Iberia has been previously studied using small mammal records from MIS 3, which always show a cold and humid climate with lower temperatures (from -7.7 °C to -2.8 °C) and higher precipitation (+75 mm and +440 mm) than present-day, independent of stadial or interstadial correlations (López-García, 2011; López-García et al., 2012b, 2012c, 2013, 2014a, 2014b, 2015; López-García and Cuenca-Bescós, 2010). The results obtained in this work globally fit

with these colder temperatures and wetter conditions, but the magnitude of these differences is reduced either when using oxygen isotopes or qualitative methods of palaeotemperature reconstruction (BM and MER). Not always coherence with previously determined stadial-interstadial fluctuations previously determined was found using the analysis of small-mammal communities and palaeotemperatures estimates. Some of the sites included in this thesis were previously studied and some reported notably colder conditions than present-day, such as unit II of Teixoneres cave, levels O and E of Abric Romaní cave and layer C4-C3 of Xaragalls cave (Burjachs et al., 2012; Fernández-García et al., 2018; López-García et al., 2012b, 2014b). The spreading of species with mid-European requirements (mainly *M. arvalis* and *M. agrestis*) and the occurrence of species currently living in northern latitudes (*Chionomys nivalis, M. (T.) gerbei, Sorex* gr. *araneus-coronatus*, *Talpa europaea*), in agreement with independent environmental proxies (pollen, charcoals, large mammals, or use wear), provide enough evidence for some of these sedimentary units to considered local and slight climatic deterioration. In most cases, biochemical analyses cannot fully support these rigorous correlations. According to $\delta^{18}O$, level G of Arbreda cave is highlighted as the most heterogenous level with the lowest MAT (9.3 °C) of all the sedimentary units analyzed, and this work points to a stadial episode, whereas previously level H was confirmed as an interstadial phase (MAT= 13.8 °C). Layer C5 of Xaragalls cave reported the second highest median $\delta^{18}O$ value, which when expressed in MAT is equal to present-day temperatures (13.6 °C), confirming the interstadial phase previously described.

Nevertheless, oxygen isotope compositions from the sequences analyzed underscore that there is little intra-site variability, mostly lower than 1‰ according to both mean and median $\delta^{18}O_p$ values. This only excludes the Arbreda cave sequence, where median $\delta^{18}O_p$ fluctuated in 2.2‰ (Fig. 9.3A). Consequently, variability in MATs through the sequences is low, especially for Abric Romaní and Teixoneres cave (<1.5 °C under $\delta^{18}O$ estimations and <2.5 °C with BM and MER methods). Abric Romaní and Teixoneres are the most homogenous sequence from the oxygen isotopic perspective. The global analyses of Abric Romaní show medium variability in median $\delta^{18}O_p$ values and low-to-medium variability in $\delta^{18}O_p$ ranges between levels. When estimations of MATs are performed, more favorable climatic conditions than other sites are recorded (9.7-12.2 °C), but if relative MAT is considered with respect to present day, the climatic change is the greatest (from -2 to -3.2 °C). Despite differences detected between unit III and II of Teixoneres, from the oxygen isotope analysis perspective and compared to contemporaneous Late Pleistocene sequences, such as Xaragalls cave and Abric Romaní, a globally stable period is reinforced. According to mean and median $\delta^{18}O_p$ values and estimated temperatures, this site represents the coldest MIS 3 sequence analyzed (10-7-11.8 °C). However, with respect to present-day conditions the difference is less marked (from -0.5 to -1.6 °C). Though in Xaragalls cave the temperatures are globally milder (11.2-13.6 °C), some variations in the $\delta^{18}O_p$ amplitudes suggest slight fluctuations in climatic conditions between -1.5 and -2.4 °C. Arbreda cave is the most heterogenous sequence but, considering median $\delta^{18}O_p$ values, not the coldest (9.3-13.8 °C). However, all methods support important decreases of temperature in the past (considering $\delta^{18}O_p$, MAT equivalent from -5.5 to -1 °C). The singularity of levels G and H are clear when they are compared to contemporaneous MIS 3 sequences.

Though temperatures oscillated during MIS3 in northeastern Iberia sites, consistent with cold- and

temperate-dependent small-mammal species, the precipitation levels and woodland estimates are always high. Previous studies on small mammal species abundances have underscored the importance of forested biotopes, usually greater than 50% (López-García, 2011; López-García et al., 2012b, 2012c, 2014b, 2015). At sites studied in northeastern Iberia, the landscape is usually described as an open woodland habitat. This is consistent with the highest abundances of forest dwellers species being during this period, mainly *Apodemus sylvaticus*, but also *Eliomys quercinus* and *Myotis myotis* (Fernández-García et al., 2016; López-García et al., 2014b). In the case of the Abric Romaní (Chapters 4 and 6), there were only slight changes in the landscape, with open forest probably always dominant with punctuated expansions of more or less humid meadows and active water courses next to the rock-shelter. The predator identified as the main accumulator of the assemblage, *Strix aluco*, is a good indicator of the forest type surrounding the site. Pine forests were probably widespread throughout the territory of Abric Romaní, with *Pinus* type *sylvestris* dominating throughout the entire sequence (Allué et al., 2017; Burjachs et al., 2012; Burjachs and Allué, 2003; Burjachs and Julià, 1994). In Xaragalls cave, the regular presence and large population of woodland-dwelling species, including the singular abundance of the wood mouse throughout the sequence (>40% in all levels), among other woodland species, supports the idea that the surrounding landscape was regularly constituted by open-forest formations. Based on results of charcoal studies of this sedimentary sequence, the forest was less taxon-diverse than the current Poblet Forest, with a clear predominance of *Pinus*-type *sylvestris* (López-García et al., 2012a).

The Teixoneres sequence is similar, where small vertebrate abundances underscore a clear predominance of a forest component (>60%) and describe an open forest landscape, in keeping with pollen, charcoal, and large-mammal dental wear analyses. Preliminary palynological data confirm a landscape dominated by woodlands composed of pines and oaks, with herbaceous taxa such as Poaceae, Chenopodicea and Astareceae, attesting some landscape openings but showing always high proportions of arboreal pollen (>50%). Progressive decreases in woodland species (*A. sylvaticus, E. quercinus*) in favor of open-environment species with mid-European requirements (*M. arvalis* and *M. agrestis*) are notable between units III and II, which could be related to the dry peak indicated by the occurrence of the steppic pollen taxon *Artemisia* in subunit IIa (López-García et al., 2012b). In contrast, during the latest stages of MIS 3, small-mammal assemblages of Arbreda cave are characterized by the predominance of species related to open environments (*Microtus (Terricola) duodemicostus*, *M. arvalis, M. agrestis*), especially from levels H to B (>70%) in opposition to the reduced presense of *A. sylvaticus* (<7%, especially reduced in levels E-C, <3%)(López-García et al., 2015). That is consistent with palynological studies which described an open and herbaceous vegetation with steppic characteristics with the emergence of Pines and Cupressaceae; in contrast, anthracological analyses point to a predominance of *Pinus sylvestris* throughout the Pleistocene sequence (Ros, 1987).

The maintenance and, usually predominance, of the forest biotope, together with wetter and cooler conditions, is a trend recurrently observed in MIS 3 Iberian archaeo-palaeontological sites. This is also supported by small-vertebrate compositions, especially from the Mediterranean area (Fernández-García et al., 2016; López-García et al., 2014), as it is recorded in Gorham's caves (Blain et al., 2013; López-García et al., 2011b), El Salt (Fagoaga et al., 2018; Marquina et al., 2017), Cova del Coll Verdaguer (Daura et al., 2017), Cova del

Gegant (López-García et al., 2012c). Small-mammal assemblages from these sites include Mediterranean species (*M. (T.) duodecimcostatus* or *I. cabrerae*) and typical woodland species (*A. sylvaticus* and *E. quercinus*), with independence of stadial-interstadial cycles. Predominance of arboreal coverage is also supported by charcoal and pollen analyses in Middle Palaeolithic levels of Cova Gran (Allué et al., 2018), where no small vertebrate data are available. This pattern is also noted at northern and northwestern Iberia, in Lezetxiki II, Askondo, Cueva del Conde, and Cova Eirós (Garcia-Ibaibarriaga, 2015; López-García et al., 2011a; Murelaga et al., 2012; Rey-Rodríguez et al., 2016); in the interior of Iberia, Los Casares (Alcaraz-Castaño et al., 2017) and even in the Atlantic coast, in Figueira Brava cave (Jeannet, 2000) and Caldeirão cave (Povoas et al., 1992). However, few sites exhibit diverse dynamics, such as El Mirón cave, Zafarraya and Ibex Cave (Denys, 2000; Barroso et al., 2003; Cuenca-Bescós et al., 2009; Barroso et al., 2014; Finlayson et al., 2016). Thus, in agreement with marine records, continental pollen studies, and small mammal abundances (e.g., Fletcher et al., 2010b; Harrison and Sanchez Goñi, 2010; Sánchez Goñi et al., 2008), Iberia never underwent a complete loss of woodland during the MIS 3, even during stadial periods or Heinrich events, when global climatic conditions deteriorate and subsequent forestall reduction occurred in northern Europe.

4. Singularity of Iberia and its importance in Prehistory

The Iberian Peninsula is a complex territory characterized by its unique environmental conditions, even though it is considered a small-scale continent. The causes lie in its geographic location in the southwestern portion of Europe surrounded by the Atlantic Ocean in the west and Mediterranean in the east, thus it receives both Atlantic and African-Mediterranean influences (Font-Tullot, 2000). In addition, its particularly complex orography with a wide-range of altitudes, favor the formation of micro-climates. The Pyrenean Mountains partially isolated this peninsula from the rest of the continent and, in addition to the Galician-Cantabrian mountains, reduced the influenced of the cold air masses coming from the northwest and the northeast. The Iberian Peninsula served as a macro-refugium for many floral and faunal species during stadial periods, sheltering them from rigorous climates until more favourable environmental conditions allowed their geographic radiation (Hewitt, 2000; Sommer and Nadachowski, 2006). In particular, the northern coast constitutes a key refuge area for a wide suite of temperate flora and fauna. Moreover, the Pyrenees acted as a natural ecogeographic barrier for the dispersion of faunas, as occurred with some cold-adapted species that could only have arrived in the peninsula through narrow corridors west and east of the Pyrenees (Álvarez-Lao et al., 2017; Álvarez-Lao and García, 2010).

The MIS 3 sequences from the northeast have shown the environmental singularities of Iberia in front northern latitudes. The maintenance of woodland covertures, besides generally wetter conditions, and not big shift in rodent communities confirms the peculiarities of northeastern Iberia during MIS 3, when globally climatic detriment and subsequent forestall reduction occurred in northern Europe. Forest biotope maintenance constitutes a singularity of Iberia and the Mediterranean area. At southernmost latitudes (<40°N), marked temperate/Mediterranean forest development occurred during MIS 3 D-O cycles and maintenance of larger local populations of temperate trees occurred even during stadials (especially, <44°), whereas at higher latitudes (>40°N) forest development was weaker and more

influenced by millennial-scale cycles (Fletcher et al., 2010; Sánchez Goñi et al., 2008). Thus, northeastern Iberian sites are placed on the limit fringe fixed for different response in forest development during interstadials events. However, despite the climate changes anthracological and palynological records inland describe well-established montane pine forest covertures, associated with components of evergreen and deciduous species, from the southern Iberian coasts to the Pyrenees during Late Pleistocene, until their decline with the begging of the Holocene (e.g., Allué et al., 2018; Carrión, 2012; Carrión et al., 2018; Daura et al., 2017).

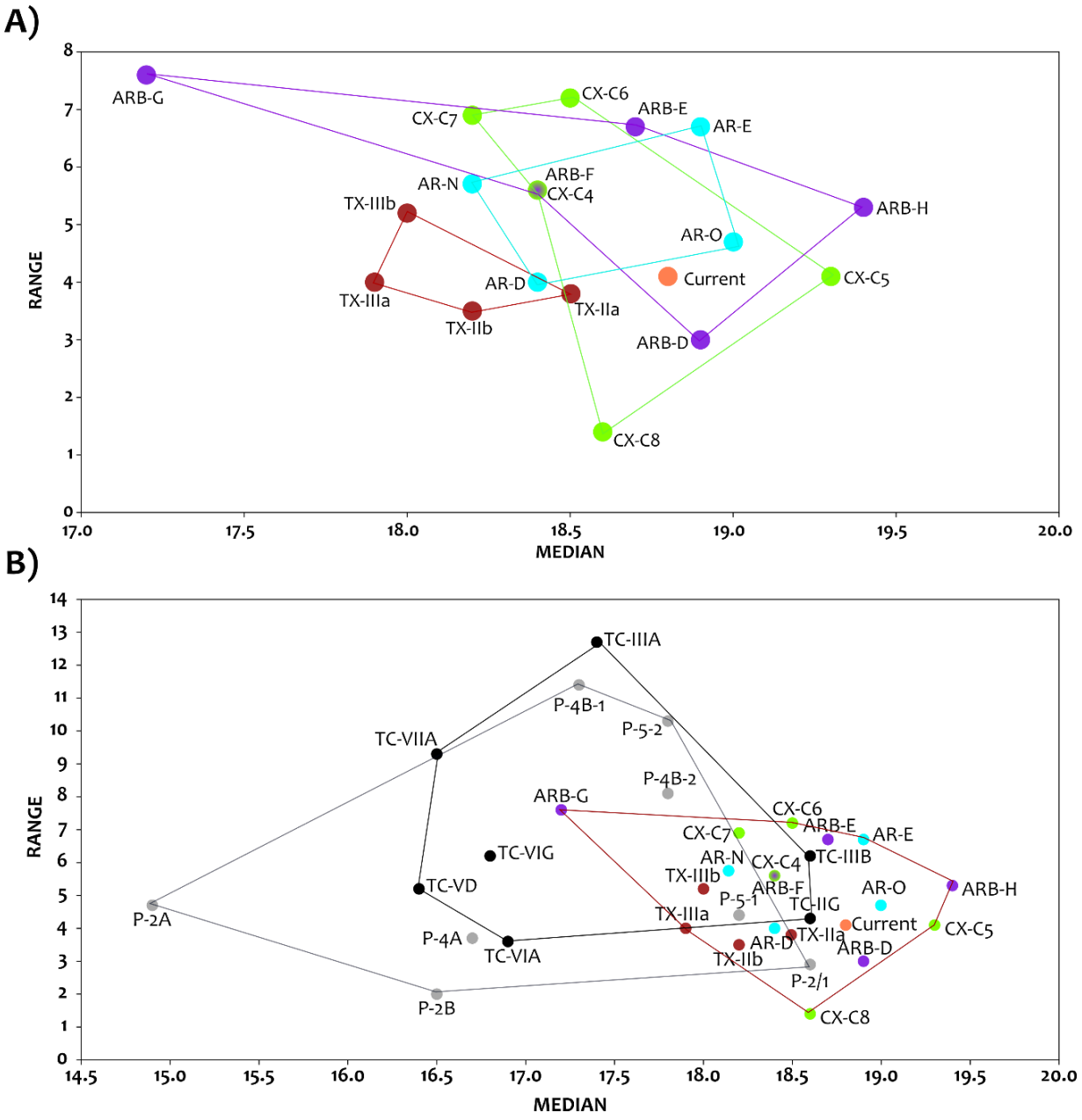

Figure 9.3 Oxygen isotope compositions of tooth enamel phosphate ($\delta^{18}O_p$; ‰ V-SMOW) comparing range of $\delta^{18}O_p$ values and $\delta^{18}O_p$ median values from modern samples and fossil deposits analyzed in the thesis: AR, Abric Romaní; TX, Teixoneres cave, CX, Xaragalls cave; ARB, Arbreda cave. In (B) $\delta^{18}O_p$ obtained in this work are compared with those obtained from Western France sites (Royer et al., 2014, 2013b): TC, Taillis des Coteaux; P, Les Pradelles.

In addition, previous isotopic studies have revealed the particular climate of the Mediterranean Basin (Dansgaard, 1964; Gat et al., 2003; Gat and Carmi, 1970; Hartman et al., 2015; Lécuyer, 2014; Lécuyer et al., 2018). The peculiar orography and climatic mode of the Iberian Peninsula is also emphasized in Chapter 5 of this study, in which it is noted that high annual amplitudes of $\delta^{18}O_{mw}$ values occur in comparison to higher latitudes in present-day (Bowen, 2017). This difference mainly lies in lower $\delta^{18}O_{mw}$ values in the cold season and notably higher $\delta^{18}O_{mw}$ values during the warm season. The cause is most likely related to the air masses operating on Iberia, such as the influence of the continental tropical air mass from North Africa that favors hot and arid summers (Font-Tullot, 2000; Gat et al., 2003). In addition, the large variability in the orography of Iberia promotes globally larger seasonal amplitudes in $\delta^{18}O_{mw}$ values than flatter territories. For these reasons, this work proposes a specific linear regression between mean annual $\delta^{18}O_{mw}$ values and mean annual air temperatures, in order to calculate mean annual temperatures for the Iberian Peninsula based exclusively on monthly GNIP data from this geographical context.

From the biochemical perspective, different patterns at northern latitudes are also detected in MIS 3 sites. As has been previously explained, analyzed fossil deposits in this thesis demonstrate stable global conditions considering oxygen isotopes compositions records. Normally low amplitudes in $\delta^{18}O$ and tiny differences between levels inside the same site and even between sites are measured (Fig. 9.3A). A total amplitude of 9.3‰ is recorded, from the lowest $\delta^{18}O_p$ value that is 14.2‰ (ARB-E) to the highest, 23.5‰ (AR-E). According to inter-level ranges in each site, Arbreda and Xaragalls caves present the most variation between levels, with amplitudes that range between 3‰ and 7.6‰ (=4.6‰) and between 1.4‰ to 7.2‰ (=5.8‰), respectively. On the contrary, Abric Romaní and especially Teixoneres cave are rather homogenous, with inter-level differences between 4‰ and 6.7‰ (=2.7‰) and between 3.5‰ and 5.3‰ (=1.8‰), respectively. Medium to small ranges of $\delta^{18}O_p$, values which are always associated with high means and relatively constant throughout these sequences, differ from a contemporaneous archaeological site in southern France, Les Pradelles (Royer et al., 2013b) (Fig. 9.3B). At the site of Les Pradelles (Charente, ca. 81-58 ka BP) the total range of $\delta^{18}O_p$ values is 12.2‰, with inter-level variations between 2‰ and 11.4‰ (=9.4‰) (Royer et al., 2013b). The same can be observed at Taillis-des-Coteaux (Vienne, 35-17 ka cal. BP), where the total range of $\delta^{18}O_p$ values is 13.1 ‰, with inter-level variations between 3.6‰ and 12.7‰ (=9.1‰) (Royer et al., 2014). Thus, only within each of these sites is the heterogeneity higher than in all the analyzed Iberian assemblages together. Moreover, both French sites tend to present lower median $\delta^{18}O_p$ values than Iberian assemblages. This is not surprising considering the existing relationship between $\delta^{18}O_p$/ $\delta^{18}O_{mw}$ and latitude. However, the offset is large. The only levels that fit with Iberian results are levels IIIB and IIG of Taillis des Coteaux and levels 5-1 and 2-1 from Les Pradelles. The restricted ranges in $\delta^{18}O_p$ values of these levels were related to hunting bias in summer, leading to calculated summer mean temperatures close to or warmer than present-day in each respective region, and resulting in each of these sites the warmest estimations. Recent research on oxygen isotopes compositions from central Iberia (Yravedra et al., 2016), also highlight the milder conditions recorded from the center of the Iberian Peninsula even during MIS 2 chronology, in comparison to the expected for this rigorous period.

In MIS 3 sites of southwestern France, species with steppe-tundra preferences are usually

predominant along the sequences (*Dicrostonyx torquatus, Microtus gregalis, Microtus oeconomus, Spermophilus* sp.). In addition to the occurrence of *M. arvalis* and *M. agrestis, A. sylvaticus* is anecdotical, thereby demonstrating a remarkably different faunal composition in association with severe climatic conditions in opposition to Southern Europe (see synthesis in Royer et al., 2016). In Northeastern Iberia, the rodent assemblages of the MIS 3 did not greatly differ from the early Holocene assemblages; the dominant species are those common in forest environments (*A. sylvaticus*) and more temperate environments or climates with a Mediterranean influence (*M. (Terricola) duodecimcotatus*) (Fernández-García et al., 2016). However, coexistence with mid-European species (mainly *M. arvalis* and *M. agrestis*) is detected, which expands or reduces its occurrence in relation to climatic fluctuations. Under multivariate statistical methods (see Chapter 3), most of the MIS 3 rodent assemblages were grouped with those of the Holocene. Their distribution depends on the dominance of *A. sylvaticus* or T. *duodecimcostatus*, and shows no particularly distinctive patterns between both these time intervals, considering major species relative abundances, apart from the reduction of mid-European species abundances with the arrival of the Holocene. Thus, it is not always simple to distinguish these two phases in rodent communities, allowing to suggest ecological similarities and underscoring the particularities of Iberia during the MIS 3 in front northern Europe environment.

5. Neanderthal subsistence in northeastern Iberia

The Late Pleistocene glacial regime and the subsequent glacial-interglacial fluctuations had an impact on both flora and fauna, including human populations throughout western Europe and the Iberian Peninsula. However, it has been shown that Iberia provides favorable environmental conditions to these living entities, with milder conditions and widespread forestall covertures. Middle Palaeolithic sites with a significant human presence are scarce in Iberia almost until the arrival of MIS 3. Some MIS 5 examples were found, such as in lower Bolomor levels, as were several MIS 5 and MIS 5/MIS 4 transition examples, as in some layers from Cova del Rinoceront, Lezetxiki II, Cueva del Camino, Arlanpe cave and Cova Eirós (Arsuaga et al., 2012a, 2012b; Blain et al., 2014; Daura et al., 2015; García-Ibaibarriaga, 2012; López-García et al., 2016; Rey-Rodríguez, 2015; Rios-Garaizar et al., 2015; Rofes et al., 2012) (Fig. 9.4). Based on the available information, human presence in these locations was relatively short and sporadic, normally in alternation with carnivore occupations. Available small-mammal studies coincide with the Iberian palaeobotanical sequences for this period, suggesting overall mild climatic conditions and a diversity of landscapes, with temperate taxa distributed according to biogeographical location. In general, it was a favorable environmental phase, characterized by a large extent of woodland landscapes over the peninsula, only declining at the end of MIS 4 with the expansion of steppe-tundra vegetation (Carrión, 2012; Daura et al., 2015; Fletcher et al., 2010; López-García et al., 2016; Rey-Rodríguez et al., 2016; Sánchez Goñi and D'Errico, 2005).

A great part of the Neanderthal occupations that occurred in northeastern Iberia occurred during the Marine Isotopic Stage 3, especially during their second half. Three of the four sequences analyzed in this thesis show recurrent Neanderthal occupation, either long-term or short-term: Abric Romaní cave (from levels Q to level B), Teixoneres cave (unit IIIb to unit IIa) and Arbreda cave (from levels N to level I). Moreover, Arbreda cave shows the first anatomically modern human occupations,

from levels H to A. The climate seems to be globally cooler than today and slight fluctuations occurred based on fluctuations in mid-European small-mammal abundances. Some of the levels, such as levels O and E from Abric Romaní rock-shelter or unit IIIa of Teixoneres cave, are considered colder and correspond to periods of more intense Neanderthal occupations at the sites. Thus, this rigorous climate does not seem to affect short- or long-term Neanderthal occupations. Furthermore, our results suggest that the climatic instability of MIS 3 within the cool global context had no real impact on the Neanderthal populations that occupied the northeastern part of the Iberian Peninsula at the time. It remains unclear what effects this instability could have exerted on their adaptive behavioral shifts.

Despite temperature oscillations, the climatic pattern associated with Neanderthal occupations in the northeast analyzed using small mammals from MIS 3 always show an important presence of the forest biotope integrated in mosaic environments with high levels of humidity (López-García et al., 2014b). This is confirmed for the Abric Romaní site, where open forest dominated the entire sequence, with only punctuated periods of opening and active water courses next to the rock-shelter (Chapter 4 and 6). Anthracological and palynological studies reported widespread *Pinus* type *sylvestris* throughout the territory (Allué et al., 2017; Burjachs et al., 2012; Burjachs and Allué, 2003; Burjachs and Julià, 1994). These forests possibly provided the necessary resources for the survival of Neanderthal groups, where they were able to develop gathering and hunting activities, along with obtaining the necessary fuel to develop their pyrotechnic activities, which has been widely documented in the occupations of the rock-shelter

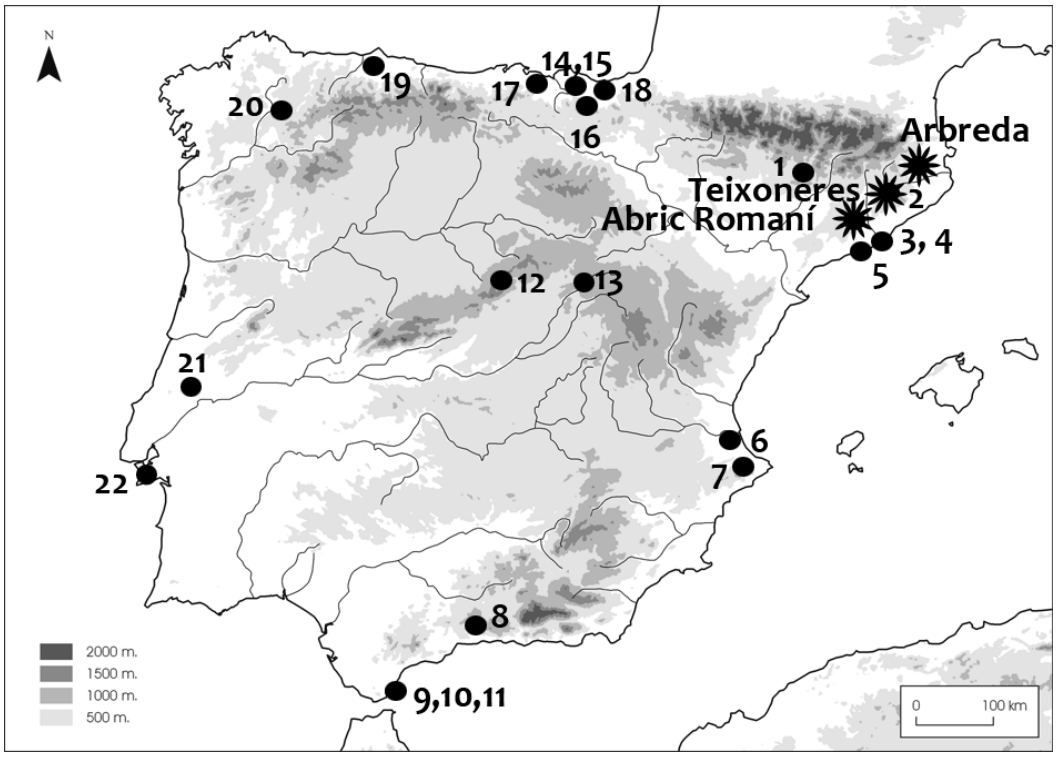

Figure 9.4 Location of Middle Palaeolithic sites with palaeoenvironmental studies discussed: 1, Cova Gran de Santa Linyà; 2, Toll cave; 3, Cova del Rinoceront; 4, Cova del Coll Verdaguer; 5, Cova del Gegant; 6, Bolomor; 7, El Salt; 8, Zafarraya cave; 9, Vanguard cave; 10, Gorham's cave; 11, Ibex cave; 12, Cueva del Camino; 13, Los Casares; 14, Askondo; 15, Arlanpe cave; 16, Lezetxiki II; 17, El Mirón; 18, Cueva Amalda; 19, Cueva del Conde; 20, Cova Eiros; 21, Caldeirão; 22, Figueira Brava.

thorough fire structures, charcoals, and fossilized wood negatives. Charcoal analysis, wood imprints and combustion structures recovered in Abric Romaní reveal that wood exploitation, as fuel or even as raw material for tools, was an organized activity related to the daily requirements of the occupations at the site, probably gathered from the areas surrounding the shelter (Allué et al., 2017; Solé et al., 2013; Vallverdú et al., 2012).

Marine records reveal that the preservation of extended woodland masses is a regional trend characteristic of Iberia and the Mediterranean Basin (e.g, Fletcher et al., 2010; Fletcher and Sánchez-Goñi, 2008; Harrison and Sanchez Goñi, 2010). This makes Iberia an optimal region for human occupation. Moreover, the detection of these forest covertures next to Mediterranean archaeological sites associated with Neanderthals may suggest an ecological preference for arboreal covertures by these populations when establishing their occupation. Neanderthal settlements are placed mainly in ecotones with high ecological diversity, procured by Iberian thermo-Mediterranean climate, with only punctuated semi-arid peaks. The maintenance of woodland cover and mosaic landscapes preserves the ecological quality of the surrounding area, providing the optimal conditions for ecological and faunal diversity. The selection of the place to establish the settlement is directly related to the availability of resources which assure the survival of the groups. Neanderthals have a good knowledge of their territory where they are able to differentially procure of available biotic resources (Chacón et al., 2007; Fernández-Laso et al., 2010). Among these resources wood for fuel was a priority in decision making regarding site occupation and the duration of those occupations (Allué et al., 2017, 2018). Forest offered to these populations the main vegetal and faunal resources for their daily subsistence.

The end of MIS 3 and the transition MIS 3/2 is also well represented in Iberia, when many sites can be integrated into a regional to global level analysis. Arbreda cave does not demonstrate sharp climatic shift between last moment of Neanderthal occupations (level I) and first anatomically modern humans' records (level H) (ca. 42-41 ka BP). López-García et al. (2015) related level H to the GI10 and describe it as milder than level I, consistent with some of the temperate phases record by palynological studies (Burjachs and Renault-Miskovsky, 1992). Oxygen isotope analysis of level H indicates that these were mild and favorable conditions. However, a slight reduction of Mediterranean species and species with woodland preferences is noticed (Fernández-García et al., 2016; López-García et al., 2015). The same trend is observed in Unit II of Teixoneres cave, which could be contemporaneous, but caution is recommended, considering the lowest chrono-stratigraphic resolution of this unit (ca.33-44) (Rosell et al., 2017; Talamo et al., 2016). If we focus on other Middle-Upper Palaeolithic transitional sites that combine small mammal studies with other climatic proxies, globally no large shifts in local climate or breaks in faunal composition are observed. Indeed, mainly slight increases in temperatures or stable climatic conditions between both types of human occupations are recorded, as occurred in Abric Romaní, Arbreda cave, El Mirón, Cova Eirós, Gorham's cave, Cueva del Conde, Cueva de Amalda, and Toll caves (Blain et al., 2013; Burjachs and Julià, 1994; Cuenca-Bescós et al., 2008, 2009; Fernández-García and López-García, 2013; López-García et al., 2011a, 2011b, 2015; Pemán, 1990; Rey-Rodríguez, 2015). Regarding the landscape, some regions experienced a little advance of forest landscapes (El Mirón and Lezetxiki II) and some others experienced a slight to intense reduction (as in Abric Romaní area, Cova Eirós, Gorham's Cave, Askondo, Arlanpe cave, Los Casares, and Toll caves) (Alcaraz-Castaño et al.,

2017; Blain et al., 2013; Cuenca-Bescós et al., 2008, 2009; Fernández-García and López-García, 2013; Garcia-Ibaibarriaga, 2015; Garcia-Ibaibarriaga et al., 2015; García-Ibaibarriaga et al., 2013; López-García et al., 2011b, 2015; Murelaga et al., 2012; Rey-Rodríguez et al., 2016; Vaquero et al., 2013).

The opening landscape trend initially observed between levels I-H of Arbreda cave through small-mammal communities continues in the latest stages of MIS 3 and early MIS 2 (levels G to C, 38.2-22.9 ka BP). Moreover, an important drop in temperatures is estimated in this region during the Evolved Aurignacian occupations of the cave (level G, 38.2-35.6 ka cal. BP). During the deposition of levels F-E (33.3-22.9 ka cal. BP), palynological and anthracological analyses suggest a landscape dominated by prairies, where *Artemisia* and Asteraceae dominated, with few river pine forest and riverbank trees (Burjachs and Renault-Miskovsky, 1992; Ros, 1987). Nevertheless, it is not until the beginning of MIS 2 in Iberia, when pollen and small-vertebrate analyses detected a clear opening of the landscape with latitudinal or local independence, underscore with the arrival of the Last Glacial Maximum. This phenomenon is recorded by decreasing levels of rainfall, landscape evolution from mesic to xeric habitats and the subsequent loss of extensive forest tracts, (Carrión, 2012; Cuenca-Bescós et al., 2008, 2009; Fernández-García et al., 2016; Finlayson and Carrión, 2007; Garcia-Ibaibarriaga et al., 2015). Therefore, a great climatic difference between Middle to Upper Palaeolithic transition assemblages is dismissed, but this shift seems to occur or at least be recorded later. Thus, the Neanderthal extinction cannot be attributed to a simple environmental factor but may have been a long-term trend. The decreasing levels of rainfall and the increasing aridity during Heinrich Event 4 (around 38 ka cal. BP; Hemming, 2004) and subsequent MIS 2 in Iberia may have caused the loss of extensive forest tracts which could have had a notable influence on Iberian Neanderthals populations used to open, and usually temperate, forest sustained by a moderate or well-balanced supply of moisture. This would have made the last Neanderthal groups more vulnerable, accelerating their fragmentation and influencing their disappearance, as Blain et al. (2013) suggest for the last surviving Neanderthals in southern Iberia (Finlayson et al., 2004, 2006; Finlayson and Carrión, 2007; López-García et al., 2011b, 2013; Sánchez Goñi and D'Errico, 2005; Sepulchre et al., 2007). Climate must have influenced these occupations/replacements in local to regional contexts but clearly not as a general environmental trend/change.

Chapter 10.
Concluding remarks and future perspectives

1. Conclusions

This thesis has completed the ecological reconstruction of four MIS 3 Iberian sequences (Abric Romaní rock-shelter, Xaragalls cave, Teixoneres cave and Arbreda cave) based on small-mammal assemblages (insectivores, bats and rodents) by applying different approaches: taphonomy, palaeoenvironmental reconstructions, and biochemical analysis. Through a detailed analysis combining these approaches both with independent proxies of palaeoecological reconstruction of each site and present-day referential studies, the following conclusions can be presented.

1.1 Oxygen isotope meaning, predator-prey interactions, and seasonality

Owls have been confirmed as the main cause of the small-mammal accumulations in the Pleistocene sequences analyzed in this work. Oxygen isotope compositions on rodent incisors suggest a preferential moment of rodent accumulation related to the season when the predator was more actively hunting. Within each sedimentary unit low $\delta^{18}O$ variability was recorded, never surpassing present-day annual $\delta^{18}O_{mw}$ variability and having a higher mean than present-day $\delta^{18}O_{mw}$ in the recovery locations. Complemented by modern ethological studies in Iberia that identified the period of maximal rodent density and the optimal period of owl hunting as being mainly in spring and early summer months, and by modern $\delta^{18}O_{mw}$ data, the parsimonious hypothesis is that this moment was within the warm season, most likely during spring-early summer months. Rodent assemblages may potentially have been accumulated in these months, reporting the incisors collected isotopic information of the last two months of life of the individual. This hypothesis does not exclude the possibility of accumulations in other seasons, but the probability of record oxygen isotope values during this period is expected to be higher. Other factors, such as spatial variability in oxygen isotope compositions (e.g. altitude) cannot be rejected due to the presence of some outliers. The $\delta^{18}O_p$ values do not seem to be biased as consequence of the physiological and dietary parameters of the wood mouse, the main species sampled. The $\delta^{18}O_p$ values reported from Arvicolinae and Glirinae remains eventually included in the analysis appear well-integrated with the values estimated by the wood mouse. According to the possible seasonal bias recorded in rodent teeth, a regression equation has been proposed here to allow the transformation of median $\delta^{18}O_{mw}$ values recorded in each sedimentary unit to mean annual $\delta^{18}O_{mw}$ approximations.

1.2 Methods for palaeotemperatures and palaeoprecipitation reconstructions with rodent assemblages

Different methods of palaeotemperature reconstruction will give different estimations, because each method has intrinsic limitations and deals with different types of data. Mutual Ecogeographic Range and Bioclimatic Model methods are species-dependent and depend on actualistic principles, whereas oxygen isotopes are strongly influenced by the spatial and temporal origin of the samples and the regression equations applied to convert $\delta^{18}O$ from rodent tooth phosphates into air temperatures. Any of these methods can be affected by taphonomic agents, but in different ways: from bias in small-mammal species composition derived either from predator preferences, or from the seasonality of the accumulation, to diagenetic processes which can alter the chemical properties of the preserved remains. Each method reflects different parameters and possible different temporal scales, depending in great part on the nature of the available or selected samples. Fossil

sedimentological units are essentially palimpsests, which could difficult the isolation of temporal events. For these reasons, a combination of different palaeoecological methods and proxies is essential to obtain faithful environmental reconstructions.

1.3 Palaeoenvironment of Late Pleistocene and MIS3 in northeastern Iberia

Based on oxygen isotopes, globally cool conditions (mean annual temperatures between 9.3 ±2.6 °C to 13.8 ±2.7 °C) were recorded for the northeastern Iberian Peninsula for a great part of the MIS 3 (ca. 30-60 ka). This is globally in agreement with other approaches based on small mammals that point to cold climate and wet environment: mean annual temperatures from 7 °C to 16.8 °C (-6.4 to +3.2 °C with respect to present-day) and mean annual precipitations between 550 mm and 1430 mm (from +682 mm to -69 mm with respect to present-day). However, biochemical results point to milder conditions, closer to present-day temperatures (from -5.5 °C to -0.5 °C) than was previously estimated, despite a layer of Xaragalls cave recording air temperatures comparable to nowadays. Not always coherence with stadial-interstadial fluctuations previously determined was found under the analysis of small mammal's communities and palaeotemperatures estimated. From a regional scale, the recorded palaeoenvironment shows global climatic stability in all sites, with only slight changes related to stadial-interstadial pulsations. This is reflected mainly in faunal communities' oscillations between Mediterranean and mid-European species abundances and usually supported by independent palaeoenvironmental proxies at the sites (e.g. pollen, charcoals, use-wear analyses). According to small-mammal species abundances, and in agreement with other palaeoenvironmental proxies, woodland formations are always abundant throughout the sequences. This environmental trend is especially clear for Xaragalls cave and Abric Romaní rock-shelter, but also in Teixoneres cave. However, the latest stages of MIS 3, represented by the Arbreda cave sequence, show a slight climatic deterioration and an opening of the landscape.

1.4 Singularity of Iberia and its importance in Prehistory

Oxygen isotope analyses underscore the particularities of Iberia in the present-day and also in the past. Firstly, present-day higher annual $\delta^{18}O_{mw}$ variability is observed, in contrast to localities from northern latitudes. This is mainly related to $\delta^{18}O_{mw}$ enrichment in summer. The influence of African air masses seems crucial in current Iberian climatic dynamics, but it is difficult to confirm whether this influence was the same in the past. A linear regression is proposed here specifically for the reconstruction of mean annual air temperatures from $\delta^{18}O$ in the Iberian Peninsula. Secondly, low variance of the $\delta^{18}O$ values was observed among fossil deposits, both within and among sites. This fact contrasts with notable heterogeneity in $\delta^{18}O$ values recorded in contemporaneous fossil assemblages from Western France. This climatic stability, besides the continuous maintenance of woodland covertures together with globally stable rodent communities, demonstrate the singularities of the Iberian Peninsula, in contrast to the high climatic instability in Eurasia, where the degree of woodland fluctuated, and cold-dependent species were frequent.

1.5 Neanderthal subsistence in northeastern Iberia

The analysis of small mammals through different ecological approaches, complemented by larger-scale proxies (Greenland ice cores and Iberian marine cores), denote more globally temperate

and stable conditions in northeastern Iberia during Neanderthal occupations within the MIS 3 (ca. 30-60 ka) than expected. The slight fluctuations mainly detected by small-mammal fauna compositions between cool-temperate climate and open-closed landscape have no special influence either in Neanderthals' short- or long-term frequentation of the analyzed sites. The important presence of woodland, integrated in mosaic environments with high levels of humidity, is clearly highlighted, indicating: 1) the preservation of this kind of landscape even in moments of European climatic detriment, transforming Iberia into an optimal region for human subsistence and/or, 2) the ecological preference of Neanderthal populations for arboreal covertures in deciding where to establish their occupations, due to woodland provided essential resources to their subsistence. Great climatic rupture between Middle and Upper Palaeolithic transition assemblages is not supported, and if this shift occurred it was after the Neanderthals' disappearance. Nevertheless, the progressive reduction of woodland in Mediterranean regions with the arrival of MIS 2 could be even more influential than climatic deterioration for these populations, especially if the milder and probably stable conditions of this region over thousands of years are considered.

2. Future perspectives

Using a $\delta^{18}O$ approach allows us to increase our knowledge of the palaeoecology of MIS3 in Iberia and complement other methods based on small mammal assemblages, including aspects such as climatic instability events, aridity, or seasonality of the accumulations. The application of the method here exposed to the other Iberian fossil sites can provide a good tool for the understanding of the ecological conditions of MIS3 in which Neanderthal populations developed, and also to acquire more information about predator-prey interactions. Nevertheless, the studies based on oxygen isotope studies on rodent teeth are still in their first phase of development and therefore more research is necessary to understand many of the problems revealed by this work. Knowledge of seasonality patterns, which necessitate more reflection on predators-prey relationship based on owl and rodent ethology and taphonomy, is needed (e.g., Andrews and Fernández-Jalvo, 2018). Modern referential coming from owl pellets, relating oxygen isotope compositions with complete taphonomic studies that evaluate the seasonal production of rodent prey, are needed to confirm or reject some of the hypotheses presented here. Histological studies on rodents (such as Klevezal, 2010; Rinaldi and Theodore, 2004) are a promising way to deal with the time period represented by rodent teeth and evaluate their preferential accumulation in fossil deposits. Moreover, some reflection is necessary regarding what this seasonality may mean for other works that focus on small mammal ecology.

Oxygen isotope studies focusing on the carbonate portion of rodent teeth can offer an interesting opportunity to deal with extensive biochemical studies, since this kind of studies allow for the processing of several samples in less time and at lower cost than phosphates. The application of this method is currently limited by ongoing uncertainties surrounding the relationship between the $\delta^{18}O$ of rodent tooth carbonate fraction and the $\delta^{18}O$ of meteoric waters, along with the preservation of this component in relation to $\delta^{18}O_{p.}$ This research is challenging and some interesting research that considers modern specimens with an archaeo-palaeonlogical objective is appearing (e.g., Jeffrey et al., 2015; Peneycad et al., 2019). Otherwise, to the author's knowledge only one study (Barham et al., 2017) has addressed the influences that chemical alteration

derived from predator digestion can have in the preservation of the original oxygen isotope composition of rodent teeth. In these sense, further studies on diagenetic alterations derived from the predator are required, as well as increases in the knowledge of how post-depositional agents can alter the conservation of isotopic compositions. Finally, only few localities in Iberia have available long-term real measurements of direct samples of $\delta^{18}O_{mw}$, collected by the International Atomic Energy Agency and World Meteorological Organization stations (IAEA/WMO, 2018), especially in northeast Spain, where only two stations are available on the coast. Considering the gaps in the spatial distribution of isotope measurements on precipitation in the Iberian Peninsula by IAEA-WMO stations, the estimated $\delta^{18}O_{mw}$ values from OIPC may not precisely reflect the oxygen isotope compositions of meteoric water at the studied sites. Measurements of $\delta^{18}O_{mw}$ values on surface water sources near studied sites are recommended for future research.

General references

AEMET & IMP, 2011. Atlas climático ibérico. Temperatura del aire y precipitación (1971-2000). Agencia Española de Meteorología & Instituto de Meteorología de Portugal.

Alcaraz-Castaño, M., Alcolea-González, J., Kehl, M., Albert, R.-M., Baena-Preysler, J., de Balbín-Behrmann, R., Cuartero, F., Cuenca-Bescós, G., Jiménez-Barredo, F., López-Sáez, J.-A., Piqué, R., Rodríguez-Antón, D., Yravedra, J., Weniger, G.-C., 2017. A context for the last Neandertals of interior Iberia: Los Casares cave revisited. Plos One 12, e0180823.

Alférez, F., 1990. Mamíferos, in: Meléndez, B. (Ed.), Paleontología 3. Volumen 1. Madrid, pp. 1–21.

Allué, E., Martínez-Moreno, J., Roy, M., Benito-Calvo, A., Mora, R., 2018. Montane pine forests in NE Iberia during MIS 3 and MIS 2. A study based on new anthracological evidence from Cova Gran (Santa Linya, Iberian Pre-Pyrenees). Review of Palaeobotany and Palynology 258, 62–72.

Allué, E., Solé, A., Burguet-Coca, A., 2017. Fuel exploitation among Neanderthals based on the anthracological record from Abric Romaní (Capellades, NE Spain). Quaternary International 431, 6–15.

Álvarez-Lao, D.J., García, N., 2010. Chronological distribution of Pleistocene cold-adapted large mammal faunas in the Iberian Peninsula. Quaternary International 212, 120–128.

Álvarez-Lao, D.J., Rivals, F., Sánchez-Hernández, C., Blasco, R., Rosell, J., 2017. Ungulates from Teixoneres Cave (Moià, Barcelona, Spain): Presence of cold-adapted elements in NE Iberia during the MIS 3. Palaeogeography, Palaeoclimatology, Palaeoecology 466, 287–302.

Amiot, R., Lécuyer, C., Buffetaut, E., Fluteau, F., Legendre, S., Martineau, F., 2004. Latitudinal temperature gradient during the Cretaceous Upper Campanian – Middle Maastrichtian: $\delta^{18}O$ record of continental vertebrates. Earth and Planetary Science Letters 226, 255–272.

Andrews, P., Whybrow, P., 2005. Taphonomic observations on a camel skeleton in a desert environment in Abu Dhabi. Palaeontologia Electronica 8, 1–17.

Andrews, P., 2006. Taphonomic effects of faunal impoverishment and faunal mixing. Palaeogeography, Palaeoclimatology, Palaeoecology 241, 572–589.

Andrews, P., 1990. Owls, Caves and Fossils. Predation, preservation and accumulation of small mammal bones in caves, with an analysis of the Pleistocene Cave Faunas from Westbury-sub-Mendip, Somerset, UK. The University of Chicago, Chicago.

Andrews, P., Cook, J., 1985. Natural modifications to bones in temperate setting. Man 20, 675–691.

Andrews, P., Evans, E.M.N., 1983. Small mammal bone accumulations produced by mammalian carnivores. Paleobiology 93, 289–307.

Andrews, P., Fernández-Jalvo, Y., 2018. Seasonal variation in prey composition and digestion in small mammal predator assemblages. International Journal of Osteoarchaeology 1–14.

Ardrey, R., 1983. La evolución del hombre: la hipótesis del cazador. Alianza, Madrid.

Arribas, Ó., 2004. Fauna y paisaje de los Pirineos en la Era Glaciar. Lynx, Barcelona.

Arrizabalaga, Á., 2004. Paleoclimatología y cronología del Würm reciente: un intento de síntesis. Zephyrus 57, 27–53.

Arsuaga, J.L., Baquedano, E., Pérez-González, A., Sala, N., Quam, R.M., Rodríguez, L., García, R., García, N., Álvarez-Lao, D.J., Laplana, C., Huguet, R., Sevilla, P., Maldonado, E., Blain, H.-A., Ruiz-Zapata, M.B., Sala, P., Gil-García, M.J., Uzquiano, P., Pantoja, A., Márquez, B., 2012a. Understanding the ancient habitats of the last-interglacial (late MIS 5) Neanderthals of central Iberia: Paleoenvironmental and taphonomic evidence from the Cueva del Camino (Spain) site. Quaternary International 275, 55–75.

Arsuaga, J.L., Fernández Peris, J., Gracia-Téllez, A., Quam, R., Carretero, J.M., Barciela González, V., Blasco, R., Cuartero, F., Sañudo, P., 2012b. Fossil human remains from Bolomor Cave (Valencia, Spain). Journal of Human Evolution 62, 629–639.

Ayliffe, L.K., Lister, A.M., Chivas, A.R., 1992. The preservation of glacial-interglacial climatic signatures in the oxygen isotopes of elephant skeletal phosphate. Palaeobiodiversity and Palaeoenvironments 99, 179–191.

Bab, I., Hajbi-Yonissi, C., Gabet, Y., Müller, R., 2007. Micro-Tomographic Atlas of the Mouse Skeleton. Springer, New York.

Bañuls-Cardona, S., Rodríguez, P.M., López-García, J.M., Morales, J.I., Cuenca-Bescós, G., Vergès, J.M., 2017. Human impact on small-mammal diversity during the middle- to late-Holocene in Iberia: The case of El Mirador cave (Sierra de Atapuerca, Burgos, Spain). The Holocene 27, 1067–1077.

Bañuls Cardona, S., López-García, J.M., Blain, H.-A., Canals Salomó, A., 2012. Climate and landscape during the Last Glacial Maximum in southwestern Iberia: The small-vertebrate association from the Sala de las Chimeneas, Maltravieso, Extremadura. Comptes Rendus Palevol 11, 31–40.

Barham, M., Blyth, A.J., Wallwork, M.D., Joachimski, M.M., Martin, L., Evans, N.J., Laming, B., McDonald, B.J., 2017. Digesting the data - Effects of predator ingestion on the oxygen isotopic signature of micro-mammal teeth. Quaternary Science Reviews 176, 71–84.

Barroso, C., Abassi, M., Bailon, S., Cheylan, M., Desclaux, E., El Gennouni, K., Fons, R., Haquart, A., Fernández Carrasquilla, F., Moigne, A.-M., Poitevin, F., Prodon, R., Vilette, P., 2003. Tafonomía: Significación Paleobiogeografía, Paleoecología y Paleoclimática de las faunas de microvertebrados del Pleistoceno Superior de la Cueva del Boquete de Zafarraya, in: Barroso Ruíz, C. (Ed.), Monografía Del Boquete de Zafarraya. pp. 289–299.

Barroso, C., Caparrós, M., Barsky, D., Moigne, A.-M., Monclova, A., 2014. Cueva del Boquete de Zafarraya: Un yacimiento de neandertales en el sur Iberia, in: Sala Ramos, R. (Ed.), Los Cazadores Recolectores Del Pleistoceno y Del Holoceno En Iberia y El Estrecho de Gibraltar: Estado Actual Del Conocimiento Del Registro Arqueológico. Universidad de Burgos, Burgos, pp. 463–472.

Behrensmeyer, A.K., 1986. Trampling as a cause of bone surface damage and pseudo-cutmarks. Nature 319, 768–771.

Behrensmeyer, A.K., 1978. Taphonomic and ecologic information from bone weathering. Paleobiology 4, 150–162.

Behrensmeyer, A.K., 1975. The taphonomy and paleoecology of Plio-Pleistocene vertebrate assemblages east of Lake Rudolf, Kenya. Bulletin of The Museum of Comparative Zoology 146, 476–578.

Bender, M.M., 1968. Mass Spectrometric Studies of Carbon 13 Variations in Corn and Other Grasses. Radiocarbon 10, 468–472.

Bennàsar, M., 2010. Tafonomía de micromamíferos del Pleistoceno Inferior de la Sierra de Atapuerca (Burgos): Sima del Elefante y Gran Dolina. Universitat Rovira i Virgili (Tarragona). Doctoral thesis (inedit).

Bennett, J.L., 1999. Thermal Alteration of Buried Bone. Journal of Archaeological Science 26, 1–8.

Bernard, A., Daux, V., Lécuyer, C., Brugal, J., Genty, D., Wainer, K., Gardien, V., Fourel, F., Jaubert, J., 2009. Pleistocene seasonal temperature variations recorded in the $\delta^{18}O$ of *Bison priscus* teeth. Earth and Planetary Science Letters 283, 133–143.

Blain, H.-A., Bailon, S., Cuenca-Bescós, G., Arsuaga, J.L., Bermúdez de Castro, J.M., Carbonell, E., 2009. Long-term climate record inferred from early-middle Pleistocene amphibian and squamate reptile assemblages at the Gran Dolina Cave, Atapuerca, Spain. Journal of Human Evolution 56, 55–65.

Blain, H.-A., Gleed-Owen, C.P., López-García, J.M., Carrión, J.S., Jennings, R., Finlayson, G., Finlayson, C., Giles-Pacheco, F., 2013. Climatic conditions for the last Neanderthals: Herpetofaunal record of Gorham's Cave, Gibraltar. Journal of Human Evolution 64, 289–299.

Blain, H.A., Laplana, C., Sevilla, P., Arsuaga, J.L., Baquedano, E., Pérez-González, A., 2014. MIS 5/4 transition in a mountain environment: Herpetofaunal assemblages from Cueva del Camino, central Spain. Boreas 43, 107–120.

Blain, H.A., Lozano-Fernández, I., Agustí, J., Bailon, S., Menéndez Granda, L., Espígares Ortiz, M.P., Ros-Montoya, S., Jiménez Arenas, J.M., Toro-Moyano, I., Martínez-Navarro, B., Sala, R., 2016. Refining upon the climatic background of the Early Pleistocene hominid settlement in western Europe: Barranco León and Fuente Nueva-3 (Guadix-Baza Basin, SE Spain). Quaternary Science Reviews 144, 132–144.

Blake, R.E., Neil, R.O., Garcia, G.A., 1997. Oxygen isotope systematics of biologically mediated reactions of phosphate: I. Microbial degradation of organophosphorus compounds. Geochimica et Cosmochimica Acta 61, 4411–4422.

Blanco, J.C., 1998. Mamíferos de España. Vol II. Cetáceos, Artiodáctilos, Roedores y Lagomorfos de la península Ibérica, Baleares y Canarias. Planeta, Barcelona.

Blumenthal, S.A., Cerling, T.E., Chritz, K.L., Bromage, T.G., Kozdon, R., Valley, J.W., 2014. Stable isotope time-series in mammalian teeth: In situ $\delta^{18}O$ from the innermost enamel layer. Geochimica et Cosmochimica Acta 124, 223–236.

Bocherens, H., 1997. Isotopic biogeochemistry as a marker of Neandertal. Anthropologischer Anzeiger 55, 101–120.

Bond, G., Heinrich, H., Broecker, W., Laberyrie, L., McManus, J., Andrews, J., Huon, S., Jantschik, R., Clasen, S., Simet, C., Tedesco, K., Klas, M., Bonani, G., Ivy, S., 1992. Evidence for massive discharges of icebergs into the North Atlantic Ocean during the last glacial period. Letters to Nature 360, 245–249.

Bowen, G.J., 2017. The Online Isotopes in Precipitation Calculator, Version 3.1 (4/2017) [WWW Document]. URL http://waterisotopes.org

Brain, C.K., 1981. The hunters or the hunted? An introduction to African Cave taphonomy. University of Chicago Press, Chicago & London.

Bromage, T.G., 1984. Interpretation of Scanning Electron Microscopic Images of abraded forming bones surfaces. American Journal of Physical Anthropology 64, 161–178.

Buikstra, J.E., Swegle, M., 1989. Bone modification due to burning: experimental evidence, in: Buikstra, J.E., Swegle, M., Bonnichsen, R., Sorg, H. (Eds.), Bone Modification. University of Maine, Orono, pp. 247–258.

Burjachs, F., Allué, E., 2003. Paleoclimatic evolution during the last glacial cycle at the NE of the Iberian Peninsula, in: Ruiz, M.B., Dorado, M., Valdeolmillos, A., Gil, M.J., Bardají, T., de Bustamante, I., Martínez, I. (Eds.), Quaternary Climatic Changes and Environmental Crises in the Mediterranean Region. Universidad de Alcalá, Ministerios de Ciencia y Tecnologia, INQUA, Alcalá de Henares (Madrid), pp. 191–200.

Burjachs, F., Julià, R., 1996. Palaeonvironmental evolution during the Middle-Upper Palaeolithic transition in the NE of the Iberian Peninsula, in: Carbonell, E., Vaquero, M. (Eds.), The Last Neandertals, the First Anatomically Modern Humans. Cultural Change and Human Evolution: The Crisis at 40 Ka BP. Gràfiques Lluc, Igualada (Barcelona), pp. 377–383.

Burjachs, F., Julià, R., 1994. Abrupt Climatic Changes during the Last Glaciation Based on Pollen Analysis of the Abric Romani, Catalonia, Spain. Quaternary Research 42, 308-315.

Burjachs, F., López-García, J.M., Allué, E., Blain, H.-A., Rivals, F., Bennàsar, M., Expósito, I., 2012. Palaeoecology of Neanderthals during Dansgaard–Oeschger cycles in northeastern Iberia (Abric Romaní): From regional to global scale. Quaternary International 247, 26–37.

Burjachs, F., Renault-Miskovsky, J., 1992. Paléoenvironnement et paléoclimatologie de la Catalogne durant près de 30,000 ans (du Würmien ancien au début de l'Holocène) d'après la Palynologie du site de l'Arbreda (Gérone, Catalogne). Quaternaire 3, 75–85.

Cáceres, I., 2002. Tafonomía de yacimientos antrópicos en karst. Complejo Galería (Sierra de Atapuerca, Burgos), Vanguard Cave (Gibraltar) y Abric Romaní (Capellades, Barcelona). Univeristat Rovira i Virgili. Doctoral thesis (inedit).

Camps, M., Higham, T., 2012. Chronology of the Middle to Upper Palaeolithic transition at Abric Romaní, Catalunya. Journal of Human Evolution 62, 89–103.

Carbonell, E., Cebrià, A., Allué, E., Cáceres, I., Castro, Z., Díaz, R., Esteban, M., Ollé, A., Pastó, I., Rodríguez, X.P., Rosell, J., Sala, R., Vallverdú, J., Vaquero, M., Vergés, J.M., 1996. Behavioural and organizational complexity in the Middle Palaeolithic from the Abric Romaní, in: Carbonell, E., Vaquero, M. (Eds.), The Last Neandertals, the First Anatomically Modern Humans. Cultural Change and Human Evolution: The Crisis at 40 Ka BP. Universitat de Tarragona, Tarragona, pp. 385–434.

Carrión, J.S., 2012. Paleoflora y paleovegetación de la Península Ibérica e Islas Baleares: Plioceno-Cuaternario. Ministerio de Economia y Competitividad - Universidad de Murcia, Murcia.

Carrión, J.S., Ochando, J., Fernández, S., Blasco, R., Rosell, J., Munuera, M., Amorós, G., Martín-Lerma, I., Finlayson, S., Giles, F., Jennings, R., Finlayson, G., Giles-Pacheco, F., Rodríguez-Vidal, J., Finlayson, C., 2018. Last Neanderthals in the warmest refugium of Europe: Palynological data from Vanguard Cave. Review of Palaeobotany and Palynology 259, 63–80.

Chacón, M.G., Fernández-Laso, M.C., García-Antón, M.D., Allué, E., 2007. Level K and L from Abric Romaní (Barcelona, Spain): procurement resources and territory management. Proceedings of the XV World UISPP Congress, Lisbon 5, 187–197.

Chaline, J., 2005. Les messages biochronologiques des faunes. Bulletin de la Société Préhistorique Française 102, 741–747.

Chaline, J., 1988. Paleocronòmetres, paleotermòmetres i paleoindicadors dels entorns prehistòrics, els rosegadors irremplaçables. Cota Zero 4, 61–64.

Chaline, J., 1974. Les proies des rapaces. Doin Éditeurs, Paris.

Chaline, J., 1972. Les rongeurs du Pléistocène moyen et supérieur de France. Éditions du Centre National de la Recherche Scientifique, Paris.

Chaline, J., 1970. La signification des rongeurs dans les dépôts quaternaires. Bull. de l'Assoc. Française pour l'Etude du Quaternaire 4, 229–241.

Climate-Data.org [WWW Document], 2018. URL https://es.climate-data.org/

Coady, J.M., Toto, P.D., Santangelo, M.V., 1967. Histology of the Mouse Incisor. Journal of Dental Research 46, 384–388.

Comay, O., Dayan, T., 2018. Taphonomic signatures of owls: New insights into micromammal assemblages. Palaeogeography, Palaeoclimatology, Palaeoecology 492, 81–91.

Coplen, T.B., 1995. Reporting od stable carbon, hydrogen, and oxygen isotopic abundances, in: Reference and Intercomparision Materials for Stable Isotopes of Light Elements. International Atomic Energy Agency, Vienna, pp. 31–34.

Courty, M.-A., Goldberg, P., MAcPhail, R., 1989. Soils and micromorphology in archaeology. Cambridge University Press, Cambridge.

Craig, H., 1961. Isotopic Variations in Meteoric Waters. Science 133, 1702–1703.

Crowson, R.A., Showers, W.J., Wright, E.K., Hoering, T.C., 1991. Preparation of Phosphate Samples for Oxygen Isotope Analysis. Analytical Chemistry 63, 2397–2400.

Cuenca-Bescós, G., Blain, H.-A., Rofes, J., López-García, J.M., Lozano-Fernández, I., Galán, J., Núñez-Lahuerta, C., 2016. Updated Atapuerca biostratigraphy: Small-mammal distribution and its implications for the biochronology of the Quaternary in Spain. Comptes Rendus Palevol 15, 621–634.

Cuenca-Bescós, G., López-García, J.M., Galindo-Pellicena, M.A., García-Perea, R., Gisbert, J., Rofes, J., Ventura, J., 2014. Pleistocene history of *Iberomys*, an endangered endemic rodent from southwestern Europe. Integrative Zoology 9, 481–497.

Cuenca-Bescós, G., Melero-Rubio, M., Rofes, J., Martínez, I., Arsuaga, J.L., Blain, H.-A., López-García, J.M., Carbonell, E., Bermudez de Castro, J.M., 2011. The Early–Middle Pleistocene environmental and climatic change and the human expansion in Western Europe: A case study with small vertebrates (Gran Dolina, Atapuerca, Spain). Journal of Human Evolution 60, 481–491.

Cuenca-Bescós, G., Rofes, J., Garcia-Pimienta, J., 2005. Environmental change across the Early-Middle Pleistocene transition: small mammalian evidence from the Trinchera Dolina cave, Atapuerca, Spain. Geological Society, London, Special Publications 247, 277–286.

Cuenca-Bescós, G., Rofes, J., López-García, J.M., Blain, H.-A., De Marfá, R.J., Galindo-Pellicena, M.A., Bennásar-Serra, M.L., Melero-Rubio, M., Arsuaga, J.L., Bermúdez de Castro, J.M., Carbonell, E., 2010. Biochronology of Spanish Quaternary small vertebrate faunas. Quaternary International 212, 109–119.

Cuenca-Bescós, G., Straus, L.G., González Morales, M.R., García Pimienta, J.C., 2009. The reconstruction of past environments through small mammals: from the Mousterian to the Bronze Age in El Mirón Cave (Cantabria, Spain). Journal of Archaeological Science 36, 947–955.

Cuenca-Bescós, G., Straus, L.G., González Morales, M.R., García Pimienta, J.C., 2008. Paleoclima y Paisaje del final del Cuaternario en Cantabria: los pequeños mamíferos de la cueva del Mirón (Ramales de la Victoria). Revista Española de Paleontología 23, 91–126.

Cuvier, G., 1817. Le Regne animal distribué d'après son organisation. Tome 1 l'introdution, les mammifères et les oiseaux. Chêz Ditriville, Paris.

D'Angela, D., Longinelli, A., 1990. Oxygen isotopes in living mammal's bone phosphate: Further results. Chemical Geology 86, 75–82.

D'Errico, F., Sánchez Goñi, M.F., 2003. Neandertal extinction and the millennial scale climatic variability of OIS 3. Quaternary Science Reviews 22, 769–788.

Daams, R., Freudenthal, M., 1987. Synopsis of the Dutch-Spanish collaboration program in the Aragonian type area, 1975-1986. Scripta Geologica 1 (Special Issue), 3–18.

Dansgaard, W., 1964. Stable isotopes in precipitation. Tellus XVI, 436–468.

Dansgaard, W., Clausen, H.B., Gundestrup, N., Hammer, U., Johnsen, S.F., Kristinsdottir, P.M., Reeh, N., 1982. A new Greenland deep ice core. Science 218, 1273–1277.

Dauphin, Y., Andrews, P., Denys, C., Fernández-Jalvo, Y., Williams, T., 2003. Structural and Chemical Bone Modifications in a Modern Owl Pellet Assemblage from Olduvai Gorge (Tanzania). Journal of Taphonomy 1, 209–232.

Dauphin, Y., Williams, C.T., 2004. Diagenetic trends of dental tissues. Comptes Rendus Palevol 3, 583–590.

Daura, J., Sanz, M., Allué, E., Vaquero, M., López-García, J.M., Sánchez-Marco, A., Domènech, R., Martinell, J., Carrión, J.S., Ortiz, J.E., Torres, T., Arnold, L.J., Benson, A., Hoffmann, D.L., Skinner, A.R., Julià, R., 2017. Palaeoenvironments of the last Neanderthals in SW Europe (MIS 3): Cova del Coll Verdaguer (Barcelona, NE of Iberian Peninsula). Quaternary Science Reviews 177, 34–56.

Daura, J., Sanz, M., García, N., Allué, E., Vaquero, M., Fierro, E., Carrión, J.S., López-García, J.M., Blain, H.A., Sánchez-Marco, A., Valls, C., Albert, R.M., Fornós, J.J., Julià, R., Fullola, J.M., Zilhão, J., 2013. Terrasses de la Riera dels Canyars (Gavà, Barcelona): The landscape of Heinrich Stadial 4 north of the " Ebro frontier" and implications for modern human dispersal into Iberia. Quaternary Science Reviews 60, 26–48.

Daura, J., Sanz, M., Julià, R., García-Fernández, D., Fornós, J.J., Vaquero, M., Allué, E., López-García, J.M., Blain, H.A., Ortiz, J.E., Torres, T., Albert, R.M., Rodríguez-Cintas, À., Sánchez-Marco, A., Cerdeño, E., Skinner, A.R., Asmeron, Y., Polyak, V.J., Garcés, M., Arnold, L.J., Demuro, M., Pike, A.W.G., Euba, I., Rodríguez, R.F., Yagüe, A.S., Villaescusa, L., Gómez, S., Rubio, A., Pedro, M., Fullola, J.M., Zilhão, J., 2015. Cova del Rinoceront (Castelldefels, Barcelona): a terrestrial record for the Last Interglacial period (MIS 5) in the Mediterranean coast of the Iberian Peninsula. Quaternary Science Reviews 114, 203–227.

Denys, C., 2000. Small mammals of Ibex Cave: biostratigraphical and palaecological remarks, in: Finlayson, C., Finlayson, G., Fa, D. (Eds.), Gibraltar during the Quaternary. Heritage Publications, pp. 215–225.

Denys, C., 1985. Nouveaux critères de reconaissance des concentrations de microvertébrés d'aprés l'étude des pelotes de chouettes du Bostwana (Afrique australe). Bulletin Muséum National d'Historie Naturelle 4, 879–933.

Denys, C., Patou-Mathis, M., 2004. Les agents taphonomiques impliqués dans la formation des sites paléontologiques et archéologiques, in: Denys, C., Patou-Mathis, M. (Eds.), Manuel de Taphonomie. Errance, Arles, pp. 31–64.

Denys, C., Williams, C.T., Dauphin, Y., Andrews, P., Fernandez-Jalvo, Y., 1996. Diagenetical changes in Pleistocene small mammal bones from Olduvai Bed I. Palaeogeography, Palaeoclimatology, Palaeoecology 126, 121–134.

Desclaux, E., Hanquet, C., El Guennouni, K., 2011. Origine(s) des accumulations de micromammiferes dans quelques sites prehistoriques du Pleistocene Moyen et Superieur d'Europe Meridionale, in: Laroulandie, V., Mallye, J.-B., Denys, C. (Eds.), Taphonomie Des Petits Vertébrés: Référentiels et Transferts Aux Fossiles. British Archaeological Reports, International Series 2269, Oxford, pp. 101–118.

Dincauza, D.F., 2000. Environmental Archaelogy. Cambridge University Press, Cambridge.

Dodson, P., 1973. The significance of small bones in paleoecological interpretation. Contributions to Geology, University of Wyoming 12.

Dodson, P., Wexlar, D., 1979. Taphonomic investigations of owl pellets. Paleobiology 5, 275–284.

Domínguez-Rodrigo, M., de Juana, S., Galán, A.B., Rodríguez, M., 2009. A new protocol to differentiate trampling marks from butchery cut marks. Journal of Archaeological Science 36, 2643–2654.

Duke, G.E., Jeers, A.A., Loft, G., Evanson, O.A., 1975. Gastric digestion in some systems. Comparative Biochemistry and Physiology 50, 649–656.

Efremov, J.A., 1940. Taphonomy: new branch of Paleontology. Pan-American Geologist 74, 81–93.

Evans, E.M.N., Van Couvering, J.A.H., Andrews, P., 1981. Palaeoecology of Miocene sites in Western Kenya. Journal of Human Evolution 10, 99–116.

Fagoaga, A., Ruiz-Sánchez, F.J., Laplana, C., Blain, H.A., Marquina, R., Marin-Monfort, M.D., Galván, B., 2018. Palaeoecological implications of Neanderthal occupation at Unit Xb of El Salt (Alcoi, eastern Spain) during MIS 3 using small mammals proxy. Quaternary International 481, 101–112.

Fernández-García, M., López-García, J.M., 2013. Palaeoecology and biochronology based on the rodents analysis from the Late Pleistocene/Holocene of Toll Cave (Moià, Barcelona). Spanish Journal of Palaeontology 28, 227–238.

Fernández-García, M., López-García, J.M., Bennàsar, M., Gabucio, M.J., Bargalló, A., Gema Chacón, M., Saladié, P., Vallverdú, J., Vaquero, M., Carbonell, E., 2018. Paleoenvironmental context of Neanderthal occupations in northeastern Iberia: The small-mammal assemblage from Abric Romaní (Capellades, Barcelona, Spain). Palaeogeography, Palaeoclimatology, Palaeoecology 506, 154–167.

Fernández-García, M., López-García, J.M., Lorenzo, C., 2016. Palaeoecological implications of rodents as proxies for the Late Pleistocene–Holocene environmental and climatic changes in northeastern Iberia. Comptes Rendus Palevol 15, 707–719.

Fernández-Jalvo, Y., 1992. Tafonomía de microvertebrados del complejo cárstico de Atapuerca (Burgos). Universidad Complutense de Madrid. Doctoral thesis (inedit).

Fernández-Jalvo, Y., Andrews, P., 2003. Experimental Effects of Water Abrasion on Bone Fragments. Journal of Taphonomy 1, 147–164.

Fernández-Jalvo, Y., Andrews, P., 1992. Small mammal taphonomy of Gran Dolina, Atapuerca (Burgos), Spain. Journal of Archaeological Science 19, 407–428.

Fernández-Jalvo, Y., Andrews, P., Denys, C., Sesé, C., Stoetzel, E., Marin-Monfort, D., Pesquero, D., 2016. Taphonomy for taxonomists: Implications of predation in small mammal studies. Quaternary Science Reviews 139, 138–157.

Fernández-Jalvo, Y., Andrews, P., Sevilla, P., Requejo, V., 2014. Digestion versus abrasion features in rodent bones. Lethaia 47, 323–336.

Fernández-Jalvo, Y., Andrews, P.J., 2016. Atlas of Taphonomic Identifications: 1001+Images of Fossil and Recent Mammal Bone Modification. Springer, Dordrecht.

Fernandez-Jalvo, Y., Avery, D.M., 2015. Pleistocene Micromammals and Their Predators at Wonderwerk Cave, South Africa. African Archaeological Review 32, 751–791.

Fernández-Jalvo, Y., Denys, C., Andrews, P., Williams, T., Dauphin, Y., Humphrey, L., 1998. Taphonomy and palaeoecology of Olduvai Bed-I (Pleistocence, Tanzania). Journal of Human Evolution 34, 137–172.

Fernández-Jalvo, Y., Marín-Monfort, M.D., 2008. Experimental taphonomy in museums: Preparation protocols for skeletons and fossil vertebrates under the scanning electron microscopy. Geobios 41, 157–181.

Fernández-Jalvo, Y., Sánchez-Chillón, B., Andrews, P., Fernández-López, S., Alcalá Martínez, L., 2002. Morphological taphonomic transformations of fossil bones in continental environments, and repercussions on their chemical composition. Archaeometry 44, 353–361.

Fernández-Jalvo, Y., Scott, L., Andrews, P., 2011. Taphonomy in palaeoecological interpretations. Quaternary Science Reviews 30, 1296–1302.

Fernández-Laso, M.C., Rivals, F., Rosell, J., 2010. Intra-site changes in seasonality and their consequences on the faunal assemblages from Abric Romaní (Middle Palaeolithic, Spain). Quaternaire 21, 155–163.

Fernández-López, S., 2000. Temas de tafonomía. Universidad Complutense de Madrid, Madrid.

Finlayson, C., Carrión, J.S., 2007. Rapid ecological turnover and its impact on Neanderthal and other human populations. Trends in Ecology and Evolution 22, 213–222.

Finlayson, C., Fa, D.A., Finlayson, G., Pacheco, F.G., Vidal, J.R., 2004. Did the moderns kill off the Neanderthals? A reply to F. d'Errico and Sánchez Goñi. Quaternary Science Reviews 23, 1205–1209.

Finlayson, C., Finlayson, S., Giles, F., Giles, F., Rodriguez, J., 2016. Using birds as indicators of Neanderthal environmental quality: Gibraltar and Zafarraya compared 421, 32–45.

Finlayson, C., Giles Pacheco, F., Rodríguez-Vidal, J., Fa, D.A., María Gutierrez López, J., Santiago Pérez, A., Finlayson, G., Allue, E., Baena Preysler, J., Cáceres, I., Carrión, J.S., Fernández Jalvo, Y., Gleed-Owen, C.P., Jimenez Espejo, F.J., López, P., Antonio López Sáez, J., Antonio Riquelme Cantal, J., Sánchez Marco, A., Giles Guzman, F., Brown, K., Fuentes, N., Valarino, C.A., Villalpando, A., Stringer, C.B., Martinez Ruiz, F., Sakamoto, T., 2006. Late survival of Neanderthals at the southernmost extreme of Europe. Nature 443, 850–853.

Flanagan, L.B., Ehleringer, J.R., Pataki, D.E., 2005. Stable isotopes and biosphere-atmosphere interactions. Processes and biological controls. Elsevier Press, San Diego.

Fletcher, W.J., Sánchez-Goñi, M.F., 2008. Orbital- and sub-orbital-scale climate impacts on vegetation of the western Mediterranean basin over the last 48,000 yr. Quaternary Research 70, 451–464.

Fletcher, W.J., Sánchez-Goñi, M.F., Peyron, O., Dormoy, I., 2010a. Abrupt climate changes of the last deglaciation detected in a Western Mediterranean forest record. Climate of the Past 6, 245–264.

Fletcher, W.J., Sánchez Goñi, M.F., Allen, J.R.M., Cheddadi, R., Combourieu-Nebout, N., Huntley, B., Lawson, I., Londeix, L., Magri, D., Margari, V., Müller, U.C., Naughton, F., Novenko, E., Roucoux, K., Tzedakis, P.C., 2010b. Millennial-scale variability during the last glacial in vegetation records from Europe. Quaternary Science Reviews 29, 2839–2864.

Fons, R., Saint Girons, M.C., 1993. Le cycle sexuel chez le mulot sylvestre, *Apodemus sylvaticus* (L., 1758), (Muridae) en region mediterraneenne. Z. Säugertierkunde 58, 38–47.

Font-Tullot, I., 2000. Climatología de España y Portugal. Universidad de Salamanca, Salamanca.

Fourel, F., Martineau, F., Lécuyer, C., Kupka, H.-J., Lange, L., Ojeimi, C., Seed, M., 2011. $^{18}O/^{16}O$ ratio measurements of inorganic and organic materials by elemental analysis–pyrolysis–isotope ratio mass spectrometry continuous-flow techniques. Rapid Communications in Mass Spectrometry 25, 2691–2696.

Freudenthal, M., García-Alix, A., Rios, M., Ruiz-Sánchez, F., Martín-Suárez, E., Delgado, A., 2014. Review of paleo-humidity parameters in fossil rodents (Mammalia): Isotopic vs. tooth morphology approach. Palaeogeography, Palaeoclimatology, Palaeoecology 395, 122–130.

García-Alix, A., 2015. A multiproxy approach for the reconstruction of ancient continental environments. The case of the Mio–Pliocene deposits of the Granada Basin (southern Iberian Peninsula). Global and Planetary Change 131, 1–10.

Garcia-Ibaibarriaga, N., 2015. Los microvertebrados en el registro arqueo-paleontológico del País Vasco: Cambios climáticos y evolución paleoambiental durante el Pleistoceno Superior. Universidad del País Vasco.

García-Ibaibarriaga, N., 2012. El registro de micromamíferos del nivel basal de Lezetxiki II (Arrasate, País Vasco). Estudios de Cuaternario 2, 71–84.

García-Ibaibarriaga, N., Murelaga, X., Bailón, S., Rofes, J., Ordiales, A., 2013. Estudio de los microvertebrados de la cueva de Arlanpe (Lemoa, Bizkaia), in: Rios-Garaizar, J., Garate, D., Gómez-Olivencia, A. (Eds.), La Cueva de Arlanpe (Lemoa): Ocupaciones Humanas Desde El Paleolítico Medio Antíguo Hasta La Prehistoria. Kobie. Bizkaiko Arkeologi Indusketak, 3, Bilbao, pp. 81–210.

García-Ibaibarriaga, N., Rofes, J., Bailon, S., Garate, D., Ríos-Garaizar, J., Martínez-García, B., Murelaga, X., 2015. A palaeoenvironmental estimate in Askondo (Bizkaia, Spain) using small vertebrates. Quaternary International 364, 244–254.

Gat, J.R., 1996. Oxygen and hydrogen isotopes in the hydrologic cycle. Annual Review of Earth and Planetary Sciences 24, 225–262.

Gat, J.R., 1980. The relationship between surface and subsurface waters: water quality aspects in areas of low precipitation. Hydrological Sciences-Butlletin des Sciences Hydrologiques 25, 257–267.

Gat, J.R., Carmi, I., 1970. Evolution of the Isotopic Composition of Atmospheric Waters in the Mediterranean Sea Area. Journal of Geophysical Research 75, 3039–3048.

Gat, J.R., Klein, B., Kushnir, Y., Roether, W., Wernli, H., Yam, R., Shemesh, A., Klein, B., Kushnir, Y., Roether, W., Wernli, H., Yam, R., Shemesh, A., 2003. Isotope composition of air moisture over the Mediterranean Sea: an index of the air-sea interaction pattern. Chemical and Physical Meteorology 55, 953–965.

Gehler, A., Tütken, T., Pack, A., 2012. Oxygen and Carbon Isotope Variations in a Modern Rodent Community - Implications for Palaeoenvironmental Reconstructions. PLoS ONE 7, 16–27.

Gehler, A., Tütken, T., Pack, A., 2011. Triple oxygen isotope analysis of bioapatite as tracer for diagenetic alteration of bones and teeth. Palaeogeography, Palaeoclimatology, Palaeoecology 310, 84–91.

Genty, D., Combourieu-nebout, N., Peyron, O., Blamart, D., Wainer, K., Mansuri, F., Ghaleb, B., Isabello, L., Dormoy, I., Grafenstein, U. Von, Bonelli, S., Landais, A., Brauer, A., 2010. Isotopic characterization of rapid climatic events during OIS3 and OIS4 in Villars Cave stalagmites (SW-France) and correlation with Atlantic and Mediterranean pollen records. Quaternary Science Reviews 29, 2799–2820.

Gonfiantini, R., 1978. Standards for stable isotope measurements in natural compounds. Nature 271, 534–536.

Gordon, C.C., Buikstra, J.E., 1981. Soil pH, bone preservation, and sampling bias at mortuary sites. American Antiquity 46, 566–571.

Gosàlbez, J., 1987. Insectívors i rosegadors de Catalunya. Metodologia d'estudi i catàleg faunístic. Ketres Editora, Barcelona.

Hall, R., 1967. Those late corn dates: isotopic fractionation as a source of error in carbon-14 dates. Michigan Archaelogist 13, 171–180.

Hammer, Ø., Harper, D.A.T., Ryan, P.D., 2001. Paleontological statistics software package for education and data analysis. Palaeontologia Electronica 4, 9–18.

Harrison, S.P., Sanchez Goñi, M.F., 2010. Global patterns of vegetation response to millennial-scale variability and rapid climate change during the last glacial period. Quaternary Science Reviews 29, 2957–2980.

Hartman, G., Hovers, E., Hublin, J.-J., Richards, M., 2015. Isotopic evidence for Last Glacial climatic impacts on Neanderthal gazelle hunting territories at Amud Cave, Israel. Journal of Human Evolution 84, 71–82.

Heinrich, H., 1988. Origin and consequences of cyclic ice rafting in the Northeast Atlantic Ocean during the past 130,000 years. Quaternary Research 29, 142–152.

Hemming, S.R., 2004. Heinrich events: Massive late Pleistocene detritus layers of the North Atlantic and their global climate imprint. Review of Geophysics 42, RG1005.

Héran, M.A., Lécuyer, C., Legendre, S., 2010. Cenozoic long-term terrestrial climatic evolution in Germany tracked by δ18O of rodent tooth phosphate. Palaeogeography, Palaeoclimatology, Palaeoecology 285, 331–342.

Hernández-Fernández, M., Azanza, B., Álvarez-Sierra, M. a, 2004. Iberian Plio-Pleistocene biochronology: micromammalian evidence for MNs and ELMAs calibration in southwestern Europe. Journal of Quaternary Science 19, 605–616.

Hernández Fernández, M., 2001. Bioclimatic discriminant capacity of terrestrial mammal faunas. Global Ecology and Biogeography 10, 189–204.

Hernández Fernández, M., Álvarez Sierra, M.Á., Peláez-Campomanes, P., 2007. Bioclimatic analysis of rodent palaeofaunas reveals severe climatic changes in Southwestern Europe during the Plio-Pleistocene. Palaeogeography, Palaeoclimatology, Palaeoecology 251, 500–526.

Hewitt, G.M., 2000. The genetic legacy of the Quarternary ice ages. Nature 405, 907–913.

Higham, T., Douka, K., Wood, R., Ramsey, C.B., Brock, F., Basell, L., Camps, M., Arrizabalaga, A., Baena, J., Barroso-Ruíz, C., Bergman, C., Boitard, C., Boscato, P., Caparrós, M., Conard, N.J., Draily, C., Froment, A., Galván, B., Gambassini, P., Garcia-Moreno, A., Grimaldi, S., Haesaerts, P., Holt, B., Iriarte-Chiapusso, M.-J., Jelinek, A., Jordá Pardo, J.F., Maíllo-Fernández, J.-M., Marom, A., Maroto, J., Menéndez, M., Metz, L., Morin, E., Moroni, A., Negrino, F., Panagopoulou, E., Peresani, M., Pirson, S., de la Rasilla, M., Riel-Salvatore, J., Ronchitelli, A., Santamaria, D., Semal, P., Slimak, L., Soler, J.,

Soler, N., Villaluenga, A., Pinhasi, R., Jacobi, R., 2014. The timing and spatiotemporal patterning of Neanderthal disappearance. Nature 512, 306–309.

Hill, A., 1979. Butchery and Natural Disarticulation: An Investigatory Technique. American Antiquity 44, 739–744.

Hill, A., Behrensmeyer, A.K., 1984. Natural Disarticulation and Bison Butchery. American Antiquity 1, 141–145.

Hillson, S., 2005. Teeth. Cambridge University Press, New York.

Hut, G., 1987. Consultants' group meeting on stable isotope reference samples for geochemical and hydrological investigations, 16-18 Sep. 1985, Report to the Director General. International Atomic Energy Agency, Vienna.

IUCN, 2018. The IUCN Red List of Threatened Species [WWW Document]. Version 2018-2. URL www.iucnredlist.org

Jeannet, M., 2000. Gruta da Figueira Brava: les Rongeurs. Memórias da Academia das Ciências de Lisboa, Classe Ciências 38, 179–243.

Jeffrey, A., Denys, C., Stoetzel, E., Lee-Thorp, J. a., 2015. Influences on the stable oxygen and carbon isotopes in gerbillid rodent teeth in semi-arid and arid environments: Implications for past climate and environmental reconstruction. Earth and Planetary Science Letters 428, 84–96.

Johnsen, S.J., Clausen, H.B., Dansgaard, W., Fuhrer, K., Gundestrup, N., Hammer, C.U., Iversen, P., Jouzel, J., Stauffer, B., Steffensen, J.P., 1992. Irregular glacial interstadials recorded in new Greenland ice core. Nature 359, 311–313.

Klevezal, G.A., 2010. Dynamics of Incisor Growth and Daily Increments on the Incisor Surface in Three Species of Small Rodents. Biology Butlletin 37, 836–845.

Klevezal, G.A., Pucek, M., Sukhovskaja, L.I., 1990. Incisor growth in voles. Acta Theriol. 35 (3-4), 331–344.

Knockaert, J., Balasse, M., Rendu, C., Burens, A., Campmajo, P., Carozza, L., Bousquet, D., Fiorillo, D., Vigne, J., 2018. Mountain adaptation of caprine herding in the eastern Pyrenees during the Bronze Age: A stable oxygen and carbon isotope analysis of teeth. Quaternary International 1–15.

Kolodny, Y., Luz, B., Navon, O., 1983. Oxygen isotope variations in phosphate of biogenic apatites, I. Fish bone apatite rechecking the rules of the game. Earth and Planetary Science Letters 64, 398–404.

Korth, W.W., 1979. Taphonomy of microvertebrate fossil assemblages. Annals of the Carnegie Museum 48, 235–285.

Kowalski, K., 1990. Some problems of the taphonomy of small mammals, in: Feijfar, O., Heinrich, W.. (Eds.), International Symposium on the Evolution, Phylogeny and Biostratigraphy of Arvicolids. Geological Survey, Prague, pp. 285–296.

Lagos, P., 2019. Predation and Its Effects on Individuals: From Individual to Species. Encyclopedia of Ecology 2, 365-368.

Laudet, F., Selva, N., 2005. Ravens as small mammal bone accumulators: First taphonomic study on mammal remains in raven pellets. Palaeogeography, Palaeoclimatology, Palaeoecology 226, 272–286.

Le Louarn, H., Quéré, J.P., 2003. Les Rongeurs de France. Faunistique et biologie. Editions d'Institut National de la Recherche Agronomique, Paris.

Lécuyer, C., 2014. Water on Earth. John Wiley & Sons Inc, London, UK and New York.

Lécuyer, C., 2004. Oxygen Isotope Analysis of Phosphate, in: Groot, P.A. de (Ed.), Handbook of Stable Isotope Analytical Techniques. Elsevier B.V., pp. 482–499.

Lécuyer, C., Atrops, F., Amiot, R., Angst, D., Daux, V., Flandrois, J., Fourel, F., Rey, K., Royer, A., Seris, M., Touzeau, A., Rousseau, D.D., 2018. Tsunami sedimentary deposits of Crete records climate during the 'Minoan Warming Period' (≈3350 yr BP). The Holocene 28, 914–929.

Lécuyer, C., Fourel, F., Martineau, F., Amiot, R., Bernard, A., Daux, V., Escarguel, G., Morrison, J., 2007. High-precision determination of $^{18}O/^{16}O$ ratios of silver phosphate by EA-pyrolysis-IRMS continuous flow technique. Journal of Mass Spectrometry 42, 36–41.

Lécuyer, C., Grandjean, P., O'Neil, J.R., Cappetta, H., Martineau, F., 1993. Thermal excursions in the ocean at the Cretaceous-Tertiary boundary (northern Morocco): $\delta^{18}O$ record of phosphatic fish debris. Palaeogeography, Palaeoclimatology, Palaeoecology 105, 235–243.

Lécuyer, C., Grandjean, P., Sheppard, S.M.F., 1999. Oxygen isotope exchange between dissolved phosphate and water at temperatures ≤135°C: Inorganic versus biological fractionations. Geochimica et Cosmochimica Acta 63, 855–862.

Lee-Thorp, J.A., van der Merwe, N.J., 1991. Aspects of the chemistry of modern and fossil biological apatites. Journal of Archaeological Science 18, 343–354.

Lindars, E.S., Grimes, S.T., Mattey, D.P., Collinson, M.E., Hooker, J.J., Jones, T.P., 2001. Phosphate $\delta^{18}O$ determination of modern rodent teeth by direct laser fluorination: An appraisal of methodology and potential application to palaeoclimate reconstruction. Geochimica et Cosmochimica Acta 65, 2535–2548.

Lloveras, L., Moreno-Garcia, M., Nadal, J., 2008a. Taphonomic study of leporid remains accumulated by the Spanish Imperial Eagle (Aquila adalberti). Geobios 41, 91–100.

Lloveras, L., Moreno-García, M., Nadal, J., 2012. Feeding the Foxes: An Experimental Study to Assess Their Taphonomic Signature on Leporid Remains. International Journal of Osteoarchaeology 22, 577–590.

Lloveras, L., Moreno-García, M., Nadal, J., 2008b. Taphonomic analysis of leporid remains obtained from modern Iberian lynx (*Lynx pardinus*) scats. Journal of Archaeological Science 35, 1–13.

Longinelli, A., 1984. Oxygen isotopes in mammal bone phosphate: A new tool for paleohydrological and paleoclimatological research? Geochimica et Cosmochimica Acta 48, 385–390.

Longinelli, A., Nuti, S., 1973. Oxygen isotope measurements of phosphate from fish teeth and bones. Earth and Planetary Science Letters 20, 337–340.

López-García, J.M., 2011. Los micromamíferos del Pleistoceno superior de la Península Ibérica. Evolución de la diversidad taxonómica y cambios paleoambientales y paleoclimáticos. Ed. Académica Española, Saarbrücken.

López-García, J.M., Blain, H.-A., Bennàsar, M., Alcover, J.A., Bañuls-Cardona, S., Fernández-García, M., Fontanals, M., Martín, P., Morales, J.I., Muñoz, L., Pedro, M., Vergés, J.M., 2014a. Climate and landscape during Heinrich Event 3 in south-western Europe: The small-vertebrate association from Galls Carboners cave (Mont-ral, Tarragona, north-eastern Iberia). Journal of Quaternary Science 29, 130–140.

López-García, J.M., Blain, H.-A., Bennàsar, M., Euba, I., Bañuls, S., Bischoff, J., López-Ortega, E., Saladié, P., Uzquiano, P., Vallverdú, J., 2012a. A multiproxy reconstruction of the palaeoenvironment and palaeoclimate of the Late Pleistocene in northeastern Iberia: Cova dels Xaragalls, Vimbodí-Poblet, Paratge Natural de Poblet, Catalonia. Boreas 41, 235–249.

López-García, J.M., Blain, H.-A., Bennàsar, M., Sanz, M., Daura, J., 2013. Heinrich event 4 characterized by terrestrial proxies in southwestern Europe. Climate of the Past 9, 1053–1064.

López-García, J.M., Blain, H.-A., Burjachs, F., Ballesteros, A., Allué, E., Cuevas-Ruiz, G.E., Rivals, F., Blasco, R., Morales, J.I., Hidalgo, A.R., Carbonell, E., Serrat, D., Rosell, J., 2012b. A multidisciplinary approach to reconstructing the chronology and environment of southwestern European Neanderthals: the contribution of Teixoneres cave (Moià, Barcelona, Spain). Quaternary Science Reviews 43, 33–44.

Lopez-Garcia, J.M., Blain, H.-A., Morales, J.I., Lorenzo, C., Banuls-Cardona, S., Cuenca-Bescós, G., Cuenca-Bescos, G., 2013. Small-mammal diversity in Spain during the late Pleistocene to early Holocene: Climate, landscape, and human impact. Geology 41, 267–270.

López-García, J.M., Blain, H.A., Allué, E., Bañuls, S., Bargalló, A., Martín, P., Morales, J.I., Pedro, M., Rodríguez, A., Solé, A., Oms, F.X., 2010. First fossil evidence of an "interglacial refugium" in the pyrenean region. Naturwissenschaften 97, 753–761.

López-García, J.M., Blain, H.A., Bennàsar, M., Fernández-García, M., 2014b. Environmental and climatic context of Neanderthal occupation in southwestern Europe during MIS3 inferred from the small-vertebrate assemblages. Quaternary International 326–327, 319–328.

López-García, J.M., Blain, H.A., Sanz, M., Daura, J., 2012c. A coastal reservoir of terrestrial resources for Neanderthal populations in north-eastern Iberia: Palaeoenvironmental data inferred from the small-vertebrate assemblage of Cova del Gegant, Sitges, Barcelona. Journal of Quaternary Science 27, 105–113.

López-García, J.M., Cuenca-Bescós, G., 2010. Évolution climatique durant le Pléistocène Supérieur en Catalogne (nord-est de l'Espagne) d'après l'étude des micromammifères. Quaternaire 21, 249–258.

López-García, J.M., Cuenca-Bescós, G., Blain, H.-A., Álvarez-Lao, D., Uzquiano, P., Adán, G., Arbizu, M., Arsuaga, J.L., 2011a. Palaeoenvironment and palaeoclimate of the Mousterian–Aurignacian transition in northern Iberia: The small-vertebrate assemblage from Cueva del Conde (Santo Adriano, Asturias). Journal of Human Evolution 61, 108–116.

López-García, J.M., Cuenca-Bescós, G., Finlayson, C., Brown, K., Pacheco, F.G., 2011b. Palaeoenvironmental and palaeoclimatic proxies of the Gorham's cave small mammal sequence, Gibraltar, southern Iberia. Quaternary International 243, 137–142.

López-García, J.M., Fernández-García, M., Blain, H.-A., Sanz, M., Daura, J., 2016. MIS 5 environmental and climatic reconstruction in northeastern Iberia using the small-vertebrate assemblage from the terrestrial sequence of Cova del Rinoceront (Castelldefels, Barcelona). Palaeogeography, Palaeoclimatology, Palaeoecology 451, 13–22.

López-García, J.M., Soler, N., Maroto, J., Soler, J., Alcalde, G., Galobart, A., Bennàsar, M., Burjachs, F., 2015. Palaeoenvironmental and palaeoclimatic reconstruction of the Latest Pleistocene of L'Arbreda Cave (Serinyà, Girona, northeastern Iberia) inferred from the small-mammal (insectivore and rodent) assemblages. Palaeogeography, Palaeoclimatology, Palaeoecology 435, 244–253.

López-González, F., Grandal-d'Anglade, A., Vidal-Romaní, J.R., 2006a. Deciphering bone depositional sequences in caves through the study of manganese coatings. Journal of Archaeological Science 33, 707–717.

López-González, F., Grandal-d'Anglade, A., Vidal-Romaní, J.R., 2006b. Deciphering bone depositional sequences in caves through the study of manganese coatings. Journal of Archaeological Science 33, 707–717.

López, M., López-Fuster, M.J., Palazón, S., Ruiz-Olmo, J., Ventura, J., 2006. Els mamífers, in: La Fauna Vertebrada a Les Terres de Lleida. Universitat de Lleida, Lleida, pp. 230–262.

Lorenzo, C., Navazo, M., Díez, J.C., Sesé, C., Arceredillo, D., Jordá Pardo, J.F., 2012. New human fossil to the last Neanderthals in central Spain (Jarama VI, Valdesotos, Guadalajara, Spain). Journal of Human Evolution 62, 720–725.

Luz, B., Kolodny, Y., 1985. Oxygen isotope variations in phosphate of biogenic apatites, IV. Mammal teeth and bones. Earth and Planetary Science Letters 75, 29–36.

Luz, B., Kolodny, Y., Horowitz, M., 1984. Fractionation of oxygen isotopes between mammalian. Geochimica et Cosmochimica Acta 48, 1689–1693.

Lyman, R.L., 2017. Paleoenvironmental Reconstruction from Faunal Remains: Ecological Basics and Analytical Assumptions. Journal of Archaeological Research 1–57.

Lyman, R.L., 2016. The mutual climatic range technique is (usually) not the area of sympatry technique when reconstructing paleoenvironments based on faunal remains. Palaeogeography, Palaeoclimatology, Palaeoecology 454, 75–81.

Lyman, R.L., 1994. Vertebrate Taphonomy. Cambridge University Press, Cambridge.

MacDonald, D., Barret, P., 2008. Guía de campo de los mamíferos de España y de Europa. Ediciones Omega, Barcelona.

Manzanares, A., 2012. Aves rapaces de la Península Ibérica, Baleares y Canarias. Ediciones Omega, Barcelona.

Margalef, R., 1974. Ecología. Omega, Barcelona.

Marín-Arroyo, A.B., Landete-Ruiz, M.D., Seva-Román, R., Lewis, M.D., 2014. Manganese coating of the Tabun faunal assemblage: Implications for modern human behaviour in the Levantine Middle Palaeolithic. Quaternary International 330, 10–18.

Marín Arroyo, A.B., Landete Ruiz, M.D., Vidal Bernabeu, G., Seva Román, R., González Morales, M.R., Straus, L.G., 2008. Archaeological implications of human-derived manganese coatings: a study of blackened bones in El Mirón Cave, Cantabrian Spain. Journal of Archaeological Science 35, 801–813.

Maroto, J., Julià, R., López-García, J.M., Blain, H.-A., 2012a. Chronological and environmental context of the Middle Pleistocene human tooth from Mollet Cave (Serinyà, NE Iberian Peninsula). Journal of Human Evolution 62, 655–63.

Maroto, J., Vaquero, M., Arrizabalaga, Á., Baena, J., Baquedano, E., Jordá, J., Julià, R., Montes, R., Van Der Plicht, J., Rasines, P., Wood, R., 2012b. Current issues in late Middle Palaeolithic chronology: New assessments from Northern Iberia. Quaternary International 247, 15–25.

Marquina, R., Fagoaga, A., Crespo, V.D., Ruiz-Sánchez, F.J., Bailon, S., Hernández, C.M., Galván, B., 2017. Amphibians and squamate reptiles from the stratigraphic unit Xb of El Salt (Middle Palaeolithic ; Alcoy, Spain): palaeoenvironmental and palaeoclimatic implications. Spanish Journal of Palaeontology 32, 291–312.

Martínez-Moreno, J., Mora, R., de la Torre, I., 2010. The Middle-to-Upper Palaeolithic transition in Cova Gran (Catalunya, Spain) and the extinction of Neanderthals in the Iberian Peninsula. Journal of Human Evolution 58, 211–226.

Maul, L.C., Masini, F., Parfitt, S.A., Rekovets, L., Savorelli, A., 2014. Evolutionary trends in arvicolids and the endemic murid Mikrotia - New data and a critical overview. Quaternary Science Reviews 96, 240–258.

Menu, H., Popelard, J.B., 1987. Utilisation des caracteres dentaires pour la determination des vespertilionines de l'ouest europeen. Butlletin de la coordination ouest pour l'étude et la protection des chauves-souris 4, 11–88.

Mikkola, H., 1983. Owls of Europe. Buteo Books, Sussex.

Moreno, A., Svensson, A., Brooks, S.J., Connor, S., Engels, S., Fletcher, W., Genty, D., Heiri, O., Labuhn, I., Perşoiu, A., Peyron, O., Sadori, L., Valero-Garcés, B., Wulf, S., Zanchetta, G., Allen, J.R.M., Ampel, L., Blamart, D., Birks, H., Blockley, S., Borsato, A., Bos, H., Brauer, A., Combourieu-Nebout, N., de Beaulieu, J.L., Drescher-Schneider, R., Drysdale, R., Elias, S., Frisia, S., Hellstrom, J.C., Ilyashuk, B., Joannin, S., Kühl, N., Larocque-Tobler, I., Lotter, A., Magny, M., Matthews, I., McDermott, F., Millet, L., Morellón, M., Neugebauer, I., Muñoz-Sobrino, C., Naughton, F., Ohlwein, C., Roucoux, K., Samartin, S., Sánchez-Goñi, M.F., Sirocko, F., van Asch, N., van Geel, B., van Grafenstein, U., Vannière, B., Vegas, J., Veres, D., Walker, M., Wohlfarth, B., 2014. A compilation of Western European terrestrial records 60-8kaBP: Towards an understanding of latitudinal climatic gradients. Quaternary Science Reviews 106, 167–185.

Moreno, S., Kufner, M.B., 1988. Seasonal Patterns in the Wood Mouse Population in Mediterranean Scrubland. Acta Theriologica 33, 79–85.

Murelaga, X., Bailón, S., Rofes, J., García-Ibaibarriaga, N., 2012. Estudio arqueozoológico de los macromamíferos del yacimiento de Askondo (Mañaria, Bizkaia), in: Garate, D., Rios-Garaizar, J. (Eds.), La Cueva de Askondo (Mañaria): Arte Parietal y Ocupación Humana Durante La Prehistoria. Kobie. Bizkaiko Arkeologi Indusketak 2, Bilbao, pp. 65–70.

Nadachowski, A., 1982. Late Quaternary rodents of Poland with special reference to morphotype dentition analysis of voles. Polska Academia Nauk, Panstwowe Wydawnictwo Naukowe, Krakow.

Naughton, F., Sánchez-Goñi, M.F., Desprat, S., Turon, J.-L., Duprat, J., 2007. Present-day and past (last 25 000 years) marine pollen signal off western Iberia. Marine micropaleontology 62, 91–114.

Navarro, N., Lécuyer, C., Montuire, S., Langlois, C., Martineau, F., 2004. Oxygen isotope compositions of phosphate from arvicoline teeth and Quaternary climatic changes, Gigny, French Jura. Quaternary Research 62, 172–182.

Ninyerola, M., Pons, X., Roure, J.M., Martín-Vide, J., Raso-Nadal, J.M., Clavero, P., 2003. Atles Climátics de Catalunya. Generalitat de Catalunya (Departament de Medi Ambient), Barcelona.

Norrdahl, K., Korpima, E., 2002. Seasonal changes in the numerical responses of predators to cyclic vole populations. Ecography 25, 428–438.

North Greenland Ice Core Project members, 2004. High-resolution record of Northern Hemisphere climate extending into the last interglacial period. Nature 431, 147–151.

O'Regan, H.J., 2008. The Iberian Peninsula - corridor or cul-de-sac? Mammalian faunal change and possible routes of dispersal in the last 2 million years. Quaternary Science Reviews 27, 2136–2144.

Olsen, S.L., Shipman, P., 1988. Surface modification on bone: Trampling versus butchery. Journal of Archaeological Science 15, 535–553.

Palomo, L.J., Gisbert, J., Blanco, C., 2007. Atlas y libro rojo de los mamíferos terrestres de España. Organismo Autónomo Parques Nacionales, Madrid.

Pemán, E., 1990. Los micromamíferos en el Pleistoceno Superior del País Vasco. Munibe 42, 259–262.

Peneycad, E., Candy, I., Schreve, D.C., 2019. Variability in the oxygen isotope compositions of modern rodent tooth carbonate: Implications for palaeoclimate reconstructions. Palaeogeography, Palaeoclimatology, Palaeoecology 514, 695–705.

Podlesak, D.W., Torregrossa, A., Ehleringer, J.R., Dearing, M.D., Passey, B.H., Cerling, T.E., 2008. Turnover of oxygen and hydrogen isotopes in the body water, CO2, hair, and enamel of a small mammal. Geochimica et Cosmochimica Acta 72, 19–35.

Potter, R.M., Rossman, G.R., 1979. Mineralogy of manganese dendrites and coatings. American Mineralogist 64, 1219–1226.

Povoas, L., Zilhao, J., Chaline, J., Brunet-Lecomte, P., 1992. La faune de rongeurs du Pleistocene superieur de la grotte de Caldeirao (Tomar, Portugal). Quaternaire 3, 40–47.

Pryor, A.J.E., Stevens, R.E., Connell, T.C.O., Lister, J.R., 2014. Quantification and propagation of errors when converting vertebrate biomineral oxygen isotope data to temperature for palaeoclimate reconstruction. Palaeogeography, Palaeoclimatology, Palaeoecology 412, 99–107.

Purroy, F.J., Varela, J., 2005. Mamíferos de España. Península, Baleares y Canarias. Lynx, Barcelona.

Rasmussen, S.O., Bigler, M., Blockley, S.P., Blunier, T., Buchardt, S.L., Clausen, H.B., Cvijanovic, I., Dahl-Jensen, D., Johnsen, S.J., Fischer, H., Gkinis, V., Guillevic, M., Hoek, W.Z., Lowe, J.J., Pedro, J.B., Popp, T., Seierstad, I.K., Steffensen, J.P., Svensson, A.M., Vallelonga, P., Vinther, B.M., Walker, M.J.C., Wheatley, J.J., Winstrup, M., 2014. A stratigraphic framework for abrupt climatic changes during the Last Glacial period based on three synchronized Greenland ice-core records: Refining and extending the INTIMATE event stratigraphy. Quaternary Science Reviews 106, 14–28.

Rey-Rodríguez, I., 2015. Reconstrucción paleoambiental y biocronológica del yacimiento del Paleolítico medio-superior de Cova Eirós (Triacastela, Lugo) a partir del análisis de las asociaiones de micromamíferos. Universitat Rovira i Virgili. Master thesis (inedit).

Rey-Rodríguez, I., López-García, J.-M., Bennàsar, M., Bañuls-Cardona, S., Blain, H.-A., Blanco-Lapaz, Á., Rodríguez-Álvarez, X.-P., de Lombera-Hermida, A., Díaz-Rodríguez, M., Ameijenda-Iglesias, A., Agustí, J., Fábregas-Valcarce, R., 2016. Last Neanderthals and first Anatomically Modern Humans in the NW Iberian Peninsula: Climatic and environmental conditions inferred from the Cova Eirós small-vertebrate assemblage during MIS 3. Quaternary Science Reviews 151, 185–197.

Rios-Garaizar, J., Maidagan, D.G., Gómez-Olivencia, A., Iriarte, E., Arceredillo-Alonso, D., Iriarte-Chiapusso, M.J., Garcia-Ibaibarriaga, N., García-Moreno, A., Gutierrez-Zugasti, I., Torres, T., Aranburu, A., Arriolabengoa, M., Bailón, S., Murelaga, X., Ordiales, A., Ortiz, J.E., Rofes, J., Pedro, Z.S., 2015. Short-term Neandertal occupations in the late Middle Pleistocene of Arlanpe (Lemoa, northern Iberian Peninsula). Comptes Rendus Palevol 14, 233–244.

Rofes, J., García-Ibaibarriaga, N., Murelaga, X., Arrizabalaga, Á., Iriarte, M.-J.J., Cuenca-Bescós, G., Villaluenga, A., 2012. The southwesternmost record of Sicista (Mammalia; Dipodidae) in Eurasia, with a review of the palaeogeography and palaeoecology of the genus in Europe. Palaeogeography, Palaeoclimatology, Palaeoecology 348–349, 67–73.

Ros, M.T., 1987. Anàlisi antracològica de la cova de l'Arbreda. Cypsela VI, 67–71.

Rosário, I.T., Mathias, M.L., 2004. Annual weight variation and reproductive cycle of the wood mouse (*Apodemus sylvaticus*) in a Mediterranean environment. Mammalia 68, 133–140.

Rosell, J., Blasco, R., Rivals, F., Cebrià, A., Morales, J.I., Rodríguez-Hidalgo, A., Serrat, D., Carbonell, E., 2010a. Las ocupaciones en la Cova de les Teixoneres (Moià, Barcelona): relaciones espaciales y grado de competencia entre hienas, osos y neandertales durante el Pleistoceno superior. Zona Arqueológica 13, 392–403.

Rosell, J., Blasco, R., Rivals, F., Chacón, M.G., Menéndez, L., Morales, J.I., Rodríguez-Hidalgo, A., Cebrià, A., Carbonell, E., Serrat, D., 2010b. A stop along the way: The role of neanderthal groups at level III of Teixoneres cave (Moià, Barcelona, Spain). Quaternaire 21, 139–154.

Rosell, J., Blasco, R., Rivals, F., Chacón, M.G., Arilla, M., Camarós, E., Rufà, A., Sánchez-Hernández, C., Picin, A., Andrés, M., Blain, H.A., López-García, J.M., Iriarte, E., Cebrià, A., 2017. A resilient landscape at Teixoneres Cave (MIS 3; Moià, Barcelona, Spain): The Neanderthals as disrupting agent. Quaternary International 435, 195–210.

Roucoux, K.H., Shackleton, N.J., Abreu, L. De, Schönfeld, J., Tzedakis, P.C., 2001. Combined marine proxy and pollen analyses reveal rapid Iberian vegetation response to North Atlantic millennial-scale climate oscillations 56, 128–132.

Royer, A., Lécuyer, C., Montuire, S., Amiot, R., Legendre, S., Cuenca-Bescós, G., Jeannet, M., Martineau, F., 2013a. What does the oxygen isotope composition of rodent teeth record? Earth and Planetary Science Letters 361, 258–271.

Royer, A., Lécuyer, C., Montuire, S., Escarguel, G., Fourel, F., Mann, A., Maureille, B., 2013b. Late Pleistocene (MIS 3-4) climate inferred from micromammal communities and $\delta^{18}O$ of rodents from Les Pradelles, France. Quaternary Research 80, 113–124.

Royer, A., Lécuyer, C., Montuire, S., Primault, J., Fourel, F., Jeannet, M., 2014. Summer air temperature, reconstructions from the last glacial stage based on rodents from the site Taillis-des-Coteaux (Vienne), Western France. Quaternary Research 82, 420–429.

Royer, A., Montuire, S., Legendre, S., Discamps, E., Jeannet, M., Lécuyer, C., 2016. Investigating the Influence of Climate Changes on Rodent Communities at a Regional-Scale (MIS 1-3, Southwestern France). Plos One 11, 1–25.

Rozanski, K., Araguás-Araguás, L., Gonfiantini, R., 1993. Isotopic Patterns in Modern Global Precipitation, in: Swart, P.K., Lohman, K.C., McKenzie, J., Savin, S. (Eds.), Climate Change in Continental Isotopic Records. Washington, pp. 1–36.

Salamolard, M., Butet, A., Leroux, A., Bretagnolle, V., 2000. Responses of an avian predator to variations in prey density at a temperature latitude. Ecology 81, 2428–2441.

Sánchez-Goñi, M.F., Eynaud, F., Turon, J.-L., Shackleton, N.J., 1999. High resolution palynological record off the Iberian margin: direct land-sea correlation for the Last Interglacial complex. Earth and Planetary Science Letters 171, 123–137.

Sánchez-Goñi, M.F., Landais, A., Cacho, I., Duprat, J., Rossignol, L., 2009. Contrasting intrainterstadial climatic evolution between high and middle North Atlantic latitudes: A close-up of Greenland Interstadials 8 and 12. Geochemistry, Geophysics, Geosystems 10, 1–16.

Sánchez-Goñi, M.F., Turon, J.-L., Eynaud, F., Gendreau, S., 2000. European climatic response to millennial-scale changes in the atmosphere-ocean system during the Last Glacial period. Quaternary Research 54, 394–403.

Sánchez Goñi, M., Cacho, I., Turon, J., Guiot, J., Sierro, F., Peypouquet, J., Grimalt, J., Shackleton, N., 2002. Synchroneity between marine and terrestrial responses to millennial scale climatic variability during the last glacial period in the Mediterranean region. Climate Dynamics 19, 95–105.

Sánchez Goñi, M.F., D'Errico, F., 2005. La historia de la vegetación y el clima del último ciclo climático (OIS5-OIS1, 140.000-10.000 años BP) en la Península Ibérica y su posible impacto sobre los grupos paleolíticos. Monografias - Museo de Altamira 20, 115–129.

Sánchez Goñi, M.F., Landais, A., Fletcher, W.J., Naughton, F., Desprat, S., Duprat, J., 2008. Contrasting impacts of Dansgaard-Oeschger events over a western European latitudinal transect modulated by orbital parameters. Quaternary Science Reviews 27, 1136–1151.

Sans-Coma, V., Gosalbez, J., 1976. Sobre la reproducción de *Apodemus sylvaticus* L, 1758 en el nordeste ibérico. Miscelánea Zoológica III, 227–233.

Sans-Fuentes, M.A., Ventura, J., 2000. Distribution patterns of the small mammals (Insectivora and Rodentia) in a transitional zone between the Eurosiberian and the Mediterranean regions. Journal of Biogeography 27, 755–764.

Sanz, M., Daura, J., Brugal, J.-P., 2014. First occurrence of the extinct deer Haploidoceros in the Iberian Peninsula in the Upper Pleistocene of the Cova del Rinoceront (Castelldefels, Barcelona). Comptes Rendus Palevol 13, 27–40.

Schoeninger, M.J., DeNiro, M.J., 1984. Nitrogen and carbon isotopic composition of bone collagen from marine and terrestrial animals. Geochimica et Cosmochimica Acta 48, 625–638.

Schrag, D.P., Adkins, J.F., Mcintyre, K., Alexander, J.L., Hodell, A., Charles, C.D., Mcmanus, J.F., 2002. The oxygen isotopic composition of seawater during the Last Glacial Maximum. Quaternary Science Reviews 21, 331–342.

Scott, L., Fernandez-Jalvo, Y., Denys, C., 1996. Owl pellets, pollen and the palaeoenvironment. South African Journal of Science 92, 223–224.

Sepulchre, P., Ramstein, G., Kageyama, M., Vanhaeren, M., Krinner, G., Sánchez-Goñi, M.F., d'Errico, F., 2007. H4 abrupt event and late Neanderthal presence in Iberia. Earth and Planetary Science Letters 258, 283–292.

Sesé, C., 2005. Aportación de los micro-mamíferos al conocimiento paleoambiental del Pleistoceno Superior en la Región Cantábrica: Nuevos datos y síntesis. Museo de Altamira. Monografías 20, 167–200.

Sesé, C., 1994. Paleoclimatical interpretation of the quaternary small mammals of Spain. Geobios 27, 753–767.

Sevilla, P., 1988. Estudio paleontológico de los Quirópteros del Cuaternario español. Paleontologia i Evolució 22, 113–233.

Shipman, P., Foster, G., Schoeninger, M., 1984. Burnt Bones and Teeth: An Experimental-Study of Color, Morphology, Crystal-Structure and Shrinkage. Journal of Archaeological Science 11, 307–325.

Shipman, P., Rose, J., 1983. Early hominid hunting, butchering, and carcass-processing behaviors: Approaches to the fossil record. Journal of Anthropological Archaeology 2, 57–98.

Solé, A., Allué, E., Carbonell, E., 2013. Hearth-related wood remains from Abric Romaní layer M (Capellades, Spain). Journal of Anthropological Research 69, 535–559.

Sommer, R.S., Nadachowski, A., 2006. Glacial refugia of mammals in Europe: Evidence from fossil records. Mammal Review 36, 251–265.

Staubwasser, M., Drăgușin, V., Onac, B.P., Assonov, S., Ersek, V., Hoffmann, D.L., Veres, D., 2018. Impact of climate change on the transition of Neanderthals to modern humans in Europe. Proceedings of the National Academy of Sciences 115, 9116–9121.

Sundell, J., Huitu, O., Henttonen, H., Kaikusalos, A., Korpimäki, E., Pietiäinen, H., Saurola, P., Hanski, I., 2004. Large-scale spatial dynamics of vole populations in Finland revealed by the breeding success of vole-eating avian predators. Journal of Animal Ecology 73, 167–178.

Sunyer, P., Muñoz, A., Mazerolle, M.J., Bonal, R., Espelta, J.M., 2016. Wood mouse population dynamics: Interplay among seed abundance seasonality, shrub cover and wild boar interference. Mammalian Biology 81, 372–379.

Svensson, A., Andersen, K.K., Bigler, M., Clausen, H.B., Davies, D.D.S.M., Johnsen, S.J., 2008. A 60000 year Greenland stratigraphie ice core chronology. Climate of the Past 4, 47–57.

Talamo, S., Blasco, R., Rivals, F., Picin, A., Chacón, M.G., Iriarte, E., López-García, J.M., Blain, H.-A., Arilla, M., Rufà, A., Sánchez-Hernández, C., Andrés, M., Camarós, E., Ballesteros, A., Cebrià, A., Rosell, J., Hublin, J.-J., 2016. The Radiocarbon Approach to Neanderthals in a Carnivore Den Site: a Well-Defined Chronology for Teixoneres Cave (Moià, Barcelona, Spain). Radiocarbon 58, 247–256.

Taylor, P.J., Denys, C., Mukerjee, M., 2004. Phylogeny of the African murid tribe Otomyini (Rodentia), based on morphological and allozyme evidence. Zoologica Scripta 33, 389–402.

Terry, R.C., 2007. Inferring predator identity from skeletal damage of small-mammal prey remains. Evolutionary Ecology Research 9, 199–219.

Tornero, C., Aguilera, M., Ferrio, J.P., Arcusa, H., Moreno-García, M., Garcia-Reig, S., Rojo-Guerra, M., 2018. Vertical sheep mobility along the altitudinal gradient through stable isotope analyses in tooth molar bioapatite, meteor water and pastures: A reference from the Ebro valley to the Central Pyrenees. Quaternary International 484, 94–106.

Tornero, C., Saña, M., 2006. Anàlisi d'isòtops estables en arqueologia: aplicació i integració a la recerca arqueològica. Cota Zero 21, 31–46.

Turner-Walker, G., Jans, M., 2008. Reconstructing taphonomic histories using histological analysis. Palaeogeography, Palaeoclimatology, Palaeoecology 266, 227–235.

Vallverdú, J., Alonso, S., Bargalló, A., Bartrolí, R., Campeny, G., Carrancho, Á., Expósito, I., Fontanals, M., Gabucio, J., Gómez, B., Prats, J.M., Sañudo, P., Solé, À., Vilalta, J., Carbonell, E., 2012. Combustion structures of archaeological level O and mousterian activity areas with use of fire at the Abric Romaní rockshelter (NE Iberian Peninsula). Quaternary International 247, 313–324.

Vaquero, M., Allué, E., Bischoff, J.L., Burjachs, F., Vallverdú, J., 2013. Environmental, depositional and cultural changes in the Upper Pleistocene and Early Holocene: The Cinglera del Capelló sequence (Capellades, Spain). Quaternaire 24, 49–64.

Vaquero, M., Carbonell, E., 2012. Some clarifications on the Middle-Upper Paleolithic transition in Abric Romaní: Reply to Camps and Higham (2012). Journal of human evolution 63, 711–717.

Vogel, J.C., van der Merwe, N.J., 1977. Isotopic evidence for early maize cultivation in New York state. American Antiquity1 42, 238–242.

von Grafenstein, U., Erlenkeuser, H., Müller, J., Trimborn, P., Alefs, J., 1996. A 200-year mid-European air temperature record preserved in lake sediments: An extension of the $^{18}O_p$-air temperature relation into the past. Geochimica et Cosmochimica Acta 60, 4025–4036.

Voorhies, M.R., 1969. Taphonomy and population dynamics of an Early Pliocene vertebrate fauna Knox County, Nebraska. Contributions to Geology, University of Wyoming 1.

Wilson, D.E., Redeer, D.M., 2005. Mammal Species of the World. A Taxonomic and Geographic Reference (3rd ed) [WWW Document]. Johns Hopkins University Press. URL http://www.departments.bucknell.edu/biology/resources/msw3/

Wolf, D., Kolb, T., Alcaraz-Castaño, M., Heinrich, S., Baumgart, P., Calvo, R., Sánchez, J., Ryborz, K., Schäfer, I., Bliedtner, M., Zech, R., Zöller, L., Faust, D., 2018. Climate deteriorations and Neanderthal demise in interior Iberia. Scientific Reports 8, 1–10.

Wolff, E.W., Chappellaz, J., Blunier, T., Rasmussen, S.O., Svensson, A., 2010. Millennial-scale variability during the last glacial: The ice core record. Quaternary Science Reviews 29, 2828–2838.

Wolff, R.G., 1973. Hydrodynamic sorting and ecology of a Pleistocene mammalian assemblage from California (U.S.A.). Palaeogeography, Palaeoclimatology, Palaeoecology 13, 91–101.

Wood, R.E., Arrizabalaga, A., Camps, M., Fallon, S., Iriarte-Chiapusso, M.J., Jones, R., Maroto, J., De la Rasilla, M., Santamaría, D., Soler, J., Soler, N., Villaluenga, A., Higham, T.F.G., 2014. The chronology of the earliest Upper Palaeolithic in northern Iberia: New insights from L'Arbreda, Labeko Koba and La Viña. Journal of Human Evolution 69, 91–109.

Yravedra, J., Julien, M.A., Alcaraz-Castaño, M., Estaca-Gómez, V., Alcolea-González, J., de Balbín-Behrmann, R., Lécuyer, C., Marcel, C.H., Burke, A., 2016. Not so deserted...paleoecology and human subsistence in Central Iberia (Guadalajara, Spain) around the Last Glacial Maximum. Quaternary Science Reviews 140, 21–38.

Zazzo, A., Balasse, M., Passey, B.H., Moloney, A.P., Monahan, F.J., Schmidt, O., 2010. The isotope record of short- and long-term dietary changes in sheep tooth enamel: Implications for quantitative reconstruction of paleodiets. Geochimica et Cosmochimica Acta 74, 3571–3586.

Zazzo, A., Lécuyer, C., Mariotti, A., 2004. Experimentally-controlled carbon and oxygen isotope exchange between bioapatites and water under inorganic and microbially-mediated conditions. Geochimica et Cosmochimica Acta 68, 1–12.

Zilhão, J., 2000. The Ebro Frontier: A Model for the Late Extinction of Iberian Neanderthals, in: Stringer, C.B., Barton, R.N.E., Finlayson, C. (Eds.), Neanderthals on the Edge: 150th Anniversary Conference of the Forbes' Quarry Discovery, Gibraltar. Oxbow Books, Oxford, pp. 111–121.

List of figures

Chapter 1. Introduction, framework and objectives

Chapter 2. Material and methods synthesis

Chapter 3. Palaeoecological implications of rodents as proxies for the Late Pleistocene – Holocene environmental and climatic changes in northeastern Iberia

Chapter 4. Paleoenvironmental context of Neanderthal occupations in northeastern Iberia: the small-mammal assemblage from Abric Romaní (Capellades, Barcelona, Spain)

Chapter 5. Unravelling the oxygen isotope signal (δ18O) from rodent teeth in northeastern Iberia, and the implications for past climate reconstructions

Chapter 6. Combined palaeoecological methods using small-mammal assemblages to decipher environmental context of a long-term Neanderthal settlement in northeastern Iberia

Chapter 8. Latest Pleistocene in northeastern Iberia: oxygen isotope analysis and palaeoenvironment inferences from rodent assemblages of Arbreda cave (Serinyà, Girona)

Chapter 9. General discussion

List of tables

Chapter 2. Material and methods synthesis

Chapter 3. Palaeoecological implications of rodents as proxies for the Late Pleistocene – Holocene environmental and climatic changes in northeastern Iberia

Chapter 4. Paleoenvironmental context of Neanderthal occupations in northeastern Iberia: the small-mammal assemblage from Abric Romaní (Capellades, Barcelona, Spain)

Chapter 5. Unravelling the oxygen isotope signal (δ18O) from rodent teeth in northeastern Iberia, and the implications for past climate reconstructions

Chapter 6. Combined palaeoecological methods using small-mammal assemblages to decipher environmental context of a long-term Neanderthal settlement in northeastern Iberia

Chapter 7. Palaeoecological reconstruction of Teixoneres site (Moià, Barcelona) based on small mammals: origin of the assemblage and palaeoclimatic inferences

Chapter 8. Latest Pleistocene in northeastern Iberia: oxygen isotope analysis and palaeoenvironment inferences from rodent assemblages of Arbreda cave (Serinyà, Girona)

Chapter 9. General discussion

Appendix 1.
Taxonomical identification

1.1 Taxonomical and terminological remarks

The description exposed on this appendix correspond to the small mammal material identified from the Abric Romaní site for this PhD thesis (Chapter 4 and 6). Descriptions and taxonomic discussion follow the terminology of van der Meulen (1973) for Arvicolinae, Pasquier (1974) for Murinae, Damms (1981) for Gliridae, Cuenca-Bescós (1988) for Scuiridae, Reumer (1984) for Soricidae, Rümke (1985) for Talpidae, Brujin and Rumke (1974) and (Menu, 1985) for Chiroptera. The general taxonomic classification considers Wilson and Redeer (2005) and Jaarola et al. (2004). Identifications follow the general criteria given by several authors (Bab et al., 2007; Brunet-Lecomte and Chaline, 1990; Chaline, 1972; Cuenca-Bescós et al., 2008; 2014; Dupuis, 1986; Felten et al., 1973; Furió, 2007; Galán et al., 2016a; 2018a; Galán, 2003; Galán et al., 2018b; Gosàlbez, 1987; López-García, 2011; López-García et al., 2011; Luzi et al., 2017; Menu and Popelard, 1987; Nadachowski, 1982; Sevilla, 1988).

The geographical distribution of extant species in the Iberian Peninsula is defined by Palomo et al. (2007) – map with species distribution is provided inside the description of each taxa – and for European distribution is based on The IUCN Red List of Threatened Species from the International Union for Conservation of Nature (IUCN, 2018). A recent revision of the species occurrence during the Late Pleistocene and the beginning of the Holocene in northeastern Iberia, can be found in Chapter 3. The ecological preference of each species considered come from different atlas and manuals of present-day mammals' species (Arribas, 2004; Blanco, 1998a, 1998b; Gosàlbez, 1987; IUCN, 2018; Le Louarn and Quéré, 2003; López et al., 2006; MacDonald and Barret, 2008; Palomo et al., 2007; Purroy and Varela, 2005).

Molars are named by a number corresponding to the situation in the mandible from front to back along with a capital letter "M" to refer to the maxilla (M1, M2 and M3) or lowercase "m" to refer to the mandible (m1, m2 and m3). Likewise, it is use with premolars ("p" or "P"). Considering dental remains faces, is uses "lingual" to refer to the internal contour that touches the tongue, "labial" or "buccal", to the external perimeter adjacent to the lip, "mesial" or "anterior" to part of the tooth closest to the mandibular symphysis and "distal" or "posterior" the opposite side, the "occlusal" surface corresponds to the chewing surface of the tooth. Following, it is provided the nomenclature and terminologies adopt for each taxonomic group.

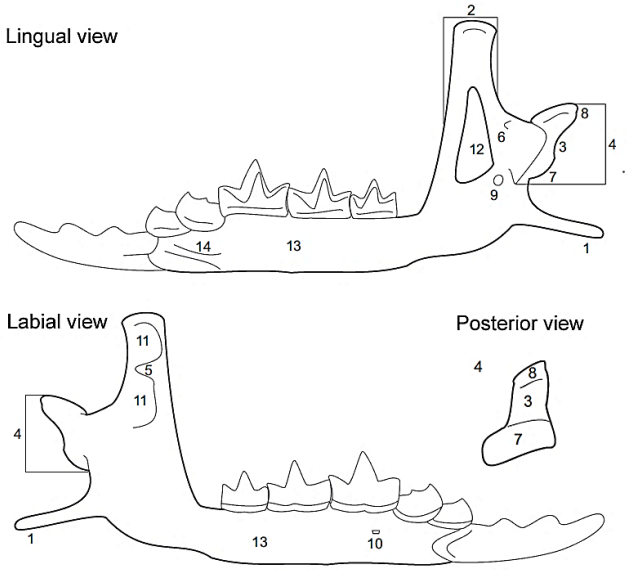

Soricidae nomenclature. Soricidae right mandible, draw modified from Furió (2007). 1, angular process; 2, coronoid process; 3, interarticular area; 4, condylar process or articular condyle; 5, condylar spicule; 6, pterygoid spicule; 7, lower articular facet; 8, upper articular facet; 9, mandibular foramen; 10, mental foramen; 11, external temporal fossa; 12, internal temporal fossa; 13, horizontal mandibular ramus or mandibular body; 14, mandibular symphysis.

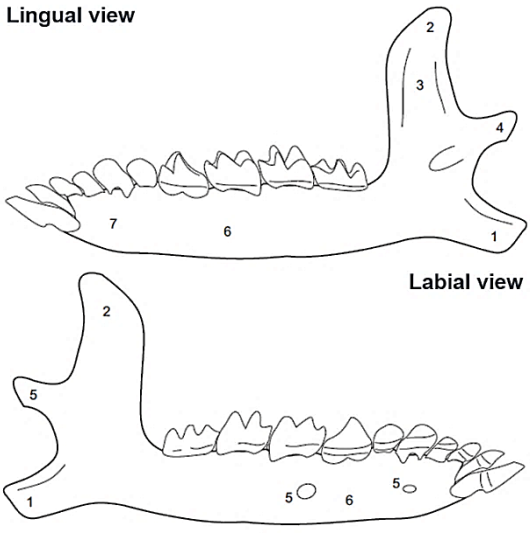

Talpidae nomenclature. Talpidae right mandible, draw modified from Furió (2007). 1, angular process; 2, coronoid process; 3, area of muscular insertion; 4, condylar process or articular condyle; 5, mental foramen; 6, horizontal mandibular ramus or mandibular body; 7, mandibular symphysis.

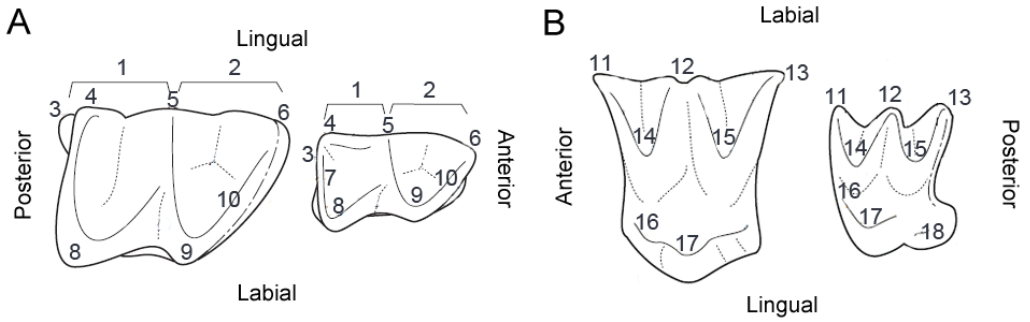

Talpidae and Soricidae nomenclature. A. Lower molars (m1 and m2) of Talpidae (left) and Soricidae (right): 1, talonid; 2, trigonid; 3, entostilid; 4, entoconid; 5, metaconid; 6, paraconid; 7, hypolophid; 8, hypoconid; 9, protoconid; 10, paralophid. B. Upper molars (M1 and M2) of Talpidae (left) and Soricidae (right): 11, parastyle; 12, mesostyle; 13, metastyle; 14, paracone; 15, metacone; 16, protoconule; 17, protocone; 18, hypocone.

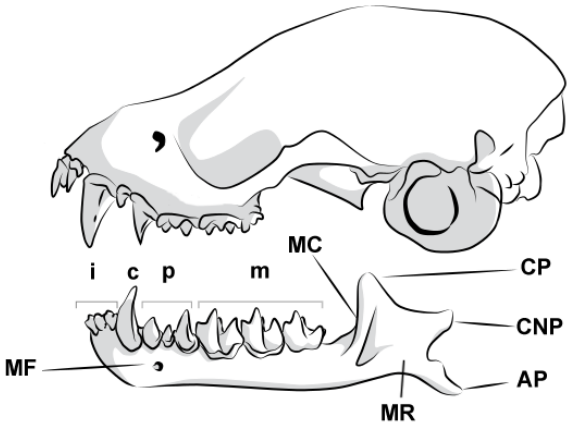

Chiroptera nomenclature. Right cranium and mandible of Chiroptera, draw modified from Galán (2003). CP, coronoid process; CNP, condylar or articular process; AP, angular process; MR, mandibular ramus; MC, masseteric crista; MF, mental foramen; i, incisors; c, canine; p, premolars; m, molars.

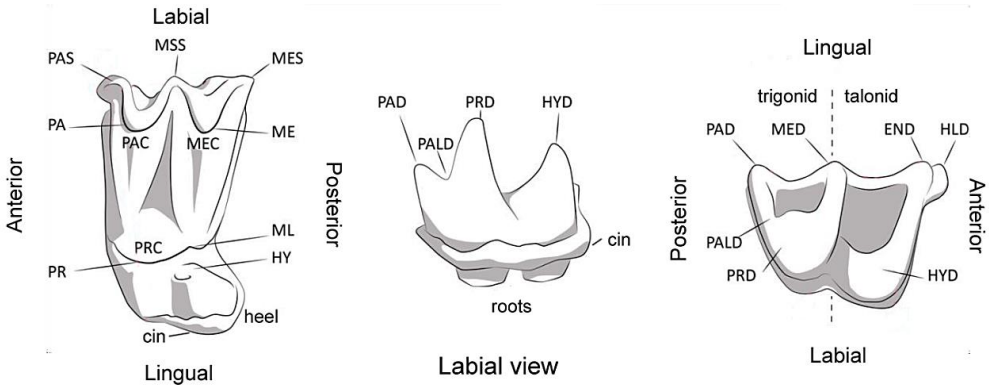

Chiroptera nomenclature. Right upper (on the left) and right lower (on the right) molars of Chiroptera, draw modified from Galán (2003). PAS, parastyle; MSS, mesostyle; MES, metastyle; PA, paracone; ME, metacone; PAC, paracrista; MEC, metacrista; PRC, protocrista; PR, protocone; ML, metaconule; HY, hypocone; cin, cingulum; PAD, paraconid; MED, metaconid; END, entoconid; HLD, hypoconulid; HYD, hypoconid; PALD, paralophid; PRD, protoconid.

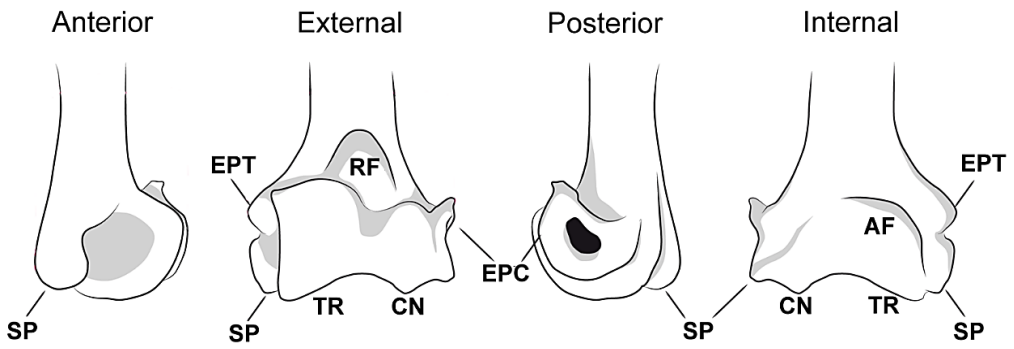

Chiroptera nomenclature. Distal epiphysis of left humerus of Chiroptera in different views, draw modified from Galán (2003). SP, styloid process; TR, trochlea; CN, condyle; EPT, epitrochlea; RF, radial fossa; EPC, epicondyle; AF, antecubital fossa.

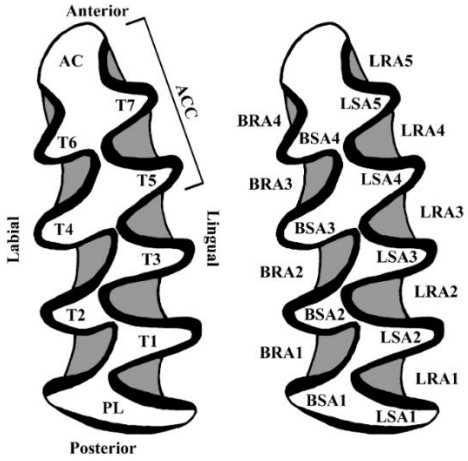

Arvicolinae nomenclature. Left first lower molar (m1) of *Microtus (Terricola) duodecimcostatus* (Abric Romaní, level D). AC, anterior cap; PL, posterior lobe; T, triangle; BRA, buccal reentrant angle; BSA, buccal salient angle; LSA, lingual salient angle; LRA, lingual reentrant angle. ACC, anteroconid complex. Black represents the enamel and grey, the cementum areas.

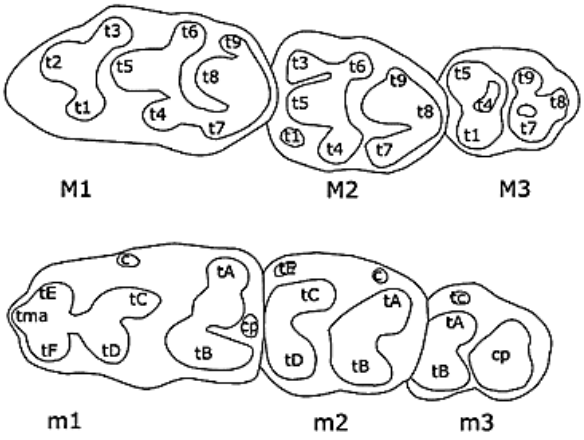

Murinae nomenclature. Upper and lower molars of *Apodemus silvaticus.* t, tubercles; t5, protocone; t6, paracone; t8, hypocone; t9, metacone; c, labial accessory cusps; cp, posterior accessory cusps; tma, medium-anterior tubercle; tF, principal antero-lingual tubercle; tE, principal antero-labial tubercle; tD, metaconid; tC, protoconid; tB, entoconid; tA, hypoconid.

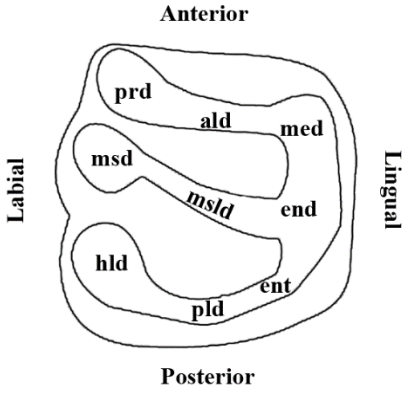

Glirinae nomenclature. Lower molar of *Eliomys quercinus*. Ald, anterolophid; End, endolophid; Ent, entoconid; Hid, hypoconid; Med, metaconid; Msd, mesoconid; Msld, mesolophid; Pld, posterolophid; Prd, protoconid.

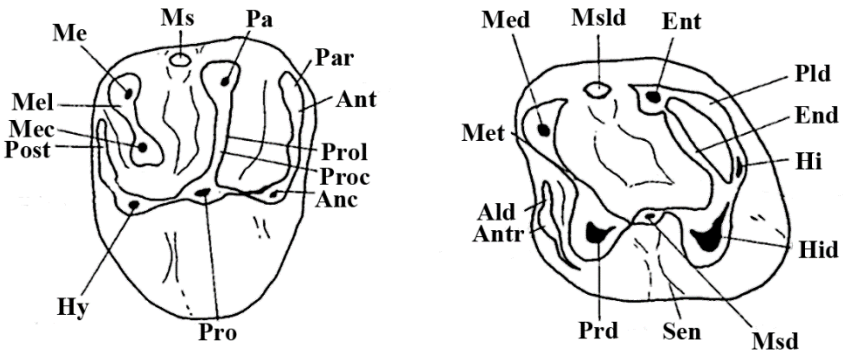

Scuiridae nomenclature. On left, first lower molar (m1) and, on right, first upper molar (M1) of Sciuridae, draw modified from Cuenca-Bescós (1988): Ms, mesostyle; Me, metacone; Mel, metaloph; Mec, metaconule; Post, posteroloph; Hy, hypocone; Pro, protocone; Pro, protocone; Anc, anteroconule; Proc, protoconule; Ant, anteroloph; Par, parastyle; Pa, paracone; Met, metalophid; Ald, anterolophid; Antr, anteroconulid; Prd, protoconulid; Sen, senid; Msd, mesoconid; Hid, Hypoconulid; Hi, hypoconid; End, entolophid; Pld, posterolophid; Ent, entoconid.

1.2 Identified species

Class MAMMALIA Linnaeus, 1758

Order SORICOMORPHA Gregory, 1910

Family SORICIDAE Fischer, 1814

Soricidae indet.

Material. – Level Q: four humeri; Level P: one mandible without teeth and one femur; Level O: two mandibles (one without teeth and one with a3-m1), one radius, three femora and one tibia-fibula; Level N: four mandibles (three without teeth and one with m2) and one humerus; Level K: one mandible without teeth; Level J: two humeri, two ulnas and two femora; Level I: one humerus; Level E: two mandibles without teeth, one humerus and one femur; Level D: two humeri.

Description. – Under this name are grouped those remains that by their general morphological characteristics seemed to be related with the Soricidae family, but their fragmentation or the absence of diagnostic characters prevented the specific identification. In the case of mandibles and in opposition to the order Chiroptera, the general slender morphology with rounded profiles and low ramus, the absence of chin and the oval shape of the alveoli have been considered. The small dimensions of post-cranial bones allow their differentiation easily from rodent remains and from the stylized and long bats remains (Chaline, 1974; Furió, 2007).

Subfamily CROCIDURINAE Milne-Edwards, 1872

Genus ***Crocidura*** Wagler, 1832

Crocidura russula Hermann, 1780

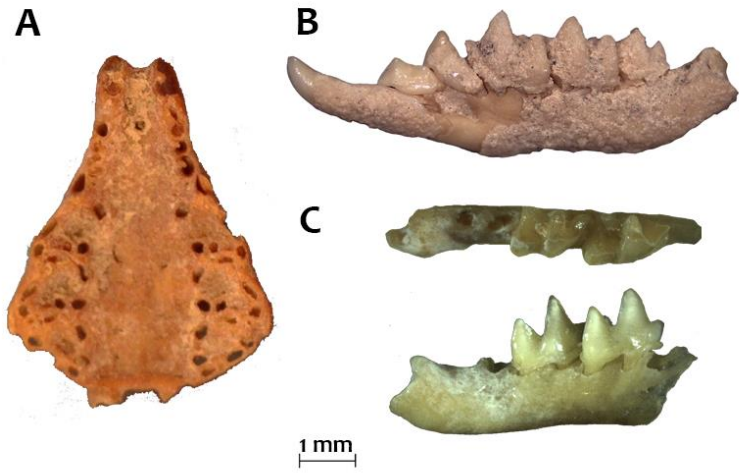

Crocidura russula remains: A) Cranial without teeth in occlusal view, from level D; B) Left mandible in labial view, from level E; C) Right mandible with m1-m2 in occlusal and labial view, from level O. Scale 1 mm.

Material. – Level O: six mandibles (one with m1-m3, two with m1-m2, one with m1 and two without teeth), one m1 and two m2; Level I: one mandible with m2-m3; Level E: two mandibles (one complete and one with m2-m3); Level D: one maxilla with P3-P4, one complete cranial and one mandible with m2.

Description. – The main characters that allow to identify this genus are the non-pigmented and completely white teeth, the straight upper edge of the lower incisor, the morphology of the cranial and the mandible. The genus *Crocidura* usually presents a more robust mandibular ramus than the genus *Sorex*. One diagnostic character is found in its condylar process, that in opposition with Soricinae subfamily, presents a unique articular facet in posterior view: presents a well-developed lower articular facet but the upper facet is less marked, both are fused on the lingual side through wide interarticular area (Furió, 2007; Gosàlbez, 1987). Currently in the Iberian Peninsula, two species assigned to this genus are documented: *C. russula* and *C. suaveolens*. The differentiation between both resides in the constriction of labial cingulum and in the morphology of P4 (López-García, 2011; Rey and Landín, 1973). The recovered molars show some constriction and the only P4 recovered in Abric Romaní show *Crocidura russula* characters, with an irregular cingulum profile, in labial view, and with the protocone separated from the hypocone, in occlusal view. The general cranial morphology recovered in level D fits also with this species. If we consider these characters, together with the current fragmentary distribution of *C. suaveolens* in northeastern Iberia, it is most likely that the identified specimens belong to *C. russula.*

Habitat and geographical distribution. – The greater white-toothed shrew (*C. russula*) is a Mediterranean species, usually associated with Mediterranean vegetation areas, such as holm oaks, cork oaks, pine forests or shrublands. It prefers open habitats with a good vegetation cover, such as forest margins, pastures or cultivated fields. It is a synanthropic species, usually living near humans. It is widely distributed in the Iberian Peninsula and in northeastern Iberia, notably abundant in the Mediterranean area, and only absent in some areas of mountain systems. It is usually found below 1000 m of altitude, because altitude is a limiting factor for this species, in relation with the consequent vegetation and climate change, different of its ecological preferences. Even so, in the Pyrenees it is located up to 1200 m a.s.l. and in the Central System up to 1700 m a.s.l..

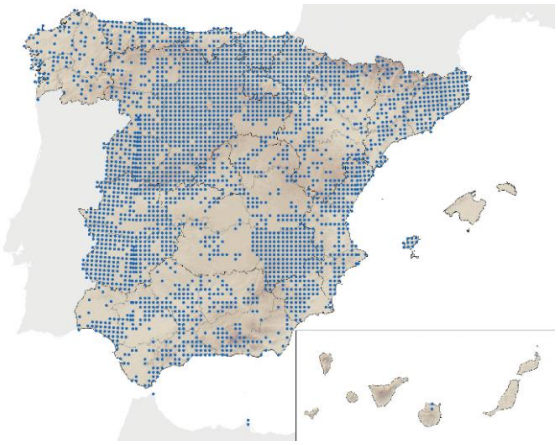

Present-day geographical distribution of *Crocidura russula* in Spain (Palomo et al., 2007).

Subfamily SORICINAE Fischer, 1814

Genus ***Sorex*** Linnaeus, 1758

Sorex minutus Linnaeus, 1766

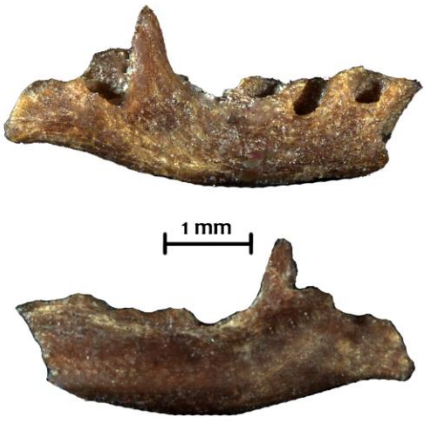

Mandible fragment of *Sorex minutus* in labial (above) and lingual (below) view, from level O. Scale 1 mm.

Material. – Level O: One mandible without teeth.

Description. – Soricinae subfamily are characterized by the red pigmentation of their teeth, lobulated lower incisors and a bi-faceted articular condyle, in posterior view, which is composed by two well-developed facets, joined by a wide interarticular area. Nevertheless, in Abric Romaní site, only one broken mandible without teeth assignable to this species was recovered. *Sorex minutus* is the smallest species of the Soricinae subfamily (Gosálbez, 1987b, Furió, 2007, López-García, 2011). Thus, the remarkable little size, the gracility and the general morphology of the recovered mandible, allow to reject other species of this genus and subfamily and are the criteria used for this attribution.

Habitat and geographical distribution. – The pigmy shrew (*S. minutus*) have mid-European climate preferences and it is adapted to cold climates. This species needs damp areas with dense vegetation cover, thus it usually lives on pastures and forest margins, although sometimes occupies coniferous or deciduous forests. The most important limiting factor of this shrew is the humidity, frequently found in areas with mean annual precipitation higher than 600 mm. Its occurrence is documented from sea level to altitudes above 2000 m a.s.l.. Although in Eurasia present a widespread distribution, its geographical distribution in the Iberian Peninsula is limited to septentrional fringe, from the northwest to the northeast, including the Montseny Massif and the Central System and always excluding areas of Mediterranean influence.

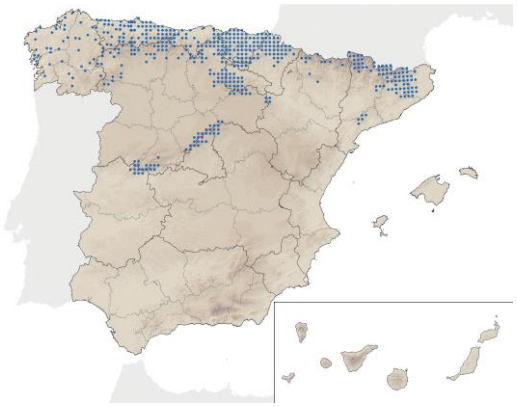

Present-day geographical distribution of *Sorex minutus* in Spain (Palomo et al., 2007).

Sorex* gr. *araneus-coronatus Linnaeus, 1758 - Millet, 1828

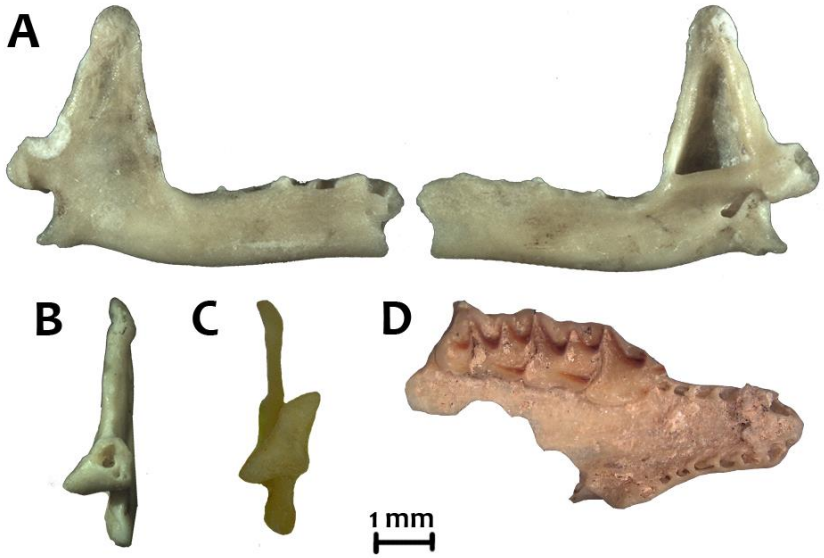

Sorex gr. *araneus-coronatus* remains: A) right mandible in labial and lingual view, from level O; B) condylar process of mandible (A) in posterior view; C) condylar process of right mandible in posterior view, from level O; D) maxilla with P4-M3 in occlusal view, from level E. Scale 1 mm.

Material. – Level O: two mandibles without teeth and one m1; Level E: one maxilla with P4-M3.

Description. – There are three current medium-size species belonging this genus in the Iberian Peninsula: *S. araneus*, *S. coronatus* and *S. granarius*. The three species share with the Soricinae subfamily some common characters: the reddish pigmentation of the teeth, the bi-faceted articular condyle and lobulated lower incisors. The differentiation between them, either considering dentition or mandibular morphology is complex. The geographical location and the general morphology of the medium-size mandibles recovered in Abric Romaní, let to reject *S. granarius*. In addition, there are certain characteristics of the mandibles for differentiating *S. araneus* and *S. coronatus*. The former has a straight coronoid process, a slender condylar process, an internal temporal fossa rather triangular and a double mandibular foramen, not very marked. Otherwise, *S. coronatus*, has a more robust mandibular body, a coronoid process slightly inclined to the distal part, a well-developed condylar process, an ovoid temporal

fossa and only one large mandibular foramen (Furió, 2007; Gosàlbez, 1987; López-García, 2011). The few recovered remains hinder a reliable differentiation between both species and are group as *Sorex* gr. *araneus-coronatus.*

Habitat and geographical distribution. – Both species, the common shrew (*S. araneus*) and the crowned shrew (*S. coronatus*) can live in similar habitats, mainly associated with humid environments with good herbaceous cover or shrubby vegetation. Both can be found in deciduous, mixed and coniferous forests, but most frequently *S. araneus*. Both have mid-European climatic requirements, preferring Atlantic and Eurosiberian climatic conditions. They do not present restrictions with respect to the altitude, living from sea level to 2200 m a.s.l.. They currently reside in the northern half of the Iberian Peninsula: *S. coronatus* in the northern fringe (from Galicia to the Catalan Pyrenees and the north of the Iberian System) and *S. araneus* is limited only to certain areas of the northeast (Pyrenees, Pre-Pyrenees and Montseny).

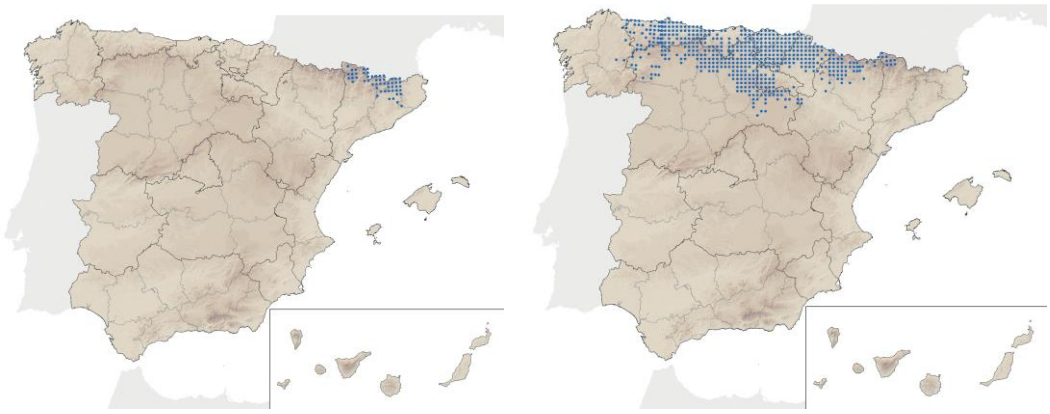

Present-day geographical distribution of *Sorex araneus* (left) and *Sorex coronatus* (right) in Spain (Palomo et al., 2007).

Genus ***Neomys*** Kaup, 1829

Neomys* gr. *fodiens-anomalus Pennant, 1711 – Cabrera, 1907

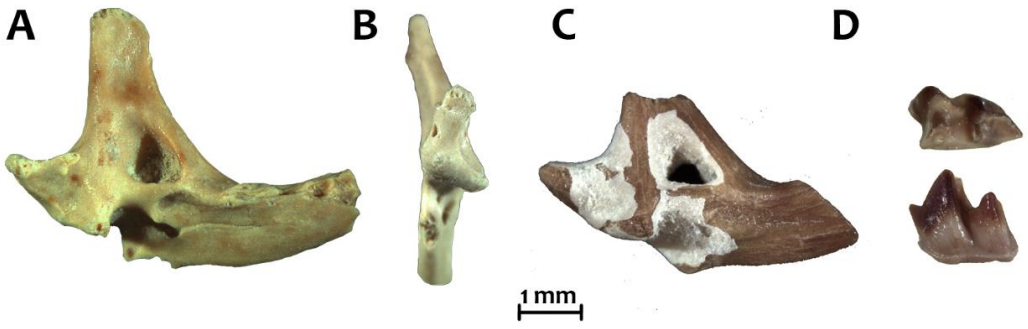

Neomys gr. *fodiens-anomalus* remains from level O: A) left mandible in lingual view; B) condylar process of mandible (A) in posterior view; C) left mandible in lingual view; D) left m2 in occlusal and labial view. Scale 1 mm.

Material. – Level O: Four mandibles without teeth, three m1 and three m2.

Description. – The genus *Neomys*, includes the largest Eurasian shrews and molars are in general more robust than in other species of shrews. Teeth of this genus are characterized by more intense and widespread red-pigmentation than *Sorex*. In posterior view, the condylar process of the mandible has two separated and marked articular facets, connected by a narrow and elongated interarticular area, with a lower facet extended towards the medial side. The internal temporal fossa is small in relation to the coronoid process and has an oval, narrow and elongated morphology, because of the arrangement of the condylar process. In addition, the coronoid process has a certain inclination toward the posterior part. It is difficult to establish diagnostic criteria to differentiate *N. fodiens* from *N. anomalus*. Their distinction usually relies on the height of the mandibular ramus, higher in *N. fodiens* (Gosálbez, 1987b, López-García, 2011). In Abric Romaní, it is not possible to reach a specific assignation, because only three mandibles are recovered, two of them broken. There remains are grouped under the name *Neomys* gr. *fodiens-anomalus*.

Habitat and geographical distribution. – The water shrew (*N. fodiens*) and the southern water shrew (*N. anomalus*) have similar habitat preferences. Both are considered species of European requirements, *N. anomalus* being better adapted to Mediterranean conditions. Usually, they are located near permanent water courses (rivers, streams, humid areas in general or even coastal areas), since they are considered semi-aquatic species, however *N. anomolus* is less dependent on aquatic environments. Also, occasionally, it can occupy humid pastures and even forest areas. *N. fodiens* usually lives in mountainous areas documented at altitudes of 900 m a.s.l.; while *N. anomalus* can occurs from sea level to above 1600 m a.s.l.. They present a discontinuous distribution in the Iberian Peninsula, with *N. fodiens* being limited to a narrow northern fringe (from Galicia to the Pyrenees) shared with *N. anomolus*, which is widely extended in the septentrional half, also penetrating in the northern area and the Iberian System until the Central System.

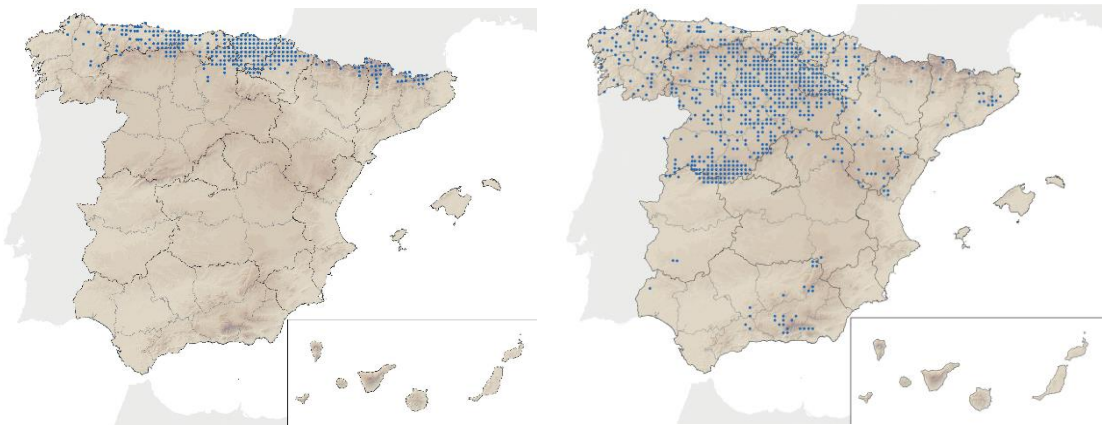

Present-day geographical distribution of *Neomys fodiens* (left) and *Neomys anomalus* (right) in Spain (Palomo et al., 2007).

Family TALPIDAE Fischer, 1814

Subfamily TALPINAE Fischer, 1814

Genus ***Talpa*** Linnaeus, 1758

Talpa europaea Linnaeus, 1758

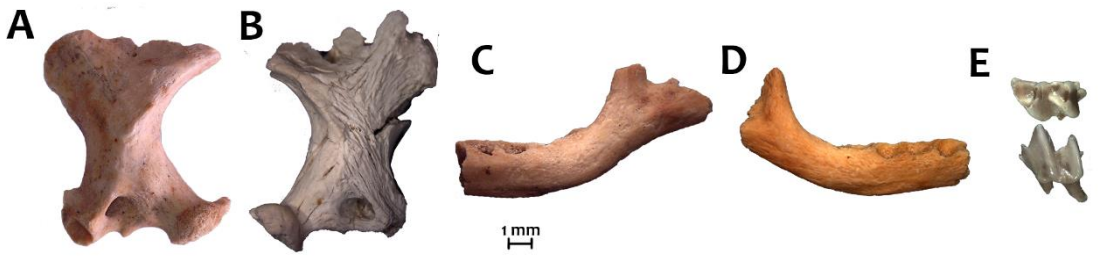

Talpa europaea remains: A) left humerus in anterior view, from level O; B) right humerus in anterior view, from level N; C) left mandible without teeth in labial view, from level N; D) right mandible without teeth in labial view, from level N; E) left m2 in occlusal and labial view, from level O. Scale 1 mm.

Material. – Level Q: one mandible without teeth, one humerus, one clavicula and one phalanx; Level O: seven mandibles without teeth, one m1, one m2, two m3, four lower molars indet., six humeri, two ulnas, two radii, three femora and three tibia-fibulas; Level N: four mandibles without teeth, one p4, one humerus and one radius; Level M: one mandible without teeth, one m1, one m2, one m3, two incisors, one canine, one clavicle, one scapula, one humerus, two radius, one sternum, one pelvis, two femora, three tibia-fibulas and two ulnas; Level J: one scapula and one radius.

Description. – The genus *Talpa* have a mandible notably larger than the rest of identified species of the order Soricomorpha. The mandible is elongated and graceful, with a mandibular body with curved profile and a mandibular ramus formed by three well-developed processes: coronoid and angular processes are robust, whereas condylar process is slender and cylindric. The dentition is composed by incisors, canines, premolars and molars. Molars are characterized by low crowns (narrower in lingual part), have dilambdodondt morphology and the location of the paracone and the metacone near the half of the crown. Upper molars have a triangular morphology, whereas lower molars are more quadrangular. Due to mole hypogeal habits, that conditions its locomotion, this genus shows remarkable adaptations in its postcranial bones, very robust, especially on the posterior limb elements. Thus, all postcranial bones allow to identify this genus, being humeri, femora, tibias and ulnas also good tools for the specific determination. The humerus is the most characteristic bone, it is wide and with the humeral head distally oriented (Furió, 2007; Gosàlbez, 1987; López-García, 2011). In the Iberian Peninsula, there are currently two species of this genus: *T. occidentalis* and *T. europaea*. The differentiation from the dental morphology or morphometry traits is complex, being the difference in the size of the humerus the best criterion to differentiate them. The measurements made by López-García (2011) determine that the Abric Romaní specimens from levels from levels M and O would be within the parameters established for *Talpa europaea*. Moreover, the first lower incisor (m1) of *T. europaea* has well-developed styles and the canine is large and characterized by a forward inclination and two roots. According to the past biogeography of

this species, there are no records of *T. occidentalis* in the Iberian northeast, where normally *Talpa europaea* is found.

Habitat and geographical distribution. – The common mole (*T. europaea*) is an hypogean species with burrowing habits. Thus, the conditional factor for its occurrence are the availability of deep, soft and humid soils to construct its extensive burrows and to find preys to feed. It mainly occupies grasslands and meadows, although it can also inhabit forests with well-formed soils, especially in deciduous forests. In the Iberian Peninsula, it is distributed through the Pyrenees and the Pre-Pyrenees, the Cantabrian Range and the Ebro Valley, the Basque Mountains and the mountains of Burgos. It can reach altitudes that extend from sea level to 2000 m a.s.l., as in the Pyrenees.

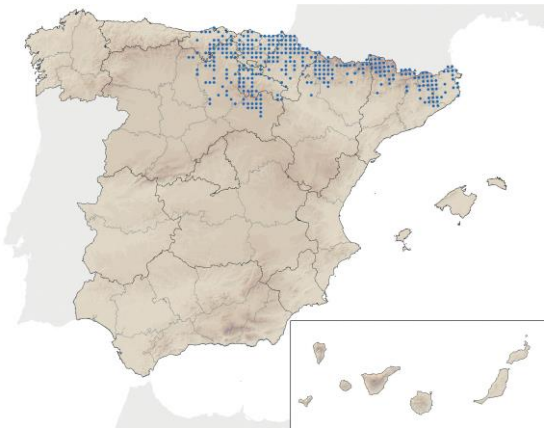

Present-day geographical distribution of *Talpa europaea* in Spain (Palomo et al., 2007).

Order CHIROPTERA Blumenbach, 1779

Chiroptera indet.

Material. – Level Q: one p4; Level O: one mandible without teeth; Level N: two mandibles without teeth, one maxilla and one long-bone; Level E: one mandible and four long-bones; Level D: five mandibles (four without teeth and one with m3), one maxilla with P4 and one p4.

Description. – Under this denomination, are grouped the remains that attending to their general morphology correspond to the order Chiroptera, but do not present diagnostic characters to be attribute to a genus or species. In the case of mandibles, their high level of fragmentation and loss of some cranial elements, difficulted the species determination, but the disposition and morphology of the alveoli and, in some occasions, the starting configuration of mandibular ramus are considered.

Suborder MICROCHIROPTERA Dobson, 1875

Family VESPERTILIONIDAE Gray, 1821

Subfamily VESPERTILIONINAE Gray, 1821

Genus ***Myotis***

Myotis* gr. *myotis-blythii Borkhausen, 1797 – Tomes, 1857

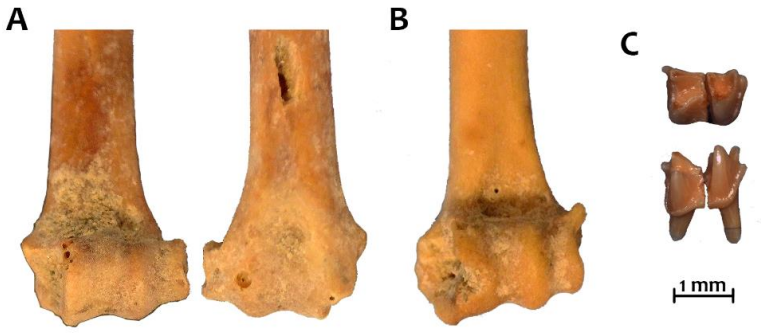

Myotis remains: A) left humerus of *Myotis* gr. *myotis-blythii* in external and internal view from level D; B) left humerus of *Myotis* gr. *myotis-blythii* in external view from level D; C) right m2 of *Myotis* sp. in occlusal and labial view, from level N. Scale 1 mm.

Material. – *Myotis* gr. *myotis-blythii*.- Level D: one M1 and two humeri. / ***Myotis* sp. –** Level N: one m2.

Description. – The genus *Myotis* is inside the family Vespertilionidae and show some of the main characters of this groups. The mandibular dental formula is three incisors, one canine, three premolars and three molars (3-1-3-3). The mandibular ramus has a triangular morphology. The lower molars have "myotodont" morphology (the hypoconulid is separated from the entoconid) and have thick and irregular cingulum. The M1 is large and characterized by the absence of talon and hypocone and the lingual cingulum is interrupted bellow the protocone. Inside this genus, there are two species of large-size in Europe: *M. myotis* and *M. blythii*. It is complex to distinguish between both species considering only morphological treats and biometrics analysis on cranial and dental elements are recommended (Galán et al., 2018a; López-García, 2011; Sevilla, 1988). The humerus distal epiphysis of these species present some diagnostical characters: the lack of the styloid process, the condyle is separated by a shallow groove from the epicondyle, the proximal edge of the trochlea does not reach the epiphyseal border and, in external view, the proximal edges between the trochlea and condyle have similar height and is straight or slightly concave (Dupuis, 1986; Felten et al., 1973; Galán et al., 2018b). Abric Romaní presented all these distinctive characters. The m2 related to genus *Myotis* sp. is myotodont with the lingual cusps aligned, closed trigonid ("V" shape) and an irregular and medium-wide cingulum (López-García, 2011; Sevilla, 1988). It has a small-size compared to that expected for *M.* gr. *myotis-blythii*. It is not possible to detail the species of this single remain, considering that there are several small-size species of this genus currently in Europe.

Habitat and geographical distribution. – The greater mouse-eared bat (*M. myotis*) is a typical forest-dweller. It foragers on mature and deciduous woodlands, woodland edges and wooded pastures. On the contrary, the lesser mouse-eared bat (*M. blythii*) is more frequent on open environments, such as steppe, meadows, grassland and scrubs, including farming lands. Both species usually roosts in underground cavities, mines or buildings, where establish hibernating colonies. *M. myotis,* occasionally, forms small colonies in trees. They have been documented up to the 2000 m a.s.l., but it is strange to find them above the 1500 m a.s.l.. Both are Palaeartic species, occurring in western, central and southern Europe. Both are widespread by the entire Iberia, but with irregular abundances and frequent confusions between both species identification. *M. myotis* is frequent in the Mediterranean area but is highly conditionate by the availability of refuges.

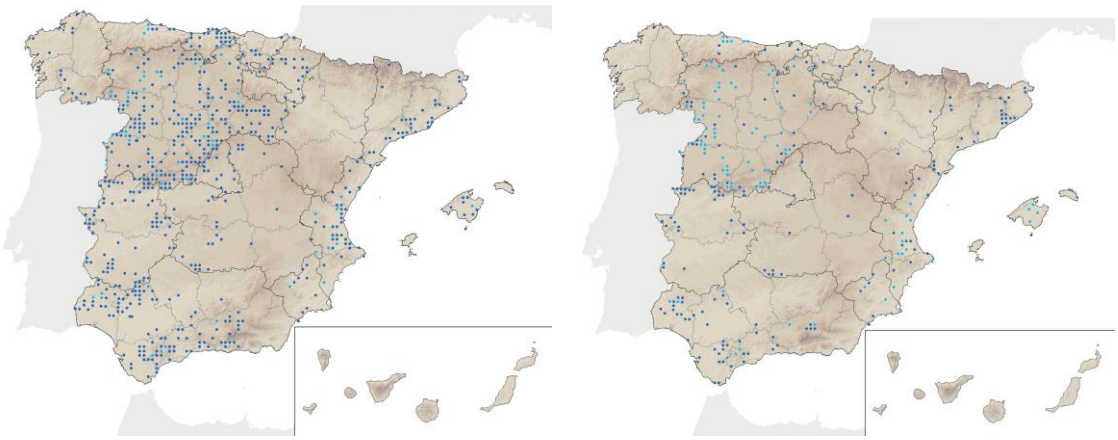

Present-day geographical distribution of *Myotis myotis* (left) and *Myotis blythii* (right) in Spain (Palomo et al., 2007). In light blue are marked areas with dubious identification between both species.

Genus ***Plecotus*** Geoffroy Saint-Hilaire, 1818

Plecotus* gr. *auritus-austriacus Linnaeus, 1758 – Fischer, 1829

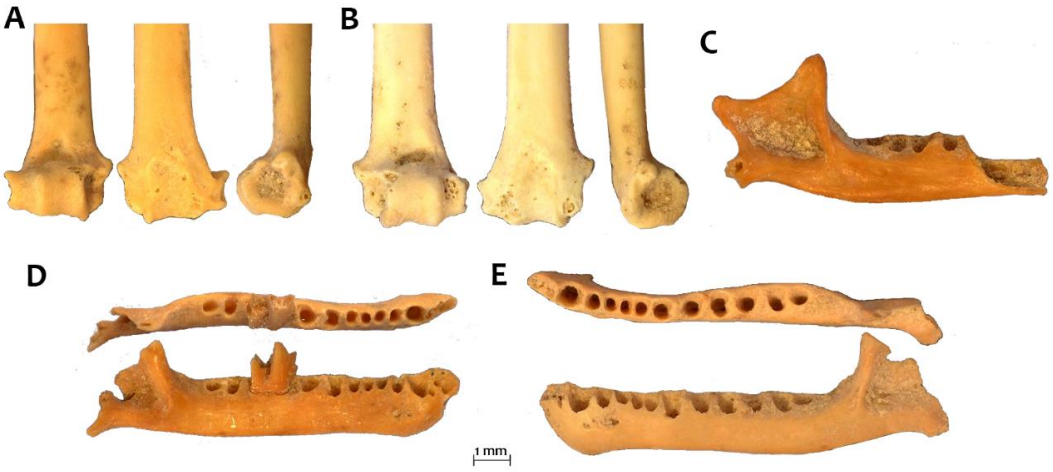

Plecotus gr. *auritus-austriacus* remains: A) right humerus in external, internal and anterior view, from level E; B) left humerus in in external, internal and anterior view, from level E; C) right mandible without teeth in labial view, from level D; D) right mandible with m2 in occlusal and labial view, from level D; E) left mandible without teeth in occlusal and labial view, from level E. Scale 1 mm.

Material. – Level E: three mandibles without teeth, one m1, one m2, one p4 and two humeri; Level D: two mandibles (one with m2 and one without teeth).

Description. – As other vespertilionids, the genus *Plecotus*, has a lower dentition composed by three incisors, one canine, three premolars and three molars (3-1-3-3). The lower molars have a myotodont morphology in occlusal view and thick and irregular cingulum in lateral view. There are some characters that allow the distinction of this genus from other medium-size myotodont species, such as the quadrangular morphology of the mandible. In addition, the mandible has high condylar process, almost at the coronoid process level, and the angular process is well-developed and robust (Dupuis, 1986; López-García, 2011; Menu and Popelard, 1987). The p4 has quadrangular morphology. The differentiation between *P. auritus* and *P. austriacus* is complex and usually relies in the P4 and the canine; but associated remains are commonly identified as *P.* gr. *auritus-austriacus* (Sevilla, 1988). The humerus distal epiphysis recovered not present styloid process (internal view), a narrow epitrochlear (posterior view), the trochlea and the condyle are separated by a shallow groove and the union is almost straight in the distal edge (external view). In opposition with the genus *Myotis*, in external view, in these remains the proximal profile form by the trochlea and the condyle is slightly convex (Dupuis, 1986; Felten et al., 1973). Considering the angular pass from the epitrochlea to the styloid procedd, in the internal view, it is most likely to attribute these remains to *P. auritus* (Dupuis, 1986). But, due to the scarce number of remains, it is preferred to consider these remains as *P. auritus-austriacus* group.

Habitat and geographical distribution. – The brown long-eared bat (*P. auritus*) main ecological preference are the deciduous and coniferous forest of Eurasia. But in the Mediterranean region is more frequent in mountain systems either in humid or dry forest. It can be found from the sea level to the 1600 m a.s.l. On the contrary, the grey long-eared bat (*P. austriacus*) tends to forager in a great variety of habitats, but prefers more open environments and it is more frequent in lowland valleys, although it can reach altitudes up to 2000 m a.s.l.. Both species, during summer, form colonies in tree holes or buildings. In winter, they hibernate in caves, mines, building and occasionally trees. *P. austriacus* is more widespread by overall Iberian, but is only frequent in the Mediterranean area, whereas *P. auritus* occupies mainly the mountain systems of the septentrional half.

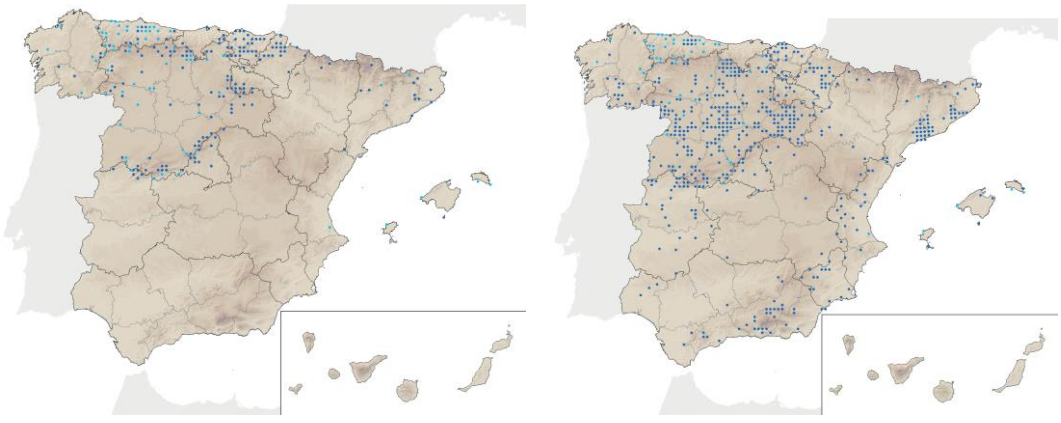

Present-day geographical distribution of *Plecotus auritus* (left) and *Plecotus austriacus* (right) in Spain (Palomo et al., 2007). In light blue are marked areas with dubious identification between both species.

Genus ***Nyctalus*** Kaup, 1829

Nyctalus lasiopterus Schreber, 1780

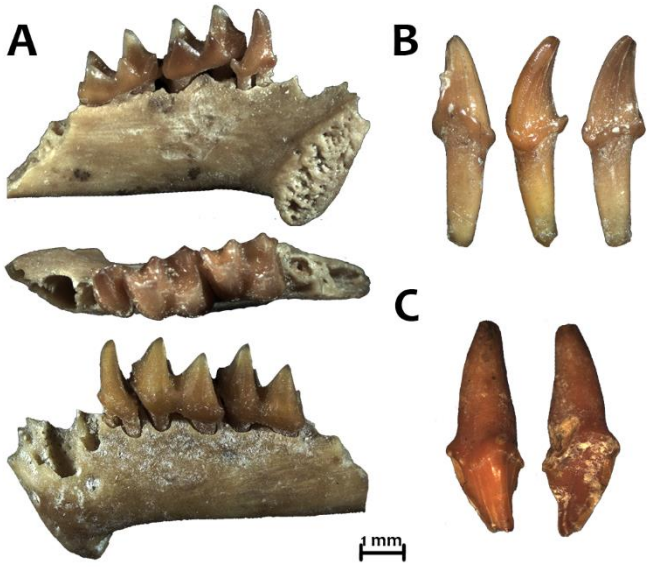

Nyctalus lasiopterus remains from level O: A) left mandible with p4-m2 in lingual, occlusal and labial view; B) left lower canine in anterior, labial and posterior view; C) left upper canine in labial and lingual view. Scale 1 mm.

Material. – Level O: one mandible with p4-m2, one lower canine (ci) and one upper canine (Ci).

Description. – The species *Nyctalus lasiopterus* is the largest European bat and their mandible and teeth can be easily distinguished by its large size. It belongs to the Vespertilionidae family, evidenced by its wide and irregular cingulum. However, this species presents certain characters typical of Rinolophidae family, such as its mandibular dental formula (composed only of two premolars) and lower molars with nyctalodont morphology (with the hypoconulid attached to the entoconid). Considering the mandible, is remarkable its large size and robustness and a marked chin with round profiles, typical of vespertilionids. The level O mandible with *in situ* teeth (p4, m1 and m2) was already identified and described by López-García (2011) and López-García et al. (2009). In this work one lower canine (ci) and one upper canine (Ci) possibly belonging to the same individual are identified. The former presents a flattened distal face, convex labial face and concave lingual face. The cingulum is thick and interrupts at the most mesial point of the crown. It has two small accessory cusps, both located in the lingual part, one in the anterior zone and the larger one in the posterior part of the canine. Both crown and root of the upper canine is more robust than in other genera and do not form an angle. It has three flat faces: the anterior-labial face, the posterior-labial face and the lingual face. The posterior edge has an angularity close to the cingulum, which is thick and irregular (Menu and Popelard, 1987; Sevilla, 1988).

Habitat and geographical distribution. – The greater noctule (*N. lasiopterus*) habitat preferences are still quite unknown. It is usually associated with forest environments, preferably with mature and well-developed trees, most often in deciduous forests, such as oak and other leafy formations. This ecological preference is related to the habit of roosting in hollows of these types of trees. It also resides in mixed and conifers forest (such as pine and fir). In the Iberian Peninsula, the species is widely distributed, but

discontinuously and the distribution is only partially known. It has been documented both in the Eurosiberian area (Cantabrian Range, Western Pyrenees and northern Iberian System) and in Mediterranean environments (Central System, Doñada and Cádiz Mountains); from sea level to above 1300 m a.s.l..

Present-day geographical distribution of *Nyctalus lasiopterus* in Spain (Palomo et al., 2007). In light blue, dubious identifications.

Genus ***Pipistrellus*** Kaup, 1829

Pipistrellus pipistrellus Schreber, 1774

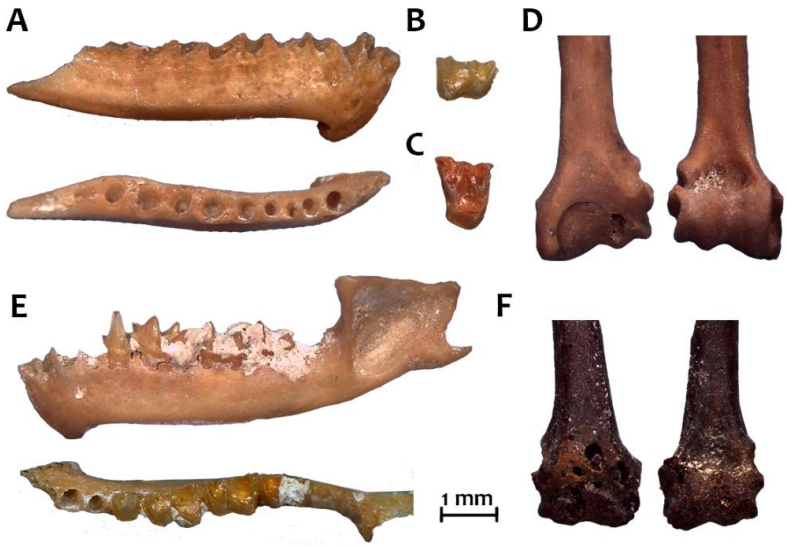

Pipistrellus pipistrellus remains from level N: A) right mandible without teeth in labial and occlusal view; B) m1 right in occlusal view; C) left M1 in occlusal view; D) right humerus in internal and external view; E) left mandible with p4-m3 in labial and occlusal view; F) left humerus in internal and external view. Scale 1 mm.

Material. – Level O: one mandible without teeth; Level N: one mandible with p4-m3, one mandible without teeth, one maxilla with P4, one canine (ci), two m1, one m3, one P4, one M1 and two humeri; Level E: one mandible without teeth.

Description. – *Pipistrellus pipistrellus* is the smallest representative of this order in Europe. Although this species is inside the Vespertilionidae family, share some characters with the Rinolophidae family, such as the mandibular dental formula, composed by three incisors, one canine, two premolars and three molars (3-1-2-3). The mandible is characterized by its small size, provide with a marked chin, a short and narrow angular process and oriented to distal part in ascending direction and a well-defined masseteric crista with a more or less uniform thickness, conferring a triangular morphology to the fossa of the anterior part of the mandible, in labial view (Dupuis, 1986; López-García, 2011; Menu and Popelard, 1987). The mental foramen is place between the canine and the p3. The lower molars of this species are "nyctadolont", with the entoconid connected with the hypoconulid, and have an irregular and wide cingulum. The m1 and m2 show a closed trigonid without lingual cingulum, a concave entocrista and lingual cusps aligned. A reduction of the talonid is expected in the m3. P4 has a triangular-polygonal shape, the labial and anterior faces are straight, the lingual has a well-developed talon and the distal face is concave. The P4 has a protuberant accessory cusp on the anterior face, where talon starts. The M1 and M2 have parastyle, mesostyle and metastyle aligned. The M1 has a straight distal edge, in opposition to *P. kulhii* (López-García, 2011; Menu and Popelard, 1987; Sevilla, 1988). All these characters have been detected in the remains recovered in Abric Romaní site. The two distal humerus epiphyses are related also to this species by the styloid process present but short, a medium width of the condyle and trochlea, a deep antecubital fossa and a epicondyle slightly surpassing the condyle in posterior view (Felten et al., 1973; Galán et al., 2016b; Menu and Popelard, 1987).

Habitat and geographical distribution. – The common pipistrelle (*P. pipistrellus*) inhabits great variety of habitats, either closed forest environment or spaces devoid of vegetation, including urban settlements, being very common in the cities. Also lives in Mediterranean shrubland, pastures and cultivated areas. Frequently, it roosts in hollows and crevices of rocks, trees or human constructions. During hibernation, in cold regions it creates large colonies in caves, while in warm regions it is only documented at the entrance of caves occasionally. It is a generalist species that can be documented from the coast to 2000 m a.s.l.. It is distributed throughout the Iberian Peninsula, including the Balearic Islands, being more frequent in the northern half.

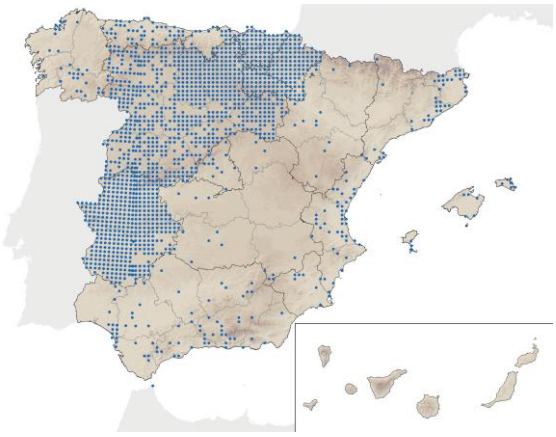

Present-day geographical distribution of *Pipistrellus pipistrellus* in Spain (Palomo et al., 2007).

Subfamily MINIOPTERINAE Dobson, 1875

Genus ***Miniopterus*** Bonaparte, 1837

Miniopterus schreibersii Kuhl, 1817

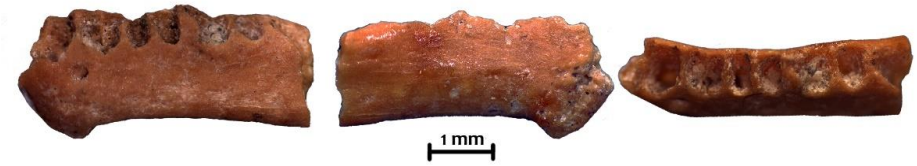

Left mandible fragment of *Miniopterus schreibersii* in labial, lingual and occlusal view, from level N. Scale 1 mm.

Material. – Level N: one mandible.

Description. – This species presents the main characters of the Vespertilionidae subfamily, as the mandibular dental formula, composed by three incisors, one canine, three premolars and three molars (3-1-3-3). Lower molars are nyctadolont and have narrow and irregular cingulum. However, the main specific characteristic of *M. schreibersii* is its large p3 sustain by two roots, providing an extra alveolus to the mandible, whereas in the rest of genus the p3 has only one root (Dupuis, 1986; Menu and Popelard, 1987; Sevilla, 1988). The single broken mandible recovered in Level N, presents these double-alveoli in correspondence with p3 position, between the canine and the two alveoli related to p4. The mandible has medium-size, is slender and has an angulate chin. The mental foramen is large and usually located under and between the alveoli of the canine and the p2 (Galán et al., 2016a). Mandibular general morphology and p3 alveoli are the characters that let to related this remain with *M. schreibersii*.

Habitat and geographical distribution. – The common bentwing bat (*M. schreibersii*) is a typical cave-dwelling species. It stablished its refuges in caves, mines and tunnels, where can form hibernation colonies with *Myotis myotis*. Occasionally, roosts in rock crevices or buildings. It forages in a variety of open and semi-open habitats, normally under Mediterranean influence, either in mountain or plain, including suburban areas. It can live from lea level to altitudes up to 1400 m a.s.l.. This species has a subtropical origin, currently widely distributed in Asia Minor, Africa and southern Europe, including all the Iberian Peninsula. It is more frequent in the Mediterranean area and in the southern half of the peninsula.

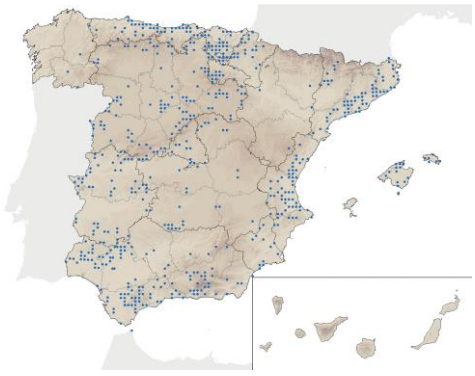

Present-day geographical distribution of *Miniopterus schreibersii* in Spain (Palomo et al., 2007).

Order RODENTIA Bowdich, 1821

Superfamily MUROIDEA Illiger, 1811

Family CRICETIDAE Fischer, 1817

Subfamily ARVICOLINAE Gray, 1821

Genus ***Arvicola*** Lacépède, 1799

Arvicola sapidus Miller, 1908

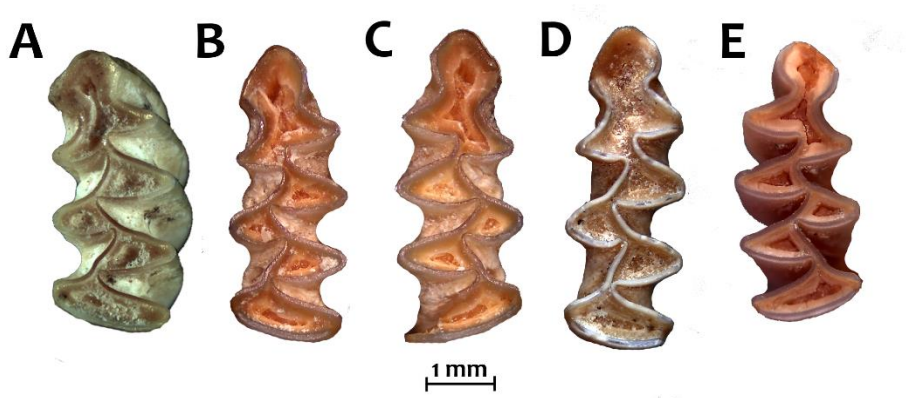

Arvicola sapidus molars in occlusal view: A) left m1 from level O; B) left m1 from level L; C) right m1 from level L; D) left m1 from level N; E) right m1 from level P. Scale 1 mm.

Material. – Level Q: three m1; Level P: thirteen m1; Level O: one hundred-seven m1; Level N: nine m1; Level L: seven m1; Level K: twenty m1; Level J: 11; Level I: four m1; Level H: one m1; Level F: one m1; Level E: five m1; Level D: fourteen m1.

Description. – The large size of this genus molars in comparison with respect to other Arvicolinae molars, facilitated the specific attribution. This large size is also reflected in other cranial and in post-cranial remains. The first lower molar (m1) is composed by five triangles: three closed triangles in the posterior part (T1-T3) and two open triangles (T4-T5) in the anteroconid complex (ACC). Two species of genus *Arvicola* are nowadays present in the Iberian Peninsula: *A. sapidus* and *A. amphibius*. The first can be recognized because T4-T5 are not parallel and T5 forms an acute angle with the anterior cap (AC), that inclines to the lingual border. Otherwise, in *A. amphibious* molars, the T5 and the AC forms an obtuse angle and the AC is rounder. In addition, *A. sapidus* possess a "*Mimomys*" enamel type, thinner in leading edges than in trailing edges of the triangles; whereas *A. amphibus* have a "*Microtus*" enamel type, thicker in leading edges with respect to trailing ones (Chaline, 1972; Cuenca-Bescós et al., 2008; Gosàlbez, 1987; López-García, 2011). Molars recovered from Abric Romaní present *Mymomys* enamel pattern and AC with an acute angulation, allowing to confirm the *A. sapidus* attribution of some previously identified remains by López-García (2011).

Habitat and geographical distribution. – The southern water vole (*A. sapidus*) is a semi-aquatic rodent always linked to water streams or stable water deposits with abundant herbaceous vegetation in its margins, preferably it occurs in margins of slow-flowing streams with argillaceous shores which allow

burrow activity. It is also found in ponds, lagoons and marshes. Occasionally, it can be found occupying wet meadows, dry ponds or slightly turbid areas. It has been detected from the sea level to 2,300 m a.s.l., in the Pyrenees. The southern water vole occurs in areas of the Iberian Peninsula, especially in the northern and eastern part, and most of France.

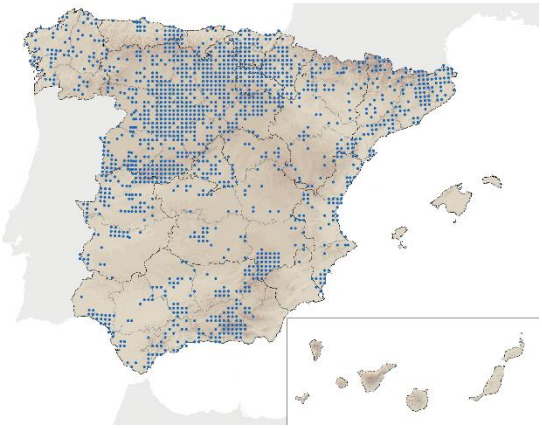

Present-day geographical distribution of *Arvicola sapidus* in Spain (Palomo et al., 2007).

Genus ***Microtus*** Schrank, 1798

Microtus arvalis Pallas, 1778 / ***Microtus agrestis*** Linnaeus, 1761

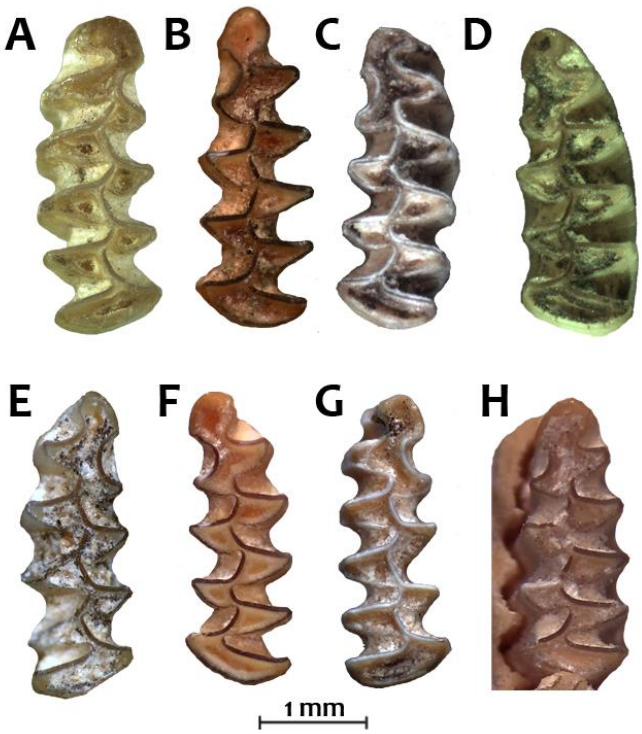

Above, *Microtus agrestis* molars in occlusal view: A) right m1 from level O; B) left m1 from level D; C) left m1 from level O; D) left m1 from level O. Bellow, *Microtus arvalis* molars in occlusal view: E) right m1 from level E; F) left m1 from level H; G) right m1 from level J; H) left m1 from level J. Scale 1 mm.

Material. – *Microtus arvalis.* – Level O: fifty-four m1; Level K: two m1; Level J: four m1; Level I: one m1; Level H: two m1; Level E: seven m1; Level D: three m1. / ***Microtus agrestis.* –** Level O: forty-five m1; Level N: one m1; Level K: one m1; Level J: two m1; Level I: one m1; Level H: one m1; Level E: four m1; Level D: four m1.

Description. – The genus *Microtus* is characterized by a m1 with seven triangles, with closed T4-T5. The enamel pattern is type "*Microtus*" (thicker in leading edges) and molars have abundant cementum. Although some morphological and morphometric characters of *M. arvalis* and *M. agrestis* overlap, both species can generally be differentiated. *M. arvalis* presents more symmetric and parallel disposition of triangles and reentrant angles, especially in the disposition of T4-T5 (BRA3-LRA4) and T6-T7 (BRA4-LRA5), and more round ACC. Otherwise, *M. agrestis* have a more asymmetric disposition and stronger alternation of reentrant angles, notable between T4-T5 and reducing the confluence between T6-T7, generating a more angular ACC (Chaline, 1972; Luzi et al., 2017; Nadachowski, 1982). These are the criteria employed to differentiate between both species for Abric Romaní molars.

Habitat and geographical distribution. – The common vole (*M. arvalis*) is usually found in wide variety of open habitats with supra-Mediterranean climate and preferred not too humid soils and high vegetation cover, such as grasslands, meadows and pastures. Usually avoid closed forests, preferably occupying alpine and subalpine meadows. The altitudinal distribution of this species is extended between 500 m and 2200 m a.s.l. In Iberia, its geographical distribution is limited to the septentrional mountainous systems (such as Pyrenees and Pre-Pyrenees), not reaching the Mediterranean fringe. The field vole (*M. agrestis*) is a Palaeartic species that lives in cool environments and needs high and dense grassland, preferable when it grows in humid places. It is common in mountain and forest areas, but its ecological preferences are meadows, grasslands, stream margins, reed beds, spines or heaths. In Iberia Peninsula, it can reach the 2000 m of altitude. Although in Eurasia present a widespread distribution, in Iberia it is limited to the northern area, from Lisbon to the Catalan coast. In northeastern Iberia, is mainly found in the Pyrenees, the Pre-Pyrenees and minor mountainous systems.

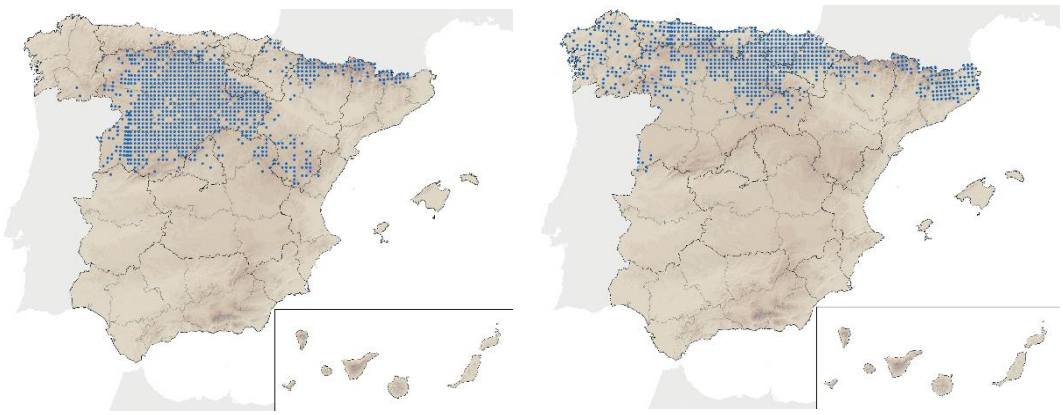

Present-day geographical distribution of *Microtus arvalis* (left) and *Microtus agrestis* (right) in Spain (Palomo et al., 2007).

Genus ***Chionomys*** Miller, 1908

Chionomys nivalis Martins, 1842

Left m1 of *Chionomys nivalis* in occlusal view, from level E. Scale 1 mm.

Material. – Level E: 1 m1.

Description. – *Chionomys nivalis* is the largest *Microtus*-type species in Iberia, but notably smaller than the species *A. sapidus*. Its molars have a *Microtus*-type enamel (thicker in leading edges) and have cementum. It can be easily distinguished from other species of the same genus because its m1s are composed by five closed triangles (T1-T5, with three BRAs and four LRAs) and have a characteristic round AC, with mushroom-shaped, strongly inclining to labial side (Cuenca-Bescós et al., 2008; Gosàlbez, 1987; López-García, 2011).

Habitat and geographical distribution. – The snow vole (*C. nivalis*) lives on mountain slopes or forest clearings, always in areas where the ground is covered with stable stones with little herbaceous cover. In this way colonizes mountain peaks, alpine refuges and the walls of subalpine meadows. After strong expansion during the Last Glacial, the current species population at Iberia are limited to small nuclei in concrete biotopes of mountainous regions of high altitudes. It is usually located between 1,000 and 2,600 m a.s.l., thus in Iberian Peninsula occupies the main mountainous areas. In northeastern Iberia, its distribution is concentrated in the Pyrenees and in the northernmost areas of the Pre-Pyrenees.

Present-day geographical distribution of *Chionomys nivalis* in Spain (Palomo et al., 2007).

Subgenus ***Terricola*** Fatio, 1867

Microtus (Terricola) duodecimcostatus Sélys-Longchamps, 1839 /

Microtus (Terricola) gerbei Gerbe, 1879

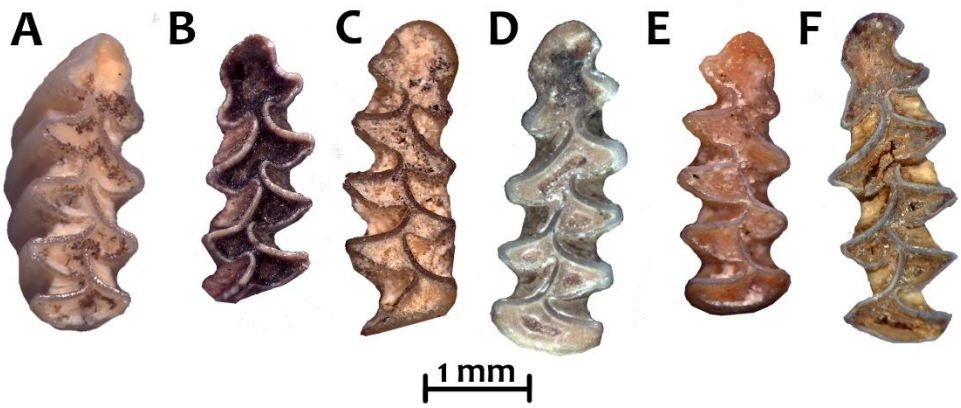

Microtus (Terricola) duodecimcostatus molars in occlusal view (from A to E): A) right m1 from level N; B) left m1 from level P; C) right m1 from level E; D) left m1 from level O; E) right m1 from level N. / *Microtus (Terricola) gerbei* molar in occlusal view (F): left m1 from level Q. Scale 1 mm.

Material. – *M. (T.) duodecimcostatus.* – Level Q: one m1; Level P: one m1; Level O: forty-six m1; Level N: ten m1; Level L: two m1; Level K: four m1; Level: sixteen m1; Level D: six m1 / ***M. (T.) gerbei.*** – Level Q: two m1.

Description. – The subgenus *Terricola* group small-size species of the genus *Microtus*, which m1 are characterized by the confluence between the fourth (T4) and the fifth (T5) triangle, conforming the commonly known as "pytiminian rhomb". The m1s presented seven triangles, with the three posterior triangles closed (T1-T3). Two species of this subgenus are currently present in northeastern Iberia: *M. (T.) duodecimcostatus* and *M. (T.) gerbei*. Both species presents in their first lower molars (m1) a second "pytyminian rhomb" with the confluence of the T6-T7, but whereas in *M. (T.) duodecimcostatus* both triangle are symmetric and parallel with the T6 open, in *M. (T.) gerbei* this confluence is asymmetric and less parallel with the T4 and, specially, the T6 inclining to the anterior part of the molar (Brunet-Lecomte and Chaline, 1990; Cuenca-Bescós et al., 2008; López-García, 2011). Considering these characters, Abric Romaní remains correspond to *M. (T.) duodecimcostatus*, only except for two remains of *M. (T.) gerbei* in level Q, with a remarkable distal inclination of the T6.

Habitat and geographical distribution. – The Mediterranean pine vole (*M. (T.) duodecimcostatus*) is a typical thermo-Mediterranean species. It usually inhabits open habitat, such as cultivated areas, abandoned fields, meadows, wooded meadows and marshes edges. Its presence is mainly conditioned by the existence of stable and humid soils, easy to excavate and with abundant herbaceous cover. It occupies altitudes from sea level to 3000 m a.s.l.. The Mediterranean pine vole is an Iberian endemism, widespread for all the peninsula reaching southern France, but exempt in the northwestern corner of Iberia and in the Pyrenees. The Pyrenean pine vole (*M. (T.) pyrenaicus*) lives on forest margins of high mountainous areas and subalpine meadows. However, it is not a species limited by altitude, since it can be found from sea level to 2000 m, but rather due to climatic factors: it usually inhabits rainy places

(MAP>1000 mm). Thus, it never achieves Mediterranean areas. Nowadays, its distribution is restricted to a narrow northern band that extend from Cantabria to Aran Valley. In northeastern Iberia, only occurs in the highest altitudes of the Pyrenees.

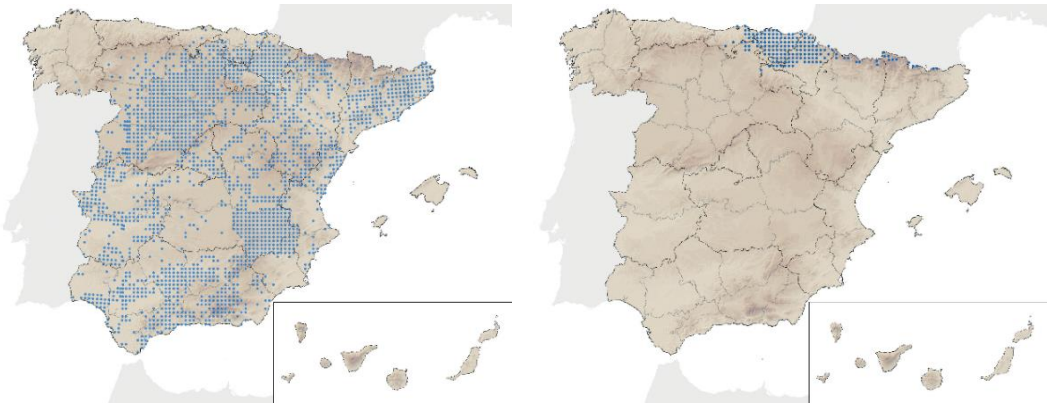

Present-day geographical distribution of *Microtus (Terricola) duodecimcostatus* (left) and *Microtus (Terricola) gerbei* (right) in Spain (Palomo et al., 2007).

Genus ***Iberomys*** Chaline, 1972

Iberomys cabrerae Thomas, 1906

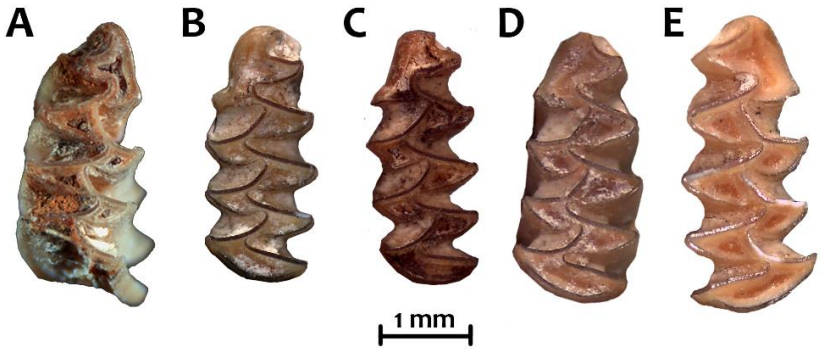

Iberomys cabrerae molars in occlusal view: A) right m1 from level O; B) left m1 from level J; C) left m1 from level N; D) left m1 from level Q; E) right m1 from level Q. Scale 1 mm.

Material. – Level Q: twelve m1; Level O: eighty-seven m1; Level N: eleven m1; Level M: one m1; Level L: one m1; Level K: three m1; Level J: five m1; Level E: 1 m1; Level D: 14.

Description. – Initially included as the subgenus *Iberomys* inside the genus *Microtus* for Chaline (1972), recent revision work of Cuenca-Bescós et al. (2014) observed enough morphological, biological and ecological differences, besides an own evolutionary history, to elevated this subgenus to the rank of genus. This genus has only one current representative: *Iberomys cabrerae*. The molars recovered from the Abric Romaní associated to this species present a large and width m1 and have abundant cementum. These molars are composed by 7 triangles, the five posterior triangles not confluent, including the fourth (T4) and the fifth (T5) triangles completely closed. These m1 show, in general, a clear asymmetry between labial triangles, narrower, and lingual triangles, wider. The salient and reentrant angles are markedly

acute. The main characteristic, however, is that the T6 is underdeveloped and inclining to the posterior part, giving to the ACC a triangular or arrowhead shape. In addition, the salient angle of T6 (BSA4) is formed by two small lobes that create a small recess, giving it a quadrangular shape, and the salient angle of T7 (LSA5) long and narrow (Chaline, 1972; Cuenca-Bescós et al., 2014; López-García, 2011).

Habitat and geographical distribution. – The Cabrera's vole (*I. cabrerae*) is an endemic species of Iberia. It inhabits strictly Mediterranean climatic areas, avoiding Eurosibereian climatic conditions. This species requires herbaceous cover grassy all the year, establishing the populations around areas with high water-table, such as reed beds, grassland and river banks, showing preference for neighborhood areas to ditches and streams. Its altitudinal range extends between 250 m and 1500 m a.s.l.. This species, currently, does not reside in northeastern Iberia. Indeed, in the Iberian Peninsula, it presents a fragmented distribution, caused by anthropic pressure, that limited its presence to the Central System, the Baetic System and the Iberian System and a small relic nucleus in the Pre-Pyrenees from Aragon.

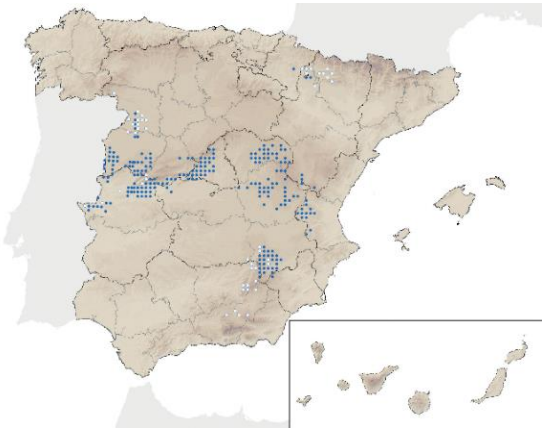

Present-day geographical distribution of *Iberomys cabrerae* in Spain (Palomo et al., 2007).

Family MURIDAE Illiger, 1811

Subfamily MURINAE Illiger, 1811

Genus ***Apodemus*** Kaup, 1829

Apodemus sylvaticus Linnaeus, 1758

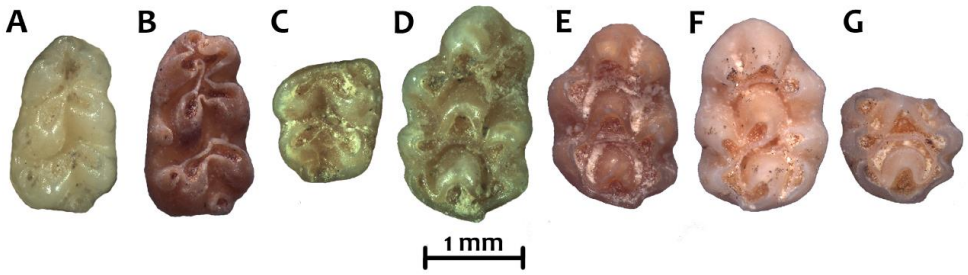

Apodemus sylvaticus molars in occlusal view: A) left m1 from level O; B) left m1 from level E; C) righ m2 from level O; D) left M1 from level O; E) left M1 from level P; F) right M1 from level N; G) left M2 from level N. Scale 1 mm.

Material. – Level Q: two m1 and four incisors; Level P: three m1, one m2, two M1, one M2 and four incisors; Level O: one hundred-ten m1, thirty-nine m2, six m3, two lower molars indet., seventy-four M1, nineteen

M2, three M3, thirty-one mandibles (three with m1, two with m2, two with m1-m2 and twenty-four without teeth), twenty-five maxillae (one with M1-M3, one with M3 and twenty-three without teeth); Level N: fifteen m1, seven m2, one m3, four M1, one M2, six mandibles (one with m1-m2, one with m2 and four without teeth) and four maxillae (one with M1, one with M2 and two without teeth) and three molars indet.; Level L: one M1 and one mandible without teeth; Level J: two M1, two mandibles (one with m1-m2 and one with m2) and two maxillae (one with M1-M3 and one with M3); Level I: one m1 and one mandible without teeth; Level E: twenty-one m1, five m2, one m3, seven M1, four M2, three M3, twenty-two mandibles (two with m1-m3, nine with m1-m2, five with m1, three with m2 and three without teeth) and maxillae (one with M1-M3, one with M1-M2, one with M2-M3, two with M1 and five without teeth); Level D: eight m1, seven m2, one m3, eleven M1, one M2, two M3, two molars indet., twenty mandibles (one with m1-m3, twelve with m1-m2, three with m1, two with m2 and two without teeth) and twelve maxillae (one with M1-3, two with M1-M2, two with M2-M3, four with M1, two with M2 and one without teeth).

Description. – The genus *Apodemus* is characterized by upper and lower molars with low occlusal surfaces composed for series of cusps or tubercles separated by narrow and deep furrows. The first lower molars (m1) have six antero-lingual and antero-labial tubercles (tF, tE, tD, tC) arranged in a "X" shape, on the labial side there are two or three secondary cusps (c), one proximal tubercle (tma) and a posterior cusp (pc) low, round and well-developed. The first upper molar (M1) is large and shows three rows of well-differentiated tubercles; while posterior upper molars (M2 and M3) are smaller and lost some tubercles with respect to M1. Two different species of genus *Apodemus* inhabit Iberia: *A. sylvaticus* and *A. flavicollis*. The conjunction between the tubercles T4 and T7 on M1 and the development of the tubercle T9 on the M2 are the morphologic characteristics that ascribe Abric Romaní remains to *A. sylvaticus* (Cuenca-Bescós et al., 1997; López-García, 2011; Pasquier, 1974).

Habitat and geographical distribution. – The wood mouse (*A. sylvaticus*) is a very adaptable species, inhabiting a wide variety of habitats, from forests, bushes, crops, meadows with tall grass, grasslands, dunes, moorland, farmland and rocky margins. It preferably occupies areas with abundant shrub or tree cover, although in homogenous forest masses areas, it prefers marginal areas. It occupies an altitudinal range that extends from sea level to 2000 m a.s.l.. The field mouse is broadly and continuously distributed throughout Iberia, including the northeast, only with the exception of the Ebro Delta.

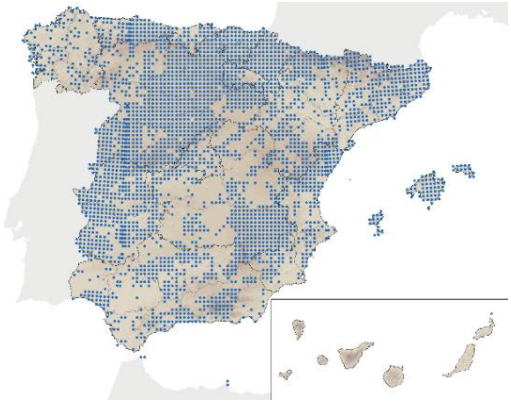

Present-day geographical distribution of *Apodemus sylvaticus* in Spain (Palomo et al., 2007).

Suborder SCIUROMORPHA Brandt, 1855

Family GLIRIDAE Muirhead, 1819

Subfamily LEITHIINAE Lydekker, 1895

Genus ***Eliomys*** Wagner, 1840

Eliomys quercinus Linnaeus, 1766

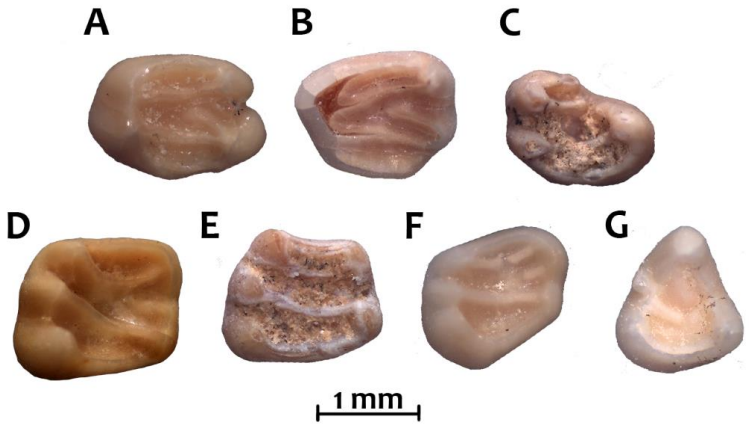

Eliomys quercinus remains in occlusal view: A) left M2 from level N; B) left M3 from level N; C) right P4 from level E; D) left m1 from level N; E) left m2 from level E; F) left m3 from level N; G) left p4 from level N. Scale 1 mm.

Material. – Level O: seven p4, nineteen m1-m2, two m3, five P4, twelve M1-M2, nine M3 and one indet; Level N: three p4, three m1-m2, two m3, two M1-M2 and two M3; Level J: one P4 and one m1; Level E: one mandible with m1-m2, two p4, three m1-m2, two m3, one P4, five M1-M2 and one M3; Level D: two p4, five m1-m2, two m3, one P4, three M1-M2 and one M3.

Description. – Currently, in Iberian Peninsula, there is only one species of the genus *Eliomys*: *E. quercinus*. The molars of this species are characterized by concave occlusal surfaces with prominent labial cusps, two for upper molars and three for lower ones. The crests that connected the mention cusps in labio-lingual sense, also called "lophos", are large and not very complex. The morphology of upper molars is quadrangular, while that of lower molars is more rounded. Have triangular premolars (p4-P4), especially the upper ones. Abric Romaní remains correspond with the main characters. Is not difficult to differentiated *Eliomys* teeth from the genus *Glis*, characterized by larger teeth, more complex crests and flat occlusal surface (Daams, 1981, Gosálbez, 1987b, Blanco, 1998b, López-García, 2011).

Habitat and geographical distribution. – The garden dormouse (*E. quercinus*) its main habitat is woodland, but is a generalist species, capable of living in numerous terrestrial and arboreal habitats. It is frequent in rocky areas, although it is also a typical species in areas of dense scrubs and in forested areas (coniferous, mixed and deciduous forests). It inhabits at altitudes ranging from the coast to 2000 m a.s.l.. It is widely distributed in Europe, including Iberia. In the northeast, it is presents, except for the Ebro Delta, and is more abundant at the Pyrenees than at sea level.

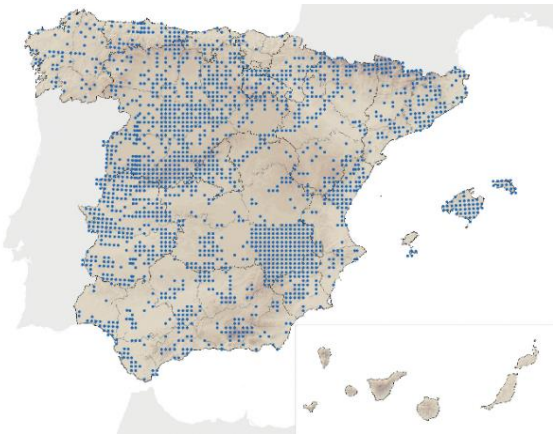

Present-day geographical distribution of *Eliomys quercinus* in Spain (Palomo et al., 2007).

Family SCIURIDAE Fischer & Waldheim, 1817

Subfamily SCIURINAE Baird, 1857

Genus ***Sciurus*** Linnaeus, 1758

Sciurus vulgaris Linnaeus, 1758

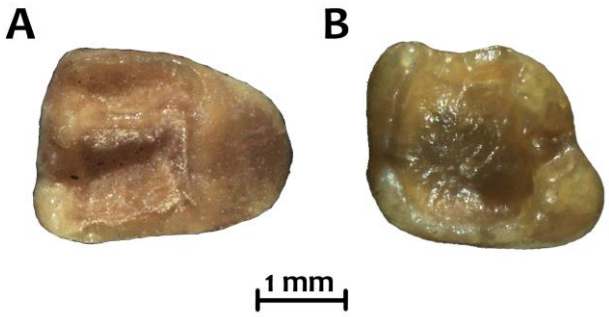

Sciurus vulgaris remains in occlusal view, from level O: A) right M1; B) right m1. Scale 1 mm.

Material. –Level Q: Broken molar; Level O: one p4, three m1, two m1, one m3, one M1, one mandible without teeth and one metacarpus.

Description. – *Sciurus vulgaris* have five molariform teeth in the upper dental series (two premolars and three molars) and four in lower one (one p4 and three molars). Their molars differed from other genus of the Sciuridae family, because they are more bunodont and lophodont and for the greater development of third molars (m3 and M3) with respect to the anterior molars. The upper molars are characterized by a well-developed tubercle (corresponding to a marked protocone and a very small hypocone) in the lingual part, from which two transverse crests connected two tubercles (paracone and metacone) located in the labial part. The anterior and posterior part of these molars are surrounded by tall crests. The M1 presents an occlusal morphology subquadrangular or triangular. In addition, they have three

roots (two on the labial side and one on the lingual). The premolars and the lower molars, in occlusal view, have a quadrangular morphology (except for the premolar that are more triangular) with variable length and width depending on the molar. The surface of these teeth is concave in the center and rises in its perimeter. In the labial part they present two large and round tubercles (hypoconid and protoconid) and one less-developed between both (mesoconid) and, in lingual side, there is a lateral crest that unites elongated metaconid and entoconid (Blanco, 1998a; Cuenca-Bescós, 1988; Gosàlbez, 1987).

Habitat and geographical distribution. – The red-squirrel (*S. vulgaris*) is a typical forest dweller, considered the most arboreal mammal of the Iberian Peninsula. It mainly lives in coniferous forests (firs, pine, larches), but also in deciduous Eurosiberian forests (oak, beech, chestnut) and in mixed forests. It is found from lowland to subalpine forest. In Iberia, it is continuously distributed by the forest areas of the Eurosiberian region, from the northeast to the northwest, the Northern Iberian System and the Central System, being absent in the south-western sector. It reaches altitudes from the littoral m to 2150 m a.s.l.

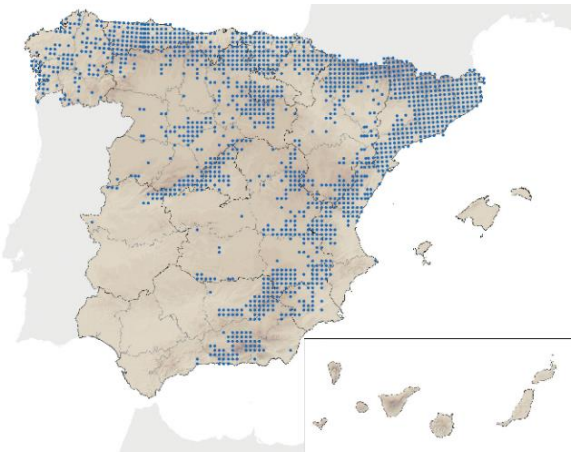

Present-day geographical distribution of *Sciurus vulgaris* in Spain (Palomo et al., 2007).

2.3 Remark about Arvicolinae and Murinae incisors

This work has selected incisors, mainly of Murinae and sometimes Arvicolinae subspecies, for oxygen isotope studies. Whenever was possible incisor persevered in its alveolar place (*in situ*) have been selected. However, the high breakage rates of some of the fossil assemblages studied, difficulted the selection of optimal *in situ* incisors, and isolated incisors were included. For this reason, in all the assemblages, during the taxonomic identification, Murinae and Arvicolinae incisors have been differentiated. The differentiation between these two subfamilies is not complex: Arvicolinae incisors are generally large and longer, have a thicker surface of enamel and are more rectilinear in longitudinal view; otherwise, Murinae incisors are smaller and shorter, with a thin enamel layer and presented a notable coverture when the longitudinal section is considered. In all the included sites, the only species of Murinae subfamily is *Apodemus sylvaticus*, thus Murinae incisors identified are usually attributed to *Apodemus* cf. *sylvaticus*, only to precise that direct identification ria is not performed but is the most probable possibility. With Arvicolinae incisors isolated is more complex to reach this assumption and are considered "Arvicolinae indet". Laterality in both cases is fixed considering that the enamel surface is wider in the labial side.

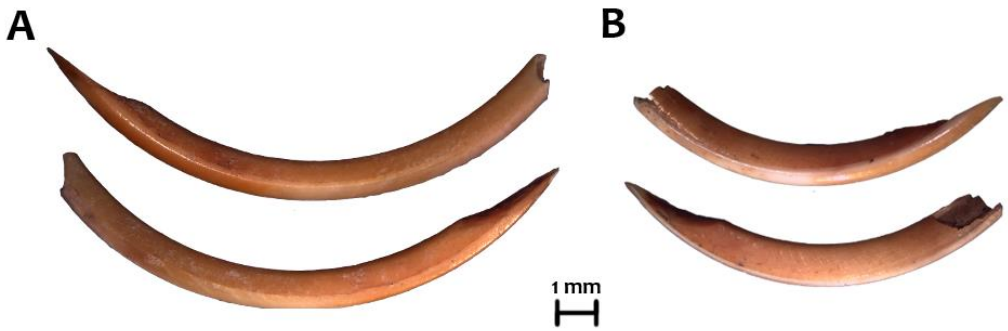

Rodent lower incisors: A) left lower incisor of Arvicolinae from level D, in labial (above) and lingual (below) view; B) right lower incisor of *Apodemus sylvaticus* from level D, in labial (above) and lingual (below) view. Scale 1 mm.

References

Arribas, Ó., 2004. Fauna y paisaje de los Pirineos en la Era Glaciar. Lynx, Barcelona.

Bab, I., Hajbi-Yonissi, C., Gabet, Y., Müller, R., 2007. Micro-Tomographic Atlas of the Mouse Skeleton, Igarss 2014. Springer, New York.

Blanco, J.C., 1998a. Mamíferos de España. Vol II. Cetáceos, Artiodáctilos, Roedores y Lagomorfos de la península Ibérica, Baleares y Canarias. Planeta, Barcelona.

Blanco, J.C., 1998b. Mamíferos de España. Vol I. Insectívoros, Quirópteros, Primates y Carnívoros de la península Ibérica, Baleares y Canarias. Planeta, Barcelona.

Brujin, H., Rumke, K., 1974. On a peculiar mammalian association from the Miocene of Oschiri (Sardinia) I and II. Konik. Nederl. Akad 71, 46–79.

Brunet-Lecomte, P., Chaline, J., 1990. Relations phylogénétiques et evolution des campagnols souterrains d'Europe (Terricola, Arvicolidae, Rodentia). Comptes Rendus l'Académie des Sci. Paris 311, 745–750.

Chaline, J., 1974. Les proies des rapaces. Doin Éditeurs, Paris.

Chaline, J., 1972. Les rongeurs du Pléistocène moyen et supérieur de France. Éditions du Centre National de la Recherche Scientifique, Paris.

Cuenca-Bescós, G., 1988. Revision de los Sciuridae del Aragoniense y del Rambliense en la fosa de Calatayud-Montalbán. Scr. Geol. 87, 1–116.

Cuenca-Bescós, G., Laplana, C., Canudo, J.-I., Arsuaga, J.L., 1997. Small mammals from Sima de los Huesos. J. Hum. Evol. 33, 175–190.

Cuenca-Bescós, G., López-García, J.M., Galindo-Pellicena, M.A., García-Perea, R., Gisbert, J., Rofes, J., Ventura, J., 2014. Pleistocene history of Iberomys, an endangered endemic rodent from southwestern Europe. Integr. Zool. 9, 481–497.

Cuenca-Bescós, G., Straus, L.G., González Morales, M.R., García Pimienta, J.C., 2008. Paleoclima y Paisaje del final del Cuaternario en Cantabria: los pequeños mamíferos de la cueva del Mirón (Ramales de la Victoria). Rev. Española Paleontol. 23, 91–126.

Damms, R., 1981. The dental pattern of the dormice Dryomys, Myomimus, Microdyromys and Peridryomys. Micropaleontol. Bull. 3, 1–115.

Dupuis, I., 1986. Le chiropteres du Quaternaire en France. 1ere partie: clespour la determination du materiel fossile. Universite de Paris.

Felten, H., Helfritch, A., Storc, G., 1973. Die bestimmung der europaischen Fledermause nach der distalen Epiphyse des Humeros. Senckenbergiana biol.

Furió, M., 2007. Los insectívoros (Soricomorpha, Erinaceomorpha, Mammalia) del Néogeno Superior del Levante peninsular. Universitat Autònoma de Barcelona. Doctoral thesis (inedit).

Galán, J., 2003. Análisis taxonómico del orden Chiroptera (Mammalia) del Pleistoceno del relleno del complejo kárstico de Aguilón. Universidad de Zaragoza. Doctoral thesis (inedit).

Galán, J., Cuenca-Bescós, G., López-García, J.M., 2016a. The fossil bat assemblage of Sima del Elefante Lower Red Unit (Atapuerca, Spain): First results and contribution to the palaeoenvironmental approach to the site. Comptes Rendus - Palevol 15, 647–657.

Galán, J., Cuenca-Bescós, G., López-García, J.M., Sauqué, V., Núñez-Lahuerta, C., 2016b. Fossil bats from the Late Pleistocene site of the Aguilón P7 Cave (Zaragoza, Spain). Comptes Rendus - Palevol 15, 501–514.

Galán, J., Núñez-Lahuerta, C., Sauqué, V., Cuenca-Bescós, G., López-García, J.M., 2018a. Cranial Biometrics of the Iberian Myotis myotis/Myotis blythii Complex: New Data for Studying the Fossil Record. J. Mamm. Evol. 1–12.

Galán, J., Núñez-Lahuerta, C., Sauqué, V., Rabal-Garcés, R., López-García, J.M., Cuenca-Bescós, G., 2018b. Los Batanes (Biescas, Spain), a roost site for horseshoe bats in the Pyrenees during the late Pleistocene. Quat. Int. 481, 135–145.

Gosàlbez, J., 1987. Insectívors i rosegadors de Catalunya. Metodologia d'estudi i catàleg faunístic. Ketres Editora, Barcelona.

IUCN, 2018. The IUCN Red List of Threatened Species [WWW Document]. Version 2018-2. URL www.iucnredlist.org

Jaarola, M., Martinkova, N., Gunduz, I., Brunhoff, C., Zima, J., Nadachowski, A., Amori, G., Bulatova, N.S., Chondropoulos, B., Fraguedakis-Tsolis, S., Others, 2004. Molecular phylogeny of the speciose vole genus Microtus (Arvicolinae, Rodentia) inferred from mitochondrial DNA sequences. Mol. Phylogenet. Evol. 33, 647–663.

Le Louarn, H., Quéré, J.P., 2003. Les Rongeurs de France. Faunistique et biologie. Editions d'Institut National de la Recherche Agronomique, Paris.

López-García, J.M., 2011. Los micromamíferos del Pleistoceno superior de la Península Ibérica. Evolución de la diversidad taxonómica y cambios paleoambientales y paleoclimáticos. Ed. Académica Española, Saarbrücken.

López-García, J.M., Blain, H.-A., Cuenca-Bescós, G., Alonso, C., Alonso, S., Vaquero, M., 2011. Small vertebrates (Amphibia, Squamata, Mammalia) from the late Pleistocene-Holocene of the Valdavara-1 cave (Galicia, northwestern Spain). Geobios 44, 253–269.

López-García, J.M., Sevilla, P., Cuenca-Bescós, G., 2009. New evidence for the greater noctule bat (Nyctalus lasiopterus) in the Late Pleistocene of western Europe. Comptes Rendus Palevol 8, 551–558.

López, M., López-Fuster, M.J., Palazón, S., Ruiz-Olmo, J., Ventura, J., 2006. Els mamífers, in: La Fauna Vertebrada a Les Terres de Lleida. Universitat de Lleida, Lleida, pp. 230–262.

Luzi, E., López-García, J.M., Blasco, R., Rivals, F., Rosell, J., 2017. Variations in Microtus arvalis and Microtus agrestis (Arvicolinae, Rodentia) Dental Morphologies in an Archaeological Context: the Case of Teixoneres Cave (Late Pleistocene, North-Eastern Iberia). J. Mamm. Evol. 24, 495–503.

MacDonald, D., Barret, P., 2008. Guía de campo de los mamíferos de España y de Europa. Ediciones Omega, Barcelona.

Menu, H., 1985. Morphotypes dentaries actuels et fossiles des Chiroptères Vespertilioninés. 1e partie: étude des morphologies dentaires. Paleovertebrata 15, 71–128.

Menu, H., Popelard, J.B., 1987. Utilisation des caracteres dentaires pour la determination des vespertilionines de l'ouest europeen. Butlletin la Coord. ouest pour l'étude la Prot. des chauves-souris 4, 11–88.

Nadachowski, A., 1982. Late Quaternary rodents of Poland with special reference to morphotype dentition analysis of voles. Polska Academia Nauk, Panstwowe Wydawnictwo Naukowe, Krakow.

Palomo, L.J., Gisbert, J., Blanco, C., 2007. Atlas y libro rojo de los mamíferos terrestres de España. Organismo Autónomo Parques Nacionales, Madrid.

Pasquier, L., 1974. Dynamique évolutive d'un sousgenere de Muridae, Apodemus (Sylvaemus). Etude biometrioque des caractères dentaires de populations fossils et actuelles d'Europe occidentale. Université de Montpellier.

Purroy, F.J., Varela, J., 2005. Mamíferos de España. Península, Baleares y Canarias. Lynx, Barcelona.

Reumer, J.W.F., 1984. Rusician and early Pleistocene Soricidae (Insectívora, Mammalia) from Tegelen (The Netherlands) and Hungary. Scr. Geol. 73, 1–173.

Rey, J.M., Landín, A., 1973. Sobre la presencia de Crocidura suaveolens en el sur de Andalucia (Mammalia, Insectivora). Bol. Real Soc. Española Hist. Nat. 71, 9–16.

Rümke, C.G., 1985. A review of fossil and recent Desmaninae (Talpidae, Insectivora). Utrech Micropaleontol. Bull. 4, 1–241.

Sevilla, P., 1988. Estudio paleontológico de los Quirópteros del Cuaternario español. Paleontol. i Evol. 22, 113–233.

van der Meulen, A.J., 1973. Middle Pleistocene small mammals from the Monte Peglia (Orvieto, Italy) with special reference to the philogeny of Microtus (Arvicolidae, Rodentia). Quaternaria 16, 1–144.

Wilson, D.E., Redeer, D.M., 2005. Mammal Species of the World. A Taxonomic and Geographic Reference (3rd ed) [WWW Document]. Johns Hopkins Univ. Press. URL http://www.departments.bucknell.edu/biology/resources/msw3/

Appendix 2.
Supplementary material

Appendix 2.1

Here is included supplementary material of "Chapter 3. Palaeoecological implications of rodents as proxies for the Late Pleistocene – Holocene environmental and climatic changes in northeastern Iberia".

2.1.A General information about sites and levels, including specific chronology, archaeological content, period classification and reference data.

Sites	Levels	Chronology	Archaeological assemblage	Period classification	Matrix data procedence	Other references
Teixoneres cave	IIII	90-60 ka BP	Middle Paleolithic (Mousterian)	ELP	López-García et al. (2012b); López-García et al. (2014)	Tissoux et al. (2006); Rossell et al. (2010)
	II	60-30 ka BP	Middle Paleolithic (Mousterian)	ELP		
Abric Romaní rockshelter	O	54.24 ±0.42 ka cal BP	Middle Paleolithic (Mousterian)	ELP	López-García (2011); Burjachs et al. (2012); Fernández-García (2014)	Bischoff et al.(1994); Vallverdú et al. (2012); Vaquero et al. (2013)
	N	54.6 ±0.4 ka cal BP	Middle Paleolithic (Mousterian)	ELP		
	D	> 44.9 ±2.5 ka cal BP	Middle Paleolithic (Mousterian)	ELP		
Cova del Gegant (old levels)	I	128-40 ka BP	Middle Paleolithic (Mousterian)	ELP	Alcalde (1986); López-García (2011); López-García et al. (2008)	Viñas&Villata (1975); López-García et al. (2008)
Cova del Gegant (new levels)	V	55.7 ka cal BP	Middle Paleolithic (Mousterian)	ELP	López-García et al. (2012c); López-García et al. (2014b)	Daura et al. (2005; 2010)
	III	49.3 ka cal BP	Middle Paleolithic (Mousterian)	ELP		
Xaragalls cave	C8		No archaeological material	ELP	López-García et al. (2012a)	
	C7		No archaeological material	ELP		
	C6	> 43.5 ka BP	No archaeological material	ELP		
	C4	45.12-48.24 ka BP	No archaeological material	ELP		
Arbreda cave	I	40-32 ka BP	Middle Paleolithic (Mousterian)	ELP	Alcalde (1986); Alcalde & Galobart (2002); López-García (2011); López-García et al. (2014b)	Maroto et al. (2012); Wood et al. (2014); Soler et al. (2014)
	H	38-34 ka BP	Upper Paleolithic (Archaic Aurignacian)	LLP		
	G	30.95 ±0.22 ka cal BP	Upper Paleolithic (Evolved Aurignacian)	LLP		
	F	28.26 ±0.28 ka cal BP	Upper Paleolithic (Gravettian)	LLP		
	E	24-25 ka BP	Upper Paleolithic (Gravettian)	LLP		
	D	22.63 ±0.1 ka cal BP	Upper Paleolithic (Middle Gravettian)	LLP		
	C	19.48 ±0.08 ka cal BP	Upper Paleolithic (Middle Solutrean)	LLP		
	B	18.86 ±0.08 ka cal BP	Upper Paleolithic (Upper Solutrean)	LLP		
	A		Upper Paleolithic (Postsolutrean)	LLP		
Gall Carboners cave	Capa 100 (Levels 105-108)	31.17-31.38 ka cal BP	No archaeological material	LLP	López-García et al. (2014a)	
Toll cave	3	35 - 13 ka BP	No archaeological material	LLP	Fernández-García & López-García (2013)	Morales et al.(2014)
	2	< 13 ka BP	No archaeological material	LLP		
Cova Colomera	CE15	13-11 ka BP	No archaeological material	LLP	Lopéz-García et al. (2010)	Oms et al.(2008)
	CE13-14	7.06 ±0.7 ka cal BP	Neolithic	HOL		
	CE12	6.87 ±0.7 ka cal BP	Neolithic	HOL		
	EE1	3.96 ±0.5 ka cal BP	Bronze Age	HOL		
	A. Sup.	3.49 ±0.5 ka cal BP	Bronze Age	HOL		
Cingle Vermell		9.76 ± 0.16 ka BP	Epipaleolithic	HOL	Alcalde (1986); Alcalde & Brunet-Lecompte (1985)	Alcalde (1986)
Cova del Frare	6	6.3 ±0.3 ka BP	Neolithic	HOL	Alcalde (1986); Alcalde & Brunet-Lecompte (1985)	Martín et al. (1981); Morales-Hidalgo et al. (2010)
	5	6.38 ±0.31 ka BP	Neolithic	HOL		
	4	4.45 ±0.1 ka BP	Neolithic	HOL		
	3	3.99 ±0.1 ka BP	Chalcolithic	HOL		
Cova 120	III	4.27 ±0.7 ka BP	Neolithic	HOL	Alcalde (1986); Alcalde & Brunet-Lecompte (1985); Agustí et al. (1991)	Alcalde (1986); Agustí et al. (1991)
	II		Chalcolithic - Bronze Age	HOL		
	I	3.19 ±0.19 ka BP	Bronze Age	HOL		

2.1.B Data associated with the principal component analysis

Eigenvalues

Principal component	Eigenvalues	% variance
1	1430.29	55.656
2	499.721	19.445
3	400.482	15.584
4	121.721	4.7364
5	82.999	3.2297

Screeplot

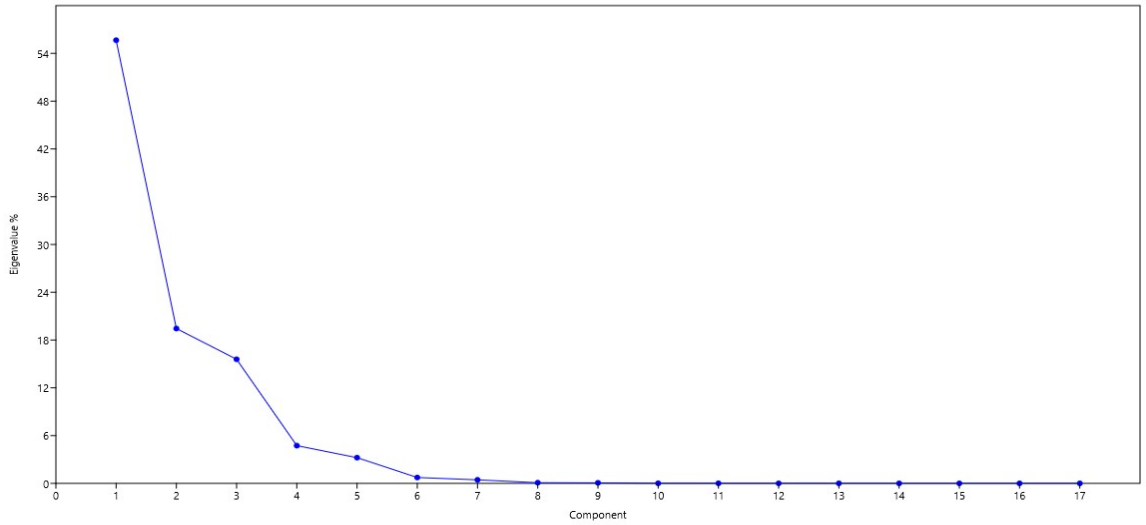

Loadings

	PC 1	PC 2	PC 3
Arvicola sapidus	0.022396	0.0021771	0.0033448
Chionomys nivalis	-0.00099281	-0.056001	**0.078456**
Microtus arvalis-agrestis	**0.80983**	**-0.28433**	**-0.23447**
Microtus (Terricola) duodecimcostatus	**-0.10434**	**0.76484**	**-0.41061**
Microtus (Terricola) gerbei	-0.0033653	0.013729	-0.007472
Microtus oeconomus	0.0039051	-0.00102	-0.0011178
Iberomys cabrerae	**-0.07569**	**0.10864**	**0.17155**
Clethrionomys glareolus	-0.0020546	0.00031775	-0.0022572
Pliomys lenki	0.00046512	-0.0002989	-0.00053013
Apodemus sylvaticus	**-0.56841**	**-0.56325**	**-0.3643**
Mus musculus	-0.013467	-0.02169	0.00075636
Eliomys quercinus	**-0.060487**	0.036039	**0.7797**
Glis glis	-0.0088098	0.0040912	-0.011383
***Hystrix* sp.**	-0.002061	-0.0020646	-0.00085254
Spermophilus* cf. *citellus	0.0031164	-0.0011605	-0.00078195
Sciurus vulgaris	-8.92E-02	5.75E-01	4.63E-01

Scores

	PC 1	PC 2	PC 3
Teixoneres_Nivel III	-12168	-0.19976	-90163
Teixoneres_Nivel II	45599	-77372	-35494
AR_Nivel O	-11774	26546	17134
AR_Nivel N	-16855	13987	14143
AR_Nivel E	-60613	11058	-4962
Gegant_Nivel I	-24396	-85385	-28256
Gegant_Nivel V	-98689	19.97	70.52
Gegant_Nivel III	-11133	73569	58083
Xaragalls_C8	-38656	-11891	-92355
Xaragalls_C7	-45806	-34252	-10643
Xaragalls_C6	-42163	-23225	-11064
Xaragalls_C4	-13938	-14107	-1696
Arbreda_Nivel I	24547	-47002	41493
Arbreda_Nivel H	62545	-24539	-80873
Arbreda_Nivel G	53401	0.23796	-51416
Arbreda_Nivel F	62542	-11623	-34948
Arbreda_Nivel E	64094	-11826	-43859
Arbreda_Nivel D	64984	-98629	-3526
Arbreda_Nivel C	69955	-11953	-43606
Arbreda_Nivel B	66737	-12.72	-36888
Arbreda_Nivel A	34098	13763	-66486
Galls Carboners_Capa 100	-98882	46124	56531
Toll_Nivel 3	23671	37602	-97259
Toll_Nivel 2	-86745	77736	-21642
Colomera_Nivel CE15	20556	-25105	67826
Colomera_Nivel CE13 -14	-16.53	-11207	-0.56738
Colomera_Nivel CE12	-16687	-13374	-0.19076
Colomera_Nivel EE1	-16567	-18984	-0.62149
Colomera_Nivel A sup.	-41694	-12776	0.50797
Cingle Vermell	-32472	-24.92	-99297
Frare_Nivel 6	-27104	46532	-24565
Frare_Nivel 5	-29889	27986	-14466
Frare_Nivel 4	-25827	30706	-80094
Frare_Nivel 3	-32318	11815	-77325
C120_Nivel III	-44.82	-25.34	-17482
C120_Nivel II	-35396	-12809	-63067
C120_Nivel I	-32635	-19007	11339

Appendix 2.2

Here is included supplementary material of "Chapter 5. Unravelling the oxygen isotope signal ($\delta^{18}O$) from rodent teeth in northeastern Iberia, and the implications for past climate reconstructions".

2.2.A Modern samples (pellets)

	Location number	Location	Altitude (m a.s.l.)	n	$\delta^{18}Op$ (‰V-SMOW)	Mean estimated $\delta^{18}Omw$ (‰V-SMOW)	$\delta^{18}Omw$ (‰ V-SMOW) - OIPC data												
							Mean	Range	Jan	Feb	Mar	Apr	May	Jun	Jul	Aug	Sept	Oct	Nov	Dec
Iberian Peninsula	1	Serinyà	108	3	19.1	-4.7	**-5.9**	**7.8**	-8.8	-8.9	-7.3	-5.8	-3.9	-2.4	-1.1	-1.5	-3	-5	-7.2	-7.9
	2	Molà	1000	4	18.3	-5.3	**-7.7**	**8.5**	-10.8	-11	-9.2	-7.7	-5.8	-4.2	-2.5	-2.8	-4.5	-6.8	-9.3	-9.9
	3	Prades	990	3	19.3	-4.5	**-7.7**	**8.5**	-10.6	-10.8	-9.1	-7.5	-5.7	-4	-2.3	-2.8	-4.4	-6.7	-9.1	-9.7
	4	Balaguer	200	2	18.1	-5.5	**-6**	**7.8**	-9.2	-9.1	-7.8	-6.2	-4.3	-2.7	-1.4	-1.9	-3.3	-5.4	-7.5	-8.2
	5	El Catllar	110	2	18.5	-5.2	**-5.6**	**7.7**	-8.7	-8.7	-7.3	-5.7	-4	-2.3	-1	-1.6	-3	-5	-7.1	-7.8
	6	Palacios de la Sierra (*)	1050	4	15	-8.1	**-8.7**	**8.3**	-11	-11.1	-9.9	-8.1	-6	-4.4	-2.8	-3.4	-4.8	-7.2	-9.5	-10.1
	7	San Martin de Valdeiglesias (*)	670	1	17.6	-5.9	**-7.1**	**8**	-9.7	-9.4	-8.7	-6.9	-4.8	-3	-1.7	-2.5	-3.8	-5.9	-8.2	-8.6
	8	Caminreal (*)	920	1	14.9	-8.2	**-7.7**	**8.3**	-10.7	-10.7	-9.2	-7.6	-5.6	-3.9	-2.4	-3	-4.5	-6.7	-9.1	-9.7
	9	Yaguas de Eresma (*)	895	1	15.7	-7.5	**-8**	**8.1**	-10.6	-10.6	-9.6	-7.8	-5.6	-3.9	-2.5	-3.1	-4.5	-6.8	-9.1	-9.6
	10	Zaragoza (*)	200	1	15.2	-7.9	**-6.3**	**7.9**	-9.4	-9.2	-8	-6.3	-4.3	-2.7	-1.5	-2	-3.4	-5.6	-7.6	-8.3
	11	Sobradiel (*)	200	1	18.2	-5.4	**-6.3**	**7.9**	-9.4	-9.2	-8	-6.3	-4.3	-2.7	-1.5	-2	-3.4	-5.6	-7.6	-8.3
	12	Cernadilla (*)	900	1	16.7	-6.7	**-8**	**7.6**	-10.5	-10.3	-9.4	-7.7	-5.5	-3.9	-2.9	-3.3	-4.5	-6.6	-8.7	-9.1
	13	Uncastillo (*)	620	1	16.7	-6.7	**-7.3**	**8.1**	-10.1	-10	-8.8	-7.1	-5	-3.4	-2	-2.5	-3.9	-6.3	-8.5	-9.1
	14	Lárrede (*)	1230	1	17.5	-6	**-8.6**	**8.6**	-11.4	-11.5	-10	-8.3	-6.3	-4.6	-2.9	-3.3	-4.9	-7.4	-9.9	-10.4
	15	Basarán (*)	1380	1	16.9	-6.5	**-8.8**	**8.7**	-11.7	-11.9	-10.3	-8.7	-6.6	-5	-3.2	-3.6	-5.2	-7.8	-10.3	-10.8
	16	Espot (*)	1500	1	19	-4.8	**-9.1**	**8.9**	-12.1	-12.4	-10.6	-9	-7	-5.4	-3.5	-3.8	-5.5	-8	-10.7	-11.2
	17	Berástegui (*)	400	1	15.6	-7.6	**-6.7**	**7.6**	-9.3	-9.3	-8.4	-6.6	-4.6	-3	-1.7	-2.3	-3.5	-5.8	-7.8	-8.4
	18	Amareleja (*)	150	1	22.2	-2.1	**-5.2**	**6.9**	-7.1	-6.8	-6.3	-4.8	-3	-1.3	-0.2	-1.4	-2.4	-3.8	-5.5	-6.1
	19	Redondo (*)	280	2	17.9	-5.7	**-5.4**	**6.9**	-7.4	-7.1	-6.6	-5.1	-3.3	-1.6	-0.5	-1.4	-2.6	-4.1	-5.8	-6.4
	20	Tomar (*)	130	1	19.2	-4.6	**-5**	**6.8**	-7.1	-6.8	-6.1	-4.9	-3.1	-1.4	-0.3	-1	-2.3	-3.9	-5.4	-5.9
Southern France and higher latitudes (*)	21	Piediquacio (Corsica)	325	1	18.4	-5.3	**-6.4**	**4.4**	-7.5	-7.4	-6.6	-6.4	-5.2	-4.7	-3.9	-3.9	-5.1	-6	-7.5	-8.3
	22	Pancheraccia (Corsica)	570	1	18.8	-4.9	**-7**	**4.6**	-8.1	-8.1	-7.3	-7	-5.7	-5.2	-4.3	-4.3	-5.5	-6.5	-8.2	-8.9
	23	Mallemort (SE France)	145	1	17.2	-6.2	**-6.5**	**4.4**	-7.7	-7.2	-6.5	-7.1	-5.8	-5.2	-4.2	-4.4	-5.4	-6.6	-7.8	-8.6
	24	La Treille (SE France)	165	1	19.7	-4.2	**-6.4**	**4.4**	-7.6	-7.1	-6.4	-7	-5.6	-5.1	-4.1	-4.3	-5.3	-6.4	-7.7	-8.5
	25	Salin-de-Giraud (SE France)	10	1	17.8	-5.8	**-6.1**	**3.9**	-7.3	-6.7	-6	-6.7	-5.4	-4.8	-3.9	-4.2	-5.1	-6.2	-7.3	-8.1
	26	Rognes (SE France)	330	1	14.8	-8.2	**-6.8**	**4.6**	-8.1	-7.7	-7	-7.5	-6.1	-5.5	-4.4	-4.6	-5.6	-6.9	-8.2	-9
	27	Caumont (SE France)	55	1	16.2	-7.1	**-6.4**	**4.4**	-7.6	-7.1	-6.3	-7	-5.7	-5.1	-4.1	-4.4	-5.3	-6.5	-7.7	-8.5
	28	Clelles (E France)	755	1	15.4	-7.7	**-8**	**5**	-9.7	-9.4	-8.8	-8.8	-7.2	-6.6	-5.4	-5.5	-6.6	-8.1	-9.7	-10.4
	29	Pointis-Inard (S France)	343	5	17.3	-6.1	**-6.6**	**4**	-7.7	-7.4	-6.8	-7.3	-6	-5	-4.4	-4.7	-5.3	-6.8	-8	-8.4
	30	Marillac-le-Franc (SW France)	112	3	17.4	-6.1	**-6.8**	**4**	-8.2	-7.6	-6.9	-7.4	-6.1	-5.3	-4.6	-4.9	-5.7	-6.9	-8.2	-8.6
	31	Montbolo (SE France)	600	1	18.8	-4.9	**-7.4**	**3.7**	-8.1	-7.9	-7.4	-7.7	-6.3	-5.5	-4.7	-4.8	-5.6	-7.1	-8.4	-9
	32	Arue (SW France)	95	1	18.2	-5.4	**-6.3**	**3.7**	-7.4	-7	-6.4	-7	-5.7	-4.7	-4.2	-4.5	-5.2	-6.5	-7.7	-7.9
	33	Artenac (W France)	145	1	20.9	-3.2	**-6.9**	**4.1**	-8.3	-7.8	-7	-7.5	-6.2	-5.4	-4.6	-4.9	-5.7	-7	-8.3	-8.7
	34	Lussant (W France)	275	1	21.7	-2.5	**-6.7**	**3.9**	-7.9	-7.3	-6.6	-7.2	-5.9	-5.2	-4.4	-4.7	-5.5	-6.7	-8	-8.3
	35	Grez-Doiceau (Belgium)	50	1	17.1	-6.3	**-7.9**	**4.2**	-9.7	-9.4	-8.2	-8.4	-7.1	-6.6	-5.7	-5.9	-6.8	-8.1	-9.4	-9.9
	36	Fontcouverte (SW France)	75	1	17.5	-6	**-6.1**	**4.1**	-7.3	-6.8	-6.1	-6.8	-5.5	-4.8	-4	-4.3	-5.1	-6.3	-7.4	-8.1
	37	Pedrech (S France)	90	1	17.8	-5.8	**-6.3**	**4**	-7.5	-7.1	-6.4	-7	-5.7	-4.9	-4.2	-4.5	-5.2	-6.5	-7.7	-8.2
	38	Sainte-Radegonde-des-Noyers (W France)	10	1	17.2	-6.2	**-6.7**	**3.9**	-8	-7.4	-6.7	-7.2	-6	-5.2	-4.5	-4.8	-5.6	-6.8	-8	-8.4
	39	Goezillio (W France)	220	1	17	-6.4	**-7.4**	**3.9**	-8.6	-7.9	-7.4	-7.7	-6.6	-5.8	-5	-5.3	-6.1	-7.4	-8.7	-8.9
	40	Fultot (N France)	130	1	17	-6.4	**-7.9**	**3.9**	-9.4	-8.9	-8.1	-8.3	-7	-6.4	-5.5	-5.8	-6.7	-7.9	-9.3	-9.7
	41	Dorset (S England)	120	1	17.8	-5.8	**-7.9**	**3.9**	-9.3	-8.7	-8.1	-8.3	-7.1	-6.5	-5.6	-5.9	-6.7	-8	-9.2	-9.5

Extended data from localities in the Iberian Peninsula, southern France and other higher-latitude localities, with oxygen isotope compositions of tooth enamel phosphate from modern rodent teeth (this work and (*) Royer et al., 2013a). Included for each locality is altitude (m a.s.l.); number of $\delta^{18}O$ samples (n); mean $\delta^{18}O$ from phosphates ($\delta^{18}O_p$; ‰ V-SMOW); mean and median estimated $\delta^{18}O$ from meteoric waters ($\delta^{18}O_{mw}$; ‰ V-SMOW) (following the Royer et al. (2013a) oxygen isotope fractionation equation); mean, ranges and monthly values of $\delta^{18}O_{mw}$ (‰ V-SMOW) (OIPC data; Bowen, 2017). In dark grey, location of estimated mean $\delta^{18}O_{mw}$ from present-day samples within present-day $\delta^{18}O_{mw}$ values throughout the year; in light grey, location of all $\delta^{18}O_{mw}$ estimated in a given locality; red square, time of pellet recovery.

2.2.B Equation for Iberia

Available dataset of Iberian sites from the Global Network of Isotopes in Precipitation created by the International Atomic Energy Agency and the World Meteorological Organization (IAEA/WMO, 2018), employed to develop the linear regression model (OLS equation) relating the monthly mean $\delta^{18}O_{mw}$ and monthly mean air temperatures (Figure 5A). Included for each site/month is latitude, longitude, altitude (m a.s.l.), number of samples (n), mean oxygen isotope composition of meteoric waters ($\delta^{18}O_{mw}$; ‰ V-SMOW) and mean air temperatures (°C). Accessible at WISER (Water Isotope System for Data Analysis, Visualization and Electronic Retrieval): https://nucleus.iaea.org/wiser.

Site	Latitude	Longitude	Altitude	Month	n	Mean δ18Omw (‰ V-SMOW)	Mean air temperature (ºC)
ALMERIA AEROPUERTO	36.85	-2.38	21	January	8	-4.83	12.68
ALMERIA AEROPUERTO	36.85	-2.38	21	February	9	-5.67	13.28
ALMERIA AEROPUERTO	36.85	-2.38	21	March	8	-4.31	14.96
ALMERIA AEROPUERTO	36.85	-2.38	21	April	11	-3.84	17.00
ALMERIA AEROPUERTO	36.85	-2.38	21	May	10	-2.44	19.98
ALMERIA AEROPUERTO	36.85	-2.38	21	June	3	-0.86	23.97
ALMERIA AEROPUERTO	36.85	-2.38	21	July	1	-0.02	26.20
ALMERIA AEROPUERTO	36.85	-2.38	21	August	1	-1.50	27.90
ALMERIA AEROPUERTO	36.85	-2.38	21	September	8	-3.09	24.06
ALMERIA AEROPUERTO	36.85	-2.38	21	October	10	-4.45	20.65
ALMERIA AEROPUERTO	36.85	-2.38	21	November	10	-5.88	16.04
ALMERIA AEROPUERTO	36.85	-2.38	21	December	11	-5.58	13.63
BARCELONA	41.38	2.12	65	January	6	-6.58	9.43
BARCELONA	41.38	2.12	65	February	7	-6.76	9.36
BARCELONA	41.38	2.12	65	March	7	-4.46	11.53
BARCELONA	41.38	2.12	65	April	9	-4.87	12.98
BARCELONA	41.38	2.12	65	Jun.	8	-4.63	16.14
BARCELONA	41.38	2.12	65	June	7	-2.37	19.83
BARCELONA	41.38	2.12	65	July	4	-4.02	23.90
BARCELONA	41.38	2.12	65	August	7	-3.19	23.93
BARCELONA	41.38	2.12	65	September	7	-3.99	21.83
BARCELONA	41.38	2.12	65	October	8	-5.01	17.46
BARCELONA	41.38	2.12	65	November	8	-5.75	12.64
BARCELONA	41.38	2.12	65	December	8	-5.73	9.90
BEJA	38.02	-7.87	246	January	2	-6.25	9.80
BEJA	38.02	-7.87	246	February	1	-4.77	11.40
BEJA	38.02	-7.87	246	March	2	-5.29	13.70
BEJA	38.02	-7.87	246	April	2	-5.93	12.65
BEJA	38.02	-7.87	246	Jul.	3	-4.03	17.57
BEJA	38.02	-7.87	246	June	2	-3.41	20.65
BEJA	38.02	-7.87	246	July	1	-5.76	23.20
BEJA	38.02	-7.87	246	October	3	-4.70	18.53
BEJA	38.02	-7.87	246	November	3	-5.41	13.77
BEJA	38.02	-7.87	246	December	2	-6.77	11.20
BRAGANCA	41.80	-6.73	690	January	2	-9.04	3.55
BRAGANCA	41.80	-6.73	690	February	2	-5.66	7.55

BRAGANCA	41.80	-6.73	690	March	2	-7.95	10.10
BRAGANCA	41.80	-6.73	690	April	2	-8.63	8.80
BRAGANCA	41.80	-6.73	690	Jun.	3	-5.41	15.00
BRAGANCA	41.80	-6.73	690	June	3	-5.10	18.03
BRAGANCA	41.80	-6.73	690	July	3	-6.06	22.20
BRAGANCA	41.80	-6.73	690	August	2	-3.28	23.10
BRAGANCA	41.80	-6.73	690	September	2	-4.72	19.50
BRAGANCA	41.80	-6.73	690	October	3	-6.78	13.83
BRAGANCA	41.80	-6.73	690	November	3	-8.63	8.80
BRAGANCA	41.80	-6.73	690	December	3	-7.08	5.87
BURGOS/VILLAFRIA	42.37	-3.63	891	January	1	-10.94	3.30
BURGOS/VILLAFRIA	42.37	-3.63	891	February	1	-9.29	3.30
BURGOS/VILLAFRIA	42.37	-3.63	891	March	1	-11.87	9.20
BURGOS/VILLAFRIA	42.37	-3.63	891	April	1	-8.82	10.20
BURGOS/VILLAFRIA	42.37	-3.63	891	Jun.	1	-4.43	13.30
BURGOS/VILLAFRIA	42.37	-3.63	891	June	1	-3.46	21.10
BURGOS/VILLAFRIA	42.37	-3.63	891	July	1	-2.79	21.00
BURGOS/VILLAFRIA	42.37	-3.63	891	August	1	-4.31	23.40
BURGOS/VILLAFRIA	42.37	-3.63	891	September	1	-8.02	17.50
BURGOS/VILLAFRIA	42.37	-3.63	891	October	1	-9.39	12.40
BURGOS/VILLAFRIA	42.37	-3.63	891	November	1	-10.40	7.90
BURGOS/VILLAFRIA	42.37	-3.63	891	December	1	-9.10	6.40
CACERES/TRUJILLO	37.60	-8.07	405	January	9	-6.54	8.23
CACERES/TRUJILLO	36.98	-8.65	405	February	10	-6.74	9.25
CACERES/TRUJILLO	42.37	-3.63	405	March	11	-5.64	12.10
CACERES/TRUJILLO	42.37	-3.63	405	April	11	-5.35	13.99
CACERES/TRUJILLO	42.37	-3.63	405	Jun.	11	-5.27	18.03
CACERES/TRUJILLO	39.47	-6.33	405	June	9	-3.77	23.79
CACERES/TRUJILLO	36.36	-9.23	405	July	3	-1.55	25.73
CACERES/TRUJILLO	35.74	-9.80	405	August	5	-4.83	26.26
CACERES/TRUJILLO	39.47	-6.33	405	September	11	-5.23	22.50
CACERES/TRUJILLO	39.47	-6.33	405	October	10	-5.39	17.11
CACERES/TRUJILLO	39.47	-6.33	405	November	11	-6.67	11.31
CACERES/TRUJILLO	38.22	-7.49	405	December	11	-7.17	8.45
CIUDAD REAL	38.98	-3.92	682	January	11	-8.34	6.11
CIUDAD REAL	38.98	-3.92	682	February	11	-7.03	8.36
CIUDAD REAL	38.98	-3.92	682	March	11	-7.72	11.49
CIUDAD REAL	38.98	-3.92	682	April	11	-6.35	13.85
CIUDAD REAL	38.98	-3.92	682	Jun.	11	-4.92	18.22
CIUDAD REAL	38.98	-3.92	682	June	9	-3.12	24.61
CIUDAD REAL	38.98	-3.92	682	July	2	-2.71	26.75
CIUDAD REAL	38.98	-3.92	682	August	6	-3.96	26.30
CIUDAD REAL	38.98	-3.92	682	September	11	-5.30	21.87
CIUDAD REAL	38.98	-3.92	682	October	11	-7.14	16.34
CIUDAD REAL	38.98	-3.92	682	November	11	-8.80	9.89
CIUDAD REAL	38.98	-3.92	682	December	9	-8.27	6.84
FARO	37.01	-7.96	9	January	15	-4.46	12.23
FARO	37.01	-7.96	9	February	13	-4.97	12.68

FARO	37.01	-7.96	9	March	10	-4.45	14.05
FARO	37.01	-7.96	9	April	12	-3.78	15.80
FARO	37.01	-7.96	9	Jun.	10	-3.21	17.22
FARO	37.01	-7.96	9	June	2	-2.29	20.90
FARO	37.01	-7.96	9	July	1	-1.06	23.80
FARO	37.01	-7.96	9	August	1	-1.11	24.00
FARO	37.01	-7.96	9	September	6	-4.09	21.75
FARO	37.01	-7.96	9	October	11	-4.09	19.25
FARO	37.01	-7.96	9	November	12	-4.35	16.00
FARO	37.01	-7.96	9	December	12	-4.60	13.92
GIBRALTAR	36.15	-5.35	5	January	37	-4.69	13.58
GIBRALTAR	36.15	-5.35	5	February	36	-4.46	13.58
GIBRALTAR	36.15	-5.35	5	March	36	-4.42	15.21
GIBRALTAR	36.15	-5.35	5	April	31	-4.22	16.50
GIBRALTAR	36.15	-5.35	5	Jun.	25	-3.28	18.96
GIBRALTAR	36.15	-5.35	5	June	13	-2.28	21.44
GIBRALTAR	36.15	-5.35	5	August	5	-3.68	24.30
GIBRALTAR	36.15	-5.35	5	September	21	-3.62	22.63
GIBRALTAR	36.15	-5.35	5	October	34	-3.88	19.68
GIBRALTAR	36.15	-5.35	5	November	39	-4.95	16.41
GIBRALTAR	36.15	-5.35	5	December	34	-4.54	14.43
GIRONA AEROPUERTO	41.90	2.75	129	January	8	-6.43	7.13
GIRONA AEROPUERTO	41.90	2.75	129	February	8	-7.40	7.88
GIRONA AEROPUERTO	41.90	2.75	129	March	9	-6.99	10.48
GIRONA AEROPUERTO	41.90	2.75	129	April	9	-5.81	13.07
GIRONA AEROPUERTO	41.90	2.75	129	Jun.	9	-5.10	17.16
GIRONA AEROPUERTO	41.90	2.75	129	June	7	-3.95	21.27
GIRONA AEROPUERTO	41.90	2.75	129	July	10	-3.44	23.82
GIRONA AEROPUERTO	41.90	2.75	129	August	9	-3.33	23.71
GIRONA AEROPUERTO	41.90	2.75	129	September	10	-3.99	20.18
GIRONA AEROPUERTO	41.90	2.75	129	October	10	-6.32	16.62
GIRONA AEROPUERTO	41.90	2.75	129	November	10	-7.08	10.86
GIRONA AEROPUERTO	41.90	2.75	129	December	9	-6.72	7.97
LA CORUÑA	43.37	-8.42	57	January	10	-5.88	11.10
LA CORUÑA	43.37	-8.42	57	February	11	-5.31	11.23
LA CORUÑA	43.37	-8.42	57	March	11	-4.98	12.67
LA CORUÑA	43.37	-8.42	57	April	11	-5.24	13.34
LA CORUÑA	43.37	-8.42	57	Jun.	11	-4.04	15.29
LA CORUÑA	43.37	-8.42	57	June	11	-4.18	18.15
LA CORUÑA	43.37	-8.42	57	July	11	-3.30	19.35
LA CORUÑA	43.37	-8.42	57	August	10	-2.71	20.01
LA CORUÑA	43.37	-8.42	57	September	11	-4.90	18.95
LA CORUÑA	43.37	-8.42	57	October	11	-5.10	16.52
LA CORUÑA	43.37	-8.42	57	November	11	-6.19	13.15
LA CORUÑA	43.37	-8.42	57	December	11	-5.54	11.35
LEON/VIRGEN DEL CAMINO	42.58	-5.65	913	January	10	-10.11	3.16
LEON/VIRGEN DEL CAMINO	42.58	-5.65	913	February	11	-10.57	4.56
LEON/VIRGEN DEL CAMINO	42.58	-5.65	913	March	10	-8.50	7.20

LEON/VIRGEN DEL CAMINO	42.58	-5.65	913	April	9	-8.26	9.19
LEON/VIRGEN DEL CAMINO	42.58	-5.65	913	Jun.	11	-6.93	12.97
LEON/VIRGEN DEL CAMINO	42.58	-5.65	913	June	10	-4.64	18.19
LEON/VIRGEN DEL CAMINO	42.58	-5.65	913	July	8	-5.88	19.43
LEON/VIRGEN DEL CAMINO	42.58	-5.65	913	August	8	-5.28	19.30
LEON/VIRGEN DEL CAMINO	42.58	-5.65	913	September	10	-6.54	16.39
LEON/VIRGEN DEL CAMINO	42.58	-5.65	913	October	11	-8.47	11.76
LEON/VIRGEN DEL CAMINO	42.58	-5.65	913	November	11	-9.50	6.38
LEON/VIRGEN DEL CAMINO	42.58	-5.65	913	December	11	-10.33	3.53
MADRID-RETIRO	40.41	-3.68	655	January	13	-8.55	6.52
MADRID-RETIRO	40.41	-3.68	655	February	14	-7.97	7.86
MADRID-RETIRO	40.41	-3.68	655	March	11	-7.04	11.40
MADRID-RETIRO	40.41	-3.68	655	April	12	-6.50	13.03
MADRID-RETIRO	40.41	-3.68	655	Jun.	14	-4.41	17.17
MADRID-RETIRO	40.41	-3.68	655	June	11	-3.03	22.13
MADRID-RETIRO	40.41	-3.68	655	July	2	-2.39	25.60
MADRID-RETIRO	40.41	-3.68	655	August	4	-1.53	25.23
MADRID-RETIRO	40.41	-3.68	655	September	11	-4.29	20.85
MADRID-RETIRO	40.41	-3.68	655	October	15	-6.39	15.41
MADRID-RETIRO	40.41	-3.68	655	November	15	-9.04	9.77
MADRID-RETIRO	40.41	-3.68	655	December	14	-7.85	6.93
MORON BASE SEVILLA	37.15	-5.62	88	January	9	-4.63	10.39
MORON BASE SEVILLA	37.15	-5.62	88	February	9	-4.40	11.57
MORON BASE SEVILLA	37.15	-5.62	88	March	10	-4.77	14.01
MORON BASE SEVILLA	37.15	-5.62	88	April	10	-3.93	15.95
MORON BASE SEVILLA	37.15	-5.62	88	Jun.	10	-3.60	19.53
MORON BASE SEVILLA	37.15	-5.62	88	June	5	-0.57	24.54
MORON BASE SEVILLA	37.15	-5.62	88	August	2	-3.40	28.45
MORON BASE SEVILLA	37.15	-5.62	88	September	8	-4.66	23.85
MORON BASE SEVILLA	37.15	-5.62	88	October	11	-4.12	19.56
MORON BASE SEVILLA	37.15	-5.62	88	November	11	-6.04	13.87
MORON BASE SEVILLA	37.15	-5.62	88	December	11	-5.49	11.28
MURCIA	38.00	-1.17	62	January	8	-5.25	10.61
MURCIA	38.00	-1.17	62	February	7	-6.03	12.46
MURCIA	38.00	-1.17	62	March	9	-5.07	14.64
MURCIA	38.00	-1.17	62	April	9	-5.05	17.00
MURCIA	38.00	-1.17	62	Jun.	10	-4.07	20.63
MURCIA	38.00	-1.17	62	June	8	-2.27	24.91
MURCIA	38.00	-1.17	62	July	4	0.12	27.03
MURCIA	38.00	-1.17	62	August	6	-3.14	27.53
MURCIA	38.00	-1.17	62	September	10	-4.79	24.28
MURCIA	38.00	-1.17	62	October	11	-3.79	20.25
MURCIA	38.00	-1.17	62	November	9	-5.27	14.89
MURCIA	38.00	-1.17	62	December	9	-5.25	11.76
PALMA DE MALLORCA	39.55	2.62	3	January	10	-6.07	11.97
PALMA DE MALLORCA	39.55	2.62	3	February	11	-5.94	11.95
PALMA DE MALLORCA	39.55	2.62	3	March	10	-5.31	13.37
PALMA DE MALLORCA	39.55	2.62	3	April	10	-4.25	15.94

PALMA DE MALLORCA	39.55	2.62	3	Jun.	10	-3.18	19.17
PALMA DE MALLORCA	39.55	2.62	3	June	7	-2.82	23.53
PALMA DE MALLORCA	39.55	2.62	3	July	6	-2.49	26.02
PALMA DE MALLORCA	39.55	2.62	3	August	5	-3.52	25.78
PALMA DE MALLORCA	39.55	2.62	3	September	11	-3.35	23.54
PALMA DE MALLORCA	39.55	2.62	3	October	11	-5.22	20.55
PALMA DE MALLORCA	39.55	2.62	3	November	10	-7.08	15.44
PALMA DE MALLORCA	39.55	2.62	3	December	9	-7.07	12.81
PENHAS DOURADAS	40.42	-7.55	1380	January	13	-8.53	2.92
PENHAS DOURADAS	40.42	-7.55	1380	February	13	-7.48	4.42
PENHAS DOURADAS	40.42	-7.55	1380	March	12	-7.04	6.39
PENHAS DOURADAS	40.42	-7.55	1380	April	12	-7.07	6.15
PENHAS DOURADAS	40.42	-7.55	1380	Jun.	13	-6.90	10.16
PENHAS DOURADAS	40.42	-7.55	1380	June	11	-5.46	13.85
PENHAS DOURADAS	40.42	-7.55	1380	July	10	-5.40	17.58
PENHAS DOURADAS	40.42	-7.55	1380	August	11	-5.08	18.24
PENHAS DOURADAS	40.42	-7.55	1380	September	14	-6.83	14.06
PENHAS DOURADAS	40.42	-7.55	1380	October	15	-7.23	9.74
PENHAS DOURADAS	40.42	-7.55	1380	November	14	-8.21	6.05
PENHAS DOURADAS	40.42	-7.55	1380	December	13	-7.43	4.05
PORTALEGRE	39.28	-7.42	597	January	14	-6.31	8.76
PORTALEGRE	39.28	-7.42	597	February	14	-5.56	10.22
PORTALEGRE	39.28	-7.42	597	March	14	-5.29	13.04
PORTALEGRE	39.28	-7.42	597	April	13	-6.17	13.12
PORTALEGRE	39.28	-7.42	597	Jun.	14	-5.10	16.43
PORTALEGRE	39.28	-7.42	597	June	12	-4.51	20.67
PORTALEGRE	39.28	-7.42	597	July	10	-1.86	23.81
PORTALEGRE	39.28	-7.42	597	August	10	-2.68	24.14
PORTALEGRE	39.28	-7.42	597	September	15	-4.20	20.69
PORTALEGRE	39.28	-7.42	597	October	15	-5.17	16.28
PORTALEGRE	39.28	-7.42	597	November	13	-6.46	12.10
PORTALEGRE	39.28	-7.42	597	December	13	-5.60	9.60
PORTO	41.13	-8.60	93	January	13	-4.96	9.67
PORTO	41.13	-8.60	93	February	10	-5.39	10.88
PORTO	41.13	-8.60	93	March	11	-4.19	12.87
PORTO	41.13	-8.60	93	April	10	-5.55	13.45
PORTO	41.13	-8.60	93	Jun.	12	-4.32	16.08
PORTO	41.13	-8.60	93	June	11	-3.01	18.45
PORTO	41.13	-8.60	93	July	11	-2.38	20.66
PORTO	41.13	-8.60	93	August	12	-2.39	20.09
PORTO	41.13	-8.60	93	September	12	-3.90	18.75
PORTO	41.13	-8.60	93	October	13	-4.89	16.18
PORTO	41.13	-8.60	93	November	13	-4.15	12.57
PORTO	41.13	-8.60	93	December	14	-4.43	10.65
SALAMANCA/MATACAN	40.95	-5.50	795	January	1	-6.95	3.50
SALAMANCA/MATACAN	40.95	-5.50	795	March	1	-9.43	9.90
SALAMANCA/MATACAN	40.95	-5.50	795	April	1	-8.48	10.80
SALAMANCA/MATACAN	40.95	-5.50	795	May	1	-6.39	15.10

SALAMANCA/MATACAN	40.95	-5.50	795	June	1	-4.89	21.60
SALAMANCA/MATACAN	40.95	-5.50	795	Agust	1	-6.51	23.50
SALAMANCA/MATACAN	40.95	-5.50	795	November	1	-10.90	8.50
SALAMANCA/MATACAN	40.95	-5.50	795	December	1	-8.70	7.20
SANTANDER	43.48	-3.80	52	January	10	-6.20	10.60
SANTANDER	43.48	-3.80	52	February	11	-6.36	10.35
SANTANDER	43.48	-3.80	52	March	11	-6.39	11.84
SANTANDER	43.48	-3.80	52	April	11	-5.18	12.72
SANTANDER	43.48	-3.80	52	Jun.	11	-3.73	14.83
SANTANDER	43.48	-3.80	52	June	11	-3.55	17.83
SANTANDER	43.48	-3.80	52	July	11	-3.89	19.56
SANTANDER	43.48	-3.80	52	August	11	-3.74	20.35
SANTANDER	43.48	-3.80	52	September	11	-4.62	18.67
SANTANDER	43.48	-3.80	52	October	11	-6.07	16.95
SANTANDER	43.48	-3.80	52	November	11	-6.33	12.90
SANTANDER	43.48	-3.80	52	December	10	-6.79	10.98
TORTOSA	40.81	0.52	48	January	9	-6.87	10.47
TORTOSA	40.81	0.52	48	February	11	-6.58	11.25
TORTOSA	40.81	0.52	48	March	11	-4.62	14.01
TORTOSA	40.81	0.52	48	April	9	-4.10	16.59
TORTOSA	40.81	0.52	48	Jun.	11	-5.59	19.85
TORTOSA	40.81	0.52	48	June	10	-2.65	24.57
TORTOSA	40.81	0.52	48	July	11	-0.94	26.78
TORTOSA	40.81	0.52	48	August	11	-2.62	26.96
TORTOSA	40.81	0.52	48	September	11	-4.47	23.31
TORTOSA	40.81	0.52	48	October	11	-6.30	19.19
TORTOSA	40.81	0.52	48	November	10	-5.82	13.81
TORTOSA	40.81	0.52	48	December	11	-6.03	10.11
VALENCIA	39.47	-0.38	13	January	8	-5.75	11.66
VALENCIA	39.47	-0.38	13	February	9	-6.25	12.39
VALENCIA	39.47	-0.38	13	March	10	-4.61	14.70
VALENCIA	39.47	-0.38	13	April	10	-4.10	16.71
VALENCIA	39.47	-0.38	13	Jun.	9	-3.61	19.58
VALENCIA	39.47	-0.38	13	June	10	-3.02	23.64
VALENCIA	39.47	-0.38	13	July	7	-0.94	25.61
VALENCIA	39.47	-0.38	13	August	9	-2.43	26.22
VALENCIA	39.47	-0.38	13	September	11	-4.47	23.45
VALENCIA	39.47	-0.38	13	October	10	-5.25	19.91
VALENCIA	39.47	-0.38	13	November	9	-6.04	14.61
VALENCIA	39.47	-0.38	13	December	10	-5.78	12.33
VALLADOLID	41.63	-4.77	735	January	10	-8.67	4.49
VALLADOLID	41.63	-4.77	735	February	11	-9.40	5.85
VALLADOLID	41.63	-4.77	735	March	10	-7.50	8.90
VALLADOLID	41.63	-4.77	735	April	9	-7.66	11.28
VALLADOLID	41.63	-4.77	735	Jun.	10	-5.75	14.96
VALLADOLID	41.63	-4.77	735	June	10	-4.11	20.56
VALLADOLID	41.63	-4.77	735	July	6	-1.97	22.23
VALLADOLID	41.63	-4.77	735	August	8	-4.50	21.80

VALLADOLID	41.63	-4.77	735	September	9	-5.93	18.27
VALLADOLID	41.63	-4.77	735	October	11	-8.16	13.36
VALLADOLID	41.63	-4.77	735	November	11	-9.46	7.49
VALLADOLID	41.63	-4.77	735	December	10	-9.40	4.59
VILA REAL	41.32	-7.73	481	January	2	-6.96	4.40
VILA REAL	41.32	-7.73	481	February	1	-4.63	10.20
VILA REAL	41.32	-7.73	481	March	2	-5.51	11.65
VILA REAL	41.32	-7.73	481	April	2	-4.64	10.20
VILA REAL	41.32	-7.73	481	Jun.	3	-6.41	15.87
VILA REAL	41.32	-7.73	481	June	3	-4.28	18.80
VILA REAL	41.32	-7.73	481	July	3	-3.05	22.90
VILA REAL	41.32	-7.73	481	August	2	-4.97	23.25
VILA REAL	41.32	-7.73	481	September	2	-5.42	19.60
VILA REAL	41.32	-7.73	481	October	3	-6.65	14.83
VILA REAL	41.32	-7.73	481	November	3	-6.86	9.87
VILA REAL	41.32	-7.73	481	December	3	-4.73	7.17
ZARAGOZA AEROPUERTO	41.67	-1.02	247	January	3	-8.37	7.60
ZARAGOZA AEROPUERTO	41.67	-1.02	247	February	3	-5.80	8.70
ZARAGOZA AEROPUERTO	41.67	-1.02	247	March	4	-5.55	12.83
ZARAGOZA AEROPUERTO	41.67	-1.02	247	April	4	-6.31	14.25
ZARAGOZA AEROPUERTO	41.67	-1.02	247	Jun.	4	-5.81	18.40
ZARAGOZA AEROPUERTO	41.67	-1.02	247	June	4	-4.81	24.18
ZARAGOZA AEROPUERTO	41.67	-1.02	247	July	3	-4.45	24.27
ZARAGOZA AEROPUERTO	41.67	-1.02	247	August	4	-2.72	25.65
ZARAGOZA AEROPUERTO	41.67	-1.02	247	September	4	-3.57	20.53
ZARAGOZA AEROPUERTO	41.67	-1.02	247	October	4	-5.96	16.28
ZARAGOZA AEROPUERTO	41.67	-1.02	247	November	4	-8.26	10.65
ZARAGOZA AEROPUERTO	41.67	-1.02	247	December	4	-6.92	7.38

2.2.C $^{18}O_{mw}$ correction

	Mean March-June - δ^{18}Omw (‰V-SMOW)	Annual Mean - δ^{18}Omw (‰V-SMOW)
Serinyà	-4.85	-5.9
Moià	-6.73	-7.7
Prades	-6.58	-7.7
Balaguer	-5.25	-6
El Catllar	-4.83	-5.6
Palacios de la Sierra	-7.1	-8.7
San Martin de Valdeiglesias	-5.85	-7.1
Caminreal	-6.58	-7.7
Yaguas de Eresma	-6.73	-8
Zaragoza	-5.33	-6.3
Sobradiel	-5.33	-6.3
Cernadilla	-6.63	-8
Uncastillo	-6.08	-7.3
Pisto Larrède Oliván	-7.3	-8.6
Basarán	-7.65	-8.8
Espot	-8	-9.1
Berástegui	-5.65	-6.7
Amareleja	-3.85	-5.2
Redondo	-4.15	-5.4
Tomar	-3.88	-5
Piediquacio (Corse)	-5.73	-6.4
Pancheraccia (Corse)	-6.3	-7

Current oxygen isotope compositions of meteoric waters ($\delta^{18}O_{mw}$; ‰ V-SMOW) from Iberian localities and Corsican localities: mean from March to June and annual mean. Data are provided by the Online Isotopes in Precipitation Calculator, derived from the International Atomic Energy Agency / World Meteorological Organization Global Network for Isotopes in Precipitation (Bowen, 2017). These data are used to develop the linear regression model (OLS equation) between current mean annual $\delta^{18}O_{mw}$ and mean March-June $\delta^{18}O_{mw}$ values (Figure 5B)..

2.2.D Owls from Iberia

Common name	Scientific name	JAN	FEB	MAR	APR	MAY	JUN	JUL	AUG	SEP	OCT	NOV	DEC	Migration behavior
Barn owl	***Tyto alba***													Sedentary
Little owl	***Athene noctua***													Sedentary
Tawny owl	***Strix aluco***													Sendentary
Long-eared owl	***Asio otus***													Sedentary in Iberia
Europan eagle owl	***Bubo bubo***													Sendentary
Short-eared owl	***Asio flammeus***													Nomad
Eurasian scops owl	***Otus scops***													Nomad

Ecological data for the most common owls from the Iberian Peninsula: breeding season (light grey), reproduction (dark grey) and migration behavior (in green, presence by migration; in orange, absence by migration). Based on: Manzanares, A. (2012).

2.2.E Bioclimatic Model apply to Xaragalls cave layers (C4-C8)

C4	I	II	II/III	III	IV	V	VI	VII	VIII	IX
Microtus agrestis	0	0	0	0	0	0	0.5	0	0.5	0
Microtus arvalis	0	0	0	0	0	0	1	0	0	0
Iberomys cabrerae	0	0	0	0	1	0	0	0	0	0
Chionomys nivalis	0	0	0	0	0.25	0	0.25	0	0.25	0.25
M. (T.) duodecimcostatus	0	0	0	0	1	0	0	0	0	0
Apodemus sylvaticus	0	0	0	0	0.5	0	0.5	0	0	0
Eliomys quercinus	0	0	0	0	0.5	0	0.5	0	0	0
Σ Climatic Restriction Index	0	0	0	0	3.25	0	2.75	0	0.75	0.25
Bioclimatic Component	0.00	0.00	0.00	0.00	46.43	0.00	39.29	0.00	10.71	3.57

Mean annual temperature (ºC)	12.2
Mean temperature of the warmest month (ºC)	20.9
Mean temperature of the coldest month (ºC)	4.6
Mean annual precipitation (mm)	815
Aridity time (months)	3.1
Thermal amplitude (ºC)	16.3

C5	I	II	II/III	III	IV	V	VI	VII	VIII	IX
Arvicola sapidus	0	0	0	0	0.5	0	0.5	0	0	0
Microtus arvalis	0	0	0	0	0	0	1	0	0	0
M. (T.) duodecimcostatus	0	0	0	0	1	0	0	0	0	0
Apodemus sylvaticus	0	0	0	0	0.5	0	0.5	0	0	0
Eliomys quercinus	0	0	0	0	0.5	0	0.5	0	0	0
Σ Climatic Restriction Index	0	0	0	0	2.5	0	2.5	0	0	0
Bioclimatic Component	0.00	0.00	0	0.00	50.00	0.00	50.00	0.00	0.00	0.00

Mean annual temperature (ºC)	16.2
Mean temperature of the warmest month (ºC)	22.1
Mean temperature of the coldest month (ºC)	11.7
Mean annual precipitation (mm)	1092
Aridity time (months)	3.1
Thermal amplitude (ºC)	10.3

C6	I	II	II/III	III	IV	V	VI	VII	VIII	IX
Arvicola sapidus	0	0	0	0	0.5	0	0.5	0	0	0
Microtus agrestis	0	0	0	0	0	0	0.5	0	0.5	0
Microtus arvalis	0	0	0	0	0	0	1	0	0	0
Iberomys cabrerae	0	0	0	0	1	0	0	0	0	0
Chionomys nivalis	0	0	0	0	0.25	0	0.25	0	0.25	0.25
M. (T.) duodecimcostatus	0	0	0	0	1	0	0	0	0	0
Apodemus sylvaticus	0	0	0	0	0.5	0	0.5	0	0	0
Eliomys quercinus	0	0	0	0	0.5	0	0.5	0	0	0
Σ Climatic Restriction Index	0	0	0	0	3.75	0	3.25	0	0.75	0.25
Bioclimatic Component	0.00	0.00	0.00	0.00	46.88	0.00	40.63	0.00	9.38	3.13

Mean annual temperature (ºC)	12.7
Mean temperature of the warmest month (ºC)	21.1
Mean temperature of the coldest month (ºC)	5.5
Mean annual precipitation (mm)	850
Aridity time (months)	3.1
Thermal amplitude (ºC)	15.5

C7	I	II	II/III	III	IV	V	VI	VII	VIII	IX
Microtus agrestis	0	0	0	0	0	0	0.5	0	0.5	0
Iberomys cabrerae	0	0	0	0	1	0	0	0	0	0
Apodemus sylvaticus	0	0	0	0	0.5	0	0.5	0	0	0
Eliomys quercinus	0	0	0	0	0.5	0	0.5	0	0	0
Σ Climatic Restriction Index	0	0	0	0	2	0	1.5	0	0.5	0
Bioclimatic Component	0.00	0.00	0.00	0.00	50.00	0.00	37.50	0.00	12.50	0.00

Mean annual temperature (ºC)	12.9
Mean temperature of the warmest month (ºC)	22.0
Mean temperature of the coldest month (ºC)	4.6
Mean annual precipitation (mm)	742
Aridity time (months)	3.5
Thermal amplitude (ºC)	17.4

C8	I	II	II/III	III	IV	V	VI	VII	VIII	IX
Microtus arvalis	0	0	0	0	0	0	1	0	0	0
Iberomys cabrerae	0	0	0	0	1	0	0	0	0	0
M. (T.) duodecimcostatus	0	0	0	0	1	0	0	0	0	0
Apodemus sylvaticus	0	0	0	0	0.5	0	0.5	0	0	0
Eliomys quercinus	0	0	0	0	0.5	0	0.5	0	0	0
Σ Climatic Restriction Index	0	0	0	0	3	0	2	0	0	0
Bioclimatic Component	0.00	0.00	0.00	0.00	60.00	0.00	40.00	0.00	0.00	0.00

Mean annual temperature (ºC)	16.8
Mean temperature of the warmest month (ºC)	23.6
Mean temperature of the coldest month (ºC)	11.4
Mean annual precipitation (mm)	816
Aridity time (months)	4.5
Thermal amplitude (ºC)	12.1

The bioclimatic model is based on the adscription of small-mammal species to ten different climatic zones. This allows the calculation first of the Climatic Restriction Index (CRIi=1/n, where i is the climatic zone inhabited by the species and n is the number of climatic zones the species inhabit) and then the Bioclimatic Component (BCi=(ΣCRIi)100/S, where S is the number of species). From the BC it is possible to calculate several climatic parameters by means of multiple linear regression developed specifically for the order Rodentia (Hernández Fernández, 2001; Hernández Fernández et al., 2007).

2.2.F Mutual Ecogeograhic Range apply to Xaragalls cave layers

	n	Max	Min	Mean	SD	CI (95%)	Standard Error
C3	6	10	6	7.92	1.69	1.35	0.69
C4	2	9	7	8	1.41	1.95	1.00
C5	52	13	6	10.36	1.58	0.43	0.22
C6	2	9	7	8	1.41	1.95	1.00
C7	3	10	7	8.67	1.53	1.73	0.88
C8	26	13	7	10.48	1.72	0.66	0.34

The mutual ecogeographic range method, determines the present-day geographical region in which a given fossil species assemblage would be located through the intersection obtained from the overlap of the current distributions of each species (Blain et al., 2009, 2016; López-García, 2011). The climatic conditions of the intersecting area are used to infer the MAT. The MER estimations of Xaragalls cave layers were published by López-García et al. (2012a). CI, Confidence Interval.

2.2.G Small vertebrates identified in Xaragalls cave

	NISP	MNI	%	NISP	MNI	%	NISP	MNI	%	NISP	MNI	%	NISP	MNI	%	NISP	MNI	%
Taxa/Layers	C3			C4			C5			C6			C7			C8		
Anura																		
Alytes obstetricans	1	1	6.7	1	1	2.8	0	0	0.0	5	2	1.8	8	2	3.8	3	1	2.7
Pelodytes cf. *punctatus*	0	0	0.0	2	0	0.0	1	1	7.1	1	1	0.9	1	1	1.9	1	1	2.7
Bufo calamita	1	1	6.7	7	1	2.8	0	0	0.0	8	1	0.9	2	1	1.9	11	1	2.7
Squamata																		
Lacertidae indet.	0	0	0.0	11	1	2.8	0	0	0.0	7	1	0.9	6	2	3.8	3	1	2.7
Anguis fragilis	1	1	6.7	1	1	2.8	0	0	0.0	3	1	0.9	6	1	1.9	1	1	2.7
Serpentes																		
Coronella girondica	0	0	0.0	9	1	2.8	2	1	7.1	18	1	0.9	7	1	1.9	7	1	2.7
Vipera cf. *latasti*	0	0	0.0	2	1	2.8	0	0	0.0	2	1	0.9	0	0	0.0	0	0	0.0
Rodentia																		
Arvicola sapidus	0	0	0.0	0	0	0.0	2	1	7.1	1	1	0.9	0	0	0.0	0	0	0.0
Microtus agrestis	2	2	13.3	2	2	5.6	0	0	0.0	2	2	1.8	2	2	3.8	0	0	0.0
Microtus arvalis	0	0	0.0	7	4	11.1	1	1	7.1	3	2	1.8	0	0	0.0	2	1	2.7
M. (Iberomys) cabrerae	0	0	0.0	1	1	2.8	0	0	0.0	4	3	2.7	1	1	1.9	4	2	5.4
Chionomys nivalis	1	1	6.7	3	2	5.6	0	0	0.0	2	1	0.9	0	0	0.0	0	0	0.0
M. (T.) duodecimcostatus	1	1	6.7	3	2	5.6	1	1	7.1	8	7	6.3	0	0	0.0	6	4	10.8
Apodemus sylvaticus	18	6	40.0	44	14	38.9	25	7	50.0	191	69	62.2	93	33	63.5	31	18	48.6
Eliomys quercinus	1	1	6.7	4	3	8.3	2	1	7.1	17	6	5.4	7	3	5.8	2	2	5.4
Insectivora																		
Sorex sp.	0	0	0.0	0	0	0.0	0	0	0.0	7	3	2.7	1	1	1.9	0	0	0.0
Sorex minutus	0	0	0.0	0	0	0.0	0	0	0.0	4	3	2.7	0	0	0.0	1	1	2.7
Neomys fodiens	0	0	0.0	0	0	0.0	0	0	0.0	0	0	0.0	2	1	1.9	0	0	0.0
Crocidura russula	0	0	0.0	0	0	0.0	0	0	0.0	2	1	0.9	1	1	1.9	1	1	2.7
Talpa europaea	0	0	0.0	2	1	2.8	0	0	0.0	0	0	0.0	1	1	1.9	0	0	0.0
Chiroptera																		
Myotis nattereri	0	0	0.0	0	0	0.0	0	0	0.0	6	3	2.7	0	0	0.0	0	0	0.0
R. euryale-mehelyi	0	0	0.0	2	1	2.8	0	0	0.0	0	0	0.0	0	0	0.0	0	0	0.0
P. auritus-austriacus	0	0	0.0	0	0	0.0	1	1	7.1	1	1	0.9	1	1	1.9	2	2	5.4
Miniopterus schreibersii	1	1	6.7	0	0	0.0	0	0	0.0	0	0	0.0	0	0	0.0	0	0	0.0
Nyctalus lasiopterus	0	0	0.0	0	0	0.0	0	0	0.0	1	1	0.9	0	0	0.0	0	0	0.0
Total	27	15	100	101	36	100	35	14	100	293	111	100	139	52	100	75	37	100

Data published by López-García et al. (2012a). NISP, number of identified specimens; MNI, minimum number of individuals (MNI) and the percentage of the MNI (%).

Appendix 2.3

Here is included supplementary material of the Abric Romaní sequence analysis exposed in "Chapter 6. Combined palaeoecological methods using small-mammal assemblages to decipher environmental context of a long-term Neanderthal settlement in northeastern Iberia".

2.3.A Taphonomic analysis of levels O, N, K, J, E and D

Recount and relative abundance index (IAR)

		Level O		Level N		Level K		Level J		Level E		Level D	
Rodents	Element (Rodents)	Recount	IAR	Recount	IAR	Recount	IAR	Recount	IAR	Recount	IAR	Recount	IAR
	Hemimaxilar	39	6.5	11	8.6	5	6.9	12	17.6	29	17.3	23	17.4
	Hemimandible	104	17.4	25	19.5	39	54.2	29	42.6	76	45.2	50	37.9
	Molar	640	35.8	188	49.0	119	55.1	118	57.8	247	49.0	170	42.9
	Incisor	557	93.5	280	218.8	67	93.1	80	117.6	197	117.3	101	76.5
	Humerus	65	21.8	45	70.3	16	44.4	30	88.2	71	84.5	33	50.0
	Radius	45	15.1	16	25.0	5	13.9	19	55.9	34	40.5	14	21.2
	Ulna	21	7.0	7	10.9	5	13.9	17	50.0	48	57.1	23	34.8
	Femur	112	37.6	27	42.2	9	25.0	33	97.1	60	71.4	43	65.2
	Tibia-fibula	93	31.2	30	46.9	14	38.9	28	82.4	63	75.0	26	39.4
	MEAN IAR		**29.6**		**54.6**		**38.4**		**67.7**		**61.9**		**42.8**
	SD IAR		**26.6**		**64.8**		**27.2**		**31.0**		**29.1**		**19.0**
	Total NISP	**1676**		**629**		**279**		**366**		**825**		**483**	
Indet	Cranial fragments	79		10		15		40		21		22	
	Cintura	13		5		4		14		34		14	
	Vertebra	30		9		27		67		99		115	
	Rib	4		1		13		31		24		26	
	Autopods	30		24		24		63		94		96	
Other	NISP Chiroptera	3		22		0		0		16		17	
	NISP Talpidae	12		7		0		2		0		0	
	NISP Soricidae	27		5		1		6		18		8	
	Total NISP	1874		712		363		589		1131		781	
	Indet	394		115		56		78		259		165	
	NR	2268		827		419		667		1390		946	

Breakage

	Breakage					
	Level O	**Level N**	**Level K**	**Level J**	**Level E**	**Level D**
Femur breakage (%)	98.2	100	100	90.9	93.3	100
Complete (n)	2	0	0	3	4	0
Total (n)	112	27	9	33	60	43
Molars breakage (%)	41.3	50.5	9.2	23.7	12.6	12.9
In situ (%)	7.7	20.0	0	0	0	0
Break (n)	3	1	0	0	0	0
Total (n)	39	5	34	30	59	47
Isolated (%)	43.4	51.4	12.9	31.8	16.5	17.9
Break (n)	264	94	11	28	31	22
Total (n)	608	183	85	88	188	123
Incisors breakage (%)	67.3	68.2	47.8	62.5	48.7	59.4
In situ (%)	0	0	28.6	63.6	24.1	29.4
Break (n)	0	0	4	7	7	5
Total (n)	8	1	14	11	29	17
Isolated (%)	68.3	68.5	52.8	62.3	53	65.5
Break (n)	375	191	28	43	89	55
Total (n)	549	279	53	69	168	84

Post-depositional processes

	Level O		Level N		Level K		Level J		Level E		Level D	
	n	%	n	%	n	%	n	%	n	%	n	%
Estriations	1055	79.6	417	81.4	97	49.7	160	68.7	404.0	77.4	243.0	74.3
Fissures	910	68.6	238	46.5	28	14.4	64	27.5	114.0	21.8	50.0	15.3
Cracks	332	25	79	15.4	7	3.6	13	5.6	25.0	4.8	9.0	2.8
Disolution	0	0	0	0	0	0	0	0	0	0	0	0
Desquamation	92	6.9	3	0.6	0	0	0	0	0.0	0	0	0
Burning	175	13.2	15	2.9	26	13.3	13	5.6	49.0	9.4	11.0	3.4
Isolated	83	47.4	8	53.3	18	69.2	11	84.6	14	28.6	3.0	27.3
Concentrated	30	17.1	5	33.3	4	15.4	1	7.7	14	28.6	3.0	27.3
Dispersed	55	31.4	1	6.7	0	0	1	7.7	9	18.4	0.0	0
Widespread	7	4	1	6.7	4	15.4	0	0	12	24.5	5.0	45.5
Manganese oxide	621	46.8	159	31.1	21	10.8	70	30	233.0	44.6	61.0	18.7
Isolated	364	58.6	142	89.3	18	85.7	61	87.1	182.0	78.1	56.0	91.8
Concentrated	54	8.7	8	5	2	9.5	1	1.4	9.0	3.9	5.0	8.2
Dispersed	202	32.5	9	5.7	1	4.8	8	11.4	42.0	18	0.0	0
Widespread	1	0.2	0	0	0	0	0	0	0	0	0.0	0
Chemical corrosion	600	45.2	138	27.0	44	22.6	130	55.8	134.0	25.7	126.0	38.5
Isolated	285	47.5	56	40.6	16	36.4	51	39.2	75.0	56.0	86.0	68.3
Concentrated	127	21.2	23	16.7	7	15.9	19	14.6	30.0	22.4	15.0	11.9
Dispersed	156	26	48	34.8	20	45.5	52	40	28.0	20.9	23.0	18.3
Widespread	32	2.4	11	8	1	2.3	8	6.2	1.0	0.7	2.0	1.6
Roots etching	409	30.8	131	25.6	43	22.1	130	55.8	131.0	25.1	122.0	37.3
Isolated	131	32	50	38.2	15	34.9	51	39.2	76.0	58.0	82.0	67.2
Concentrated	120	29.3	23	17.6	7	16.3	19	14.6	27.0	20.6	15.0	12.3
Dispersed	131	32	47	35.9	20	46.5	52	40	27.0	20.6	23.0	18.9
Widespread	27	6.6	11	8.4	1	2.3	8	6.2	1.0	0.8	2.0	1.6
Water abrasion	73	5.5	8	1.6	1	0.5	4	1.7	8	1.5	2	0.6
Rounding	73	5.5	8	1.6	1	0.5	4	1.7	8	1.5	2	0.6
R1	72	98.6	6	75	1	100	4	100	8	100	2	100
R2	1	1.4	2	25	0	0	0	0	0	0	0	0
Polished	20	1.5	3	0.6	0	0	3	1.3	2	0.4	2	0.6
P1	20	100	3	100	0	0	3	100	2	100	2	100
Burning	192	14.5	32	6.3	0	0	6	2.6	60	11.5	9	2.8
Degree 1	96	50	16	50	0	0	5	83.3	32	53.3	2	22.2
Degree 2	68	35.4	3	9.4	0	0	1	16.7	24	40	4	44.4
Degree 3	25	13	8	25	0	0	0	0	4	6.7	3	33.3
Degree 4	3	1.6	5	15.6	0	0	0	0	0	0	0	0
Trampling	0	0	0	0	0	0	0	0	0	0	0	0
Weathering	3	0.2	0	0	0	0	0	0	0	0	0	0

2.3.B Evenness and Simpson's Diversity Index

	D	E	F	H	I	J	K	L	M	N	O	P	Q
Taxa (n)	10	12	1	3	5	7	5	4	3	10	15	3	7
Individuals (n)	52	47	1	5	7	18	18	7	5	39	276	11	14
Simpson Index	0.813	0.724	0	0.64	0.734	0.772	0.58	0.612	0.64	0.844	0.841	0.43	0.755
Shannon Index	1.916	1.799	0	1.055	1.475	1.69	1.165	1.154	1.055	2.023	2.053	0.76	1.673

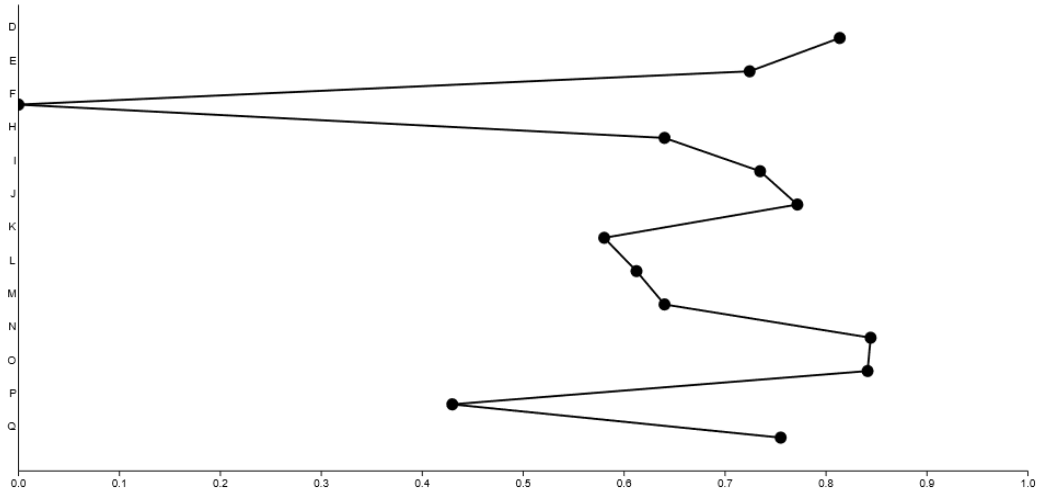

The species evenness and diversity is calculated, using Paleontological Statistics (PAST) software (Hammer et al., 2001). The evenness of a community can be represented by Simpson's Diversity Index [$(1 - \Sigma pi^2)$, where pi is the proportion of individuals in i species)]. This index allows us to quantify how equal communities are through numerical and increases when the specific diversity of a community increases, and the result will always be between 0 and 1

2.3.C Mutual Ecogeographic Range of levels O, N, E and D

	Level O		Level N		Level E		Level D	
	MAT	MAP	MAT	MAP	MAT	MAP	MAT	MAP
n	*7*	*7*	*166*	*166*	*5*	*5*	*110*	*110*
Mean	**11.1**	**871**	**12.2**	**615**	**9.7**	**760**	**11.6**	**606**
Min	7.5	700	7.5	300	7.5	700	7.5	300
Max	12.5	1000	17.5	1400	12.5	1000	15	1000
SD	2.0	160	2	169	2.6	134	1.6	159
Error (C.I.95%)	1.8	41	0.3	9	3.2	40	0.3	10
Current data	14.8	619	14.8	619	14.8	619	14.8	619
Respect to present-day	**-3.7**	**252**	**-2.6**	**-4**	**-5.1**	**141**	**-3.2**	**-13**

Mean annual temperature - Level O

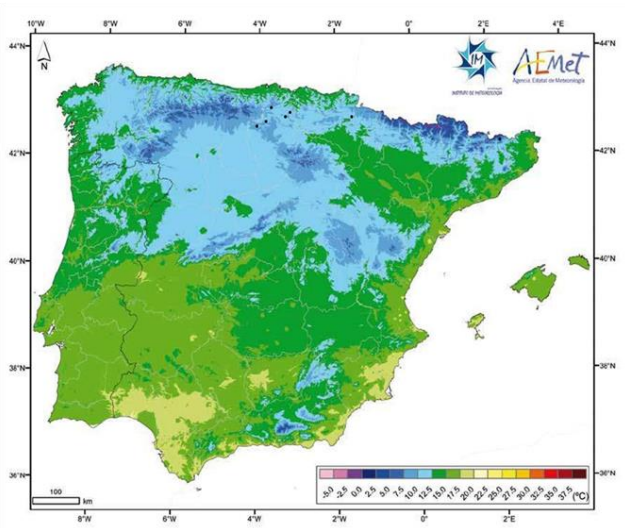

Mean annual precipitation - Level O

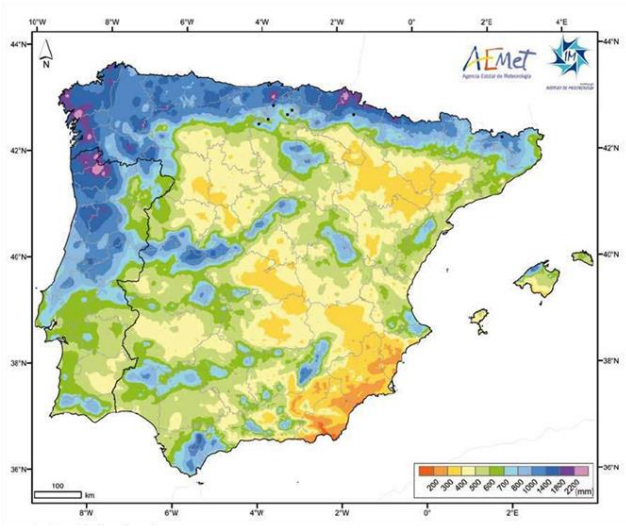

Mean annual temperature - Level N

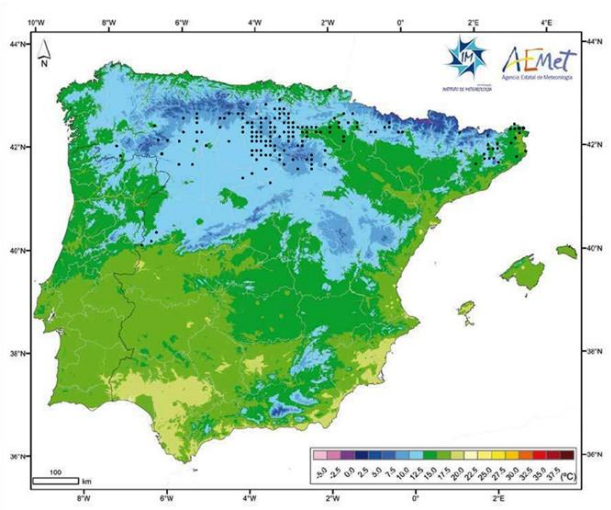

Mean annual precipitation - Level N

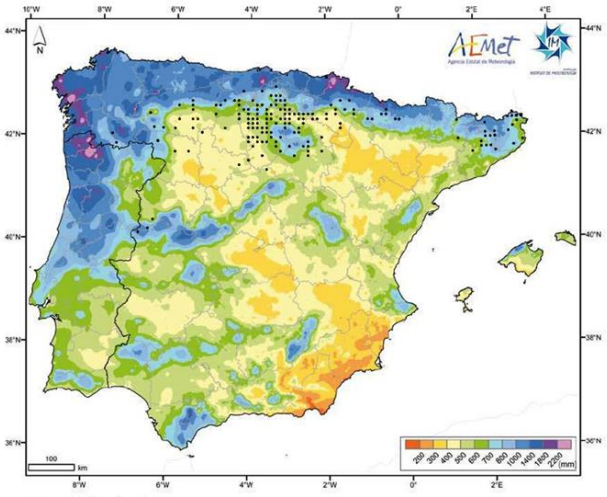

Mean annual temperature - Level E

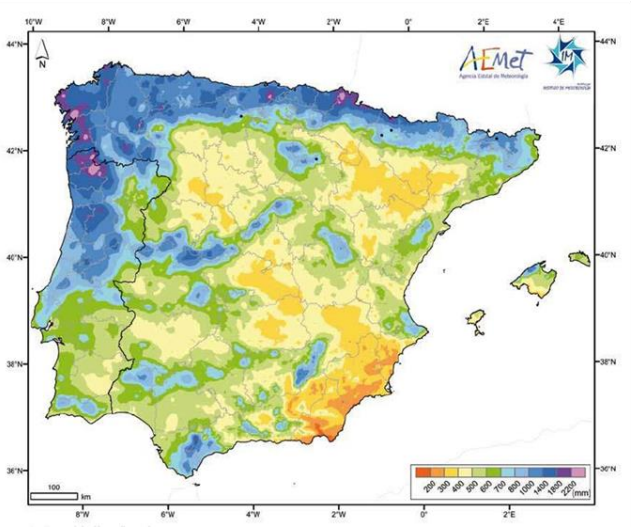

Mean annual precipitation - Level E

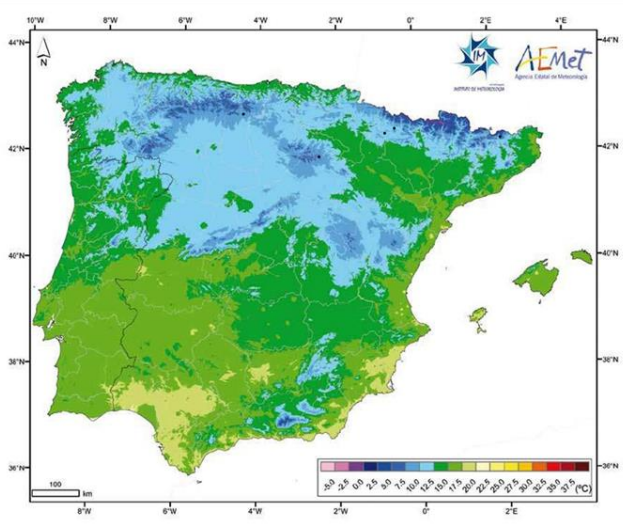

Mean annual temperature - Level D

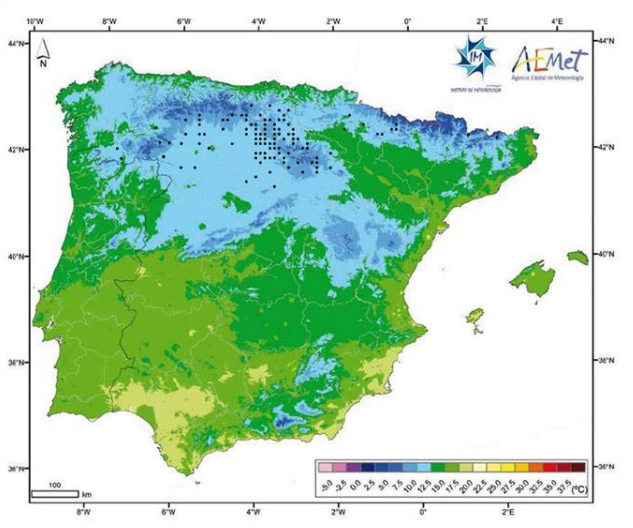

Mean annual precipitation - Level D

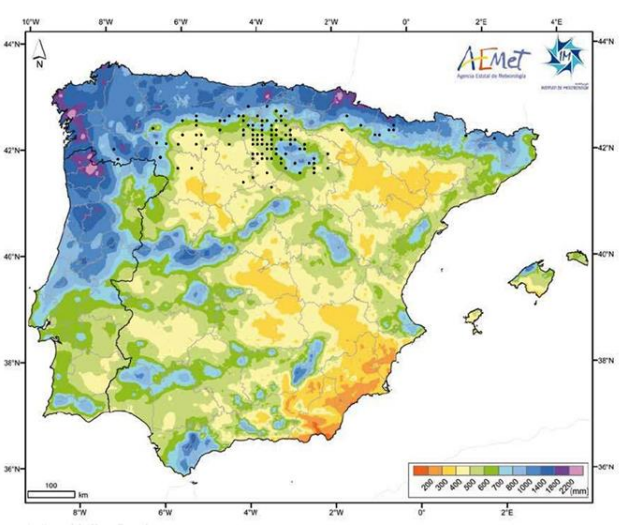

The mutual ecogeographic range method, determines the present-day geographical region in which a given fossil species assemblage would be located through the intersection obtained from the overlap of the current distributions of each species (Blain et al., 2009, 2016; López-García, 2011). The Iberian species distribution maps are obtained from Palomo et al. (2007) and the current Mean Annual Temperatures (MAT) and Mean Annual Precipitations (MAP) are obtained from AEMET & IMP (2011).

2.3.D Bioclimatic Model of levels O, N, E and D

D	I	II	II/III	III	IV	V	VI	VII	VIII	IX
Arvicola sapidus	0	0	0	0	0.5	0	0.5	0	0	0
Microtus agrestis	0	0	0	0	0	0	0.5	0	0.5	0
Microtus arvalis	0	0	0	0	0	0	1	0	0	0
Iberomys cabrerae	0	0	0	0	1	0	0	0	0	0
M. (T.) duodecimcostatus	0	0	0	0	1	0	0	0	0	0
Apodemus sylvaticus	0	0	0	0	0.5	0	0.5	0	0	0
Eliomys quercinus	0	0	0	0	0.5	0	0.5	0	0	0
Σ Climatic Restriction Index	0	0	0	0	3.5	0	3	0	0.5	0
Bioclimatic Component	0.00	0.00	0.00	0.00	50.00	0.00	42.86	0.00	7.14	0.00

Mean annual temperature (ºC)	14.3
Mean temperature of the warmest month (ºC)	22.1
Mean temperature of the coldest month (ºC)	7.7
Mean annual precipitation (mm)	892
Aridity time (months)	3.3
Thermal amplitude (ºC)	14.3

E	I	II	II/III	III	IV	V	VI	VII	VIII	IX
Arvicola sapidus	0	0	0	0	0.5	0	0.5	0	0	0
Microtus agrestis	0	0	0	0	0	0	0.5	0	0.5	0
Microtus arvalis	0	0	0	0	0	0	1	0	0	0
Iberomys cabrerae	0	0	0	0	1	0	0	0	0	0
Chionomys nivalis	0	0	0	0	0.25	0	0.25	0	0.25	0.25
M. (T.) duodecimcostatus	0	0	0	0	1	0	0	0	0	0
Apodemus sylvaticus	0	0	0	0	0.5	0	0.5	0	0	0
Eliomys quercinus	0	0	0	0	0.5	0	0.5	0	0	0
Sumatorio de CRI	0	0	0	0	3.75	0	3.25	0	0.75	0.25
Espectro bioclimático	0.00	0.00	0.00	0.00	46.88	0.00	40.63	0.00	9.38	3.13

Mean annual temperature (ºC)	12.7
Mean temperature of the warmest month (ºC)	21.1
Mean temperature of the coldest month (ºC)	5.5
Mean annual precipitation (mm)	850
Aridity time (months)	3.1
Thermal amplitude (ºC)	15.5

N	I	II	II/III	III	IV	V	VI	VII	VIII	IX
Arvicola sapidus	0	0	0	0	0.5	0	0.5	0	0	0
Microtus agrestis	0	0	0	0	0	0	0.5	0	0.5	0
Iberomys cabrerae	0	0	0	0	1	0	0	0	0	0
M. (T.) duodecimcostatus	0	0	0	0	1	0	0	0	0	0
Apodemus sylvaticus	0	0	0	0	0.5	0	0.5	0	0	0
Eliomys quercinus	0	0	0	0	0.5	0	0.5	0	0	0
Sumatorio de CRI	0	0	0	0	3.5	0	2	0	0.5	0
Espectro bioclimático	0.00	0.00	0.00	0.00	58.33	0.00	33.33	0.00	8.33	0.00

Mean annual temperature (ºC)	14.5
Mean temperature of the warmest month (ºC)	23.3
Mean temperature of the coldest month (ºC)	6.7
Mean annual precipitation (mm)	629
Aridity time (months)	4.5
Thermal amplitude (ºC)	16.5

O	I	II	II/III	III	IV	V	VI	VII	VIII	IX
Arvicola sapidus	0	0	0	0	0.5	0	0.5	0	0	0
Microtus agrestis	0	0	0	0	0	0	0.5	0	0.5	0
Microtus arvalis	0	0	0	0	0	0	1	0	0	0
Iberomys cabrerae	0	0	0	0	1	0	0	0	0	0
M. (T.) duodecimcostatus	0	0	0	0	1	0	0	0	0	0
Apodemus sylvaticus	0	0	0	0	0.5	0	0.5	0	0	0
Eliomys quercinus	0	0	0	0	0.5	0	0.5	0	0	0
Sciurus vulgaris	0	0	0	0	0.333	0	0.333	0	0.333	0
Sumatorio de CRI	0	0	0	0	3.833	0	3.333	0	0.833	0
Espectro bioclimático	0.00	0.00	0.00	0.00	47.91	0.00	41.66	0.00	10.41	0.00

Mean annual temperature (ºC)	13.3
Mean temperature of the warmest month (ºC)	21.7
Mean temperature of the coldest month (ºC)	5.9
Mean annual precipitation (mm)	858
Aridity time (months)	3.1
Thermal amplitude (ºC)	15.8

The bioclimatic model is based on the adscription of small-mammal species to ten different climatic zones. This allows the calculation first of the Climatic Restriction Index (CRIi=1/n, where i is the climatic zone inhabited by the species and n is the number of climatic zones the species inhabit) and then the Bioclimatic Component (BCi=(ΣCRIi)100/S, where S is the number of species). From the BC it is possible to calculate several climatic parameters by means of multiple linear regression developed specifically for the order Rodentia (Hernández Fernández, 2001; Hernández Fernández et al., 2007).

Appendix 2.4. Here is included supplementary material of "Chapter 7. Palaeoecological reconstruction of Teixoneres site (Moià, Barcelona) based on small mammals: origin of the assemblage and palaeoclimatic inferences".

2.4.A Taphonomic analysis

Recount and relative abundance index (IAR)

		IIIb		IIIa		IIb		IIa	
	Element (Rodents)	Recount	IAR	Recount	IAR	Recount	IAR	Recount	IAR
Rodents	Hemimaxilar	13	14.8	20	16.1	15	16.3	8	10.0
	Hemimandible	27	30.7	54	43.5	20	21.7	29	36.3
	Molar	138	52.3	178	47.8	81	29.3	104	43.3
	Incisor	141	160.2	200	161.3	59	64.1	64	80.0
	Humerus	25	56.8	41	66.1	17	37.0	25	62.5
	Radius	3	6.8	13	21.0	5	10.9	6	15.0
	Ulna	19	43.2	21	33.9	10	21.7	16	40.0
	Femur	22	50.0	38	61.3	17	37.0	21	52.5
	Tibia-fibula	29	65.9	30	48.4	12	26.1	15	37.5
	MEAN IAR		**53.4**		**55.5**		**29.3**		**41.9**
	SD IAR		**44.5**		**43.0**		**15.7**		**21.8**
	Total NISP	**417**		**595**		**236**		**288**	
Indet	Cranial fragments	4		10		2		13	
	Cintura	4		26		3		5	
	Vertebra	44		76		20		22	
	Rib	7		8		7		7	
	Autopods	28		39		7		10	
Other	NISP Chiroptera	42		33		34		54	
	NISP Talpidae	8		0		1		2	
	NISP Soricidae	19		4		13		1	
	Total NISP	573		791		323		402	
	Indet	209		197		65		82	
	NR	782		988		388		484	

Breakage

	Breakage			
	Subunit IIIb	Subunit IIIa	Subunit IIb	Subunit IIa
Postcranial breakage (%)	100.0	100	100	100.0
Complete (n)	0	0	0	0
Total (n)	47	79	34	46
Molars breakage (%)	11.7	8.3	17.1	6.9
In situ (%)	0	0	0	0
Break (n)	0	0	0	0
Total (n)	29	30	8	12
Isolated (%)	14.8	9.9	19.1	7.9
Break (n)	16	16	13	7
Total (n)	108	162	68	89
Incisors breakage (%)	68.1	68.0	45.8	42.0
In situ (%)	22	27	25.0	20.0
Break (n)	2	3	1	1
Total (n)	9	11	4	5
Isolated (%)	71.2	70.4	47.3	43.8
Break (n)	94	131	26	28
Total (n)	132	186	55	64

Post-depositional processes

	Level IIIb		Level III		Level IIb		Level II	
	n	%	n	%	n	%	n	%
Estriations	295	79.1	381	79.0	167	79.5	171	77.4
Fissures	104	27.9	141	29.3	34	16.2	46	20.8
Cracks	33	8.8	56	11.6	10	4.8	4	1.8
Disolution	0	0	0	0	0	0	0	0
Desquamation	1	0.3	0	0	0	0	0	0
Burning	20	5.4	57	11.8	2	1.0	3	1.4
Isolated	15	75	31	54.4	2	100	2	66.7
Concentrated	5	25	21	36.8	0	0	1	33.3
Dispersed	0	0	2	3.5	0	0	0	0
Widespread	0	0	3	5.3	0	0	0	0
Manganese oxide	175	46.9	177	36.7	121	57.6	108	48.9
Isolated	134	76.6	148	83.6	92	76.0	84	77.8
Concentrated	5	2.9	12	6.8	6	5.0	4	3.7
Dispersed	36	20.6	16	9.0	23	19.0	20	18.5
Widespread	0	0	1	0.6	0	0	0	0
Chemical corrosion	126	33.8	105	21.8	34	16.2	35	15.8
Isolated	86	68.3	73	69.5	27	79.4	28	80
Concentrated	19	15.1	11	10.5	5	14.7	3	8.6
Dispersed	20	15.9	19	18.1	2	5.9	4	11.4
Widespread	1	0.1	2	1.9	0	0	0	0
Roots etching	122	32.7	77	16.0	21	10	26	11.8
Isolated	82	67.2	51	66.2	14	66.7	20	76.9
Concentrated	19	15.6	9	11.7	5	23.8	2	7.7
Dispersed	20	16.4	16	20.8	2	9.5	4	15.4
Widespread	1	0.8	1	1.3	0	0	0	0
Water abrasion	0	0	0	0	0	0	0	0
Rounding	6	0.5	1	0.2	1	0.5	2	0.9
R1	4	66.7	1	100	0	0	1	50
R2	1	16.7	0	0	1	100	1	50
R3	1	16.7	0	0	0	0	0	0
Polished	3	0.2	1	0.2	1	0.5	2	0.9
P1	2	66.7	1	100	1	100	2	100
P2	0	0	0	0	0	0	0	0
P3	1	33.3	0	0	0	0	0	0
Burning	7	1.9	2	0.4	2	1.0	0	0
Degree 1	2	28.6	0	0	1	50	0	0
Degree 2	1	14.3	1	50	1	50	0	0
Degree 3	2	28.6	1	50	0	0	0	0
Degree 4	2	28.6	0	0	0	0	0	0
Trampling	0	0	0	0	0	0	0	0
Weathering	0	0	0	0	0	0	0	0

2.4.B Small vertebrates identified in Texioneres cave

	II			IIb			III			IIIb		
	NISP	MNI	%	NISP	MNI	%	NISP	MNI	%	NISP	MNI	%
Salamandra salamandra	11	2	4.65	19	30	8.77	0	0	0	0	0	0
Alytes obstetricans	19	4	9.3	27	12	3.51	2	2	1.59	1	1	0.7
Pelodytes punctatus	10	4	9.3	8	5	1.46	0	0	0	0	0	0
Bufo bufo	3	1	2.33	5	3	0.88	1	1	0.79	0	0	0
Bufo calamita	51	5	11.6	117	34	9.94	47	28	22.2	2	2	1.4
Rana temporaria	11	4	9.3	35	14	4.09	15	11	8.73	5	3	2.1
Anura indet.	0	0	0	9	0	0	4	0	0	0	0	0
Lacerta s.l.	0	0	0	0	0	0	2	2	1.59	3	1	0.7
Lacertidae indet.	2	1	2.33	10	9	2.63	4	4	3.17	3	1	0.7
Anguis fragilis	1	1	2.33	5	4	1.17	2	2	1.59	0	0	0
Natrix cf. *natrix*	0	0	0	0	0	0	0	0	0	1	1	0.7
Coronella austriaca	1	1	2.33	7	5	1.46	0	0	0	7	1	0.7
Malpolon monspessulanus	0	0	0	2	1	0.29	0	0	0	0	0	0
Vipera aspis	14	2	4.65	20	8	2.34	0	0	0	0	0	0
Ophidia indet.	0	0	0	8	0	0	2	0	0	6	0	0
Arvicola sapidus	0	0	0	4	2	0.58	4	2	1.59	2	1	0.7
Microtus arvalis	10	5	11.6	95	53	15.5	18	10	7.94	3	2	1.4
Microtus agrestis	9	7	16.3	53	30	8.77	11	6	4.76	19	15	11
M. arvalis-agrestis	0	0	0	28	17	4.97	2	2	1.59	0	0	0
Pliomys lenki	0	0	0	3	1	0.29	1	1	0.79	0	0	0
Chionomys nivalis	0	0	0	14	8	2.34	1	1	0.79	0	0	0
Iberomys cabrerae	0	0	0	0	0	0	3	2	1.59	0	0	0
Terricola duodecimcostatus	0	0	0	14	9	2.63	21	15	11.9	39	20	14
Terricola gerbei	0	0	0	0	0	0	1	1	0.79	0	0	0
Apodemus sylvaticus	5	2	4.65	51	17	4.97	43	17	13.5	116	58	41
Eliomys quercinus	1	1	2.33	15	7	2.05	8	4	3.17	15	7	4.9
Glis glis	0	0	0	0	0	0	0	0	0	14	7	4.9
Erinaceus europaeus	0	0	0	1	1	0.29	0	0	0	0	0	0
Talpa europaea	0	0	0	6	2	0.58	3	1	0.79	10	2	1.4
Crocidra russula	0	0	0	9	7	2.05	2	1	0.79	4	2	1.4
Neomys fodiens	0	0	0	1	1	0.29	0	0	0	0	0	0
Sorex minutus	0	0	0	2	2	0.58	0	0	0	0	0	0
Sorex coronatus	0	0	0	4	2	0.58	1	1	0.79	1	1	0.7
Rhinolophus ferrumequinum	0	0	0	2	1	0.29	0	0	0	1	1	0.7
R. euryale-mehelyi	0	0	0	2	2	0.58	0	0	0	0	0	0
Myotis myotis-blythii	3	3	6.98	140	47	13.7	27	10	7.94	29	14	9.9
Pipistrellus sp.	0	0	0	4	2	0.58	0	0	0	0	0	0
Miniopterus schreibersii	0	0	0	17	5	1.46	2	1	0.79	1	1	0.7
Quiroptera indet.	0	0	0	2	1	0.29	1	1	0.79	1	1	0.7
Total	151	43	100	739	342	100	228	126	100	283	142	100

Data published by López-García et al. (2012b). NISP, number of identified specimens; MNI, minimum number of individuals (MNI) and the percentage of the MNI (%).

2.4.C Mutual Ecogeographic Range

MAT	n	Max	Min	Mean	SD	CI (95%)	Standard Error
IIa	132	12	4	**9**	1.9	0.33	0.17
IIb	5	10	7	**8.8**	1.3	1.14	0.58
IIIa	2	8	6	**7**	1.4	1.96	1.00
IIIb	5	10.5	8	**9.4**	1.1	0.95	0.48

MAP	n	Max	Min	Mean	SD	CI (95%)	Standard Error
IIa	132	2500	500	**981**	539	92	47
IIb	5	1200	850	**950**	154	135	69
IIIa	2	1000	850	**925**	106	147	75
IIIb	5	1200	600	**840**	227	199	102

The mutual ecogeographic range method, determines the present-day geographical region in which a given fossil species assemblage would be located through the intersection obtained from the overlap of the current distributions of each species (Blain et al., 2009, 2016; López-García, 2011). The climatic conditions of the intersecting area are used to infer the MAT. The MER estimations of Xaragalls cave layers were published by López-García et al. (2012b). CI, Confidence Interval.

2.4.D Bioclimatic Model

Subunit IIa	I	II	II/III	III	IV	V	VI	VII	VIII	IX
Microtus agrestis	0	0	0	0	0	0	0.5	0	0.5	0
Microtus arvalis	0	0	0	0	0	0	1	0	0	0
Apodemus sylvaticus	0	0	0	0	0.5	0	0.5	0	0	0
Eliomys quercinus	0	0	0	0	0.5	0	0.5	0	0	0
Σ Climatic Restriction Index	0	0	0	0	1	0	2.5	0	0.5	0
Bioclimatic Component	0.00	0.00	0.00	0.00	25.00	0.00	62.50	0.00	12.50	0.00

Mean annual temperature (ºC)	11.3
Mean temperature of the warmest month (ºC)	18.4
Mean temperature of the coldest month (ºC)	5.5
Mean annual precipitation (mm)	1431
Aridity time (months)	0.1
Thermal amplitude (ºC)	12.9

Subunit IIb	I	II	II/III	III	IV	V	VI	VII	VIII	IX
Arvicola sapidus	0	0	0	0	0.5	0	0.5	0	0	0
Microtus agrestis	0	0	0	0	0	0	0.5	0	0.5	0
Microtus arvalis	0	0	0	0	0	0	1	0	0	0
Chionomys nivalis	0	0	0	0	0.25	0	0.25	0	0.25	0.25
M. (T.) duodecimcostatus	0	0	0	0	1	0	0	0	0	0
Apodemus sylvaticus	0	0	0	0	0.5	0	0.5	0	0	0
Eliomys quercinus	0	0	0	0	0.5	0	0.5	0	0	0
Pliomys coronensis	0	0	0	0.2	0.2	0	0.2	0.2	0.2	0
Σ Climatic Restriction Index	0	0	0	0.2	2.95	0	3.45	0.2	0.95	0.25
Bioclimatic Component	0.00	0.00	0.00	2.50	36.88	0.00	43.13	2.50	11.88	3.13

Mean annual temperature (ºC)	11.5
Mean temperature of the warmest month (ºC)	20.1
Mean temperature of the coldest month (ºC)	3.9
Mean annual precipitation (mm)	927
Aridity time (months)	2.5
Thermal amplitude (ºC)	16.2

Subunit IIIa	I	II	II/III	III	IV	V	VI	VII	VIII	IX
Arvicola sapidus	0	0	0	0	0.5	0	0.5	0	0	0
Microtus agrestis	0	0	0	0	0	0	0.5	0	0.5	0
Microtus arvalis	0	0	0	0	0	0	1	0	0	0
Iberomys cabrerae	0	0	0	0	1	0	0	0	0	0
Chionomys nivalis	0	0	0	0	0.25	0	0.25	0	0.25	0.25
M. (T.) duodecimcostatus	0	0	0	0	1	0	0	0	0	0
Apodemus sylvaticus	0	0	0	0	0.5	0	0.5	0	0	0
Eliomys quercinus	0	0	0	0	0.5	0	0.5	0	0	0
Pliomys coronensis	0	0	0	0.2	0.2	0	0.2	0.2	0.2	0
Σ Climatic Restriction Index	0	0	0	0.2	3.95	0	3.45	0.2	0.95	0.25
Bioclimatic Component	0.00	0.00	0.00	2.22	43.89	0.00	38.33	2.22	10.56	2.78

Mean annual temperature (ºC)	12.4
Mean temperature of the warmest month (ºC)	21.1
Mean temperature of the coldest month (ºC)	4.6
Mean annual precipitation (mm)	793
Aridity time (months)	3.4
Thermal amplitude (ºC)	16.5

Subunit IIIb	I	II	II/III	III	IV	V	VI	VII	VIII	IX
Arvicola sapidus	0	0	0	0	0.5	0	0.5	0	0	0
Microtus agrestis	0	0	0	0	0	0	0.5	0	0.5	0
Microtus arvalis	0	0	0	0	0	0	1	0	0	0
M. (T.) duodecimcostatus	0	0	0	0	1	0	0	0	0	0
Apodemus sylvaticus	0	0	0	0	0.5	0	0.5	0	0	0
Eliomys quercinus	0	0	0	0	0.5	0	0.5	0	0	0
Glis glis	0	0	0	0	0	0	1	0	0	0
Σ Climatic Restriction Index	0	0	0	0	2.5	0	4	0	0.5	0
Bioclimatic Component	0.00	0.00	0.00	0.00	35.71	0.00	57.14	0.00	7.14	0.00

Mean annual temperature (ºC)	13.4
Mean temperature of the warmest month (ºC)	20.0
Mean temperature of the coldest month (ºC)	8.2
Mean annual precipitation (mm)	1286
Aridity time (months)	1.4
Thermal amplitude (ºC)	11.8

The bioclimatic model is based on the adscription of small-mammal species to ten different climatic zones. This allows the calculation first of the Climatic Restriction Index (CRIi=1/n, where i is the climatic zone inhabited by the species and n is the number of climatic zones the species inhabit) and then the Bioclimatic Component (BCi=(ΣCRIi)100/S, where S is the number of species). From the BC it is possible to calculate several climatic parameters by means of multiple linear regression developed specifically for the order Rodentia (Hernández Fernández, 2001; Hernández Fernández et al., 2007).

Appendix 2.5

Here is included supplementary material of "Chapter 8. Latest Pleistocene in northeastern Iberia: oxygen isotope analysis and paleoenvironment inferences from rodent remains of Arbreda cave (Serinyà, Girona)".

2.5.A Small mammals identified in Arbreda cave

	Levels									
	Level I	Level H	Level G	Level F	Level E	Level D	Level C	Level B	Level A	Terra Rossa
Erinaceus europaeus	0.00	0.31	1.05	0.35	0.40	0.46	0.17	0.00	0.26	0.00
Talpa europaea	1.37	0.00	0.21	0.00	0.00	0.00	0.00	0.00	0.00	0.00
Sorex minutus	0.00	0.63	0.21	0.71	0.79	0.00	0.99	1.28	0.26	0.00
Sorex gr. *coronatus-araneus*	0.00	0.63	0.42	0.00	1.59	0.46	0.99	0.64	0.51	0.00
Neomys gr. *fodiens-anomalus*	0.00	0.63	0.00	0.00	0.00	0.00	0.00	0.00	0.00	0.00
Crocidura russula	0.00	0.00	0.84	0.00	0.40	0.00	0.17	0.00	3.08	3.35
Arvicola sapidus	6.16	3.13	0.84	1.42	2.78	5.48	2.15	2.56	2.06	0.84
Arvicola amphibius	0.00	0.00	0.00	0.00	0.00	0.00	0.17	0.32	0.00	0.21
Microtus arvalis	21.23	23.75	17.99	24.82	38.49	28.08	31.95	26.92	17.87	7.95
Microtus agrestis	20.55	43.13	54.60	53.19	44.84	50.68	53.64	50.64	41.26	12.55
Microtus arvalis-agrestis	2.05	6.25	2.72	3.55	1.98	3.65	3.64	5.45	1.54	0.42
Microtus oeconomus	0.00	0.31	0.21	0.00	0.40	0.00	0.33	0.32	0.00	0.00
Microtus gregalis	0.00	0.00	0.00	0.00	0.00	0.23	0.00	0.00	0.00	0.00
Chionomys nivalis	5.48	4.69	1.46	0.35	0.00	0.46	0.33	0.00	0.26	0.00
Iberomys cabrerae	0.00	0.00	0.42	0.35	0.00	0.46	0.00	0.32	0.51	2.93
Microtus (Terricola) duodecimcostatus	8.22	7.19	5.23	1.06	0.79	0.68	0.33	0.64	15.30	44.35
Microtus (Terricola) gerbei	0.68	0.00	0.00	0.00	0.00	0.00	0.00	0.00	0.00	0.00
Apodemus sylvaticus	19.18	4.38	7.95	7.45	3.97	3.42	1.16	6.73	11.95	20.50
Eliomys quercinus	15.07	5.00	5.86	6.03	3.57	5.25	3.64	3.85	5.01	5.86
Glis glis	0.00	0.00	0.00	0.35	0.00	0.00	0.00	0.00	0.00	0.84
Spermophilus cf. *citellus*	0.00	0.00	0.00	0.00	0.00	0.00	0.33	0.32	0.00	0.00
Total	**100**	**100**	**100**	**100**	**100**	**100**	**100**	**100**	**100**	**100**
NISP	**146**	**317**	**480**	**280**	**252**	**434**	**603**	**311**	**777**	**477**
MNI	**73**	**160**	**239**	**141**	**126**	**219**	**302**	**156**	**389**	**239**

Data published by López-García et al. (2015). Percentage of minimum number of individuals (%) of small vertebrates of Arbreda cave.

2.5.B Mutual Ecogeographic Range

	MAT					MTC				MTW				MAP			
	n	Mean	Max	Min	SD	Mean	Max	Min	SD	Mean	Max	Min	SD	Mean	Max	Min	SD
Terra Rossa	15	**9.6**	11	7	1.3	**2.3**	3	1	0.9	**17.8**	19	15	1.1	**926.7**	1500	700	256
Level A	5	**8.4**	10	6	1.5	**1.6**	3	0	1.1	**18.8**	21	17	1.6	**950**	1200	850	154
Level B	15	**9.6**	11	7	1.3	**2.3**	3	1	0.9	**17.8**	19	15	1.1	**926.7**	1500	700	256
Level C	1	**9**	–	–	–	**1**	–	–	–	**17**	–	–	–	**850**	–	–	–
Level D	5	**8.4**	10	6	1.5	**1.6**	3	0	1.1	**18.8**	21	17	1.6	**950**	1200	850	154
Level E	102	**10.09**	12	5	1.42	**2.49**	5	0	1.1	**18.97**	22	16	1.3	**714**	1500	350	200
Level F	1	**10**	–	–	–	**1**	–	–	–	**17**	–	–	–	**1200**	–	–	–
Level G	3	**8.7**	10	7	1.5	**0.7**	1	0	0.6	**16.7**	17	16	0.6	**966.7**	1200	850	202
Level H	5	**8.4**	10	6	1.5	**1.6**	3	0	1.1	**18.8**	21	17	1.6	**950**	1200	850	154
Level I	2	**6**	6	6	0	**0**	0	0	0	**17**	17	17	0	**1500**	1500	1500	0

The mutual ecogeographic range method, determines the present-day geographical region in which a given fossil species assemblage would be located through the intersection obtained from the overlap of the current distributions of each species (Blain et al., 2009, 2016; López-García, 2011). The climatic conditions of the intersecting area are used to infer the MAT. The MER estimations of Arbreda cave layers were published by López-García et al. (2015).

2.5.C Bioclimatic Model

Level Rossa	I	II	II/III	III	IV	V	VI	VII	VIII	IX
Arvicola sapidus	0	0	0	0	0.5	0	0.5	0	0	0
Arvicola terrestris	0	0	0	0	0.25	0	0.25	0.25	0.25	0
Microtus agrestis	0	0	0	0	0	0	0.5	0	0.5	0
Microtus arvalis	0	0	0	0	0	0	1	0	0	0
Iberomys cabrerae	0	0	0	0	1	0	0	0	0	0
M. (T.) duodecimcostatus	0	0	0	0	1	0	0	0	0	0
Apodemus sylvaticus	0	0	0	0	0.5	0	0.5	0	0	0
Eliomys quercinus	0	0	0	0	0.5	0	0.5	0	0	0
Glis glis	0	0	0	0	0	0	1	0	0	0
Σ Climatic Restriction Index	0	0	0	0	3.75	0	4.25	0.25	0.75	0
Bioclimatic Component	0.00	0.00	0.00	0.00	41.67	0.00	47.22	2.78	8.33	0.00

Mean annual temperature (ºC)	13.3
Mean temperature of the warmest month (ºC)	21.1
Mean temperature of the coldest month (ºC)	6.5
Mean annual precipitation (mm)	1023
Aridity time (months)	2.4
Thermal amplitude (ºC)	14.5

Level A	I	II	II/III	III	IV	V	VI	VII	VIII	IX
Arvicola sapidus	0	0	0	0	0.5	0	0.5	0	0	0
Microtus agrestis	0	0	0	0	0	0	0.5	0	0.5	0
Microtus arvalis	0	0	0	0	0	0	1	0	0	0
Iberomys cabrerae	0	0	0	0	1	0	0	0	0	0
Chionomys nivalis	0	0	0	0	0.25	0	0.25	0	0.25	0.25
M. (T.) duodecimcostatus	0	0	0	0	1	0	0	0	0	0
Apodemus sylvaticus	0	0	0	0	0.5	0	0.5	0	0	0
Eliomys quercinus	0	0	0	0	0.5	0	0.5	0	0	0
Σ Climatic Restriction Index	0	0	0	0	3.75	0	3.25	0	0.75	0.25
Bioclimatic Component	0.00	0.00	0.00	0.00	46.88	0.00	40.63	0.00	9.38	3.13

Mean annual temperature (ºC)	12.7
Mean temperature of the warmest month (ºC)	21.1
Mean temperature of the coldest month (ºC)	5.5
Mean annual precipitation (mm)	850
Aridity time (months)	3.1
Thermal amplitude (ºC)	15.5

Level B	I	II	II/III	III	IV	V	VI	VII	VIII	IX
Arvicola sapidus	0	0	0	0	0.5	0	0.5	0	0	0
Arvicola terrestris	0	0	0	0	0.25	0	0.25	0.25	0.25	0
Microtus agrestis	0	0	0	0	0	0	0.5	0	0.5	0
Microtus arvalis	0	0	0	0	0	0	1	0	0	0
Iberomys cabrerae	0	0	0	0	1	0	0	0	0	0
M. (T.) duodecimcostatus	0	0	0	0	1	0	0	0	0	0
Microtus oeconomus	0	0	0	0	0	0	0.333	0	0.333	0.333
Apodemus sylvaticus	0	0	0	0	0.5	0	0.5	0	0	0
Eliomys quercinus	0	0	0	0	0.5	0	0.5	0	0	0
Spermophilus citellus	0	0	0	0	0.333	0	0.333	0.333	0	0
Σ Climatic Restriction Index	0	0	0	0	4.083	0	3.916	0.583	1.083	0.333
Bioclimatic Component	0.00	0.00	0.00	0.00	40.83	0.00	39.16	5.83	10.83	3.33

Mean annual temperature (ºC)	11.5
Mean temperature of the warmest month (ºC)	20.6
Mean temperature of the coldest month (ºC)	3.2
Mean annual precipitation (mm)	836
Aridity time (months)	-0.7
Thermal amplitude (ºC)	0.5

Level C	I	II	II/III	III	IV	V	VI	VII	VIII	IX
Arvicola sapidus	0	0	0	0	0.5	0	0.5	0	0	0
Arvicola terrestris	0	0	0	0	0.25	0	0.25	0.25	0.25	0
Microtus agrestis	0	0	0	0	0	0	0.5	0	0.5	0
Microtus arvalis	0	0	0	0	0	0	1	0	0	0
Chionomys nivalis	0	0	0	0	0.25	0	0.25	0	0.25	0.25
M. (T.) duodecimcostatus	0	0	0	0	1	0	0	0	0	0
Microtus oeconomus	0	0	0	0	0	0	0.333	0	0.333	0.333
Apodemus sylvaticus	0	0	0	0	0.5	0	0.5	0	0	0
Eliomys quercinus	0	0	0	0	0.5	0	0.5	0	0	0
Spermophilus citellus	0	0	0	0	0.333	0	0.333	0.333	0	0
Σ Climatic Restriction Index	0	0	0	0	3.333	0	4.166	0.583	1.333	0.583
Bioclimatic Component	0.00	0.00	0.00	0.00	33.33	0.00	41.66	5.83	13.33	5.83

Mean annual temperature (ºC)	9.7
Mean temperature of the warmest month (ºC)	19.0
Mean temperature of the coldest month (ºC)	1.2
Mean annual precipitation (mm)	920
Aridity time (months)	1.9
Thermal amplitude (ºC)	17.8

Level D	I	II	II/III	III	IV	V	VI	VII	VIII	IX
Arvicola sapidus	0	0	0	0	0.5	0	0.5	0	0	0
Microtus agrestis	0	0	0	0	0	0	0.5	0	0.5	0
Microtus arvalis	0	0	0	0	0	0	1	0	0	0
Iberomys cabrerae	0	0	0	0	1	0	0	0	0	0
Chionomys nivalis	0	0	0	0	0.25	0	0.25	0	0.25	0.25
M. (T.) duodecimcostatus	0	0	0	0	1	0	0	0	0	0
Apodemus sylvaticus	0	0	0	0	0.5	0	0.5	0	0	0
Eliomys quercinus	0	0	0	0	0.5	0	0.5	0	0	0
Microtus gregalis	0	0	0	0	0	0	0	0.333	0.333	0.333
Σ Climatic Restriction Index	0	0	0	0	3.75	0	3.25	0.333	1.083	0.583
Bioclimatic Component	0.00	0.00	0.00	0.00	41.67	0.00	36.11	3.70	12.03	6.48

Mean annual temperature (ºC)	10.6
Mean temperature of the warmest month (ºC)	20.0
Mean temperature of the coldest month (ºC)	2.1
Mean annual precipitation (mm)	763
Aridity time (months)	2.9
Thermal amplitude (ºC)	17.9

Level E	I	II	II/III	III	IV	V	VI	VII	VIII	IX
Arvicola sapidus	0	0	0	0	0.5	0	0.5	0	0	0
Microtus agrestis	0	0	0	0	0	0	0.5	0	0.5	0
Microtus arvalis	0	0	0	0	0	0	1	0	0	0
M. (T.) duodecimcostatus	0	0	0	0	1	0	0	0	0	0
Apodemus sylvaticus	0	0	0	0	0.5	0	0.5	0	0	0
Eliomys quercinus	0	0	0	0	0.5	0	0.5	0	0	0
Microtus oeconomus	0	0	0	0	0	0	0.333	0	0.333	0.333
Σ Climatic Restriction Index	0	0	0	0	2.5	0	3.333	0	0.833	0.333
Bioclimatic Component	0.00	0.00	0.00	0.00	35.71	0.00	47.61	0.00	11.90	4.76

Mean annual temperature (ºC)	11.0
Mean temperature of the warmest month (ºC)	19.1
Mean temperature of the coldest month (ºC)	3.9
Mean annual precipitation (mm)	1053
Aridity time (months)	1.7
Thermal amplitude (ºC)	15.2

Level F	I	II	II/III	III	IV	V	VI	VII	VIII	IX
Arvicola sapidus	0	0	0	0	0.5	0	0.5	0	0	0
Microtus agrestis	0	0	0	0	0	0	0.5	0	0.5	0
Microtus arvalis	0	0	0	0	0	0	1	0	0	0
Iberomys cabrerae	0	0	0	0	1	0	0	0	0	0
Chionomys nivalis	0	0	0	0	0.25	0	0.25	0	0.25	0.25
M. (T.) duodecimcostatus	0	0	0	0	1	0	0	0	0	0
Apodemus sylvaticus	0	0	0	0	0.5	0	0.5	0	0	0
Eliomys quercinus	0	0	0	0	0.5	0	0.5	0	0	0
Glis glis	0	0	0	0	0	0	1	0	0	0
Σ Climatic Restriction Index	0	0	0	0	3.75	0	4.25	0	0.75	0.25
Bioclimatic Component	0.00	0.00	0.00	0.00	41.67	0.00	47.22	0.00	8.33	2.78

Mean annual temperature (ºC)	12.8
Mean temperature of the warmest month (ºC)	20.4
Mean temperature of the coldest month (ºC)	6.4
Mean annual precipitation (mm)	1030
Aridity time (months)	2.3
Thermal amplitude (ºC)	13.9

Level G	I	II	II/III	III	IV	V	VI	VII	VIII	IX
Arvicola sapidus	0	0	0	0	0.5	0	0.5	0	0	0
Microtus agrestis	0	0	0	0	0	0	0.5	0	0.5	0
Microtus arvalis	0	0	0	0	0	0	1	0	0	0
Iberomys cabrerae	0	0	0	0	1	0	0	0	0	0
Chionomys nivalis	0	0	0	0	0.25	0	0.25	0	0.25	0.25
M. (T.) duodecimcostatus	0	0	0	0	1	0	0	0	0	0
Apodemus sylvaticus	0	0	0	0	0.5	0	0.5	0	0	0
Eliomys quercinus	0	0	0	0	0.5	0	0.5	0	0	0
Microtus oeconomus	0	0	0	0	0	0	0.333	0	0.333	0.333
Σ Climatic Restriction Index	0	0	0	0	3.75	0	3.583	0	1.083	0.583
Bioclimatic Component	0.00	0.00	0.00	0.00	41.67	0.00	39.81	0.00	12.03	6.48

Mean annual temperature (ºC)	10.9
Mean temperature of the warmest month (ºC)	19.7
Mean temperature of the coldest month (ºC)	3.1
Mean annual precipitation (mm)	849.1
Aridity time (months)	2.6
Thermal amplitude (ºC)	16.6

Level H	I	II	II/III	III	IV	V	VI	VII	VIII	IX
Arvicola sapidus	0	0	0	0	0.5	0	0.5	0	0	0
Microtus agrestis	0	0	0	0	0	0	0.5	0	0.5	0
Microtus arvalis	0	0	0	0	0	0	1	0	0	0
Chionomys nivalis	0	0	0	0	0.25	0	0.25	0	0.25	0.25
M. (T.) duodecimcostatus	0	0	0	0	1	0	0	0	0	0
Apodemus sylvaticus	0	0	0	0	0.5	0	0.5	0	0	0
Eliomys quercinus	0	0	0	0	0.5	0	0.5	0	0	0
Microtus oeconomus	0	0	0	0	0	0	0.333	0	0.333	0.333
Σ Climatic Restriction Index	0	0	0	0	2.75	0	3.583	0	1.083	0.583
Bioclimatic Component	0.00	0.00	0.00	0.00	34.38	0.00	44.79	0.00	13.54	7.29

Mean annual temperature (ºC)	9.8
Mean temperature of the warmest month (ºC)	18.5
Mean temperature of the coldest month (ºC)	2.2
Mean annual precipitation (mm)	991
Aridity time (months)	1.7
Thermal amplitude (ºC)	16.2

Level I	I	II	II/III	III	IV	V	VI	VII	VIII	IX
Arvicola sapidus	0	0	0	0	0.5	0	0.5	0	0	0
Microtus agrestis	0	0	0	0	0	0	0.5	0	0.5	0
Microtus arvalis	0	0	0	0	0	0	1	0	0	0
Chionomys nivalis	0	0	0	0	0.25	0	0.25	0	0.25	0.25
M. T. duodecimcostatus	0	0	0	0	1	0	0	0	0	0
Apodemus sylvaticus	0	0	0	0	0.5	0	0.5	0	0	0
Eliomys quercinus	0	0	0	0	0.5	0	0.5	0	0	0
Σ Climatic Restriction Index	0	0	0	0	2.75	0	3.25	0	0.75	0.25
Bioclimatic Component	0.00	0.00	0.00	0.00	39.29	0.00	46.43	0.00	10.71	3.57

Mean annual temperature (ºC)	11.8
Mean temperature of the warmest month (ºC)	19.9
Mean temperature of the coldest month (ºC)	4.8
Mean annual precipitation (mm)	1012
Aridity time (months)	2.1
Thermal amplitude (ºC)	15.0

References

Agustí , B., Alcalde, G., Güell, A., Juan-Muns, N., Rueda, J.M., Terradas, X., 1991. La cova 120, parada de caçadors-recol·lectors del paleolític mitjà. Cypsela IX, 7-20.

Alcalde, G., 1986. Les faunes de rongeurs du Pléistocène supérieur et de l'Holocène de Catalogne (Espagne) et leurs significations paléoécologiques et paléoclimatiques. PhD. École pratique des Hautes études-Sciences de la Vie et de la Terre IIIème section, Paris, 114p

Alcalde, G., Brunet-Lecomte, P., 1985. Contribució al coneixement del medi i el clima durant el Plesitocè superior i l'Holocè a Catalunya, amb l'aplicació de l'ànalisis factorial de correspondencies a les associacions de rosegadors. Paleontologia i Evolució 19, 49-55.

Alcalde, G., Galobart, A., 2002. Els petits mamífers del Plistocè superior. In: Maroto, J., Ramió, S., Galobart, A. (Eds.), Els vertebrats fossils del Pla de l'Estany. Quaderns. Centre d'Estudis Comarcals de Banyoles 23, 141-154.

Bischoff, J., Ludwig, L., García, J., Carbonell, E., Vaquero, M., Stafford, T.W., Jull, A., 1994. Dating of the basal Aurignacians and wich at Abric Romaní (Catalonia, Spain) by radiocarbon and Uranium-series. Journal of Archaeological Science 21, 541-551.

Blain, H.-A., Bailon, S., Cuenca-Bescós, G., Arsuaga, J.L., Bermúdez de Castro, J.M., Carbonell, E., 2009. Long-term climate record inferred from early-middle Pleistocene amphibian and squamate reptile assemblages at the Gran Dolina Cave, Atapuerca, Spain. J. Hum. Evol. 56, 55–65.

Blain, H.A., Lozano-Fernández, I., Agustí, J., Bailon, S., Menéndez Granda, L., Espígares Ortiz, M.P., Ros-Montoya, S., Jiménez Arenas, J.M., Toro-Moyano, I., Martínez-Navarro, B., Sala, R., 2016. Refining upon the climatic background of the Early Pleistocene hominid settlement in western Europe: Barranco León and Fuente Nueva-3 (Guadix-Baza Basin, SE Spain). Quat. Sci. Rev. 144, 132–144.

Bowen, G.J., 2017. The Online Isotopes in Precipitation Calculator, Version 3.1 (4/2017): http://waterisotopes.org.

Burjachs, F., López-García, J.M., Allué, E., Blain, H.-A., Rivals, F., Bennàsar, M., Expósito, I., 2012. Palaeoecology of Neanderthals during Dansgaard-Oeschger cycles in northeastern Iberia (Abric Romaní): From regional to global scale. Quaternary International 247, 26-37.

Daura, J., Sanz, M., Subirà, M.E., Quam, R., Fullola, J., Arsuaga, J.L., 2005. A Neandertal mandible form the Cova del Gegant (Sitges, Barcelona, Spain). Journal of Human Evolution 49, 56-70.

Daura, J., Sanz, M., Pike, A.W.G., Subirà, M.E., Fornós, J., Fullola, J.M., Julià, R., Zilhao, J., 2010. Stratigraphic context and direct dating of the Neandertal mandible from Cova del Gegant (Sitges, Barcelona). Journal of Human Evolution 59, 109-122.

Fernández-García, M., 2014. Análisis paleoecológico en relación a las ocupaciones humanas del Nivel O del Abric Romaní (Capellades, Barcelona) mediante el estudio de los micromamífero y sus mecanismos de acumulación. Master thesis. Tarragona, 179p. Inedit.

Fernández-García, M., López-García, J.M., 2013. Palaeoecology and biochronology based on the rodents analysis from the Late Pleistocene/Holocene of Toll Cave (Moià, Barcelona). Spanish Journal of Palaeontology 28 (2), 227-238.

Hernández Fernández, M., 2001. Bioclimatic discriminant capacity of terrestrial mammal faunas. Glob. Ecol. Biogeogr. 10, 189–204.

Hernández Fernández, M., Álvarez Sierra, M.Á., Peláez-Campomanes, P., 2007. Bioclimatic analysis of rodent palaeofaunas reveals severe climatic changes in Southwestern Europe during the Plio-Pleistocene. Palaeogeogr. Palaeoclimatol. Palaeoecol. 251, 500–526.

IAEA/WMO, 2018. Global Network of Isotopes in Precipitation. The GNIP Database. Accessible at WISER (Water Isotope System for Data Analysis, Visualization and Electronic Retrieval): https://nucleus.iaea.org/wiser.

López-García, J.M., 2011. Los micromamíferos del Pleistoceno superior de la Península Ibérica. Evolución de la diversidad taxonómica y cambios paleoambientales y paleoclimáticos. Editorial Académica Española, Saarbrücken, 368p.

López-García, J,M., Blain, H.A., Cuenca-Bescós, G., Arsuaga, J.L., 2008. Chronological, environmental, and climatic precisions on Neanderthal site of the Cova del Gegant (Sitges, Barcelona, Spain). Journal of Human Evolution 55, 1151-1155.

López-García, J.M., Blain, H.A., Allúe, E., Bañuls, S., Bargalló, A., Martín, P., Morales, J.I., Pedro, M., Rodríguez, A., Solé, A., Oms, F.X., 2010. First fossil evidence of an "interglacial refugium" in the Pyrenean región. Naturwissensehaften 97, 753-761.

López-García, J.M., Blain, H.-A., Bennàsar, M., Euba, I., Bañuls, S., Bischoff, J., López-Ortega, E., Saladié, P., Uzquiano, P., Vallverdú, P., 2012a. A multiproxy reconstruction of the palaeoenvironment and paleoclimate of the Late Pleistocene in northeastern Iberia: Cova dels Xaragalls, Vimbodí-Poblet, Paratge Natural de Poblet, Catalonia. Boreas 41, 235-249.

López-García, J.M., Blain, H.-A., Burjachs, F., Ballesteros, A., Allue, E., Cuevas-Ruiz, G. E., Rivals, F., Blasco, R., Morales, J.I., Hidalgo, A. R., Carbonell, E., Serrat, E., Rosell, J., 2012b. A multidisciplinary approach to reconstructing the southwestern European Neanderthals: the contribution of Teixoneres cave (Moià, Barcelona). Quaternary Science Reviews 43, 33-44.

López-García, J.M., Blain, H.-A., Sanz, M., Daura, J., 2012c. A coastal reservoir of terrestrial resources for Neanderthal populations in north-eastern Iberia: palaeoenvironmental data inferred from the small-vertebrate assemblage of Cova del Gegant, Sitges, Barcelona. Journal of Quaternary Science 27 (1), 105-113.

López-García, J., Blain, H.A., Bennàsar, M., Alcover, J.A., Bañuls-Cardona, S., Fernández-García, M., Fontanals, M., Martín, P., Morales, J.I., Muñoz, L., Pedro, M., Vergés, J.M., 2014a. Climate and landscape during Heinrich Event 3 in south-western Europe: the small-vertebrate association from Galls Carboners cave (Mont-ral, Tarragona, north-eastern Iberia). Journal of Quaternary Science 29 (2), 130-140.

López-García, J., Blain, H.A., Bennàsar, M., Fernández-García, M., 2014b. Environmental and climatic context of Neanderthal occupation in southwestern Europe during MIS3 inferred from the small-vertebrate assemblages. Quaternary International 326-327, 319-328.

Manzanares, A. (2012) Aves rapaces de la Península Ibérica, Baleares y Canarias. Barcelona: Ediciones Omega, pp. 262.

Maroto, J., Vaquero, M., Arrizabalaga, A., Baena, J., Baquedano, E., Jordá, J., Julià, R., Montes, R., Van Der Plicht, J., Rasines, P., Wood, R., 2012. Current issues in late Middle Palaeolithic chronology: New assessments from Northern Iberia. Quaternary International 247, 15-25

Martín, A., Guilaine, J., Thommeret, J., Thommeret, Y., 1981. Estratigrafía y dataciones C14 del yacimiento de la "Cova del Frare" de St. Llorenç del Munt (Matadepera, Barcelona). Zephyrus XXXII-XXXIII, 101-111.

Morales Hidalgo, J.I., Fontanals Torroja, M., Oms Arias, X., Vergès Bosch, J.M., 2010. La chronologie du Néolithique ancien cardial du nord-est de la península Ibérique. Datations, problématique et méthodologie. L'anthropologie 114, 427-444.

Morales, J.I., Rodríguez-Hidalgo, A., Cebrià, A., Oms, F.X., Allué, E., Fernández-García, M., López-García, J.M., Soto, M., García-Barbo, A.B., 2014. Intervencions sistemàtiques als dipòsits holocens i pleistocens de la Cova del Toll (Moià, Bages) entre els anys 2006 i 2011. In: II Jornades d'Arqueologia de la Catalunya Central. Museu Episcopal de Vic, pp. 68-73.

Oms, X., Bargalló, A., Chaler, M., Fontanals, M., García, M.S., López-García, J.M., Morales, J.M., Nievas, T., Rodríguez, A., Serra, J., Solé, A., Vergès, J.M. 2008. La Cova Colomera (Sant Esteve de la Sarga, Lleida), una cueva-redil en el Prepirineo de Lérida. Primeros resultados y perspectivas de futuro. In: Hernández-Pérez, M.S., Soler-Díez, J.A., Padilla, J.A. (Eds.) Actas IV Congreso Neolítico Peninsular. Museo Arqueológico de Alicante, pp. 230-236.

Rosell, J., Blasco, R., Rivals, F., Chacón, M.G., Menéndez, L., Morales, J.I.,Rodríguez, A., Cebrià, A., Carbonell, E., Serrat, D., 2010. A stop alongthe way: the role of Neanderthal groups at Level III of Teixoneres Cave(Moià, Barcelona, Spain). Quaternaire 21 (2), 139–154.

Royer, A.; Lécuyer, C.; Montuire, S.; Amiot, R.; Legendre, S.; Cuenca-Bescós, G..; Jeannet, M.; Martineau, F., 2013, What does the oxygen isotope composition of rodent teeth record? Earth and Planetary Science Letters, 361: 258-271.

Soler, J., Soler, N., Solés, A., Niell, X., 2014. Arbreda cave from the Middle Paleolithic to the Neolithic. In: Sala, R. (Ed.) Los cazadores recolectores del Pleistoceno y del Holoceno en Iberia y el Estrecho de Gibraltar: Estado actual del conocimiento del registro arqueológico. Universidad de Burgos & Fundación Atapuerca, Burgos, pp. 221-231.

Tissoux, H., Falguères, C., Bahain, J.-J., Rosell, J., Cebria, A., Carbonell, E.,Serrat, D., 2006. Datation par les séries de l'Uranium des occupa-tions moustériennes de la grotte de Teixoneres (Moia, Province deBarcelone, Espagne). Quaternaire 17 (1), 27–33.

Vallverdú-Poch, J., Gómez, B., Vaquero, M., Bischoff, J.L., 2012. Chapter 2. The Abric Romaní site and the Capellades Region. In: Carbonell, E. (Ed.) High resolution Archaeology and Neanderthal Behaviour: Time and Space in Level J of the Abric Romaní (Capellades, Spain). Springer, New York, pp. 135-147.

Vaquero, M., Allué, E., Bischoff, J.L., Burjachs, F., Vallverdú, J., 2013. Environmental, despositional and cultural changes in the Upper Pleistocene and Early Holocene: The Cinglera del Capelló sequence (Capellades, Spain). Quaternaire 24, 49-64.

Viñas, R., Villalta, J.F., 1975. El depósito cuaternario de la "Cova del Gegant". Speleon I, 19-33.

Wood, R.E., Arrizabalaga, A., Camps, M., Fallon, S., Iriarte-Chiapusso, M.J., Jones, R., Maroto, J., De la Rasilla, M., Santamaría, D., Soler, J., Soler, N., Villaluenga, A., Higham, T.F.G., 2014. The chronology of the earliest Upper Palaeolithic in northern Iberia: New insights from L'Arbreda, Labeko Koba and La Viña. J. Hum. Evol. 69, 91–109.

Appendix 3. Manuscripts

In the following pages (349-377) are included the scientific manuscripts already published and related to Chapter 3 and 4 of this doctoral thesis, maintain with the journal editions.

C. R. Palevol 15 (2016) 707–719

Contents lists available at ScienceDirect

Comptes Rendus Palevol

www.sciencedirect.com

General Palaeontology, Systematics and Evolution (Vertebrate Palaeontology)

Palaeoecological implications of rodents as proxies for the Late Pleistocene–Holocene environmental and climatic changes in northeastern Iberia

Implications paléoécologiques des rongeurs comme indicateurs des changements environnementaux et climatiques du Pléistocène supérieur à l'Holocène dans le Nord-Est de la péninsule Ibérique

Mónica Fernández-García[a,b,*], Juan Manuel López-García[b], Carlos Lorenzo[a,b]

[a] *Àrea de Prehistòria, Universitat Rovira i Virgili (URV), Avenue Catalunya, 35, 43002 Tarragona, Spain*
[b] *Institut Català de Paleoecologia Humana i Evolució Social (IPHES), C/Marcel·lí Domingo s/n, Campus Sescelades URV (Edifici W3), 43007 Tarragona, Spain*

ARTICLE INFO

Article history:
Received 16 March 2015
Accepted after revision 20 August 2015
Available online 5 November 2015

Handled by Hugues A. Blain

Keywords:
Rodentia
MIS 2
Palaeoenvironment
Middle Palaeolithic
Upper Palaeolithic
Late Glacial Maximum

ABSTRACT

Rodents are among the most useful proxies for reconstructing the ecology and environment of the Quaternary. The present paper focuses on a series of fossil rodent assemblages from northeastern Iberia of the Late Pleistocene (ca. 128–11.7 ka BP) and the beginning of the Holocene (< 11.7 ka BP). Descriptive and multivariate statistical methods have been applied to expand what is known about the species involved and their palaeoecological implications. The results show the importance of the three predominant species: *Microtus arvalis*, *Microtus agrestis* and *Apodemus sylvaticus*. A transition in the ecological conditions is shown in the studied area during the course of this interval: from open environments and cooler climatic conditions to more forested landscapes and temperate conditions. The beginning of the Late Pleistocene and the Holocene share similarities, and both differ clearly from the end of the Late Pleistocene, showing the singular nature of the environmental conditions of Marine Isotope Stage 2 in the northeastern sector of the Iberian Peninsula.

Mots clés :
Rongeurs
SIM 2
Paléoenvironnement
Paléolithique moyen
Paléolithique supérieur
Dernier maximum glaciaire

RÉSUMÉ

Les rongeurs sont parmi les marqueurs les plus significatifs pour la reconstruction de l'écologie et de l'environnement du Quaternaire. Ce travail prend en compte une série d'assemblages de rongeurs fossiles du Pléistocène supérieur (environ 128 à 11,7 ka BP) et du début de l'Holocène (< 11,7 ka BP), provenant du Nord-Est de la péninsule Ibérique. Des méthodes statistiques descriptives et multivariées ont été appliquées, afin d'obtenir une meilleure connaissance des espèces concernées et de leurs implications paléoécologiques. Les résultats obtenus indiquent l'importance de trois espèces dominantes : *Microtus arvalis*, *Microtus agrestis* et *Apodemus sylvaticus*. Une transition des conditions écologiques est mise en évidence dans la région étudiée pendant cet intervalle : depuis des environnements

* Corresponding author. Institut Català de Paleoecologia Humana i Evolució Social, C/Marcel·lí Domingo s/n, Campus Sescelades URV (Edifici W3), 43007 Tarragona, Spain.
E-mail address: monica.fernandez.garcia.90@gmail.com (M. Fernández-García).

http://dx.doi.org/10.1016/j.crpv.2015.08.005
1631-0683/

ouverts avec un climat plutôt frais vers des paysages plus boisés traduisant un climat tempéré. Les ressemblances mises en évidence parmi les sites datant du début du Pléistocène supérieur et de l'Holocène se démarquent nettement de ceux de la fin du Pléistocène supérieur, soulignant la singularité des conditions environnementales pendant le stade isotopique marin 2 dans le Nord-Est de la péninsule Ibérique.

1. Introduction

The Late Pleistocene (128–11.7 ka BP) is an interval characterized by high climate instability, which alternates cold and warm phases and isolated climatic episodes (such as Heinrich Events or Dansgaard-Oeschger events) (Sánchez-Goñi and D'Errico, 2005). Theses fluctuations are likely to have had impacts on flora, fauna and human societies. The transition from the Latest Pleistocene to the Holocene, characterized by a sharp increase in temperatures occurring around 11,700 years ago, also constituted an environmental break with major consequences (Bradley and England, 2008).

Different proxies (such as Greenland ice cores, marine pollen cores or continental records) have increased what is known of the Quaternary environment. In the continental domain, the temporal discontinuity of sedimentary records limits the reconstruction of reliable climatic parameters. Many proxies have been developed in order to quantify climatic parameters, on the basis either of palaeobiological approaches or geochemical methods. Over the last two decades, multidisciplinary approaches have been developed in order to improve the reconstruction of continental climate models and understand the responses of living organisms to climatic changes (Sánchez-Goñi and D'Errico, 2005; Sánchez-Goñi et al., 2008). For the Iberian Peninsula, climatic particularities have been discussed that differed from the dynamics of the rest of Europe on account of geographical situation and as a consequence of the condition of southern Europe as particularities that can also be found in the Italian Peninsula and the Balkans (Fletcher et al., 2010; Harrison and Sánchez-Goñi, 2010).

Rodents are one of the most noteworthy groups of mammals in the European Quaternary, and they have become one of the most useful tools for reconstructing the ecology and environment of the Quaternary. Species from this order tend to undergo an accelerated evolution and are generally characterized by short life spans (Van Dam et al., 2006), a close relationship with their environment and strict ecological requirements. These factors make them extremely good markers for studies that focus on evolution, biochronology and particularly for inferring a record of their local living environments. Moreover, their widely ranging geographical distribution and the high presence of their remains in Quaternary sedimentary deposits makes it possible to apply multiple statistical approaches and quantitative methods (Alcalde and Galobart, 2002; Chaline, 1988; López-García, 2011). In the present study, the statistical analysis of rodent assemblages from Late Pleistocene (128–11.7 ka BP) and Holocene (< 11.7 ka BP) sites from the northeastern Iberian Peninsula increases what is known of the species in question during this time frame, taking into account the specific palaeoecological implications of the assemblages with the aim of understanding the environmental evolution of this region. On the basis of this methodology, our aim is to ascertain the differences and similarities between these sites/levels depending on the occurrence of species and also establish which species assemblages are the most common and which are the dominant ones.

2. Materials and methods

2.1. Data matrix

The data matrix employed corresponds to specimens recovered from 37 levels from 12 archaeological sites from the Northeast of the Iberian Peninsula, chronologically located in the Late Pleistocene and the beginning of the Holocene. For each species, the minimum number of individuals (MNI) has been taken into account. Only levels with an NMI greater than or equal to 15 have been included in these analyses. This NMI limit has been decided as the optimal point to remove the assemblages with low individuals but not loss to many levels from this region (Fig. 1; Table 1) (Appendix A1).

Corrections have been applied to the data matrix in order to simplify the interpretation and reduce the dispersion of the results. Firstly, the specimens of *Microtus arvalis* and *Microtus agrestis* are integrated into a single group because it is common, especially in older publications, not to differentiate between these two species (identified as *Microtus arvalis-agrestis*). In order not to overlook the importance of the presence of these two species, the adopted solution is to put these categories into a single group. As regards the ecological restrictions on the two species, both are mid-European species associated with cool climates, high altitudes and open landscapes; they only differ in their preference for moisture (Palomo et al., 2007; Sans-Fuentes and Ventura, 2000).

Secondly, all specimens identified as *Arvicola* sp. in previous publications (Alcalde, 1986) have been interpreted as belonging to the species *Arvicola sapidus*, because this is the only species from this genus present during this interval in the Northeast of Iberia (López-García, 2011). The only example of *Arvicola terrestris*, the other extant species from this genus, is located in Cova d'Olopte B (Villalta, 1972), and this is probably misidentified, also corresponding to *A. sapidus*, a species widely extended in Catalonia during the Late Pleistocene–Holocene. Finally, the specimens identified as *Terricola* sp. have been considered to be *Microtus (Terricola) duodecimcostatus*. The other known species of

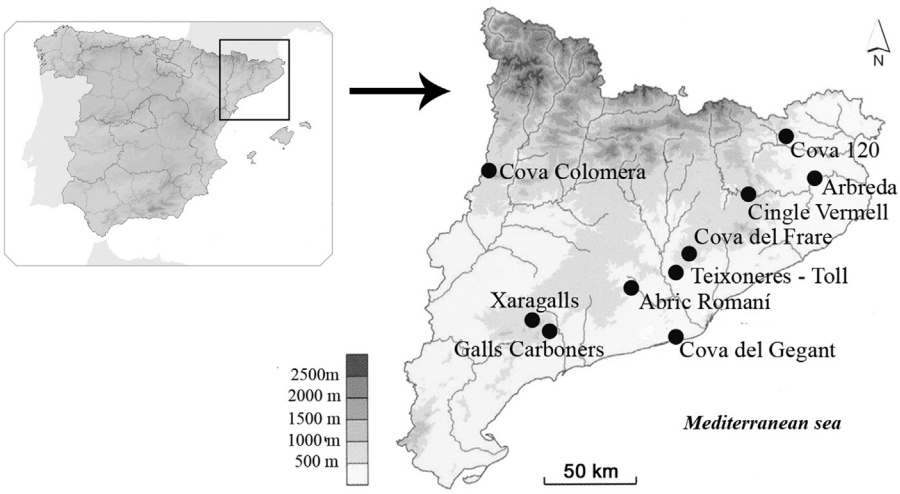

Sites	Levels	Chronology
Teixoneres cave	III, II	90-30 ka BP
Abric Romani rockshelter	O, N, E	55-49 ka BP
Cova del Gegant (old levels)	I	128-40 ka BP
Cova del Gegant (new levels)	V, III	55.7-49.3 ka cal BP
Xaragalls cave	C8, C7, C6, C4	45-13 ka BP
Arbreda cave	I, H, G, F, E, D, C, B, A	40-18.8 ka BP
Galls Carboners cave	Capa 100	31.17-31.38 ka cal BP
Toll cave	3, 2	<35 - >13
Cova Colomera	CE15, CE13-14, CE12, EE1, A. sup	13-3.5 ka BP
Cingle Vermell		9.76 ±0.16 ka BP
Cova del Frare	6, 5, 4, 3	6.3-3.9 ka BP
Cova 120	III, II, I	4.27-3.1 ka BP

Fig. 1. Location of Late Pleistocene–Holocene archaeological sites included from the northeast of the Iberian Peninsula, and table showing the site and the corresponding levels, with their general chronology.
Fig. 1. Localisation des sites archéologiques du Pléistocène supérieur–Holocène dans le Nord-Est de la péninsule Ibérique, et tableau montrant les noms des sites, leurs niveaux correspondants et leurs chronologies.

this genus that is close morphologically, *Microtus (T.) gerbei*, is not an abundant species in the region and is commonly associated with cooling temperatures (Palomo et al., 2007). The reason for this grouping is not to lose sight of the importance of *M. (T.) duodecimcostatus* as a result of fragmentation of the information associated with this species, which is dominant in some assemblages.

2.2. Classification of levels

The 37 studied levels have been grouped, in accordance with their chronology, in three time intervals:

- Early Late Pleistocene (ELP). This includes all archaeological levels from ca. 128 to 40 ka BP, generally related to the Middle Palaeolithic and consequently to *Homo neanderthalensis* activity. Since in the Northeast of Iberia there are only a few Middle Palaeolithic sites with chronologies older than 60 ka BP, the greater part of the assemblages belong to MIS 3 (ca. 60–30 ka BP). Thirteen levels of five different fossil sites are included: Levels III and II from Teixoneres cave (López-García et al., 2012b); Levels O, N and E from Abric Romaní (López-García, 2011; Fernández-García, 2014); Levels I, V and III from Cova del Gegant (López-García et al., 2012c); Levels C8, C7, C6 and C4 from Xaragalls Cave (López-García et al., 2012a) and Level I from Arbreda cave (Alcalde, 1986; López-García, 2011). This group represents a total of 946 individuals.
- Latest Late Pleistocene (LLP). This comprises all archaeological levels from ca. 40 to 11.7 ka BP, commonly related to the Upper Palaeolithic and the presence of Anatomically Modern Humans. This time interval is equivalent to end of MIS 3 and the complete MIS 2 (ca. 30–14 ka BP). Twelve levels from four different fossil sites are included: Levels I, H, G, F, E, D, C, B and A from Arbreda cave (Alcalde, 1986; López-García, 2011); the assemblage from Galls Carboners cave (López-García et al., 2014b); Levels 3 and 2 from Toll cave (Fernández-García and López-García, 2013) and Level CE15 from Cova Colomera (López-García et al., 2010). This group represents a total of 1455 individuals.
- Holocene (HOL). Groups all archaeological sites recent than 11.7 ka BP, including Epipalaeolithic, Neolithic, Chalcolithic and Bronze Age sites. All these levels belong to MIS 1. Twelve levels from four different fossil sites are included: Level CE13–14, CE12, EE1 and A. sup. from Cova Colomera (López-García et al., 2010); the assemblage from Cingle Vermell (Alcalde, 1986); Level 6, 5, 4

Table 1
Data matrix for the occurrence of species in Late Pleistocene–Holocene archaeological levels in the northeastern of Iberia. The occurrence of the species is expressed as the minimum number of individuals (MNI).
Tableau 1
Matrice de données pour la présence d'espèces dans les niveaux archéologiques du Pléistocène supérieur–Holocène dans le Nord-Est de l'Ibérie. La présence de l'espèce est exprimée en nombre minimum d'individus (NMI).

	Arvicola sapidus	*Chionomys nivalis*	*Microtus arvalis-agrestis*	*M. (Terricola) duodecim-costatus*	*Microtus (Terricola) gerbei*	*Microtus oeconomus*	*Iberomys cabrerae*	*Clethrionomys glareolus*	*Pliomys lenki*	*Apodemus sylvaticus*	*Mus musculus*	*Eliomys quercinus*	*Glis glis*	*Hystrix* sp.	*Spermophilus* cf. *citellus*	*Sciurus vulgaris*	Total MNI
Early Late Pleistocene (128–40 ka BP)																	
Teixoneres – Level III	3	1	35	35	1	0	2	0	1	75	0	11	7	0	0	0	171
Teixoneres – Level II	2	8	100	9	0	0	0	0	1	19	0	8	0	0	0	0	147
Abric Romaní – Level O	55	0	55	25	0	0	45	0	0	69	0	8	0	0	0	1	258
Abric Romaní – Level N	3	0	0	1	0	0	8	0	0	3	0	0	0	0	0	0	15
Abric Romaní – Level E	3	0	3	4	1	0	0	0	0	5	0	1	0	0	0	0	17
Cova del Gegant – Level I	0	0	5	5	2	0	4	0	0	24		4	0	2	0	0	46
Cova del Gegant – Level V	0	0	0	1	0	0	5	0	0	1	0	17	0	0	0	0	24
Cova del Gegant – Level III	0	0	1	0	0	0	3	0	0	3	0	11	0	0	0	0	18
Xaragalls – C8	0	0	1	4	0	0	2	0	0	18	0	2	0	0	0	0	27
Xaragalls – C7	0	0	2	0	0	0	1	0	0	33	0	3	0	0	0	0	39
Xaragalls – C6	1	1	4	7	0	0	3	0	0	69	0	6	0	0	0	0	91
Xaragalls – C4	0	2	6	2	0	0	1	0	0	14	0	3	0	0	0	0	28
Arbreda – Level I	5	7	30	4	0	0	0	0	0	12	0	7	0	0	0	0	65
Latest Late Pleistocene (40–11 ka BP)																	
Arbreda – Level H	4	0	95	12	0	0	0	0	0	3	0	2	0	0	0	0	116
Arbreda – Level G	0	0	41	7	0	1	0	0	0	3	0	3	1	0	0	0	56
Arbreda – Level F	2	0	89	2	0	0	0	0	0	7	0	6	0	0	0	0	106
Arbreda – Level E	6	0	98	1	0	1	0	0	0	6	0	4	0	0	0	0	116
Arbreda – Level D	16	0	192	4	0	0	0	0	0	7	0	9	0	0	0	0	228
Arbreda – Level C	13	0	248	0	0	2	0	0	0	5	0	8	0	0	2	0	278
Arbreda – Level B	2	0	61	0	0	0	0	0	0	3	0	3	0	0	1	0	70
Arbreda – Level A	6	0	125	60	0	0	2	0	0	22	0	15	0	0	1	0	231
Galls Carboners	0	9	3	0	0	0	0	0	0	9	0	33	0	0	0	0	54
Toll – Level 3	0	1	16	19	0	0	1	0	0	1	0	2	1	0	0	0	41
Toll – Level 2	0	0	3	61	2	0	3	0	0	2	0	0	0	0	0	0	71
Colomera – Level CE15	0	34	33	4	0	0	0	0	0	12	0	5	0	0	0	0	88
Holocene (< 11 ka BP)																	
Colomera – Level CE13–14	0	24	11	5	0	0	1	0	0	36	0	4	0	0	0	0	81
Colomera – Level CE12	0	11	11	4	0	0	2	0	0	32	0	6	0	0	0	0	66
Colomera – Level EE1	0	6	8	1	0	0	1	0	0	22	0	4	0	0	0	0	42
Colomera – Level A sup.	0	0	0	6	0	0	1	0	0	32	0	9	0	0	0	0	48
Cingle Vermell	3	0	6	2	0	0	1	1	0	37	0	3	0	0	0	0	53
Cova del Frare – Level 6	0	0	0	16	0	0	0	0	0	8	0	0	0	0	0	0	24
Cova del Frare – Level 5	0	0	0	33	0	0	8	0	0	29	0	2	0	0	0	0	72
Cova del Frare – Level 4	0	0	0	25	0	0	9	1	0	19	0	3	1	0	0	0	58
Cova del Frare – Level 3	0	0	0	5	0	0	2	0	0	8	0	1	1	0	0	0	17
Cova 120 – Level III	0	0	3	6	0	0	0	0	0	49	0	2	0	0	0	0	60
Cova 120 – Level II	0	3	4	11	0	0	11	0	0	70	2	6	7	0	0	0	114
Cova 120 – Level I	1	0	1	0	0	0	1	0	0	18	6	3	1	0	0	0	31
Early Late Pleistocene	72	19	242	97	4	0	74	0	2	345	0	81	7	2	0	1	946
Latest Late Pleistocene	49	44	1004	170	2	4	6	0	0	80	0	90	2	0	4	0	1455
Holocene	4	44	44	114	0	0	37	2	0	360	8	43	10	0	0	0	666
Total MNI	125	107	1290	381	6	4	117	2	2	785	8	214	19	2	4	1	3067

and 3 from Cova del Frare (Alcalde, 1986) and Level III, II and I from Cova 120 (Alcalde, 1986). This group represents a total of 666 individuals.

2.3. Multivariable statistical methodology

To provide a better understanding of such a large corpus of data, multivariate statistical methods have been applied, allowing us to reduce the number of variables involved in order to facilitate our ecological interpretations. Methods of multivariate analysis without previous assumptions of dependence and independence have been selected, with the aim of defining coherent patterns in space and time (Shennan, 1997). The original data correspond to absolute frequency variables, so the most recommended multivariate statistics proxy is correspondence analysis (López-Roldan and Lozares-Colina, 2000). However, this method has been shown to have limitations for the studied data, such as its low representativeness and the low explanatory capacity of its results. Consequently, other methods have been applied.

On the one hand, a principal component analysis (PCA) has been applied. This analysis has been performed after the transformation of the data from absolute frequency variables to ratio variables, replacing the original values by percentages. This data for which the sum over the variables is 100% is equivalent to compositional data (Baxter, 2003). The PCA makes it possible to analyse the sample in standardized form and yields advantages in interpretation by placing the different variables on a coordinate axis, distinguishing different components (the resulting variables) that indicate the weight of each original variable in the graphical representation obtained (Jolliffe, 2002). The covariance matrix has been used, because it proves to be the most appropriate to increase the total variance obtained in the first, second and third components (López-Roldan and Lozares-Colina, 2000; Shennan, 1997).

On the other hand, for a better and more visual compression of the data, a cluster analysis has been applied. Behind this method lies the idea that objects can be similar to one another at different levels; accordingly, the results can be represented in the form of a dendrogram, where the hierarchical relationships can be detected (Shennan, 1997). In the both cluster analyses presented, the original values have also been transformed into ratio variables. The first one have included the same data than the PCA; whereas in the second, the levels have been group in the three time intervals distinguished, including totals. A Euclidean Index is selected for grouping the data in both; this index is recommended for quantitative measures and ratio variables. The "paired group linkage" has been applied in all cases. For all the statistical approaches, the Paleontological Statistics program has been used (PAST3) (Hammer et al., 2001).

3. Results

3.1. Previous data

A preliminary view of the occurrence of species in different levels from the Late Pleistocene–Holocene epoch clearly shows the dominance of some taxa over other, more poorly represented taxa. The most abundant taxa, listed in increasing order, are: the group of the common vole and the field vole (*Microtus arvalis-agrestis*), the wood mouse (*Apodemus sylvaticus*), the Mediterranean pine vole (*M. (T.) duodecimcostatus*), Cabrera's vole (*Iberomys cabrerae*), the garden dormouse (*Eliomys quercinus*), the European snow vole (*Chionomys nivalis*) and the southwestern water vole (*Arvicola sapidus*). However, in many cases their dominance do not extend for long intervals of time and are restricted to the singularities of certain sites (Table 1). The important presence of *M. arvalis-agrestis* is clear, but it combines an abundant presence in some levels with being very scarce in others. Meanwhile, *A. sylvaticus* is dominant in some levels but always at lower rates than in intervals of *M. arvalis-agrestis* dominance (Table 1; Fig. 2).

Leaving aside the peculiarities of each site and taking into account the species representativeness during the different time intervals, various trends have been observed (Fig. 3). Notable changes in species abundance are observed for certain intervals, particularly regarding the presence of these two domain species. During the early Late Pleistocene, both species show a roughly equal representation: *A. sylvaticus* (36.5%) and *M. arvalis-agrestis* (25.6%). However, with the arrival of the latest Late Pleistocene, a significant shift is detected, involving a remarkable decrease in *A. sylvaticus* (5.5%) and the almost complete dominance of *M. arvalis-agrestis* (69%). In the Holocene, by contrast, the opposite situation occurs: *A. sylvaticus* undergoes a revival (54%) and *M. arvalis-agrestis* loses in importance (6.6%). The other species barely exceed 1% in any of the intervals considered, except for *M. (T.) duodecimcostatus*, *E. quercinus*, *C. nivalis*, *A. sapidus* and *I. cabrerae*, which are better represented but remain more or less constant in the different intervals.

3.2. Multivariate statistics

3.2.1. Principal component analysis

Interesting results were obtained when principal component analysis was applied (Fig. 4). Considering the eigenvalues attributed to each of the components (Appendix A2), the first three should be included. The scree plot clearly shows that Component 4 is not relevant (PC4, less than 5% of variance). In contrast, the first three principal components present high representativeness, summarizing more than 90% of the variance of the studied sample (PC1, 55.6%; PC2, 19.4%; PC3, 15.5%; Appendix A2).

PC1 arranges the archaeological levels in relation to high values of MNI of two main groups of species (Fig. 4A): *M. arvalis-agrestis* for positive values of this axis and *A. sylvaticus* for negative values. The *M. arvalis-agrestis* group of species can be related with open environments, low humidity rates and cold temperatures, whereas the second is adapted to forest environments in a temperate climate without major climatic constraints (Palomo et al., 2007). Nevertheless, it is also remarkable the importance of *M. (T.) duodecimcostatus*, *E. quercinus* and *I. cabrerae* for negative values. *M. (T.) duodecimcostatus* and *I. cabrerae* are species typical of Mediterranean areas, while *E. quercinus* is a generalist species but usually related to forest cover

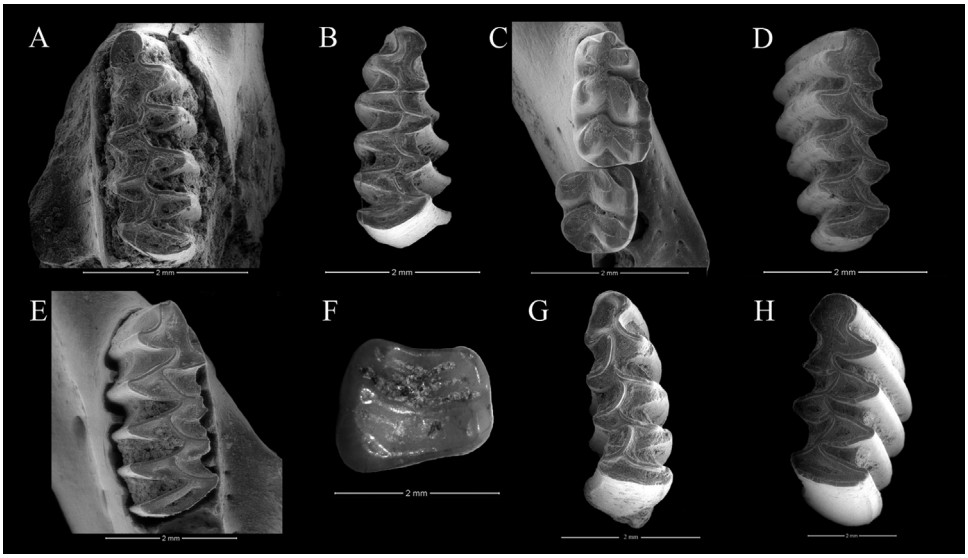

Fig. 2. Most common rodent species from northeastern Iberia during the Late Pleistocene–Holocene. A. Left m1 of *Microtus arvalis* (Toll cave). B. Right m1 of *Microtus agrestis* (Cova del Gegant). C. Right m1 and m2 of *Apodemus sylvaticus* (Toll cave). D. Right m1 of *Microtus (Terricola) duodecimcostatus* (Cova del Gegant). E. Right m1 of *Iberomys cabrerae* (Abric Romaní). F. Right m2 of *Eliomys quercinus* (Toll cave). G. Left m1 of *Chionomys nivalis* (Toll cave). H. Left m1 of *Arvicola sapidus* (Toll cave). Occlusal view: scale 2 mm.

Fig. 2. Espèces de rongeurs les plus communes du Nord-Est de la péninsule Ibérique au cours du Pléistocène supérieur–Holocène. A. m1 gauche de *Microtus arvalis* (grotte du Toll). B. m1 droite de *Microtus agrestis* (Cova del Gegant). C. m1 et m2 droites de *Apodemus sylvaticus* (grotte du Toll). D. m1 droite de *Microtus* (*Terricola*) *duodecimcostatus* (Cova del Gegant). E. m1 droite de *Iberomys cabrerae* (Abric Romaní). F. m2 droite de *Eliomys quercinus* (grotte du Toll). G. m1 gauche de *Chionomys nivalis* (grotte du Toll). H. m1 gauche de *Arvicola sapidus* (grotte du Toll). Vues occlusales : échelle = 2 mm.

(Palomo et al., 2007; Purroy and Varela, 2003; Sans-Fuentes and Ventura, 2000). From a palaeoenvironmental point of view, a distribution of sites along the PC1 can be inferred between a more open and possibly colder climate, represented by "the *M. agrestis-arvalis* tendency", to forested areas and more temperate weather, represented by "the *A. sylvaticus* tendency". Accordingly, the simplest interpretation for the distribution of levels on the graph would be a gradient from more closed environments (negative values on PC1 axis) to more open environments (positive values of PC1 axis), with the climatic implications that this might entail.

In addition, positive PC2 values are determined by the occurrence of *M. (T.) duodecimcostatus* and secondly by *I. cabrerae*. Both are commonly associated with Mediterranean conditions and related forest or wet grassland habitats (Palomo et al., 2007; Sans-Fuentes and Ventura, 2000). On the other hand, negative values depend on *A. sylvaticus* and *M. arvalis-agrestis* and in lesser proportion on *C. nivalis*. The latter three are mid-European species nowadays living in areas at notable altitudes, with cold temperatures and lower rainfall; by contrast, *A. sylvaticus* is a generalist species, related to the forest and not restricted by altitudinal factors (Palomo et al., 2007; Purroy and Varela, 2003; Sans-Fuentes and Ventura, 2000). In this sense, it proves difficult to develop a palaeoecological interpretation for PC2. Nevertheless, the contrast between PC1 and PC2 suggests a classification of assemblages in terms of the three most dominant species (*M. arvalis-agrestis, A. sylvaticus* and *M. (T.) duodecimcostatus*) in the Northeast of the Iberian Peninsula during the Late Pleistocene and Early Holocene.

As regards the three above-defined time intervals, it can be observed that the closest associations over time within each time interval tend to appear together on the graph. Specifically, LLP levels appear separated from the rest of the associations and concentrated together in relation to *M. arvalis-agrestis*. Moreover, ELP and HOL levels are grouped together, their distribution depends on the dominance of *A. sylvaticus* or *T. duodecimcostatus*, showing no particularly distinctive patterns between these two time intervals. In complementary form, the ELP and HOL samples tend to appear far away from *M. arvalis-agrestis*, and the LLP ones from *A. sylvaticus*, showing the respective low presence of these species. This demonstrates the great similarity of these two climatic phases (ELP and HOL), or rather the high particularity of LLP.

On the one hand, all the LLP levels from Arbreda cave and Level CE15 from Cova Colomera are grouped together in the "*M. arvalis-agrestis* tendency". The location of some LLP levels shows that, in spite of the above-noted clear bipolarization between the two main groups of species, there are other determinant taxa during this interval, such as the Mediterranean pine vole (*M. (T.) duodecimcostatus*). The high presence of this taxon is evident in levels from Toll cave and is the reason about its position in the graph. The only incoherent level is Galls Carboners cave assemblage, which appears somewhat distant, because is the oldest site from the LLP samples and is affected by the Mediterranean influence on its location.

On the other hand, among the ELP and HOL levels, two levels appear closer to the LLP group: Level I from Arbreda cave and Level II from Teixoneres cave. These correspond to the latest and earliest levels, respectively, among the ELP

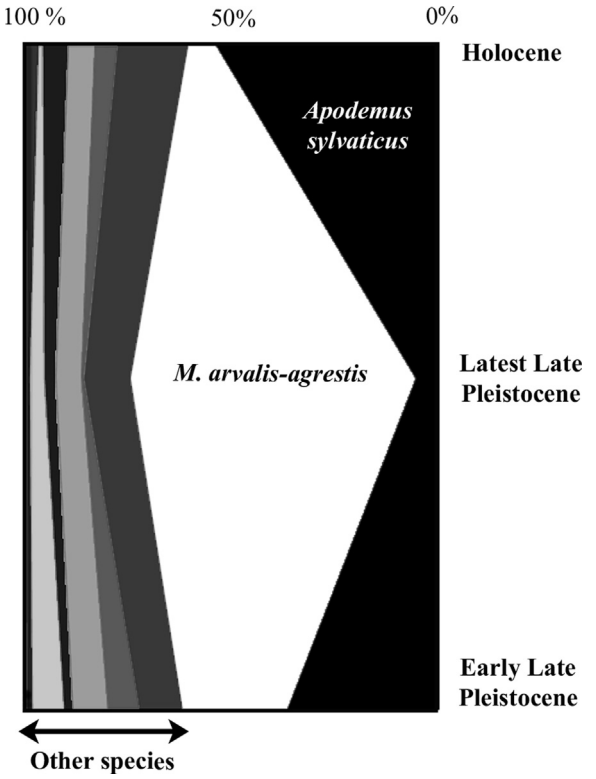

Fig. 3. Relative frequency of Late Pleistocene–Holocene rodent species in northeastern Iberia throughout the three chronological periods differentiated. From left to right: non-significant species (*Microtus (Terricola) gerbei*, *Microtus oeconomus*, *Clethrionomys glareolus*, *Pliomys lenki*, *Mus musculus*, *Glis glis*, *Hystrix* sp., *Spermophilus citellus*, *Sciurus vulgaris*); *Arvicola sapidus*; *Chionomys nivalis*; *Eliomys quercinus*; *Iberomys cabrerae*; *Microtus (Terricola) duodecimcostatus*; *Microtus arvalis-agrestis*; *Apodemus sylvaticus*.
Fig. 3. Fréquence relative des espèces de rongeurs au cours du Pléistocène supérieur–Holocène dans le Nord-Est de la péninsule Ibérique à travers les trois périodes chronologiques différenciées. De gauche à droite : espèces non significatives (*Microtus (Terricola) gerbei*, *Microtus oeconomus*, *Clethrionomys glareolus*, *Pliomys lenki*, *Mus musculus*, *Glis glis*, *Hystrix* sp., *Spermophilus citellus*, *Sciurus vulgaris*) ; *Arvicola sapidus* ; *Chionomys nivalis* ; *Eliomys quercinus* ; *Iberomys cabrerae* ; *Microtus (Terricola) duodecimcostatus* ; *Microtus arvalis-agrestis* ; *Apodemus sylvaticus*.

assemblages. The reasons could be related both to chronological and geographical influences. The former could be interpreted as a marker for a progressive trend on decrease of temperatures and changing conditions associated with the beginning of the LLP and the resulting glacial acceleration. Level II from Teixoneres cave has been linked in previous publications (López-García et al., 2014c) with Heinrich Event 2 or 3, a cooling episode that led to a high presence of mid-European species such as *M. arvalis* and *M. agrestis*. This phenomenon is also found in Levels O and E of the Abric Romaní rock-shelter, previously associated with cold episodes: Stadial 17-15 and Heinrich Event 5, respectively (Fernández-García, 2014; López-García, 2011).

By combining PC1 and PC3, we can observe small differences in the association of levels (Fig. 4B). Positive values for PC3 are related with the occurrence of *E. quercinus* and, less importantly, with *C. nivalis* and *I. cabrerae*, while negative values are defined by the proportionally greater occurrence of *M. (T.) duodecimcostatus*, *A. sylvaticus* and *M. arvalis-agrestis*. As occurred in the PC2, this makes an ecological interpretation somewhat more complex, but a chronological trend is conserved, clustering LLP closer to *M. arvalis-agrestis* and the rest (ELP and HOL) closer to *A. sylvaticus*. The only exceptions are the Galls Carboners assemblage and levels III and V from Cova del Gegant, a result of the tendency established by the predominance of *E. quercinus* in these samples, which is a particularity of these locations. However, the chronological distribution detected by the combination of PC1 and PC2 is in general terms maintained in the combination of PC1 and PC3, revealing the great influence of the *M. arvalis-agrestis* and *A. sylvaticus* bipolarization shown by PC1.

3.2.2. Cluster analysis

The results obtained by the cluster analysis of the total occurrences of species by time intervals are congruent with those obtained through the PCA (Fig. 5). Certainly, the divergence of the assemblages from the LLP from the other two time intervals can be appreciated, with the ELP and the HOL assemblages appearing closer to each other (Fig. 5B). This phenomenon can be observed clearly if the relative presence of the species by interval is tested, but also if we cluster their occurrence by isolated levels (Fig. 5A). The clustering level analysis shows only three possible outliers. The possible reasons for this anomaly have already been explained for the PCA. In the case of Level 2 from Toll cave (LLP), the high presence of *M. (T.) duodecimcostatus* would be determinant in its association.

Once again, the trend showed is probably related to the high occurrence of mid-European species during the LLP, while in the other two time intervals the dominant species are those common in forest environments and more temperate environments or climates with a Mediterranean influence. If we pay attention to how the graph shows the association of species (Fig. 5B), *M. arvalis-agrestis* is clearly far from the rest, as is *A. sylvaticus*. *M. (T.) duodecimcostatus* is also somewhat further away from the rest but to a lower degree. These relations demonstrate the singular character of these three species, which are commonly more abundant in northeastern assemblages, as has been observed by means of the PCA. The rest of the species appear much more clustered, with only *E. quercinus, A. sapidus, I. cabrerae* and *C. nivalis* showing a certain distance from the rest (but always within this group of unrepresentative species).

4. Discussion

There are some species that dominate in specific archaeological records as a result of the precise conditions of each site, including parameters such as the altitude, the proximity to the coast or to river courses. In the light of the results obtained in this study, however, it seems consistent to interpret an ecological trend reflected in the rodent associations, a trend that is relatively independent of the precise conditions of the archaeological sites in the Northeast of Iberia. In short, one can observe a gradient in the environmental conditions running from open spaces such as meadows or grasslands and linked to the presence of *M. arvalis-agrestis*, to more wooded areas or areas with greater vegetation cover associated with *A. sylvaticus*.

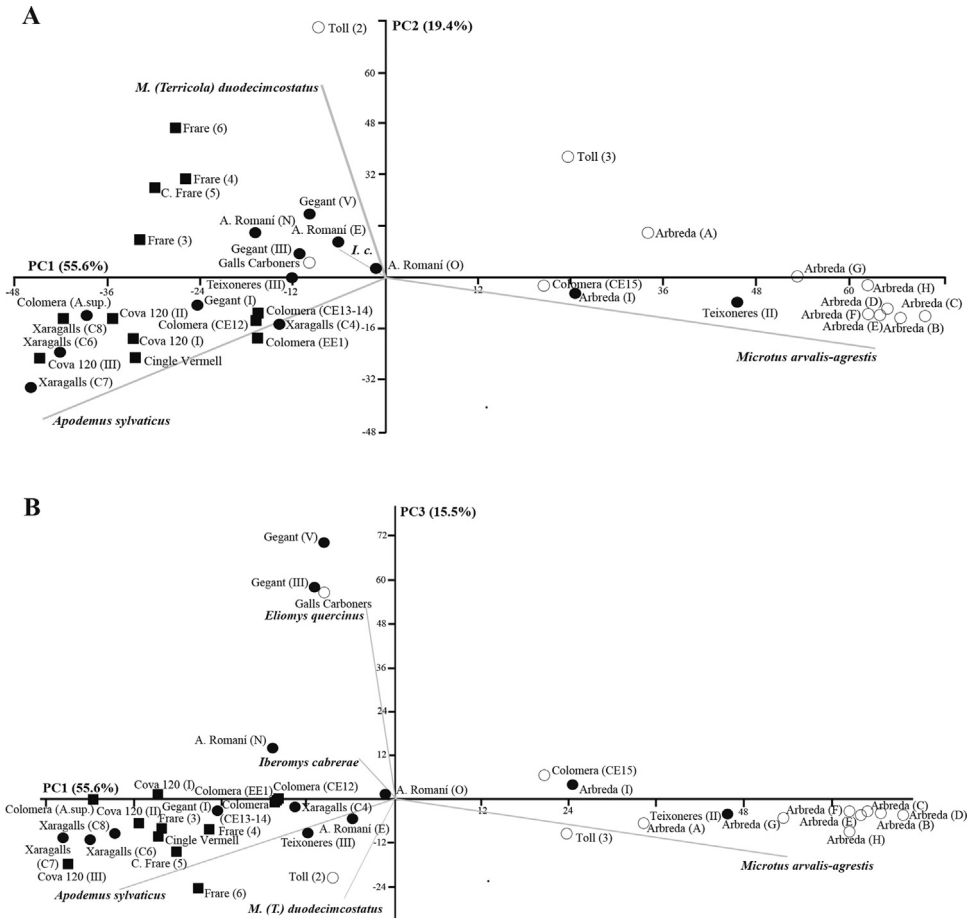

Fig. 4. Principal component analysis of Late Pleistocene–Holocene levels from northeastern Iberia according to rodent species occurrence. A. Graphical representation of components 1 (x) and 2 (y). B. Graphical representation of components 1 (x) and 3 (y). Early Late Pleistocene levels in black dots, Latest Late Pleistocene levels in white dots, and Holocene levels in squares.

Fig. 4. Analyse en composantes principales des niveaux du Pléistocène supérieur–Holocène des sites du Nord-Est de la péninsule Ibérique, selon la présence des espèces de rongeurs. A. Représentation graphique des composantes 1 (x) et 2 (y). B. Représentation graphique des composantes 1 (x) et 3 (y). Niveaux du début du Pléistocène supérieur en points noirs, derniers niveaux du Pléistocène supérieur tardif en points blancs, et niveaux de l'Holocène en carrés.

Nonetheless, the particularities of the Iberian Peninsula make some Mediterranean species (such as *M. (T.) duodecimcostatus* and *I. cabrerae*) or woodland species (such as *E. quercinus*) crucial in the interpretation of the environment (Palomo et al., 2007; Purroy and Varela, 2003). The continuous transitions in the ecological conditions between open and cooling environments and more forested and temperate ones constitute a common tendency in the western Mediterranean during the Late Pleistocene cycles (Harrison and Sánchez-Goñi, 2010). Overall, the Late Pleistocene is in general terms considered colder than the Holocene because of the alternation of glacial and interglacial cycles, whereas the Holocene constitutes an interval of climatic recovery, identified as the last interglacial before the present (Uriate, 2003). However, we can see a greater proximity in the overall association of species during the HOL and ELP than during the LLP. The singularity of the LLP can be observed in its fauna composition characterized by species related with mid-European requirements and open environments (*M. arvalis, M. agrestis* and *C. nivalis*). By contrast, the ELP (Middle Palaeolithic) assemblages are not as different from the HOL ones as might have been expected, presenting similar proportions of woodland species (*A. sylvaticus*) and Mediterranean species (*M. (T.) duodecimcostatus* and *I. cabrerae*). This can be understood in terms of climate issues related with MIS 2 and the Last Glacial Maximum (LGM), which testifies to the largest drop in temperature experienced during this time interval and the subsequent reduction of wood cover (Sánchez-Goñi and D'Errico, 2005). However, it should be borne in mind that this phenomenon occurs in lower intensity in Iberia than in the rest of Europe, where the conditions of aridity in cold moments are more pronounced, as reflected in faunal communities and other proxies (Fletcher and Sánchez-Goñi, 2008; Sommer and Nadachowski, 2006). The maintenance of woodland cover remains a constant in Iberia in spite of the intervals of instability.

4.1. Early Late Pleistocene environment (128–40 ka BP)

During MIS 4, solar insolation was minimal, initiating a global cold period. Long-term pollen records obtained

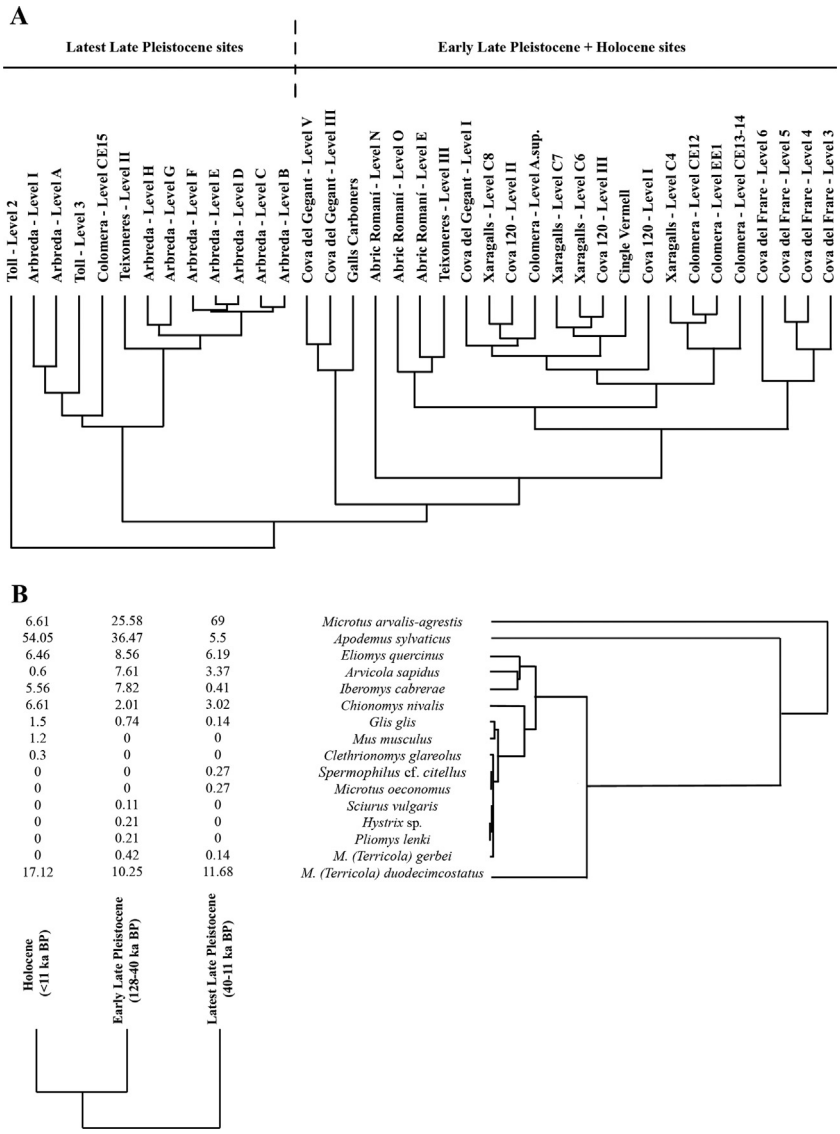

Fig. 5. Late Pleistocene–Holocene species occurrence in northeastern Iberia by cluster analysis in different levels (A) and associated by chronological periods (B) (on the top right, the species groups and, on the lower left margin, the periods grouped).
Fig. 5. Analyse de groupes montrant la présence des espèces dans les différents niveaux des sites du Nord-Est de la péninsule Ibérique au Pléistocène supérieur–Holocène (A) et associées par périodes chronologiques (B) (en haut à droite, les groupes d'espèces et, sur la marge inférieure gauche, les périodes regroupées).

from French lacustrine deposits, such as La Grande Pile and the Velay Maars, indicate the predominance of boreal forests during MIS 4, declining at the end of MIS 4 with the expansion of steppe–tundra vegetation (Fletcher et al., 2010; Sánchez-Goñi et al., 2008). According to pollen analysis, MIS 3 is characterized in southern Europe by a dynamic that alternates between phases of forest development and the expansion of semi-arid areas in accordance with the warming and cooling, respectively, of the sea-surface temperatures (Fletcher et al., 2010; Harrison and Sánchez-Goñi, 2010). However, various proxies, including pollen and small mammals, have shown that this alternation of dryness and wetness and the consequent reduction-extension of forest are not straightforward.

There are many Middle Palaeolithic sites located in the Northeast of Iberia during MIS 3. Some of them present interesting climatic reconstructions based on small mammals, such as Level II from Teixoneres cave (60–30 ka BP), Level IV from Cova del Gegant (60 ± 3.8 ka BP), Level O from Abric Romaní (54.24 ± 0.42 ka BP), Level C8 from Xaragalls cave (> 43.5 ka BP), Level I from Arbreda cave (40–32 ka BP) and Galls Carboners (31.38–31.17 ka BP) (Fernández-García, 2014; López-García, 2011; López-García et al., 2012a,b,c, 2014b). As has previously been reported by López-García et al. (2014c), small-mammal proxies show lower mean annual temperatures and higher precipitation levels throughout this period in this region (Fernández-García, 2014). Coexistence is also

observed between temperate and cold rodent species, which underwent changes in proportion depending on the stadial-interstadial fluctuations. Moreover, Mediterranean species (*M. (T.) duodecimcostatus* or *I. cabrerae*) are always present in the assemblages. However, the predominance of typical woodland species (*A. sylvaticus* and *E. quercinus*) in MIS 3 assemblages becomes a defining characteristic of the environment conditions, independent of whether it was a stadial or interstadial phase. These two latter trends are probably related with the clustering of the ELP sites with HOL assemblages in the statistical proxy in this paper.

This is coherent with palynological studies that have suggested that southern Europe (below 40°N) never underwent a complete loss of woodland, even in stadials or Heinrich Events (Fletcher et al., 2010). During interstadials the forest recovered extremely quickly, though depending on regional climatic conditions (Fletcher et al., 2010; Sánchez-Goñi and D'Errico, 2005). The Mediterranean coast was where the forest development was most pronounced, as a result of the influence of the Mediterranean climate and the smaller effect of North Atlantic fluctuations (Fletcher et al., 2010; Harrison and Sánchez-Goñi, 2010). In fact, important differences from the rodent communities of southwestern France can be noted. The typical rodent species in sedimentary sequences from MIS 4 and MIS 3 in these areas are *M. arvalis, Microtus gregalis* and *Dicrostonyx torquatus* (Chaline, 1972; Marquet, 1993; Royer et al., 2013). These three species today live in open habitats (tundras, forested tundras or steppes) and have a distribution that is latitude-dependent (MacDonald and Barrett, 2008). Their presence thus argues in favour of a very cold and arid environment, different from that detected for the Northeast of Iberia during this interval.

4.2. Latest Late Pleistocene (40–14.7 ka BP)

The LLP is basically represented by the end of MIS 3, the complete MIS 2 and the beginning of MIS 1 (ca. 14.7 ka BP) (Lisiecki and Raymo, 2005). These stages are highlighted in all geological sources as the most intense glacial phases, characterized by rapid and major climatic changes (Vermeersch, 2005), and ranging chronologically from ca. 27 to 11.7 ka BP. MIS 2 contains two Heinrich Events (H2 and H1), dated respectively to ca. 24 ka BP (H2) and to 16 ka BP (Oldest Dryas or H1), and also the Last Glacial Maximum (LGM) (ca. 22–19 ka BP), the moment of maximum cold in the Northern Hemisphere which represents the time of maximum extension of ice sheets at the polar caps (Fletcher and Sánchez-Goñi, 2008). This singularity of the LLP (Upper Palaeolithic) can be observed beyond the changes in the fauna composition and is clear in our statistical proxy, associated with an important increase in the species related with mid-European requirements and open environments (*M. arvalis, M. agrestis* and *C. nivalis*) and a lower representation of woodland species (*A. sylvaticus*).

According to the available data, the rodent species present in the northeastern Iberian Peninsula during the LLP were predominantly mid-European taxa with an ecological preference for cold environmental conditions (*M. arvalis* and *M. agrestis*), humid meadows (*M. agrestis* and *M. (T.) gerbei*) and, to a lesser extent, open forests (*A. sylvaticus* and *E. quercinus*) (Alcalde, 1986; López-García, 2011). Assemblages with such characteristics have been described in Levels C4–C1 of Cova dels Xaragalls (48.2–13.7 ka BP) (López-García et al., 2012a), Level III of Balma de la Griera (21.2 ka BP) (Nadal, 2000) and the oldest levels of Arbreda cave (39.9–17.3 ka BP) (Alcalde, 1986; López-García, 2011). LLP levels from Arbreda cave (39.9–17.32 ka BP) present a clear predominance of rodent species associated with open humid conditions (*M. arvalis*, *M. agrestis* and *M. (T.) duodecimcostatus*), whereas species associated with forest conditions are present in much lower proportions (*A. sylvaticus*, *G. glis* and *E. quercinus*). The association is also characterized by a strong representation of mid-European species (*M. arvalis* and *M. agrestis*), meaning cold conditions and open landscapes (Alcalde, 1986; Alcalde and Brunet-Lecomte, 1985). This great relative abundance of *M. arvalis* and *M. agrestis* is a common trend in other sites in Iberia (López-García, 2011). Additionally, it has been detected in some southern French sequences, accompanied by a high presence of *Microtus gregalis*, as at Tailles-des-Coteaux (Jeannet, 2011; Royer et al., 2014), and is also common in the LLP sites of the Italian Peninsula, such as Grotta della Serratura, Cava Filo, Grotta de la Ferrovia, Grotta Paglicci, Riparo Tagliente and Grotta del Romito (Berto, 2013; Bertolini et al., 1996; López-García et al., 2014a).

However, mention should be made of the Galls Carboners (López-García et al., 2014b) assemblage, which is located somewhat further away from the rest of the LLP levels in our PCA proxy. Associated with Heinrich Event 3, this level is at a distance from the rest of the sites as a result of the high presence of *E. quercinus*, a generalist species that is nonetheless linked with woodland cover, and the scarce representation of *M. arvalis-agrestis* group. This site provides an example of the particularities of small-mammal proxies in the Iberian Peninsula. Firstly, it warns us that there are other species, generally less abundant than *A. sylvaticus*, which should also be taken into account in the definition of open *vs*. closed landscape changes; in other words, that we cannot reduce the northeastern Iberian scenario to the bipolarization between *M. arvalis-agrestis* and *A. sylvaticus*. In this case, *E. quercinus* is the predominant species, indicating the importance of woodland cover, as well as *C. nivalis*, a species that is scarcely present in the northeastern Iberian Peninsula but is extremely indicative of cool periods (nowadays being restricted to the Pyrenean region) (Palomo et al., 2007; Pérez-Aranda, 2009). Secondly, it warns us that, within the cool and open environmental tendency of the LLP, some Iberian sites were exceptions to the global European pattern, showing the importance of a Mediterranean influence, also influenced by their geographical location. This finds expression in the maintenance of woodland cover even in the coldest episodes, such as Heinrich Event 3 or the LGM.

In fact, the Iberian Peninsula enjoyed a milder climate than the rest of Europe and served as a refugium for certain mid-European species (Sommer and Nadachowski, 2006), such as *C. nivalis* or *M. oeconomus*. Marine cores close to the coast of Iberia Peninsula reveal that during the LGM the Iberian Peninsula was characterized by

conditions that were slightly more humid than in the rest of Europe (Fletcher and Sánchez-Goñi, 2008; Kageyama et al., 2005; Sánchez-Goñi and D'Errico, 2005). The study of pollen fluctuations has established that the climate was cold and wet during the LGM (Kageyama et al., 2005), while the analysis of lakes has shown a greater degree of humidity than in other areas of Europe during the same interval. The study of small-mammal faunas from Iberia has also suggested a predominance of woodland during this time interval, with small-mammal species indicating an environment with a high level of humidity. This has been shown by small-mammal studies from four Iberian sites dated to the LGM: El Mirón Cave (Ramales de Victoria, Cantabria), Valdavara-1 (Becerreá, Lugo), El Portalón (Sierra de Atapuerca, Burgos) and Sala de las Chimeneas (Maltravieso, Cáceres) (Bañuls-Cardona et al., 2014; Cuenca-Bescós et al., 2009; López-García et al., 2011, 2012b). In general, these sites show a combination of species associated with mid-European requirements (*M. arvalis, M. agrestis, M. oeconomus* and *C. nivalis*) and species associated with Mediterranean climatic conditions (*I. cabrerae* and *M. (T.) duodecimcostatus*). As regards the landscape, there is a high presence of species associated with open woodland areas and wet environments. In short, it is suggested that the climate was harsher than nowadays during the LLP, though not as rigorous as elsewhere in Europe, with mean annual temperatures lower than at present and an environment dominated by wet open meadows (with species associated with humidity: *A. terrestris* and *M. agrestis*). However, it is also considered a more humid period than in the rest of Europe with higher precipitation levels than nowadays.

4.3. Pleistocene–Holocene transition (< 14.7 ka BP)

This glacial maximum phase is followed by the Late Glacial (corresponding to the beginning of MIS 1), which precedes the Holocene and ranges chronologically from ca. 14.7 to 11.7 ka BP (Bradley and England, 2008; Lisiecki and Raymo, 2005; Walker et al., 2009). The Younger Dryas–Holocene transition is dated to ca. 10–11 ka BP, and is characterized by a sharp increase in temperatures and precipitation, constituting a definitive break from Pleistocene climatic dynamics and leading to the climatic improvement related to the Holocene, an overall stable period from the thermal point of view (Bradley and England, 2008; Walker et al., 2009). Many studies demonstrate a clear change in the landscape composition of the Iberian Peninsula during this period, which culminated in the current composition of the flora and fauna. In the Iberian Peninsula a variety of pollen and anthracological sequences reveal this sudden rupture, with the majority agreeing that there was a change in landscape composition marked in most places by the substitution of certain taxa by others (Carrión et al., 2010; Fernández et al., 2007; Gil García et al., 2002). There is clear increase in thermophilous plant species indicative of a warm climate and in species associated with vegetation cover, with a greater expansion of forests to the detriment of open spaces (Burjachs and Renault-Miskovsky, 1992; Carrión et al., 2010).

This change is also manifest in the small-vertebrate associations from the Northeast of the Iberian Peninsula. The general pattern observed throughout rodent communities is a sharp increase in taxa with warmer requirements or a Mediterranean character (*M. (T.) duodecimcostatus* and *I. cabrerae*) and others linked to forest habitats (*A. sylvaticus* and *E. quercinus*), together with a decrease in mid-European species with cold requirements and open habitat preferences (*M. arvalis, M. agrestis* and *C. nivalis*). This transition is detected in several localities, such as Toll Cave (35–13 ka BP), Balma de la Griera (21.25 ± 0.35 ka BP), Cova Colomera (13–3 ka BP), Cingle Vermell (9.76 ± 0.16 ka BP) and Cova de la Guineu (9.8 ± 0.8 ka BP) (Alcalde, 1986; Alcalde and Brunet-Lecomte, 1985; Fernández-García and López-García, 2013; López-García, 2011; López-García et al., 2010). The greater or lesser descent in mid-European species depends on the particular characteristics of the sites in question (latitude, altitude, proximity to coast); sites of mid-European influence and at high altitude will preserve adequate conditions for the preservation of some of these specimens, as at Cova Colomera (López-García et al., 2010).

The Pleistocene–Holocene faunal transition can also be detected in other small-mammal associations from Iberia. There is a break in the faunal assemblage at the cave of El Mirador in Burgos (López-García et al., 2008), where this transition is marked by the disappearance of micromammal species with mid-European requirements such as *C. nivalis* and *M. oeconomus*, taxa with mid-European requirements and nowadays only found at higher altitudes. It is also in evidence at El Mirón in Cantabria (Cuenca-Bescós et al., 2009). This transition is also present in other southern European localities; a turning point is detected in faunal assemblages from this period in southern Italy. There, the general trend is the replacement of *M. arvalis* and *M. agrestis* by a strictly Mediterranean species, *M. (T.) savii*. This phenomenon is observed in Grotta de la Serratura, Riparo Salvini, Grotta Paglicci, Caballo Cave and Grotta delle Mura (Berto, 2013; Bertolini et al., 1996). However, in Grotta del Romito (Calabria) this substitution is related with the dominance of a glirid species, *Glis glis*, associated with woodland formations (López-García et al., 2014a). However, both species indicate a climatic improvement, with an increase in forest cover.

5. Conclusions

Both descriptive statistical methods and more complex statistical methods bring to light that there are three dominant species during the studied chronology: *Microtus arvalis, Microtus agrestis* and *Apodemus sylvaticus*. *M. arvalis* and *M. agrestis* are species associated with mid-European requirements that were especially dominant at the end of the Late Pleistocene (ca. 40–11.7 ka BP), whereas *A. sylvaticus*, a generalist species but mainly associated with wooded areas and temperate environments, was dominant at the beginning of the Late Pleistocene (ca. 128–30 ka BP) and regained its importance with the arrival of the Holocene (< 11.7 ka BP). Accordingly, this bipolarization between *M. arvalis-agrestis* and *A. sylvaticus* could be interpreted as a transition in the ecological conditions at the different sites

between open, cooling environments and more forested and temperate ones. Nevertheless, there are other species that seem determinant to evaluate the faunal dynamics of this time interval (*M. (T.) duodecimcostatus, E. quercinus* and *I. cabrerae*). The results also show that the beginning of the Late Pleistocene and the Holocene have similarities in common and differ clearly from the end of the Late Pleistocene, demonstrating the singular nature of the environment associated with the extreme environmental conditions of MIS 2 and the Late Glacial Maximum in the Northeast of the Iberian Peninsula. Other palaeoenvironmental proxies and small-mammal studies from Iberia and southern Europe confirm the singular nature of the latest Late Pleistocene and the general increase in woodland cover with the arrival of the Holocene period.

Acknowledgements

This paper is part of the projects CGL2012-38358, CGL2012-38434, 2014 SGR900 and 2014 SGR899 and 2014 SGR900. J.M. López-García is a beneficiary of a Beatriu de Pinós postdoctoral fellowship (2011BP-A200001) from the Generalitat de Catalunya, a grant co-funded by the European Union through the Marie Curie Actions of the 7th Framework Program for R + D.

Appendix A. Supplementary data

Supplementary data associated with this article can be found, in the online version, at http://dx.doi.org/10.1016/j.crpv.2015.08.005.

References

Alcalde, G., (PhD dissertation) 1986. Les faunes de rongeurs du Pléistocène supérieur et de l'Holocène de Catalogne (Espagne) et leurs significations paléoécologiques et paléoclimatiques. École pratique des Hautes études – Sciences de la Vie et de la Terre III[e] section, Paris.

Alcalde, G., Brunet-Lecomte, P., 1985. Contribució al coneixement del medi i el clima durant el Pleistocè superior i l'Holocè a Catalunya, amb l'aplicació de l'ànalisis factorial de correspondencies a les associacions de rosegadors. Paleontologia i Evolució 19, 49–55.

Alcalde, G., Galobart, A., 2002. Els petits mamífers del Plistocè superior. In: Maroto, J., Ramió, S., Galobart, A. (Eds.), Els vertebrats fossils del Pla de l'Estany, 23. Centre d'Estudis Comarcals de Banyoles, Quaderns, pp. 141–154.

Bañuls-Cardona, S., López-García, J.M., Blain, H.-A., Lozano-Fernández, I., Cuenca-Bescós, G., 2014. The end of the Last Glacial Maximum in the Iberian Peninsula characterized by the small-mammal assemblages. J. Iber. Geol. 40 (1), 19–27.

Baxter, M., 2003. Statistics in Archaeology. Arnold Publishers, London.

Berto, C., (PhD dissertation) 2013. Distribuzione ed evoluzione delle associazioni a piccoli mammiferi nella penisola italiana durante il Pleistocene superiore. Università degli Studi di Ferrara, Ferrara.

Bertolini, M., Fedozzi, S., Martini, F., Sala, B., 1996. Late Glacial and Holocene climatic oscillations inferred from the variations in the micromammal associations at Grotta della Serratura (Marina di Camerota, Salerno, S Italy). Il Quat. 9 (2), 561–566.

Bradley, R.S., England, J.H., 2008. The Younger Dryas and the Sea if Ancient Ice. Quat. Res. 70, 1–10.

Burjachs, F., Renault-Miskovsky, J., 1992. Paléonvironnement et paléoclimatologie de la Catalogne durant près de 30 000 ans (du Würmien ancien au début de l'Holòcene) d'après la Palynologie du site de L'Arbreda (Gérone, Catalogne). Quaternaire 3 (2), 75–85.

Carrión, J.S., Fernández, S., González-Sampériz, P., Gil-Romera, G., Badal, E., Carrión-Marco, Y., López-Merino, L., López-Sáez, J.A., Fierro, E., Burjachs, F., 2010. Expected trends and surprises in the Late Glacial and Holocene vegetation history of the Iberian Peninsula and Balearic Islands. Rev. Palaeobot. Palynol. 162, 458–475.

Chaline, J., 1972. Les rongeurs du Pléistocène moyen et supérieur de France. Éd. CNRS, Paris.

Chaline, J., 1988. Paleocronòmetres, paleotermòmetres i paleoindicadors dels entorns prehistòrics, els rosegadors irremplaçables. Cota Zero 4, 61–64.

Cuenca-Bescós, G., Straus, L.G., González Morales, M., García Pimineta, J.C., 2009. The reconstruction of past environments through small mammals: From the Mousterian to Bronze Age in El Mirón cave. J. Archaeol. Sci. 36, 947–955.

Fernández, S., Fuentes, N., Carrión, J.S., González-Sampériz, P., Montoya, E., Gil, G., Vega-Toscano, G., Riquelme, J.A., 2007. The Holocene and Upper Pleistocene pollen sequence of Carihuela Cave, southern Spain. Geobios 40, 75–90.

Fernández-García, M., (Master Thesis) 2014. Análisis paleoecológico en relación a las ocupaciones humanas del Nivel O del Abric Romaní (Capellades, Barcelona) mediante el estudio de los micromamíferos y sus mecanismos de acumulación. Universitat Rovira i Virgili, Tarragona.

Fernández-García, M., López-García, J.M., 2013. Palaeoecology and biochronology based on the rodent analysis from the Late Pleistocene/Holocene of Toll Cave (Moià, Barcelona). Span. J. Palaeontol. 28 (2), 227–238.

Fletcher, W.J., Sánchez-Goñi, M.F., 2008. Orbital and sub-orbital-scale climate impacts on vegetation of the western Mediterranean basin over the last 48,000 years. Quat. Res. 70, 451–464.

Fletcher, W.J., Sánchez-Goñi, M.F., Allen, J.R.M., Cheddadi, R., Combourieu-Nebout, N., Huntley, B., Lawson, I., Londeix, L., Magri, D., Margari, V., Müller, U.C., Naughton, F., Novenko, E., Roucoux, K., Tzedakis, P.C., 2010. Millennian-scale variability during the last glacial in vegetation records from Europe. Quat. Sci. Rev. 29, 2839–2864.

Gil García, M.J., Dorado, M., Valdeolmillos, A., Ruiz-Zapata, M.B., 2002. Late-glacial and Holocene palaeoclimatic record from Sierra de Cebollera (northern Iberian Range, Spain). Quat. Internat. 93–94, 13–18.

Hammer, Ø., Harper, D.A.T., Ryan, P.D., 2001. PAST: Paleontological statistics software package for education and data analysis. Palaeontol. Electron. 4 (1), 1–9.

Harrison, S.P., Sánchez-Goñi, M.F., 2010. Global patterns of vegetation response to millennnial-scale variability and rapid climate change during the last glacial period. Quat. Sci. Rev. 29, 2957–2980.

Jeannet, M., 2011. La grotte du Taillis des Coteaux à Antigny (Vienne). Taphonomie et Paléo-environnement selon les microvertébrés. Bilan Sci., 304–313.

Jolliffe, I.T., 2002. Principal Component Analysis, Second Edition. Springer Text in Statistics. Springer, New York.

Kageyama, M., Combourieu-Nebout, N., Sepulchre, P., Peyron, O., Krinner, G., Ramstein, G., Cazet, J.-P., 2005. The Last Glacial Maximum and Heinrich Event 1 in terms of climate and vegetation around the Alborán sea: a preliminary model-data comparison. C. R. Geoscience 337, 983–992.

Lisiecki, L.E., Raymo, M.E., 2005. A Pliocene–Pleistocene stack of 57 globally distributed benthic $\delta^{18}O$ records. Paleoceanography 20, PA 1003.

López-García, J.M., 2011. Los micromamíferos del Pleistoceno superior de la Península Ibérica. Evolución de la diversidad taxonómica y cambios paleoambientales y paleoclimáticos. Editorial Académica Española, Saarbrücken.

López-García, J.M., Cuenca-Bescós, G., Rosell-Ardèvol, J., 2008. Resultados del estudio de microvertebrados del Neolítico de la Cueva del Mirador (Ibeas de Juarros, Sierra de Atapuerca, Burgos). In: Hernández-Pérez, M.S., Soler-Díaz, J.A., López-Padilla, J.A. (Eds.), Actas IV Congreso del Neolítico Peninsular. Museo Arqueológico de Alicante, pp. 338–344.

López-García, J.M., Blain, H.A., Allúe, E., Bañuls, S., Bargalló, A., Martín, P., Morales, J.I., Pedro, M., Rodríguez, A., Solé, A., Oms, F.X., 2010. First fossil evidence of an "interglacial refugium" in the Pyrenean region. Naturwissenschaften 97, 753–761.

López-García, J.M., Blain, H.A., Cuenca-Bescós, G., Alonso, C., Alonso, S., Vaquero, M., 2011. Small vertebrates (Amphibia, Squamata, Mammalia) from the Late Pleistocene-Holocene of the Valdavara-1 cave. Geobios 44, 253–269.

López-García, J.M., Blain, H.-A., Bennàsar, M., Euba, I., Bañuls, S., Bischoff, J., López-Ortega, E., Saladié, P., Uzquiano, P., Vallverdú, P., 2012a. A multiproxy reconstruction of the palaeoenvironment and paleoclimate of the Late Pleistocene in northeastern Iberia: Cova dels Xaragalls, Vimbodí-Poblet, Paratge Natural de Poblet, Catalonia. Boreas 41, 235–249.

López-García, J.M., Blain, H.-A., Burjachs, F., Ballesteros, A., Allue, E., Cuevas-Ruiz, G.E., Rivals, F., Blasco, R., Morales, J.I., Hidalgo, A.R., Carbonell, E., Serrat, E., Rosell, J., 2012b. A multidisciplinary approach to reconstructing the southwestern European Neanderthals: the contribution of Teixoneres cave (Moià, Barcelona). Quat. Sci. Rev. 43, 33–44.

López-García, J.M., Blain, H.-A., Sanz, M., Daura, J., 2012c. A coastal reservoir of terrestrial resources for Neanderthal populations in north-eastern Iberia: palaeoenvironmental data inferred from the small-vertebrate assemblage of Cova del Gegant, Sitges, Barcelona. J. Quat. Sci. 27 (1), 105–113.

López-García, J.M., Berto, C., Colamussi, V., Dalla Valle, C., Lo Vetro, D., Luzi, E., Malavasi, G., Martini, F., Sala, B., 2014a. Palaeoenvironmental and palaeoclimatic reconstruction of the Latest Pleistocene-Holocene sequence from Grotta del Romito (Calabria, southern Italy) using the small-mammal assemblages. Palaeogeogr. Palaeoclimatol. Palaeoecol. 409, 169–179.

López-García, J., Blain, H.A., Bennàsar, M., Alcover, J.A., Bañuls-Cardona, S., Fernández-García, M., Fontanals, M., Martín, P., Morales, J.I., Muñoz, L., Pedro, M., Vergés, J.M., 2014b. Climate and landscape during Heinrich Event 3 in south-western Europe: the small-vertebrate association from Galls Carboners cave (Mont-ral, Tarragona, north-eastern Iberia). J. Quat. Sci. 29 (2), 130–140.

López-García, J., Blain, H.A., Bennàsar, M., Fernández-García, M., 2014c. Environmental and climatic context of Neanderthal occupation in southwestern Europe during MIS3 inferred from the small-vertebrate assemblages. Quat. Internat. 326–7, 319–328.

López-Roldan, P., Lozares-Colina, C., 2000. Anàlisis multivariable de dades estadístiques. Universitat Autònoma de Barcelona, Bellaterra.

MacDonald, D., Barrett, P., 2008. Guía de campo de los mamíferos de España y de Europa. Ediciones Omega, Barcelona.

Marquet, J.-C., 1993. Paléoenvironnement et chronologie des sites du domaine atlantique français d'âge Pléistocène moyen et supérieur d'après l'étude des rongeurs. Les Cahiers de la Claise, Supplément 2, Tours.

Nadal, J., 2000. La fauna mamífera al Garraf i els seus voltants a través del registre arqueològic. III Trobada d'estudiosos del Garraf 30, 165–170.

Palomo, L.J., Gisbert, J., Blanco, C., 2007. Atlas y libro rojo de los mamíferos terrestres de España. Dirección General para la Biodiversidad – SECEM-SECEMU, Madrid.

Pérez-Aranda, D., (PhD dissertation) 2009. Biología, ecología, genética y conservación del topillo nival ("Chionomys nivalis") en Peñalara y en Sierra Nevada. Universidad Complutense de Madrid, Madrid.

Purroy, F.J., Varela, J.M., 2003. Mamíferos de España. Península, Baleares y Canarias. Lynx, Barcelona.

Royer, F.J., Lécuyer, C., Montuire, S., Escarguel, G., Foruel, F., Mann, A., Maureille, B., 2013. Late Pleistocene (MIS 364) climate inferred from micromammal communities and $\delta^{18}O$ of rodents from les Padrelles, France. Quat. Res. 80, 113–124.

Royer, A., Lécuyer, C., Montuire, S., Primault, J., Foruel, F., Jeannet, M., 2014. Summer air temperature, reconstruction from the last glacial stage based on rodents from the site Taillis-des-Coteaux (Vienne), Western France. Quat. Res. 82, 420–429.

Sánchez-Goñi, M.F., D'Errico, F., 2005. La historia de la vegetación y el clima del último ciclo climático (OIS5-OIS1, 140.000–10.000 años BP) en la Península Ibérica y su posible impacto sobre los grupos paleolíticos. Museo de Altamira. Monografías 20, 115–129.

Sánchez-Goñi, M.F., Landais, A., Fletcher, W.J., Naughton, F., Desprat, S., Duprat, J., 2008. Contrasting impacts of Dansgaard-Oeschger event over a western Europe latitudinal transect modulated by orbital parameters. Quat. Sci. Rev. 27, 1136–1151.

Sans-Fuentes, M.A., Ventura, J., 2000. Distribution patterns of the small mammals (Insectivora and Rodentia) in a transitional zone between the Eurosiberian and the Mediterranean regions. J. Biogeogr. 27, 755–764.

Shennan, S., 1997. Quantifying Archaeology. Edinburgh University Press, Edinburgh.

Sommer, R.S., Nadachowski, A., 2006. Glacial refugia of mammals in Europe: evidence from fossil recors. Mamm. Rev. 36, 251–265.

Uriate, A., 2003. Historia del clima de la Tierra. Servicio Central de Publicaciones del Gobierno Vasco, Vitoria-Gasteiz.

Van Dam, J.A., Aziz, H.A., Sierra, M.Á.Á., Hilgen, F.J., van den Hoek Ostende, L.W., Lourens, L.J., Mein, P., van der Meulen, Albert, J., Pelaez-Campomanes, P., 2006. Long-period astronomical forcing of mammal turnover. Nature 443 (7112), 687–691.

Vermeersch, P.M., 2005. European population changes during the Marine Isotope Stage 2 and 3. Quat. Internat. 137, 77–85.

Villalta, J.F., 1972. Presencia de la Marmota y otros elementos de la fauna esteparia en el Pleistocena catalán. Acta Geol. Hisp. 7 (6), 170–173.

Walker, M., Johnsen, S., Rasmussen, S.O., Popp, T., Steffensen, J.-P., Gibbard, P., Hoek, W., Lowe, J., Andrews, J., Björck, S., Cwynar, Les, C., Hughen, K., Kershaw, P., Kromer, B., Litt, T., Lowe, D.J., Nakagawa, T., Newham, R., Schwander, J., 2009. Formal definition and dating of the GSSP (Global Stratotype Section and Point) for the base of the Holocene using the Greendland NGRIP ice core, and selected auxiliary records. J. Quat. Sci. 24 (1), 3–17.

Palaeogeography, Palaeoclimatology, Palaeoecology 506 (2018) 154–167

Contents lists available at ScienceDirect

Palaeogeography, Palaeoclimatology, Palaeoecology

journal homepage: www.elsevier.com/locate/palaeo

Paleoenvironmental context of Neanderthal occupations in northeastern Iberia: The small-mammal assemblage from Abric Romaní (Capellades, Barcelona, Spain)

Mónica Fernández-García[a,*], Juan Manuel López-García[b], Maria Bennàsar[b,c], Maria Joana Gabucio[b,c], Amèlia Bargalló[d], M. Gema Chacón[b,c,e], Palmira Saladié[b,c,f,g], Josep Vallverdú[b,c,g], Manuel Vaquero[b,c], Eudald Carbonell[b,c]

[a] Sezione di Scienze Preistoriche e Antropologiche, Dipartimento di Studi Umanistici, Università degli Studi di Ferrara, C/ so Ercole I d'Este 32, 44121 Ferrara, Italy
[b] Institut Català de Paleoecologia Humana i Evolució Social (IPHES), Zona Educacional 4, Campus Sescelades URV (Edifici W3), 43007 Tarragona, Spain
[c] Àrea de Prehistòria, Universitat Rovira i Virgili (URV), Av. Catalunya 35, 43002 Tarragona, Spain
[d] Institute of Archaeology, University College London, Gordon Square 31-34, London WC1H OPY, United Kingdom of Great Britain and Northern Ireland
[e] UMR7194 – HNHP (CNRS – MNHN – UPVD – Sorbonne Universités), 1 rue René Panhard, 75013 Paris, France
[f] GQP-CG, Grupo Quaternáario e Pré-História do Centro de Geociências (uI&D 73 - FCT), Portugal
[g] Unit Associated to CSIC, Departamento de Paleobiología, Museo Nacional de Ciencias Naturales (MNCN), Consejo Superior de Investigaciones Científicas (CSIC), Calle José Gutiérrez Abascal 2, 28006 Madrid, Spain

ARTICLE INFO

Keywords:
Level O
Taphonomy
Climate
Landscape
Middle Paleolithic
Marine Isotope Stage 3

ABSTRACT

The Abric Romaní site (Capellades, Barcelona, Spain) constitutes a key site for understanding the latest Neanderthal occupations in Western Europe. Here we present a comprehensive systematic and taphonomic analysis of a small-mammal assemblage from Level O of the Abric Romaní site, with the aim of reconstructing the paleoecological context in which the Neanderthals lived. The assemblage, which probably dates from a stadial episode between Interstadial 15 and Interstadial 14, contains fifteen small mammal species, including species uncommon for the northeast of Iberia, such as *Sciurus vulgaris*, *Nyctalus lasiopterus* and *Pipistrellus pipistrellus*. Taphonomic studies suggest a predatory origin for the assemblage, probably related to *Strix aluco*, and paleoecological inferences suggest lower temperatures (−3/−4 °C) and higher rainfall (+70/+170 mm) than at present and a landscape dominated by an open forest with watercourses. The new data improve our knowledge of trends associated with Marine Isotope Stage 3 that affected Neanderthal populations in the Iberian Peninsula, showing that the Neanderthals were well adapted to cooler and wetter conditions across Iberia.

1. Introduction

Given the close relationship between hunter-gatherer societies and the prevailing climate and environment, knowledge of the ecological landscapes in the vicinity of occupations is essential to reach a better understanding of evolutionary processes. The changing paleoenvironmental conditions that occurred during the Middle Paleolithic tend to be related with Neanderthal dynamics and their extinction (Baena et al., 2012; D'Errico and Sánchez Goñi, 2003; Leroyer and Leroi-Gourhan, 1983; Mellars, 1998; Sánchez Goñi and D'Errico, 2005; Sepulchre et al., 2007; Zilhão, 2000). Neanderthals inhabited Europe for more than 100,000 years (from Marine Isotope Stages, [MIS] 6/5 to 3/2) and are usually associated with the Mousterian technocomplexes. The end of the Mousterian Phase occurred at ca. 40 ka across Europe. The late survival of Neanderthals in southern Iberia is suggested at sites such as Gorham's Cave (Gibraltar), although this hypothesis has recently been challenged (Finlayson et al., 2006; Higham et al., 2014; Wood et al., 2014). Northern Iberia also contains some late Mousterian sites, such as El Esquilleu, Cova Gran, Abric Romaní and L'Arbreda cave (Martínez-Moreno et al., 2010; Camps and Higham, 2012; Maroto et al., 2012; Vaquero and Carbonell, 2012; Wood et al., 2014). Some authors have connected these relict populations with the favorable environmental conditions associated with peninsulas and the preservation of larger open woodland areas than in the rest of Europe (Burjachs and Julià, 1994; Zilhão, 2000; Finlayson et al., 2006; Finlayson and Carrión, 2007; Fletcher et al., 2010; López-García et al., 2014b).

The Abric Romaní rock-shelter is a key site for understanding the last Neanderthal populations and their relationships with the

* Corresponding author.
E-mail address: frnmnc@unife.it (M. Fernández-García).

https://doi.org/10.1016/j.palaeo.2018.06.031
Received 16 March 2018; Received in revised form 18 June 2018; Accepted 19 June 2018
Available online 20 June 2018

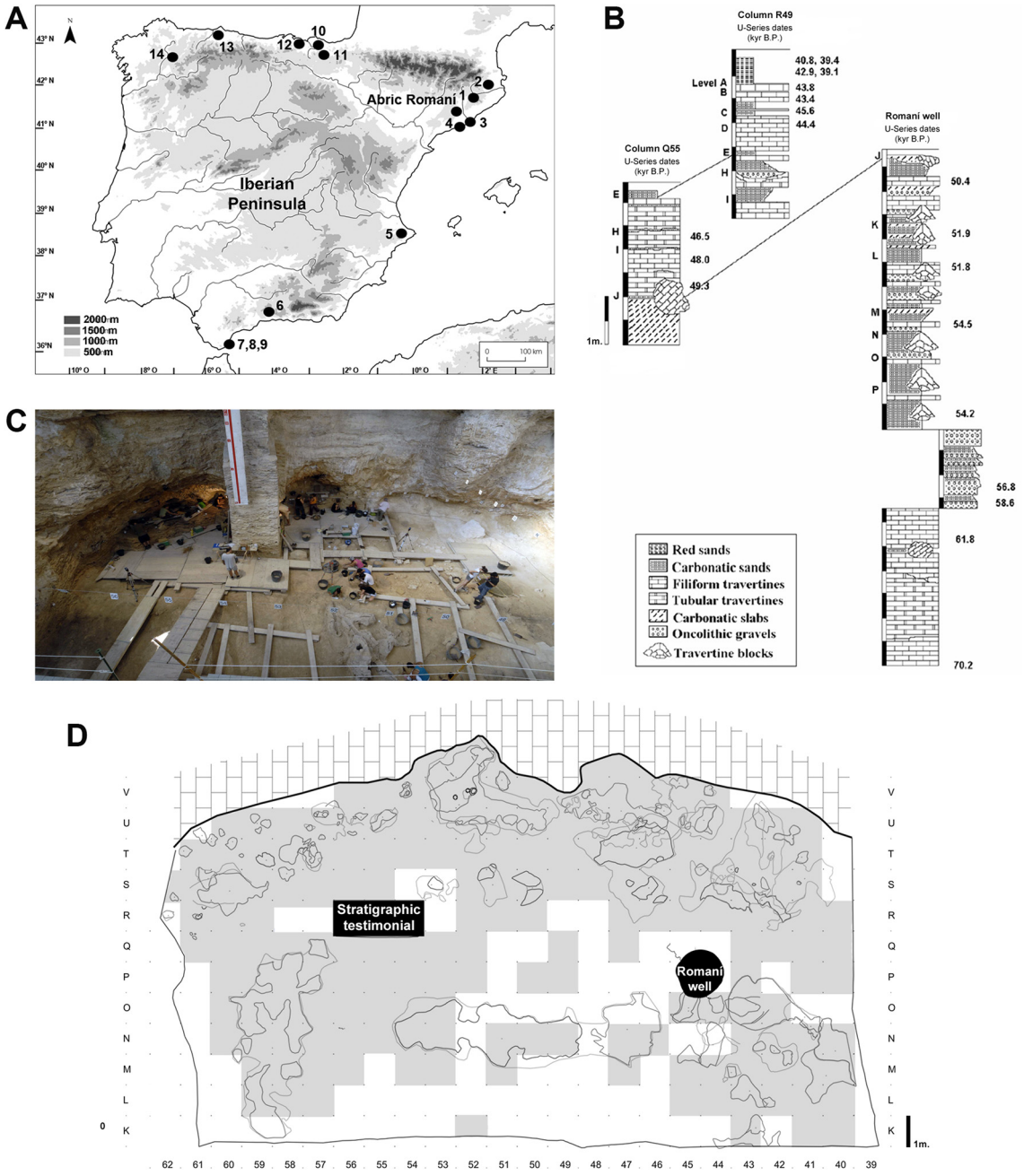

Fig. 1. (A) Location of the Abric Romaní site in Iberia and the locations of other Middle Paleolithic sites: 1, Teixoneres cave; 2, Arbreda cave; 3, Cova del Gegant; 4, Cova del Coll Verdaguer; 5, El Salt; 6, Zafarraya cave; 7, Vanguard cave; 8, Gorham's cave; 9, Ibex cave; 10, Askondo; 11, Lezetxiki II; 12, El Mirón; 13, Cueva del Conde; 14, Cova Eirós (Barroso et al., 2014; Daura et al., 2017; Fagoaga et al., 2017; Finlayson et al., 2016; Garcia-Ibaibarriaga, 2015; López-García, 2011; López-García et al., 2011b, 2011c, 2012b, 2012c, 2014b, 2015; Murelaga et al., 2012; Rey-Rodríguez et al., 2016; Talamo et al., 2016) (B) Stratigraphy of Abric Romaní with U/Th dates (Bischoff et al., 1988); (C) Level O surface in the excavation campaign of 2010; (D) Level O surface. Lines indicate areas with combustion structures; brick pattern corresponds to rock-shelter wall; in gray, areas included in the small-mammal taphonomic sample of this study.

paleoenvironment of southwestern Europe. In this paper, we analyze the paleoenvironment of Level O, the richest level for both archaeological and paleontological remains, undertaking the first complete analysis of the small-mammal assemblage, and considering the implications of these environmental conditions for Neanderthal occupations. A combination of paleontological approaches, including the taxonomic identification of small-mammal bone remains and their taphonomic characterization, is used to identify the origin of the assemblage and post-depositional processes. The analysis also takes into account other paleoenvironmental proxies for the Middle Paleolithic Abric Romaní sequence (from B to O; ca. 70–30 ka) and the paleoenvironmental context of the Iberian Peninsula, especially the northeastern part, during MIS 3.

2. Site description

The Abric Romaní archaeological site is a rock-shelter in the Quaternary travertine formation known as “Cinglera del Capelló”, located on the west bank of the Anoia River, near the town of Capellades (Barcelona, Spain). Its coordinates are 41°32′N and 1°41′E and its

altitude is 280 m.a.s.l. (Fig. 1A). The deposit was discovered in 1909 by Amador Romaní and the present excavations started in 1983 (Bartrolí et al., 1995; Carbonell et al., 1996, 1994). The exposed section is made up of a minimum thickness of 17 m of well-stratified travertine sediments. At present, sixteen levels have been excavated completely (labeled from A to P), most of them belonging to the Middle Paleolithic, with the exception of the uppermost Level A, which has been attributed to the Protoaurignacian (Carbonell et al., 1996; Giralt and Julià, 1996; Vaquero and Carbonell, 2012; Vaquero et al., 2013) (Fig. 1B). The Mousterian lithics, the faunal remains derived from butchering activities and the combustion structures preserved in the succession of layers indicate that Neanderthals occupied this site at different periods during MIS 4 and MIS 3. Dates obtained by U-series and ^{14}C AMS provide calendar ages from ca. 40 ka (Level A) to ca. 70 ka (from the base sediments) (Bischoff et al., 1988). However, new data from Sharp et al. (2016) have suggested that carbonate tufas extend at least 30 m beneath the current base of the excavation, reaching ~110 ka at the base of the core, with a possible human occupation as old as ~100 ka. The sequence can be considered a natural sequence punctuated by short periods of human occupation using the rock-shelter as a residential camp-site (Vaquero et al., 2013). The sedimentary rate is estimated to be approximately 0.46 mm/yr (Bischoff et al., 1988; Vaquero et al., 2013). Palynological analyses indicate a succession of five different climatic phases, between the final phase of MIS 4 and the Hengelo Interstadial (Burjachs and Julià, 1994). The pollen analysis is complemented by analyses of charcoals, phytoliths, herpetofauna, small mammals and ungulate tooth wear (Allué et al., 2017; Burjachs et al., 2012; Vaquero et al., 2013). The milder conditions documented at the bottom of the sequence progressed towards the interstadial climate in evidence in the topmost levels through cycles of warmer and colder events.

Archaeological Level O comprises poorly stratified sand and fine gravel with a weathered surface (Fig. 1C, D). These finer-grained deposits lie above a basal succession composed of gravel, blocks and megablocks originating from the fall of travertine rocks from the cliff above the rock-shelter (Vallverdú et al., 2012). The underlying and overlying travertine layers have been U-series dated to 54.24 ± 0.42 ka and 54.60 ± 0.40 ka, respectively (Bischoff et al., 1988). The excavated surface covers most of the originally occupied surface with an area of 271 m^2, and more than 40,000 archaeological remains have been reported, including lithic artifacts, faunal remains, charcoal, wood negatives and combustion structures have been reported. Malacofauna and small-mammal remains have also been recovered (Vallverdú et al., 2012; Chacón et al., 2013). Previous zooarchaeological and taphonomic analyses suggest that Neanderthals were the principal accumulator of large-mammal carcasses, with a small degree of intervention by carnivores and a humid fossilization microenvironment (Gabucio et al., 2018, 2012). Level O exhibits an elaborate technology based on the use of the Levallois flaking method, showing a marked technological difference with respect to the overlying levels, in which discoid knapping is dominant (Chacón et al., 2013; Bargalló, 2014; Bargalló et al., 2016; Picin and Carbonell, 2016). This technological shift is associated with a different use of the space in the settlement and could be related to a modification in the mobility patterns of the Neanderthals (Chacón et al., 2013; Picin and Carbonell, 2016). The paleoenvironmental conditions of Level O fall within the framework of pollen zone 3 (56.8–49.5 ka) (from Level O to J), characterized by short and abrupt oscillations within warmer and wetter episodes at intervals of about 10 kyr (Burjachs and Julià, 1994; Burjachs et al., 2012; López-García et al., 2014b). Previous works have included preliminary small-mammal analyses of Level O when fieldwork on this level was still in progress (Burjachs et al., 2012; Fernández-García et al., 2016; López-García, 2011, 2008; López-García et al., 2009; López-García and Cuenca-Bescós, 2010; López García, 2007).

3. Materials and methods

3.1. Recovery and taxonomic study of the material

The small mammal remains included in this analysis consist mainly of isolated teeth and disarticulated bones obtained from a random sediment sampling of the 271 m^2 surface of Level O, which take place over the course of eight excavation seasons (2004–2011). The remains were collected by washing and sieving the sediment, with two superimposed meshes of 5 mm and 1 mm, and selected by the subsequent sorting. The taxonomic identification is based on various reference criteria (Bab et al., 2007; Chaline, 1972; Cuenca-Bescós et al., 2014; Gosàlbez, 1987; López-García, 2011; Menu and Popelard, 1987; Nadachowski, 1982; Sevilla, 1988) and on a comparison with the reference collections of the *Institut Català de Paleoecologia Humana i Evolució Social* (*IPHES*) and the *Università degli Studi di Ferrara* (*UNIFE*). Specific identifications are based mainly on the best diagnostic elements: isolated teeth for Murinae, Glirinae and Sciuridae; first lower molars (m1) for Arvicolinae; mandible, maxilla and isolated teeth for Chiroptera and Soricomorpha; and mandible, isolated teeth and postcranial material for Talpidae. The remains were counted (NISP) and grouped using the minimum number of individuals (MNI) method, determined by counting the most highly represented diagnostic element, taking into account laterality, for each species.

3.2. Taphonomic analysis

The taphonomic study is based on the observation and description of the superficial alterations of skeletal elements (Andrews, 1990; Fernández-Jalvo et al., 2016), differentiating between alterations caused by predation (biostratinomic origin) and post-depositional alterations (biostratinomic or fossil diagenetic origin). According to Andrews (1990) and Fernandez-Jalvo and Andrews (1992), taphonomic effects of predation can be detected through the skeletal representation, breakages and, particularly, features of digestion. To determine the skeletal representation and the proportions of elements present, all the elements of the sample are considered (Andrews, 1990; Fernández-Jalvo and Andrews, 1992).

To evaluate the patterns of breakage and digestion, only incisors, molars and femora are included. For each skeletal element, the number of complete elements is compared to the number of fractured elements (Andrews, 1990; Fernández-Jalvo and Andrews, 1992). Nevertheless, the most important indicator in determining a predatory origin is the corrosion marks produced by gastric juices during digestion, which is the only type of alteration that cannot be confused with other agents. Digestion is a directional and progressive process (Fernández-Jalvo et al., 2016, 2014). In the present analysis, the proportion of fossil bones affected together with the degree of alteration is considered, distinguishing between light, moderate, heavy and extreme digestion (Fernández-Jalvo and Andrews, 1992; Fernández-Jalvo et al., 2016). The obtained results are compared with indices obtained for current reference predation collections developed by Andrews (1990). After the accumulation of the small mammal assemblage, post-depositional taphonomic processes occurred, including effects associated with roots, water abrasion, cementation, combustion, manganese oxide pigmentation and weathering (Fernández-López, 2000). To identify and

characterize these alterations, we used the criteria published by Shipman et al. (1984), Andrews and Cook (1985), Andrews (1990), Fernández-Jalvo (1992), Lyman (1994), Bennàsar (2010), Fernández-López (2000) and Cáceres (2002), among others. Our analysis evaluates molars, incisors and femora in terms of the absence/presence of these alterations and, in some cases, their degree and location.

3.3. Paleoenvironmental and paleoclimatic reconstruction

To reconstruct the ecological conditions prevalent during the deposition of Level O, several methodologies are used. Firstly, to assess the homogeneity of the environment, the species evenness and diversity is calculated (Margalef, 1974), using Paleontological Statistics (PAST) software (Hammer et al., 2001). Williams et al. (2002) associated a highly even community with complex and heterogeneous vegetation. The evenness of a community can be represented by Simpson's Diversity Index ($1 - \Sigma((n_i / n)^2)$, where n_i is the number of individuals of taxon *i*. This, allows us to quantify how equal communities are through numerical representation (between 0 and 1). A larger difference in species within communities results in a higher value for the evenness index (Simpson, 1949).

Climatic conditions prevailing during the formation of the assemblage are inferred by quantitative and qualitative methods. The quantitative method involves the chorotypes previously established for small-mammal faunas in Catalonia by López et al. (2006) and Sans-Fuentes and Ventura (2000), assigning each taxon to one chorotype according to its current climatic requirements and geographical distribution. The chorotypes differentiated are as follows: *chorotype 1* includes species with mid-European requirements; *chorotype 2* includes mid-European species tolerant of Mediterranean conditions; *chorotype 3* includes Mediterranean species; *chorotype 4* includes generalist species with a broad distribution (*Eliomys quercinus*, *Apodemus sylvaticus* and *Sciurus vulgaris*) or species with a particular habitat (such as *Arvicola sapidus*, *Pipistrellus pipistrellus* and *Nyctalus lasiopterus*), which in general provide little climatic information (Table 1) (Fernández-García and López-García, 2013).

The qualitative Mutual Ecogeographic Range (MER) method is used for a similar purpose. This method determines in which present geographical regions a given fossil species assemblage would be located through the intersection obtained from the overlap of the current distributions of each species, obtained from Palomo et al. (2007). The current climatic conditions of the intersecting area (Font-Tullot, 2007) are used to infer the past temperatures and precipitation levels, including the mean annual temperature (MAT), the mean temperature of the coldest month (MTC), the mean temperature of the warmest month (MTW), the mean annual precipitation (MAP), the mean precipitation of the winter months (DJF) and the mean precipitation of the summer months (JJA). Careful attention is paid to ensure that the real current distribution of each species corresponds to the potential ecological distribution and has not been strongly affected by other limiting or perturbing parameters (such as human impact or predation). Accordingly, *Iberomys cabrerae* is excluded because its current distribution is conditioned by anthropic factors. The little-known and generally fragmentary distribution of bat species precludes this order of mammals (Palomo et al., 2007). This method has already been applied to assemblages containing extant reptile and amphibian taxa (Blain et al., 2009, 2016) and to Late Pleistocene small-mammal assemblages (López-García, 2011). The results of our analysis were compared to the present climatic conditions for the Capellades region provided by Ninyerola et al. (2003).

Finally, the landscape is reconstructed using the Habitat Weighting Method, employed by Evans et al. (1981) and Andrews (2006). This method is based on the distribution of each taxon in the habitat(s) in which it is currently present on the Iberian Peninsula (Palomo et al., 2007), considering five main habitat types: open dry, open humid, woodland, rocky and water (López-García et al., 2011a). Each species is given a maximum score of 1.00, which is divided among the habitat types according to its habitat preferences (Table 1).

4. Results and discussion

4.1. Origin of the small-mammal assemblage

The taphonomic analysis includes 2268 elements (MNI: 160). The differential anatomical representation (the relative abundance and the proportional elements representation), the high presence of fragmentation, and especially the detection of digestion marks on the analyzed elements indicate that a considerable portion of the small-mammal

Table 1
Number of identified specimens (NISP), minimum number of individuals (MNI) and the percentage of MNI through the assemblage of small mammals of level O from Abric Romaní. C1, chorotype 1; C2, chorotype 2; C3, chorotype 3; C4, chorotype 4; OD, open dry; OH, open humid; WO, woodland; R, rocky; WA, water.

	Recount			Chorotypes				Habitat				
Taxon	NISP (n)	MNI (n)	MNI (%)	C1	C2	C3	C4	OD	OH	WO	R	WA
Microtus agrestis	47	25	8.8		x				0.5	0.5		
Microtus arvalis	54	30	10.56	x				0.5		0.5		
Iberomys cabrerae	87	45	15.85			x			0.5	0.5		
M. (Terricola) duodecimcostatus	46	25	8.8			x			0.25	0.5	0.25	
Arvicola sapidus	284	55	19.37				x					1
Apodemus sylvaticus	327	69	24.3				x			1		
Eliomys quercinus	55	8	2.82				x			0.5	0.5	
Sciurus vulgaris	10	2	0.7				x			1		
Rodentia indet.	1195											
Crocidura russula	17	3	1.06			x		0.5		0.5		
Sorex gr. *araneus-coronatus*	3	2	0.7	x					0.5	0.5		
Sorex minutus	1	1	0.35		x				0.5	0.5		
Neomys gr. *fodiens-anomalus*	10	2	0.7	x					0.25			0.75
Talpa europaea	31	7	2.46		x				0.75	0.25		
Soricidae indet.	10	7	2.46									
Pipistrellus pipistrellus	1	1	0.35				x			0.5	0.5	
Nyctalus lasiopterus	6	1	0.35				x			1		
Chiroptera indet.	1	1	0.35									
Indet.	481											
Total	2666	284	100									

Table 2
Taphonomic analysis synthesis, including recount (number of identified specimens; minimum number of individuals), predation alterations (skeletal representation, proportion representation indexes, breakage and digestion) and post-depositional alterations. The Relative Abundance Index compare the number of skeletal elements recovered with the expected number of each element multiplied by MNI; the proportion postcranial/cranial ratio relates the number of postcranial elements (humerus, radius, ulna, femur and tibia) to cranial ones (mandible, maxillae and isolated molars). Digestion and post-depositional analyses are performed on incisors, molars and femurs (NISP: 1327).

Recount	
NISP (n)	2268
MNI (n)	160
Skeletal representation	
Relative Abundance Index (%)	29.1
SD of Relative Abundance Index	24.9
Proportional representation indexes	
Postcranial/cranial Index	0.69
Humerus + femur/maxilla + mandible index	0.03
Radius + tibia/humerus + femur index	0.78
Isolated molars/empty alveolus index	1.47
Breakage	
Incisors fracture (%)	67.3
Molars fracture (%)	41
Femora fracture (%)	96.5

Digestion	(n)	(%)
Total of digested elements	401	39.3
Light degree	277	27
Moderate degree	101	10
Heavy degree	23	2.3
Extreme degree	0	0
Digested incisors	151	40.5
Light degree	115	31
Moderate degree	30	8
Heavy degree	6	1.5
Extreme degree	0	0
Digested molars	191	33
Light degree	119	20.5
Moderate degree	55	9.5
Heavy degree	17	3
Extreme degree	0	0
Digested femora	59	89.4
Light degree	43	65.2
Moderate degree	16	24.2
Heavy degree	0	0
Extreme degree	0	0

Post-depositional agents	(n)	(%)
Cracking for humidity and temperature changes	332	79.6–25
Desquamation	92	6.9
Manganese oxide pigmentation	625	47.1
Plant activity	600	45.2
Cementation	175	13.2
Burned	192	14.5
Water abrasion	73	5.5
Weathering	3	0.2

accumulation in Level O is associated with predation (Table 2; Fig. 2). The breakage rates and the proportional skeletal representation are not coherent with the expected pattern for any of the predators considered by Andrews (1990) and are probably related with post-depositional agents, as is common in archaeological contexts. Indeed, only 6% of the molars and 2% of the incisors were found *in situ*. These results reinforce the importance of digestion marks, such as the only diagnostic alteration, over other proxies in the determination of predation (Bennàsar, 2010; Bennàsar et al., 2016; Fernández-Jalvo, 1992; Fernández-Jalvo et al., 2016, 2014; López-García et al., 2014a). At least 40% of the elements exhibit digestion marks, demonstrating the predatory origin of the assemblage: 40% of incisors, 32% of molars and 89% of femora. The predominant digestion marks are light in degree (27%), but a significant presence of moderate (10%) and some heavy digestion marks (2.3%) are also observed.

Digestion is progressive, sequential and dependent on several parameters, such as digestion time, predator age or even the position in the predator's stomach (Andrews, 1990; Duke et al., 1975; Fernández-Jalvo et al., 2014). The homogeneity observed in the assemblage, considering the progressive proportion of degrees of digestion, is indicative of a single predator and rules out mixtures of different predator types (Bennàsar, 2010). The percentage of small-mammal incisors, molars and femora showing digestion marks and the degree of alteration point to the presence of a category 3 predator as defined by Andrews (1990), capable of intermediate modification. Candidates include two different nocturnal raptors: the tawny owl (*Strix aluco*) or the Eurasian eagle-owl (*Bubo bubo*) (Andrews, 1990; Fernández-Jalvo and Andrews, 1992; Fernández-Jalvo et al., 2016). Both are currently present in the Anoia region (Jiménez, 2003) and have been common in Iberia since the Early Pleistocene (Arribas, 2004). It is difficult to differentiate between the accumulations produced by these two avian predators, although there are small differences. In general terms, *S. aluco* tends to produce concentrations with higher rates of breakage, higher percentages of digested elements and a higher number of strongly digested teeth than *B. bubo*, which rarely produces alterations exceeding the moderate degree (Andrews, 1990; Fernández-Jalvo and Andrews, 1992; López-García et al., 2014a). For these reasons, *S. aluco* is considered the probable accumulator of the small-mammal remains from Level O. Additionally, the general range and size of the species in the fossil assemblage are coherent with the modern tawny owl diet (Olsson, 1979; Andrews, 1990; Kowalski, 1995; Palomo et al., 2007).

The tawny owl is a strongly territorial and sedentary raptor that remains year round in the nesting territory, which is restricted in size (8–75 ha). This owl nests in rocky soil, in rock crevices or in tree holes (Mikkola, 1983; Andrews, 1990; Svensson, 2010). The hunting behavior of this predator involves no preferential criteria in selecting taxa, as it is an extremely opportunistic feeder. It adjusts its behavior to the environment and its diet to whatever is available in its particular hunting territory. Usually, its hunting range is restricted to less than 1 km from the nest (Andrews, 1990; König et al., 1999; Mikkola, 1983; Svensson, 2010). Consequently, its prey assemblage is extremely diverse (coherent with the high diversity detected in the studied assemblage) and constitutes a good record of the nearby ecosystem inhabited by this predator. The enlarged sample of the present work provides enough remains to undertake a complete taphonomic analysis and rule out preliminary attribution to a Category 1 predator (such as *Asio otus* or *Tyto alba*) (López-García et al., 2014b). Even though the tawny owl inflicts major digestion damage on the remains, it is also an eclectic predator and, like *Asio otus* and *Tyto alba*, is not likely to have produce a significant representation bias in the fossil assemblage. Therefore, the fossil assemblage from Level O is assumed to preserve consistent relative species abundances from the past environment of the Abric Romaní region and can be used to develop paleoecological interpretations.

4.2. Post-depositional processes and taphonomic history

After the deposition of pellets by the predator, post-depositional agents will affect the small-mammal remains (Fernández-López, 2000) (Fig. 3). The most common effects detected in Level O are related to changes in temperature and humidity (striations, 79.6%; fissures, 68.6%; cracks, 25%), the presence of water (manganese oxide, 47.1%; abrasion, 5.5%), plant activity (chemical corrosion, 45.2%) and the use of fire at the site (burned bones, 14.5%) (Table 2). To a lesser degree, cementation is also observed (13.2%). None of the alterations shows a taxonomic or anatomical preference, and the alterations are homogeneously distributed across the surface of the level. All the post-

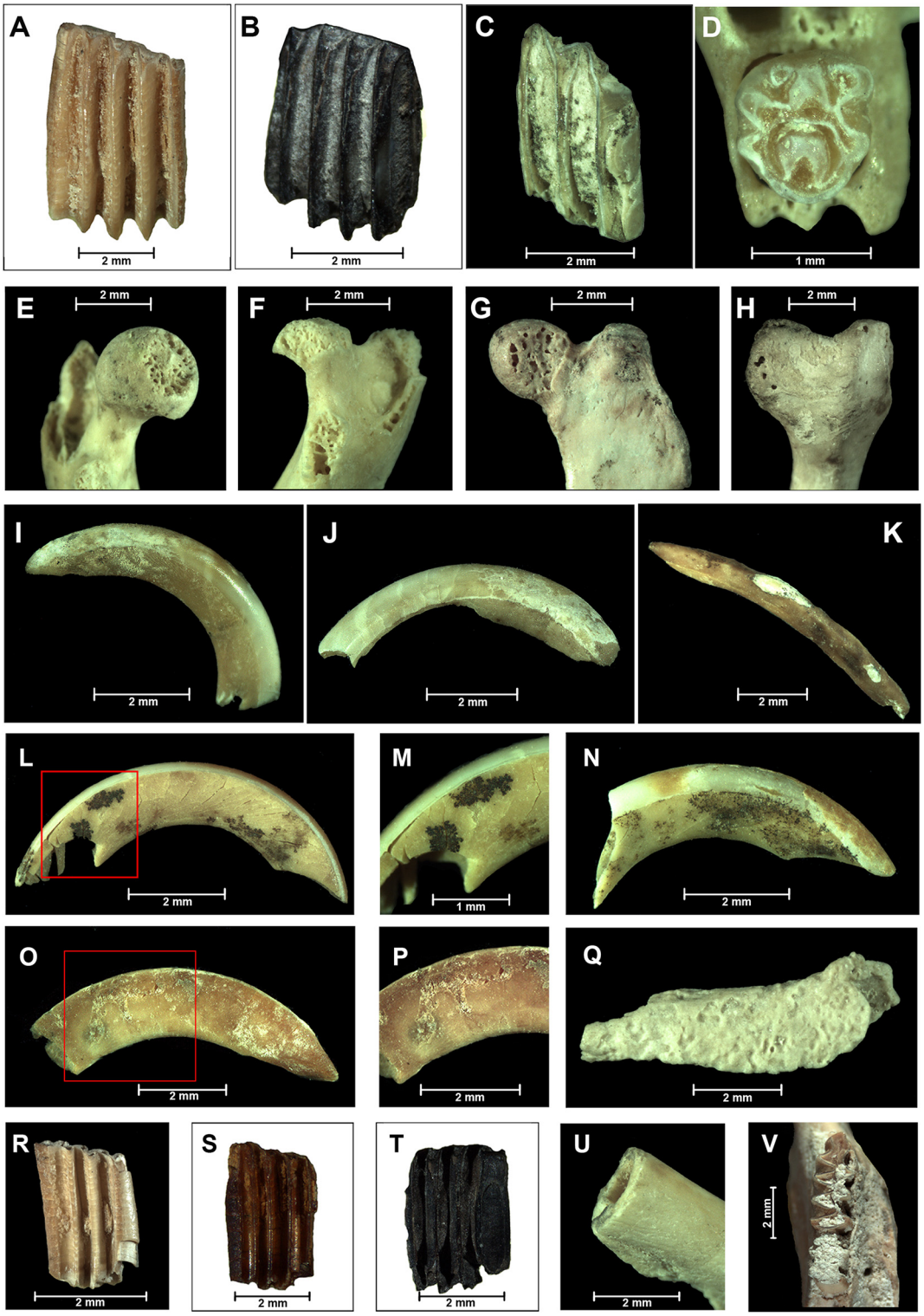

Fig. 2. Taphonomic features associated with the small-mammal remains from Level O. (A) right m1 *Arvicola sapidus* with light digestion; (B) left m1 *Iberomys cabrerae* with moderate digestion; (C) upper molar Arvicolinae with heavy digestion; (D) right M2 *Apodemus sylvaticus* with moderate digestion; (E) proximal epiphysis of a rodent left femur with light digestion; (F) proximal epiphysis of a rodent right femur with moderate digestion; (G) proximal epiphysis of *Talpa europaea* left femur with light digestion; (H) distal epiphysis of *Talpa europaea* left femur with light digestion; (I) rodent upper incisor with light digestion; (J) rodent upper incisor with moderate digestion; (K) rodent lower incisor with heavy digestion; (L) rodent upper incisor with dispersed manganese oxide pigmentation; (M) detail of manganese oxide pigmentation; (N) rodent upper incisor with dispersed manganese oxide pigmentation; (O) rodent upper incisor with chemical corrosion associated with roots; (P) detail of chemical corrosion; (Q) rodent left femur with generalized root corrosion; (R) left m1 *Arvicola sapidus* with cracking due to changes in humidity; (S) left m1 *Iberomys cabrerae*, burned (Grade 2); (T) Arvicolinae molar, burned (Grade 3); (U) rodent right femur with rounded breaking edge; (V) right mandible *Arvicola sapidus* with cement concretion.

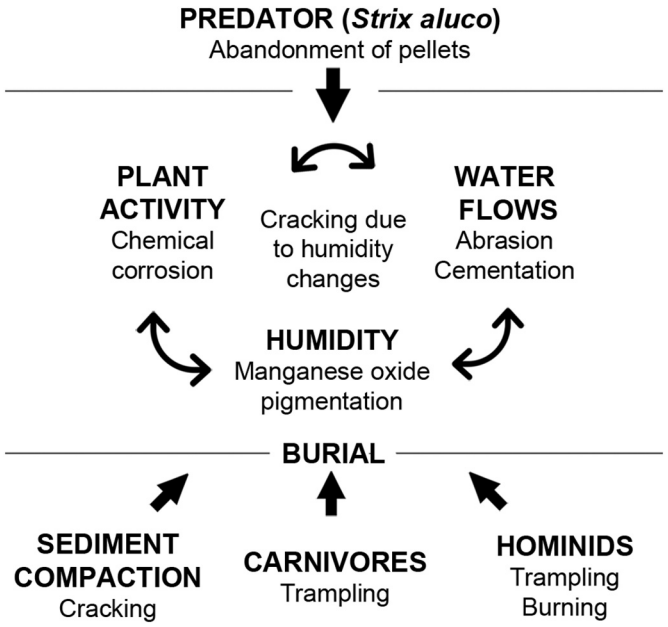

Fig. 3. Simplified taphonomic sequence to explain the formation of the Level O small mammal assemblage.

depositional alterations are coherent with a fossiliferous rock-shelter environment (Fernández-Jalvo, 1992) that combines open-environment agents (such as plant activity) with common karst agents characterized by humidity patterns (for instance, manganese oxide precipitation).

Some of the alterations suggest an important presence of water, related to a wet environment (evidenced by chemical corrosion), abrupt humidity changes (evidenced by cementation and fissures) or flooding (evidenced by manganese oxide). Marín-Arroyo et al. (2014) also associated manganese oxide with a high proportion of abandoned organic matter produced by intensive human occupations. According to Gabucio et al. (2012), this site can be described as a humid fossiliferous microenvironment, characterized by wet conditions and the reactivation of water flows and flooding, which is consistent with the underground streams responsible for the formation of the travertine rock-shelter (Vallverdú et al., 2012). The high rates of breakage, previously noted as incoherent with any of the predation patterns defined by Andrews (1990) (Table 2), are probably related to changes in the humidity level and possibly trampling and sediment compaction. Chemical corrosion, evidence of plant activity, is probably associated with mosses (Gabucio et al., 2012, 2018; Vallverdú et al., 2012; Vaquero et al., 2013). Even though water was present, no transport is detected, due to the low presence of abrasion modifications (with consistently low degrees of polishing and rounding) (Cáceres, 2002). Nevertheless, differential dynamic transport could be related to the low weight and density of small-mammal remains (Korth, 1979; Fernández-Jalvo and Andrews, 2003). In any case, all the taphonomic evidence confirms an *in situ* accumulation of remains, ruling out considerable transport dynamics. Therefore, *S. aluco* likely established its roost in one of the fissures of the rock-shelter, leaving the pellets in the substrate (Olsson, 1979; Svensson, 2010). Moreover, the absence of desquamation and weathering rules out long and continuous exposure to meteorological agents (Fernández-Jalvo et al., 2002), coherent with the site conditions and with the inferred rapid burial dynamics (Bischoff et al., 1988; Vaquero et al., 2013; Sharp et al., 2016).

In comparison with previous zooarchaeological studies (Gabucio et al., 2012, 2018), with the exception of anthropic, carnivore and rodent modifications, all the alterations observed in the large-mammal assemblage are present in the small-mammal assemblage. This confirms the *in situ* nature of the whole deposit. A comparison in spatial terms (Bargalló et al., 2016; Gabucio et al., 2014, 2018) shows homogeneity between small- and large-mammal remains in the spatial distribution of alterations, indicating a unitary taphonomic pattern, with only a few differences probably related to short-distance water transport. In any case, post-depositional alterations have not caused considerable damage to the assemblage as a whole.

4.3. Identified species of small mammals

Level O presents the richest small-mammal assemblage in the whole archaeological sequence (López-García, 2011; Burjachs et al., 2012). From the number of identified specimens (NISP) of 2666, 990 elements have been identified at the species level, representing 284 individuals (MNI) that belong to 15 different taxa: five insectivores (*Crocidura* cf. *russula*, *Sorex* gr. *araneus-coronatus*, *Sorex minutus*, *Neomys* gr. *fodiens-anomalus* and *Talpa europaea*); two chiropters (*Pipistrellus pipistrellus* and *Nyctalus lasiopterus*) and eight rodents (*Apodemus sylvaticus*, *Arvicola sapidus*, *Iberomys cabrerae*, *Microtus* (*Terricola*) *duodecimcostatus*, *Microtus agrestis*, *Microtus arvalis*, *Eliomys quercinus* and *Sciurus vulgaris*) (Table 1; Fig. 4). With respect to preliminary published works (López-García et al., 2014b), the present study has incorporated 2451 remains, at least 175 individuals, and found four new taxa not previously identified in Level O: *P. pipistrellus*, *S. vulgaris*, *N.* gr. *fodiens-anomalus* and *S. minutus*. The latter three are identified for the first time in the Abric Romaní sequence.

The wood mouse (*A. sylvaticus*) is the most abundant taxon in Level O (24%). This species is a generalist but is usually associated with forested environments in a temperate climate without major climatic constraints (Palomo et al., 2007). Consequently, this species is currently highly widespread on the Iberian Peninsula, and its occurrence in the Late Pleistocene sites of northeastern Iberia is common (Palomo et al., 2007; Fernández-García et al., 2016). The second most frequent species (19%), the southwestern water vole or *A. sapidus*, is an endemic Gallaic-Iberian species that occurs only in freshwater habitats, without specific climatic restrictions (Louarn and Quéré, 2003; Palomo et al., 2007). Cabrera's vole (*I. cabrerae*; 15%) and the Mediterranean pine vole (*M.* (*T.*) *duodecimcostatus*; 8%) are endemic Iberian species with typically Mediterranean requirements. Representing lower proportions of the assemblage, both the common vole (*M. arvalis*; 10%) and the field vole (*M. agrestis*; 8%) are associated with open environments, low humidity and cold temperatures. Currently, they are present in the mountainous regions in the north and the center of the Iberian Peninsula (Palomo et al., 2007; Fernández-García et al., 2016).

All the species from Level O are common in the Late Pleistocene Iberian sites (Sesé, 1994; Cuenca-Bescós et al., 2010; López-García, 2011; Fernández-García et al., 2016), with the exception of the chiropters and the red squirrel (*S. vulgaris*). Level O of Abric Romaní includes one of the most ancient records of *I. cabrerae* in northeastern Iberia (López-García, 2011). *N. lasiopterus* and *P. pipistrellus* are unusual taxa in Late Pleistocene sites. *N. lasiopterus* has been recorded in Cueva del Agua (Sevilla, 1988) and Cova dels Xaragalls (López-García et al., 2012a); being the specimen from Level O the second oldest in Catalonia (López-García, 2011; López-García et al., 2009). *P. pipistrellus* is only recorded in other levels of Abric Romaní, in Cova Colomera (López-García et al., 2010) and in Cueva del Agua (Sevilla, 1988). The occurrence of *S. vulgaris*, as ascertained in Abric Romaní (Fernández-García et al., 2016), is also rare in the Pleistocene of the Iberian Peninsula. Although nowadays it is common in the north, it is strange to find this species in fossil deposits prior to Holocene (López-García, 2011; Sesé, 2011). Its presence in northern Iberia is only recorded in Cova del Coll Verdaguer (Daura et al., 2017) and in old excavations at Cova del Gegant (Estévez, 1980), however it has not been detected in the subsequent revisions of the small-mammal assemblage of Cova del Gegant (López-García et al., 2012c, 2008).

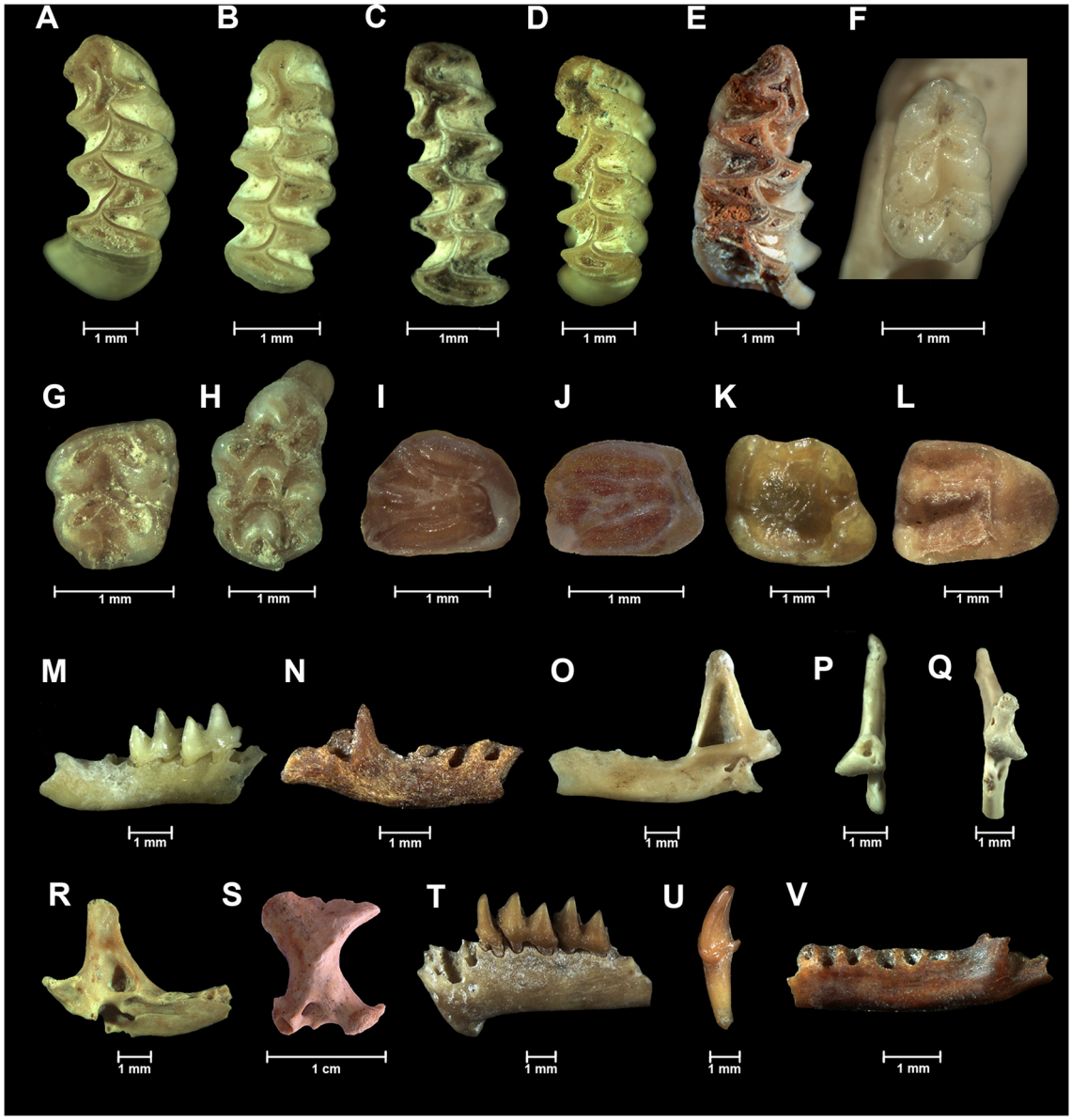

Fig. 4. Small-mammal species identified in Level O of Abric Romaní. (A) left m1 *Arvicola sapidus* (occlusal view); (B) left m1 *Microtus arvalis* (occlusal view); (C) left m1 *Microtus agrestis* (occlusal view); (D) left m1 *Microtus* (*Terricola*) *duodecimcostatus* (occlusal view); (E) right m1 *Iberomys cabrerae* (occlusal view); (F) left m1 *Apodemus sylvaticus* (occlusal view); (G) right m2 *Apodemus sylvaticus* (occlusal view); (H) left M1 *Apodemus sylvaticus* (occlusal view); (I) left m1-m2 *Eliomys quercinus* (occlusal view); (J) right M1-M2 *Eliomys quercinus* (occlusal view); (K) right m1 *Sciurus vulgaris* (occlusal view); (L) right M1 *Sciurus vulgaris* (occlusal view); (M) right mandible *Crocidura russula* (buccal view); (N) right mandible *Sorex minutus* (buccal view); (O) right mandible *Sorex* gr. *araneus-coronatus* (lingual view); (P) right mandible *Sorex* gr. *araneus-coronatus* (posterior view); (Q) left mandible *Neomys* gr. *fodiens-anomalus* (posterior view); (R) left mandible *Neomys* gr. *fodiens-anomalus* (lingual view); (S) left humerus *Talpa europaea*; (T) left mandible *Nyctalus lasiopterus* (buccal view); (U) left Ci *Nyctalus lasiopterus* (buccal view); (V) left mandible *Pipistrellus pipistrellus* (buccal view).

4.4. Paleoenvironmental reconstruction

Level O possesses a high species richness and diversity. Fifteen small-mammal taxa are recorded in the assemblage, and the Simpson's Diversity Index is 0.84, indicating that the species are approximately numerically equal and that no one species dominates the assemblage. From a paleoecological perspective, this may be related to stable environmental conditions and heterogeneous vegetation (woodland) capable of sustaining such diversity (Margalef, 1974); evenness is usually coherent with a high presence of forest species (Williams et al., 2002). Comparison of our results with the species currently present in the site area (Gosàlbez, 1987; Jiménez and Tomás, 2009; Palomo et al., 2007) reveals a slight decrease in the diversity and several faunal replacements, as well as the disappearance of mid-European species such as *M. agrestis* and *M. arvalis*.

The small-mammal chorotype distribution in Level O indicates a preponderance of generalist taxa or taxa without particular climatic requirements (chorotype 4: 49.3%) (Fig. 5), as evidenced by the high proportion of *A. sylvaticus* and *A. sapidus*. Nevertheless, the similar proportion of Mediterranean (chorotype 3: 26.4%) and mid-European species (chorotype 1 and 2: 24.3%) is remarkable. Concurrently, the Mutual Ecogeographic Range (MER), connects this assemblage with

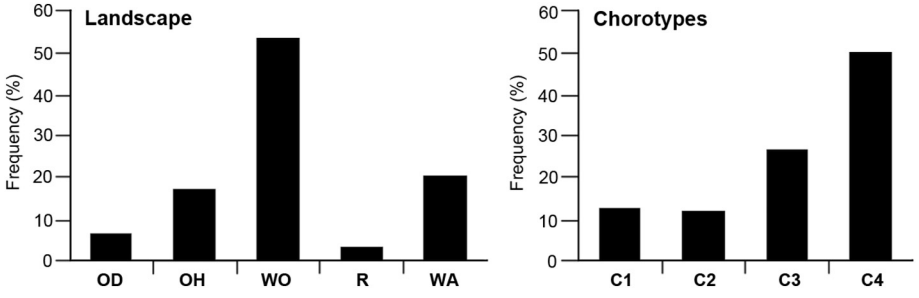

Fig. 5. Distribution by chorotype and landscape preferences of the small mammals from Level O of Abric Romaní. C1, chorotype 1 (mid-European species); C2, chorotype 2 (mid-European species tolerant of Mediterranean conditions); C3, chorotype 3 (Mediterranean species); C4, chorotype 4 (generalist species or species with a particular habitat, which provide little climatic information); OD, open dry (meadows with seasonal change); OH, open humid (evergreen meadows with dense pastures and suitable topsoils); WO, woodland (mature forest including woodland margins and forest patches, with moderate ground cover); R, rocky (areas with suitable rocky or stony substratum); WA, water (areas along streams, lakes and ponds).

seven geographical points (10 × 10 km UTM) located in the northern Iberian region: five in the Cantabrian area (30TVN12; 30TVN33; 30TVN46; 30TVN74; 30TVN85), one in the Ebro Valley (30TVN14), and one in the Catalan Pre-Pyrenees (30TDG38). The present climatic data for these regions, when compared with current climatic information for Capellades (Ninyerola et al., 2003), show lower temperatures (MAT between − 3 and −4 °C; MTC between −2 and −3 °C; MTW between −3 and −4 °C). However, the annual precipitation levels are only slightly higher than at present for Capellades (MAP: between +70 and +170 mm), and the winter precipitation is also slightly higher (DJF: between +60 and +80 mm) (Table 3). Notable differences are detected between this reconstruction and previous paleotemperature estimations for Level O (Burjachs et al., 2012; López-García, 2011; López-García et al., 2014b), such as an increase of +2.5 °C in the MAT and a decrease of -100 mm in the MAP. This is related to new identified species, warning us of the effect that a larger small-mammal sampling can have in drawing paleoenvironmental inferences. For the habitat reconstruction, the Habitat Weighting Method indicated that the area surrounding the site featured an extended open-woodland environment, as confirmed by the presence of forest dwellers (52%) (*A. sylvaticus*, *S. vulgaris* and *N. lasiopterus*) and open-environment taxa (18%) (*M. arvalis*, *M. agrestis* and *T. europaea*). The existence of stable watercourses close to the rock-shelter is confirmed by water-dependent specimens (20%) (*A. sapidus* and *N.* gr. *fodiens-anomalus*) recovered from Level O (Fig. 5). The presence of water is likely related to the Anoia River, which flows at the foot of the site, and to the hydrologic dynamics (i.e., water streams) directly associated with the formation of the site (Vallverdú et al., 2012). The landscape reconstruction undertaken in the present study differs substantially from previous reconstructions (Burjachs et al., 2012; López-García, 2011), underlining the importance of forest at the expense of open spaces (wet and dry) and the aquatic component. The ecological behavior of the predator responsible for the small-mammal assemblage, *Strix aluco*, coincides with this habitat. In fact, the tawny owl is considered the most common woodland owl in Europe (Mikkola, 1983; Andrews, 1990); it is usually found in deciduous and mixed forests with forest clearings (Jutglar and Masó, 1999; König et al., 1999; Mikkola, 1983; Svensson, 2010). Presently, it is widely distributed on the Iberian Peninsula. It is considered a Palearctic species, and its distribution in the past was likely similar to its present distribution but reaching more southern latitudes during cold periods (Arribas, 2004).

Table 3
Temperatures and precipitation estimates of the for Level O of Abric Romaní, using the Mutual Ecogeographic Range based on 10 × 10 km UTM squares with equivalent species presence, and modern climatic data of the site. The 10 × 10 km UTM square names (e.g., 30TDG38) are taken from http://www.aitorgaston.com/utm10.php. Mean, average values obtained; Max, maximum values obtained; Min, minimum values obtained; SD, standard deviation; MAT, mean annual temperature; MTC, mean temperature of coldest month; MTW, mean temperature of warmest month; MAP, mean annual precipitation; DJF, mean precipitation of winter months; JJA, mean precipitation of summer months. Temperature data in degrees centigrade (°C) and precipitation data in millimeters (mm).

	MAT	MTC	MTW	MAP	DJF	JJA
30TDG38	11	4	19	1000	129	138
30TXN14	11	4	21	1000	204	131
30TVN74	11	3	18	1000	204	131
30TVN85	11	3	18	1000	204	131
30TVN33	12	3	18	700	136	71
30TVN46	12	2	17	700	256	102
30TVN12	12	5	17	700	136	71
Mean	**11.4**	**3.4**	**18.3**	**871**	**181**	**111**
Max	12	5	21	1000	256	138
Min	11	2	17	700	129	71
SD	± 0.53	± 0.97	± 1.38	± 160	± 48	± 29
Current data	**14-15**	**5-6**	**21-22**	**700-800**	**100-120**	**100-120**

MIS 3 is characterized by large climatic oscillations within a cool general context. After the cold episodes, large and rapid temperature increases occurred, followed by a progressive cooling (Arrizabalaga, 2004; Harrison and Sanchez Goñi, 2010). The lower temperature estimates (MAT: −4/−3 °C; MTC: −2/−3 °C) and the large differences between winter and summer temperatures (a difference of 15 °C between MTC and MTW), which are features more common for Atlantic areas than for the Mediterranean coast (Fletcher et al., 2010), relate Level O with a cool period. Moreover, the presence of some species that currently inhabit high latitudes (*S.* gr. *araneus-coronatus*, *T. europaea*, *M. arvalis*, *M. agrestis* and *Rana temporaria*) (Burjachs et al., 2012; López-García et al., 2014b; Sans-Fuentes and Ventura, 2000) and the equal proportion of Mediterranean and mid-European taxa are common features in Iberia during cold episodes (Sommer and Nadachowski, 2006). Considering the chronology of Level O (54.24 ± 0.42 ka; 54.60 ± 0.40 ka) (Bischoff et al., 1988; Vaquero et al., 2013), it could be related with a stadial episode, probably between IS15 (55.8 ± 1.2 ka b2k) and IS14 (54.2 ± 1.2 ka b2k) (Svensson et al., 2008; López-García et al., 2014b), enclosing previous correlations based on archaeobotanical analysis (Burjachs et al., 2012). The high levels of precipitation and the forested habitat indicate humid conditions for this cool period. The correlation agrees with the palynological and anthracological studies (Burjachs and Julià, 1994; Burjachs et al., 2012), which characterize this phase as generally cool, interrupted by short, hot, wet episodes. Both proxies reflect equivalent landscapes and humid environments for the level, with the arboreal taxa (*Artemisia*, Poaceae and *Pinus*) representing between 62 and 81% of the total pollen in the palynological studies. Finally, it is interesting to observe the climatic conditions of Level O whitin the Abric Romaní sequence (Table 4.) According to previous small-mammal data from the site (Burjachs et al., 2012; López-García et al., 2014a, 2014b), all the levels present lower temperatures than currently (−2.5 °C and −4.7 °C), but

Table 4
Mean annual temperature (MAT) and mean annual precipitation (MAP) estimates for Abric Romaní levels with high MNI content. Level O data belong to this work estimations; previous works provided upper levels estimates: (*) López-García et al., 2014b; (**) Burjachs et al., 2012. To allow comparison with previous small-mammal studies, corrections related to the climatic source are apply (this work uses Ninyerola et al. (2003) rather than Font-Tullot (2000) employed in previous works).

Level	Chronology (ka BP)	Climatic event	MAT (°C)	MAP (mm)
D	49–44.9	Interstadial 12**	−3.3/−4.3	−160/−60
E	49	Heinrich event 5*	−3.7/−4.7	−48/+48
J	51–49		−3.4/−4.4	−160/−60
N	54.6	Interstadial 16**	−2.5/−3.5	−130/−30
O	54.2	Stadial 17–15	−3/−4	+70/+170

not all of them are more humid than at present (between −160 mm and +170 mm). Level O is the most humid level but not the coldest, which is Level E (−3.3 °C to −4.3 °C), correlated with Heinrich Event 5 by López-García et al. (2014b). Regarding the landscape, species associated with woodland are always present. This is also confirmed by the pollen and charcoal analyses, which indicate that arboreal coverage was maintained throughout the sequence, with just brief decreases (Burjachs et al., 2012; Vaquero et al., 2013; Allué et al., 2017). Instead of the differential occupational pattern detected for Level O in relation to the upper levels (Gabucio and Bargallo, 2012; Chacón et al., 2013; Picin and Carbonell, 2016), major changes are not detected in the environment by small-mammal analysis. Even so, it has been shown that when the sample size is increased for a particular level, the estimations of the climatic parameters may well differ; accordingly, paleotemperature reconstructions of these levels should be taken with caution, since the MNI is low throughout the sequence (MNI = 16–39), with the sole exception of Level O.

4.5. Environmental aspects of the Neanderthal occupations in Iberia during MIS 3

Middle Paleolithic sites with a significant human presence are scarce in Iberia almost until the arrival of MIS 3. This period is related to globally warm conditions characterized by extended forest cover and interrupted by semiarid and cool phases (Burjachs and Julià, 1994; D'Errico and Sánchez Goñi, 2003; Sánchez Goñi and D'Errico, 2005; Sánchez Goñi et al., 2008; Fletcher et al., 2010). There are many Middle Paleolithic sites located in the northeast of Iberia during MIS 3. In some cases, complete climatic reconstructions have been based on small mammals, such as level III (45,870–44,840 cal yr B.P.) and II (44,210–33,060 cal yr B.P.) of Teixoneres cave, level IV of Cova del Gegant (60,000 ± 3800 cal yr B.P.) and level I of Arbreda cave (45,840–41,410 cal yr B.P.) (López-García, 2011; López-García et al., 2015, 2014b, 2012b, 2012c; Talamo et al., 2016) (Fig. 1A; Fig. 6). Irrespective of whether they shown a stadial or an interstadial correlation, all these assemblages indicate a cold (6–10 °C) and humid climate (870–1500 mm precipitation) related to major presence of forest (always greater than 60%). The temperatures are lower than at present (between −9.1 and −5.3 °C) and the precipitation levels are higher (between +692 and +349 mm). Level O fits within this general climatic context.

This is in accordance with the climatic pattern that López-García

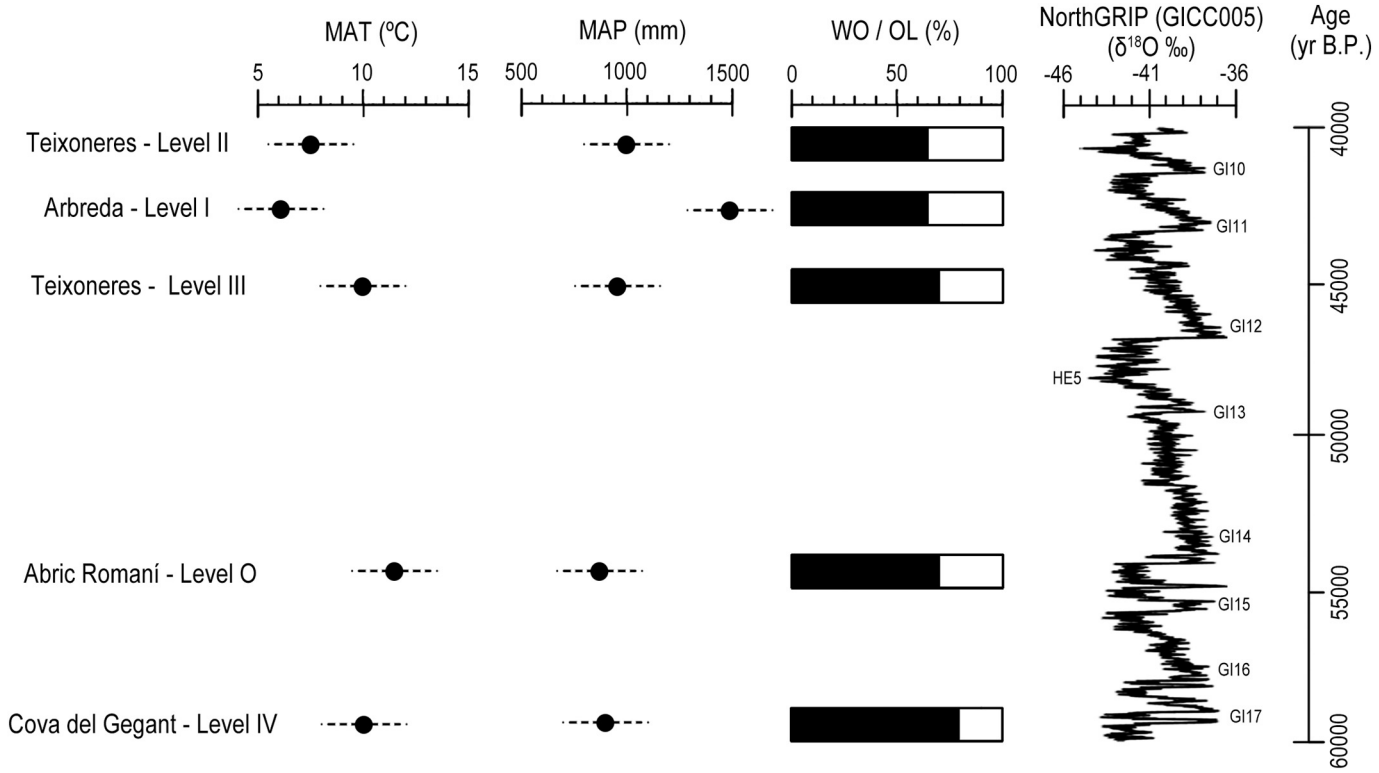

Fig. 6. Mean annual temperature (MAT) and mean annual precipitation (MAP) estimates and woodland (WO) vs. open landscape (OL) proportions from five northeastern Iberian sites, provided by previous small vertebrate studies (López-García, 2011; López-García et al., 2015, 2014b, 2012b, 2012c; Talamo et al., 2016). The assemblages are correlated with the NorthGRIP $\delta^{18}O$ curve, published by Svensson et al. (2008).

et al. (2014b) associated with Neanderthals in northeastern Iberia during MIS 3, based on lower temperatures and higher precipitations than at present and a major presence of an open woodland habitat. In all these Middle Paleolithic sites, temperatures oscillated but the precipitation levels and woodland estimates were always high. This is evidenced by assemblages with oscillations in the balance of Mediterranean and mid-European taxa but the continuous presence of woodland dwellers. This scheme seems to become a little more complex when other MIS 3 archaeological sites with small-vertebrate studies from throughout Iberia are considered. The considerable environmental differences among the different regions of the Iberian Peninsula, with a mix of Atlantic, Mediterranean and continental influences, have to be taken into account. Some archaeological sites exhibit diverse dynamics, such as El Mirón cave, Zafarraya and Ibex cave (Barroso et al., 2014; Finlayson et al., 2016), but the overall trend seems to fit well with the northeastern pattern of lower temperatures than at present and the major presence of the forest biotope integrated within mosaic environments with high levels of humidity. This pattern is recorded at Lezetxiki II, Askondo, Cueva del Conde, Vanguard cave and Gorham's cave (López-García et al., 2011b, 2011c; Murelaga et al., 2012; Blain et al., 2013; Garcia-Ibaibarriaga, 2015; Finlayson et al., 2016). Similar environmental characteristics are also in evidence in level 3 of Cova Eirós (Rey-Rodríguez et al., 2016), subunit Xb of El Salt (Fagoaga et al., 2017) and Cova del Coll Verdaguer (Daura et al., 2017), three sites with chronologies close to Level O but geographically and climatically different.

This general situation is coherent with palynological studies that have suggested that southern Europe (below 40°N) never experienced a complete loss of woodland, even in stadials or Heinrich Events (Fletcher et al., 2010; Harrison and Sanchez Goñi, 2010), making Iberia an optimal region for human occupation. The maintenance of woodland cover or at least mosaic landscapes preserves the ecological quality of the surrounding area. Indeed, the Neanderthal occupations at Abric Romaní are probably more closely related to the conditions of ecological and faunal diversity that an open woodland landscape allows, than to any specific climatic condition. Also, it is well-known that fuel wood for fire production played an important role in Neanderthal settlements, as occurs in Abric Romaní (Vallverdú et al., 2012; Allué et al., 2017). Bearing in mind other Iberian Middle Paleolithic sites, our results suggest that the climate instability of MIS 3 within the cool global context had no real impact on the Neanderthal populations that occupied the northeastern part of the Iberian Peninsula at the time, remaining unclear what effects this instability could have exerted on their shifts in adaptive behavior that are evidenced in the Abric Romaní sequence. In environmental terms and in accordance with previous studies of the Late Pleistocene in the northeastern Iberia, a general preference for woodland landscapes is confirmed, probably in relation with Neanderthal habits of adaptation.

5. Conclusions

Level O represents the richest level in small-mammal remains from the Abric Romaní rock-shelter, a fundamental archaeological site for the understanding of the last Neanderthals occupations in Iberia. A detailed study of this assemblage reveals that:

- The origin of the assemblage is related to the activity of the tawny owl (*Strix aluco*), and post-depositional alterations indicate a fossiliferous microenvironment of relative environmental humidity and occasional water flows. Both taphonomic analyses confirm the reliability of the assemblage for paleoecological reconstructions.
- During the deposition of this level, the region of Capellades was colder (MAT: −3/−4 °C) and slightly wetter (MAP: +70/+170 mm; DJF: +60/+80 mm) than at present and featured semi-open woodland with a watercourse in the vicinity of the site. Further, the equal proportion of Mediterranean and mid-European species and the chronology of the level suggest a correlation with a cool climatic phase, probably between interstadials IS15 and IS14.
- Considering the Abric Romaní sequence and other Iberian MIS3 sites, it is suggested that these hominid groups were well adapted to the instability of this period. It is not clear what direct impact the climate had on their adaptive shifts on a local scale, as occurred in Abric Romaní. However, a general preference for occupying forest biotopes is detected.

Acknowledgments

We are grateful to the Abric Romaní excavation team. Additionally, we want to thank Joan Caparrós and Marc Torres for their contributions to the sorting of the material. This research was supported by the Ministry of Science, Innovation and Universities of the Spanish Government, project n° HAR2016-76760-C3-1-P, and the Catalonian Government, project n° SGR 2017-836. The Departament de Cultura (Servei d'Arqueologia i Patrimoni) of the Generalitat de Catalunya (2014/100576), the Diputació de Barcelona, the Ajuntament de Capellades, and Arts Gràfiques Romanyà-Valls S.A. provided support for the excavations. We are also grateful to two anonymous reviewers and to the editor (Dr. Falcon-Lang) for their comments which helped in improving the scientific content of this study. We want to thank Rupert Glasgow for reviewing the English language of the manuscript. M. Fernández-García is the beneficiary of a PhD scholarship funded under the Erasmus Mundus Programme – International Doctorate in Quaternary and Prehistory. J.M. López-García was supported by a Ramón y Cajal contract (RYC-2016- 19386) with financial sponsorship from the Spanish Ministry of Science, Innovation and Universities. A. Bargalló was funded by the European Union's Horizon 2020 research and innovation programme under the Marie Sklodowska-Curie Action grant agreement (PREKARN n° 702584).

References

Allué, E., Solé, A., Burguet-Coca, A., 2017. Fuel exploitation among Neanderthals based on the anthracological record from Abric Romaní (Capellades, NE Spain). Quat. Int. 431, 6–15. https://doi.org/10.1016/j.quaint.2015.12.046.

Andrews, P., 1990. Owls, Caves and Fossils. Predation, Preservation and Accumulation of Small Mammal Bones in Caves, With an Analysis of the Pleistocene Cave Faunas From Westbury-sub-Mendip, Somerset, UK. The University of Chicago, Chicago.

Andrews, P., 2006. Taphonomic effects of faunal impoverishment and faunal mixing. Palaeogeogr. Palaeoclimatol. Palaeoecol. 241, 572–589. https://doi.org/10.1016/j.palaeo.2006.04.012.

Andrews, P., Cook, J., 1985. Natural modifications to bones in temperate setting. Man 20, 675–691.

Arribas, Ó., 2004. Fauna y paisaje de los Pirineos en la Era Glaciar. Lynx, Barcelona.

Arrizabalaga, Á., 2004. Paleoclimatología y cronología del Würm reciente: un intento de síntesis. Zephyrus 57, 27–53.

Bab, I., Hajbi-Yonissi, C., Gabet, Y., Müller, R., 2007. Micro-tomographic Atlas of the Mouse Skeleton, Igarss 2014. Springer, New York. https://doi.org/10.1007/s13398-014-0173-7.2.

Baena, J., Carrión, E., Cuartero, F., Fluck, H., 2012. A chronicle of crisis: the Late Mousterian in North Iberia (Cueva del Esquilleu, Cantabria, Spain). Quat. Int. 247, 199–211. https://doi.org/10.1016/j.quaint.2011.07.031.

Bargalló, A., 2014. Technological Analysis of Neanderthal Settlement of the Level O Abric Romaní (Barcelona, Spain). Universitat Rovira i Virgili.

Bargalló, A., Gabucio, M.J., Rivals, F., 2016. Puzzling out a palimpsest: testing an interdisciplinary study in level O of Abric Romaní. Quat. Int. 417, 51–65. https://doi.org/10.1016/j.quaint.2015.09.066.

Barroso, C., Caparrós, M., Barsky, D., Moigne, A.-M., Monclova, A., 2014. Cueva del Boquete de Zafarraya: Un yacimiento de neandertales en el sur Iberia. In: Sala Ramos, R. (Ed.), Los Cazadores Recolectores Del Pleistoceno y Del Holoceno En Iberia y El Estrecho de Gibraltar: Estado Actual Del Conocimiento Del Registro Arqueológico. Universidad de Burgos, Burgos, pp. 463–472.

Bartrolí, R., Cebria, A., Muro, I., Riu-Barrera, E., Vaquero, M., 1995. A frec de ciencia. L'Atles d'Amador Romaní i Guerra. Ajuntament de Capellades, Capellades

(Barcelona).
Bennàsar, M., 2010. Tafonomía de micromamíferos del Pleistoceno Inferior de la Sierra de Atapuerca (Burgos): Sima del Elefante y Gran Dolina. Universitat Rovira i Virgili, Tarragona.
Bennàsar, M., Cáceres, I., Cuenca-Bescós, G., 2016. Paleoecological and microenvironmental aspects of the first European hominids inferred from the taphonomy of small mammals (Sima del Elefante, Sierra de Atapuerca, Spain). C.R. Palevol 15, 635–646. https://doi.org/10.1016/j.crpv.2015.07.006.
Bischoff, J.L., Julia, R., Mora, R., 1988. Uranium-series dating of the Mousterian occupation at Abric Romani, Spain. Nature 332, 68–70.
Blain, H.-A., Bailon, S., Cuenca-Bescós, G., Arsuaga, J.L., Bermúdez de Castro, J.M., Carbonell, E., 2009. Long-term climate record inferred from early-middle Pleistocene amphibian and squamate reptile assemblages at the Gran Dolina Cave, Atapuerca, Spain. J. Hum. Evol. 56, 55–65. https://doi.org/10.1016/j.jhevol.2008.08.020.
Blain, H.-A., Gleed-Owen, C.P., López-García, J.M., Carrión, J.S., Jennings, R., Finlayson, G., Finlayson, C., Giles-Pacheco, F., 2013. Climatic conditions for the last Neanderthals: Herpetofaunal record of Gorham's Cave, Gibraltar. J. Hum. Evol. 64, 289–299. https://doi.org/10.1016/j.jhevol.2012.11.003.
Blain, H.A., Lozano-Fernández, I., Agustí, J., Bailon, S., Menéndez Granda, L., Espígares Ortiz, M.P., Ros-Montoya, S., Jiménez Arenas, J.M., Toro-Moyano, I., Martínez-Navarro, B., Sala, R., 2016. Refining upon the climatic background of the Early Pleistocene hominid settlement in western Europe: Barranco León and Fuente Nueva-3 (Guadix-Baza Basin, SE Spain). Quat. Sci. Rev. 144, 132–144. https://doi.org/10.1016/j.quascirev.2016.05.020.
Burjachs, F., Julià, R., 1994. Abrupt climatic changes during the last glaciation based on pollen analysis of the Abric Romani, Catalonia, Spain. Quat. Res. 42, 308–315. https://doi.org/10.1006/qres.1994.1081.
Burjachs, F., López-García, J.M., Allué, E., Blain, H.-A., Rivals, F., Bennàsar, M., Expósito, I., 2012. Palaeoecology of Neanderthals during Dansgaard–Oeschger cycles in Northeastern Iberia (Abric Romaní): from regional to global scale. Quat. Int. 247, 26–37. https://doi.org/10.1016/j.quaint.2011.01.035.
Cáceres, I., 2002. Tafonomía de yacimientos antrópicos en karst. Complejo Galería (Sierra de Atapuerca, Burgos), Vanguard Cave (Gibraltar) y Abric Romaní (Capellades, Barcelona). Univeristat Rovira i Virgili.
Camps, M., Higham, T., 2012. Chronology of the Middle to Upper Palaeolithic transition at Abric Romaní, Catalunya. J. Hum. Evol. 62, 89–103. https://doi.org/10.1016/j.jhevol.2011.10.010.
Carbonell, E., Giralt, S., Vaquero, M., 1994. Abric Romani (Capellades, Barcelone, Espagne): une importante séquence anthropisée au Pléistocène supérieur. Bull. Soc. Préhist. Fr. 91, 47–55. https://doi.org/10.3406/bspf.1994.9703.
Carbonell, E., Cebrià, A., Allué, E., Cáceres, I., Castro, Z., Díaz, R., Esteban, M., Ollé, A., Pastó, I., Rodríguez, X.P., Rosell, J., Sala, R., Vallverdú, J., Vaquero, M., Vergés, J.M., 1996. Behavioural and organizational complexity in the Middle Palaeolithic from the Abric Romaní. In: Carbonell, E., Vaquero, M. (Eds.), The Last Neandertals, the First Anatomically Modern Humans. Cultural Change and Human Evolution: The Crisis at 40 Ka BP. Universitat de Tarragona, Tarragona, pp. 385–434.
Chacón, M.G., Bargalló, A., Gómez, B., Picin, A., Vaquero, M., Carbonell, E., 2013. Continuity or discontinuity of neanderthal technological behaviours During MIS 3: level M and level O of the Abric Romani site (Capellades, Spain). In: Pleistocene Foragers on the Iberian Peninsula: Their Culture and Environment. Festschrift in Honour of Gerd-Christian Weniger for his sixtieth birthday. Wissenschaftliche Schriften des Neanderthal Museums 7, pp. 55–84.
Chaline, J., 1972. Les rongeurs du Pléistocène moyen et supérieur de France. Éditions du Centre National de la Recherche Scientifique, Paris.
Cuenca-Bescós, G., Rofes, J., López-García, J.M., Blain, H.-A., De Marfá, R.J., Galindo-Pellicena, M.A., Bennásar-Serra, M.L., Melero-Rubio, M., Arsuaga, J.L., Bermúdez de Castro, J.M., Carbonell, E., 2010. Biochronology of Spanish Quaternary small vertebrate faunas. Quat. Int. 212, 109–119. https://doi.org/10.1016/j.quaint.2009.06.007.
Cuenca-Bescós, G., López-García, J.M., Galindo-Pellicena, M.A., García-Perea, R., Gisbert, J., Rofes, J., Ventura, J., 2014. Pleistocene history of Iberomys, an endangered endemic rodent from southwestern Europe. Integr. Zool. 9, 481–497. https://doi.org/10.1111/1749-4877.12053.
Daura, J., Sanz, M., Allué, E., Vaquero, M., López-García, J.M., Sánchez-Marco, A., Domènech, R., Martinell, J., Carrión, J.S., Ortiz, J.E., Torres, T., Arnold, L.J., Benson, A., Hoffmann, D.L., Skinner, A.R., Julià, R., 2017. Palaeoenvironments of the last Neanderthals in SW Europe (MIS 3): Cova del Coll Verdaguer (Barcelona, NE of Iberian Peninsula). Quat. Sci. Rev. 177, 34–56. https://doi.org/10.1016/j.quascirev.2017.10.005.
D'Errico, F., Sánchez Goñi, M.F., 2003. Neandertal extinction and the millennial scale climatic variability of OIS 3. Quat. Sci. Rev. 22, 769–788. https://doi.org/10.1016/S0277-3791(03)00009-X.
Duke, G.E., Jeers, A.A., Loft, G., Evanson, O.A., 1975. Gastric digestion in some systems. Comp. Biochem. Physiol. 50, 649–656.
Estévez, J., 1980. El aprovechamiento de los recursos faunísticos: Aproximación a la economía en el Paleolítico catalán. Cypsela 3, 9–30.
Evans, E.M.N., Van Couvering, J.A.H., Andrews, P., 1981. Palaeoecology of Miocene sites in Western Kenya. J. Hum. Evol. 10, 99–116. https://doi.org/10.1016/S0047-2484(81)80027-9.
Fagoaga, A., Ruiz-Sánchez, F.J., Laplana, C., Blain, H.-A., Marquina, R., Marin-Monfort, M.D., Galván, B., 2017. Palaeoecological implications of Neanderthal occupation at Unit Xb of El Salt (Alcoi, eastern Spain) during MIS 3 using small mammals proxy. Quat. Int. 1–12. https://doi.org/10.1016/j.quaint.2017.10.024.
Fernández-García, M., López-García, J.M., 2013. Palaeoecology and biochronology based on the rodents analysis from the Late Pleistocene/Holocene of Toll Cave (Moià, Barcelona). Span. J. Palaeontol. 28, 227–238.
Fernández-García, M., López-García, J.M., Lorenzo, C., 2016. Palaeoecological implications of rodents as proxies for the Late Pleistocene–Holocene environmental and climatic changes in northeastern Iberia. C.R. Palevol 15, 707–719. https://doi.org/10.1016/j.crpv.2015.08.005.
Fernández-Jalvo, Y., 1992. Tafonomía de microvertebrados del complejo cárstico de Atapuerca (Burgos). Universidad Complutense de Madrid.
Fernández-Jalvo, Y., Andrews, P., 1992. Small mammal taphonomy of Gran Dolina, Atapuerca (Burgos), Spain. J. Archaeol. Sci. 19, 407–428. https://doi.org/10.1016/0305-4403(92)90058-B.
Fernández-Jalvo, Y., Andrews, P., 2003. Experimental effects of water abrasion on bone fragments. J. Taphon. 1, 147–164.
Fernández-Jalvo, Y., Sánchez-Chillón, B., Andrews, P., Fernández-López, S., Alcalá Martínez, L., 2002. Morphological taphonomic transformations of fossil bones in continental environments, and repercussions on their chemical composition. Archaeometry 44, 353–361. https://doi.org/10.1111/1475-4754.t01-1-00068.
Fernández-Jalvo, Y., Andrews, P., Sevilla, P., Requejo, V., 2014. Digestion versus abrasion features in rodent bones. Lethaia 47, 323–336. https://doi.org/10.1111/let.12061.
Fernández-Jalvo, Y., Andrews, P., Denys, C., Sesé, C., Stoetzel, E., Marin-Monfort, D., Pesquero, D., 2016. Taphonomy for taxonomists: implications of predation in small mammal studies. Quat. Sci. Rev. 139, 138–157. https://doi.org/10.1016/j.quascirev.2016.03.016.
Fernández-López, S., 2000. Temas de tafonomía. Universidad Complutense de Madrid, Madrid.
Finlayson, C., Carrión, J.S., 2007. Rapid ecological turnover and its impact on Neanderthal and other human populations. Trends Ecol. Evol. 22, 213–222. https://doi.org/10.1016/j.tree.2007.02.001.
Finlayson, C., Giles Pacheco, F., Rodríguez-Vidal, J., Fa, D.A., María Gutierrez López, J., Santiago Pérez, A., Finlayson, G., Allue, E., Baena Preysler, J., Cáceres, I., Carrión, J.S., Fernández Jalvo, Y., Gleed-Owen, C.P., Jimenez Espejo, F.J., López, P., Antonio López Sáez, J., Antonio Riquelme Cantal, J., Sánchez Marco, A., Giles Guzman, F., Brown, K., Fuentes, N., Valarino, C.a., Villalpando, A., Stringer, C.B., Martinez Ruiz, F., Sakamoto, T., 2006. Late survival of Neanderthals at the southernmost extreme of Europe. Nature 443, 850–853. https://doi.org/10.1038/nature05195.
Finlayson, C., Finlayson, S., Giles, F., Giles, F., Rodriguez, J., 2016. Using birds as indicators of Neanderthal environmental quality: Gibraltar and Zafarraya compared. 421, 32–45.
Fletcher, W.J., Sánchez Goñi, M.F., Allen, J.R.M., Cheddadi, R., Combourieu-Nebout, N., Huntley, B., Lawson, I., Londeix, L., Magri, D., Margari, V., Müller, U.C., Naughton, F., Novenko, E., Roucoux, K., Tzedakis, P.C., 2010. Millennial-scale variability during the last glacial in vegetation records from Europe. Quat. Sci. Rev. 29, 2839–2864. https://doi.org/10.1016/j.quascirev.2009.11.015.
Font-Tullot, I., 2007. Climatología de España y Portugal. Universidad de Salamanca, Salamanca.
Gabucio, M.J., Bargallo, A., 2012. Neanderthal subsistence change around 55 kyr. In: Actas das IV Jornadas Jovens em Investig. Archeol. - JIA 2011. vol. II. pp. 193–200.
Gabucio, M.J., Cáceres, I., Rosell, J., 2012. Evaluating post-depositional processes in level O of the Abric Romaní archaeological site. Neues Jahrb. Geol. Palaontol. Abh. 265, 147–163. https://doi.org/10.1127/0077-7749/2012/0252.
Gabucio, M.J., Cáceres, I., Rosell, J., Saladié, P., Vallverdú, J., 2014. From small bone fragments to Neanderthal activity areas: the case of Level O of the Abric Romaní (Capellades, Barcelona, Spain). Quat. Int. 330, 36–51. https://doi.org/10.1016/j.quaint.2013.12.015.
Gabucio, M.J., Cáceres, I., Rivals, F., Bargalló, A., Saladié, P., Vallverdú, J., Vaquero, M., Carbonell, E., 2018. Unraveling a Neanderthal palimpsest from a zooarcheological and taphonomic perspective. Archaeol. Anthropol. Sci. 10, 197–222. https://doi.org/10.1007/s12520-016-0343-y.
Garcia-Ibaibarriaga, N., 2015. Los microvertebrados en el registro arqueo-paleontológico del País Vasco: Cambios climáticos y evolución paleoambiental durante el Pleistoceno Superior. Universidad del País Vasco.
Giralt, S., Julià, R., 1996. The sedimentary record of the middle/upper Paleolithic transition in the Capellades area (NE Spain). In: Carbonell, E., Vaquero, M. (Eds.), The Last Neanderthals, the First Anatomically Modern Humans: Cultural Change and Human Evolution: The Crisis at 40 Ka BP. Universitat de Tarragona, Tarragona, pp. 356–376.
Gosàlbez, J., 1987. Insectívors i rosegadors de Catalunya. Metodologia d'estudi i catàleg faunístic. Ketres Editora, Barcelona.
Hammer, Ø., Harper, D.A.T., Ryan, P.D., 2001. Paleontological statistics software package for education and data analysis. Palaeontol. Electron. 4, 9–18. https://doi.org/10.1016/j.bcp.2008.05.025.
Harrison, S.P., Sanchez Goñi, M.F., 2010. Global patterns of vegetation response to millennial-scale variability and rapid climate change during the last glacial period. Quat. Sci. Rev. 29, 2957–2980. https://doi.org/10.1016/j.quascirev.2010.07.016.
Higham, T., Douka, K., Wood, R., Ramsey, C.B., Brock, F., Basell, L., Camps, M., Arrizabalaga, A., Baena, J., Barroso-Ruíz, C., Bergman, C., Boitard, C., Boscato, P., Caparrós, M., Conard, N.J., Draily, C., Froment, A., Galván, B., Gambassini, P., Garcia-Moreno, A., Grimaldi, S., Haesaerts, P., Holt, B., Iriarte-Chiapusso, M.-J., Jelinek, A., Jordá Pardo, J.F., Maíllo-Fernández, J.-M., Marom, A., Maroto, J., Menéndez, M., Metz, L., Morin, E., Moroni, A., Negrino, F., Panagopoulou, E.,

Peresani, M., Pirson, S., de la Rasilla, M., Riel-Salvatore, J., Ronchitelli, A., Santamaria, D., Semal, P., Slimak, L., Soler, J., Soler, N., Villaluenga, A., Pinhasi, R., Jacobi, R., 2014. The timing and spatiotemporal patterning of Neanderthal disappearance. Nature 512, 306–309. https://doi.org/10.1038/nature13621.
Jiménez, C., 2003. Guía dels ocells de Vilanova del Camí. Ajuntament de Vilanova del Camí, Vilanova del Camí (Barcelona).
Jiménez, C., Tomás, M., 2009. Mamífers de Vilanova del Camí. Ajuntament de Vilanova del Camí, Vilanova del Camí (Barcelona).
Jutglar, F., Masó, A., 1999. Aves de la Península Ibérica. Guía de campo. Planeta, Barcelona.
König, C., Weick, F., Becking, J.H., 1999. Owls. A Guide to the Owls of the World. Pica press, New Haven.
Korth, W.W., 1979. Taphonomy of microvertebrate fósil assemblages. Ann. Carnegie Museum 48, 235–285.
Kowalski, K., 1995. Taphonomy of bats (Chiroptera). Geobios 18, 251–256. https://doi.org/10.1016/S0016-6995(95)80172-3.
Leroyer, C., Leroi-Gourhan, A., 1983. Problèmes de chronologie. Le Castelperronien et l'Aurignacien. Bull. Soc. Préhist. Fr. 80, 41–44.
López García, J.M., 2007. Primeros datos sobre los microvertebrados del Pleistoceno Superior del Abric Romaní (Capellades, Barcelona). In: Cambra-Moo, O. (Ed.), Cantera Paleontológica. Diputación Provincial de Cuenca, Cuenca, pp. 235–245.
López, M., López-Fuster, M.J., Palazón, S., Ruiz-Olmo, J., Ventura, J., 2006. Els mamífers. In: La Fauna Vertebrada a Les Terres de Lleida. Universitat de Lleida, Lleida, pp. 230–262.
López-García, J.M., 2008. Late Pleistocene small mammals from Abric Romaní (Barcelona, Spain). Ann. dell'Università degli Stud. di Ferrara vol.spec., pp. 105–110.
López-García, J.M., 2011. Los micromamíferos del Pleistoceno superior de la Península Ibérica. Evolución de la diversidad taxonómica y cambios paleoambientales y paleoclimáticos. Ed. Académica Española, Saarbrücken.
López-García, J.M., Cuenca-Bescós, G., 2010. Évolution climatique durant le Pléistocène Supérieur en Catalogne (nord-est de l'Espagne) d'après l'étude des micromammifères. Quaternaire 21, 249–258.
López-García, J.M., Blain, H.-A., Cuenca-Bescós, G., Arsuaga, J.L., 2008. Chronological, environmental, and climatic precisions on the Neanderthal site of the Cova del Gegant (Sitges, Barcelona, Spain). J. Hum. Evol. 55, 1151–1155. https://doi.org/10.1016/j.jhevol.2008.08.001.
López-García, J.M., Sevilla, P., Cuenca-Bescós, G., 2009. New evidence for the greater noctule bat (Nyctalus lasiopterus) in the Late Pleistocene of western Europe. C.R. Palevol 8, 551–558. https://doi.org/10.1016/j.crpv.2009.05.004.
López-García, J.M., Blain, H.A., Allué, E., Bañuls, S., Bargalló, A., Martín, P., Morales, J.I., Pedro, M., Rodríguez, A., Solé, A., Oms, F.X., 2010. First fossil evidence of an "interglacial refugium" in the pyrenean region. Naturwissenschaften 97, 753–761. https://doi.org/10.1007/s00114-010-0695-6.
López-García, J.M., Blain, H.-A., Cuenca-Bescós, G., Alonso, C., Alonso, S., Vaquero, M., 2011a. Small vertebrates (Amphibia, Squamata, Mammalia) from the late Pleistocene-Holocene of the Valdavara-1 cave (Galicia, northwestern Spain). Geobios 44, 253–269. https://doi.org/10.1016/j.geobios.2010.10.001.
López-García, J.M., Cuenca-Bescós, G., Blain, H.-A., Álvarez-Lao, D., Uzquiano, P., Adán, G., Arbizu, M., Arsuaga, J.L., 2011b. Palaeoenvironment and palaeoclimate of the Mousterian–Aurignacian transition in northern Iberia: the small-vertebrate assemblage from Cueva del Conde (Santo Adriano, Asturias). J. Hum. Evol. 61, 108–116. https://doi.org/10.1016/j.jhevol.2011.01.010.
López-García, J.M., Cuenca-Bescós, G., Finlayson, C., Brown, K., Pacheco, F.G., 2011c. Palaeoenvironmental and palaeoclimatic proxies of the Gorham's cave small mammal sequence, Gibraltar, southern Iberia. Quat. Int. 243, 137–142. https://doi.org/10.1016/j.quaint.2010.12.032.
López-García, J.M., Blain, H.-A., Bennàsar, M., Euba, I., Bañuls, S., Bischoff, J., López-Ortega, E., Saladié, P., Uzquiano, P., Vallverdú, J., 2012a. A multiproxy reconstruction of the palaeoenvironment and palaeoclimate of the Late Pleistocene in northeastern Iberia: Cova dels Xaragalls, Vimbodí-Poblet, Paratge Natural de Poblet, Catalonia. Boreas 41, 235–249. https://doi.org/10.1111/j.1502-3885.2011.00234.x.
López-García, J.M., Blain, H.-A., Burjachs, F., Ballesteros, A., Allué, E., Cuevas-Ruiz, G.E., Rivals, F., Blasco, R., Morales, J.I., Hidalgo, A.R., Carbonell, E., Serrat, D., Rosell, J., 2012b. A multidisciplinary approach to reconstructing the chronology and environment of southwestern European Neanderthals: the contribution of Teixoneres cave (Moià, Barcelona, Spain). Quat. Sci. Rev. 43, 33–44. https://doi.org/10.1016/j.quascirev.2012.04.008.
López-García, J.M., Blain, H.A., Sanz, M., Daura, J., 2012c. A coastal reservoir of terrestrial resources for neanderthal populations in north-eastern Iberia: Palaeoenvironmental data inferred from the small-vertebrate assemblage of Cova del Gegant, Sitges, Barcelona. J. Quat. Sci. 27, 105–113. https://doi.org/10.1002/jqs.1515.
López-García, J.M., Blain, H.-A., Bennàsar, M., Alcover, J.A., Bañuls-Cardona, S., Fernández-García, M., Fontanals, M., Martín, P., Morales, J.I., Muñoz, L., Pedro, M., Vergés, J.M., 2014a. Climate and landscape during Heinrich Event 3 in south-western Europe: the small-vertebrate association from Galls Carboners cave (Mont-ral, Tarragona, north-eastern Iberia). J. Quat. Sci. 29, 130–140.
López-García, J.M., Blain, H.A., Bennàsar, M., Fernández-García, M., 2014b. Environmental and climatic context of neanderthal occupation in southwestern Europe during MIS3 inferred from the small-vertebrate assemblages. Quat. Int. 326–327, 319–328.
López-García, J.M., Soler, N., Maroto, J., Soler, J., Alcalde, G., Galobart, A., Bennàsar, M., Burjachs, F., 2015. Palaeoenvironmental and palaeoclimatic reconstruction of the Latest Pleistocene of L'Arbreda Cave (Serinyà, Girona, northeastern Iberia) inferred from the small-mammal (insectivore and rodent) assemblages. Palaeogeogr. Palaeoclimatol. Palaeoecol. 435, 244–253. https://doi.org/10.1016/j.palaeo.2015.06.022.
Louarn, H.L., Quéré, J.-P., 2003. Les Rongeurs de France. Faunistique et biologie. Institut National de la Recherche Agronomique, Paris.
Lyman, R.L., 1994. Vertebrate Taphonomy. Cambridge University Press, Cambridge.
Margalef, R., 1974. Ecología. Omega, Barcelona.
Marín-Arroyo, A.B., Landete-Ruiz, M.D., Seva-Román, R., Lewis, M.D., 2014. Manganese coating of the Tabun faunal assemblage: implications for modern human behaviour in the Levantine Middle Palaeolithic. Quat. Int. 330, 10–18. https://doi.org/10.1016/j.quaint.2013.07.016.
Maroto, J., Vaquero, M., Arrizabalaga, Á., Baena, J., Baquedano, E., Jordá, J., Julià, R., Montes, R., Van Der Plicht, J., Rasines, P., Wood, R., 2012. Current issues in late Middle Palaeolithic chronology: New assessments from Northern Iberia. Quat. Int. 247, 15–25. https://doi.org/10.1016/j.quaint.2011.07.007.
Martínez-Moreno, J., Mora, R., de la Torre, I., 2010. The Middle-to-Upper Palaeolithic transition in Cova Gran (Catalunya, Spain) and the extinction of Neanderthals in the Iberian Peninsula. J. Hum. Evol. 58, 211–226. https://doi.org/10.1016/j.jhevol.2009.09.002.
Mellars, P., 1998. The Neanderthal Legacy: An Archaeological Perspective From Western Europe. Princeton University Press, Princeton (NY).
Menu, H., Popelard, J.B., 1987. Utilisation des caracteres dentaires pour la determination des vespertilionines de l'ouest europeen. Bull. Coord. Ouest l'étude Prot. Chauves-Souris 4, 11–88.
Mikkola, H., 1983. Owls of Europe. Buteo Books, Sussex.
Murelaga, X., Bailón, S., Rofes, J., García-Ibaibarriaga, N., 2012. Estudio arqueozoológico de los macromamíferos del yacimiento de Askondo (Mañaria, Bizkaia). In: Garate, D., Rios-Garaizar, J. (Eds.), La Cueva de Askondo (Mañaria): Arte Parietal y Ocupación Humana Durante La Prehistoria. Kobie. Bizkaiko Arkeologi Indusketak 2, Bilbao, pp. 65–70.
Nadachowski, A., 1982. Late Quaternary Rodents of Poland with Special Reference to Morphotype Dentition Analysis of Voles. Polska Academia Nauk, Panstwowe Wydawnictwo Naukowe, Krakow.
Ninyerola, M., Pons, X., Roure, J.M., Martín-Vide, J., Raso-Nadal, J.M., Clavero, P., 2003. Atles Climátics de Catalunya. Generalitat de Catalunya (Departament de Medi Ambient), Barcelona.
Olsson, V., 1979. Studies on a population of Eagle owls in southeast Sweden. Viltrevy 11, 1–99.
Palomo, L.J., Gisbert, J., Blanco, C., 2007. Atlas y libro rojo de los mamíferos terrestres de España. Organismo Autónomo Parques Nacionales, Madrid.
Picin, A., Carbonell, E., 2016. Neanderthal mobility and technological change in the northeastern of the Iberian Peninsula: The patterns of chert exploitation at the Abric Romaní rock-shelter. C.R. Palevol 15, 581–594. https://doi.org/10.1016/j.crpv.2015.09.012.
Rey-Rodríguez, I., López-García, J.-M., Bennàsar, M., Bañuls-Cardona, S., Blain, H.-A., Blanco-Lapaz, Á., Rodríguez-Álvarez, X.-P., de Lombera-Hermida, A., Díaz-Rodríguez, M., Ameijenda-Iglesias, A., Agustí, J., Fábregas-Valcarce, R., 2016. Last Neanderthals and first Anatomically Modern Humans in the NW Iberian Peninsula: Climatic and environmental conditions inferred from the Cova Eirós small-vertebrate assemblage during MIS 3. Quat. Sci. Rev. 151, 185–197. https://doi.org/10.1016/j.quascirev.2016.08.030.
Sánchez Goñi, M.F., D'Errico, F., 2005. La historia de la vegetación y el clima del último ciclo climático (OIS5-OIS1, 140.000-10.000 años BP) en la Península Ibérica y su posible impacto sobre los grupos paleolíticos. Monogr. - Mus. Altamira 20, 115–129.
Sánchez Goñi, M.F., Landais, A., Fletcher, W.J., Naughton, F., Desprat, S., Duprat, J., 2008. Contrasting impacts of Dansgaard-Oeschger events over a western European latitudinal transect modulated by orbital parameters. Quat. Sci. Rev. 27, 1136–1151. https://doi.org/10.1016/j.quascirev.2008.03.003.
Sans-Fuentes, M.A., Ventura, J., 2000. Distribution patterns of the small mammals (Insectivora and Rodentia) in a transitional zone between the Eurosiberian and the Mediterranean regions. J. Biogeogr. 27, 755–764. https://doi.org/10.1046/j.1365-2699.2000.00421.x.
Sepulchre, P., Ramstein, G., Kageyama, M., Vanhaeren, M., Krinner, G., Sánchez-Goñi, M.F., d'Errico, F., 2007. H4 abrupt event and late Neanderthal presence in Iberia. Earth Planet. Sci. Lett. 258, 283–292. https://doi.org/10.1016/j.epsl.2007.03.041.
Sesé, C., 1994. Paleoclimatical interpretation of the quaternary small mammals of Spain. Geobios 27, 753–767. https://doi.org/10.1016/S0016-6995(94)80060-X.
Sesé, C., 2011. Micromamíferos (Erinaceomorfos y Roedores) del final del Pleistoceno Superior y primera parte del Holoceno de Cova Fosca (Alto Maestrazgo, Castellón): Reconstrucción paleoambiental del entorno del yacimiento. 20, 119–137.
Sevilla, P., 1988. Estudio paleontológico de los Quirópteros del Cuaternario español. Paleontol. Evol. 22, 113–233.
Sharp, W.D., Mertz-Kraus, R., Vallverdu, J., Vaquero, M., Burjachs, F., Carbonell, E., Bischoff, J.L., 2016. Archeological deposits at Abric Romaní extend to 110 ka: U-series dating of a newly cored, 30 meter-thick section. J. Archaeol. Sci. Rep. 5, 400–406. https://doi.org/10.1016/j.jasrep.2015.12.015.
Shipman, P., Foster, G., Schoeninger, M., 1984. Burnt bones and teeth: an experimental-study of color, morphology, crystal-structure and shrinkage. J. Archaeol. Sci. 11, 307–325. https://doi.org/10.1016/0305-4403(84)90013-x.
Simpson, E.H., 1949. Measurement of diversity. Nature 163, 688.

Sommer, R.S., Nadachowski, A., 2006. Glacial refugia of mammals in Europe: evidence from fossil records. Mammal Rev. 36, 251–265. https://doi.org/10.1111/j.1365-2907.2006.00093.x.

Svensson, L., 2010. Guía de aves. España, Europa y región mediterránea. Omega, Barcelona.

Svensson, A., Andersen, K.K., Bigler, M., Clausen, H.B., Davies, D.D.S.M., Johnsen, S.J., 2008. A 60000 year Greenland stratigraphie ice core chronology. Clim. Past 4, 47–57.

Talamo, S., Blasco, R., Rivals, F., Picin, A., Chacón, M.G., Iriarte, E., López-García, J.M., Blain, H.-A., Arilla, M., Rufà, A., Sánchez-Hernández, C., Andrés, M., Camarós, E., Ballesteros, A., Cebrià, A., Rosell, J., Hublin, J.-J., 2016. The radiocarbon approach to Neanderthals in a carnivore Den site: a well-defined chronology for Teixoneres cave (Moià, Barcelona, Spain). Radiocarbon 58, 247–256. https://doi.org/10.1017/RDC.2015.19.

Vallverdú, J., Alonso, S., Bargalló, A., Bartrolí, R., Campeny, G., Carrancho, Á., Expósito, I., Fontanals, M., Gabucio, J., Gómez, B., Prats, J.M., Sañudo, P., Solé, À., Vilalta, J., Carbonell, E., 2012. Combustion structures of archaeological level O and mousterian activity areas with use of fire at the Abric Romaní rockshelter (NE Iberian Peninsula). Quat. Int. 247, 313–324. https://doi.org/10.1016/j.quaint.2010.12.012.

Vaquero, M., Carbonell, E., 2012. Some clarifications on the Middle-Upper Paleolithic transition in Abric Romaní: Reply to Camps and Higham (2012). J. Hum. Evol. 63, 711–717. https://doi.org/10.1016/j.jhevol.2012.07.007.

Vaquero, M., Allué, E., Bischoff, J.L., Burjachs, F., Vallverdú, J., 2013. Environmental, depositional and cultural changes in the Upper Pleistocene and Early Holocene: the Cinglera del Capelló sequence (Capellades, Spain). Quaternaire 24, 49–64.

Williams, S.E., Marsh, H., Winter, J., 2002. Spatial scale, species diversity, and habitat structure: small mammals in Australian tropical rain forest. Ecology 83, 1317–1329. https://doi.org/10.2307/3071946.

Wood, R.E., Arrizabalaga, A., Camps, M., Fallon, S., Iriarte-Chiapusso, M.J., Jones, R., Maroto, J., De la Rasilla, M., Santamaría, D., Soler, J., Soler, N., Villaluenga, A., Higham, T.F.G., 2014. The chronology of the earliest Upper Palaeolithic in northern Iberia: New insights from L'Arbreda, Labeko Koba and La Viña. J. Hum. Evol. 69, 91–109. https://doi.org/10.1016/j.jhevol.2013.12.017.

Zilhão, J., 2000. The ebro frontier: a model for the late extinction of Iberian Neanderthals. In: Stringer, C.B., Barton, R.N.E., Finlayson, C. (Eds.), Neanderthals on the Edge:150th Anniversary Conference of the Forbes' Quarry Discovery, Gibraltar. Oxbow Books, Oxford, pp. 111–121. https://doi.org/10.1109/ICELMACH.2008.4800248.